NASA TECHNICAL MEMORANDUM

NASA TM X-71692

NASA TM X-71692

TITAN/CENTAUR T/C-1
POST FLIGHT EVALUATION REPORT

by Lewis Research Staff
Lewis Research Center
Cleveland, Ohio 44135
April, 1975

This information is being published in preliminary form in order to expedite its early release.

CONTENTS

I. SUMMARY

by S. V. Szabo, Jr., and L. J. Ross

The first Titan/Centaur launch vehicle, TC-1, was launched from the Eastern Test Range Complex 41 at 09:48:01.46 hours Eastern Daylight Time on February 11, 1974. The vehicle carried a dynamic mass model of the Viking spacecraft and a SPHINX spacecraft, intended to study high voltage interactions in space. This launch was a Proof Flight of a vehicle configuration integrating the Air Force Titan booster and the NASA Centaur upper stage. It also was the first flight of the Centaur Standard Shroud developed for the Titan/Centaur.

The countdown for the launch proceeded normally except for an additional 45 minute hold which was required to resolve a question concerning interpretation of booster hydraulic system data. The launch window opened at 09:03:00 hours Eastern Daylight Time. The vehicle was launched on a flight azimuth of 105°.

The Titan boost phase of flight was satisfactory. Solid Motor operation, Stage I and Stage II operation were normal. Venting of the Centaur Standard Shroud during ascent was successful and shroud separation and jettison was accomplished without incident. At the completion of the Titan Stage II burn, the Centaur successfully separated from the Titan.

At this time, the Centaur main engines were sequenced through the first planned starting cycle, but failed to achieve steady state operation. The vehicle flight control system, not sensing vehicle acceleration, commanded engine shutdown, and recycled, as programmed, through a back-up engine start attempt. The second engine start attempt was also unsuccessful. The flight control system then placed the vehicle in a coast-phase mode and the vehicle continued downrange in free fall. The vehicle was destroyed by Range Safety when the impact point was approximately 2200 nautical miles downrange, 12 minutes, 28.5 seconds after liftoff.

E-8293

II. INTRODUCTION

by S. V. Szabo, Jr., and L. J. Ross

The Titan/Centaur vehicle number one (TC-1) was the first vehicle launched combining the Air Force Titan III booster and the National Aeronautics and Space Administration's Centaur Upper Stage. In addition, the configuration utilized a newly developed Centaur Standard Shroud.

The Centaur D was originally developed starting in the late 1950, early 1960 time period as a second stage for the Atlas D missile. During the 1960's, the Atlas/Centaur combination was used successfully to launch Surveyor, OAO, ATS, Intelsat, Pioneer, and Mariner spacecraft. An updated version of Centaur, designated D-1, which incorporated a new avionics system began operation as the Atlas upper stage in 1973. The D-1 Centaur when serving as an Atlas upper stage is designated D-1A while the version that flies with the Titan is the D-1T. The D-1T Centaur also incorporates certain redundancy and reliability/quality improvements in selected mechanical systems. These improvements are scheduled for incorporation into D-1A in 1975.

The Titan III booster was developed by the United States Air Force and has been in use successfully since 1964. Modifications were required to the Titan IIID configuration to integrate it with the Centaur. The Titan used with the Centaur is designated the Titan IIIE.

The Centaur Standard Shroud was developed to accommodate the larger payloads capable of being carried by the Titan/Centaur. The design of this shroud was based on similar shrouds used by the Air Force in the Titan III programs.

The unique capabilities of the Titan/Centaur which provide a high-energy restartable upper stage fills the performance and cost need for a launch vehicle capable of delivering heavier payloads beyond the capability of Atlas/Centaur but less than that of the Saturn V to interplanetary trajectories and synchronous orbit. The Titan/Centaur will be used to launch operational payloads such as: Helios, a joint undertaking between NASA and the Federal Republic of Germany Space Agency, to investigate space near the Sun; Viking, a combination Martian orbiter and lander; and Mariner Jupiter/Saturn, a flyby of these planets.

The Titan/Centaur TC-1 vehicle was intended as a proof flight of the Titan/Centaur combination. The vehicle was to perform four burns of the Centaur engines, perform settled propellant and zero-g coast periods, and in general obtain data on the Titan, Centaur, and Centaur Standard Shroud

during the flight.

The major objectives of the flight were:

Primary: Demonstrate the capability of the Titan/Centaur launch vehicle and the Integrate/Transfer/Launch facilities to support operational missions.

Secondary: Demonstrate Centaur capability to perform an operational two-burn mission, with an extended parking orbit coast, and an operational three-burn synchronous orbit mission.

Deliver a spacecraft (SPHINX) into the mission transfer orbit at a specified spacecraft without compromising the other mission objectives.

Although the Centaur did not achieve orbit, a large part of the primary objective of the mission was achieved, since the countdown, Titan stage of flight, Centaur Standard Shroud Jettison, and Titan/Centaur separation were successfully accomplished. These events represented the major new operations and hardware associated with the Titan/Centaur. Since the Centaur stage, in the D-1A configuration, had successfully flown in three previous missions, its operational objectives were secondary. None of the secondary objectives were achieved since the vehicle never became orbital.

The limited proof flight, however, provided the following overall accomplishments:

Titan/Centaur Integration Design Verification

1. Demonstrated ability of launch complex 41 to support a launch. (Hardware and software) Proved the ability of the complex, multi-organizational (government and contractor) launch team to function successfully.

2. Demonstrated the steering interface between the Centaur and the Titan in roll and wind bias during Stage 0 and closed loop guidance during Stages I and II phases of flight.

3. Satisfactorily demonstrated Titan/Centaur staging.

4. Verified the structural integrity of all vehicle stages and the Centaur interstage adapter through the launch and boost environment.

Centaur Standard Shroud

1. Demonstrated successful flight operation of all shroud systems.

2. Successfully jettisoned shroud.

3. Demonstrated operation of all umbilicals, chutes, and doors on shroud.

Analytical

1. Obtained data that confirms estimates of launch/flight environment. (Loads, acoustics, thermal, and vibration)

2. Obtained all data required for the Viking Dynamic Simulator program.

In addition to the above overall accomplishments, the performance of the following new D-1T Centaur designs was demonstrated:

Structural

1. Interstage adapter
2. Centaur truss adapter
3. Viking transition adapter including thermal diaphragm
4. Encapsulation bulkhead
5. Pyrotechnic forward seal releaser
6. Titanium stub adapter
7. Forward bearing reactor system
8. Centaur radiation shield integrity
9. Centaur and Centaur standard shroud compartment venting systems

Avionics/Software

1. Coast phase autopilot operation
2. Main engine start failure logic
3. Titan/Centaur interface
   *Discretes
   *Steering
4. Guidance/stabilization/sequencing
5. Telemetry system
6. Electrical power supply
7. Computer controlled vent and pressurization system (CCVAPS) program
8. RF antenna switch at shroud jettison
9. Computer controlled launch set (CCLS) operation during countdown

Fluid Systems

1. Redundant hydrogen peroxide system
2. Reaction control thrusters
3. Computer controlled venting and pressurization system in the pressurization mode

*New solenoid valves
*LO_2 tank bubbler
*LH_2 tank helium energy dissipator
*Pyrotechnic shutoff valves
*Control pressure transducers

4. LH_2 tank vent system and disconnects
5. LO_2 tank vent system and disconnects

This report presents an evaluation of the Titan/Centaur-1 in support of the mission objectives. Titan, Centaur, and Centaur Standard Shroud Systems are described, and their performance evaluated.

III. LAUNCH VEHICLE DESCRIPTION

General

The combination of the Titan IIIE and Centaur D-1T, called the Titan/Centaur, is illustrated in figure III-1. An Interstage Adapter supports the Centaur stage and the Centaur Standard Shroud (CSS) atop the Titan IIIE. The interstage remains with the Titan at Centaur separation. The Centaur Standard Shroud covers the spacecraft, the Centaur, and part of the Interstage Adapter.

As discussed previously, the Titan/Centaur was added to the NASA family of launch vehicles to fill a performance gap between the Atlas/Centaur and Saturn V vehicles.

The remainder of this section of the report presents overall descriptions of the Titan IIIE, Centaur D-1T, Centaur Standard Shroud, and the TC-1 payload. For detailed systems descriptions, see the respective sections in this report.

Centaur D-1T

The improved Centaur (fig. III-2) is built by General Dynamics' Convair Aerospace Division. It incorporates design changes over the original Centaur D model necessary to meet new mission requirements and to incorporate certain redundancy and reliability improvements.

The Centaur uses liquid hydrogen and liquid oxygen as the propellants. These are contained in pressure-stabilized thin wall tanks. The propellant tanks are separated by a vacuum-insulated common bulkhead. An equipment module mounted on the forward end of Centaur provides for the support of the electronic and guidance equipment.

Increased Centaur coast (up to $5\frac{1}{4}$ hr), to provide improved synchronous orbit capability, is obtained by adding an aluminized mylar radiation shield to the hydrogen tank sidewalls. Radiation shielding and insulation have been added to cover the exposed portions of the aft and forward ends of the Centaur tanks.

Vehicle thrust is provided by two Pratt & Whitney Aircraft Corporation engines developing 66 720 newtons (15 000 lb) thrust each. The Centaur tank pressurization and venting systems were modified to incorporate redundancy features and are controlled by the Centaur Digital Computer Unit (DCU). Reliability improvements were made to the hydraulic

system which provides the necessary force to gimbal the Centaur engines in response to guidance commands. The hydrogen-peroxide system for the propellant boost pumps and attitude control engines has been redesigned to incorporate redundancy features. Attitude control and propellant settling thrust are provided by 26.7 newtons (6 lb) thrust hydrogen-peroxide engines mounted on the vehicle aft bulkhead. The engine arrangement, in conjunction with the Centaur computer software, can maintain vehicle stability in the event of a single engine failure to fire.

The Centaur updated astrionics system, integrates many former hardware functions into the airborne computer software. Guidance and control are accomplished using a newly developed Centaur Digital Computer Unit (DCU) built by Teledyne Systems Company. This computer is an advanced, high speed digital computer with extensive input and output capabilities. From the DCU, discrete signals are provided to the Sequence Control Unit (SCU). The SCU provides the necessary interface between the DCU and the vehicle systems that require switched and/or timed commands. Engine steering commands go to the Servo Inverter Unit (SIU). The SIU contains four servo-amplifiers. Each amplifier operates in conjunction with the hydraulic system to gimbal the engines. The SIU also contains the electronics for the propellant utilization system and an inverter which supplies vehicle a.c. power. Electrical power is provided by battery. Up to three batteries can be used to meet expanded mission requirements.

A stable platform and its electronics unit make up the Honeywell, Inc. Inertial Measurement Group (IMG). The IMG measures acceleration and provides a time reference for the DCU to make navigational computations. The IMG consists of two packages: the Systems Electronic Unit (SEU) and the Inertial Reference Unit (IRU). The SEU contains filters, power supplies, and mode control relays for the IRU. The IRU contains a four gimbal all-attitude stable platform. Three gyros stabilize this platform on which are mounted three pulse-rebalanced accelerometers. The IMG, in conjunction with the DCU, performs the navigation and guidance functions for the Titan/Centaur vehicle and also performs the flight control for the Centaur phase of flight. During the Titan boost phase of flight, guidance steering commands are provided by the Centaur guidance system to the Titan flight control system.

The flight software is modularized into several special purpose subroutines that operate under the control of a real time executive program. The executive calls on subroutines to perform various tasks such as guidance and navigation, sequencing telemetry, attitude control, and propellant mixture ratio management. This results in a flexible system readily adaptable to new missions through software rather than hardware changes.

The Centaur pulse code modulation telemetry system is a time division multiplexed system controlled by the DCU. Remote multiplexer units provide a convenient means for handling Centaur instrumentation.

Prelaunch checkout of the Centaur is accomplished using a ground computer called the Computer Controlled Launch Set (CCLS). The CCLS functions include calibration and alinement of the inertial measurement group, loading and verifying storage of Centaur computer programs, and testing of electronic systems.

Titan IIIE

The Titan/Centaur booster, designated Titan IIIE, was developed from the family of Titan III vehicles in use by the Air Force since 1964. The Titan IIIE is a modified version of the Titan IIID. Modifications were made to the Titan to accept steering commands and discretes from the Centaur inertial guidance system instead of a radio guidance system. In addition, a redundant programmer and sequence system were added. The Titan IIIE, illustrated in figure III-3 consists of two solid rocket motors designated Stage 0 and the Titan III core vehicle Stages I and II.

The two Solid Rocket Motors (SRM's) provide a thrust of 10.6 million newtons (2.4 million lb) at liftoff. These motors, built by United Technology Center, use propellants which are basically aluminum and ammonium perchlorate in a synthetic rubber binder. Flight control during the Stage 0 phase of flight is provided by a Thrust Vector Control (TVC) system in response to commands from the Titan flight control computer. Nitrogen tetroxide injected into the SRM nozzle through TVC valves deflects the thrust vector to provide control. Pressurized tanks attached to each solid rocket motor supply the thrust vector control fluid. Electrical systems on each SRM provide power for the TVC system.

Titan core Stages I and II are built by the Martin Marietta Corporation. The Stages I and II propellant tanks are constructed of welded aluminum panels and domes while interconnecting skirts use conventional aluminum sheet and stringer construction. The Stage II forward skirt provides the attach point for the Centaur stage and also houses a truss structure supporting most of the Titan IIIE electronics. A thermal barrier was added to isolate the Titan IIIE electronics compartment from the Centaur engine compartment.

Stages I and II are both powered by liquid rocket engines made by the Aerojet Liquid Rocket Company. Propellants for both stages are nitrogen tetroxide and a 50/50 combination of hydrazine and unsymmetrical dimethylhydrazine. The Stage I engine consists of dual thrust chambers and turbopumps producing 2.3 million newtons (520 000 lb) thrust at altitude.

Independent gimbaling of the two thrust chambers, using a conventional hydraulic system, provides control in pitch, yaw, and roll during Stage I flight. The Stage II engine is a single thrust chamber and turbopump producing 445 000 newtons (100 000 lb) thrust at altitude. The thrust chamber gimbals for flight control in pitch and yaw and the turbopump exhaust duct rotates to provide roll control during Stage II flight.

The Titan flight control computer provides pitch, yaw, and roll commands to the solid rocket motor's thrust vector control system and the Stages I and II hydraulic actuators. The flight control computer receives attitude signals from the three-axis reference system which contains three displacement gyros. Vehicle attitude rates in pitch and yaw are provided by the rate gyro system located in Stage I. In addition, the flight control computer generates preprogrammed pitch and yaw signals, provides signal conditioning, filtering and gain changes, and controls the dump of excess thrust vector control fluid. With the addition of the Centaur inertial guidance system interface, a roll axis interface was added to provide a variable flight azimuth capability for planetary launches. The Centaur computer provides steering programs for Stage 0 wind load relief and guidance steering for Titan Stages I and II.

A flight programmer provides timing for flight control programs, gain changes, and other discrete events. A staging timer provides acceleration-dependent discretes for Stage I ignition and timed discretes for other events keyed to staging events. The flight programmer and staging timer, operating in conjunction with a relay package and enable-disable circuits, comprise the electrical sequencing system. On Titan IIIE a second programmer, relay package, and other circuits were added to provide redundancy. Also, interfaces were added with the Centaur and Centaur Standard Shroud for staging and shroud jettison.

The Titan uses three batteries: one for flight control and sequencing, one for telemetry and instrumentation, and one for ordnance. On Titan IIIE separate redundant Range safety command system batteries were added to satisfy Range requirements.

The Titan telemetry system is an S-band frequency, pulse code modulation/frequency modulation (PCM/FM) system consisting of one control converter and remote multiplexer units. The PCM format is reprogrammable.

Many of the modifications to the Titan for Titan/Centaur were made to incorporate redundancy and reliability improvements. In addition to those modifications previously mentioned, a fourth retrorocket was added to Stage II in order to ensure proper Titan/Centaur separation if one motor does not fire. All redundancy modifications to Titan IIIE utilized Titan flight proven components. This feature, coupled with the large degree of commonality between the various configurations of the Titan, retains for the Titan IIIE the proven reliability of the Titan family.

Centaur Standard Shroud

The Centaur Standard Shroud is a jettisonable fairing designed to protect the Centaur vehicle and its payloads for a variety of space missions. The Centaur Standard Shroud, as shown in figure III-4, consists of three major segments: a payload section, a tank section, and a boattail section. The 4.27 meters (14 ft) diameter of the shroud was selected to accommodate the Viking spacecraft requirements. The separa-

tion joints sever the shroud into clamshell halves.

The shroud basic structure is a ring stiffened aluminum and magnesium shell. The cylindrical sections are constructed of two light gage aluminum sheets. The outer sheet is longitudinally corrugated for stiffness. The sheets are joined by spot welding through an epoxy adhesive bond. Sheet splices, ring attachments, and field joints employ conventional rivet and bolted construction. The biconic nose is a semi-monocoque magnesium-thorium single skin shell. The nose dome is stainless steel. The boattail section accomplishes the transition from the 4.27 meters (14 ft) shroud diameter to the 3.05 meters (10 ft) Centaur interstage adapter. The boattail is constructed of a ring stiffened aluminum sheet conical shell having external riveted hat section stiffeners.

The Centaur Standard Shroud modular concept permits installation of the tank section around the Centaur independent of the payload section. The payload section is installed around the spacecraft in a special clean room, after which the encapsulated spacecraft is transported to the launch pad for installation on the Centaur.

The lower section of the shroud provides insulation for the Centaur liquid hydrogen tank during propellant tanking and prelaunch ground hold operations. This section has seals at each end which close off the volume between the Centaur tanks and the shroud. A helium purge is required to prevent formation of ice in this volume.

The shroud is separated from the Titan/Centaur during Titan Stage II flight. Jettison is accomplished when an electrical command from the Centaur initiates the separation system detonation. Redundant dual explosive cords are confined in a flattened steel tube which lies between two notched plates around the circumference of the shroud near the base and up the sides of the shroud to the nose dome. The pressure produced by the explosive cord detonation expands the flattened tubes, breaking the two notched plates and separating the shroud into two halves.

To ensure reliability, two completely redundant electrical and explosive systems are used. If the first system should fail to function, the second is automatically activated as a backup within one half second.

The Titan pyrotechnic battery supplies the electrical power to initiate the Centaur Standard Shroud electric pyrotechnic detonators. Primary and back-up jettison discrete signals are sent to the Titan squib firing circuitry by the Centaur Sequence Control Unit (SCU). A tertiary jettison signal, for additional redundancy, is derived from the Titan staging timer.

Four base-mounted, coil-spring thrusters force each of the two severed shroud sections to pivot about hinge points at the base of the shroud. After rotating approximately 60°, each shroud half separates from its hinges and continues to fall back and away from the launch vehicle.

Two additional sets of springs are installed laterally across the Centaur Standard Shroud split lines; one set of two springs in the upper nose cone to assist in overcoming nose dome rubbing friction and one set of two springs at the top of the Tank Section to provide additional impulse during Centaur/Shroud jettison disconnect breakaway.

VDS and SPHINX Spacecraft

The payload for the TC-1 launch was a passive mass and dynamic representation of the Viking Spacecraft referred to as the Viking Dynamic Simulator (VDS). A piggy-back satellite called SPHINX (Space Plasma High Voltage Interaction Experiment) was mounted on the forward end of the VDS. Figure III-5 illustrates the VDS-SPHINX configuration.

The VDS was designed to duplicate the Viking Spacecraft mass properties (weight, cg, and moments of inertia) and first longitudinal oscillatory mode. Strain gage, microphone and accelerometer instrumentation were located on the VDS and channeled into a special FM/FM telepak installed on the Orbiter Simulator to permit verification of the analytical model developed to predict VDS inflight loads. This verification is pertinent in that the same techniques are used to estimate Viking spacecraft loads. The VDS is not separated in flight.

The Proof Flight Payload is made up of six main elements: a Centaur truss adapter, Viking transition adapter, and Viking spacecraft adapter (provided by JPL); each in, or very nearly in, Viking operational flight configuration; structure especially built to simulate the Viking orbiter and lander (VODS and VLDS, respectively); and, an adapter built by Langley to join the VODS and VLDS. This adapter referred to as the Proof Flight Lander Adapter (PFLA) is identical to the Viking flight configuration adapter in overall geometry but is fabricated of steel instead of aluminum (Viking flight configuration) to afford better load carrying capability. The total VDS weight above the Viking transition adapter was 7959 pounds.

The SPHINX (Space Plasma High Voltage Interaction Experiment) is a satellite developed and built by Lewis Research Center to obtain engineering data necessary to design high voltage systems that can be exposed directly to the space environment. The SPHINX configuration is that of a 30-inch octagonal baseplate which supports components mounted on top and bottom. The components are covered with thermal surfaces which give the satellite an overall height of 18.9 inches. Four solar arrays are permanently mounted on the baseplate edges. The SPHINX was to have been separated from the VDS by means of a spring ejector mechanism with a velocity of 2 feet per second and a spin rate of 30 rpm. Total SPHINX weight was 250 pounds.

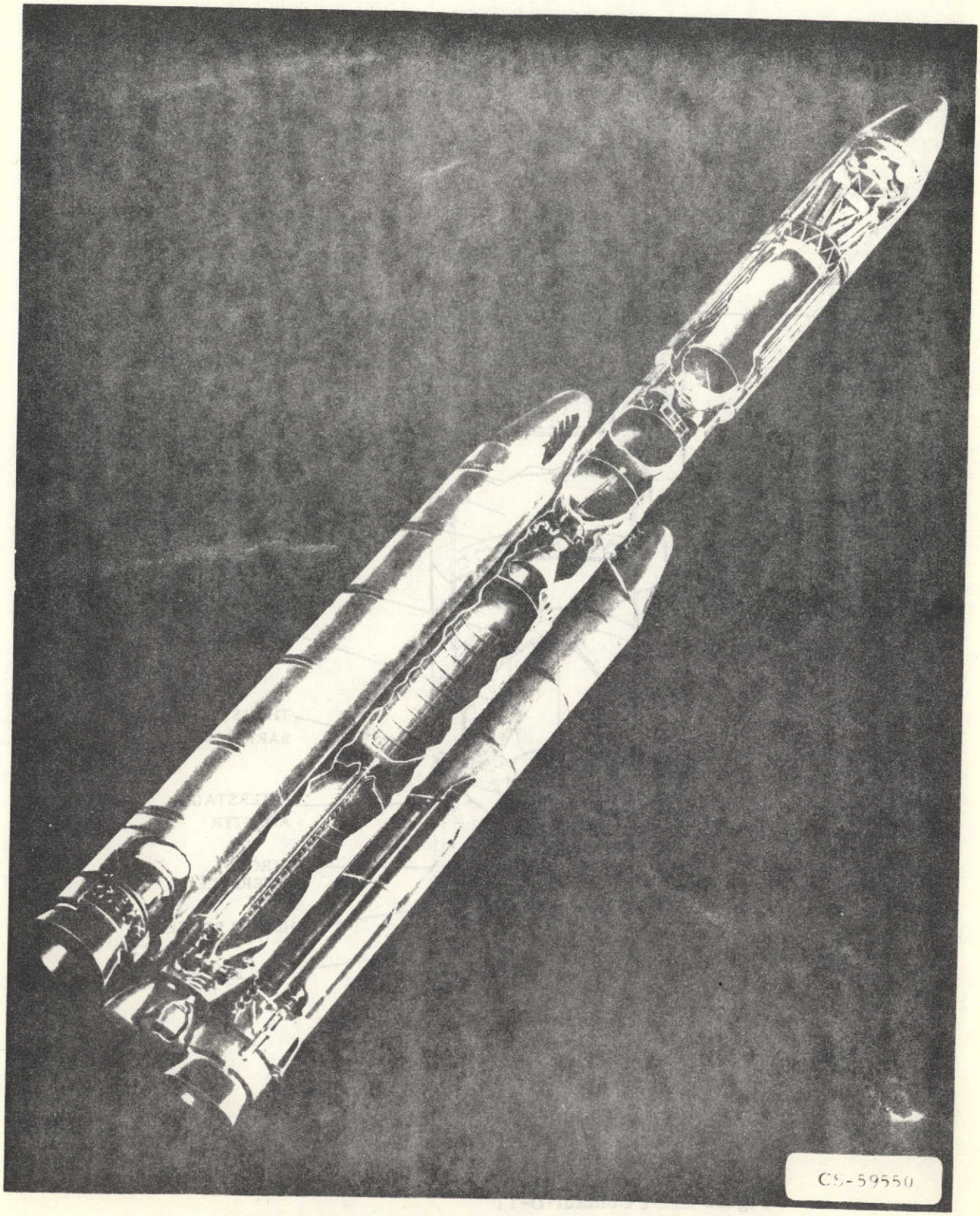

FIGURE III-1. - THE TITAN/CENTAUR VEHICLE

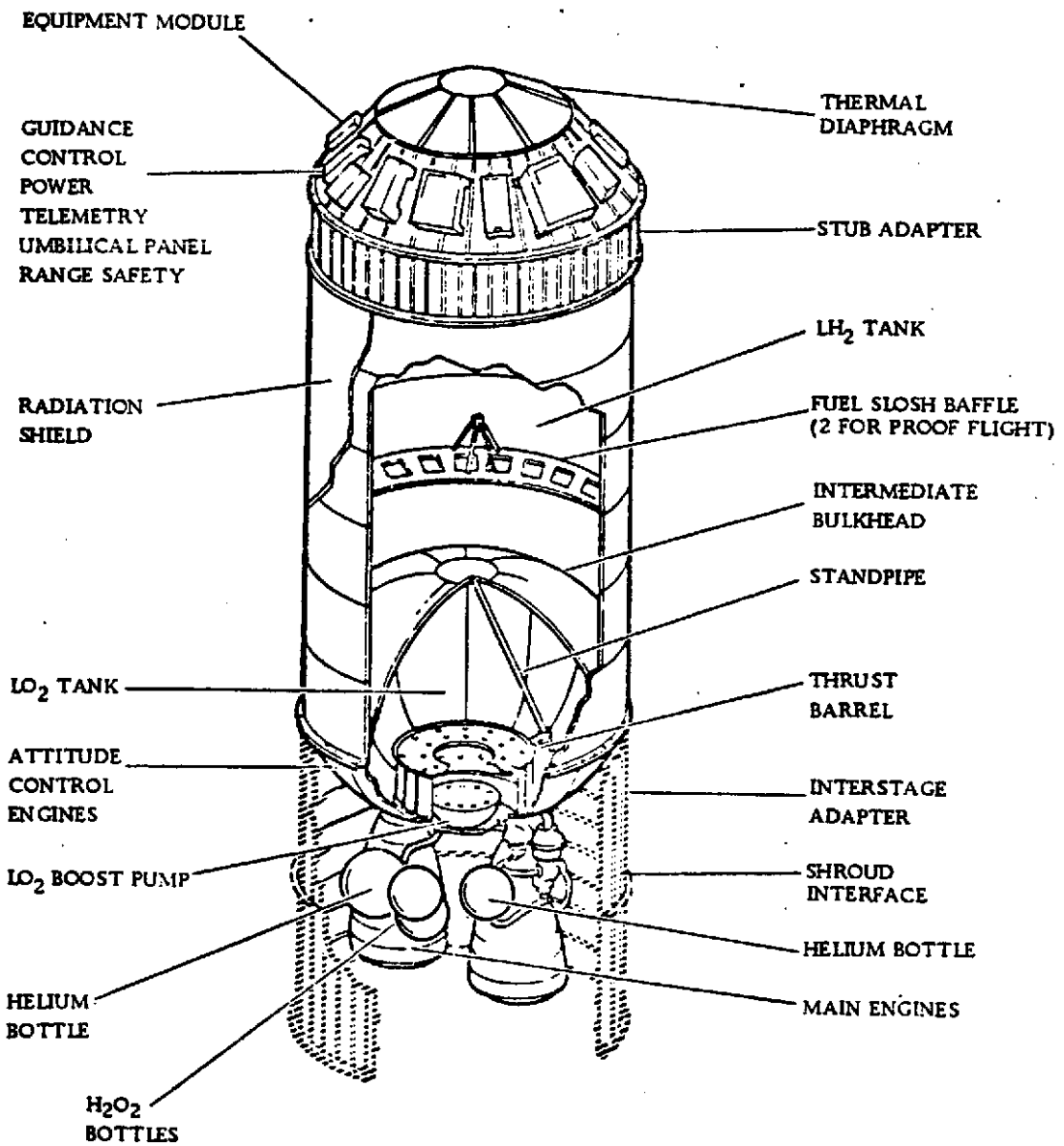

Figure III-2 Centaur D-1T

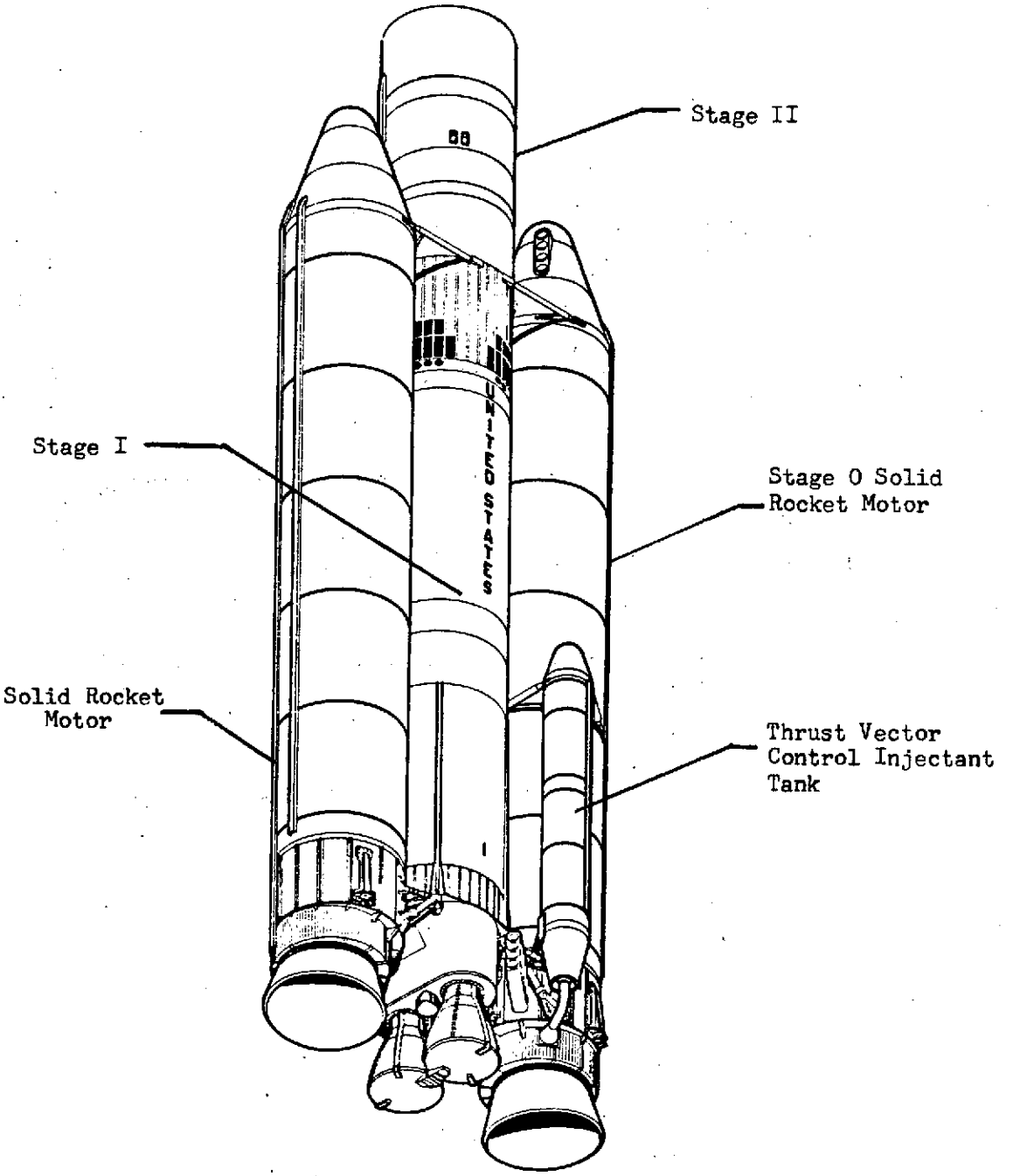

Figure III-3 Titan IIIE.

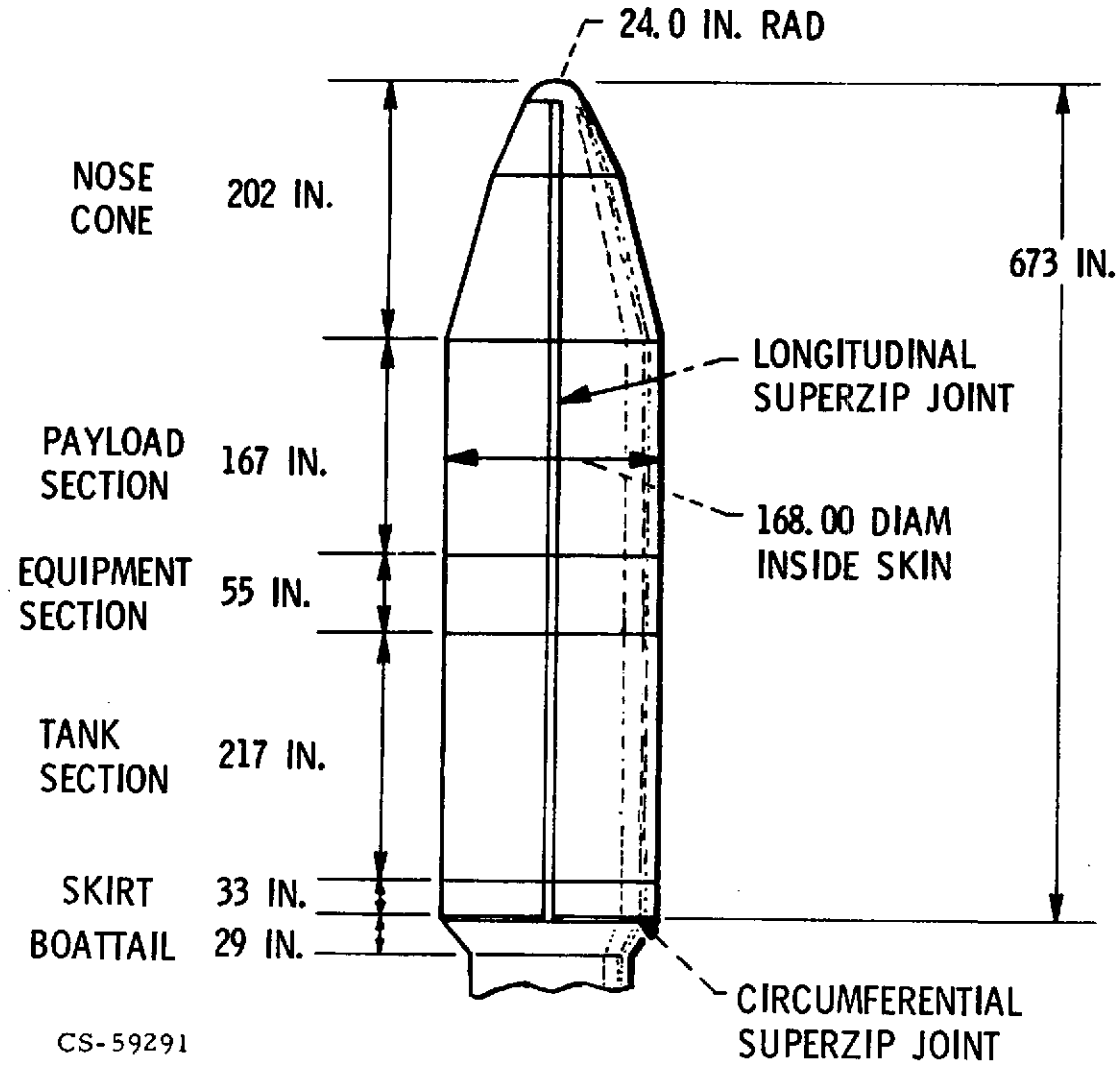

FIGURE III-4. - CENTAUR STANDARD SHROUD CONFIGURATION

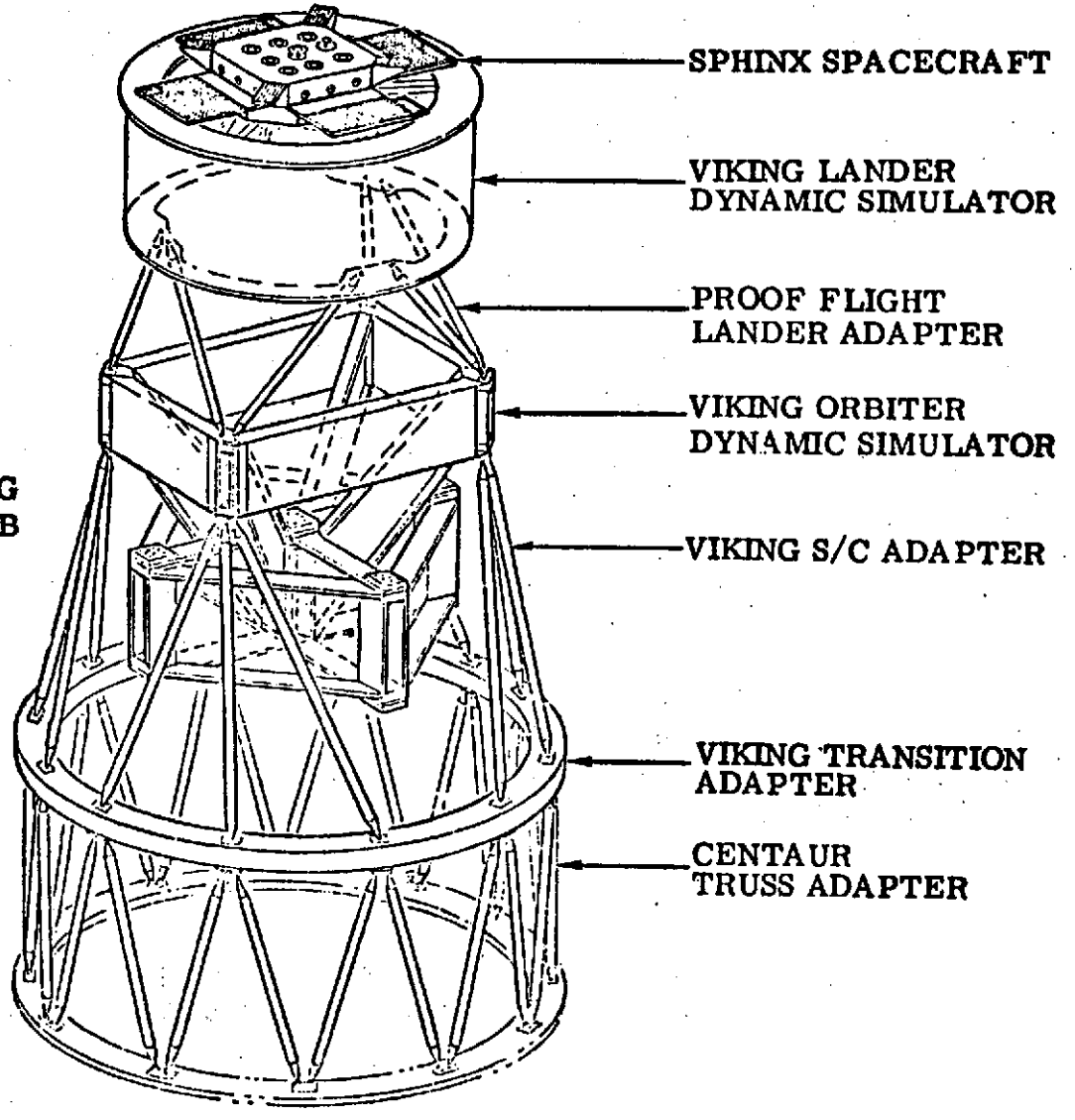

TOTAL WEIGHT, ABOVE VIKING TRANSITION ADAPTER 7,959 LB

FIGURE III-5 TITAN/CENTAUR PROOF FLIGHT PAYLOAD

IV. MISSION PROFILE AND PERFORMANCE SUMMARY

by S. V. Szabo, Jr., and R. P. Kuivenen

Mission Profile

The planned Titan/Centaur Proof Flight Mission Profile or Compendium is shown in figure IV-1. Also shown on the figure is an approximate time for the occurrence of each event listed.

Launch is from Complex 41 at Cape Kennedy, Florida with ignition of the Titan Solid Rocket Motors (SRM's). These motors burn for about 120 seconds, and then are jettisoned. They provide an initial liftoff thrust of about 2.4 million pounds.

During the final seconds of the SRM's burn, the two liquid rocket engines are ignited on the Titan Core Stage I. They provide about 520 000 pounds of thrust and burn for about 150 seconds. At the completion of Stage I burn, Stage II is ignited and Stages I and II separate.

Stage II engine burn provides about 100 000 pounds of thrust for an additional 200 seconds. During Stage II burn at about T + 270 seconds the Centaur Standard Shroud is jettisoned.

Prior to Stage II burnout and separation, preparations for Centaur Engine Start are initiated at Stage II burnout, the Centaur and Stage II are separated, and the Centaur engines ignited.

The Centaur phase of flight profile is mission dependent. Following is described the plan for the Proof Flight. The first Centaur engine burn was to have been about 135 seconds long. This burn would have placed the Centaur and spacecraft into a 100 nautical mile parking orbit. The vehicle would then remain in this orbit with continuous propellant settling thrust for 12 minutes. At the end of the 12-minute coast, the Centaur engines would have been reignited. This burn would place the vehicle in an intermediate transfer orbit in a "zero g" coasting configuration. The vehicle coast was planned to be 80 minutes. The engines would then have been reignited for a third time placing the vehicle in a transfer orbit to synchronous altitude. At the end of the third burn, the Centaur was programmed to reorient and separate the SPHINX spacecraft along a vector corresponding to the Earth to Sun alinement at launch plus 30 days. The Centaur then was intended to reorient for Sun alinement and antenna pointing and coast in "zero g" for $5\frac{1}{4}$ hours to near synchronous altitude. During this coast a series of "thermal maneuvers" to maintain

vehicle temperatures would have occurred. At near synchronous altitude, the engines were scheduled to ignite for a fourth time for about 60 seconds. At the end of this burn a series of boost pump and other experiments were to have been performed to complete the mission.

Performance Summary

TC-1 liftoff occurred at 1348:01.8 GMT (0948.01.8 EDT) on Monday, February 11, 1974, 0.4 seconds after stage SRM ignition. The launch was delayed 45 minutes from the planned launch time of 1303 GMT (0903 EDT) because of launch equipment problems. The ADDJUST designed Titan Stage 0 steering programs for aerodynamic load relief were based on a Windsonde balloon which was released 2.5 hours prior to the planned launch time.

The Stage 0 phase of flight appeared to be near normal. The ignition of the Step I engines occurred at 114.5 seconds into the flight which was 0.4 seconds earlier than predicted. 12.1 seconds after Step I ignition (126.6 sec) the solid rocket motors (SRM's - Step 0) were jettisoned. The comparison of the guidance reconstructed trajectory with the preflight predicted trajectory at SRM jettison showed the vehicle position was 30.5 meters (100 ft) high but the velocity was 11.3 meters per second (37.0 ft/sec) lower than predicted.

The duration of the Stage I solo portion of flight was 0.6 second longer than predicted. The Stage I/Stage II staging sequence commenced at 263.1 seconds and was completed 0.7 second later (263.8 sec after SRM ignition) with the jettison of Stage I. At Stage I shutdown, the guidance reconstructed trajectory showed that the vehicle position and velocity were 823.0 meters (2700 ft) and 45.1 meters per second (148 ft/sec) lower than predicted. During the Titan Stage II portion of flight, at 274.4 seconds, the Centaur Standard Shroud was jettisoned. The Centaur SCU commands this event 10 seconds after the Centaur DCU senses shutdown of the Titan Stage I.

The Titan Stage II portion of flight was 3.6 seconds longer in duration than predicted, with Stage II shutdown occurring at 469.5 seconds into flight. The Centaur DCU commanded Stage II separation 5.6 seconds after Centaur DCU sensed the shutdown deceleration.

The vehicle was 1341.1 meters (4400 ft) low in altitude and 73.8 meters per second (242 ft/sec) low in velocity at Stage II shutdown. These dispersions were within the expected tolerances.

The Centaur Main Engine Start (MES-1) for first-burn occurred at 486.0 seconds; however, the Centaur did not achieve a successful start. The Centaur guidance system cycled into the restart mode and a second start of the Centaur engines (RMES-1) was attempted 70 seconds later at 556.0 seconds into the flight. This attempt also failed.

The Range Safety Officer terminated the flight and destroyed the

Centaur at 748.5 seconds into the mission. Table IV-1 lists the major flight events as they occurred through flight termination. Table IV-2 presents the targeted orbits at the end of each of the four Centaur burns which were selected to accomplish the objectives of the Proof Flight mission.

TABLE IV-1. - MARK EVENTS TITAN/CENTAUR PROOF FLIGHT

Event	Predicted	Actual
	T + Sec.	T + Sec.
Stage 0 ignition (SRM ignition)	0.0	0.0
Lift-off	.23	.4
Stage I ignition	114.9	114.16
Step 0 jettison (SRM jettison)	126.2	126.70
Stage I shutdown (stage II ignition command)	262.0	263.1
Step I jettison	262.7	263.8
Centaur standard shroud (CSS) jettison	273.0	274.4
Stage II shutdown	464.8	469.5
Step II jettison	470.7	475.1
Centaur main engine start (MES-1) (first attempt)	481.2	486.0
Centaur main engine restart (RMES-1) (second attempt)	------	556.0
Flight termination (destruct)	------	748.5

TABLE IV-2. - FINAL PROOF FLIGHT PREDICTED ORBITAL PARAMETERS

Parameter	MECO			
	1	2	3	4
Epoch (T + sec; MECO + 0.5 sec)	618.2	1388.7	6371.2	25 335.0
Semi-major axis, nmi	3531.97	4004.075	12 940.11	18 759.37
Eccentricity	0.000495	0.118150	0.696004	0.170474
Inclination, deg	31.768	31.792	31.743	29.725
Apogee radius, nmi	3533.72	4477.16	21 946.47	21 957.36
Perigee radius, nmi	3530.22	3530.99	3933.74	12 117.44
Apogee height, nmi	80.79	1033.22	18 502.54	18 513.43
Perigee height, nmi	86.29	87.06	489.81	12 117.44
Longitude of ascending node, deg	158.81	155.57	134.79	71.41
Period, min	87.750	105.919	615.357	1074.108
Energy, C_3, km^2/sec^2	-60.9369	-53.7521	-16.6326	-11.4731
Argument of perigee, deg	281.939	190.11	109.85	90.04
True anomaly, deg	216.065	0.688	351.75	187.27
Eccentric anomaly, deg	216.082	0.611	356.50	188.635
Argument of latitude, deg	138.004	190.803	101.598	277.31
Mean anomaly, deg	216.099	0.539	358.93	190.101
Semi-latus rectum, nmi	3531.97	3948.18	6671.64	18 214.19

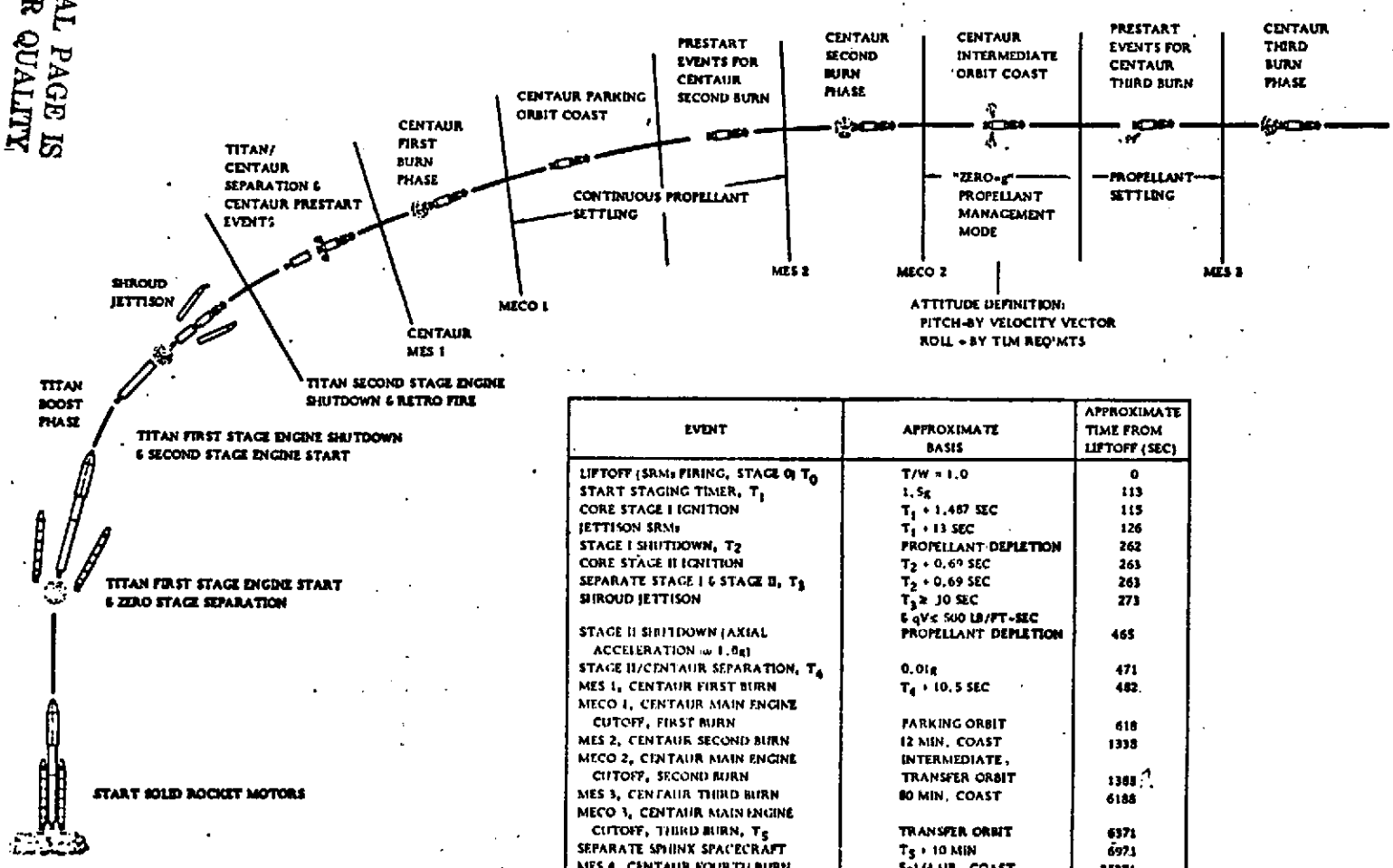

EVENT	APPROXIMATE BASIS	APPROXIMATE TIME FROM LIFTOFF (SEC)
LIFTOFF (SRMs FIRING, STAGE I) T_0	T/W = 1.0	0
START STAGING TIMER, T_1	1.5g	113
CORE STAGE I IGNITION	T_1 + 1.487 SEC	115
JETTISON SRMs	T_1 + 13 SEC	126
STAGE I SHUTDOWN, T_2	PROPELLANT DEPLETION	262
CORE STAGE II IGNITION	T_2 + 0.69 SEC	263
SEPARATE STAGE I & STAGE II, T_3	T_2 + 0.69 SEC	263
SHROUD JETTISON	$T_3 \geq$ 10 SEC & qV $\leq$ 500 LB/FT-SEC	273
STAGE II SHUTDOWN (AXIAL ACCELERATION = 1.0g)	PROPELLANT DEPLETION	465
STAGE II/CENTAUR SEPARATION, T_4	0.01g	471
MES 1, CENTAUR FIRST BURN	T_4 + 10.5 SEC	482
MECO 1, CENTAUR MAIN ENGINE CUTOFF, FIRST BURN	PARKING ORBIT	618
MES 2, CENTAUR SECOND BURN	12 MIN. COAST	1338
MECO 2, CENTAUR MAIN ENGINE CUTOFF, SECOND BURN	INTERMEDIATE, TRANSFER ORBIT	1388
MES 3, CENTAUR THIRD BURN	80 MIN. COAST	6188
MECO 3, CENTAUR MAIN ENGINE CUTOFF, THIRD BURN, T_5	TRANSFER ORBIT	6971
SEPARATE SPHINX SPACECRAFT	T_5 + 10 MIN	6971
MES 4, CENTAUR FOURTH BURN	5-1/4 HR. COAST	25271
MECO 4, CENTAUR MAIN ENGINE CUTOFF, FOURTH BURN	TERMINAL ORBIT	25335

FIGURE IV-1a TITAN/CENTAUR PROOF FLIGHT COMPENDIUM

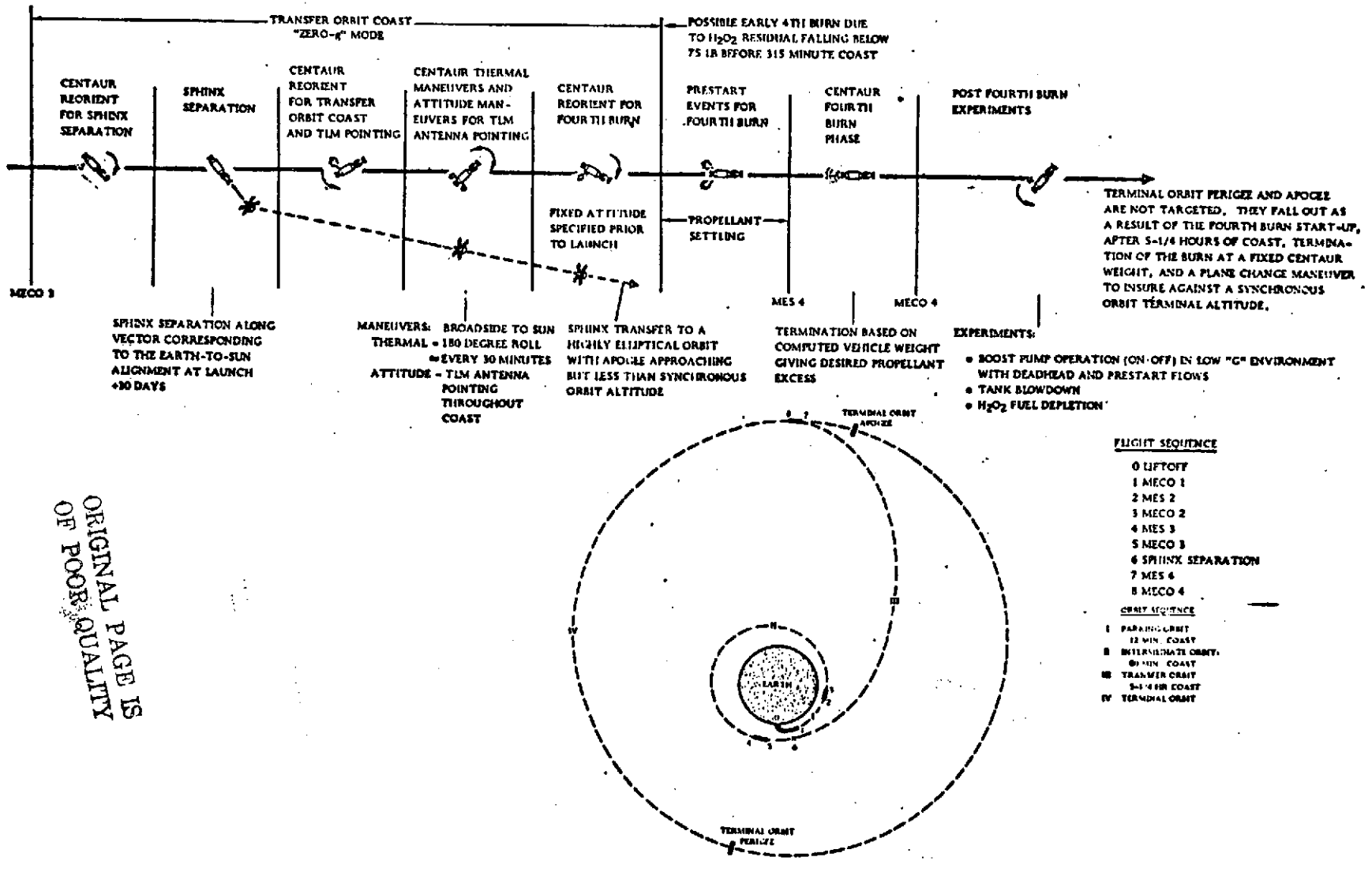

FIGURE IV-1b TITAN/CENTAUR PROOF FLIGHT COMPENDIUM

V. TITAN IIIE SYSTEMS

V-1. TITAN MECHANICAL SYSTEMS

V-1A. AIRFRAME STRUCTURE

by R. W. York

Summary

The Titan vehicle maintained structural integrity throughout all phases of booster ascent flight. The propellant tank ullage pressures were normal. All compartments vented as expected. The Titan Compartment 2A thermal barrier experienced a lower-than-expected differential pressure, indicating preflight predictions were conservative.

System Description

The Titan IIIE vehicle consists of a two-stage core vehicle with solid rocket motors (SRM's) on either side (fig. V-1A-1).

The structural design of the IIIE core vehicle is of frame stabilized monocoque and conventional "skin-stringer-frame" construction (fig. V-1A-2). The primary material of construction is aluminum alloy. Alloys 2014 and 7075 are used in all primary structural members. Alloy 7075 is used predominately for extruded or forged frames, stringers, and longerons.

The stages are composed of major assemblies or segments within the stages. These major assemblies are provided with bolt-together interfaces called tension splices.

Stage I airframe includes four major assemblies; the fuel tank assembly, the oxidizer tank assembly, interstage structure, and the engine heat shield.

The fuel tank assembly includes an aft skirt with longerons, the tank assembly, and a forward skirt with a tension splice interface frame. The tank wall also serves as the vehicle exterior wall.

The oxidizer tank assembly includes an aft skirt with tension splice frame, the tank assembly, and a forward skirt with transportation splice frame. The interstage structure is considered an extension of the oxidizer tank forward skirt.

Stage II airframe includes two major assemblies; the fuel tank assembly and the oxidizer tank assembly.

The fuel tank assembly has an aft skirt with an aft staging interface, the fuel tank, and a forward skirt with tension splice interface.

The oxidizer tank assembly includes an aft skirt with tension splice frame, the oxidizer tank, and a forward skirt with a forward interface for the Centaur interstage adapter structure. An internal truss mounted in the Stage II forward skirt provides mounting for the flight controls, power supply, telemetry, and other electronic equipment. A structural thermal barrier (fig. V-1A-3), is attached to the forward end of the Stage II airframe. The barrier is constructed of formed aluminum stringers that support a 10-foot diameter cover of thin Dacron-polyester coated material. The equipment truss is protected by an aluminum cover. The purpose of the barrier is to prevent the environment of the Centaur thrust compartment from adversely affecting the Titan electronic components and the Stage II ullage gas and propellant and, conversely, the barrier prevents the Titan compartment environment from adversely affecting the Centaur thrust compartment during prelaunch and flight.

The engine heat shield assembly protects the Stage I engine from the high temperatures radiated from the SRM nozzles. The engine heat shield is composed of an upper engine shroud which attaches to the aft frame of Stage I and encloses the major portion of the engine from the thrust chamber throats up. Two lace-on jackets to cover the thrust chamber nozzles, covers to close the open end of the chambers and turbine tail pipes and flexible boots to close the openings around thrust chambers and turbine tail pipes complete the assembly.

Flight Performance

The ullage pressures within the oxidizer and fuel tanks of both Stage I and Stage II were sufficient to maintain structural integrity throughout flight. The pressures did not exceed the design limits of the vehicle.

Compartment IIA internal pressure vented as expected and achieved essentially zero psi at approximately 125 seconds after lift-off (fig. V1-2-2).

The eight Titan Compartment IIA wall differential pressure measurements (fig. V1-2-2) indicated a steady-state maximum of 0.8 psid crush at 40 to 45 seconds and 1.3 psid burst at 43 seconds in the pitch plane. In the yaw plane, Compartment IIA experienced steady-state maximums of 1.1 psid crush and 1.45 psid burst during the same times. By 80 seconds all measurements were recording less than 0.2 psid steady-state. The Titan Compartment IIA design limit differential pressures are defined in figure VI-2-2. All maximum wall differential pressures measured were within design limits.

The differential pressure across the Compartment IIA thermal barrier remained steady at 0.15 psid collapse throughout flight. This was well within the design limit of 1.3 psid.

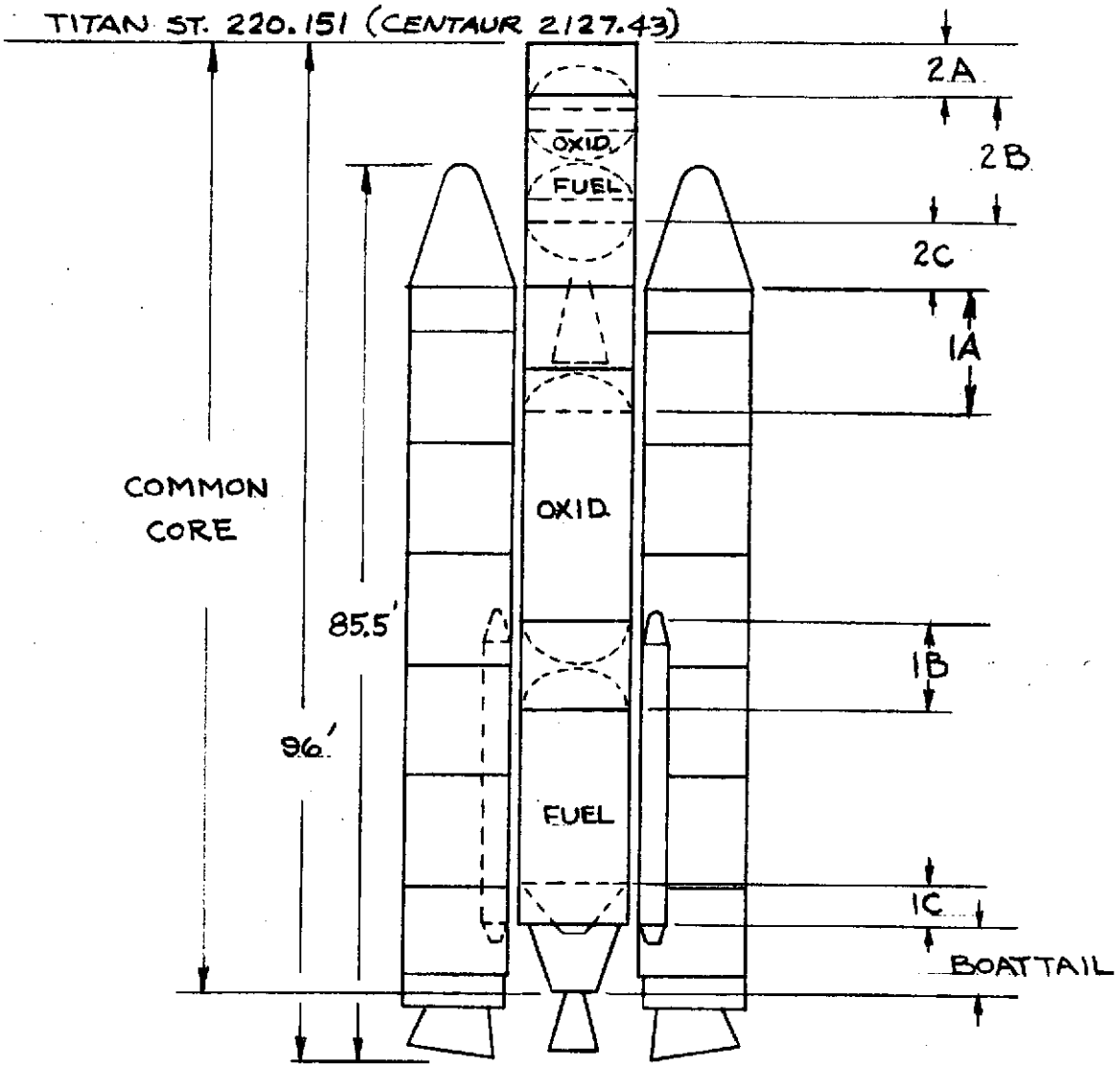

FIGURE V-1A-1 TITAN III E VEHICLE DIMENSIONS AND COMPARTMENTS

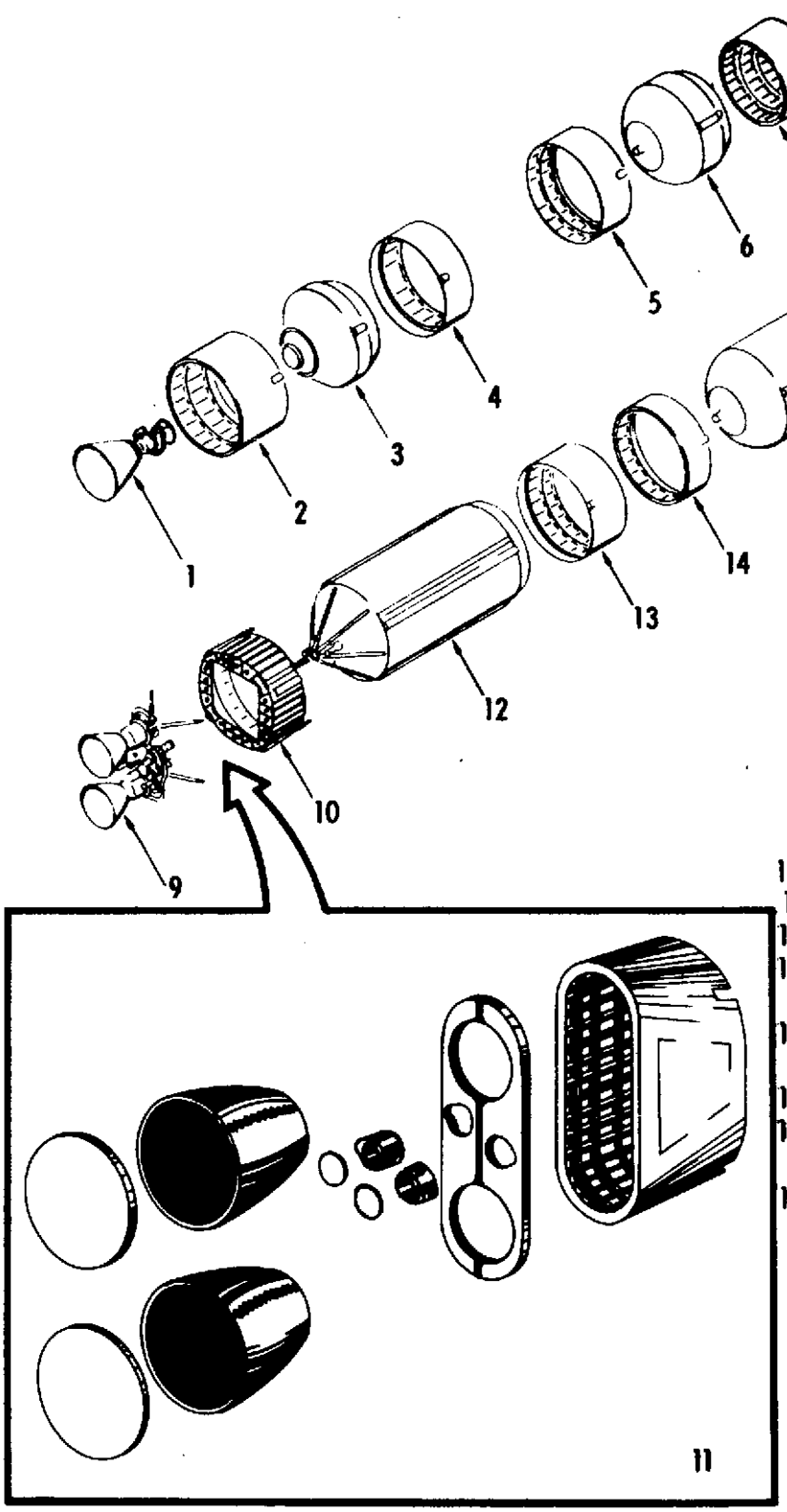

1. STAGE II ROCKET ENGINE
2. STAGE II AFT SKIRT
3. STAGE II FUEL TANK
4. STAGE II BETWEEN TANKS STRUCTURE
5. STAGE II BETWEEN TANKS STRUCTURE
6. STAGE II OXIDIZER TANK
7. FORWARD SKIRT
8. TRUSS ASSEMBLY
9. STAGE I ROCKET ENGINES
10. STAGE I TAIL SKIRT
11. STAGE I HEAT SHIELD
12. STAGE I FUEL TANK
13. STAGE I BETWEEN TANKS STRUCTURE
14. STAGE I BETWEEN TANKS STRUCTURE
15. STAGE I OXIDIZER TANK
16. STAGE I OXIDIZER TANK FORWARD SKIRT
17. INTER-STAGE STRUCTURE

FIGURE V-1A-2 TITAN AIRFRAME STAGES I AND II

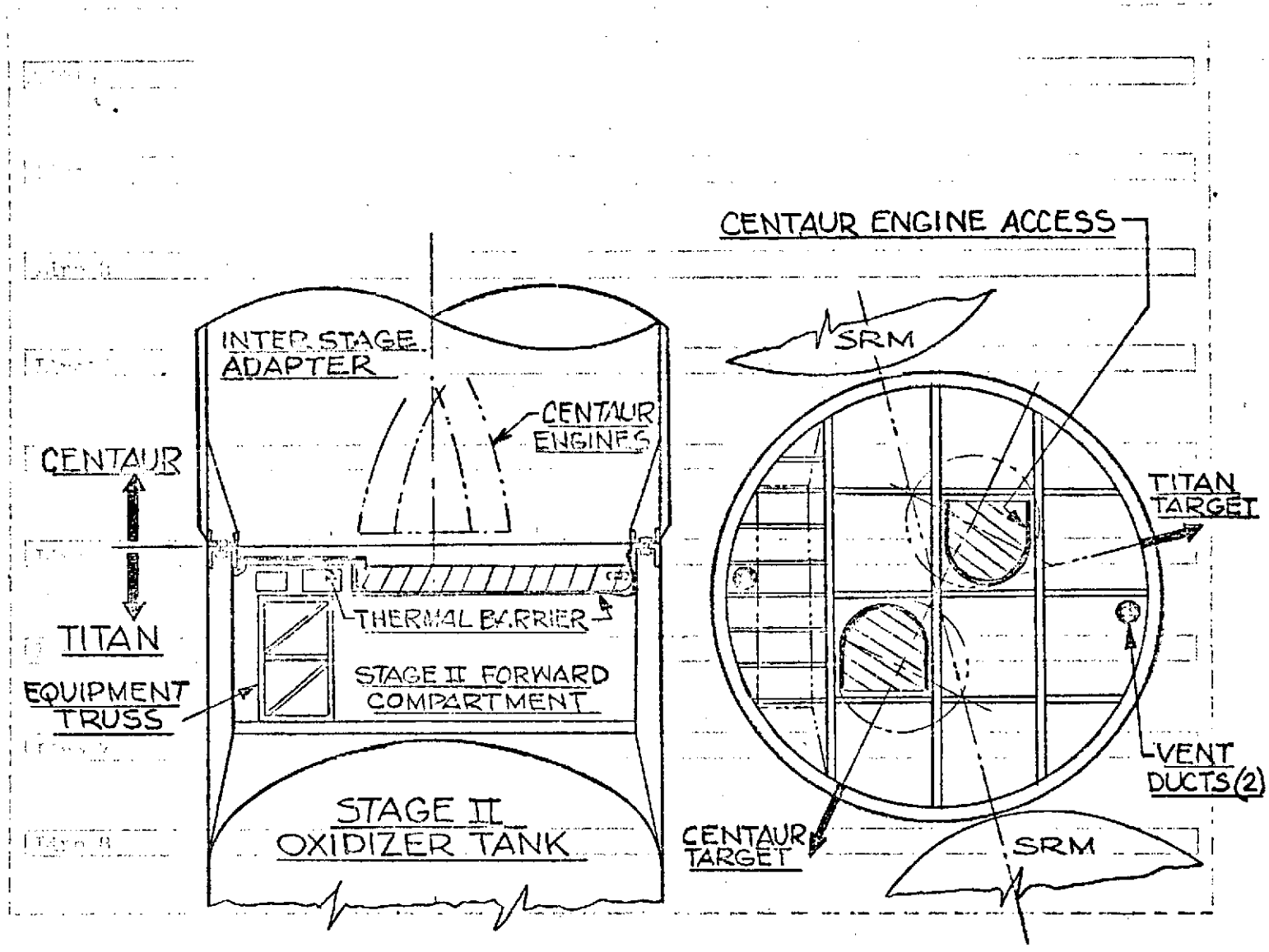

FIGURE V-1A-3 TITAN/CENTAUR STRUCTURAL INTERFACE AND THERMAL BARRIER

V-1B. TITAN PROPULSION AND HYDRAULIC SYSTEMS

by R. J. Salmi and R. J. Schroeder

Summary

All Titan IIIE-1 Stage 0 systems and components functioned as expected and no failures or anomalies were observed. The actual flight trajectory performance was on the low side but within the 3-sigma limits of the normal predicted values. At Stage 0 separation the relative velocity was 37 feet per second (0.88 percent) less than nominal and the separation occurred 0.52 second later than predicted.

Stage I engine performance was slightly lower than expected with average thrust 1.26 percent low and average specific impulse 0.69 second low. Engine operating time was 0.6 second longer than expected. Subassembly two exhibited an anomaly at FS_1 + 65 seconds when the thrust chamber pressure, oxidizer and fuel pump discharge pressures, and gas generator pressure dropped 1 to 2 percent. Postflight investigation concluded that the most likely cause of this anomaly was a hot gas leak through an instrumentation fitting on the turbine inlet manifold used during engine acceptance testing.

Performance of the Stage II engine was satisfactory. Average thrust was 1.65 percent lower than expected and average specific impulse was 0.49 second higher than expected. Engine operating time was 3.4 seconds longer than expected.

Prelaunch propellant loading and pressurization of the Stages I and II propellant tanks were within the acceptable limits. The autogenous pressurization system on each stage supplied adequate pressurization gases to the propellant tanks during engine operation.

The Stages I and II hydraulic systems performed satisfactorily during countdown operation and flight operation. Hydraulic reservoir level measurement on Stage II exhibited a 5 percent bandwidth of noise during Stage II engine operation. Structural loads transmitted into the hydraulic actuators during Stages I and II engine start transients were within the capability of the actuators.

System Description

Stage 0. - The initial Titan boost phase (Stage 0) was provided by two solid propellant rocket motors (SRM's) which developed approximately 1 200 000 pounds thrust each. The SRM's are a matched pair; that is, they had similar combustion characteristics which were determined from propellant burning rate tests made during the propellant manufacturing process. The basic solid motors were built up from five cylindrical segments plus an aft and forward closure, as shown in figure V-1B-1. Each

segment was 10 feet in diameter and 10 feet long. The segment grain port is circular and is slightly larger at the aft end of the segment than at the forward end.

The solid propellant grain is a mixture of polybutadiene-acrylic acid acrylonitride terpolymer (PBAN), ammonium perchlorate, aluminum powder, an epoxy based binder and small amounts of iron oxide to control the burn rate. At room temperatures, the nominal design web action time (time from 75 percent of maximum chamber pressure to the knee of the tail-off break) is approximately 105 seconds. The total burn time to the end of tail-off is about 125 seconds. During the web action time, the thrust of each SRM decays from the initial 1 200 000 pounds to about 820 000 pounds.

The forward closures had star grain ports to provide rapid initial thrust buildup and they also housed the igniters as shown in figure V-1B-2. The nose support skirts and nose fairings were also supported by the forward closures. The aft closures were strong structural members which supported the nozzle assemblies, as shown in figure V-1B-3. The aft closures were cast with circular grain ports.

The steel nozzle assemblies consisted of throat sections with exposed surfaces fabricated from disk shaped layers of graphite and expansion sections lined with phenolic impregnated silica cloth ablative materials plus other insulating materials. The nozzle expansion ratios were 8:1 and their centerlines were canted 6° from the SRM centerlines so that the SRM thrust vectors intersected near the vehicle center of gravity to reduce yawing moments resulting from thrust differences in the two motors.

The aft support skirts were strong ring-beam reinforced cylindrical sections attached to the aft closures. Attached to the aft support skirts were the core support longerons, the ground support longerons, the TVC tank supports, aft staging rockets and the aft heat shields. The core support longerons transmit the thrust of the SRM's to the core vehicle.

At the end of the SRM burn time, the solid rockets are separated from the core vehicle by firing explosive bolts at the core support longeron ball joints and at the forward outriggers and by firing the forward and aft staging rockets. Each SRM has eight staging rockets with clusters of four located in the nose support skirt as indicated in figure V-1B-1. Each staging rocket has a thrust of approximately 4800 pounds and a burn time of about 2.6 seconds.

Both the SRM's and the TVC injectant tanks have a destruct system which consists of linear shaped charges that are mounted longitudinally along their external surfaces. The destruct charges are fired automatically if inadvertent SRM separation occurs or they can be fired by ground control prior to SRM separation.

Stage I. - Thrust for the Titan Stage I was provided by one Aerojet Liquid Rocket Company engine Model LR87-AJ-11 shown schematically in figure V-1B-4. The engine assembly consisted of two identical engines attached to a single frame and mounted on the vehicle. These individual engines, designated as Subassembly 1 and Subassembly 2, were designed to operate simultaneously to provide a vacuum rated thrust of 520 000 pounds with a 15:1 expansion ratio.

Each subassembly consisted of the following major components and subsystems: pump suction lines, turbopump assembly, pump discharge lines, regeneratively cooled thrust chamber assembly, thrust chamber valves, gas generator, autogenous pressurization system, an ablative skirt to provide a 15:1 expansion ratio, an exit closure with separation systems, engine control and instrumentation harnesses.

Subassembly performance (thrust, weight flow rates, mixture ratio) were preset by the use of fixed orifices in the propellant discharge lines and cavitating venturis in the gas generator feed lines. Autogenous pressurization gas flow rates were also preset by a sonic nozzle in the fuel autogenous line and a cavitating venturi in the oxidizer autogenous line.

Engine start was provided by a solid propellant start cartridge in each subassembly to initiate pump operation and drive the turbine until the engine became self-sustaining.

Engine shutdown was initiated by the thrust chamber pressure switch (one in each subassembly) when it sensed a decay in thrust chamber pressure due to propellant depletion.

Thrust vector control (pitch, yaw, and roll) was provided by gimballing each subassembly thrust chamber with two hydraulic actuators.

Stage II. - The Titan Stage II rocket engine was Aerojet Liquid Rocket Company Model LR91-AJ-11 shown schematically in figure V-1B-5. This engine develops a vacuum rated thrust of 100 000 pounds with a 49.2:1 expansion ratio. Except for being somewhat smaller, the Stage II engine is similar in construction and operation to a single subassembly of the Stage I engine.

The Stage II engine consists of the following major components and subsystems: pump suction lines, turbopump assembly, pump discharge lines, regeneratively cooled thrust chamber, thrust chamber valves, gas generator, autogenous pressurization system, an ablative skirt to provide a 49.2:1 expansion ratio, roll control nozzle assembly, engine control, and instrumentation harnesses.

Engine performance (thrust, weight flow rates, mixture ratio) were preset by the use of fixed orifices in the propellant discharge lines and cavitating venturis in the gas generator feed lines. Autogenous pressurization gas flow rates were also preset by a sonic nozzle in the fuel autogenous line and a cavitating venturi in the oxidizer autogenous line.

Engine start was provided by a solid propellant start cartridge to initiate pump operation and drive the turbine until the engine became self-sustaining. The electrical command for Stage II engine start was issued at the same time as Stage I shutdown, resulting in what is known as "fire-in-the-hole" for Stage II engine start.

Stage II engine shutdown was initiated by propellant depletion sensed by a reduction in acceleration to approximately 1.0 g level.

Thrust vector control in pitch and yaw was provided by gimballing the thrust chamber with two hydraulic actuators. Roll control was accomplished by swiveling the turbine exhaust nozzle with a single hydraulic actuator.

Stages I and II propellant feed systems. - The Titan propellant feed systems for Stages I and II is shown in figures V-1B-6 and V-1B-7. Both stages used the same storable, hypergolic liquid propellants. The fuel was a mixture of 50 percent hydrazine with 50 percent unsymmetrical dimethyl hydrazine and the oxidizer was nitrogen tetroxide.

Propellant feed lines for both stages terminated at a set of electrically operated reclosable prevalves. This was the first Titan III flown with this type of prevalve. Other Titan III vehicles used an ordnance operated, nonreclosable type of valve. Propellants were loaded into the vehicle tanks through manually operated fill and drain disconnects with the prevalves in the closed position. The prevalves were opened during the automatic portion of the terminal countdown to provide propellants to the engine pumps.

The Stage I propellant feed system included a set of toroidal accumulators in the fuel feed lines to reduce the "pogo" effect between the engine and the vehicle structure. Stage II propellant feed system did not have the toroidal accumulators in the fuel feed line.

Ullage volumes in each propellant tank were pressurized with gaseous nitrogen before liftoff. During engine operation the required tank pressurization gas was supplied at a controlled rate by the engine autogenous system to make up for the removal of propellant from the tanks. Fuel tanks were pressurized by hot turbine exhaust gas that was cooled in a heat exchanger before entering the fuel tanks. Oxidizer tanks were pressurized by heating liquid oxidizer to the gaseous state in a heat exchanger located in the turbine exhaust stack.

Stages I and II hydraulic systems. - The Titan Stages I and II hydraulic systems shown schematically in figures V-1B-8 and V-1B-9 provided the mechanical force necessary to gimbal the Stages I and II thrust chambers and to swivel the Stage II turbine exhaust nozzle for thrust vector control. Both systems are nearly identical except for the size of the turbine driven hydraulic pumps and the linear actuators. Each system supplied a nominal 2950 psi pressure to the hydraulic actuators during ground checkout operations and during flight. An electric motor driven

pump supplied the hydraulic pressure required for ground checkout of the flight control system. The in-flight hydraulic pressure was supplied by a variable delivery, pressure-compensated, piston type pump, mechanically driven by the rocket engine turbine. The remaining elements common to both hydraulic systems were a regulating unit that included an accumulator and reservoir, a filter, a manually operated ground disconnect, check valves, and instrumentation.

Flight Performance

Stage 0. - The nominal flight trajectory based on the predicted SRM performance class, projected a relative velocity of 4185 feet per second and an elapsed time of 126.067 seconds at Stage 0 separation. The flight performance based on Digital Computer Unit (DCU) data indicated that at separation the relative velocity was 37 feet per second below nominal (0.88 percent) and that the time at separation was 126.585 seconds (0.14 percent long). SRM's 19 and 20 were known to be of the slow-burner SRM family which was assigned a nominal class web action time (WAT) of 109.0 seconds at 60° F SRM bulk temperature instead of the specification nominal WAT of 106.9 seconds. As shown in table V-1B-1, the actual flight WAT's are 110.0 and 108.9 seconds for SRM's 19 and 20, respectively. Corrected to the nominal temperature of 60° F, the WAT's are 110.0 and 108.9 seconds, well within the bounds of the 109-second performance class. Table I also shows that all of the performance parameters involving the delivered impulse were within the specification limits. Table V-1B-I and figures V-1B-10 and V-1B-11, show that the maximum chamber pressure/thrust at lift-off was below the specification value. The thrust was within the specified limits for most of the remaining burn time but was generally near the lower limit. Figures V-1B-10 and V-1B-11, also show the thrust time (burn time) extending beyond the specification limits. Differences in the thrust developed by the two SRM's result in yawing moments which must be overcome by the thrust vector control (TVC) system. Critical times occur during thrust buildup and tail-off when TVC is lowest. The maximum measured thrust differentials were 43 251 pounds during thrust buildup and 65 000 pounds during tail-off, which are very low when compared to the allowable values of 168 000 and 290 000 pounds, respectively.

Stage I. - Flight performance of the Titan Stage I engine was satisfactory. Engine start signal (87 FS_1) occurred at T + 114.6 seconds when the accelerometer in the Titan flight programmer sensed a reduction in acceleration to 1.5 g's during the tail-off period of the Stage 0 solid rocket motors.

Separation of the thrust chamber exit closure was satisfactory as indicated by the normal engine start transient. The time differential between subassembly one ignition and subassembly two ignition was 0.07 second. Eighty percent rated thrust level for each subassembly was reached with a 0.03 second time differential. There was no thrust overshoot produced in either subassembly. Stage I engine start transient

data is shown in table V-1B-2.

Engine performance during the steady-stage period was satisfactory. Average engine thrust was 1.26 percent lower than expected, average specific impulse was 0.69 second lower than expected, and average engine mixture ratio was 0.98 percent higher than expected. The corresponding 3 sigma dispersion about the expected values were ±3.27 percent on thrust, ±2.3 seconds on specific impulse, and ±2.17 percent on mixture ratio. Stage I engine steady-state performance data is shown in table V-1B-3.

An anomaly occurred during steady-state operation on subassembly two at approximately 65 seconds after engine ignition. This anomaly exhibited itself as a sudden decreased shift of one to two percent of full scale reading of the following subassembly two telemetry measurements: thrust chamber pressure, oxidizer and fuel pump discharge pressures, and gas generator pressure. A postflight investigation of this anomaly concluded that it could have resulted from contamination entering the fuel or oxidizer bootstrap venturi inlet screen or from the loss of a B-nut cap on an unused instrumentation port on the turbine inlet manifold. The most likely cause appears to be the loss of the B-nut cap since similar instances have been encountered during ground tests. An interim corrective action to prevent future reoccurrences of this problem requires safety wiring all critical B-nuts on Stage I and Stage II engines.

Stage I engine shutdown occurred at T + 263.1 seconds when the thrust chamber pressure switches sensed a reduction in chamber pressure and issued the engine shutdown signal (87 FS_2). Engine shutdown was the result of oxidizer exhaustion as planned. The shutdown transient was normal for an oxidizer exhaustion mode. Stage I engine operating time (FS_1 to FS_2) was 0.6 second longer than expected.

Stage II. - Flight performance of the Titan Stage II engine was satisfactory. Engine start signal (91 FS_1) occurred at T + 263.1 seconds (simultaneous with Stage I engine shutdown signal, 87 FS_2). The Stage II engine start transient was normal as shown in table V-1B-4.

Engine steady-state performance was satisfactory. Average engine thrust was 1.65 percent lower than expected, average specific impulse was 0.49 second higher than expected and average engine mixture ratio was 0.71 percent higher than expected. The corresponding 3 sigma dispersions about the expected values were ±3.80 percent on thrust, ±3.5 seconds on specific impulse, and ±2.66 percent on mixture ratio. Steady-state engine performance data is shown in table V-1B-5.

Stage II engine shutdown (91 FS_2) occurred at T + 469.6 seconds when the sensed vehicle acceleration dropped to 1.0 g's. Engine shutdown was the result of oxidizer exhaustion. The shutdown transient was normal for an oxidizer exhaustion mode.

Stage II engine operating time (FS_1 to FS_2) was 3.4 seconds longer than expected.

Stages I and II propellant feed systems. - The Titan Stages I and II propellant tanks were loaded with propellants based on an average expected in-flight propellant bulk temperature of 67.5° F. In addition, Stage I propellant tanks were loaded to provide a 2 sigma probability of having an oxidizer depletion shutdown. This was done to minimize the risk of encountering high Stage II actuator loads during the Stage II engine start transient. A comparison of the actual loaded propellant weights for each tank with the expected loaded weights is shown in table V-1B-6. Loaded propellant weights were within the allowable tolerance of ±0.4 percent for the oxidizer and ±0.3 percent for the fuel.

The Titan Stages I and II propellant tanks were initially pressurized within the required prelaunch limits on F-1 day. Table V-1B-7 shows the prelaunch tank pressurization limits compared with the recorded telemetry tank pressures just prior to lift-off. All four propellant tanks were pressurized satisfactorily and the final prelaunch values were 0.5 to 2.0 psi above the midband of the launch limits.

The autogenous pressurization systems on Stages I and II supplied adequate pressurization gases to the propellant tanks during engine operation. Average tank pressures were 0.3 to 3.7 psi higher than expected. Table V-1B-8 shows the expected average tank pressures during engine operation with the actual flight values.

Stages I and II hydraulic systems. - Performance of the hydraulic systems on Stages I and II were normal. The electric motor driven pump in each stage supplied normal hydraulic pressure for the flight control system tests performed during countdown. Hydraulic pressures supplied by the turbine driven pump on each stage during engine operation were normal. Hydraulic reservoir levels were satisfactory except Stage II measurement exhibited approximately a five percent bandwidth of noise during Stage II engine operation. Table V-1B-9 shows Stages I and II hydraulic system performance data.

The structural loads transmitted into the hydraulic actuators during the Stage I engine start transient were normal. A maximum load of 16 000 pounds tension was applied to subassembly 1 pitch actuator 4-1. This load was considerably below the allowable tension load of 50 000 pounds on the Stage I actuators. Stage II engine start transient resulted in a maximum load of 9700 pounds compression applied to the Stage II pitch actuator 1-2. Compared with other Titan III flights, the Stage II actuator load on TC-1 was the third highest load. It was also the highest load experienced with a Stage I oxidizer depletion shutdown but was below the 14 400 pound load encountered with a Stage I fuel depletion shutdown. Recent tests performed on the Stage II actuator have demonstrated an actuator capability of approximately 18 000-pound load. Table V-1B-X shows the maximum actuator loads encountered on TC-1 during the Stages I and II engine start transients.

TABLE V-1B-1

TITAN SOLID ROCKET MOTOR PERFORMANCE SUMMARY

Parameter	Rocket Motor Specification		SRM 19			SRM 20		
	Nominal	Allowable Deviation, %	Measured	Corrected	Deviation, %	Measured	Corrected	Deviation, %
Test condition	Vacuum	–	Flight	Vacuum	–	Flight	Vacuum	–
Firing condition, °F	60	–	64.6	60	–	65.3	60	–
Web action time, sec	106.9	±2.16	109.4	110.0	+2.90	108.1	108.9	+1.87
Action time, sec	116.8	±3.43	119.6	120.4	+3.08	119.8	120.6	+3.25
Maximum forward end chamber pressure, psia	791	±3.76	739	730	-7.71	731	720	-8.98
Maximum initial sea level thrust, lb x 10^{-6}	1.1638	±6.23	1.0784	1.0625	-8.70	1.0650	1.0476	-9.98
Web action time total impulse, lb-sec x 10^{-6}	108.43	±1.0	102.388	108.160	-0.25	101.668	107.437	-0.92
Action time total impulse, lb-sec x 10^{-6}	112.52	±1.0	106.625	112.411	-0.10	106.548	112.333	-0.17
Web action time delivered specific impulse, sec	266.0	±0.7	252.3	266.6	+0.23	252.0	266.3	+0.11

NOTE: All thrust and impulse values are nozzle centerline.

TABLE V-1B-2 TITAN STAGE I ENGINE START TRANSIENT DATA, TC-1

Parameter	Units	Flight Values		
		Allowable	Actual	
			Subassembly 1	Subassembly 2
FS_1 to Ignition	Sec	0.6 to 1.0	.76	.83
Ignition to 80% Rated Thrust Level	Sec	0.125 minimum	.20	.23
Thrust Overshoot	Lbf	323,000 maximum	No over-shoot	No over-shoot

TABLE V-1B-3 TITAN STAGE I ENGINE STEADY-STATE PERFORMANCE, TC-1

Parameter	Units	Average Steady-State Flight Values	
		Expected (2)	Actual
Thrust, total	lbf	527649	520986
Specific impulse	sec	302.33	301.64
Mixture ratio, $^{o}/F$	units	1.9079	1.9266
Overboard propellant flow rate, total (1)	lbm/sec	1745.28	1727.18
Oxidizer flow rate, total	lbm/sec	1147.71	1139.60
Fuel flow rate, total	lbm/sec	601.55	591.51
Propellant outage	lbm	1138 mean 2971 max.	2186 (fuel)
Oxidizer temperature	^{o}F	65	56.1
Fuel temperature	^{o}F	65	56.6
FS_1 to FS_2	sec	147.9	148.5

NOTES: 1) Excludes autogenous pressurant flow
2) Expected values are those used in the final preflight targeted trajectory

TABLE V-1B-4 TITAN STAGE II ENGINE START TRANSIENT DATA, TC-1

Parameter	Units	Flight Values	
		Allowable	Actual
FS1 to ignition	Sec	0.5 to 0.9	0.70
10% to 80% rated thrust	Sec	0.150 minimum	.20
Thrust at overshoot	lbf	128000 max.	103790

TABLE V-1B-5 TITAN STAGE II ENGINE STEADY-STATE PERFORMANCE TC-1

Parameter	Units	Average Steady-State Flight Values	
		Expected(3)	Actual
Thrust, total	lbf	104263	102542
Specific impulse(1)	Sec	315.14	316.63
Mixture ratio, $^{o}/F$	Units	1.7888	1.8015
Overboard propellant flowrate, total (2)	lbm/sec	328.06	321.12
Oxidizer flowrate, total	lbm/sec	211.25	207.34
Fuel flowrate, total	lbm/sec	118.09	115.09
Propellant outage	lbm	153 mean 623 max.	284(fuel)
Oxidizer temperature	^{o}F	65	58.5
Fuel temperature	^{o}F	65	58.9
FS_1 to FS_2	Sec	203.1	206.5

NOTES: 1) Excludes roll nozzle thrust

2) Excludes autogenous pressurant flow

3) Expected values are those used in the final pre-flight targeted trajectory

TABLE V-1B-6 TITAN LOADED PROPELLANT WEIGHTS STAGE I AND STAGE II, TC-1

	Expected (Lbs.)	Actual (Lbs.)
Stage I		
Oxidizer	168,766	168,739
Fuel	90,140	90,079
Stage II		
Oxidizer	42,796	42,781
Fuel	24,190	24,178

TABLE V-1B-7 TITAN PROPELLANT TANK PRELAUNCH PRESSURIZATION, STAGE I AND STAGE II, TC-1

	Prelaunch Limits (psia)		Value at T-30 Sec. (psia)
	Lower	Upper	
Stage I			
Oxidizer Tank	33.6	45.0	40.0
Fuel Tank	24.0	32.0	30.0
Stage II			
Oxidizer Tank	45.0	57.0	52.0
Fuel Tank	50.0	56.0	54.5

TABLE V-1B-8 TITAN PROPELLANT TANK AVERAGE PRESSURES DURING ENGINE OPERATION, TC-1

	Expected Value[1] (psia)	Actual Value (psia)
Stage I		
Oxidizer Tank	33.9	34.6
Fuel Tank	25.7	26.0
Stage II		
Oxidizer Tank	50.5	53.5
Fuel Tank	53.0	56.7

(1) Expected values are based on an average in-flight propellant bulk temperature of 65° F

TABLE V-1B-9 TITAN HYDRAULIC SYSTEMS FLIGHT DATA, TC-1

Parameter	Units	Expected	Stage I	Stage II
Hydraulic Supply Pressure				
Max. at Pump Start	psi	4500 Max(1)	3420	4072
Average Steady-State	psi	2900-3000	2970	2950
Reservoir Level				
Prior to Pump Start	%	22-47	47.5	50
At Max. Pump Start Pres.	%	22-47	33	34
Shutdown Minus 5 Sec.	%	22-47	35	36

(1) Proof pressure limit

TABLE V-1B-10 TITAN HYDRAULIC ACTUATOR MAXIMUM LOADS DURING ENGINE START TRANSIENTS, TC-1

	Units	Stage I Actuators				Stage II Actuators	
		Subassembly One		Subassembly Two			
		Pitch 1-1	Yaw-Roll 2-1	Yaw-Roll 3-1	Pitch 4-1	Pitch 1-2	Yaw 2-2
Load	lbf	+8250	+11000	+11000	-16000	+9700	+5860

+ sign indicates compression load
- sign indicates tension load

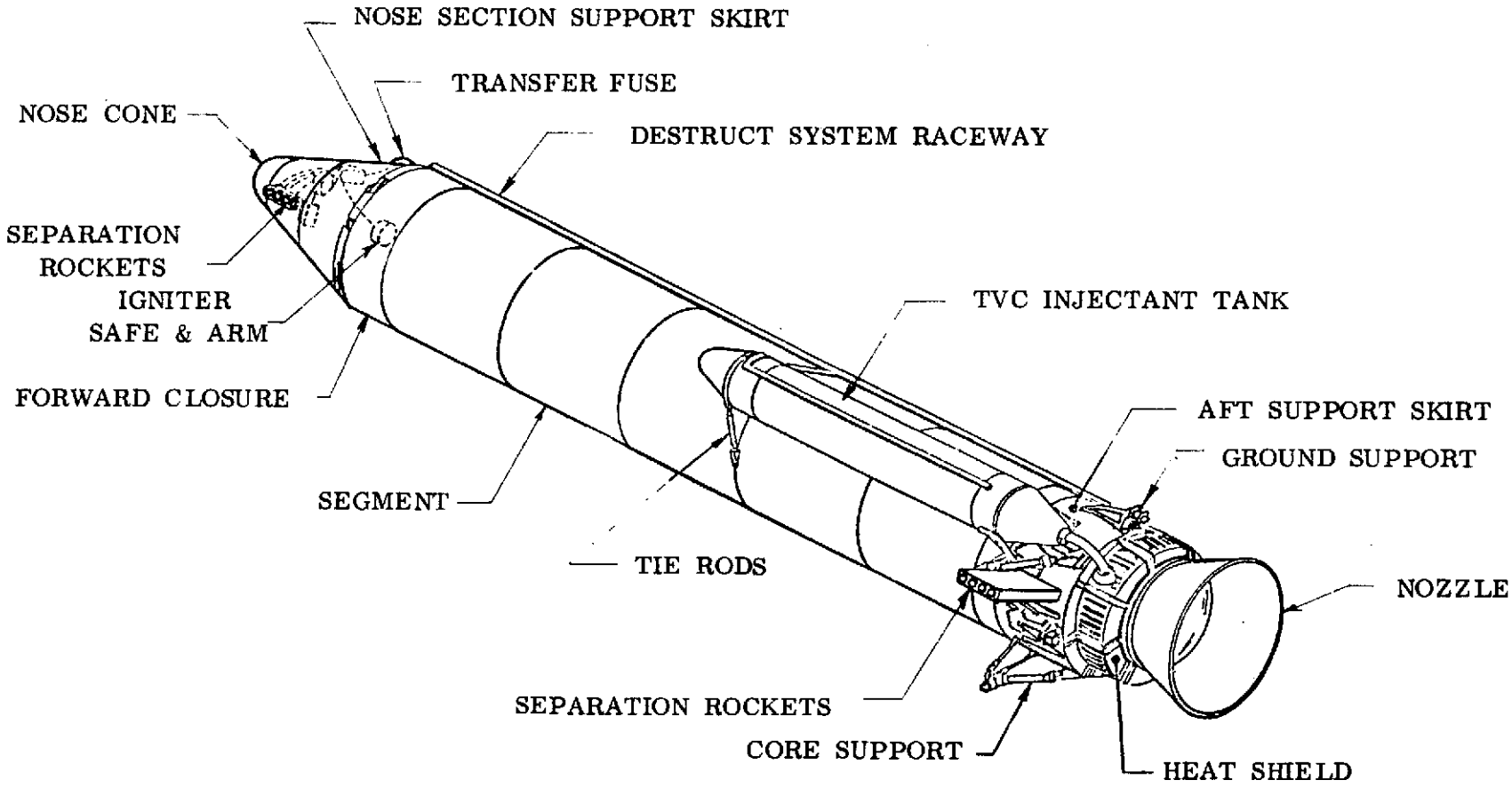

FIGURE V-1B-1 - STAGE 0 SOLID ROCKET MOTOR

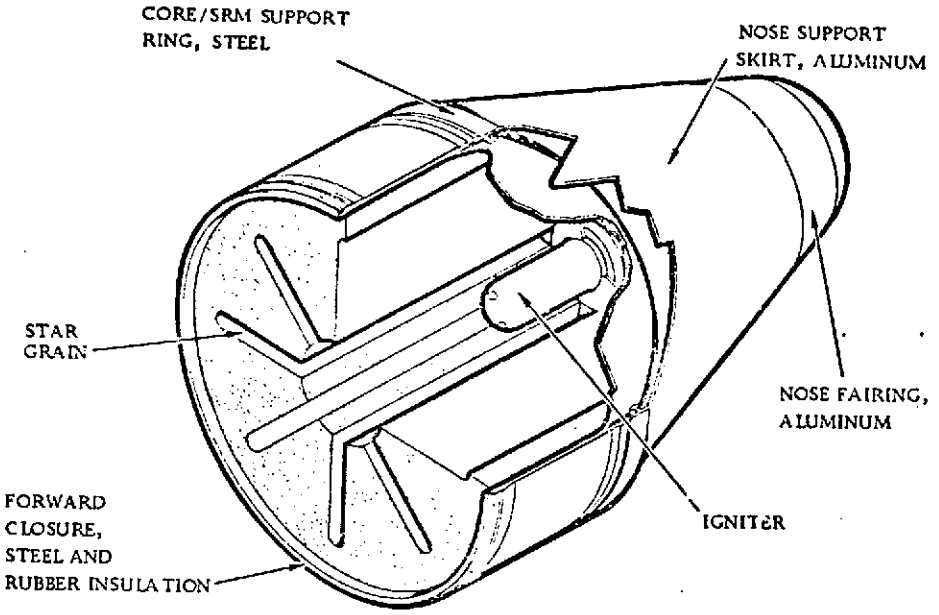

FIGURE V-1B-2 SRM FORWARD CLOSURE

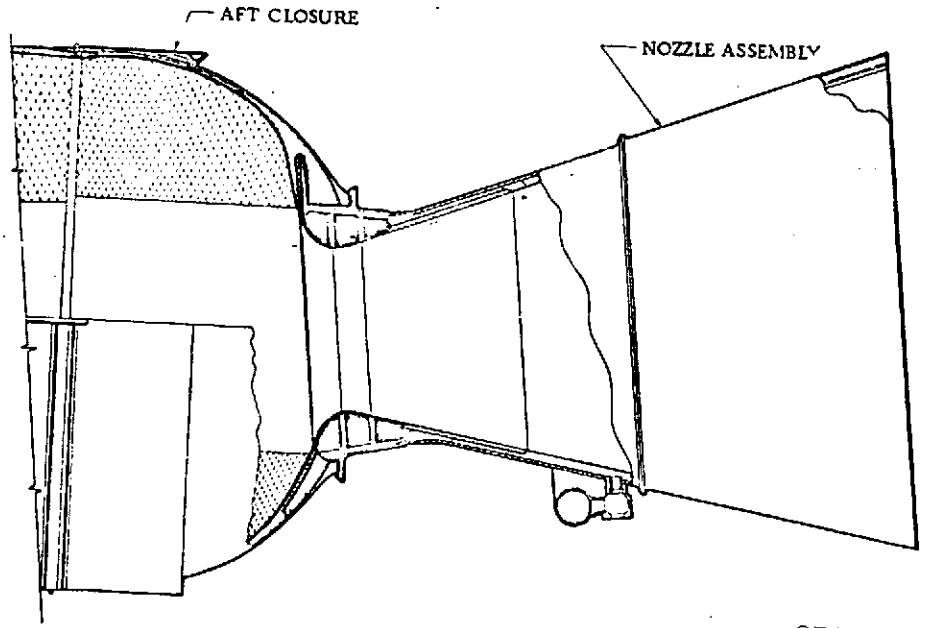

FIGURE V-1B-3 SRM AFT CLOSURE ASSEMBLY

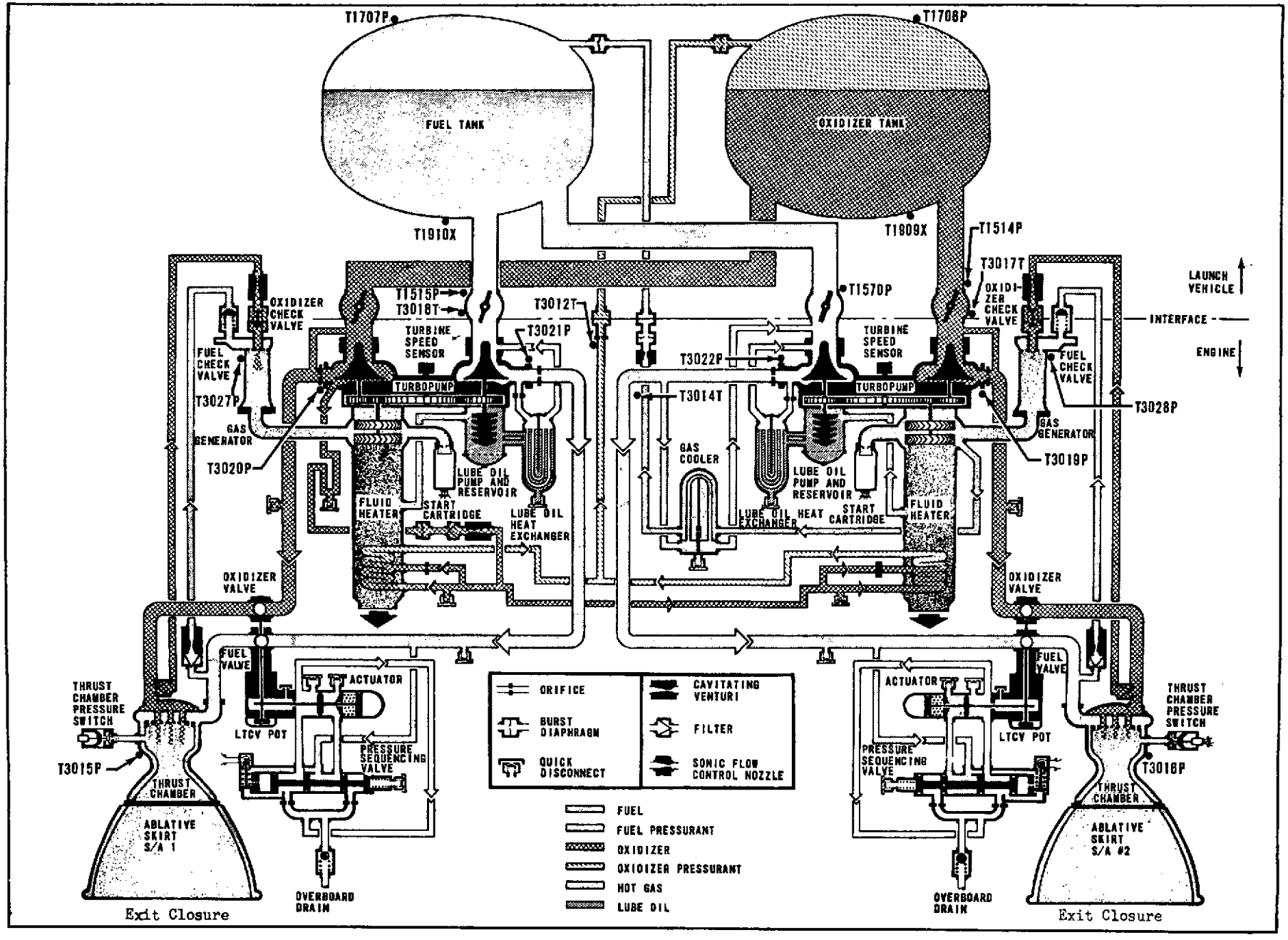

Figur V-1[illegible] Titan Stage I Engin Sch atic

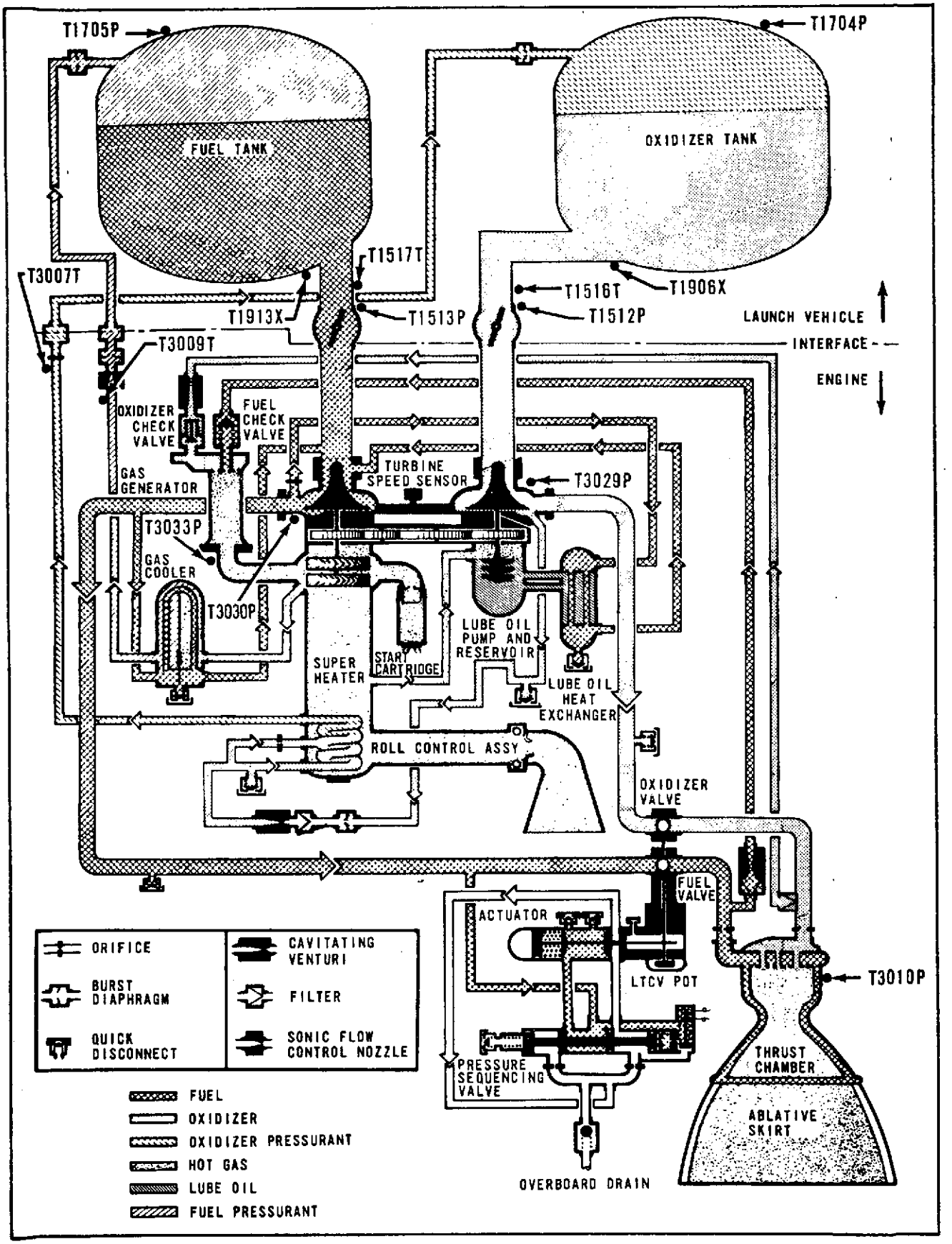

Figure V-1B-5 Titan Stage II Engine Schematic

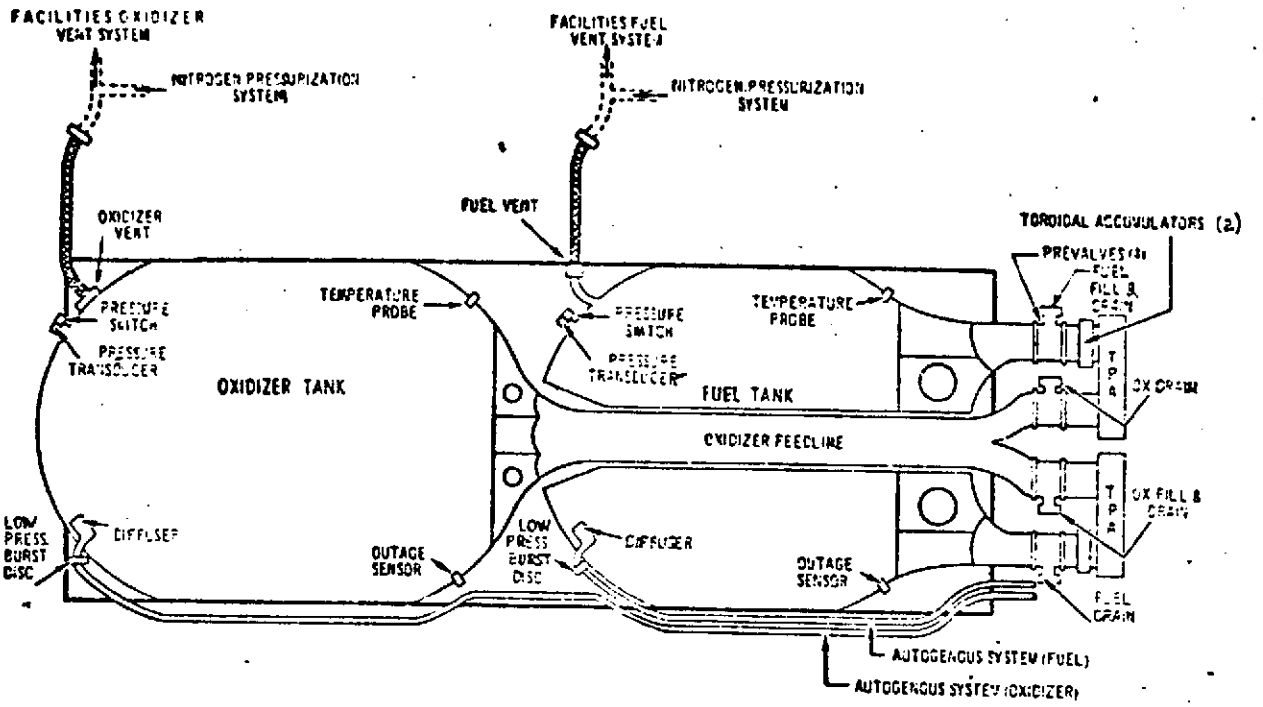

FIGURE V-1B-6 TITAN STAGE I PROPELLANT FEED SYSTEM

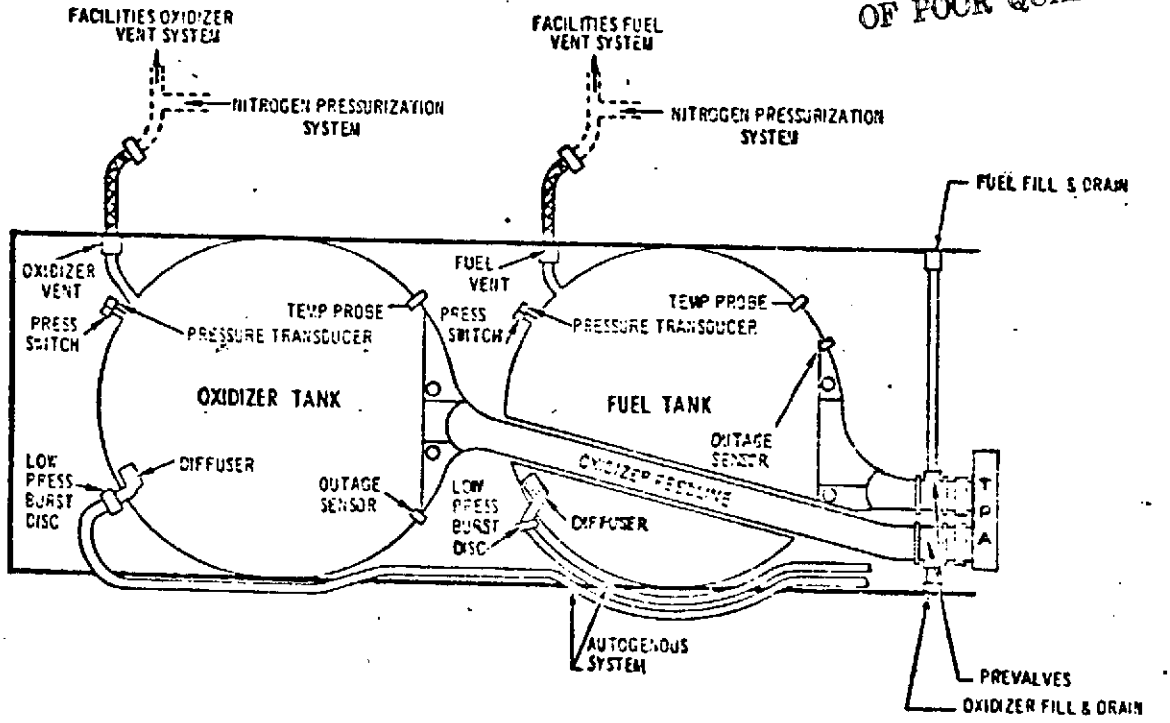

FIGURE V-1B-7 TITAN STAGE II PROPELLANT FEED SYSTEM

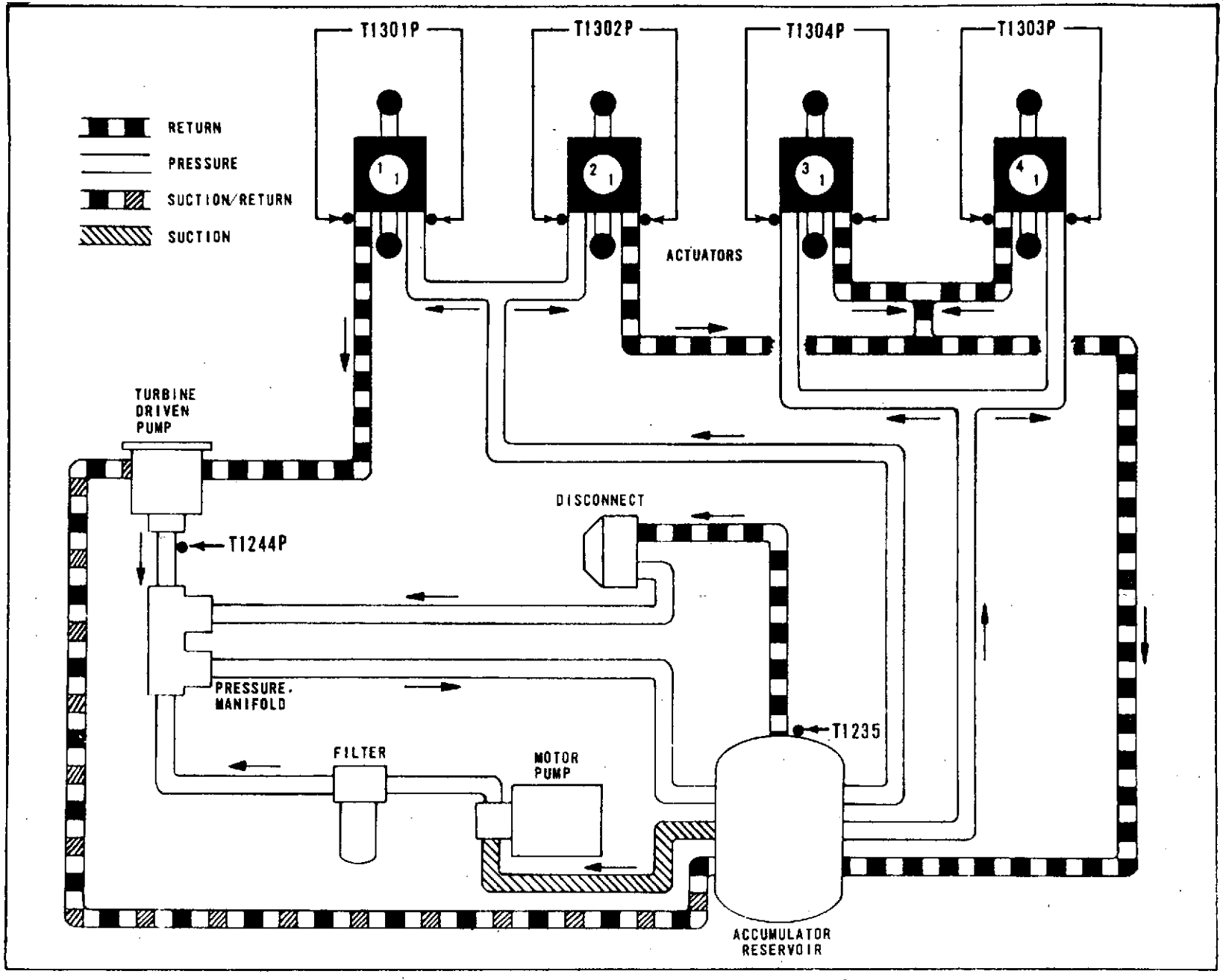

Figure V-1B-8 TITAN Stage I Hydraulic Schematic

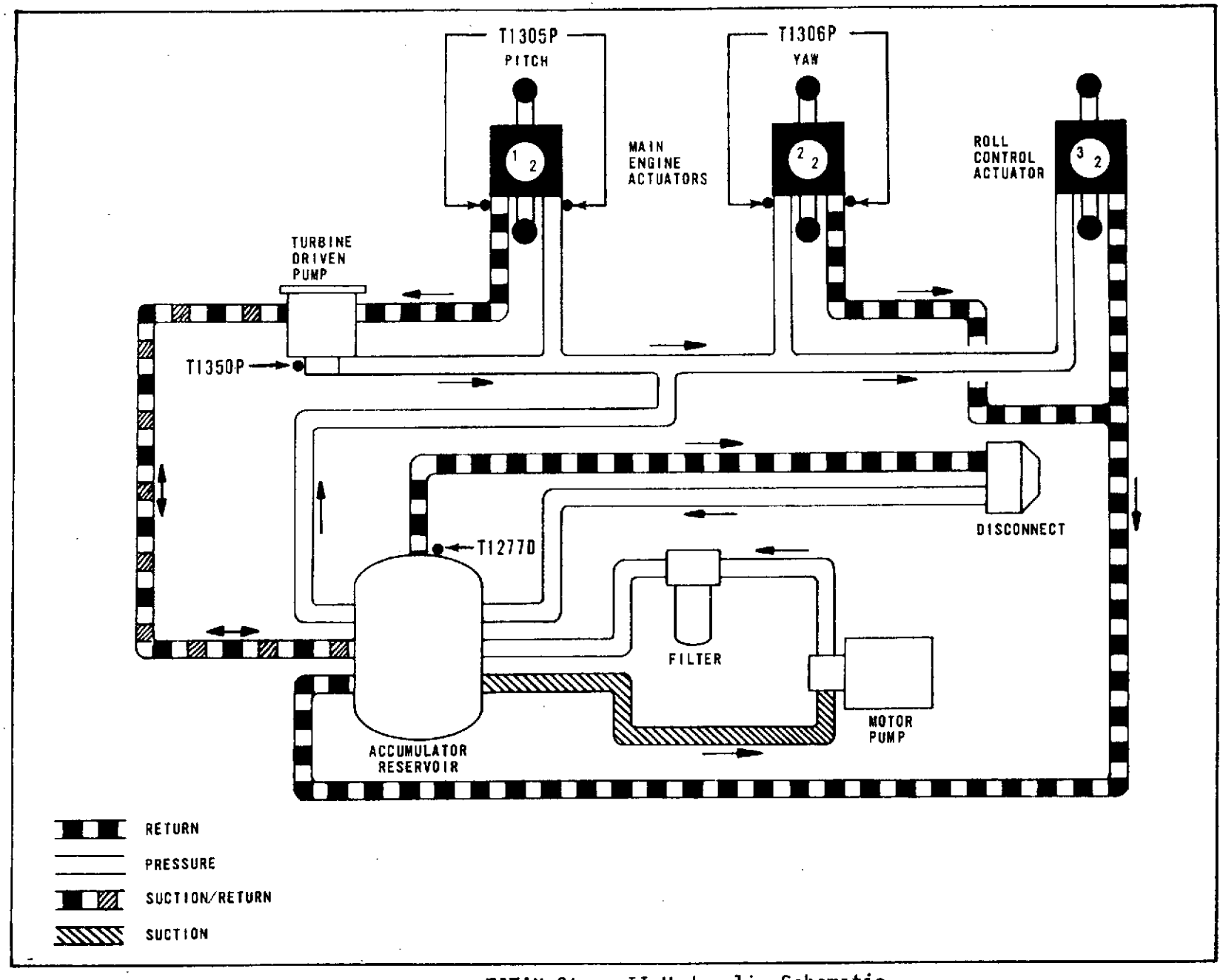

Figure V-1B-9 TITAN Stage II Hydraulic Schematic

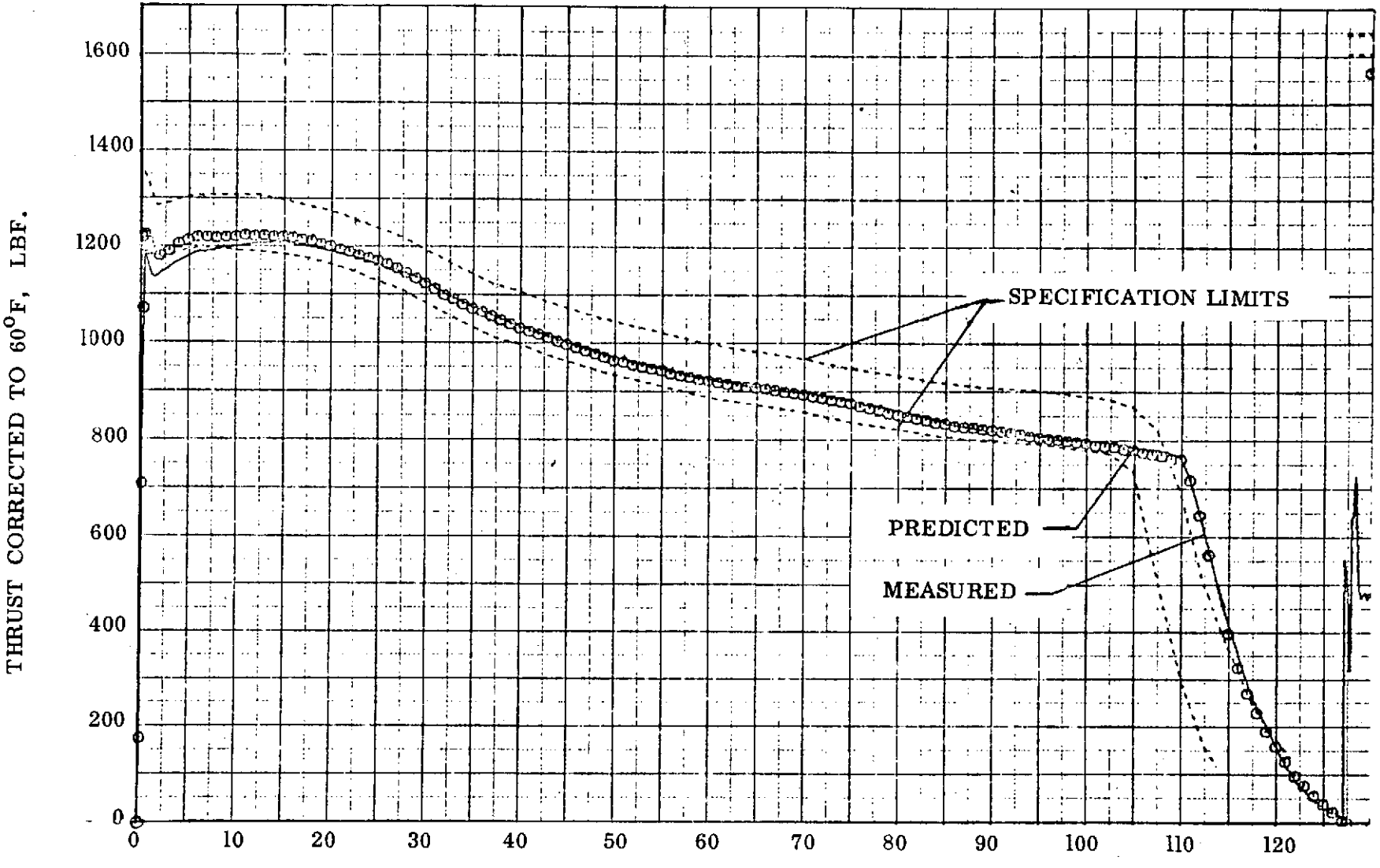

FIGURE V-1B-10 UNAUGMENTED NOZZLE CENTERLINE VACUUM THRUST vs TIME, CORRECTED TO 60° F, SRM 19.

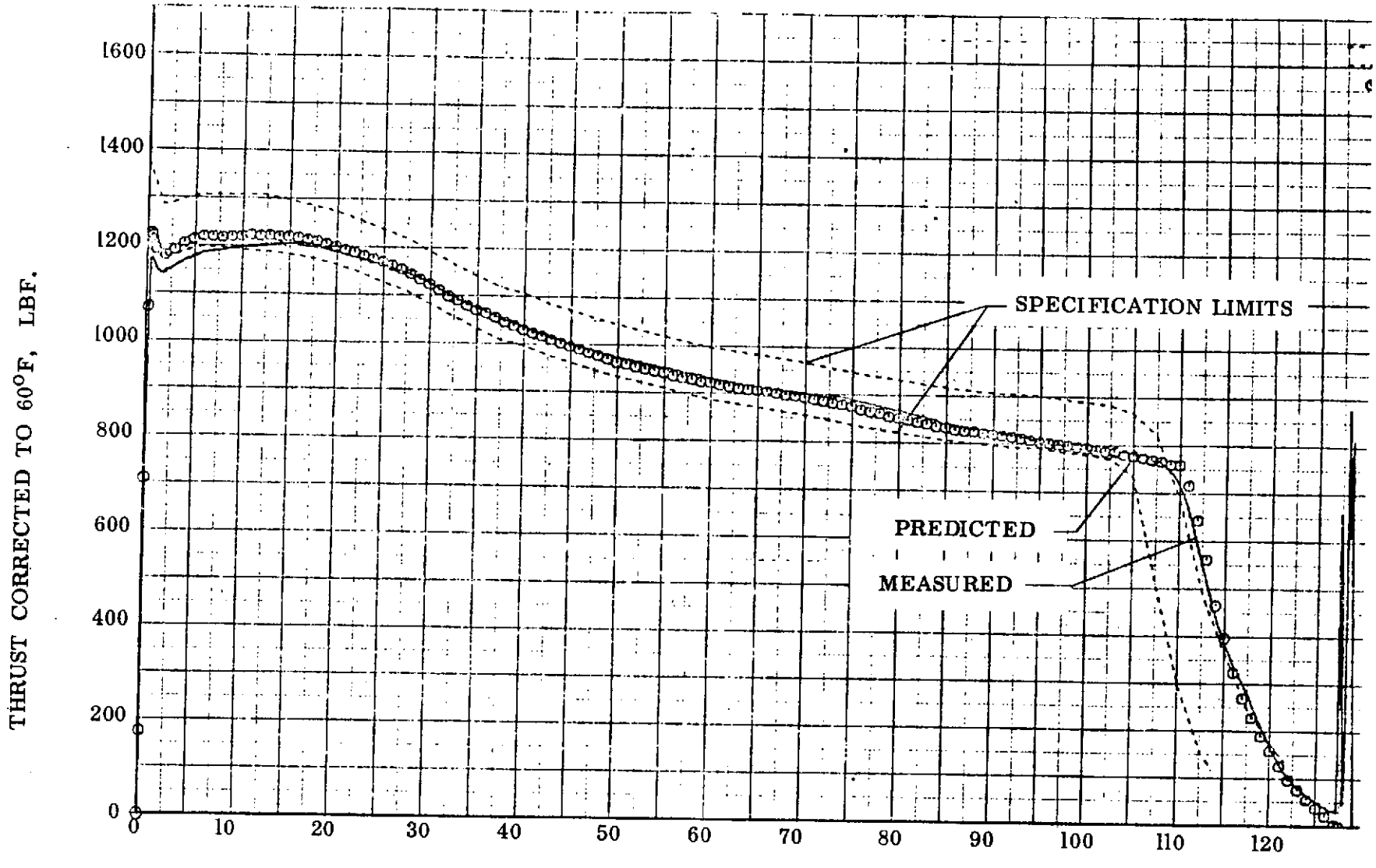

FIGURE V-18-11 UNAUGMENTED NOZZLE CENTERLINE VACUUM THRUST vs TIME, CORRECTED TO 60° F, SRM 20.

V-1C. TITAN STAGE 0 THRUST VECTOR CONTROL SYSTEMS

by R. J. Salmi

Summary

The Stage 0 thrust vector control systems performed as expected. No anomalies in the performance of the electromechanical valves were detected. Thrust vector control fluid usage and dump were normal.

System Description

The Stage 0 thrust vector control system provides side forces in response to steering commands by means of fluid injection into the SRM nozzles. Each nozzle has an injectant manifold with 24 electromechanical valves (EMV's) that operate in groups of six to provide four steering quadrants as shown in figure V-1C-1. The injectant fluid (N_2O_4) interferes with the nozzle supersonic flow causing flow turning through an oblique shock wave as shown in figure V-1C-2. The reaction of the N_2O_4 with the fuel rich exhaust increases the pressure in the separated flow region thereby enhancing both the flow turning effectiveness and the thrust.

The EMV's respond to steering commands from the core vehicle. Failure of one valve in a quadrant does not compromise the system effectiveness. In normal operation, all EMV's are opened to provide a steady flow of N_2O_4. The valve openings are set by the control computer to provide a scheduled dump rate. Steering commands to open the valves in a given quadrant also reduce the openings of the EMV's in the remaining quadrants to minimize the amount of injectant required for steering and to maintain the dump rate.

The TVC system details are shown in figure V-1C-3. The injectant flow is maintained by the high GN_2 ullage pressure (952 to 1107 psia at liftoff) which decays to about 630 psia at separation. Leakage of N_2O_4 from the EMV's into the nozzle during ground hold is prevented by pyroseal end caps on the valve outlets. The pyroseal caps burn off at engine startup before any steering control is required.

Flight Performance

The operation of the EMV's is determined by monitoring the valve positions during flight. The outputs from the EMV position indicators are read as group averages for two groups of three valves each for each quadrant. If any valve is in an incorrect position, the two group outputs from that quadrant will have different average values. For SRM's 19 and 20, no valve anomalies were detected.

The TVC system fluid inventories are summarized in table V-1C-1. The values shown are all within the expected range of values.

TABLE V-1C-1

	SRM 19	SRM 20
Nitrogen tetroxide load, lb	8446	8439
Total expended, lb	6725	6522
Total dumped, lb	4145	3938
Total TVC steering, lb	2580	2584
Manifold pressure at ignition, psia	1024	1001
Manifold pressure at separation, psia	560	556

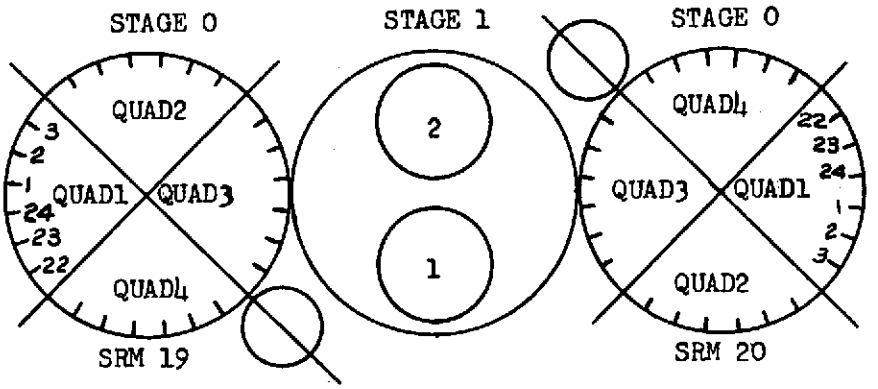

VIEW LOOKING FORWARD

FIGURE V-1C-1 SRM STEERING QUADRANT AND EMV ORIENTATION

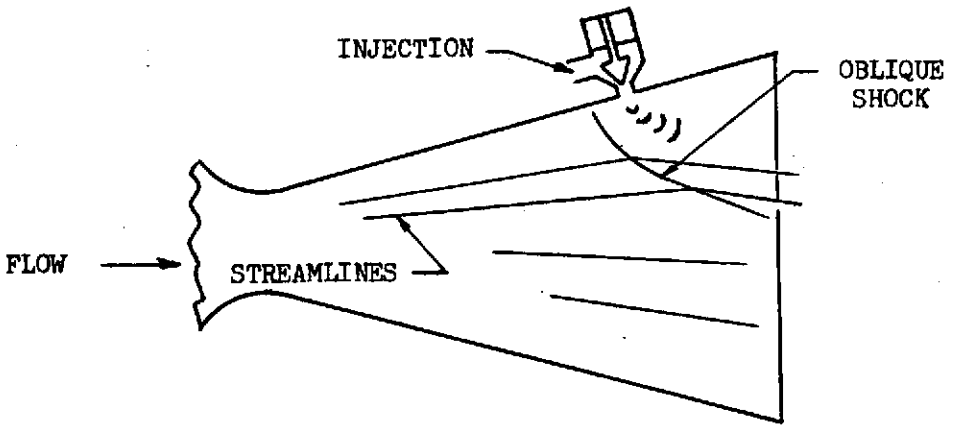

FIGURE V-1C-2 SRM THRUST VECTOR CONTROL INJECTION.

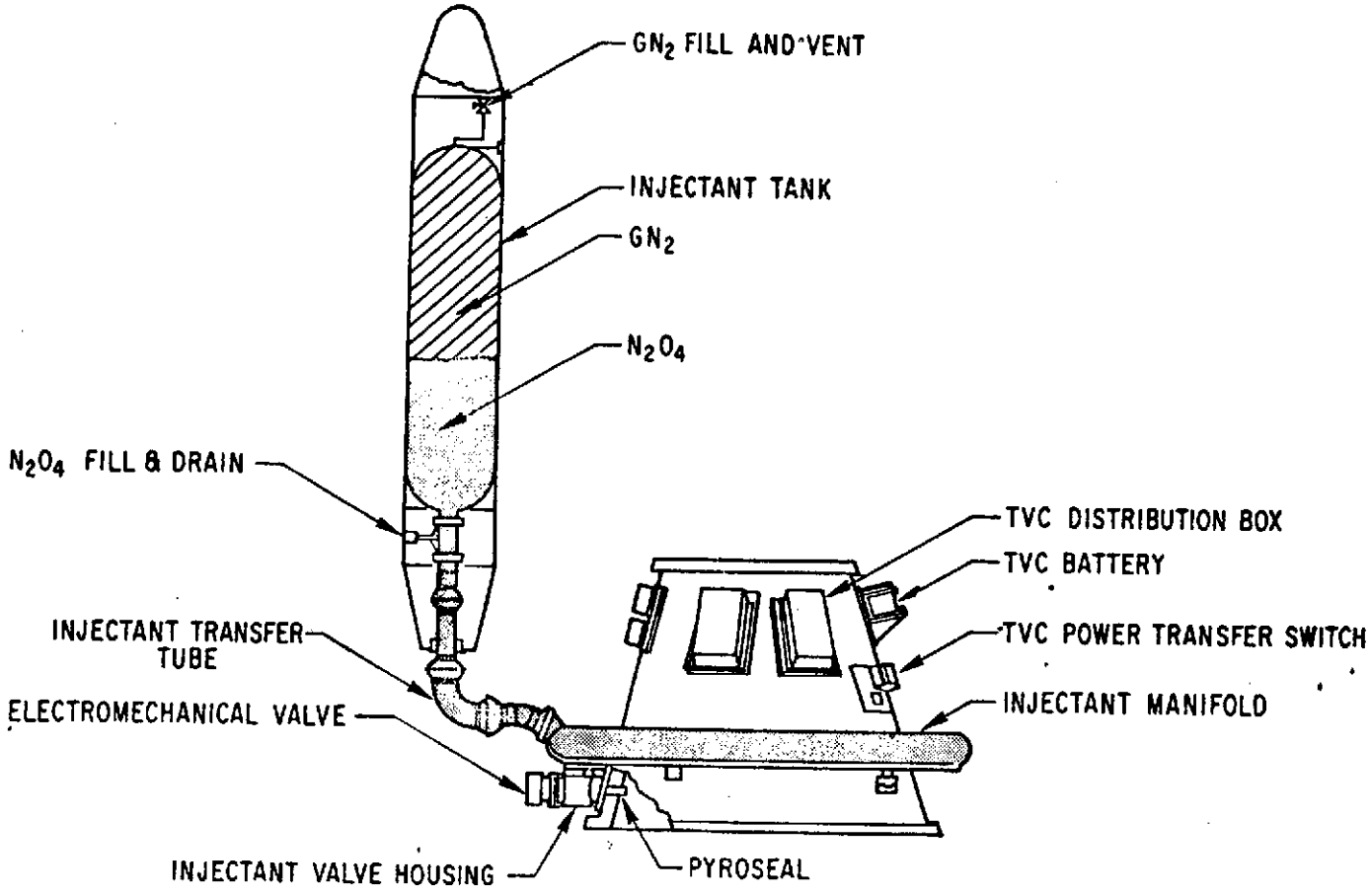

FIGURE V-1C-3. - THRUST VECTOR CONTROL SYSTEM DETAILS

V-2. TITAN FLIGHT CONTROL AND SEQUENCING SYSTEM

by E. Jeris and T. Porada

Summary

The Flight Control System maintained vehicle stability throughout powered flight. Control system responses due to the roll to launch azimuth, ADDJUST and closed loop guidance steering commands from Centaur were well within the control system capabilities. All open loop pitch rates and preprogrammed events were issued as planned. Dump programming of TVC injectant fluid was satisfactory. No system or component anomalies occurred.

System Description

The Flight Control System consists of a three-axis reference system (TARS), flight control computer (FCC), a rate gyro system, two flight programmers, and a staging timer. The rate gyro system package is located between tanks on Stage I. All other flight control system components are mounted on the equipment truss located in the forward compartment of Stage II. A block diagram of the flight control system is shown in figure V-2-1.

The function of the flight control system is to provide vehicle attitude stability, provide discrete commands, issue an open loop pitch program, and regulate SRM thrust vector control fluid usage. The flight control system responds to steering commands from Centaur for the roll to launch azimuth maneuver and ADDJUST steering during Stage 0 and closed loop guidance steering during Stages I and II.

TARS gyros provide analog attitude error signal proportional to the angular displacement of the vehicle from an established reference in each of the pitch, yaw, and roll axes to the flight control computer. Torquer windings are provided in each gyro to change the reference as commanded by a preprogrammed rate history generated by the Titan flight programmer. In addition separate torquer windings are provided in each gyro to accept commands from Centaur guidance.

The rate gyro package senses rate of change of vehicle attitude in pitch and yaw during Stages 0 and I flight. Rate gyro output is a signal voltage proportional to vehicle angular rate sent to the flight control computer.

Two flight programmers (A and B) provide momentary (0.1 or 1 sec) and continuous discrete commands. Each programmer has the capability of issuing thirty (30) time-based and one (1) acceleration based discrete. Command system redundancy is provided by the two programmers. Flight

programmer "A" accelerometer provides for Stage II shutdown command (redundant with a Centaur command) and programmer "B" accelerometer provides a Stage I start command (redundant with the staging timer).

The flight control computer accepts attitude error signals from the TARS and angular rate signals from the rate gyro system. These signals are conditioned (filtered and integrated), amplified, mixed, and distributed to the thrust vector control devices (SRM TVC valves and Stages I and II hydraulic actuators). Flight programmers and the electrical sequencing system provide discrete commands to the flight control computer. These discrete commands change gains and pitch rates at appropriate flight times. The flight control computer also controls the dump programming of the TVC injectant fluid. Dump is controlled by comparing commanded TVC valve opening with a nominal profile, remembering the difference between commanded and nominal, and using the memory to issue the appropriate dump command. The computer provides ten (10) in-flight gain states, ten (10) pitch rates, derived rate information in pitch, yaw, and roll from TARS output, and attitude integrators to compensate for hardware offsets and structural misalinement, and vehicle center of gravity offsets.

The staging timer provides one acceleration based and three time based discretes. The acceleration based discrete is used to start the Stage I engines during Stage 0 deceleration. Stage I start command results from a majority vote of any two of three accelerometers. The first time-based discrete is used for SRM jettison, the second for CSS jettison backup and the third is a spare.

Flight Performance

The Titan flight control system maintained stable control using a peak of 24, 16.6, and 16.7 percent of command capability for Stages 0, I, and II, respectively. Command voltage to each SRM quadrant and dynamic and static stability limits are shown in figures V-2-2 and V-2-3. The stability limits represent the TIIIE-1 side force constraint in terms of TVC system quadrant voltage. This constraint is used in conjunction with launch day wind/synthetic vehicle simulations as a go/no-go criterion with respect to vehicle stability and control authority. Simulation responses satisfying the constraint assures a 3-sigma probability of acceptable control authority and vehicle stability. Maximum command during Stage 0 flight was 2.4 volts which is 24 percent of the control system capability and 34 percent of the dynamic stability limit. The peak command (pitch down) resulted from the Titan open loop pitch program and Centaur ADDJUST pitch down wind load relief steering.

For Stages I and II, the control system limit is the maximum gimbal angle associated with the actuator stop. Actual gimbal angle used for Stages I and II against flight time is plotted in figures V-2-4 through V-2-8. During Stage I flight the maximum gimbal angle required for control was 16.6 of full travel at SRM jettison. During Stage II 15 percent of full gimbal angle was the maximum used for control. This occurred in

the roll channel during CSS jettison.

The control system response to vehicle dynamics was evaluated for each significant flight event. The amplitude, frequency, and duration of vehicle transients and the control system output in terms of SRM commands and Stages I and II gimbal angle is shown in table V-2-1.

Both flight programmers (A and B) and the staging timer issued all preprogrammed discretes at the proper times. The Centaur sent four discretes to the Titan at the proper times. The complete sequence of events with actual and nominal times from SRM ignition is shown in table V-2-2.

TABLE V-2-1 VEHICLE DYNAMIC RESPONSE

Event	Time Sec.	Axis	Zero to Peak Amplitude Deg./Sec.	Transient Frequency Hz	Transient Duration Sec.	Required Control % of Capability
Lift-off	0	P	2.0	Mixed (30-40)	< 1	2
		R	1.2	10	< 1	
		Y	2.6	Mixed (30-40)	1	< 1
Roll Maneuver	6.6	R	5.8	.25	7	23.5
Peak TARS Offset (Result of ADDJUST Steering and Winds)	27.5	P				24
Maximum Aerodynamic Pressure (45-60 Sec.)	48	P	6.2	Mixed	15	11.7
	46.5	Y	6.0	Mixed	15	11.5
SRM Tail-off through Stage I Start	113-115.2	Y	.36	Drift	2.2	7.8
Stage I Ignition	115.4	P	.6		.5	<2
	115.4	Y	.6		.5	2
SRM Jettison	126.6	Y	1.2	3.0	1.75	16.6
		R	5.2	.3	5	
Start of PR 7 (Only Pitch up Program)	130.1	P	1.2	N/A	N/A	14.7
Enable Guidance Steering (2.8^{o} Pitch Down $.7^{o}$YL)	156.3	P	1.56	N/A	N/A	10.5
		Y	.6	N/A	N/A	10.6

TABLE V-2-1 Cont.

Event	Time Sec.	Axis	Zero to Peak Amplitude Deg./Sec.	Transient Frequency Hz	Transient Duration Sec.	Required Control % of Capability
Stage I Shutdown Stage II Start	263.1	R	.24	N/A	N/A	4.2
CSS Jettison	274	P	.76	10	.5	4
	275	P	.12	.25	4	4
	274	Y	.48	10	.6	<1
	274	R	1.2	10	.5	10.5
	275		.60	3	1.5	15.0
	276.5	R	.8			15.0
Enable Guidance (3^{o} PU .10 YL Command)	284	P	.84		6	13
	284	Y	.12		5	3
Stage II Tailoff		P	1.2	Drift	5.5	N/A
		Y	2.4	Drift	5	N/A
		R	2	Drift	5	N/A

TABLE V-2-2

SEQUENCE OF EVENTS - TITAN/CENTAUR - PROOF FLIGHT

	EVENT	SIGNAL SOURCE F/P A	F/P B	S/T	SCU	TIME FROM SRM IGNITION TIME ZULU	ACTUAL SEC.	NOM. SEC.	REMARKS
1.	PROGRAM INITIATE					48:00:4	-1.0	-1.0	SUPPLIED BY AGE (CMG)
2.	VERIFICATION DISCRETE	P	S			48:00.9	-0.5	-0.5	HOLD FUNCTIONS
3.	SRM IGNITION; START TVC DUMP RATE 1; START ATT. INT.; UNCAGE TARS					48:01.44 48:01.6	0.0	0.0	SUPPLIED BY AGE DCU T-0 REF
	A. LIFTOFF (1C1E UMB)					48:01:81	0.4	0.21	THRUST/WEIGHT 1.0
	B. START TVC DUMP RATE 1 B/U					48:01.85	0.41	0.53	2A1E UMB. DISC.
4.	START ROLL PROGRAM				P	48:08.0	6.6	6.50	
5.	STOP ROLL PROGRAM				P	48:08.5	7.1	6.98	4.8° TOTAL ROLL ANGLE
	BEGIN DCU P-Y PROGRAM					48:12.6	11.2	10.0	CENTAUR FUNCTION (1050 FT. ALT.)

NOTE: REFERENCE TIME 1300 ZULU

TABLE V-2-2

SEQUENCE OF EVENTS - TITAN/CENTAUR - PROOF FLIGHT

	EVENT	SIGNAL SOURCE F/P A	F/P B	S/T	SCU	TIME FROM SRM IGNITION TIME ZULU	ACTUAL SEC.	NOM. SEC.	REMARKS
6.	PITCH RATE 1	P(1)				48:11.4	10.0	10.0	1.17°/SEC PD
			S(1)			48:11.4	10.0	10.0	(1.14°/SEC ACTUAL)
7.	PITCH RATE 2	P(2)				48:21.4	20.0	20.0	0.53°/SEC PD
			S(2)			48:21.4	20.0	20.0	(0.51°/SEC ACTUAL)
8.	GAIN CHANGE 1; DUMP RATE 2	P(5)				48:30.4	29.0	29.0	
			S(5)			48:30.4	29.0	29.0	
9.	PITCH RATE 3	P(3)				48:31.4	30.0	30.0	0.73°/SEC PD
			S(3)			48:31.4	30.0	30.0	(0.72°/SEC ACTUAL)
10.	PITCH RATE 4	P(10)				49:03.4	62.0	62.0	0.63°/SEC PD
			S(10)			49:03.5	62.1	62.0	(0.62°/SEC ACTUAL)
11.	GAIN CHANGE 2; DUMP RATE 3	P(6)				49:11.4	70.0	70	
			S(6)			49:11.5	70.1	70	
12.	PITCH RATE 5; ENABLE S/T ACC. SW'S.; TPS PWR. SWITCH CLOSED; ENABLE STG. I START	P(21)				49:16.5	75.1	75.0	0.52°/SEC PD
			S(11)			49:16.5	75.1	75.0	(0.51°/SEC ACTUAL)

NOTE: REFERENCE TIME 1300 ZULU

TABLE V-2-2

SEQUENCE OF EVENTS - TITAN/CENTAUR - PROOF FLIGHT

	EVENT	SIGNAL SOURCE F/P A	F/P B	S/T	SCU	TIME FROM SRM IGNITION TIME ZULU	ACTUAL SEC.	NOM. SEC.	REMARKS
13.	ENABLE STG. I START B/U; ENABLE S/T ACC. SW'S. B/U; TPS PWR. CLOSED B/U		P(9)			49:16.5	75.1	75	
14.	GAIN CHANGE 3;	P(7)				49:31.5	90.1	90	
	DUMP RATE 4		S(8)			49:31.5	90.1	90	
15.	PITCH RATE 6	P(12)				49:36.5	95.1	95.0	0.38°/SEC PD
			S(15)			49:36.5	95.1	95.0	(0.39°/SEC ACTUAL)
16.	END F/P B TIME BASE 1; ENABLE F/P B ACC. SW.		P(16)			49:37.5	96.1	96	INTERNAL DISC. REQUIRED FOR PROG. B ONLY
	SEP. FWD. BRG. REACTORS					49:41.6	100.2	100	CENTAUR FUNCTION
17.	ACC. DECAY TO 1.5 G'S					49:55.1	114.1	113.4	ACCELEROMETER VEHICLE
	INHIBIT TITAN STEER.					49:56.0	114.6	114.0	CENTAUR FUNCTION

NOTE: REFERENCE TIME 1300 ZULU

TABLE V-2-2

SEQUENCE OF EVENTS - TITAN/CENTAUR - PROOF FLIGHT

	EVENT	SIGNAL SOURCE F/P A	F/P B	S/T	SCU	TIME FROM SRM IGNITION TIME ZULU	ACTUAL SEC.	NOM. SEC.	REMARKS
18.	STAGE I START (87FS1); SRM ISDS DISABLE; INITIATE F/P B T/B 2; INITIATE S/T T/B 1; SEP. EXIT CLOSURE CMD.		S(A)	P		49:56.3 49:56.0	114.9 114.6	114.1 114.1	SENSED BY ACC. SW'S. (723 MS AFTER VEHICLE + 1.5 G'S ± 0.1 G'S)
	A. EXIT CLOSURE SEP.							114.9	784 MS AFTER S7FS1
19.	STAGE I ISDS SAFE ENABLE; REMOVE F/P B ACC. DISCRETE		P(27)			50:02.0	120.6	120.1	6 SEC FROM STAGE I START (6.0 SEC. ACTUAL)
20.	STAGE O/I SEP. CMD.; GAIN CHANGE 4; REMOVE S/T ACC. DISC.		S(18)	P		50:08.0	126.6	126.1	TIMED FROM STG I START (12.0 SEC)
21.	STG I ISDS SAFE ENABLE	S(8)				DATA DROPOUT		126.1	ACTIVATED FROM S/T STG O/I SEP. DISCRETE
22.	SRM JETTISON					50:08.1	126.7	126.2	FROM STG O/I SEP. DISC.
23.	PITCH RATE 7	P(15)	S(19)			50:11.5 50:15.8	130.1 134.4	130.0 133.9	0.75°/SEC PU (0.72°/SEC ACTUAL)

NOTE: REFERENCE TIME 1300 ZULU

TABLE V-2-2

SEQUENCE OF EVENTS - TITAN/CENTAUR - PROOF FLIGHT

	EVENT	SIGNAL SOURCE F/P A	F/P B	S/T	TIME FROM SRM IGNITION TIME ZULU	ACTUAL SEC.	NOM. SEC.	REMARKS
24.	PITCH RATE 9	P(19)			50:21.5	140.1	140.0	0.09°/SEC PD (0.09° ACT)
			S(20)		50:25.8	144.4	143.867	29.9 SEC FROM STG I START (29.9 SEC. ACT.)
	ENABLE TITAN STEER.						146.0	CENTAUR FUNCTION
25.	START CLOSED LOOP GUIDANCE				50:37.7	156.3	146.2	CENTAUR FUNCTION
	PITCH RATE 8	P(11)					—	NOT USED
			S(21)				—	NOT USED
26.	GAIN CHANGE 5	P(13)			51:13.6	192.2	192	
			S(23)		51:18.0	196.6	196.0	82 SEC FROM STG I START (82.0 SEC. ACT.)
	RELEASE FORWARD SEAL				51:36.6	215.2	214.0	CENTAUR FUNCTION
27.	GAIN CHANGE 6	P(14)			51:53.6	232.2	232	
			S(25)		51:58.0	236.6	236.0	122 SEC FROM STG I START (122.0 SEC ACT.)
	INHIBIT TITAN STEER.				51:33.8	212.4	236.0	CENTAUR FUNCTION

NOTE: REFERENCE TIME 1300 ZULU

TABLE V-2-2

SEQUENCE OF EVENTS - TITAN/CENTAUR - PROOF FLIGHT

	EVENT	SIGNAL SOURCE F/P A	SIGNAL SOURCE F/P B	SIGNAL SOURCE S/T	SCU	TIME FROM SRM IGNITION TIME ZULU	TIME FROM SRM IGNITION ACTUAL SEC.	TIME FROM SRM IGNITION NOM. SEC.	REMARKS
28.	STG I S/D ENABLE; STG I ISDS SAFE; ENABLE STG I/II STG'ING; ENABLE SAFE STG I DEST. INIT; ENABLE STG II ENGINE START; ENABLE CSS SEP.	P(16)	S(24)			52:03.5 52:11.0	245.1 249.6	245 249.0	135 SEC FROM STG I START (135.0 SEC. ACT.)
29.	STG I S/D (87FS2); STG II START (91 FS1); FIRE STG'ING ORDNANCE					52:24.5	263.1	261.9	TCPS INITIATED WHEN P_c IS 77% OF STEADY STATE
	A. STG I DEST. INIT. SAFED							262.1	0.24 SEC AFTER 87FS2
	B. STG II IGNITION					52:25.3	263.9	262.6	0.69 SEC AFTER 87FS2
	C. STG I JETTISON					52:24.5	263.1	262.6	STG'ING ORDNANCE FIRED
30.	GAIN CHANGE 7; PITCH RATE 10; (START S/T TB2)					52:25.3	263.9	262.6	STG I/II ELECT. DISC. PR NO. 10 0.11°/SEC PD (0.09°/SEC ACTUAL)
31.	FIRE SHROUD SEP. PRI. ORD.				P	52:35.4	274.04	273.0	STG I THRUST DECAY TO 1.5 G + 10 SEC

NOTE: REFERENCE TIME 1300 ZULU

TABLE V-2-2

SEQUENCE OF EVENTS - TITAN/CENTAUR - PROOF FLIGHT

	EVENT	SIGNAL SOURCE F/P A	F/P B	S/T	SCU	TIME FROM SRM IGNITION TIME ZULU	ACTUAL SEC.	NOM. SEC.	REMARKS
32.	FIRE SHROUD SEP. SEC. ORD.				P	52:35.9	274.54	275.5	500 ± 50 MILLISEC. AFTER PRIMARY CSS SEP. SIGNAL
	ENABLE TITAN STEER S2A ON (H_2O_2)					52:45.7	284.3	276.0	CENTAUR FUNCTIONS
33.	FIRE SHROUD SEP. PRI. ORD. B/U			S		52:54.3	292.9	291.6	STG I/II SEP + 29.0 SEC
	S2A OFF (H_2O_2) Y1 ON (H_2O_2)							293.0	CENTAUR FUNCTIONS
34.	REMOVE GAIN CHANGE 7;	P(24)				53:11.6	310.2	310	DOES NOT CHANGE STATUS OF GAIN STATE OR PITCH RATE ON FCC
	PITCH RATE 10 ENABLE		S(26)			53:15.9	314.5	313.9	199.8 SEC FROM STG I START (199.9 ACTUAL)
	Y1 OFF (H_2O_2) Y2 ON (H_2O_2) Y2 OFF (H_2O_2)							318.0 318.0 338.0	CENTAUR FUNCTION CENTAUR FUNCTION CENTAUR FUNCTION
35.	GAIN CHANGE 8	P(18)	S(28)			53:41.6 53:46.2	340.2 344.8	340 344.1	230 SEC FROM STG I START (230.2 ACTUAL)
	S2B ON (H_2O_2)							381.0	CENTAUR FUNCTION

NOTE: REFERENCE TIME 1300 ZULU

TABLE V-2-2

SEQUENCE OF EVENTS - TITAN/CENTAUR - PROOF FLIGHT

	EVENT	SIGNAL SOURCE F/P A	F/P B	S/T	SCU	TIME FROM SRM IGNITION TIME ZULU	ACTUAL SEC.	NOM. SEC.	REMARKS
36.	GAIN CHANGE 9	P(22)				54:41.6	400.2	400	
			S(29)			54:46.2	404.3	404.1	290 SEC FROM STG I START (290.2 ACTUAL)
	S2B OFF (H_2O_2)							431.0	CENTAUR FUNCTION
	INHIBIT TITAN STEER.					55:09.8	428.4	434.5	CENTAUR FUNCTION
	BOOST PUMPS ON					55:13.3	437.9	436.7	CENTAUR FUNCTION
37.	STG II S/D ENABLE;	P(25)				55:29.7	448.3	448	
	ENABLE F/P A ACC. SW.;		S(30)			55:33.2	451.8	451.2	337.1 SEC FROM STG I START (337.2 ACTUAL)
	STOP PITCH RATE 1D;								
	ARM CENTAUR 91FS2 B/U;								
	ENABLE SAFE STG II DEST. INIT.;								
	ENABLE RETROFIRE;								
	ENABLE STG II/CENTAUR SEP.;								
	END F/P "A" TB 1;								
	END F/P "B" TB 2								
38.	STG II PROP. EXH.							464.67	
39.	ACC. DECAY TO 1.0 G'S					55:50.9	469.5	464.98	VEHICLE ACCELEROMETER

NOTE: REFERENCE TIME 1300 ZULU

TABLE V-2-2

SEQUENCE OF EVENTS - TITAN/CENTAUR - PROOF FLIGHT

	EVENT	SIGNAL SOURCE F/P A	SIGNAL SOURCE F/P B	SIGNAL SOURCE S/T	SCU	TIME FROM SRM IGNITION TIME ZULU	ACTUAL SEC.	NOM. SEC.	REMARKS
40.	STG II S/D SIGNAL (91FS2); SAFE STG II DEST. INIT.; ENABLE RETROFIRE; ENABLE STG II/CENTAUR SEP.; START F/P A T/B 2 (P(A) ONLY)	P(A)			S	55:51.0	469.6	465.1	ACC. DECAY TO 1.0 + 0.0/-0.9 G'S SENSED BY CENTAUR GUIDANCE
						55:51.6	470.2	467.7	725 MILLISEC. AFTER ACC. DECAY TO 1.0 ± 0.1 G
41.	STG II CENTAUR SEP. CMD. FIRE STG II RETROS				P	55:56.6	475.24	470.5	+ 0.022 G TO 1.0 SEC AFTER 0.01 G OR 7.0 SEC AFTER SENSING 1.0 G
		S(30)				55:59.0	477.6	473.1	7.4 SEC AFTER SENSING 1.0 G

NOTES: REFERENCE TIME 1300 ZULU

* P = PRIMARY S = SECONDARY F/P A = FLIGHT PROGRAMMER A S/T = STAGING TIMER
SCU = SEQUENCE CONTROL UNIT, CENTAUR GUIDANCE
( ) = DENOTES FLIGHT PROGRAMMER DISCRETE NUMBER OR ACCELERATION SWITCH OUTPUT

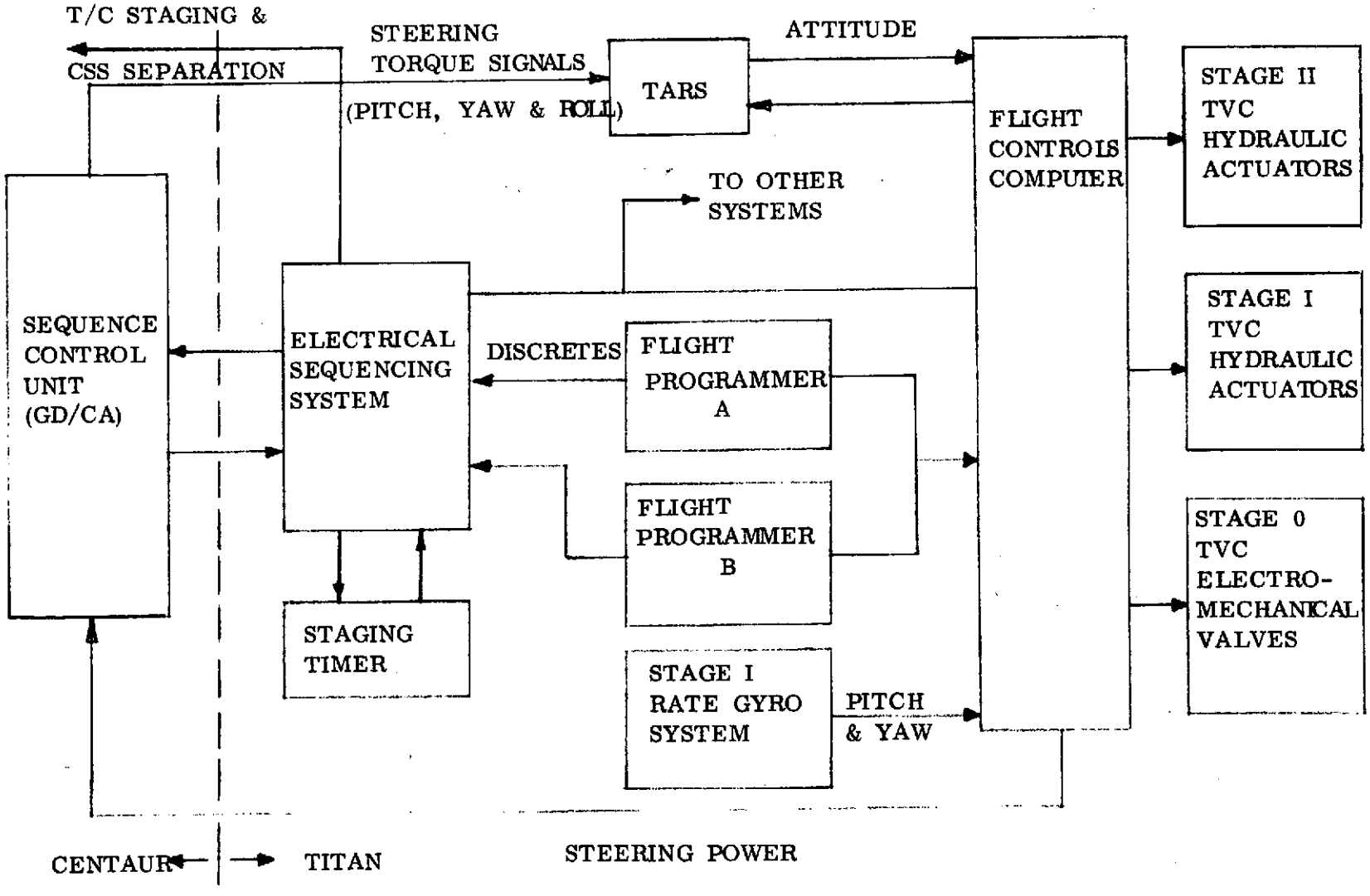

FIGURE V-2-1 FLIGHT CONTROLS AND SEQUENCING SYSTEM

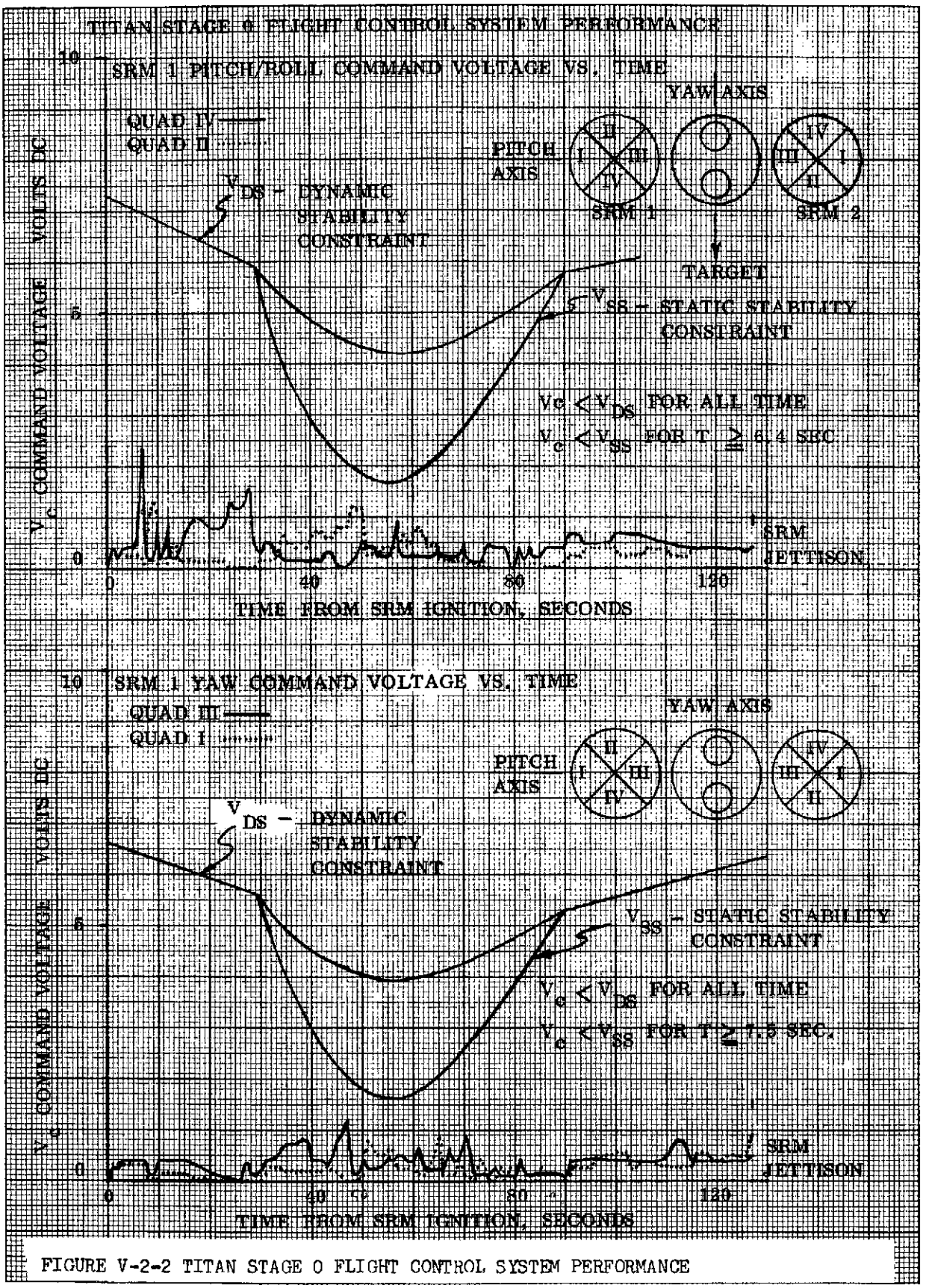

FIGURE V-2-2 TITAN STAGE 0 FLIGHT CONTROL SYSTEM PERFORMANCE

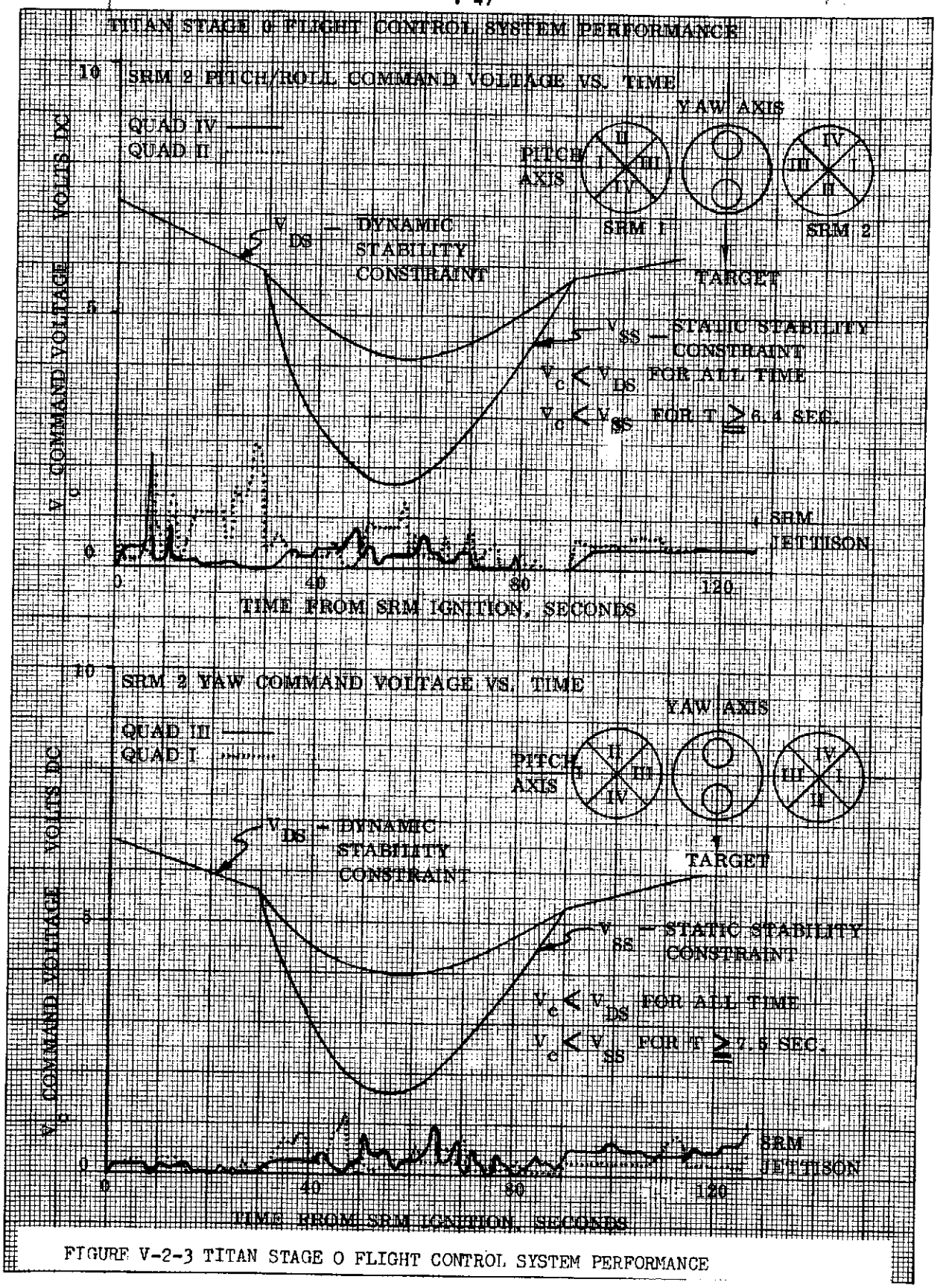

FIGURE V-2-3 TITAN STAGE 0 FLIGHT CONTROL SYSTEM PERFORMANCE

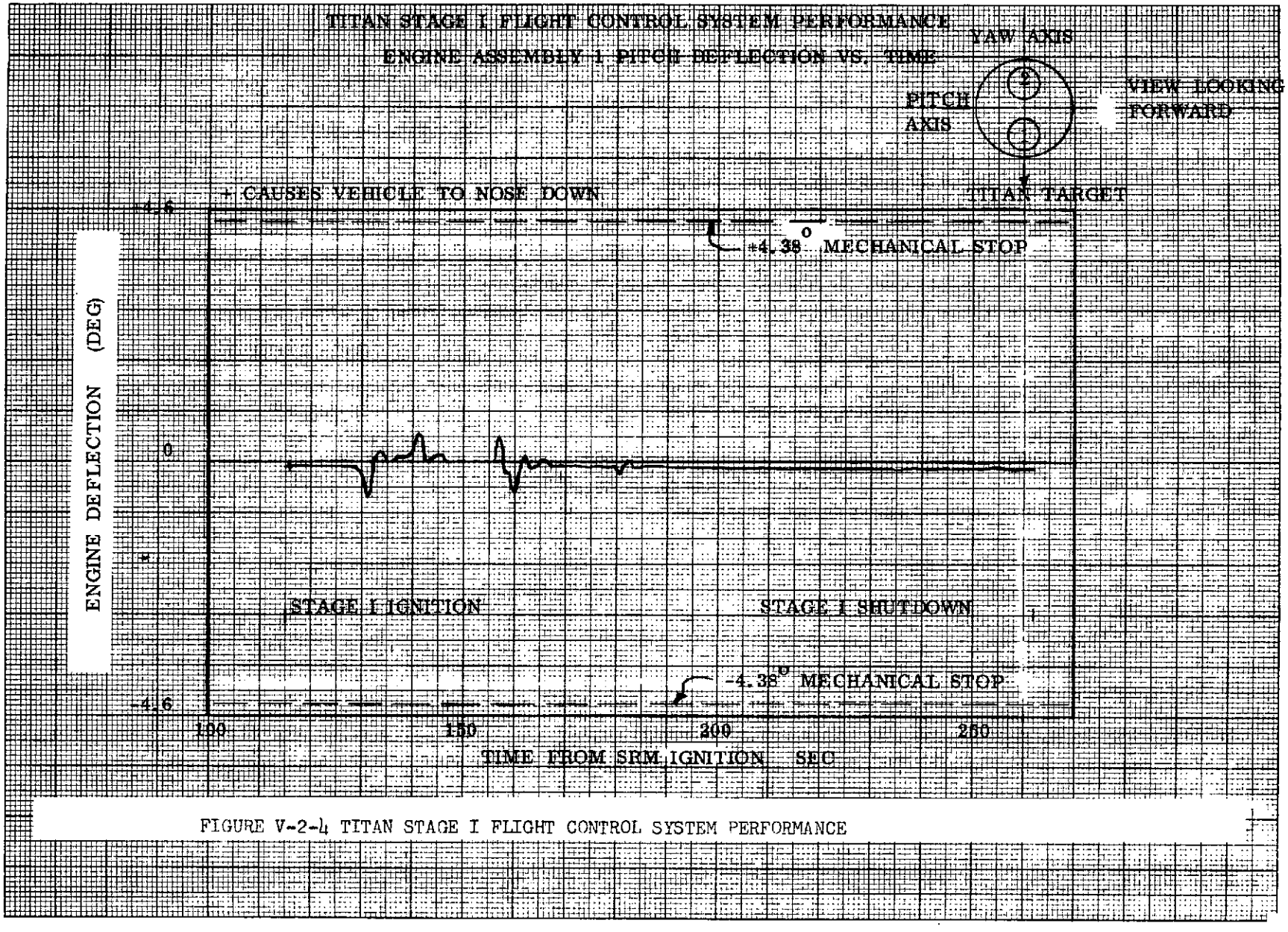

FIGURE V-2-4 TITAN STAGE I FLIGHT CONTROL SYSTEM PERFORMANCE

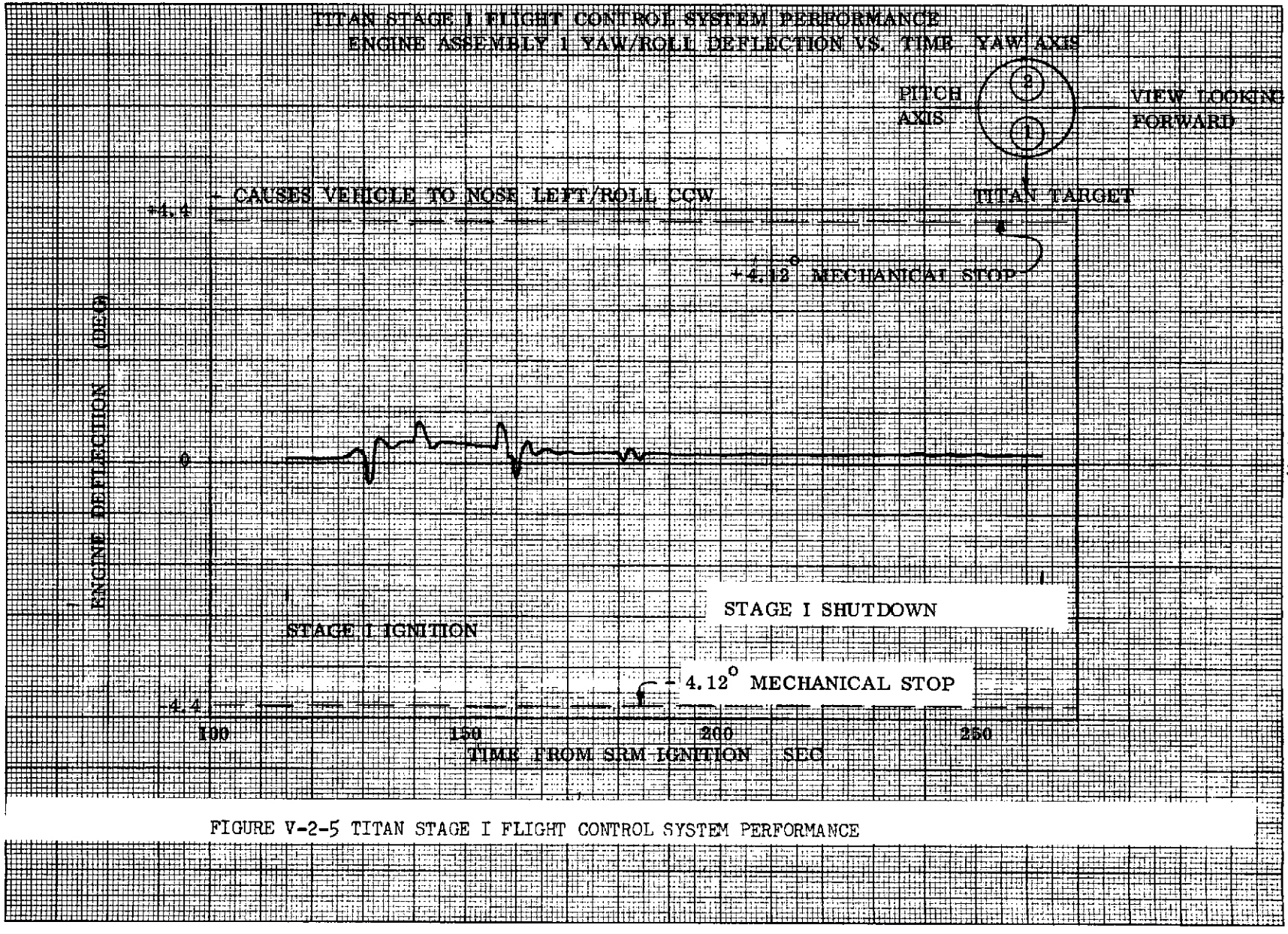

FIGURE V-2-5 TITAN STAGE I FLIGHT CONTROL SYSTEM PERFORMANCE

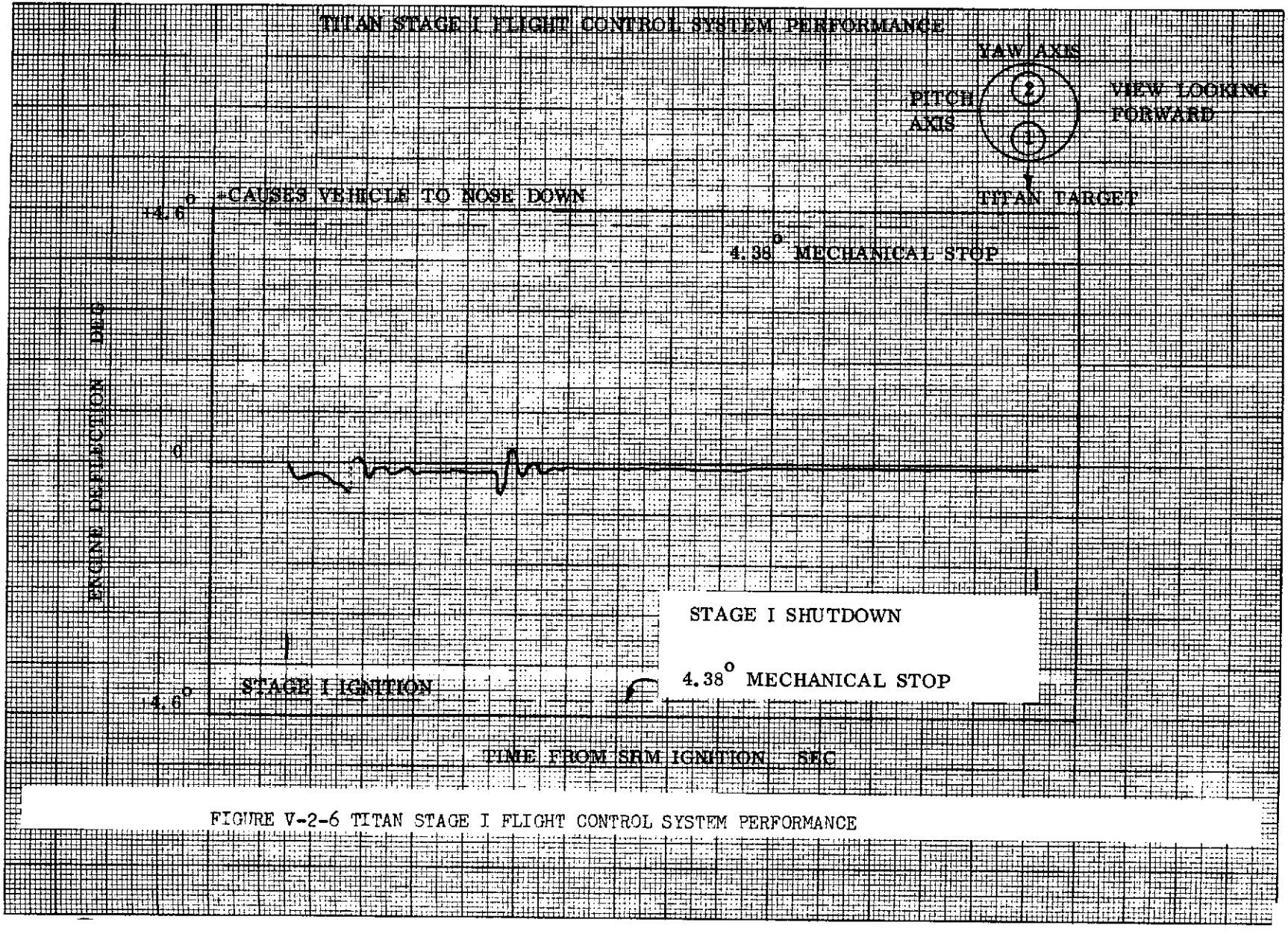

FIGURE V-2-6 TITAN STAGE I FLIGHT CONTROL SYSTEM PERFORMANCE

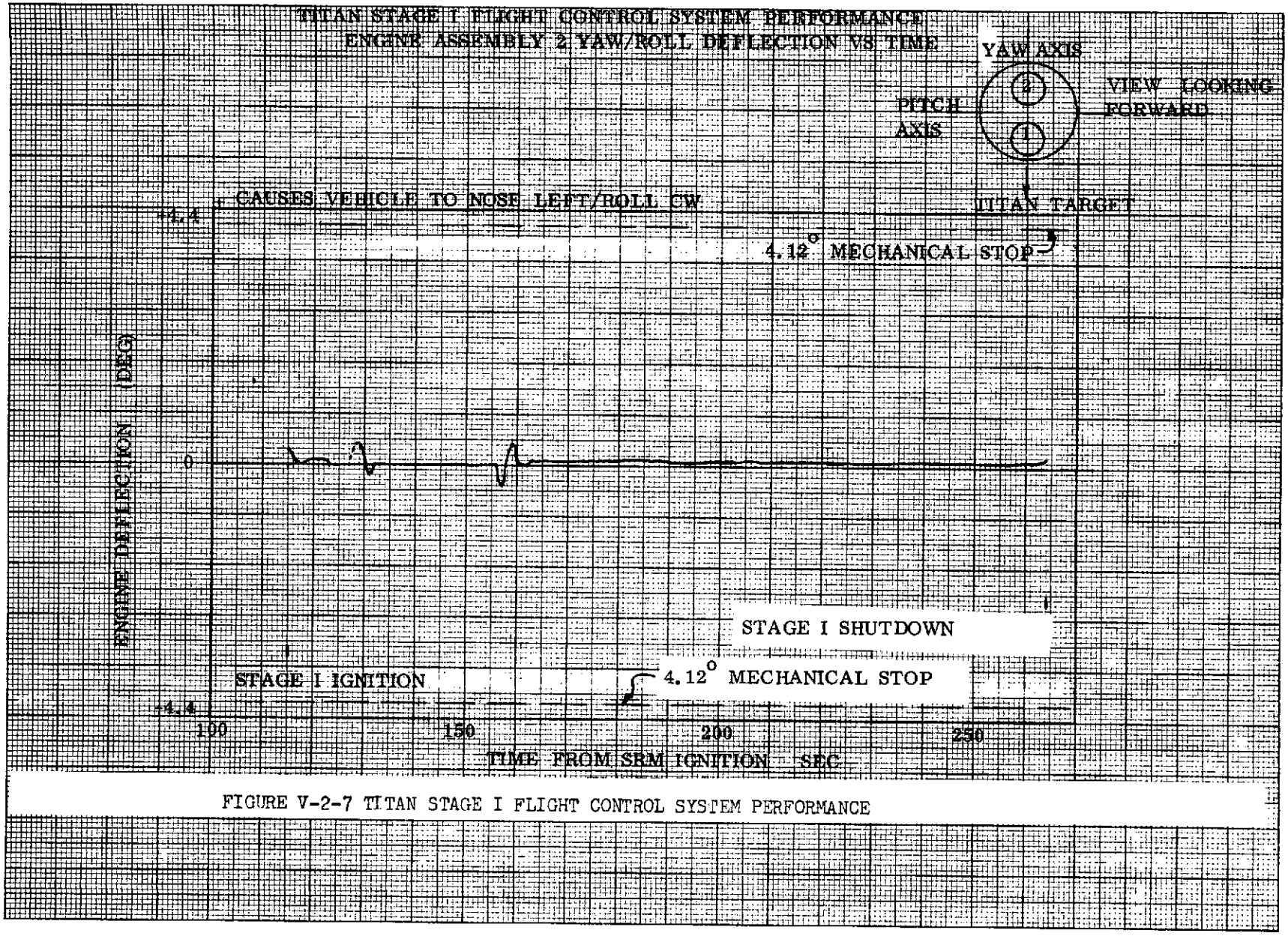

FIGURE V-2-7 TITAN STAGE I FLIGHT CONTROL SYSTEM PERFORMANCE

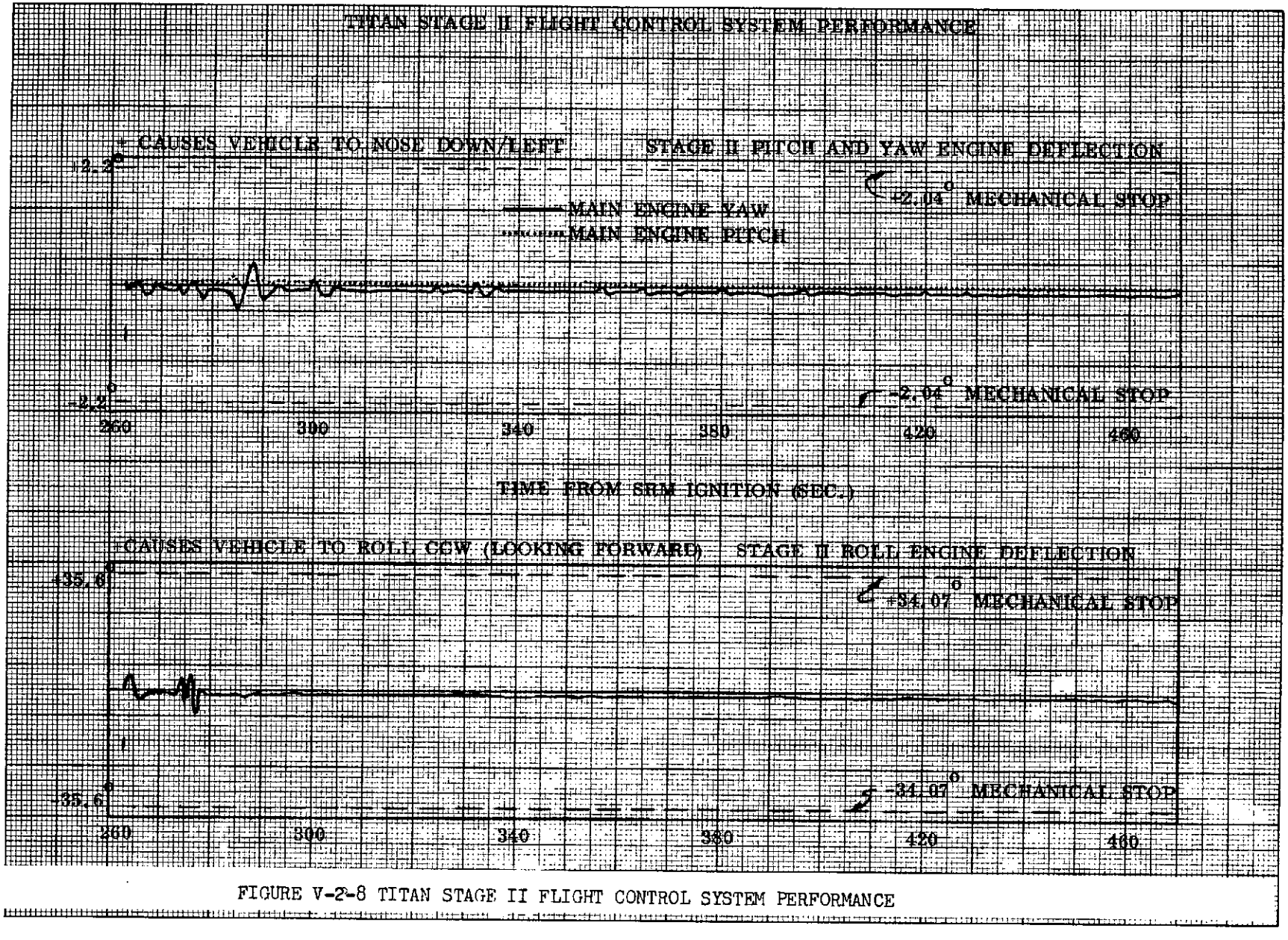

FIGURE V-2-8 TITAN STAGE II FLIGHT CONTROL SYSTEM PERFORMANCE

V-3. TITAN ELECTRICAL/ELECTRONIC SYSTEMS

by B. L. Beaton and R. E. Orzechowski

V-3A. Solid Rocket Motor Electrical System

Summary

The solid rocket motor (SRM) electrical system performance was satisfactory with no significant anomalies. All power requirements of the SRM electrical system were satisfied. One minor anomaly occurred at SRM ignition when a bridgewire apparently shorted to structure after initiation and simultaneous shorting occurred in the ignitor safe and arm device.

System Description

The SRM electrical system consists of batteries, power transfer switches, distribution boxes, and associated harnessing. The batteries are 28 volts d.c. silver zinc, manually activated power supplies. The SRM electrical system block diagram is shown in figure V-3A-1.

The SRM aft instrumentation power system (AIPS) battery has a 2 ampere-hour capacity and is located within the aft skirt section of each SRM. It provides the power requirements of the instrumentation components of the motor.

The thrust vector control (TVC) battery has a 27 ampere-hour capacity and is located within the aft skirt section of each SRM. It provides the power requirements to drive the 24 electromechanical thrust vector control valves on each SRM.

The AIPS power is transferred to internal power during the automatic sequence at T - 31.7 seconds. The thrust vector control power transfer switch transfers TVC power from ground power to airborne battery power at T - 22 seconds. At T - 0 the SRM ignition commands and power are transmitted through the Stage II electrical system and the ISDS distribution box to the igniter safe-arm device which ignites the SRM igniter. During SRM burn, the Titan flight control system provides commands through the TVC distribution box to control the opening and closing of the electromechanical valves.

Power for the SRM staging functions is provided by the core vehicle transient power supply. This power ignites the forward and aft SRM separation ordnance and also provides power through the ISDS distribution box for ignition of the forward and aft staging motors.

The AIPS battery provides power through the instrumentation distribution box to transducers, signal conditioners, and other instrumentation system components.

Flight Performance

The SRM electrical system supplied the requirements of the dependent systems at normal voltage levels. All monitored system voltages were the same for both SRM's. The TVC bus voltage was 31.2 volts d.c. following transfer to internal power and was 32.0 volts d.c. at SRM separation. The AIPS bus voltage was 29.4 volts d.c. and the instrumentation regulated bus voltage was 10.0 volts d.c. throughout the entire SRM burn portion of flight.

The anomaly at SRM ignition was apparently caused by a short from an SRM igniter bridgewire positive to structure and simultaneous shorting from the transient return to readiness return within the igniter safe and arm device. As a result, the Titan core transfer current shunt indicated 15 amps for approximately 400 milliseconds. The current dropped to zero simultaneous with the removal of the current path when the SRM umbilicals were ejected. This anomaly had no adverse effect on any airborne system.

V-3B. Titan Core Electrical System

Summary

The core electrical system performance was satisfactory with no major anomalies. All power requirements of the core electrical system were satisfied. All voltage and current measurements indicated expected values. Some bridgewire shorting (after initiation) was observed at every ordnance event.

System Description

The Titan electrical system consists of batteries, motor driven switches, static inverter, relay assemblies, enable-disable circuits, squib firing circuits, diode and resistor assemblies, staging connectors and associated harnessing. The Titan core electrical system block diagram is depicted in figure V-3B-1.

The function of the electrical system is to provide and distribute power to various airborne systems. Power is provided to these systems from ground power supplies during checkout and readiness procedures. Power transfer switches transfer the systems to airborne power supplies during the automatic sequence. An electrical sequencing system consisting of relay assemblies converts command signals from the flight control programmers and/or guidance into events signals to perform flight operations.

The Titan electrical system has three airborne power systems and associated distribution systems. They are as follows:

Accessory Power System (APS)
Instrumentation Power System (IPS)
Transient Power System (TPS)

The batteries used in the airborne electrical system are 28 volts d.c. silver-zinc manually activated batteries. Both the APS and the IPS batteries have a 4-ampere-hour capacity while the TPS battery is rated at 25 ampere-hours.

The APS provides power for equipment essential to flight. The battery and associated power transfer switch are located on the Stage II forward compartment equipment truss. The battery provides power to the gyro heater on both Stages I and II, the flight controls static inverter and the sequencing system. The system also provides the power and signal requirements to the flight controls system, the liquid rocket engine interface and the Centaur vehicle interface.

The IPS provides power for the instrumentation components on the core vehicle. The IPS battery is located on the Stage II forward compartment equipment truss. The IPS shares the Stage II power transfer switch with the APS. In addition to its primary function, the IPS battery provides redundancy for the APS battery. The IPS battery is diode-coupled to the APS bus such that the IPS battery can support both the APS and IPS loads in the event of an APS battery failure.

The TPS battery and associated TPS power transfer switch are also located on the forward equipment truss. The TPS battery provides power for the ordnance bus through the TPS power transfer switch. Power transfer on this bus is accomplished in flight by discretes from the flight programmers approximately 75 seconds after lift-off. The TPS then provides power for all ordnance functions during the remainder of the flight. The ordnance functions and associated number of actuated bridgewires are as follows:

Stage I engine start	8
Stage 0/I separation	32
Stage 0 retrorockets	32
Stage II engine start	2
Stage I/II separation	48
CSS jettison (primary system)	8
Titan/Centaur separation	4
Stage II retrorockets	8

The static inverter converts 28 volts d.c. from the APS bus to 800 hertz for the flight controls computer, staging timer, TARS and rate gyros, and the acceleration sensors.

Squib firing circuits are solid state devices used to provide high current switching to ordnance devices.

Enable/disable circuits provide electronic switching capability for loads up to 1 ampere.

Two relay assemblies are mounted on the forward equipment truss. Each relay assembly contains 20 relays which are used as required to provide signal or power for the vehicle sequencing system.

Flight Performance

The Titan core electrical system supplied the requirements of the dependent system at normal voltage and current levels. The Titan core electrical system performance is summarized in table V-3B-1. The data presented is essentially steady state with no attempt to present transients. The TPS voltage and current measurements during ordnance events are difficult to present due to their short duration and low sampling rates.

The transfer current indicated 15 amperes at T - 0 as previously discussed under SRM electrical system performance. The transfer current indicated that during maximum loads on the APS bus, the IPS battery provided a small amount of load sharing.

The TPS bus voltage was 31.3 volts d.c. at TPS bus enable and rose to 33.0 volts d.c. at Titan/Centaur staging. This condition is normal due to increasing battery temperature since the battery internal heater and the TPS bus are enabled concurrently.

Following the Titan/Centaur staging event, the TPS current measurement exhibited an offset of approximately 9 percent (54 amps). This condition can be attributed to ordnance bridgewire shorting to vehicle structure. In this case one of the many parallel return paths to TPS negative is through the TPS current signal conditioner resistance network where allowable resistor tolerances would permit a worst case offset of as much as 29 percent. This condition was also in evidence on the TPS current measurement during the anomaly at T - 0 when a bridgewire shorted to vehicle structure after initiation.

V-3C. Titan Flight Termination System

Summary

All Titan Flight Termination System (FTS) measurements indicated proper system operation. Range Safety Command battery voltages were steady throughout the flight. The receiver AGC voltages were nominal throughout the flight. Safing commands to the Inadvertent Separation Destruct System (ISDS) were issued by the flight programmer in the proper sequence. The Range Safety Officer's (RSO) command to destroy the Centaur stage at approximately T + 750 seconds had no effect on the Titan since the Stage II Destruct Initiators are "safed" at Stage II shutdown.

System Description

The flight termination system is comprised of two safety systems - the command control system and the inadvertent separation destruct system. The command control system functions to shutdown the Stages I and II engines and to destroy the entire booster vehicle upon command. The inadvertent separation destruct system functions to automatically destroy Stage 0 and/or Stage I in case of a vehicle break-up or premature separation. A simplified block diagram of the Flight Termination System is shown in figure V-3C-1.

Command Shutdown and Destruct System (CSDS). - The Command Shutdown and Destruct System receives and responds to ground originated commands from the RSO. These commands may either be engine shutdown, or engine shutdown together with vehicle destruct. The command system consists of an omnidirectional antenna system, two command receivers, engine shutdown circuitry, destruct circuitry, and redundant command receiver power supply systems. Except for elements of the antenna system, the command destruct system is independently redundant.

Command control antennas 1 and 2 receive the signal transmitted from the ground. The 4-port junction distributes the two antenna inputs equally to command receiver sets 1 and 2. The command receiver sets then independently interpret the input and provide an output to cause the appropriate flight terminating action.

When the ground originated command calls for engine shutdown alone, the command receivers each cause a current to flow through Stages I and II engine shutdown solenoids via diode assemblies that maintain command receivers electrical isolation. When the command is for vehicle destruct, shutdown occurs as above, and power is routed to Stages I and II destruct safe/arm devices and to SRM destruct circuitry via current limiting resistor assemblies.

Inadvertent Separation Destruct System (ISDS). - Should physical separation occur between Stages 0/I and I/II before normal staging for any

reason, the ISDS will cause rupture of the propellant tanks of Stage 0/I, and possibly, of Stage II. Two squib firing circuits (SFC) redundantly route power through a resistor assembly to the Stage 0 and/or Stage I destruct safe/arm devices upon inadvertent separation.

During normal staging, the flight programmer provides a disable signal which prevents the ISDS from initiating destruct. The programmer also "safes" the safe/arm device on initiation of staging.

Instrumentation of the Flight Termination System. - To monitor the performance of the FTS while in flight the following measurements are telemetered: Automatic Gain Control (AGC), voltage and engine shutdown (ESD) signal of each CRS. Also the ESD signals, originated by either the flight programmer or a CRS, are monitored in Compartment 1C for Stage I ESD and in Compartment 2C for Stage II ESD by telemetry. The SRM telemetry system monitors the destruct commands from each receiver as well as the ISDS disable commands from the programmer. The voltage of each of the two command receiver batteries located in Stage II are also telemetered in flight.

Flight Termination System Performance

The Titan flight termination system performance was nominal throughout the flight. Monitoring of the receiver AGC voltages by telemetry indicated that sufficient signal was present throughout the powered flight to assure that any destruct or engine shutdown commands would have been properly executed. An engine shutdown and a destruct command was issued by the Range Safety Offices at approximately T + 750 seconds to destroy the Centaur vehicle. These commands had no effect on the Titan stage since the Stage II Destruct Initiators were "safed" at Stage II separation. A list of commands against time and station switching times as issued by the Range are given in tables V-3C-1 and V-3C-2.

The Range Safety command battery voltages were 32.2 volts d.c. at liftoff and remained steady throughout the flight. The commands from the flight programmer to safe the Stage I and the two SRM Inadvertent Separation Destruct Systems (ISDS) were issued at their expected times. The flight programmer also issued the command to safe the Destruct Initiator on Stage II prior to the Titan/Centaur separation.

V-3D. Titan Instrumentation and Telemetry System

Summary

All 197 Titan vehicle measurements yielded acceptable qualitative and quantitative data. Two measurements did exhibit minor problems during the flight. The Stage II longitudinal acceleration measurement indicated a stiction problem and the Stage II hydraulic reservoir level measurement had some noise evident during the flight.

Adequate telemetry coverage of the Titan vehicle was provided by the KSC and AFETR ground stations from liftoff to beyond Titan/Centaur separation. Data dropout, due to plume attenuation occurred, as expected, for 1.5 seconds at Stage 0 separation.

System Description

The airborne instrumentation and telemetry system consists of transducers, signal conditioners, the remote multiplexer instrumentation system (RMIS), the transmitter and the antenna. The RMIS consists of the remote multiplexer units (RMU's) and a converter unit (CU). A simplified block diagram of system components is shown in figure V-3D-1. The system collects, multiplexes, encodes, and transmits analog and 28 volts d.c. bilevel measurements made on the airborne systems during checkout, launch, and flight of the vehicle.

Test data inputs to the instrumentation system originate from sensors monitoring physical parameters and electrical signals from various vehicle subsystems. The sensors convert mechanical conditions, liquid levels, gas and liquid pressure, temperature, and acceleration to proportional electrical signals. All data signals are either analog or bilevel d.c. Signals not compatible with the required input to the encoding equipment are routed to signal conditioners.

The data signals are sampled and encoded by the RMIS (fig. V-3D-2), which is comprised of eight remote multiplexer units and a single converter unit. The CU is capable of accepting up to 80 bilevel inputs in addition to the analog RMU outputs. Up to 32 analog signals having a range of 0 to 40 millivolt d.c. can be accepted by each RMU. The RMU samples, amplifies, and holds the assigned low-level input signals to provide a serial pulse amplitude modulated (PAM) output train to the converter unit. The output of each RMU is connected to a pair of redundant data lines that feed the multiplexed PAM data to the converter. Logic control signals are addressed and transmitted from the converter programmer to each of the RMU's on a pair of redundant address lines. Each RMU has a unique address. The converter performs analog-to-digital conversion of the PAM input signal and provides a serial PCM data train output to a S-band PCM/FM transmitter.

The transmitter accepts the RMIS serial pulse train from the converter and generates a frequency modulated RF signal for transmission to ground receiving stations. The RF output of the transmitter is routed by coaxial cable to a single broad-beam antenna.

Flight Performance

A total of 197 measurements were telemetered by the Titan Remote Multiplexed Instrumentation System (RMIS). A summary of the types of measurements against the systems in which they were monitored is given in table V-3D-1. Of these 197 measurements all but two performed without any anomalies. Measurement 2325, Stage II longitudinal acceleration, did not respond to small levels of vibration indicating that some stiction was present within the accelerometer. Measurement 1227, Stage II hydraulic reservoir level, exhibited noise spikes in flight. The measurement had exhibited the same type of noise during ground systems testing. The problem has been attributed to the resistance potentiometer within the transducer. Although anomalies did occur with these two transducers useful data was obtained from both measurements throughout the flight.

Adequate telemetry coverage of the Titan vehicle was provided from liftoff to beyond Titan/Centaur separation. A summary of the predicted data coverage against actual data coverage of Titan telemetry link is given in table V-3D-2.

There was a data dropout at 13:50:08 for a period of approximately 1.5 seconds. This dropout was expected and is due to plume attenuation at the time of Stage 0 separation.

TABLE V-3B-1 TITAN CORE VEHICLE ELECTRICAL SYSTEM PERFORMANCE SUMMARY

	POWER ON INTERNAL	LIFTOFF	ENABLE TPS	STAGE I START	STG. 0/I SEP.	STG. I/II SEP.	CSS JETT.	STG. II S/D	T/C STAGING
	T-31.7	T-0	T+75	T+114.6	T+126.6	T+263.9	T+273.1	T+469.6	T+475.3
APS VOLTAGE	27.8	28.6	28.3	27.5	27.9	27.3	28.3	28.2	27.9
APS CURRENT	8.2	8.2	8.8	10.2	10.5	13.1	7.5	8.5	9.6
IPS VOLTAGE	28.6	28.9	28.6	28.5	28.5	28.3	28.5	28.6	28.6
IPS CURRENT	10.7	10.6	10.7	10.7	10.7	10.7	10.0	10.0	10.0
TRANSFER CURRENT	0	15.1	0.3	0.3	0.2	0.5	0.1	0.1	0.1
TPS VOLTAGE	0	0	31.3	31.5	32.1	32.5	32.5	33.0	33.0

TABLE V-3c-1 FUNCTIONS VERSUS TIME

FUNCTIONS	TIME
Engine Shutdown	14:00:25 Z
Destruct	14:00:30.0 Z
Functions Off	14:00:46.5 Z

TABLE V-3C-2 STATION SWITCHING TIMES

STATION	CARRIER ON	CARRIER OFF
Mainland (Sta. 1)	13:15:34 Z	13:50:42.52 Z
Grand Bahama Is. (Sta. 3)	13:50:42.5 Z	13:51:03 Z
Mainland	13:51:03 Z	13:51:23 Z
G.B.I.	13:51:21.5 Z	13:55:40 Z
Antigua (Sta. 91)	13:55:39.5 Z	14:00:57.5 Z

TABLE V-3D-1 TITAN BOOSTER MEASUREMENTS SUMMARY

SYSTEM	TYPE OF MEASUREMENT ACCELERATION	VOLTAGE	CURRENT	PRESSURE	TEMPERATURE	DISPLACEMENT	RATES	DISCRETES	TOTAL
AIRFRAME	7			10				2	19
RANGE SAFETY		3						6	9
ELECTRICAL		15	10						25
HYDRAULICS				8		2			10
PROPULSION				29	8			4	41
FLIGHT CONTROL		32				33	11	10	86
TELEMETRY		6			1				7
TOTAL	7	56	10	47	9	35	11	22	197

TABLE V-3D-2

SUMMARY OF PREDICTED DATA COVERAGE
VERSUS ACTUAL DATA COVERAGE
TITAN 2287.5 MHz LINK

STATION	PREDICTED		ACTUAL	
	AOS	LOS	AOS	LOS
CIF (Mainland)	Turn On	450 Sec	Turn On	489 Sec
GBI (Grand Bahama)	76 Sec	487 Sec	40 Sec	540 Sec
GTK (Grand Turk)	279 Sec	608 Sec	281 Sec	664 Sec

AOS - Acquisition of Signal

LOS - Loss of Signal

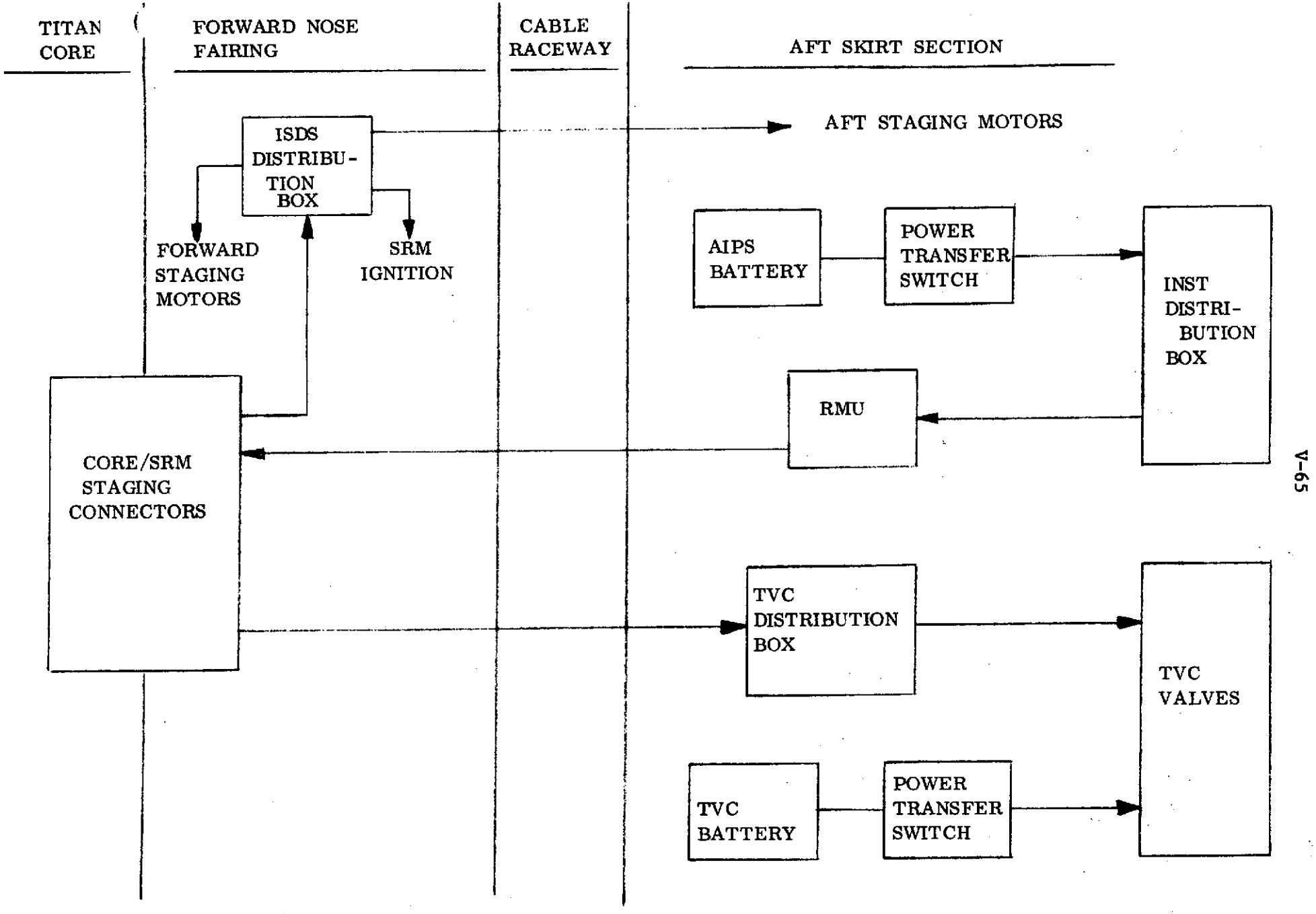

FIGURE V-3A-1 SOLID ROCKET MOTOR ELECTRICAL SYSTEM

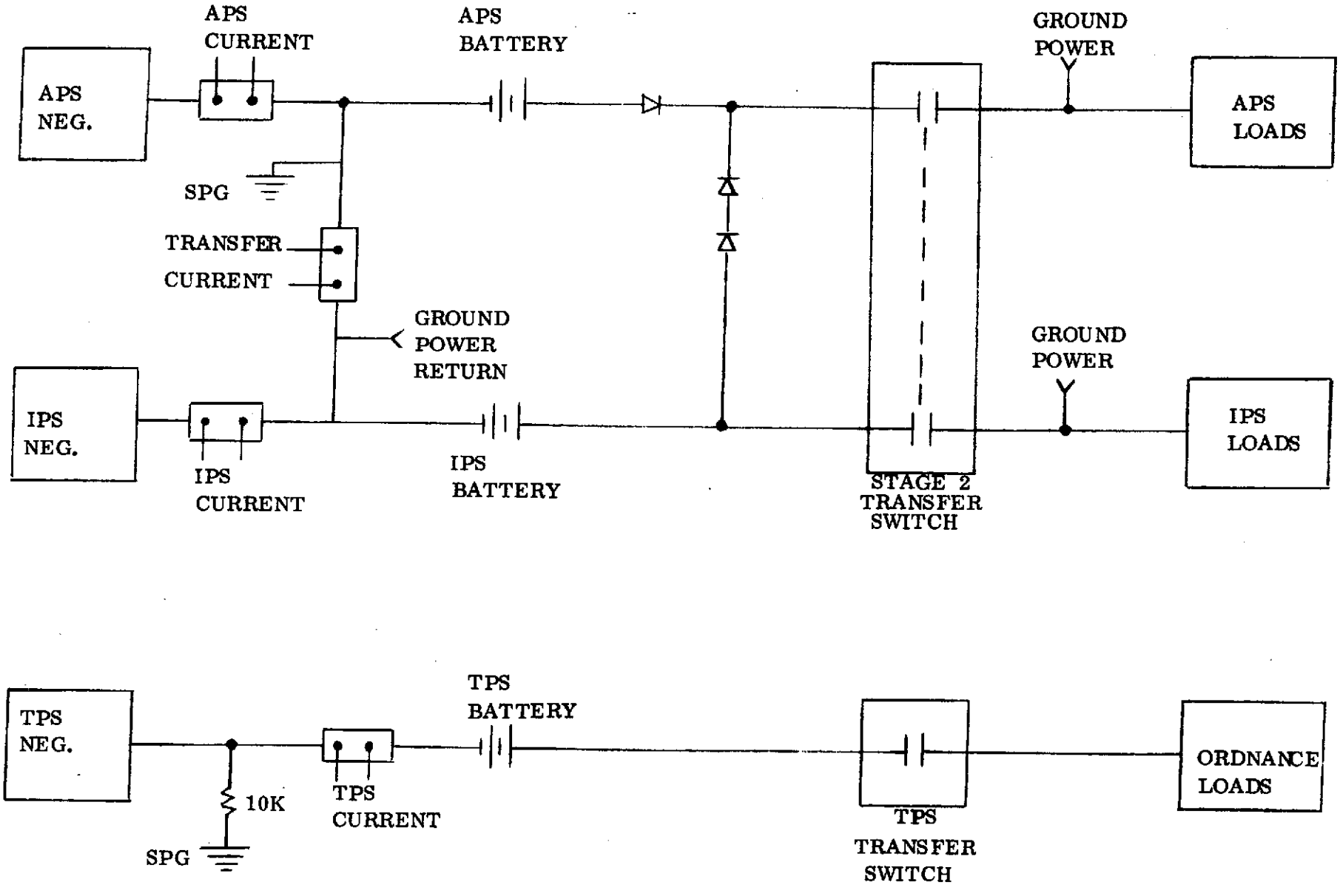

FIGURE V-3B-1 TITAN CORE ELECTRICAL SYSTEM

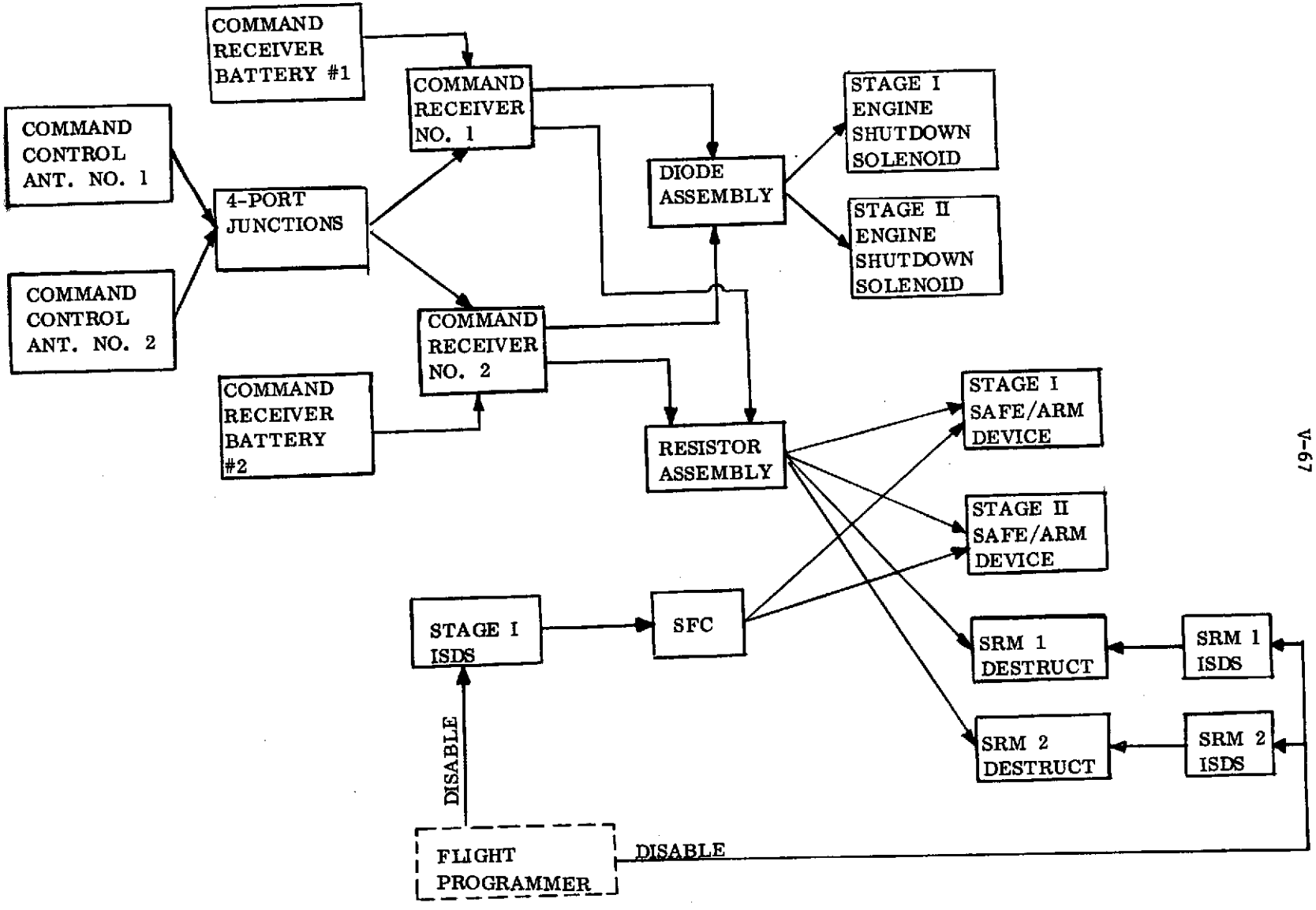

FIGURE V-3C-1 FLIGHT TERMINATION SYSTEM BLOCK DIAGRAM

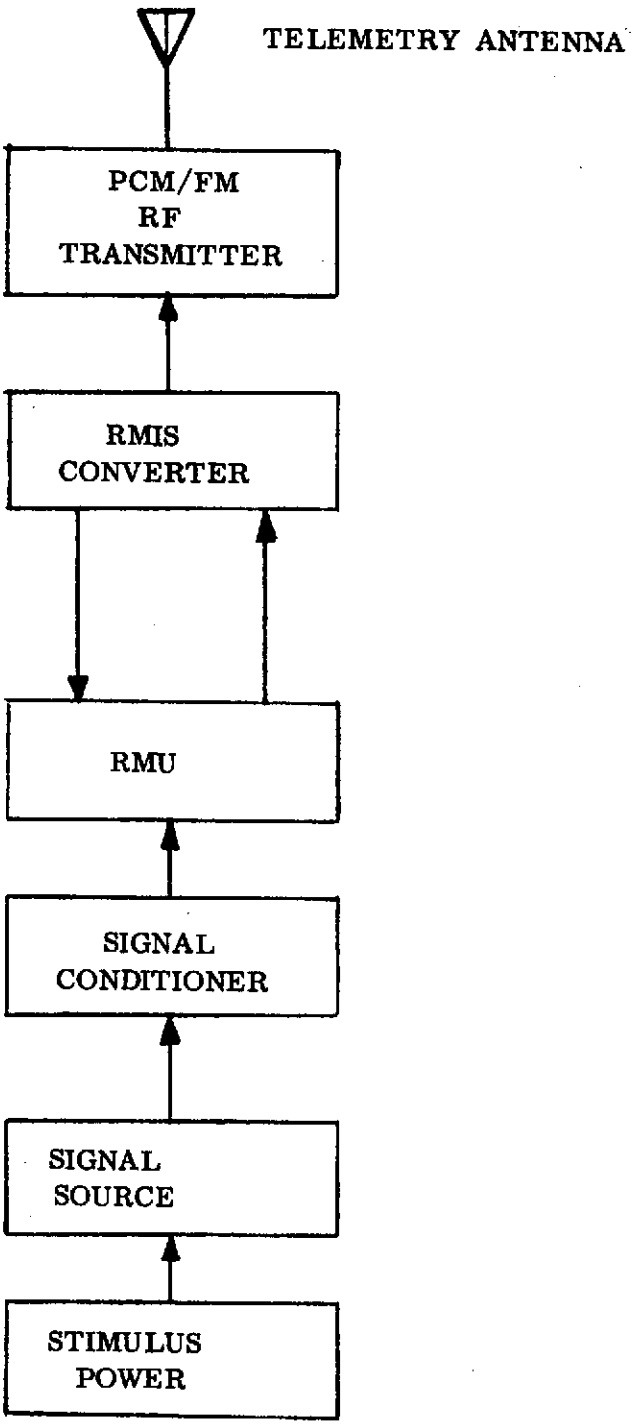

FIGURE V-3D-1 SIMPLIFIED BLOCK DIAGRAM, AIRBORNE INSTRUMENTATION SYSTEM

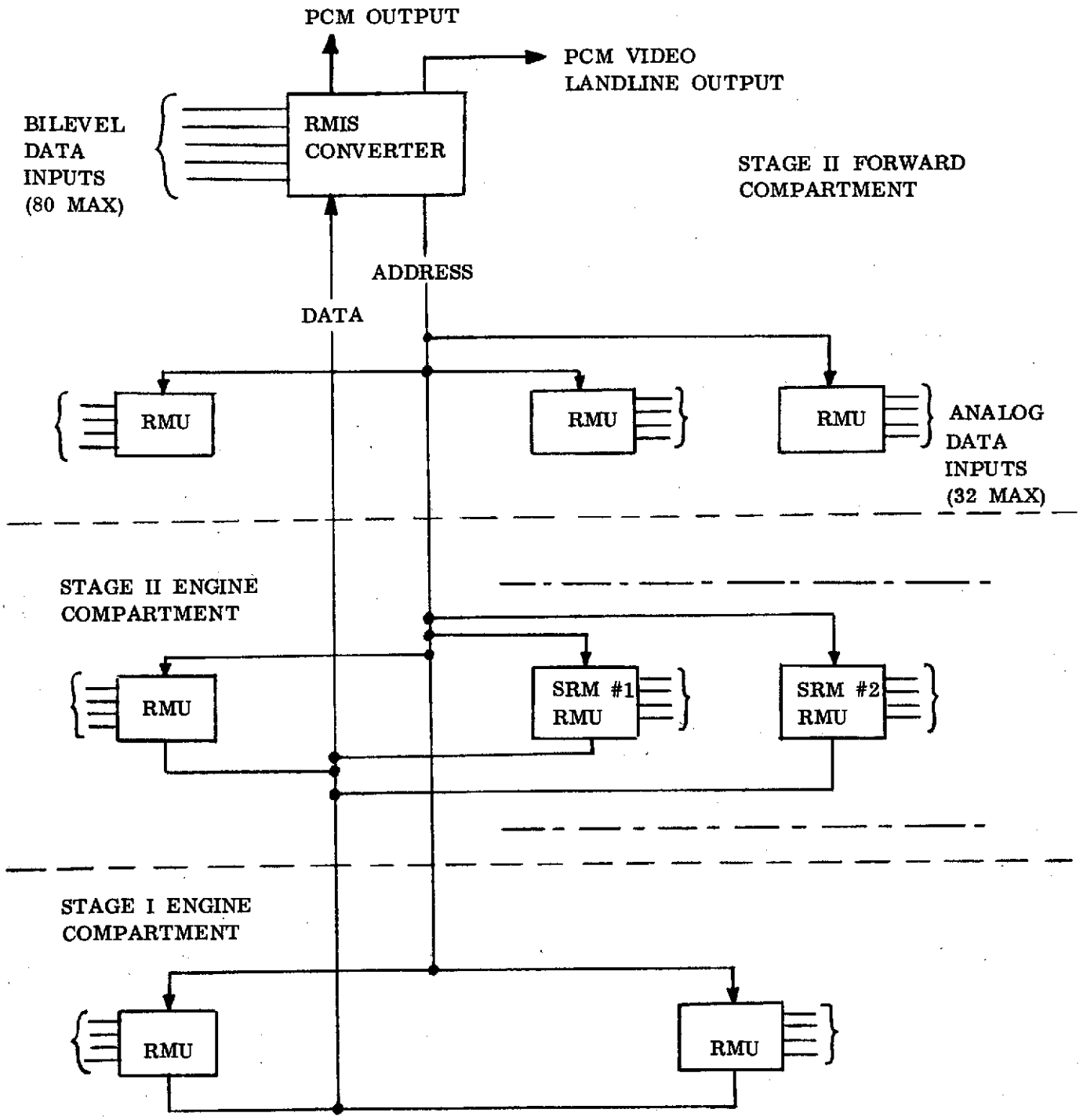

FIGURE V-3D-2 TITAN IIIE RMIS BLOCK SYSTEM DIAGRAM

VI. CENTAUR STANDARD SHROUD AND BOLT-ON HARDWARE

VI-1. CENTAUR STANDARD SHROUD DISCONNECTS AND DOOR CLOSURES

by T. L. Seeholzer

Summary

All Centaur Standard Shroud (CSS) disconnects and door closures occurred satisfactorily on the TC-1 flight.

System Description

There are two groups of disconnects and door closures on the Centaur Standard Shroud (CSS). The first group includes those that occur prior to vehicle liftoff. The second group are those that occur concurrent with vehicle liftoff.

The first group consists of the T - 4 aft and the T - 4 forward electrical and helium purge umbilicals shown in figures VI-1-1, VI-1-2, and VI-1-3. Umbilical disconnect and door closings are accomplished by lanyards that are retracted by hydraulic cylinders. The forward T - 4 door is closed by torsion springs and door weights and incorporates two secondary and two primary latches as shown in figure VI-1-4. The T - 4 aft umbilical door (fig. VI-1-5) is closed by a door closing lanyard and incorporates two primary and one secondary latch.

The second group of disconnects that occur at vehicle liftoff (T - 0) are:

(1) Payload air conditioning. - Disconnect of the payload air conditioning duct was accomplished by deflating the connecting seal and retracting the duct by a lanyard system as shown in figure VI-1-6. The door is closed by torsion springs. Both outer and inner doors are incorporated for redundancy.

(2) RTG cooling and gas lines. - Disconnect is accomplished by a fly-a-way lanyard pull system. The disconnect incorporates three shear pins and a rotating door to seal the opening as shown in figure VI-1-7.

(3) Encapsulation seal. - This seal, which isolates the payload from the Centaur vehicle, is released at T - 0 by means of a fly-a-way lanyard retract system. Two lanyard release systems are incorporated for

redundancy (reference figs. VI-1-8 and VI-1-9).

(4) Equipment module air conditioning and line of sight. - Disconnect of the equipment module air conditioning duct is similar to the payload air conditioning disconnect function. Door closure is accomplished by torsion springs and door weight. The door incorporates one primary and one secondary latch as shown in figures VI-1-10 and VI-1-11.

(5) Forward electrical umbilical. - Identical to the T - 4 forward umbilical (reference figs. VI-1-2 and VI-1-4)

(6) LH_2 vent fin disconnect. - Disconnect of this duct is accomplished by a fly-a-way lanyard system (reference fig. VI-1-12).

(7) LH_2 and LO_2 fill and drain valve disconnects and doors. - Disconnect of the valve is accomplished by a lanyard system which disconnects the valve by fracturing frangible bolts. Doors are closed by lanyards and incorporate two primary and one secondary latches as shown in figures VI-I-13 and VI-1-14.

(8) Interstage adapter air conditioning. - Disconnect and door closing are similar to the payload air conditioning (reference fig. VI-1-6).

System Performance

Movie and television coverage verified proper disconnect of the T - 4 forward umbilicals and the closing of these CSS doors on the primary latches. Microswitches mounted on the T - 4 aft door verified that the door closed on the primary latches following umbilical disconnect.

All functions of the T - 0 disconnects and doors were verified by movie and television camera data. The T - 4 and T - 0 forward door latches had been modified prior to flight to improve reliability of primary latching.

Following this modification, a reference line was painted on the primary latch housing and a dot was painted on the pawl retaining pin to assist in determining primary door latching. Enlargements of movie frames covering these doors verified primary latching.

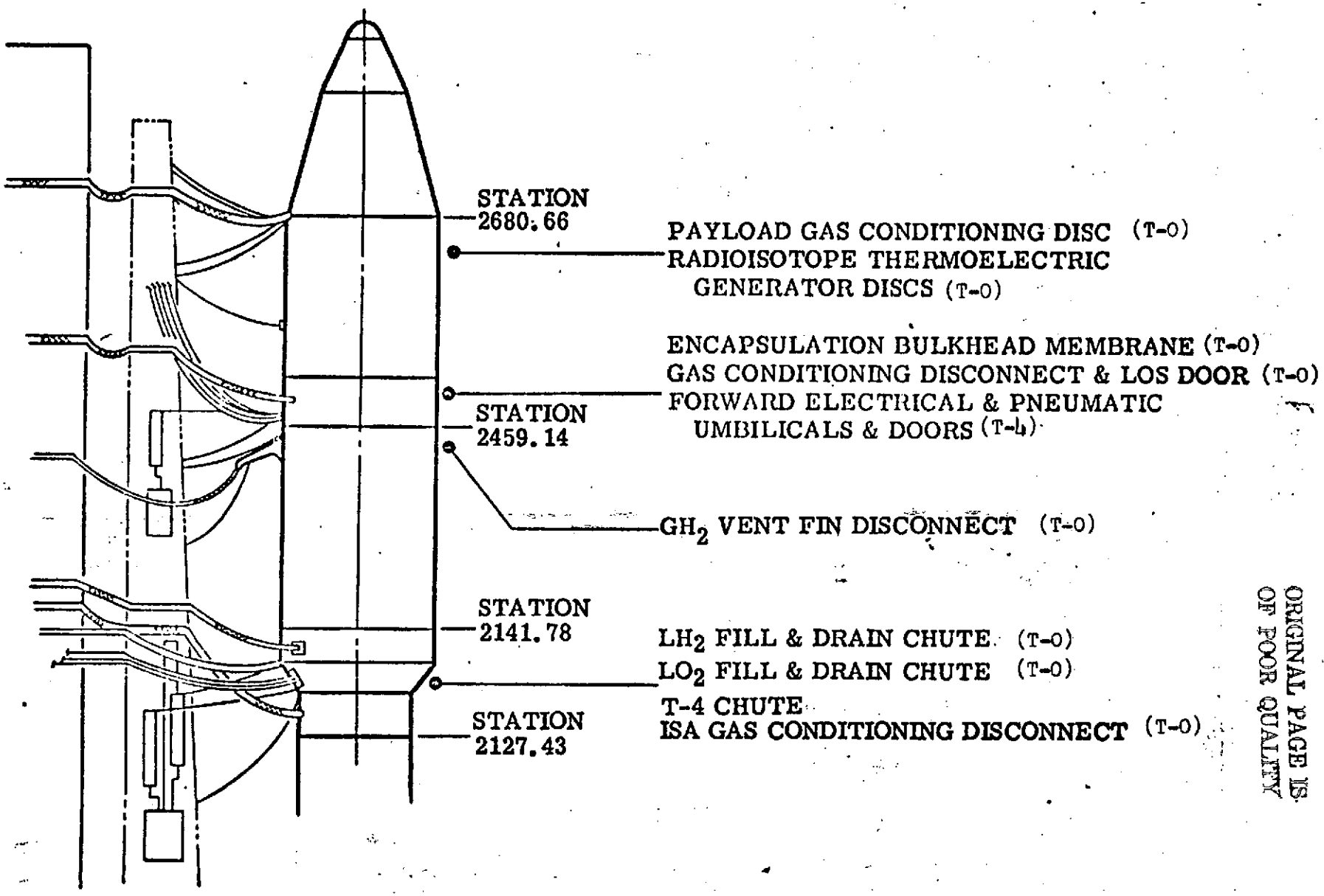

FIGURE VI-1-1 CENTAUR STANDARD SHROUD DISCONNECTS AND DOOR CLOSURES

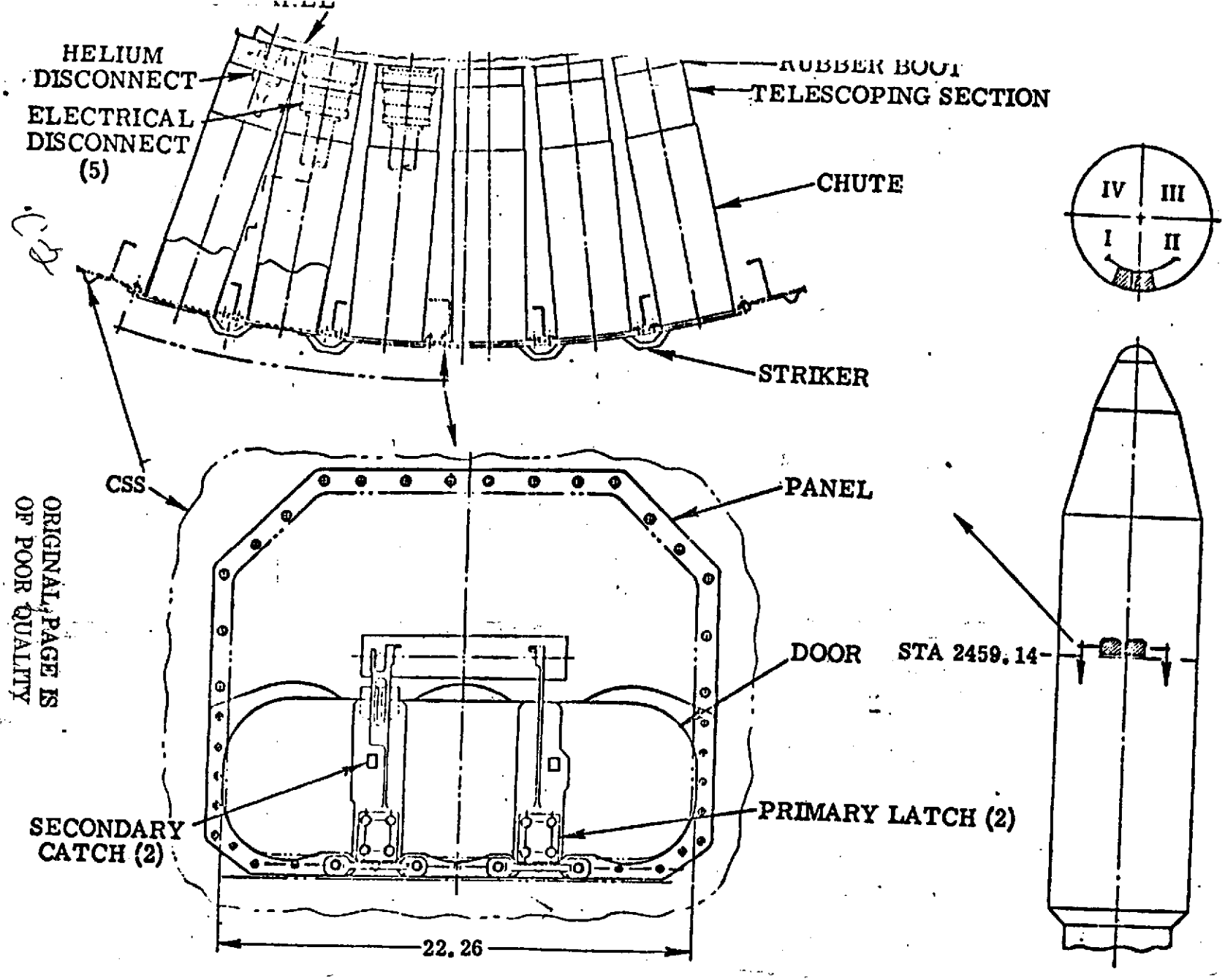

FIGURE VI-1-2 T-4 FORWARD UMBILICAL CHUTES AND DOOR

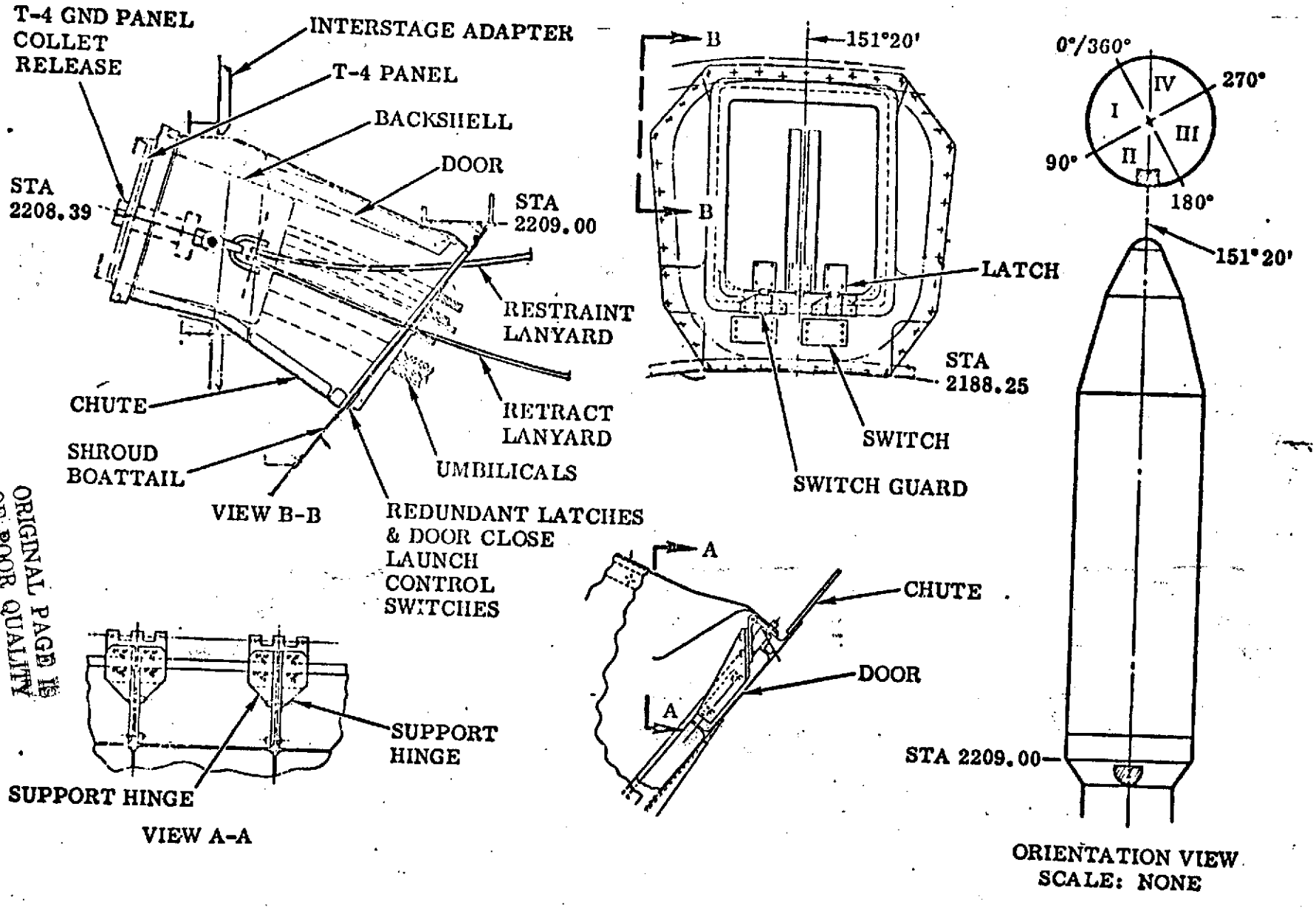

FIGURE VI-1-3 T-4 AFT PANEL AND DOOR

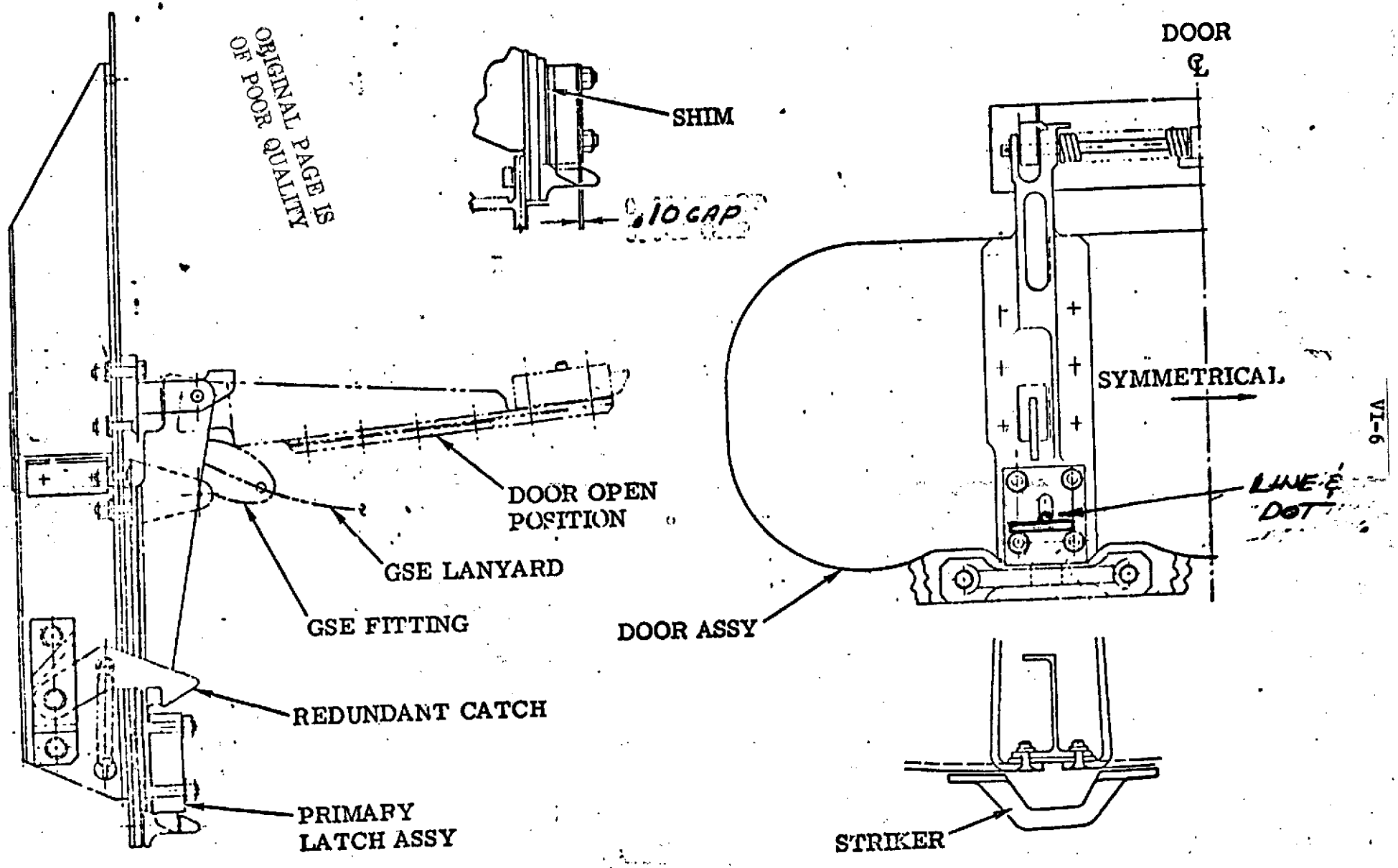

FIGURE VI-1-4 FORWARD DOOR LATCHES

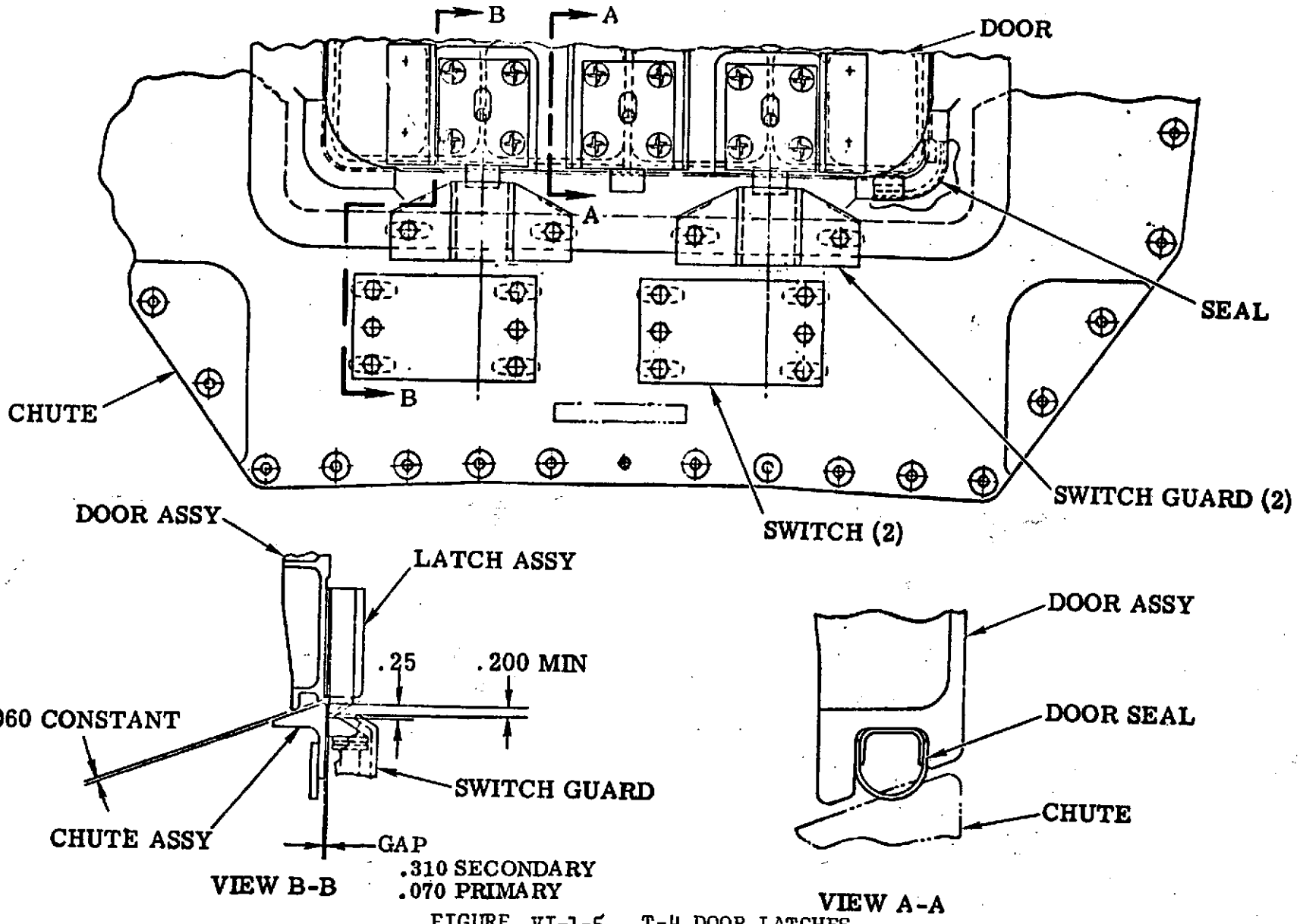

FIGURE VI-1-5 T-4 DOOR LATCHES

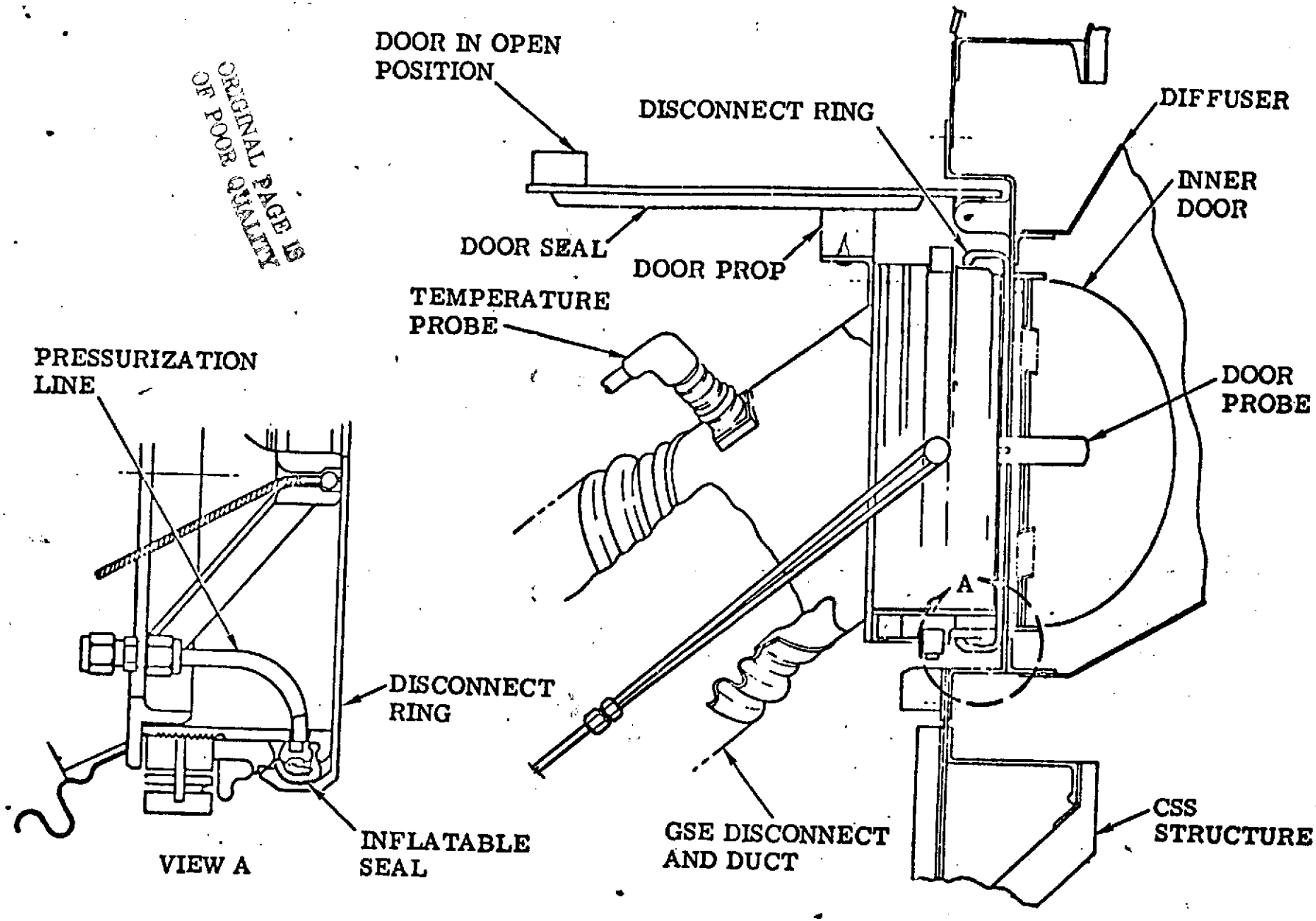

FIGURE VI-1-6 PAYLOAD AIR CONDITIONING DISCONNECT

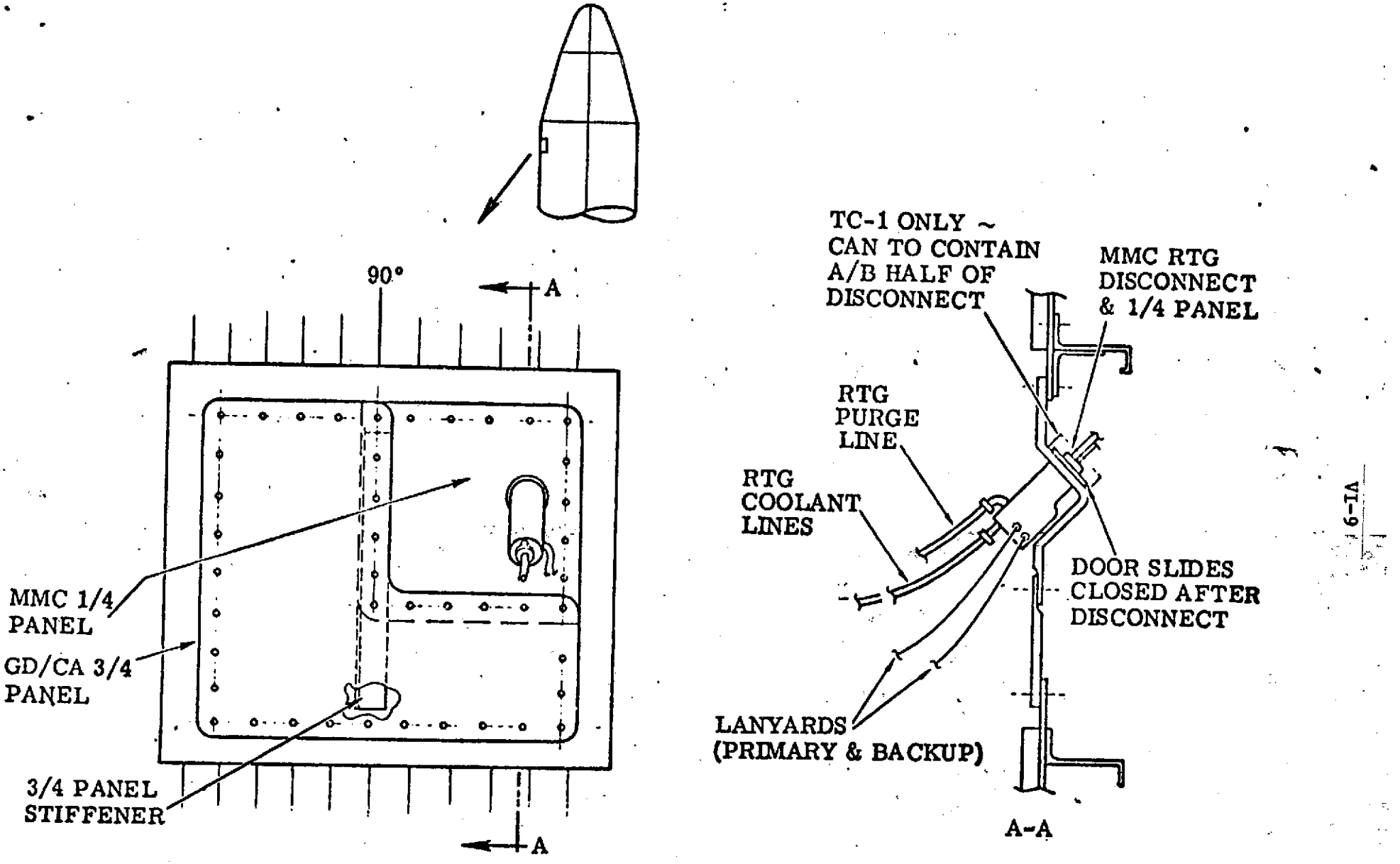

FIGURE VI-1-7 SHROUD RTG DISCONNECT

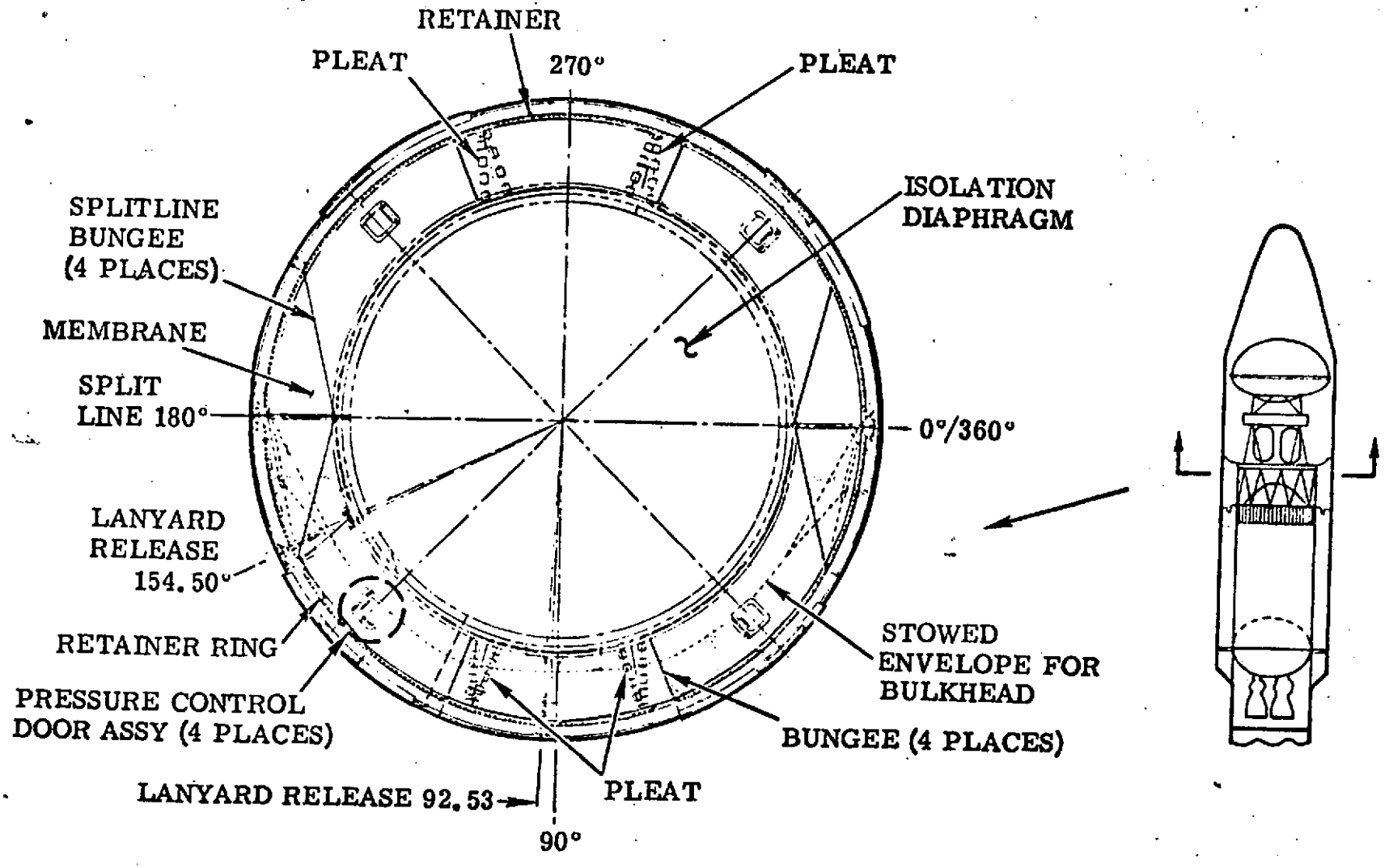

FIGURE VI-1-8 ENCAPSULATION SEAL

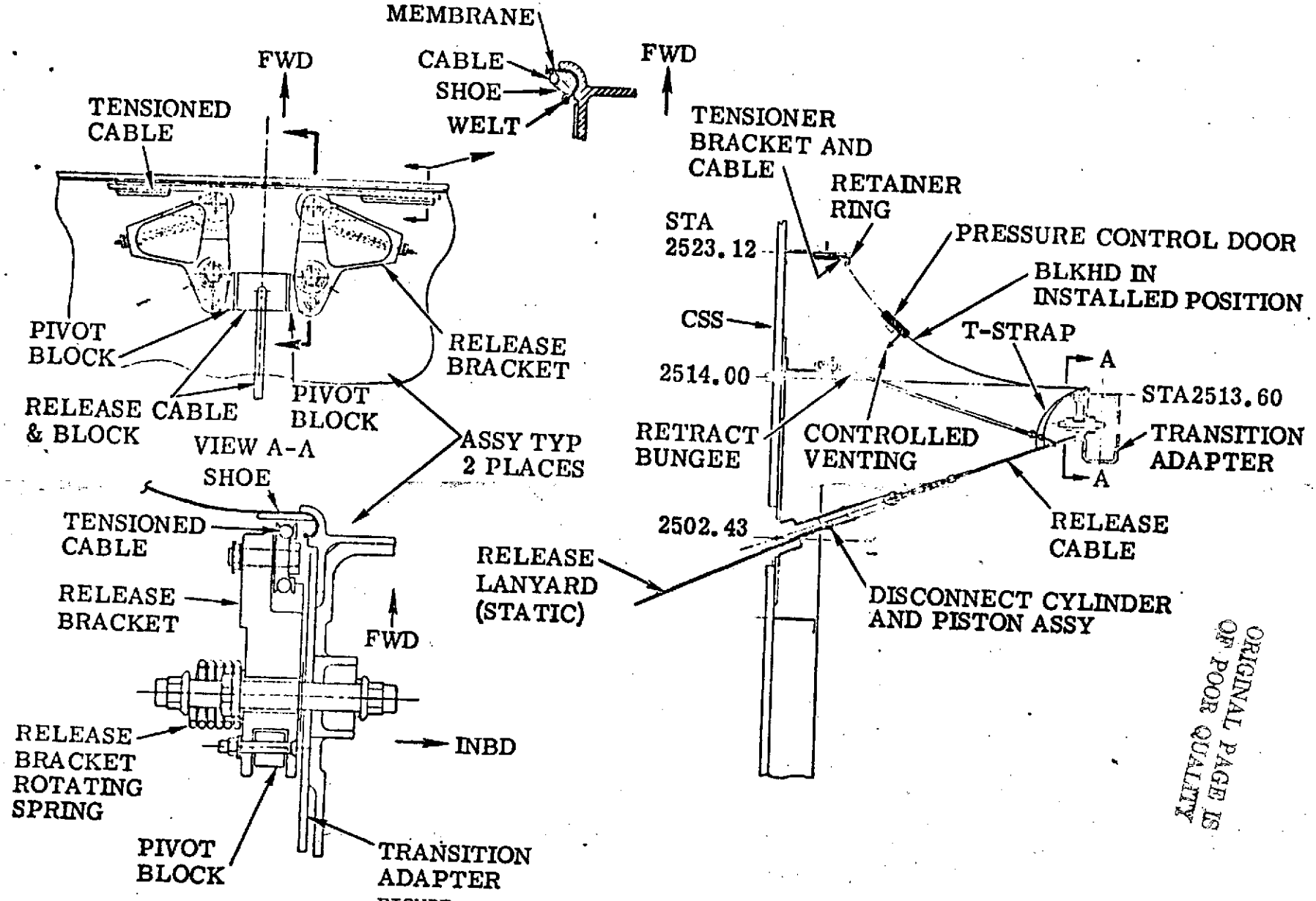

FIGURE VI-1-9 ENCAPSULATION SEAL DETAILS

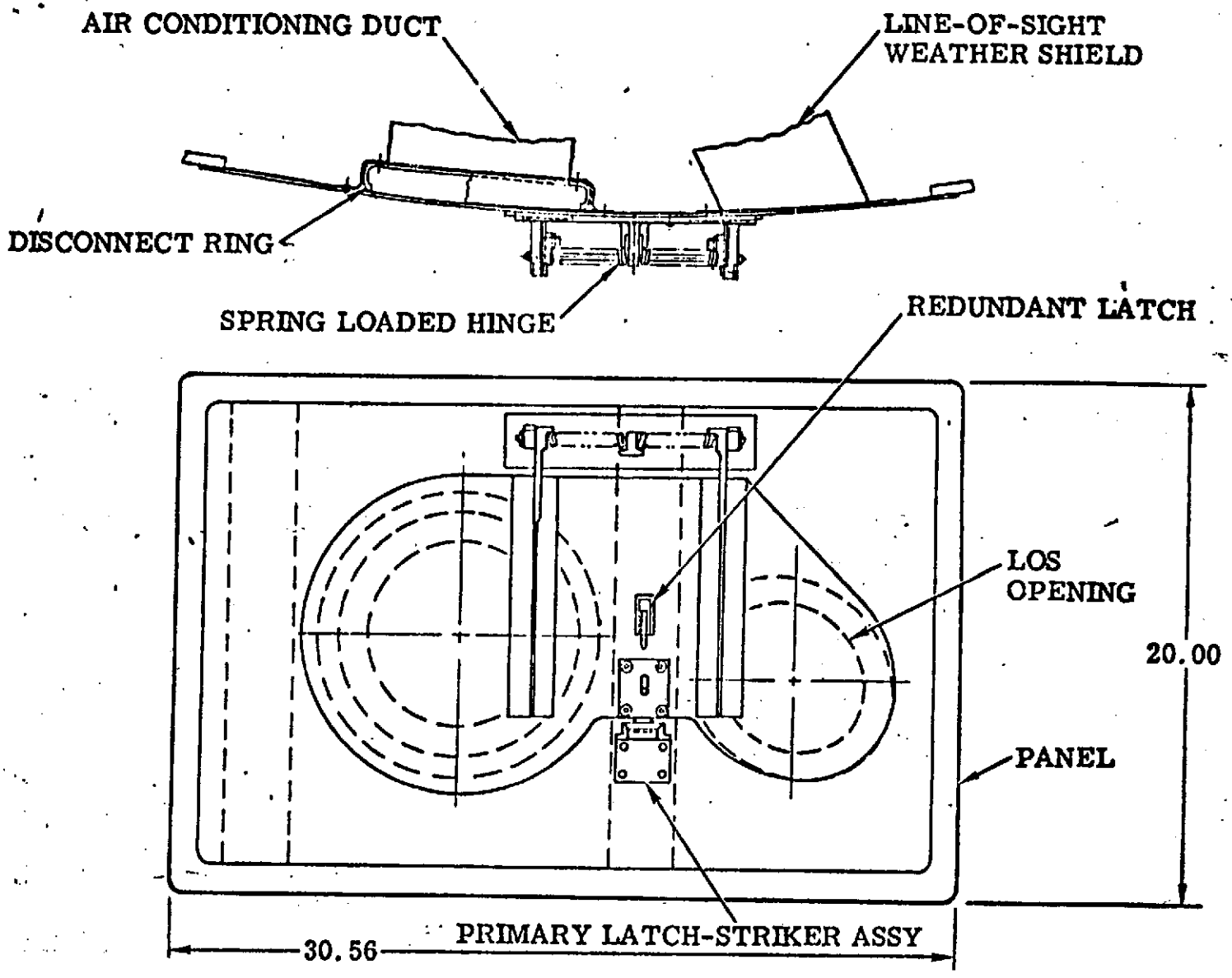

FIGURE VI-1-10 AIR CONDITIONING LINE OF SIGHT DOOR

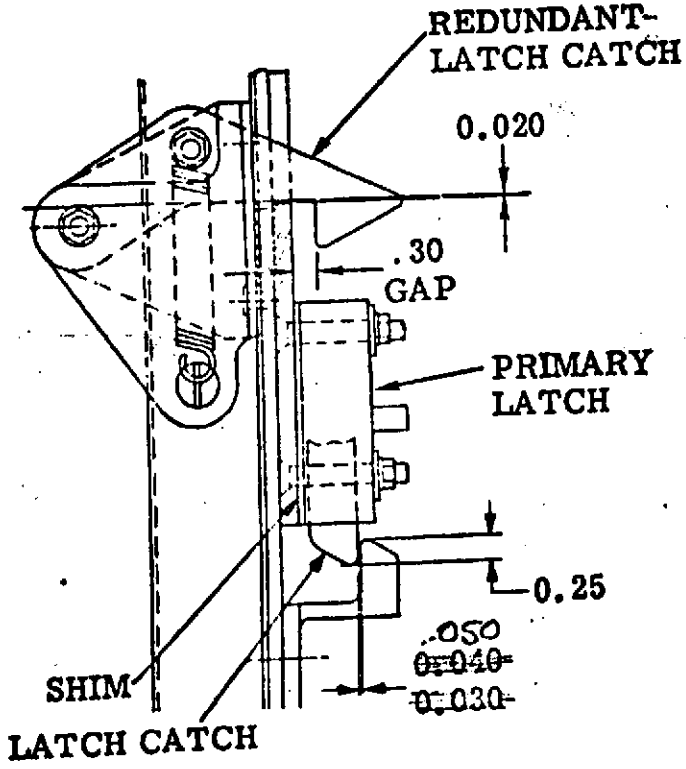

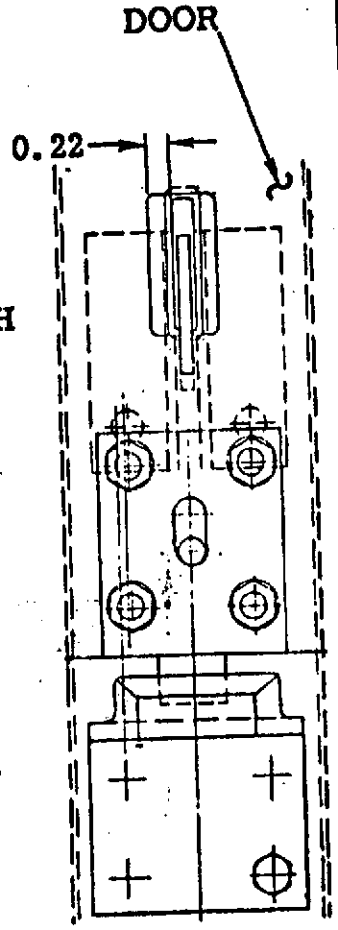

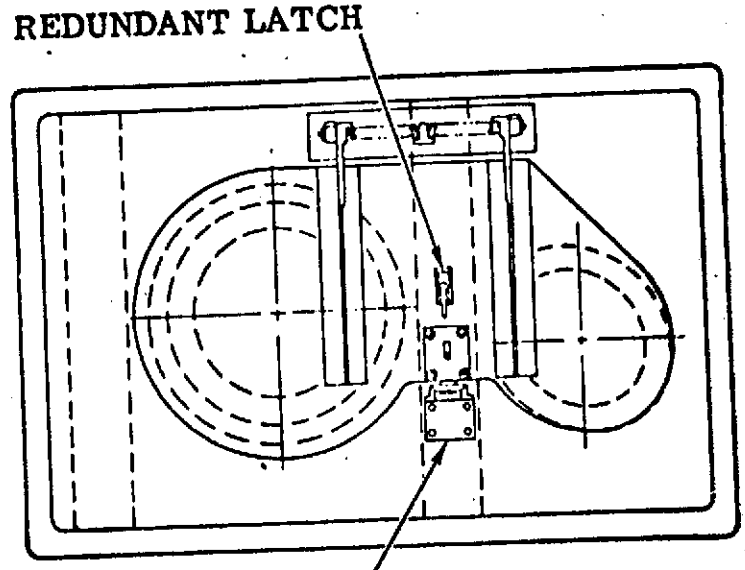

AFTER DOOR IS SEATED, SHIM AS REQUIRED TO OBTAIN SPECIFIED GAP BETWEEN LATCH CATCH AND STRIKER

FIGURE VI-1-11 AIR CONDITIONING LINE OF SIGHT DOOR LATCHES

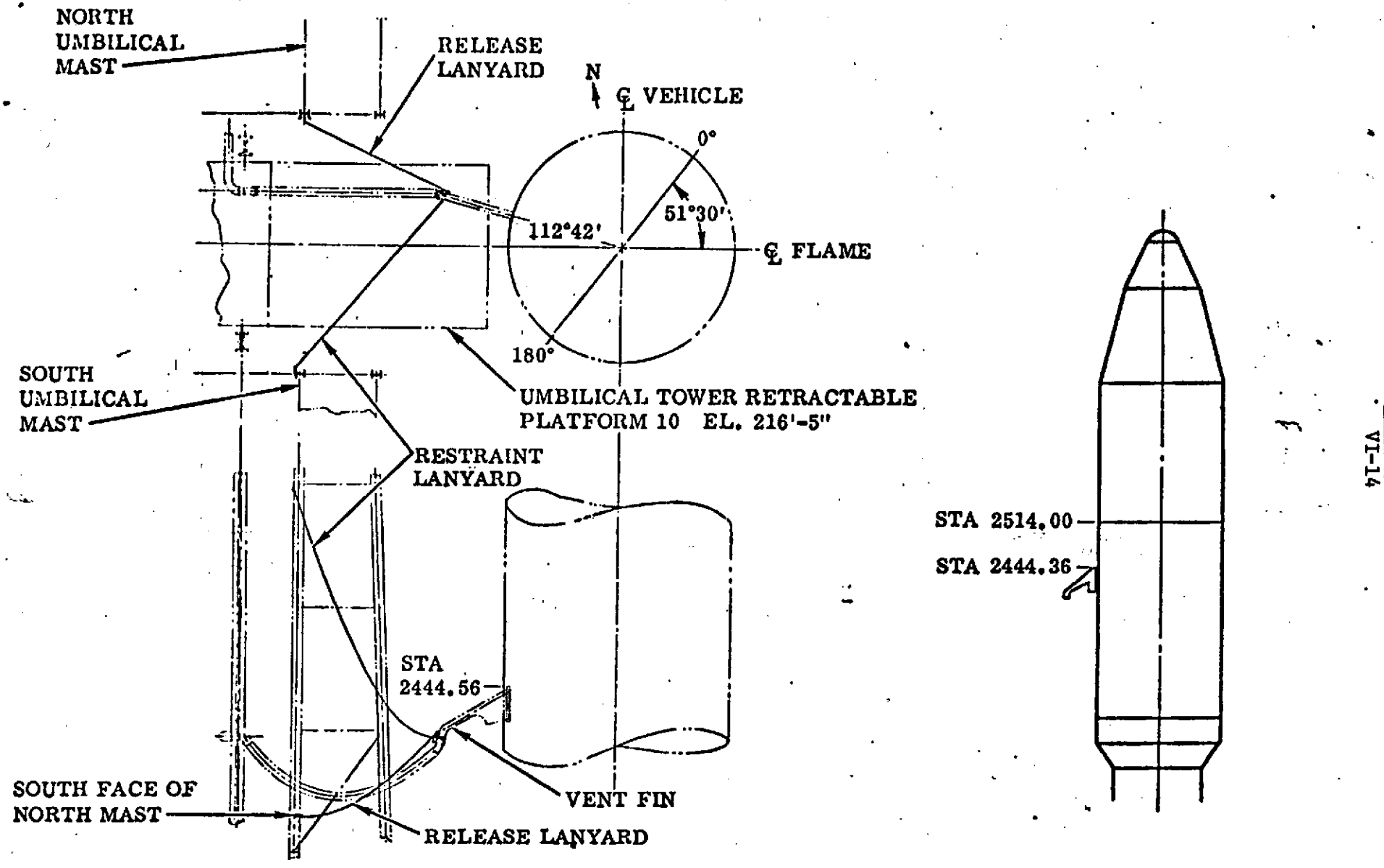

FIGURE VI-1-12 VENT FIN DISCONNECT

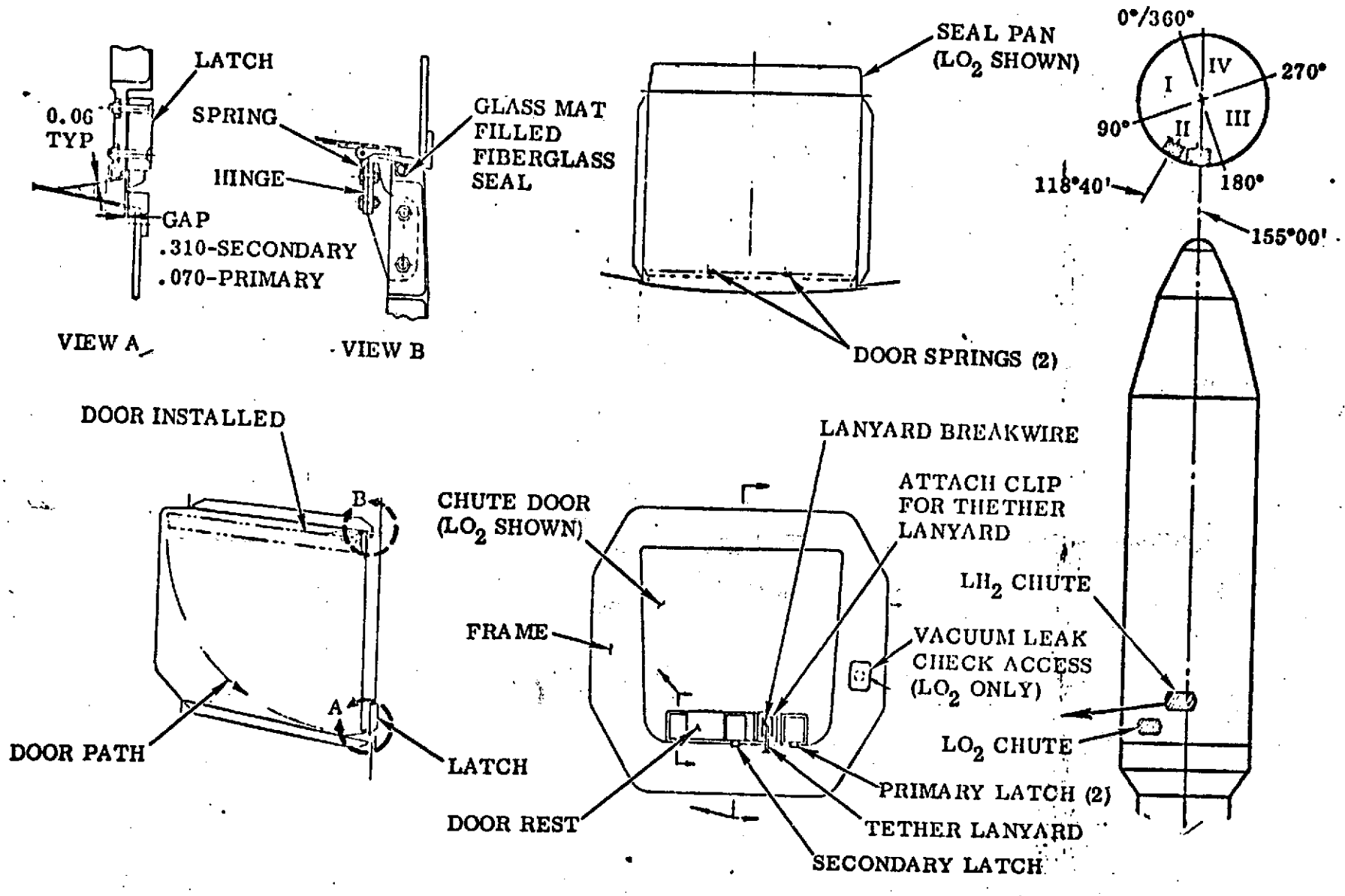

FIGURE VI-1-13 LH_2 AND LOX FILL AND DRAIN VALVE CHUTE AND DOOR

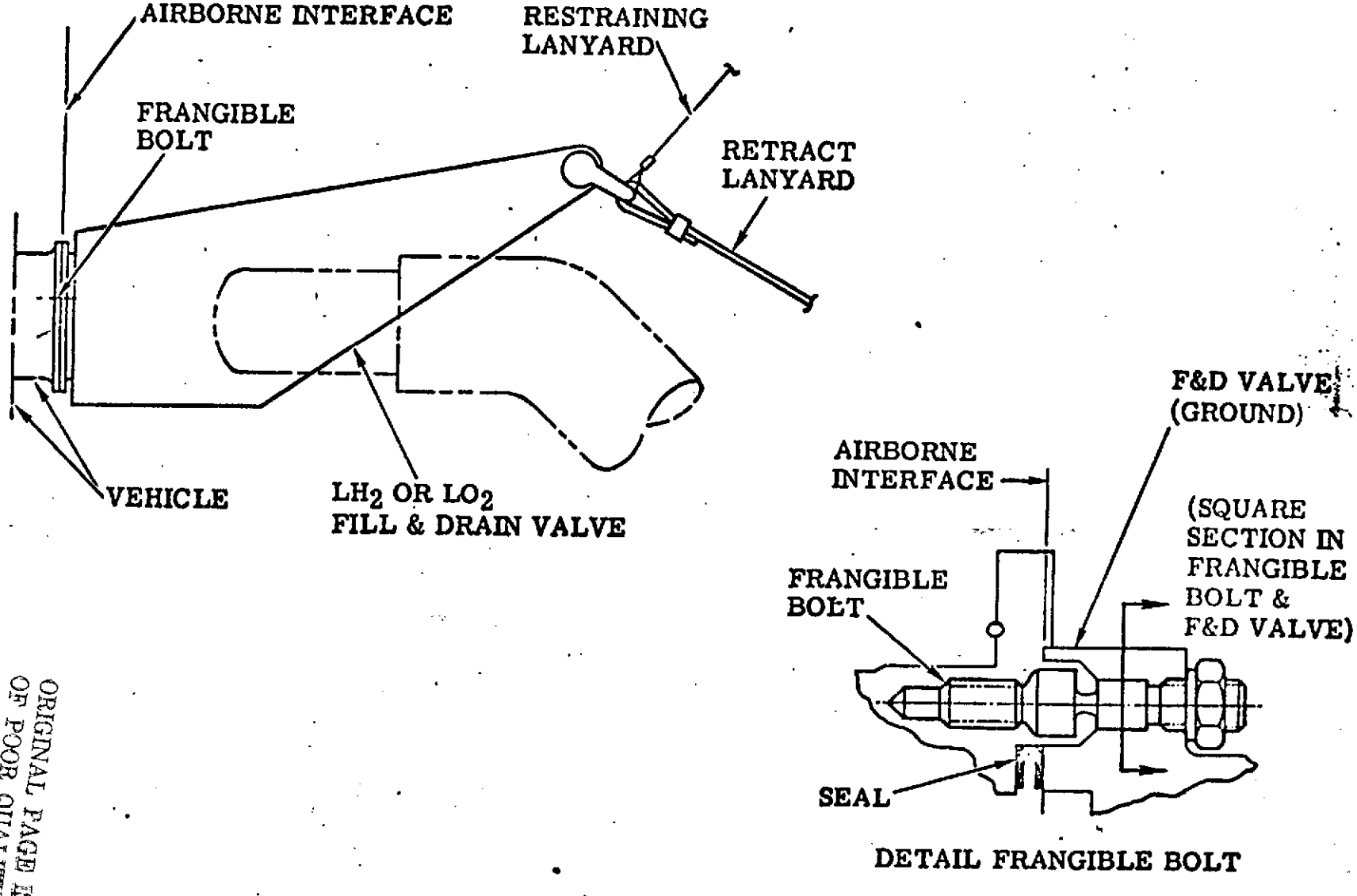

FIGURE VI-1-14 LH_2 AND LOX FILL AND DRAIN VALVE DISCONNECT DETAILS

VI-2. CENTAUR STANDARD SHROUD ASCENT VENT SYSTEM

by W. K. Tabata

Summary

The ascent vent system on the Centaur Standard Shroud functioned satisfactorily. Crushing and bursting pressures were well within allowables. Maximum pressure decay rate near Mach 1 was at the expected value of about 0.7 psi per second.

System Description

The ascent vent system for the Centaur Standard Shroud (CSS) is a passive but complex system involving many separate compartments that must be vented in a controlled manner to minimize vehicle and spacecraft structural differential pressures. The various vented compartments along with gas media, volumes, vent areas, and number of vents are shown in figure VI-2-1.

For TC-1, Compartment 1 or the spacecraft (Viking Dynamic Simulator and SPHINX) had a negligible internal volume and presented no venting problems.

The payload compartment (Compartment 2) and the Centaur electronics compartment (Compartment 3) are separated prior to liftoff by an encapsulation bulkhead for spacecraft sterilization reasons. At liftoff, this bulkhead is opened with the result that in flight, compartments 2 and 3 comprise one volume of 3853 cubic feet of gaseous nitrogen and are vented through eleven vent openings in the shroud. The total vent area for these two compartments is 125 square inches.

The Centaur equipment module compartment (Compartment 4A) and the LH_2 tank compartment (Compartment 4) are separated from the adjacent compartments by the shroud forward and aft seals and the Centaur Equipment Module. Separation is required since these two compartments are purged with helium on the ground to prevent cryopumping of GN_2 into the LH_2 tank area. Compartment 4A (78 cu ft) is then vented in flight through one 24 square inch vent in the LH_2 fill and drain valve chute door. This one vent is actually composed of five circular orifices in the door.

The Centaur Interstage is Compartment 5. This 839 cubic foot volume is purged on the ground with 120° F gaseous nitrogen for thermal conditioning Centaur propulsion system components after the Centaur stage is tanked with cryogenics. In flight, this compartment is vented through nine vents with a total area of 90 square inches in the CSS.

At the same station on the CSS as the Centaur Interstage vents are four vents for the Titan forward skirt (Compartment 6). These four vents

have a total area of 40 square inches and are located costation with Compartment 5 vents in order to minimize the differential pressure across the thermal barrier which separates the two compartments. The thermal barrier is required since Compartment 6 is air conditioned with 68° F air on the ground. The volume of Compartment 6 is 338 cubic feet.

As mentioned earlier, the CSS ascent vent system is passive. All the vents are rectangular in shape, are canted aft at 30 degrees, and contain a fiberglass honeycomb insert. The only different vent is the LH_2 tank compartment vent which is five circular holes in the LH_2 fill and drain valve chute door.

Flight Performance

The TC-1 measured internal pressure-flight time history of Compartments 2/3 (payload/Centaur electronics compartments) is shown in figure VI-2-2. The agreement between the two flight measurements CA890P and CA891P is good. The comparison of flight data to the preflight estimate is also quite good.

A Viking spacecraft design criteria for the Centaur standard shroud ascent vent system is that the spacecraft compartment maximum pressure decay rate (DP/Dt) during the transonic portion of flight should not exceed -0.7 psi per second and should be less than -0.5 psi per second for the other portions of flight. For TC-1, the predicted maximum decay rate during transonic was -0.85 psi per second. This predicted decay rate exceeded the -0.7 psi per second requirement for the following reasons:

(1) Pressure decay rates greater than -0.7 psi per second were not a problem for the TC-1 payloads.

(2) After ascent vent system hardware was built and installed on the TC-1 vehicle:

(a) Wind tunnel tests at Lewis Research Center indicated the flow coefficients of the flight vents were slightly greater than that assumed in the venting analyses

(b) The CSS forward umbilical door latch gaps were increased to insure proper door closing. This increased gap resulted in a larger leakage area in Compartment 3.

An expanded time plot of the spacecraft/electronics compartments pressure during the transonic portion of flight is shown in figure VI-2-3. As indicated in the figure, the maximum decay rate was approximately -0.7 psi per second for a 1.0 second period. Prior to and after this transonic portion of flight, the pressure decay rates were less than -0.3 psi per second.

Pressure-time history plots for Compartment 4A (CA881P forward bulk-

head or equipment module compartment), Compartment 4 (CA879P LH_2 tank compartment), Compartment 5 (CA894P Centaur interstage), Compartment 6 (TA2207P Titan forward skirt compartment), and the respective preflight estimates predicted by analyses are presented in figures VI-2-4 through 6. Again in all cases, the comparison between flight data and preflight estimates are quite good.

Another meaningful comparison of flight data and preflight estimates can be seen by examining the various compartment separator differential pressures.

In figure VI-2-7 are presented the differential pressure data for the CSS forward seal (Compartment 4 - Compartment 2/3) and the Centaur equipment module (Compartment 4A - Compartment 2/3). The forward seal and equipment module differential pressures agree well with the preflight estimates. The peak differential pressures measured in flight were +1.20 psi for the equipment module and +1.0 psi for the forward seal. The preflight estimate was +0.95 psi. The venting analyses also predicted worse-case differential pressures for both the forward seal and the equipment module of +2.8 and -1.6 psi. The flight pressures measured indicate sufficient margin.

The CSS aft seal differential pressures (Compartment 4 - Compartment 5) are shown in figure VI-2-8. The maximum differential pressure measured in flight (+0.6 psi) was half of the preflight estimate (+1.2 psi) and well below the analyses worse-case limits of +2.8 and -1.3 psi.

The thermal barrier differential pressures (Compartment 5 - Compartment 6) are shown in figure VI-2-9. Sufficient margin is again indicated by comparing the maximum differential pressure measured in flight (+0.15 psi) to the analyses limits of +1.3 and -1.0 psi. The preflight estimate was +0.3 psi.

The GD/CA ascent venting analyses assumed an isothermal expansion based on previous Atlas/Centaur flight data. There was concern before the TC-1 flight that the larger volumes in the Centaur standard shroud would behave more as an isentropic expansion. The TC-1 flight data for the payload compartment gas temperature (measurement CY112T) and an average gas temperature for the LH_2 tank compartment calculated from radiation shield measurements are shown in figure VI-2-10. Plotted on the figure are also the corresponding gas temperature history for the two compartments calculated with the GD/CA venting analyses assuming an isentropic expansion. The TC-1 flight data are similar to previous Atlas/Centaur flight data and verify the venting analyses assumption to be correct. The temperature histories are more isothermal than isentropic.

The Centaur standard shroud wall differential pressures due to compartment venting are not covered in this section of the report, but are discussed in the Centaur Standard Shroud Aerodynamics Section.

Conclusions

The TC-1 Centaur standard shroud ascent vent system performed satisfactorily and as designed.

(1) Compartment pressure histories and compartment separator differential pressures were approximately as the preflight estimates.

(2) The spacecraft compartment pressure decay rate (DP/Dt) during the transonic portion of flight was less than the preflight prediction.

(3) The compartment gas temperature histories matched more closely the isothermal expansion assumption used in the venting analyses rather than an isentropic expansion.

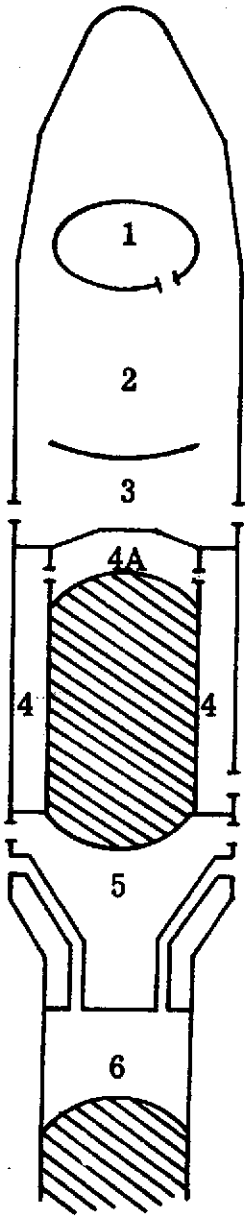

	Compartment	Media	Vol(ft^3)	Vent Area(in^2)	No. Vents
1	Spacecraft	GN_2	- - -	- - -	- - -
2	Payload Compartment	GN_2	3291	125	11
3	Centaur Electronics	GN_2	562		
4A	Equipment Module	GHe	78	20	10
4	LH_2 Tank Compartment	GHe	1370	24	1
5	Centaur Interstage	GN_2	839	90	9
6	Titan Forward Skirt	Air	338	40	4

FIGURE VI -2-1 CENTAUR STANDARD SHROUD ASCENT VENT SYSTEM

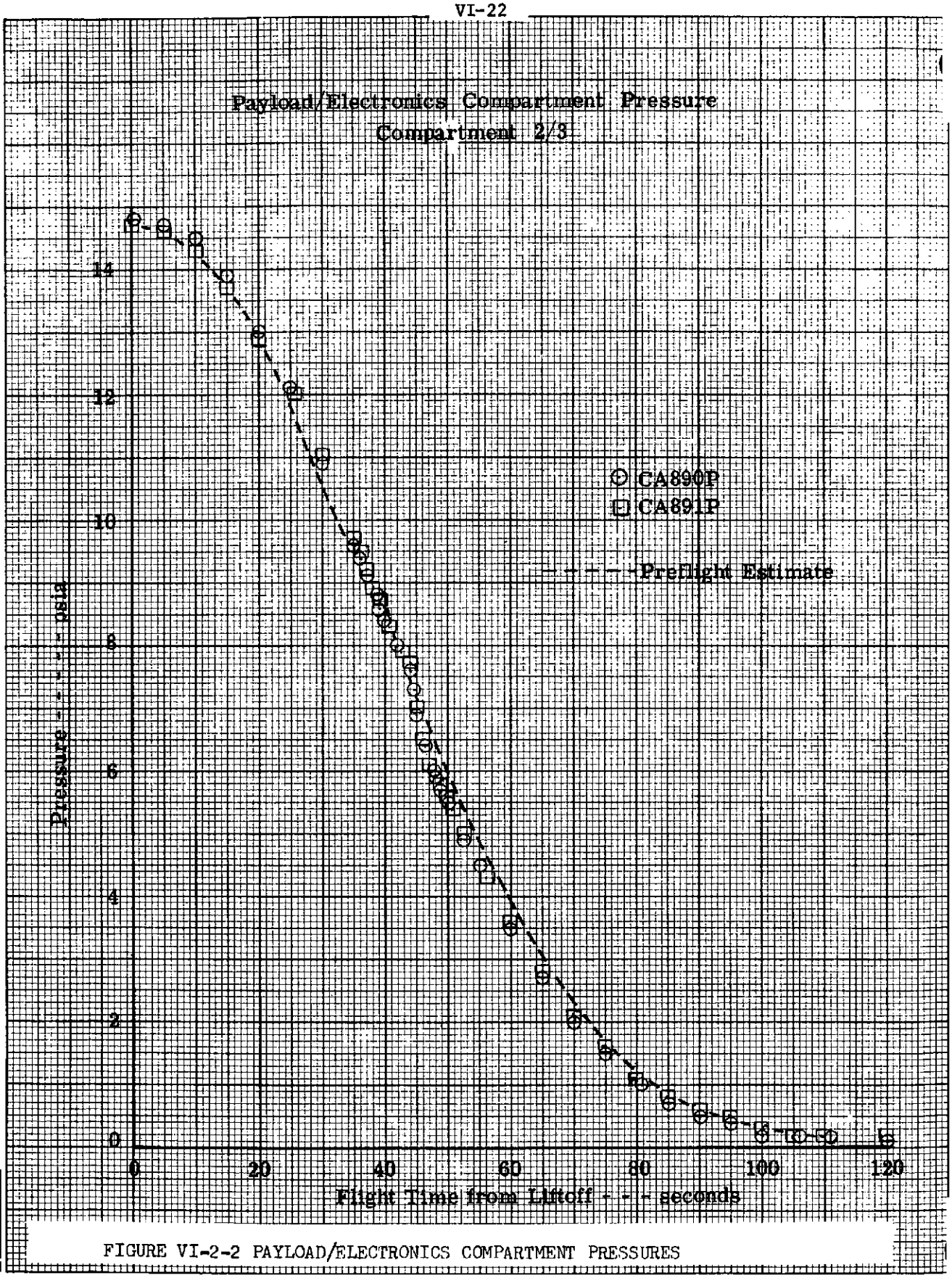

FIGURE VI-2-2 PAYLOAD/ELECTRONICS COMPARTMENT PRESSURES

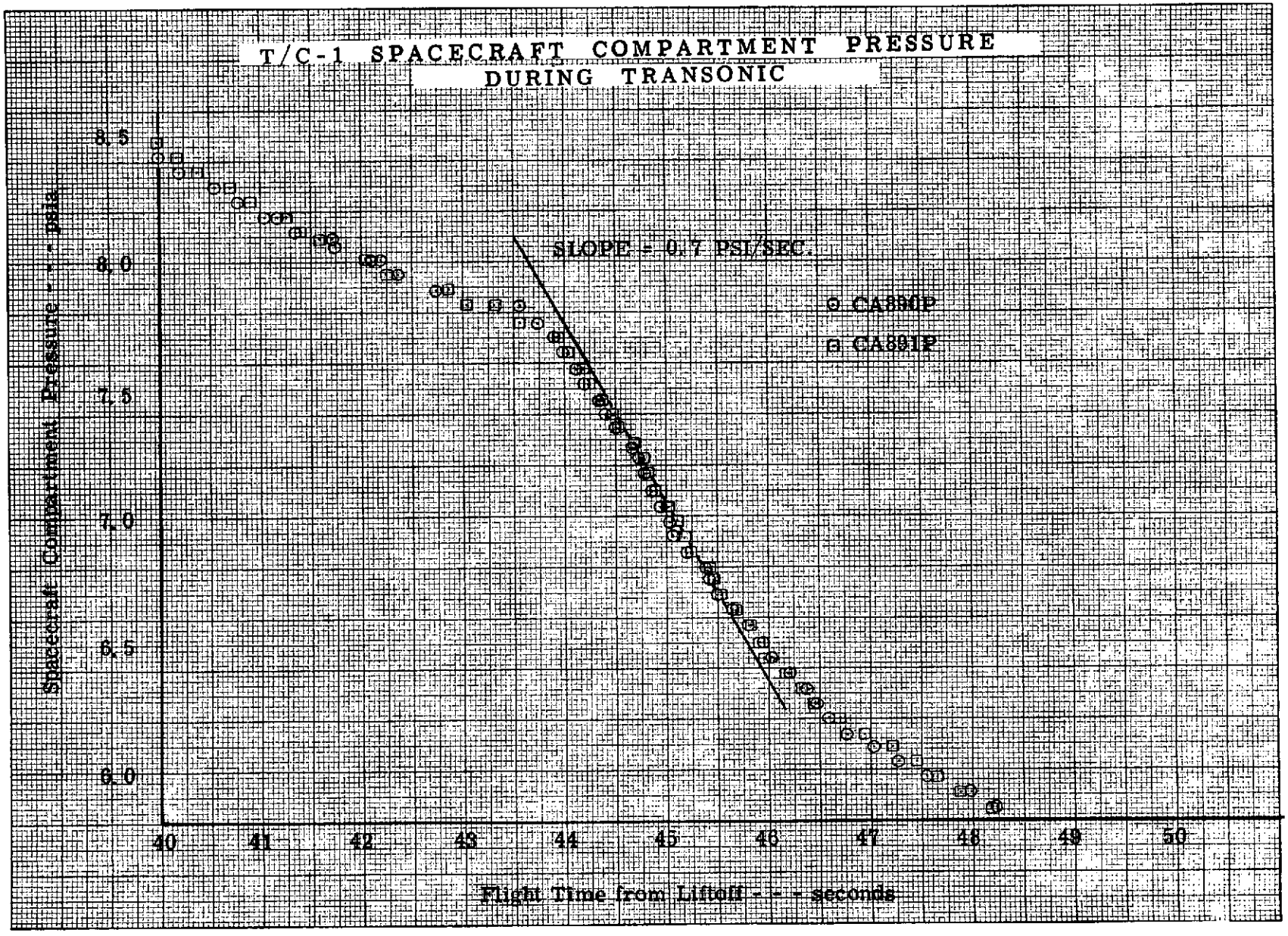

FIGURE VI-2-3 SPACECRAFT COMPARTMENT MAXIMUM PRESSURE DECAY RATE

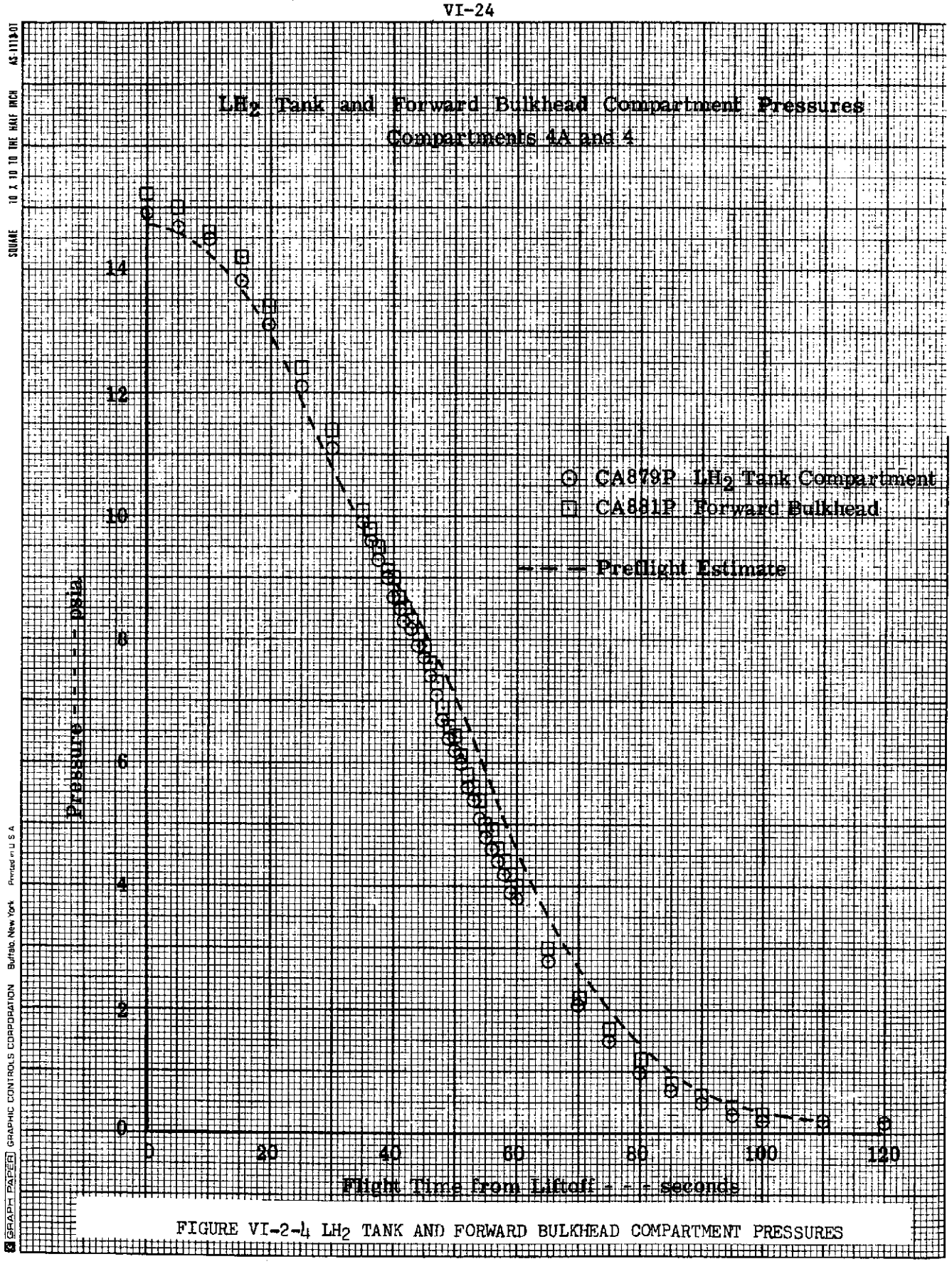

FIGURE VI-2-4 LH_2 TANK AND FORWARD BULKHEAD COMPARTMENT PRESSURES

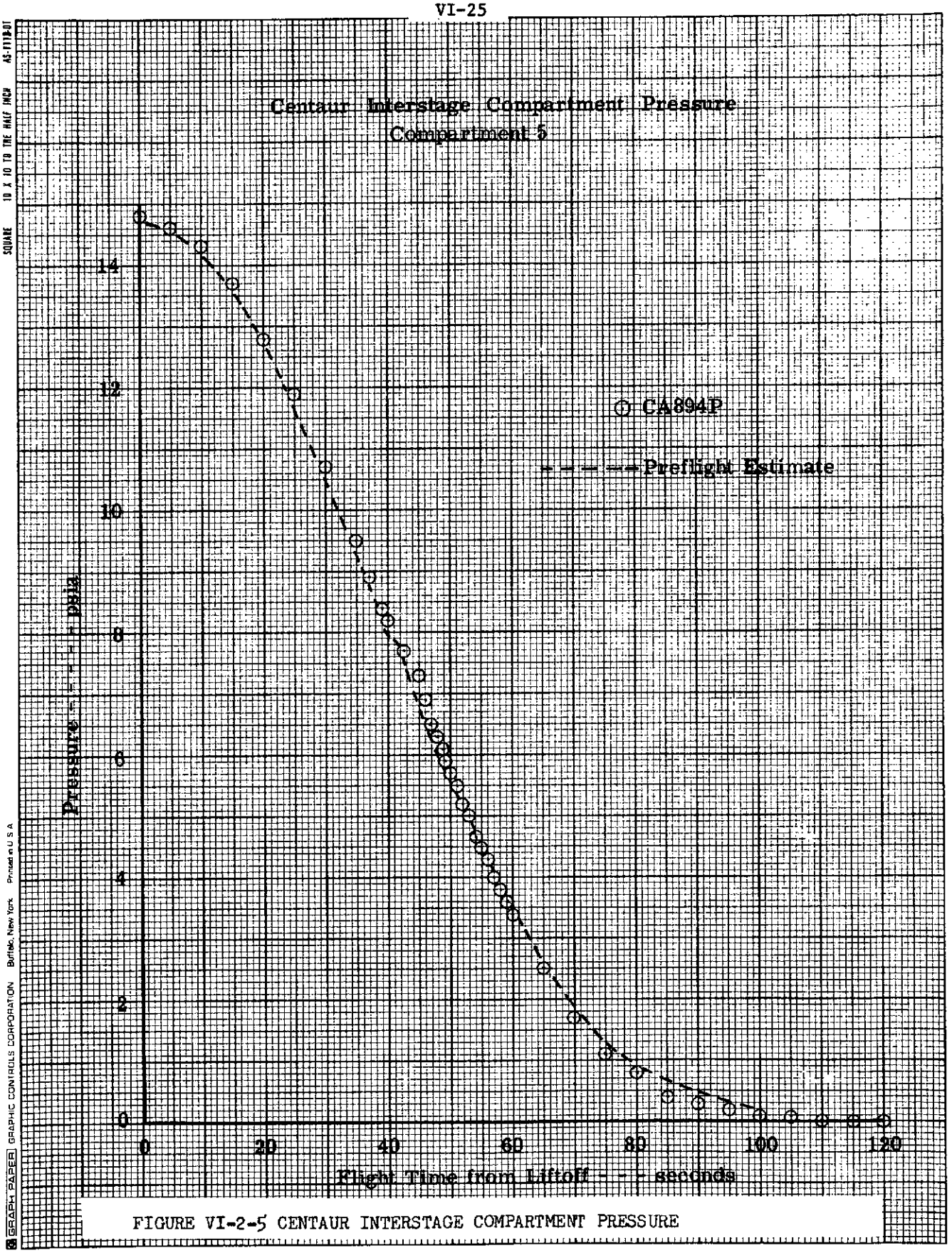

FIGURE VI-2-5 CENTAUR INTERSTAGE COMPARTMENT PRESSURE

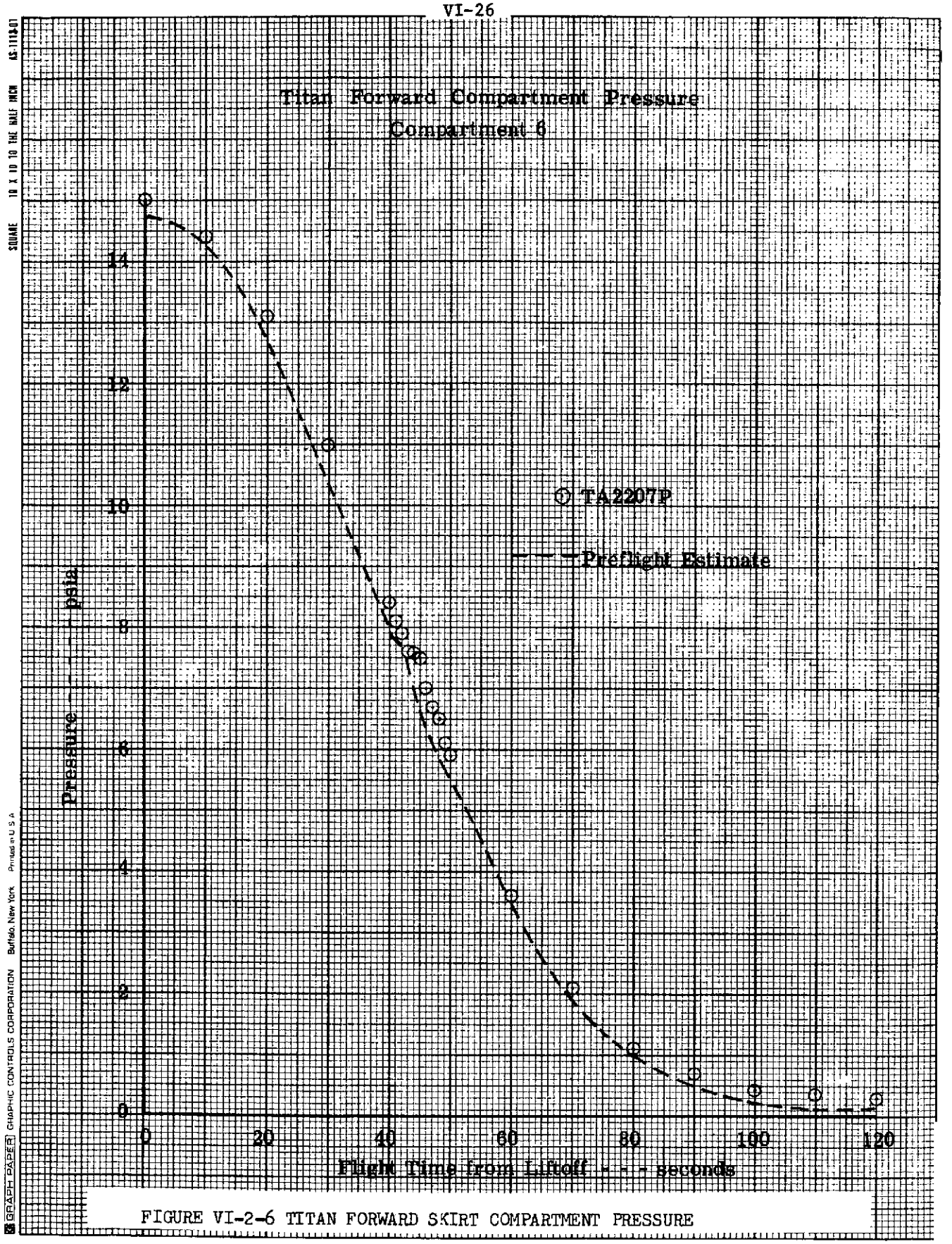

FIGURE VI-2-6 TITAN FORWARD SKIRT COMPARTMENT PRESSURE

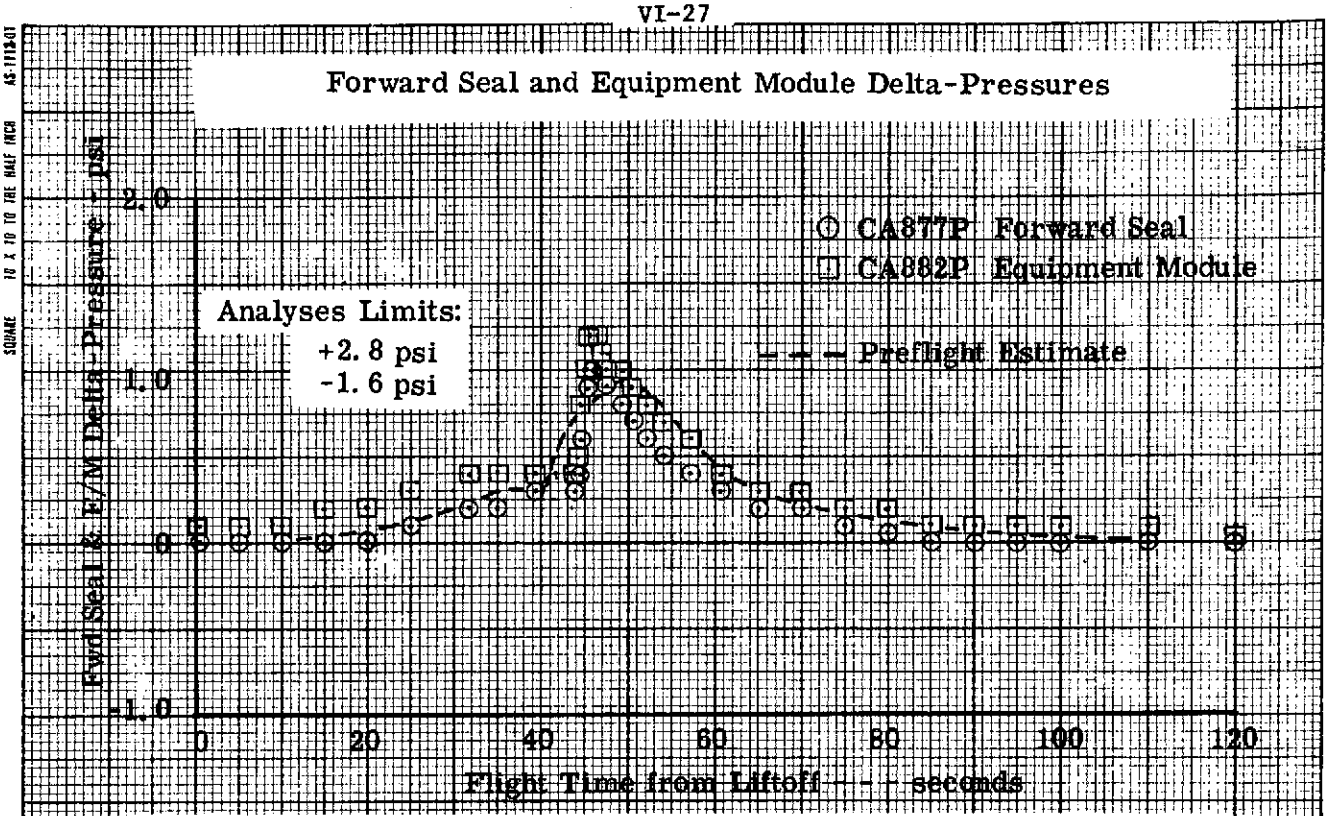

FIGURE VI-2-7 CSS FORWARD SEAL AND EQUIPMENT MODULE DELTA PRESSURES

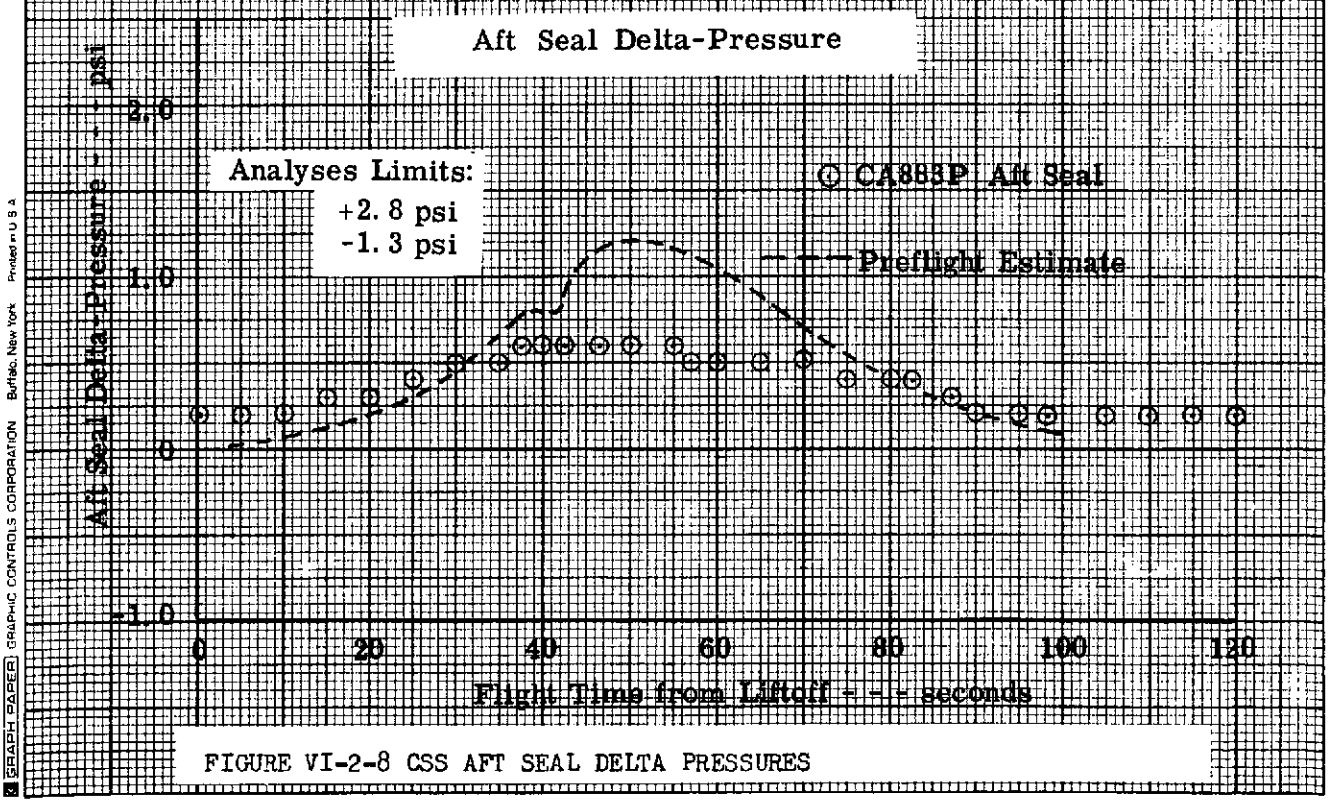

FIGURE VI-2-8 CSS AFT SEAL DELTA PRESSURES

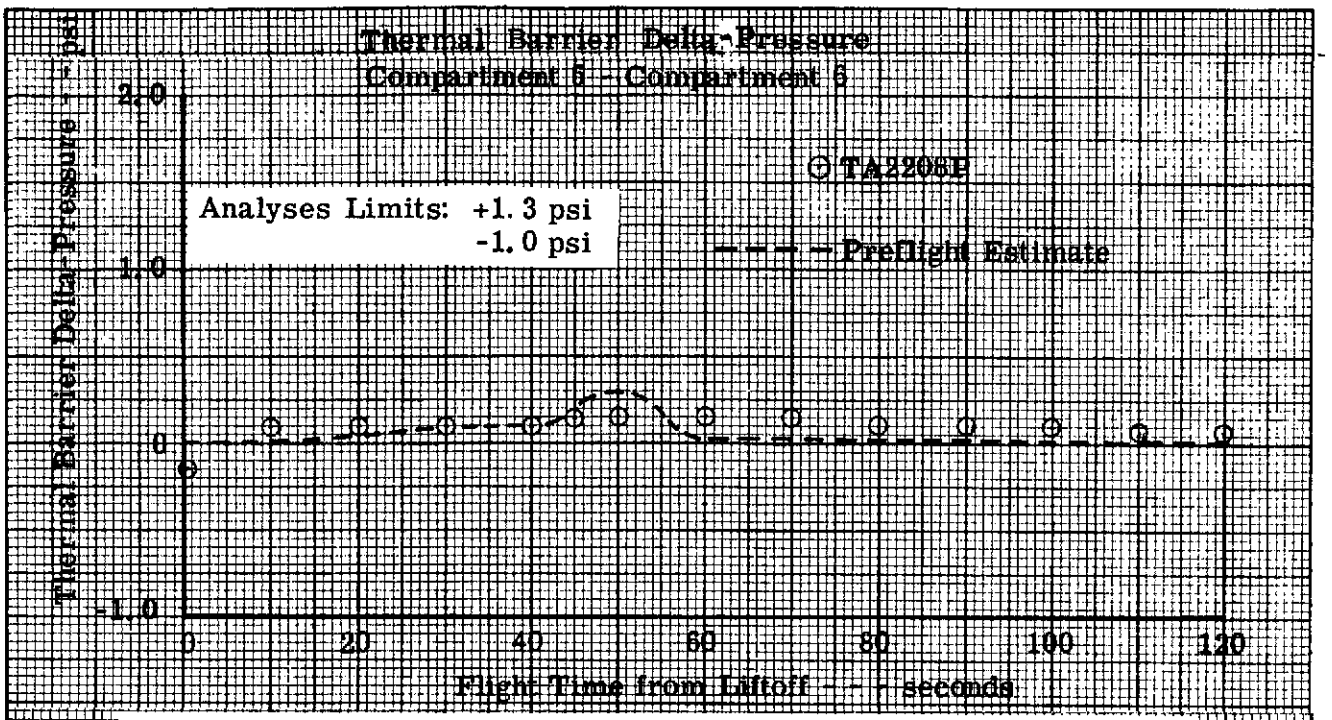

FIGURE VI-2-9 THERMAL BARRIER DELTA PRESSURES

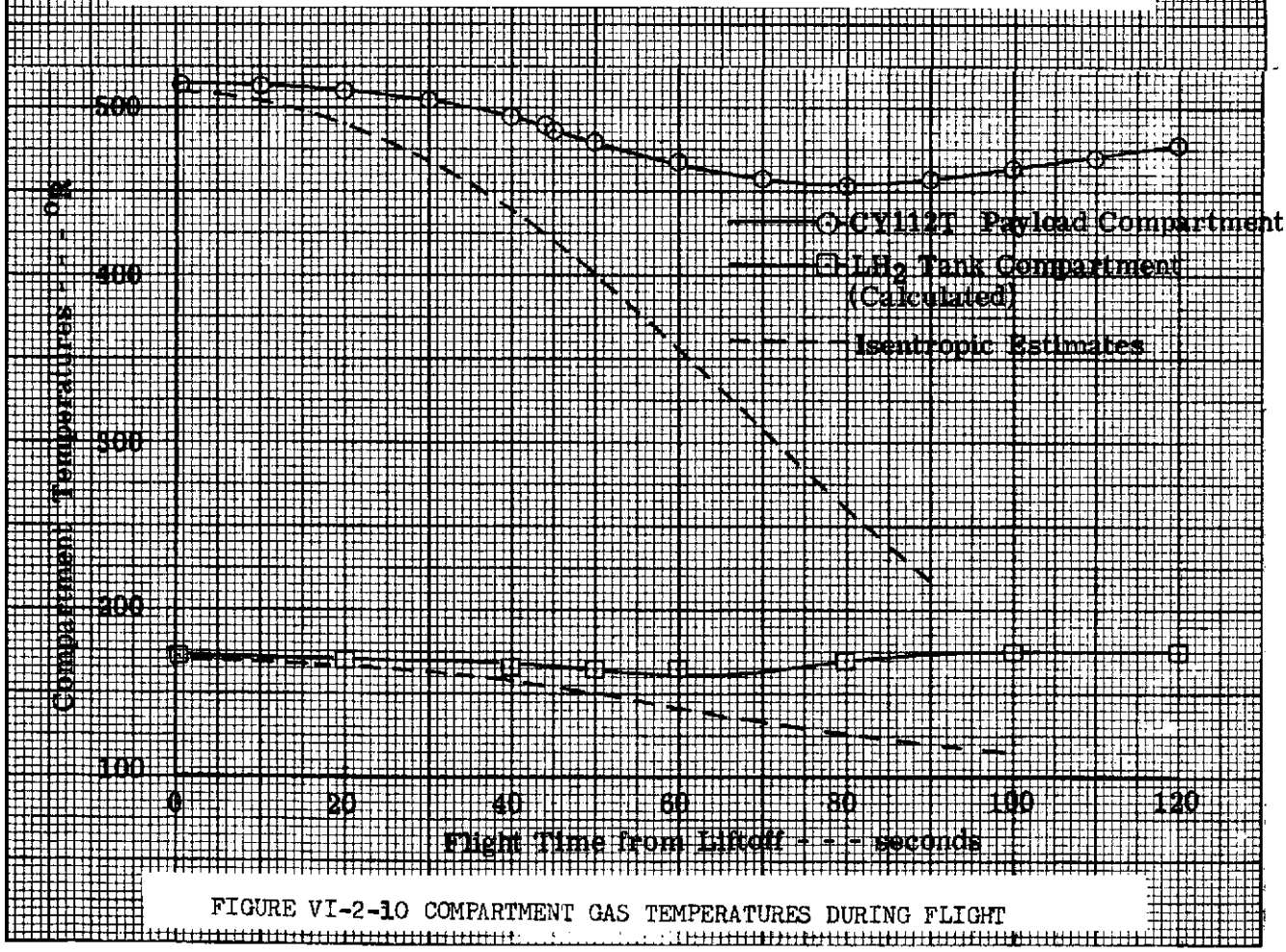

FIGURE VI-2-10 COMPARTMENT GAS TEMPERATURES DURING FLIGHT

VI-3. CENTAUR STANDARD SHROUD AND VEHICLE AERODYNAMICS

by M. L. Jones and J. C. Estes

Summary

All aerodynamic pressures and temperatures compared well with predicted values and were well within allowable limits.

Aerodynamic Pressures

The location and arrangement of the instrumentation used to measure the differential pressures across the walls of the CSS, the ISA, and the Titan forward compartment is shown in figure VI-3-1. Figure VI-3-2(a) through (z) present the time history of these differential pressures. Included on the figure are the applicable design limits in both burst and crush. The differential pressures remained below the design limits throughout the atmospheric ascent portion of the flight. Also shown for some of the stations along the CSS are plots of preflight calculated differential pressures based upon a nominal trajectory at zero angle of attack. The flight pressures remained within the calculated values except at Station 2750, where the maximum flight crush pressure exceeded the calculated value by 1.25 psi.

At Station 2678, measurement CA419P became noisy from approximately 33.5 to 38 seconds (fig. VI-3-2(a)). The exact cause of the noise is not known, but it is highly probable that it was caused by a separated flow field at the cone/cylinder juncture (Station 2680.66) at or near the transonic speed range.

The proximity of the Titan forward compartment instrumentation to the solid rocket motors created a considerable amount of high frequency pressure oscillations throughout the first seventy seconds of flight. Consequently, the data shown for these measurements represent envelopes of the maximum burst and crush pressures.

It can be seen from the data at those stations where there was multiple instrumentation that there were only minor circumferential variations of pressure, indicating a very low vehicle angle of attack during the portion of the flight that had aerodynamic significance.

Aerodynamic Temperatures

Measured external shroud temperatures against flight time are shown in figure VI-3-3(a) through (i). The shroud station and circumferential location of each temperature sensor is indicated on the figures. Measurements from CA169T (fig. VI-2-3(b)) are believed to be invalid data in the time range of 65 to 80 seconds.

Figure VI-2-3(c) compares flight measurements at Station 2672 with windward control temperatures used on the shroud for the heated jettison tests conducted at Plum Brook Station. The jettison test control temperatures were indicative of a design heating (very hot) trajectory. Note that the shroud was jettison-tested at much higher temperatures than were observed in the flight. Figure VI-2-3(c) also shows predicted shroud temperatures based on a TC-1 preflight nominal trajectory simulation. These temperatures, too, are much higher than the actual flight observations.

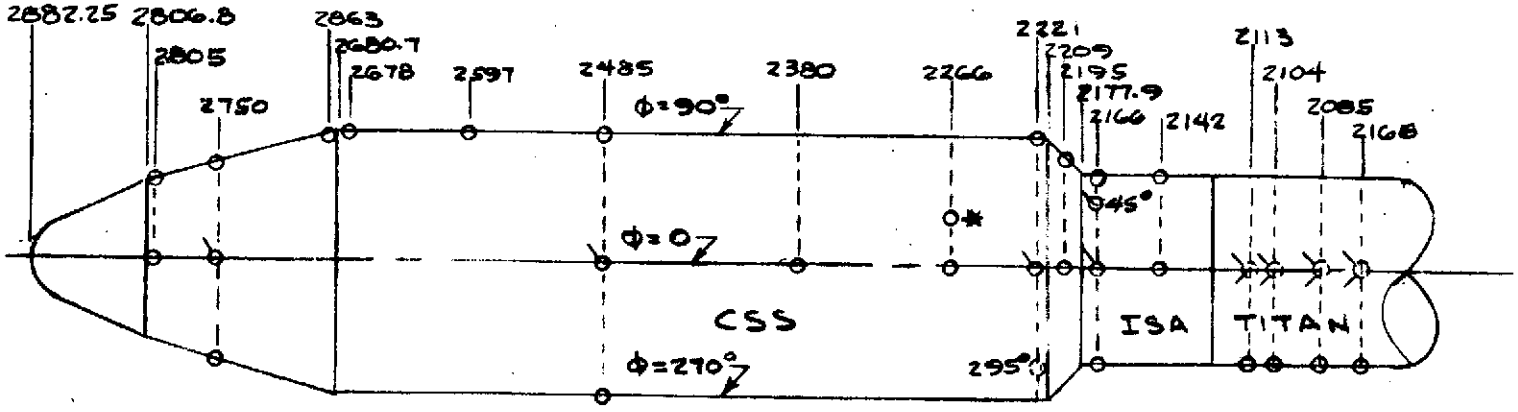

* LOCATED ADJACENT TO LH2 FILL & DRAIN VALVE DOOR

TWO LOCATIONS - NEAR & FAR SIDES

ONE LOCATION - FAR SIDE

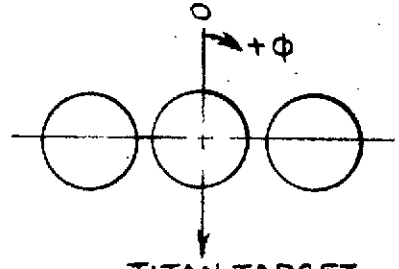

TITAN TARGET

VIEW LOOKING FORWARD

FIGURE VI-3-1 LOCATION OF CSS, ISA, & TITAN FORWARD COMPARTMENT DIFFERENTIAL PRESSURE MEASUREMENTS

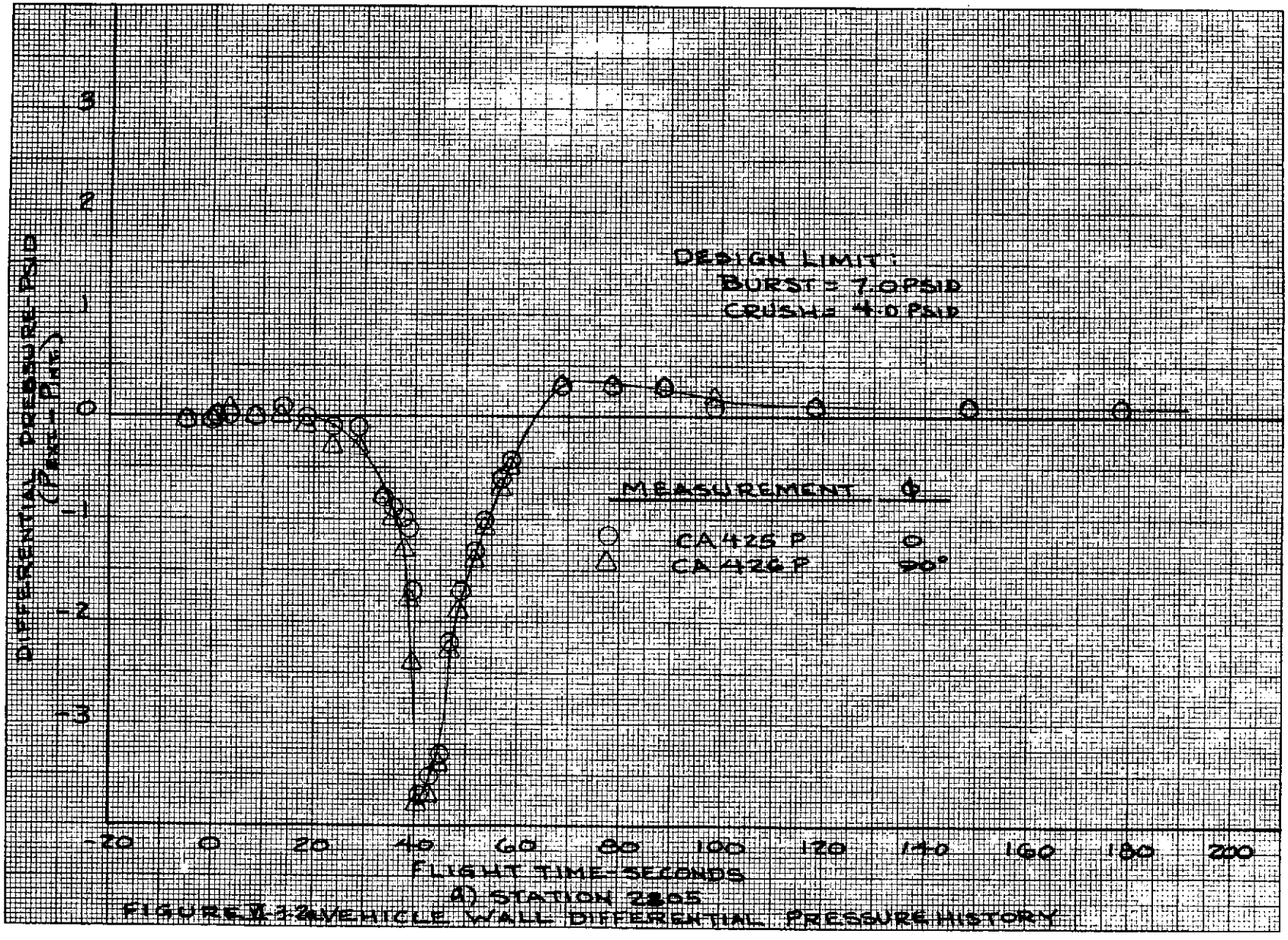

a) STATION 2305

FIGURE VI-12 VEHICLE WALL DIFFERENTIAL PRESSURE HISTORY

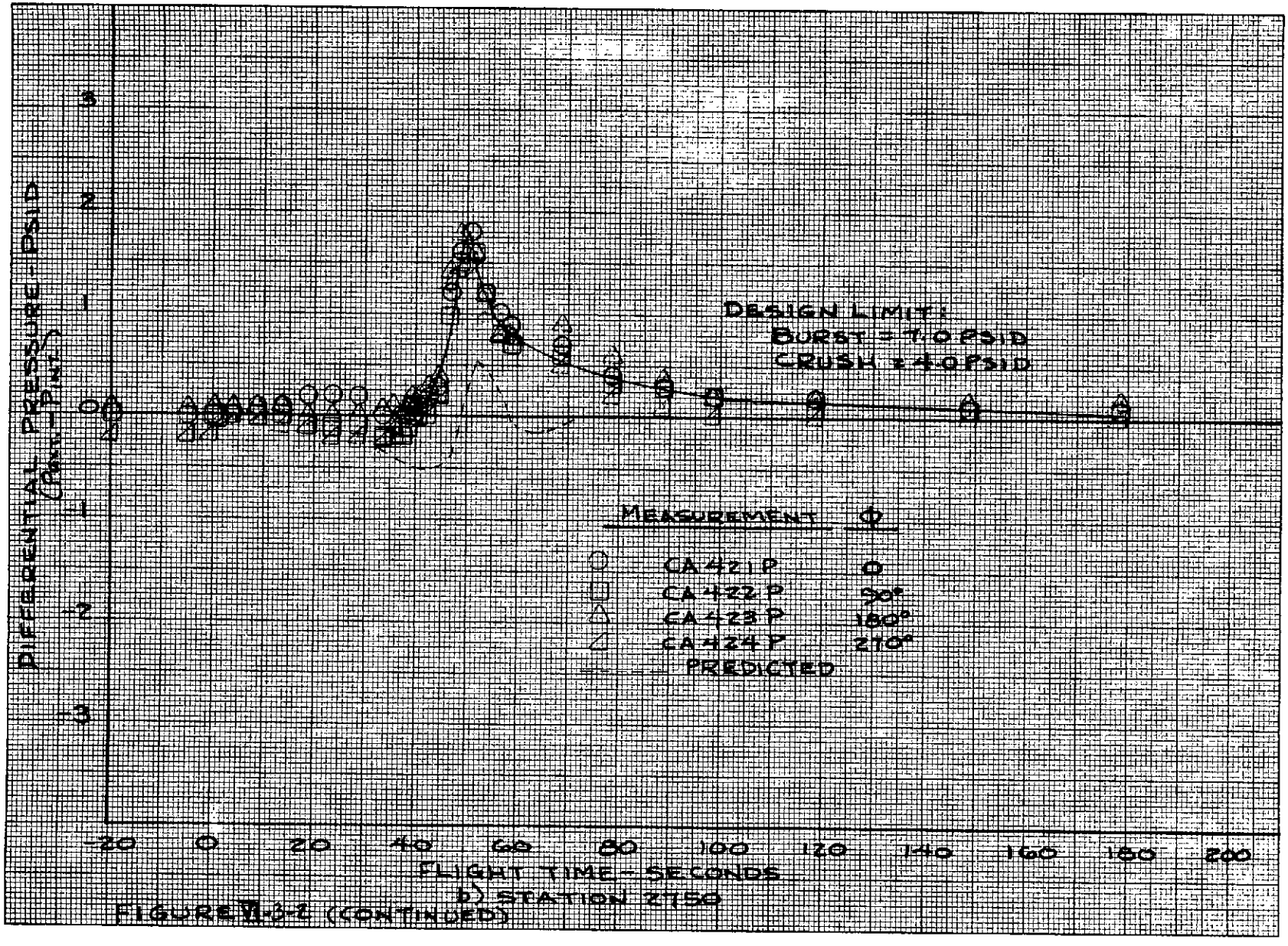

FIGURE VI-3-2 (CONTINUED)

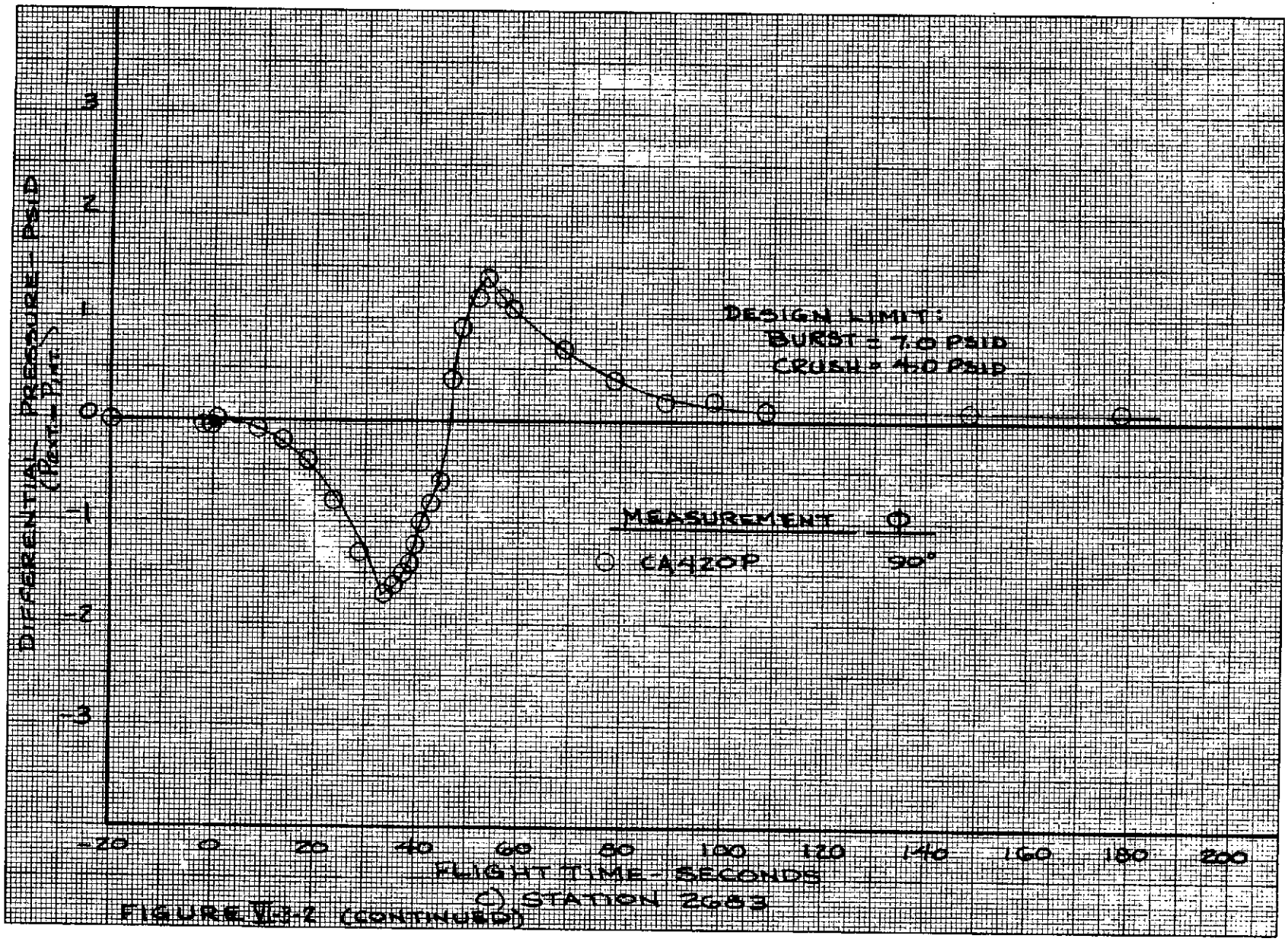

FIGURE VI-2 (CONTINUED) STATION 2083

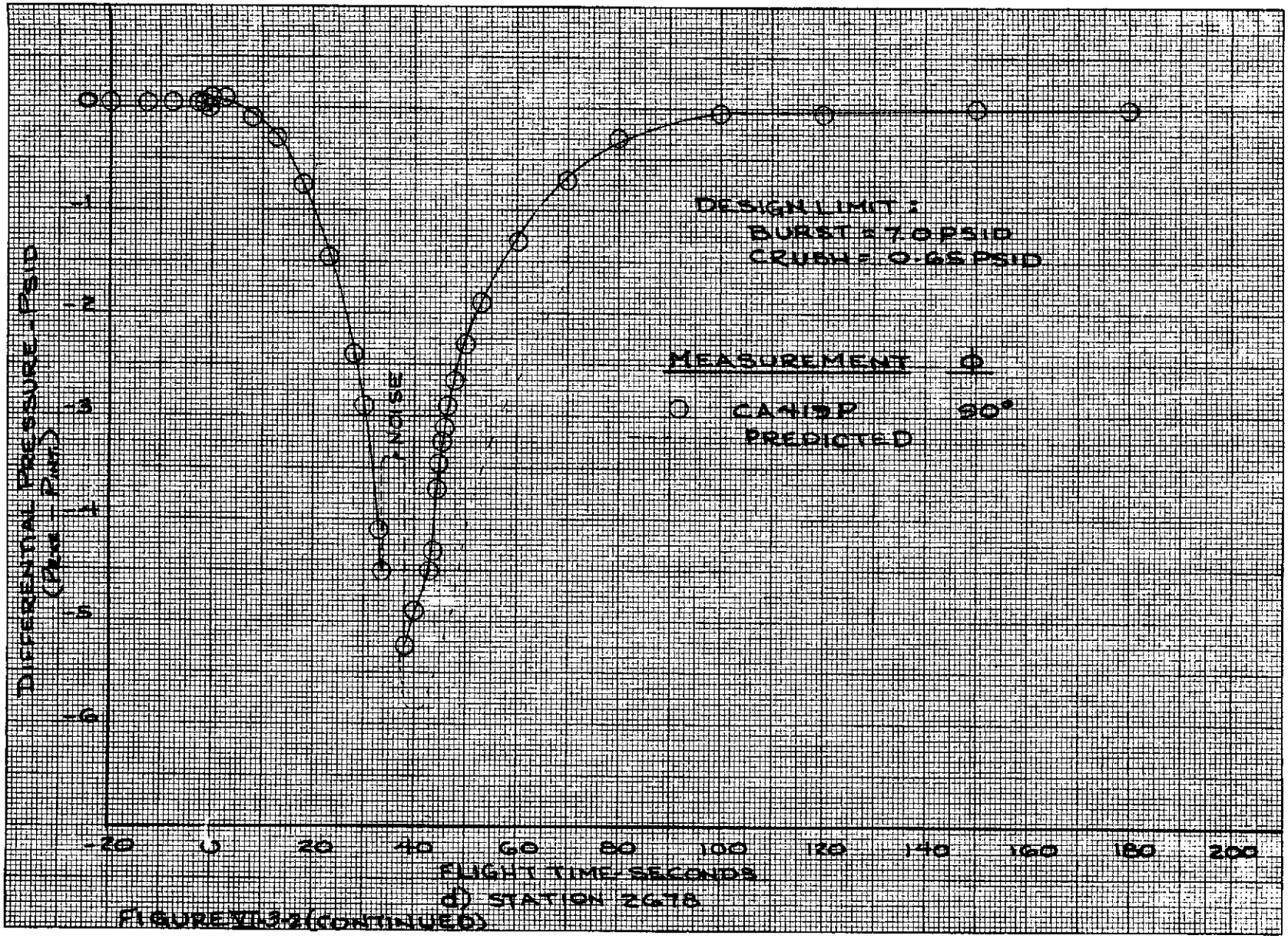

d) STATION 2678

FIGURE VI-3-2 (CONTINUED)

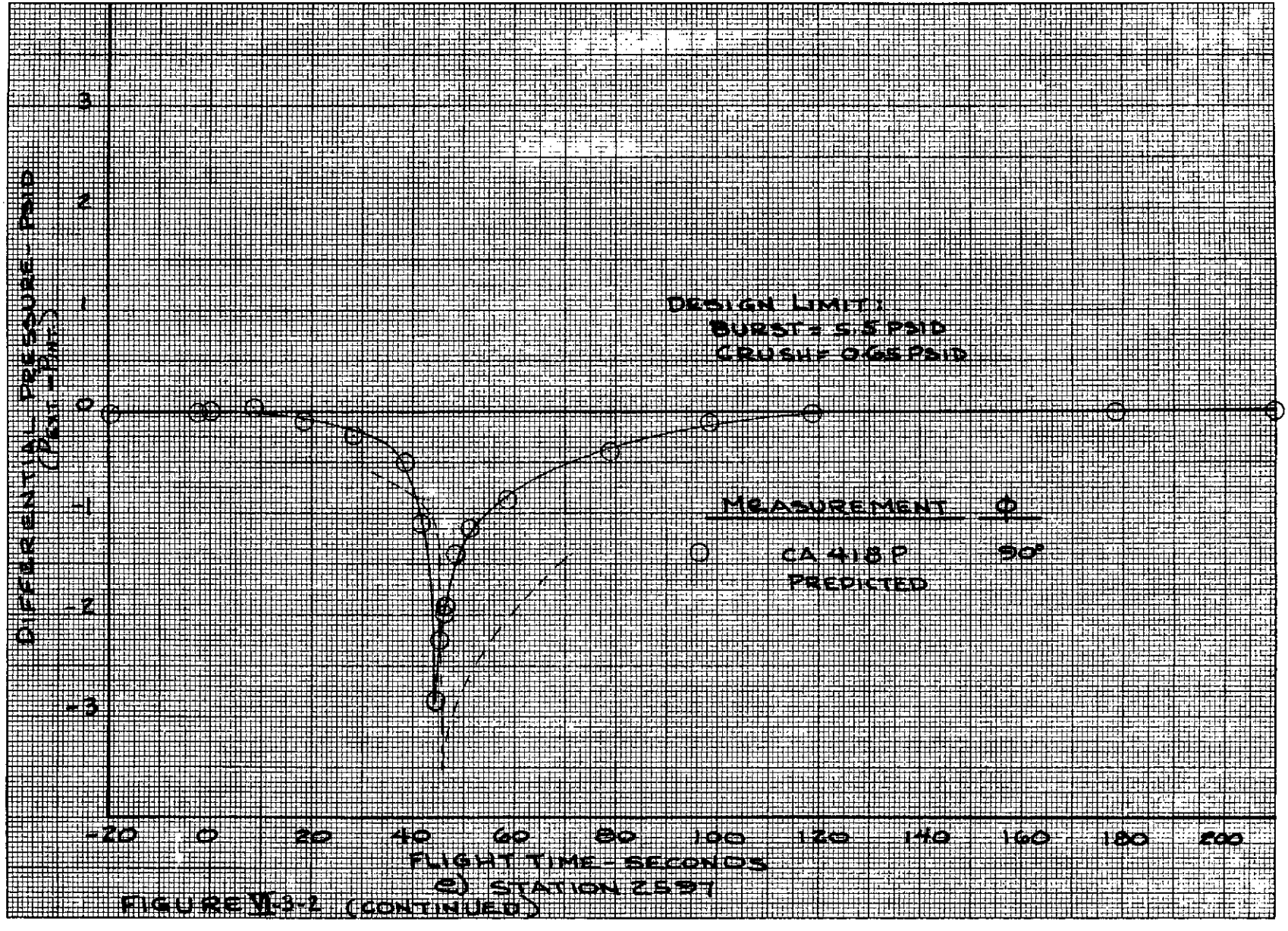

FIGURE VI-3-2 (CONTINUED)
e) STATION 2597

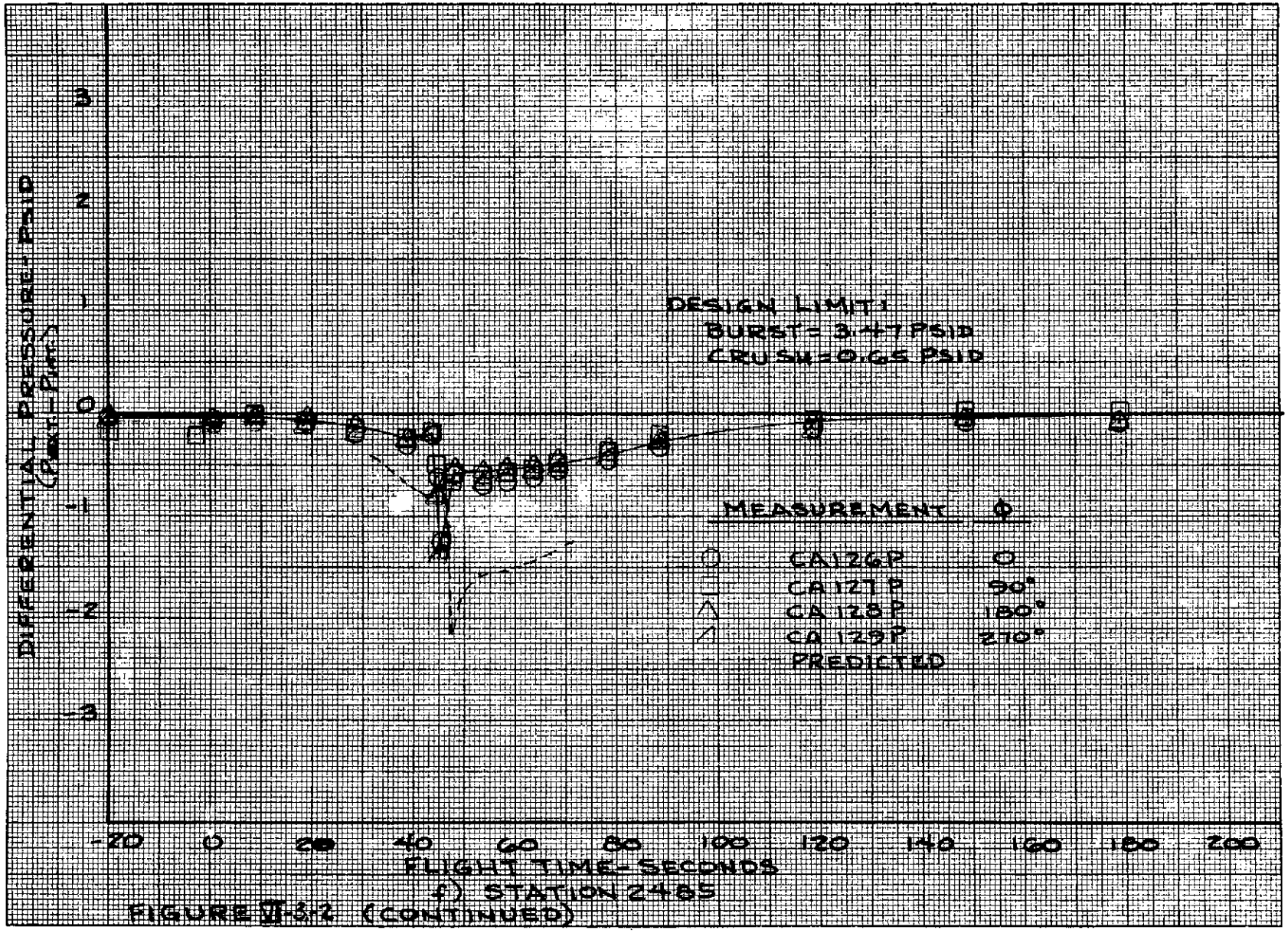

f) STATION 2465

FIGURE VI-3-2 (CONTINUED)

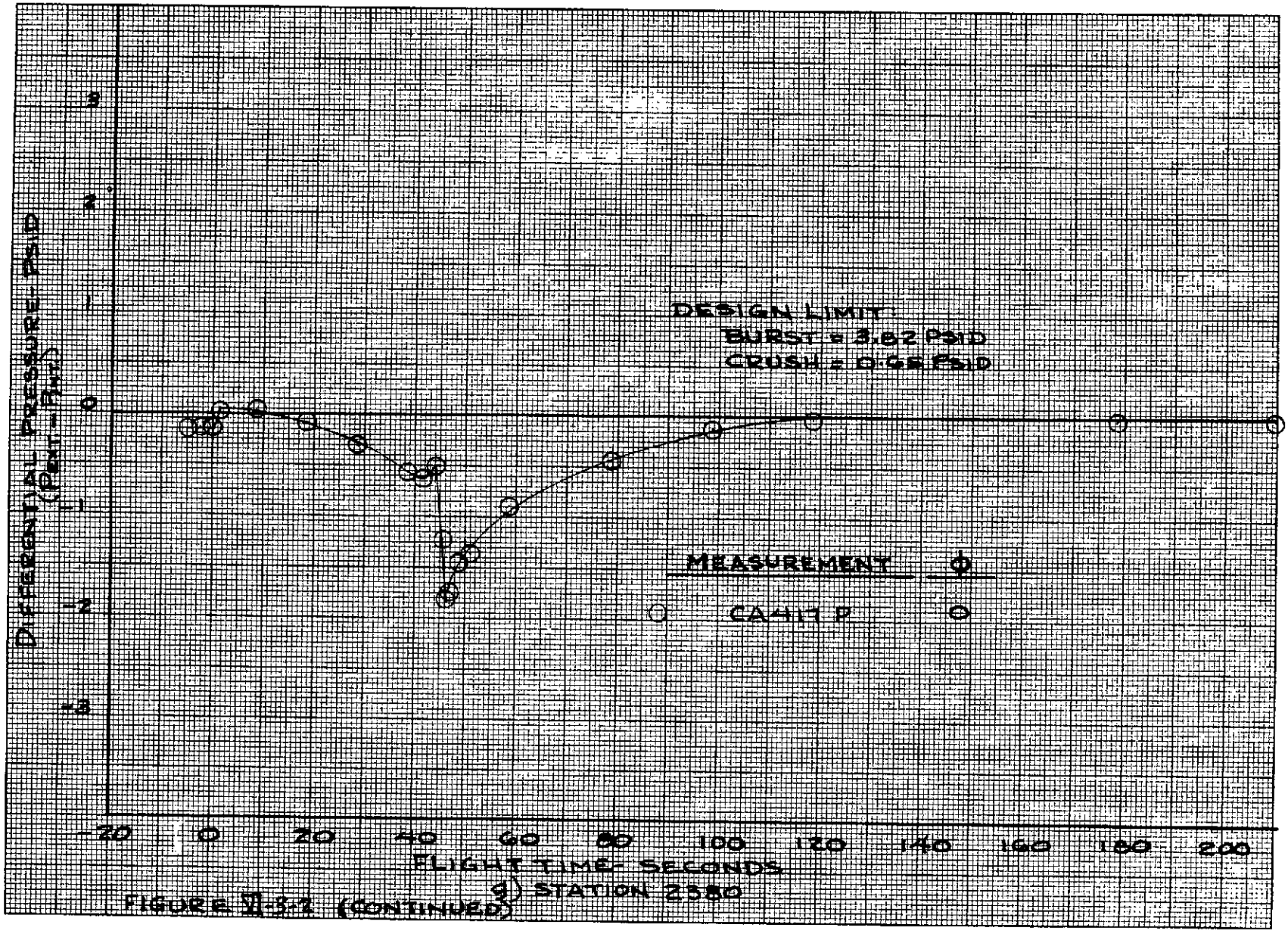

FIGURE VI-3-2 (CONTINUED)
g) STATION 2380

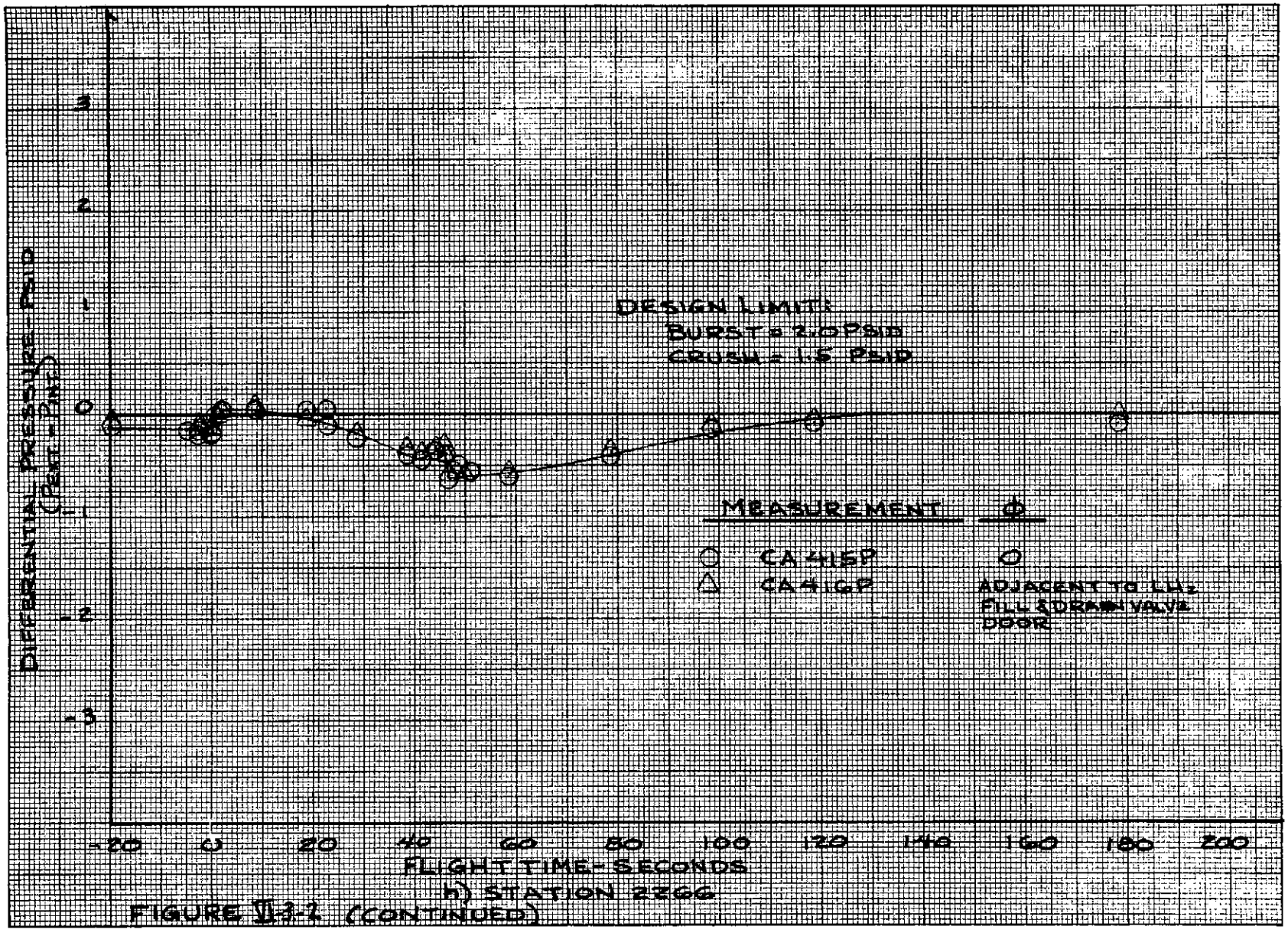

b) STATION 2266

FIGURE VI-3-2 (CONTINUED)

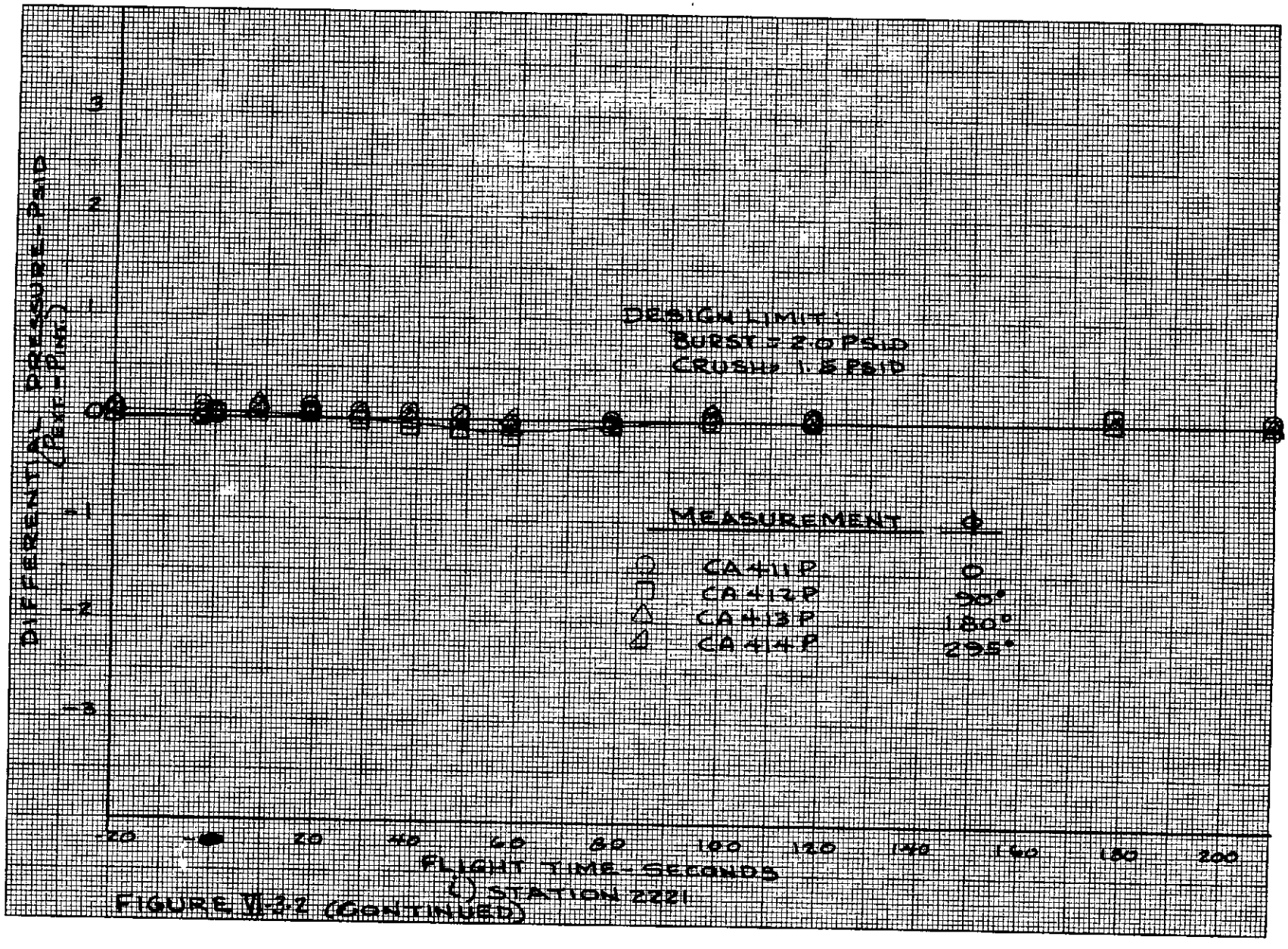

FIGURE VI-2.2 (CONTINUED)
c) STATION 2221

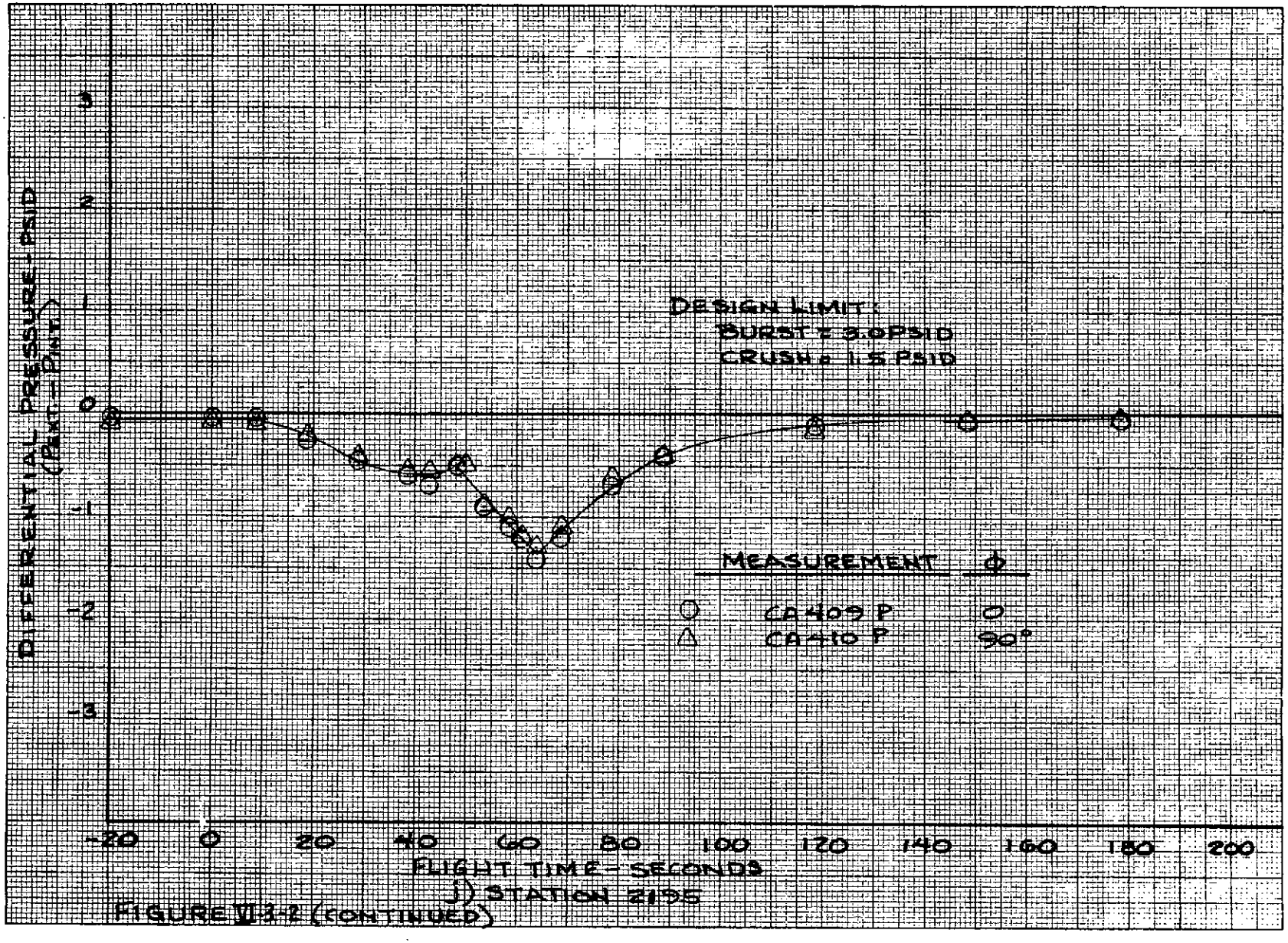

j) STATION 2195

FIGURE VI 3-2 (CONTINUED)

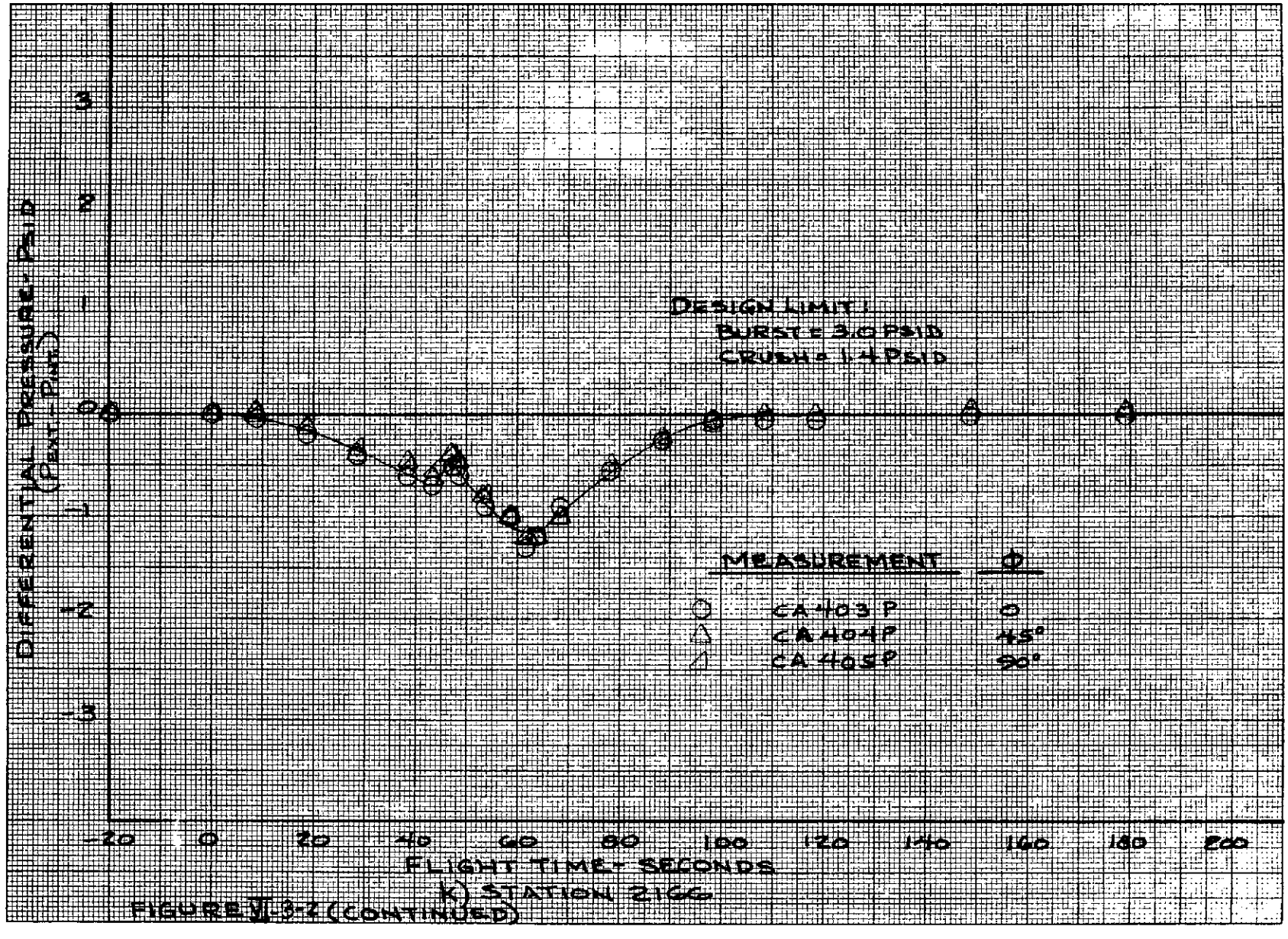

K) STATION 216.

FIGURE VI-3-2 (CONTINUED)

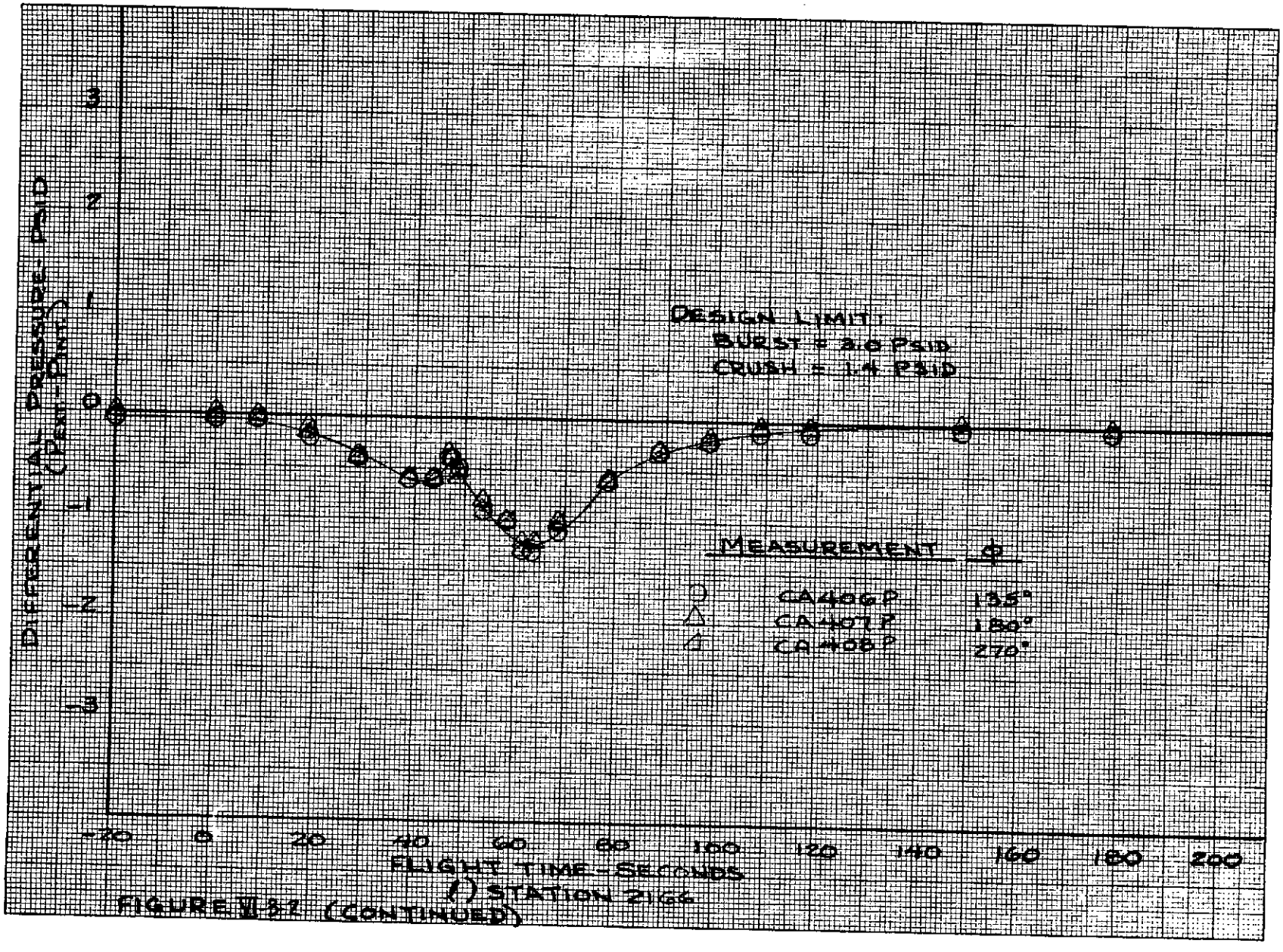

FIGURE VI-22 (CONTINUED)

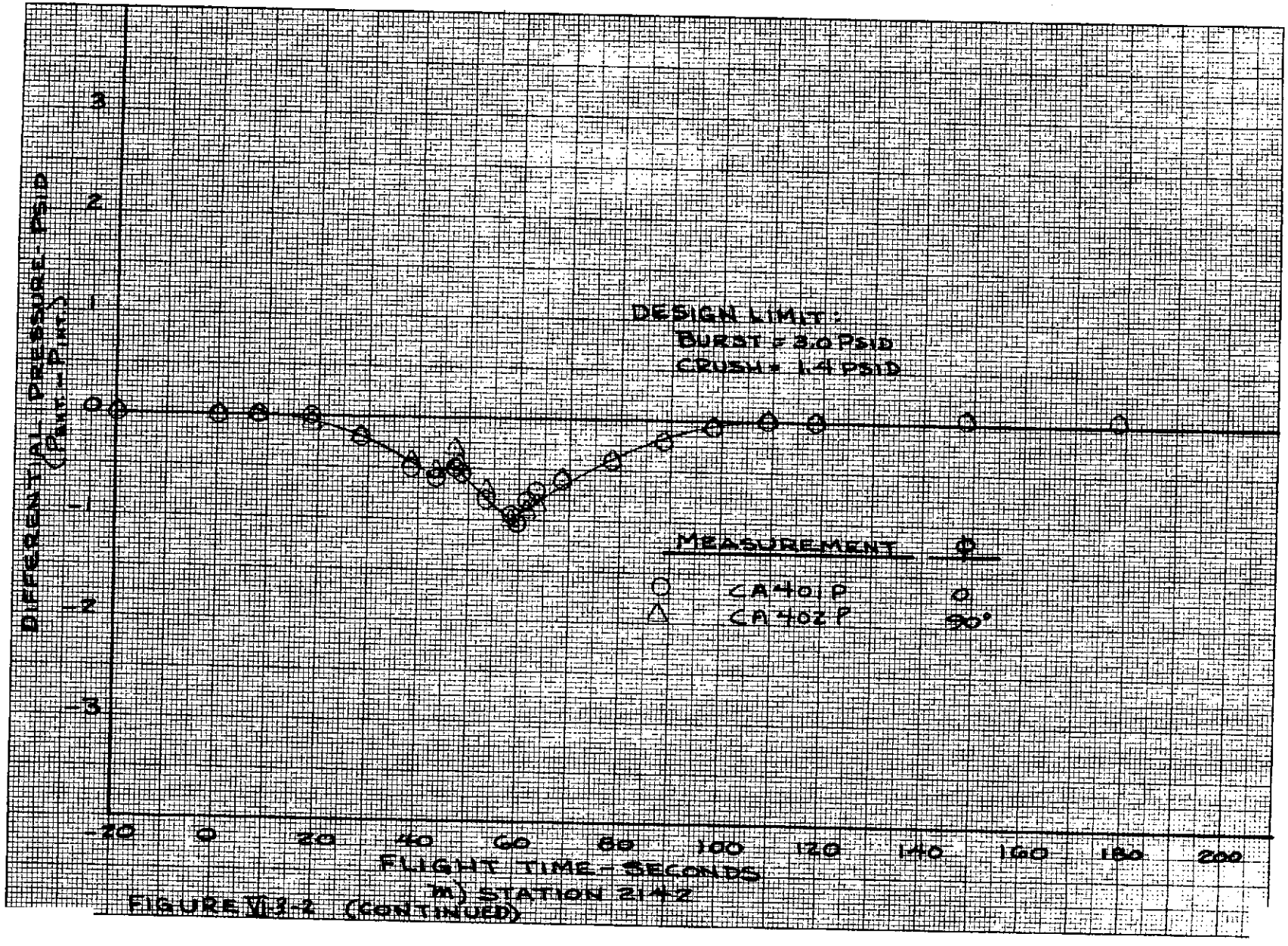

m) STATION 2142

FIGURE VI-2-2 (CONTINUED)

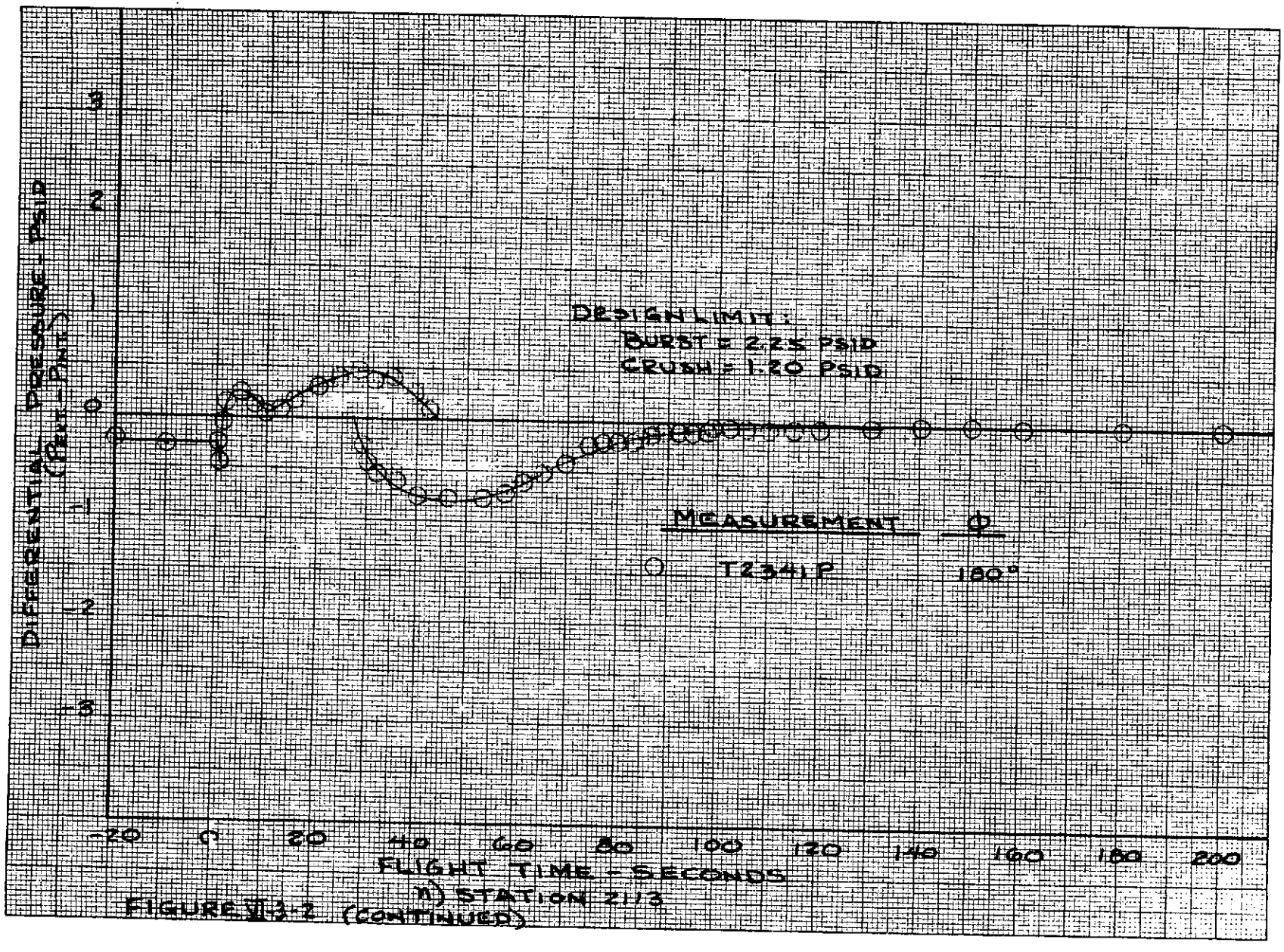

FIGURE VI-2 (CONTINUED)
A) STATION 2113

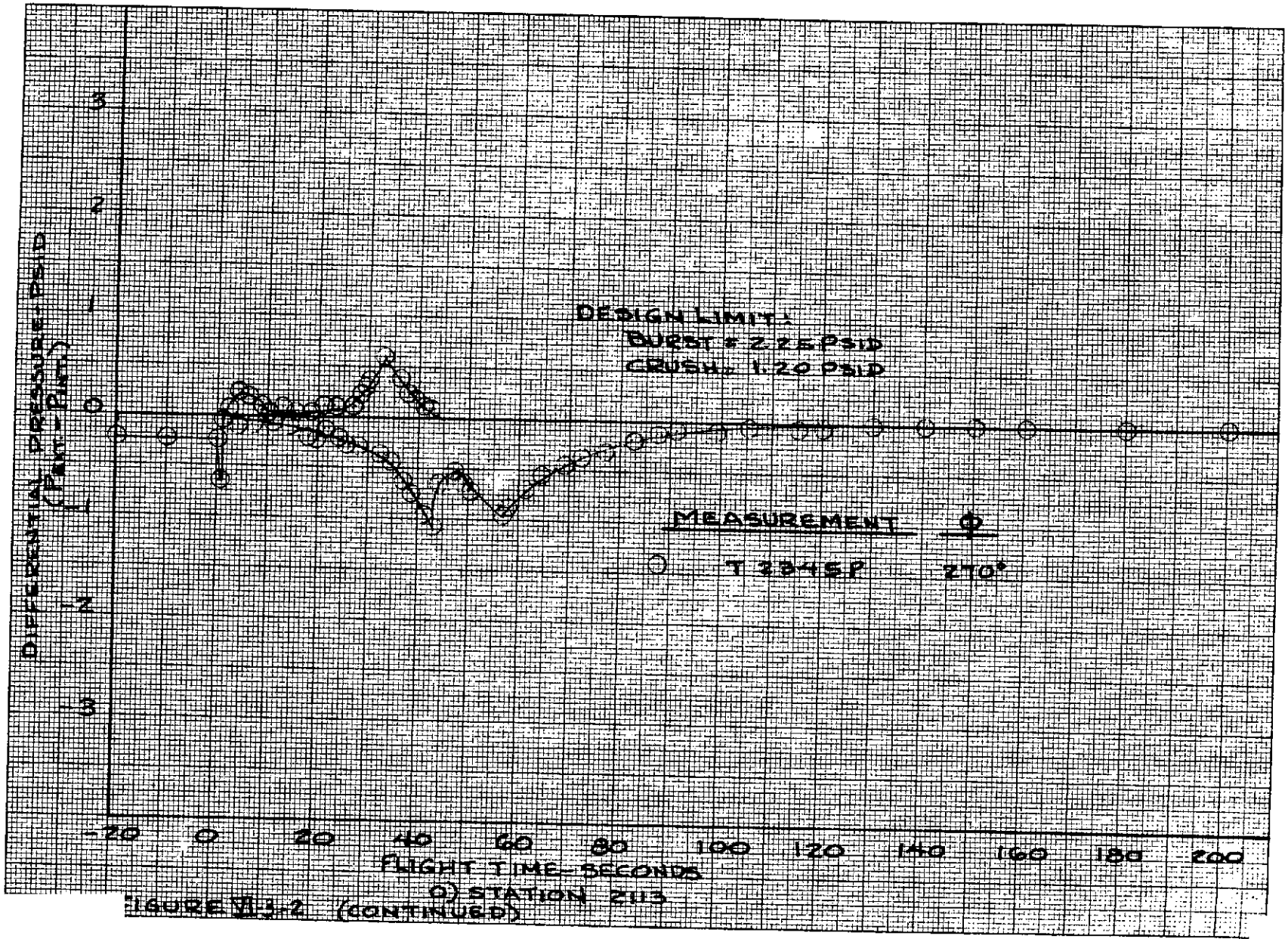

FIGURE VI.3-2 (CONTINUED)
c) STATION 2113

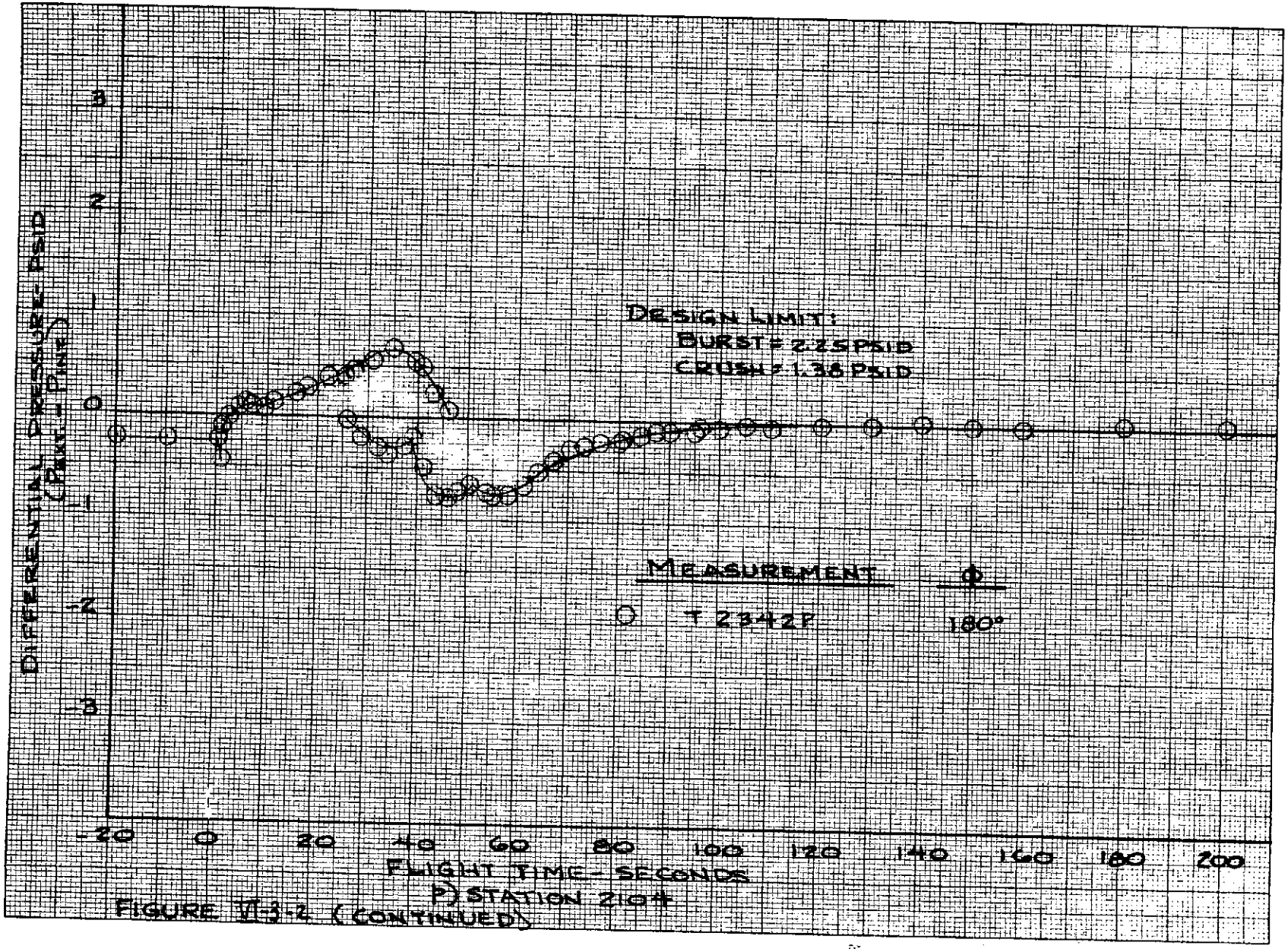

P) STATION 2104

FIGURE VI-3-2 (CONTINUED)

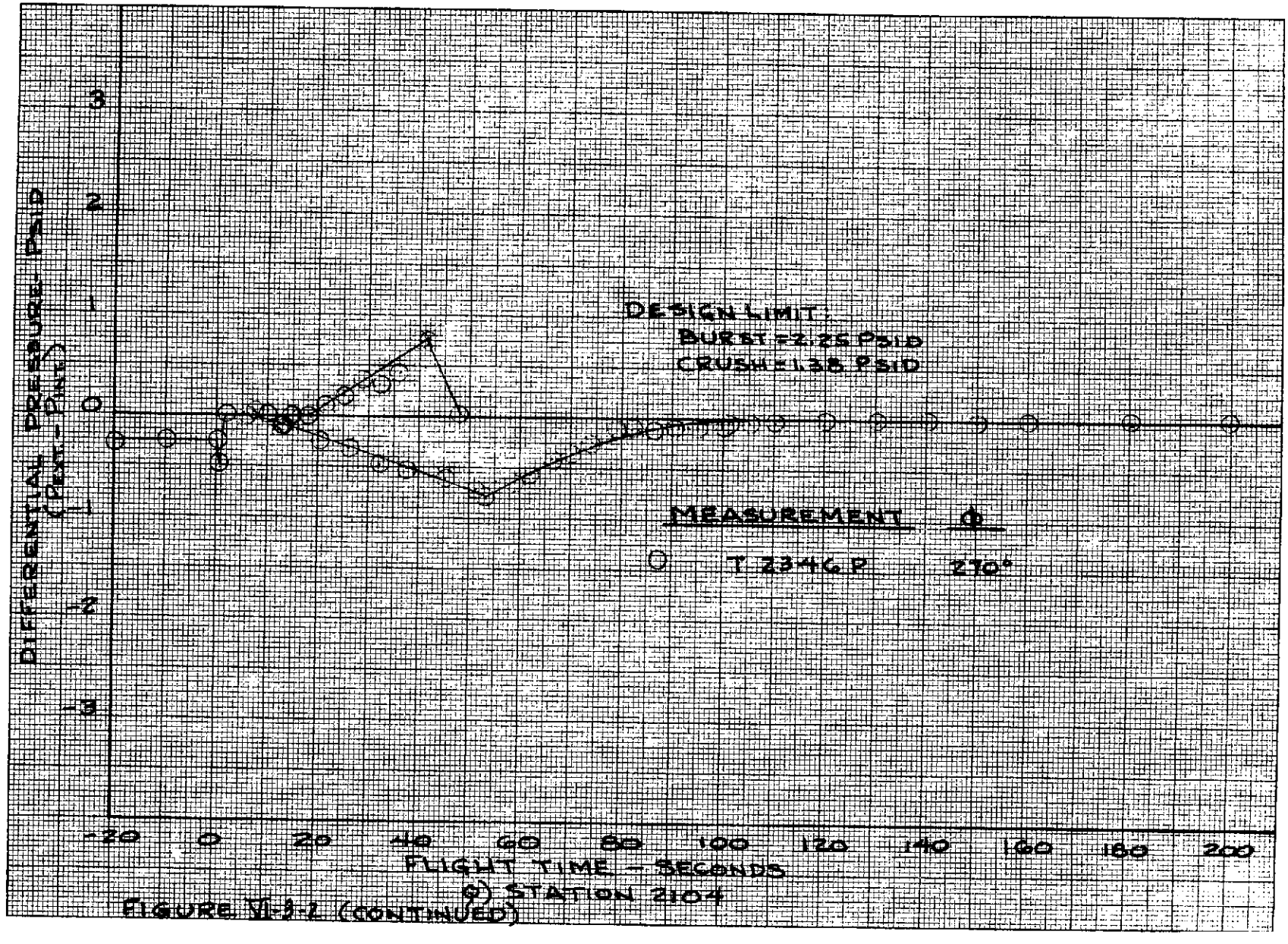

FIGURE VI-3-2 (CONTINUED)

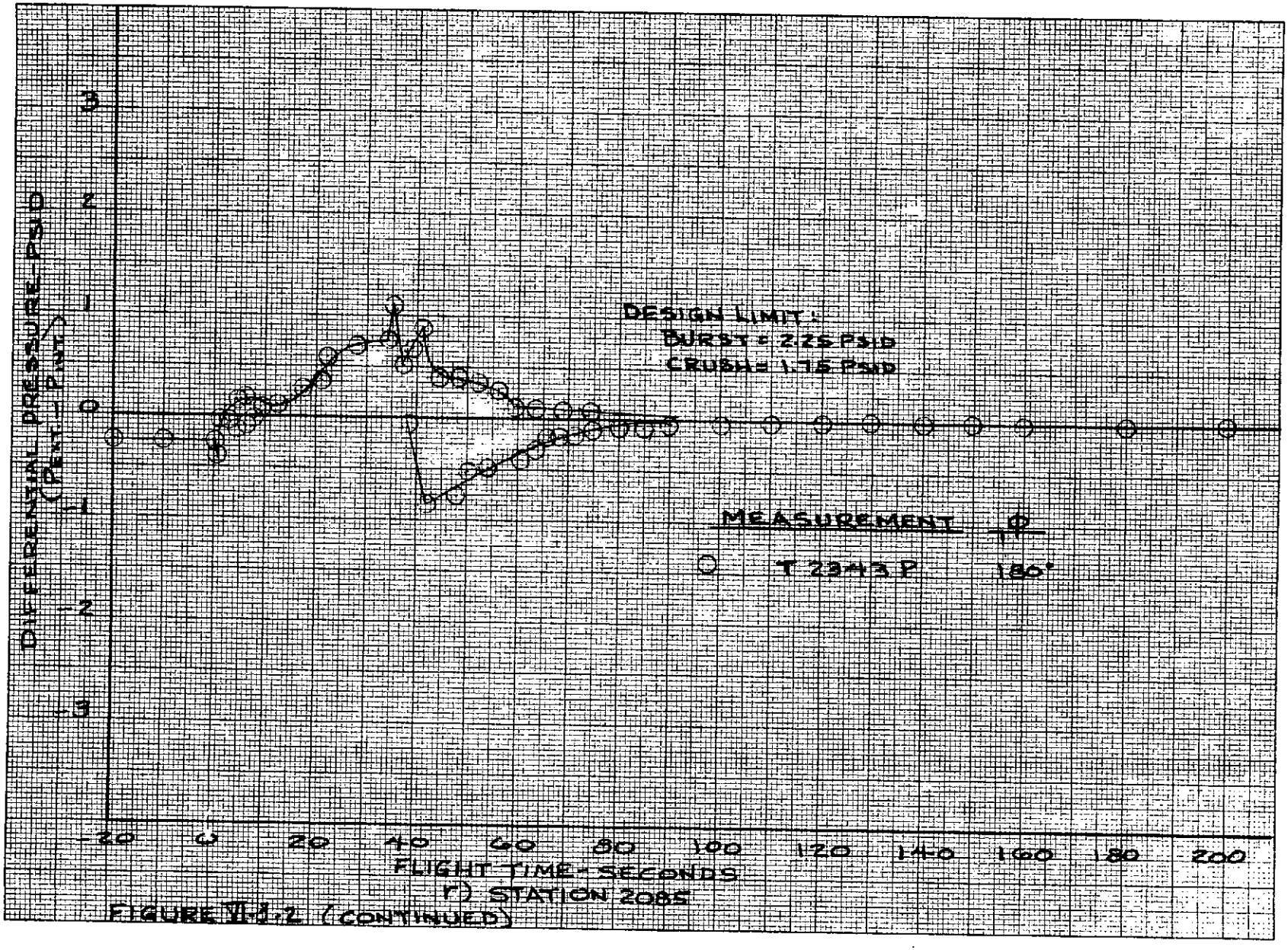

r) STATION 2085

FIGURE VI-3-2 (CONTINUED)

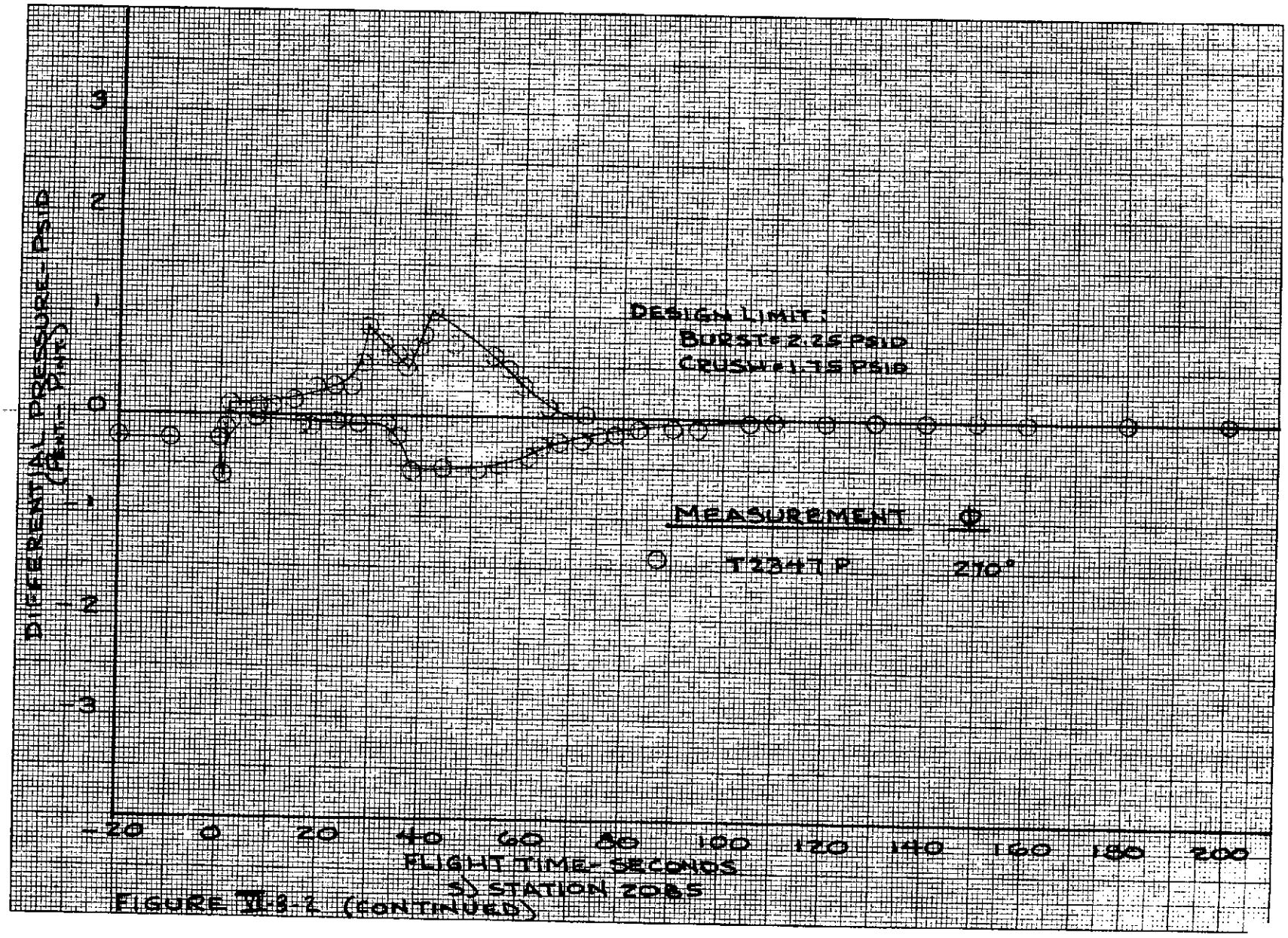

FIGURE VI-3-2 (CONTINUED)
3) STATION 2085

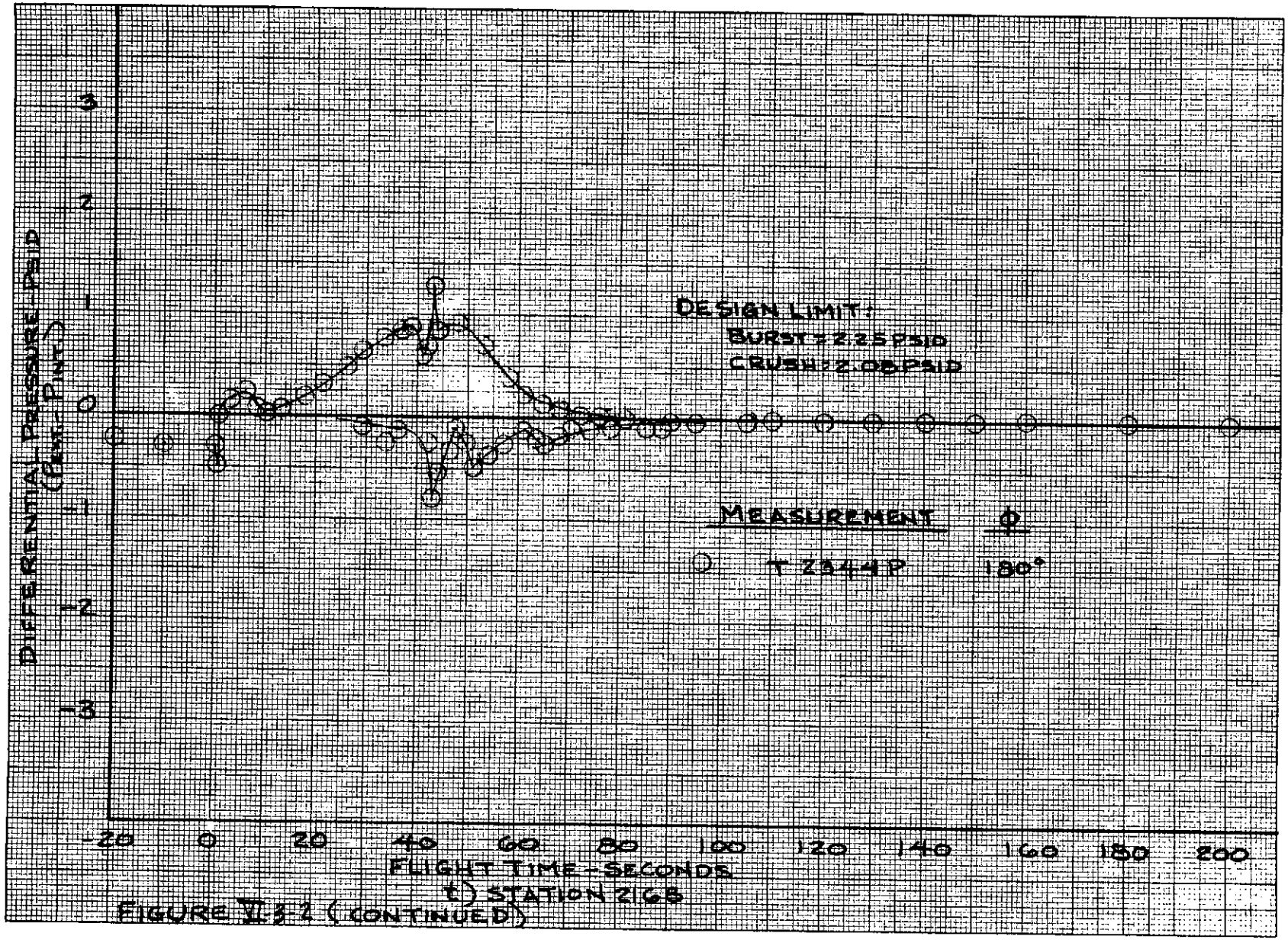

t) STATION 2165

FIGURE VI-2 (CONTINUED)

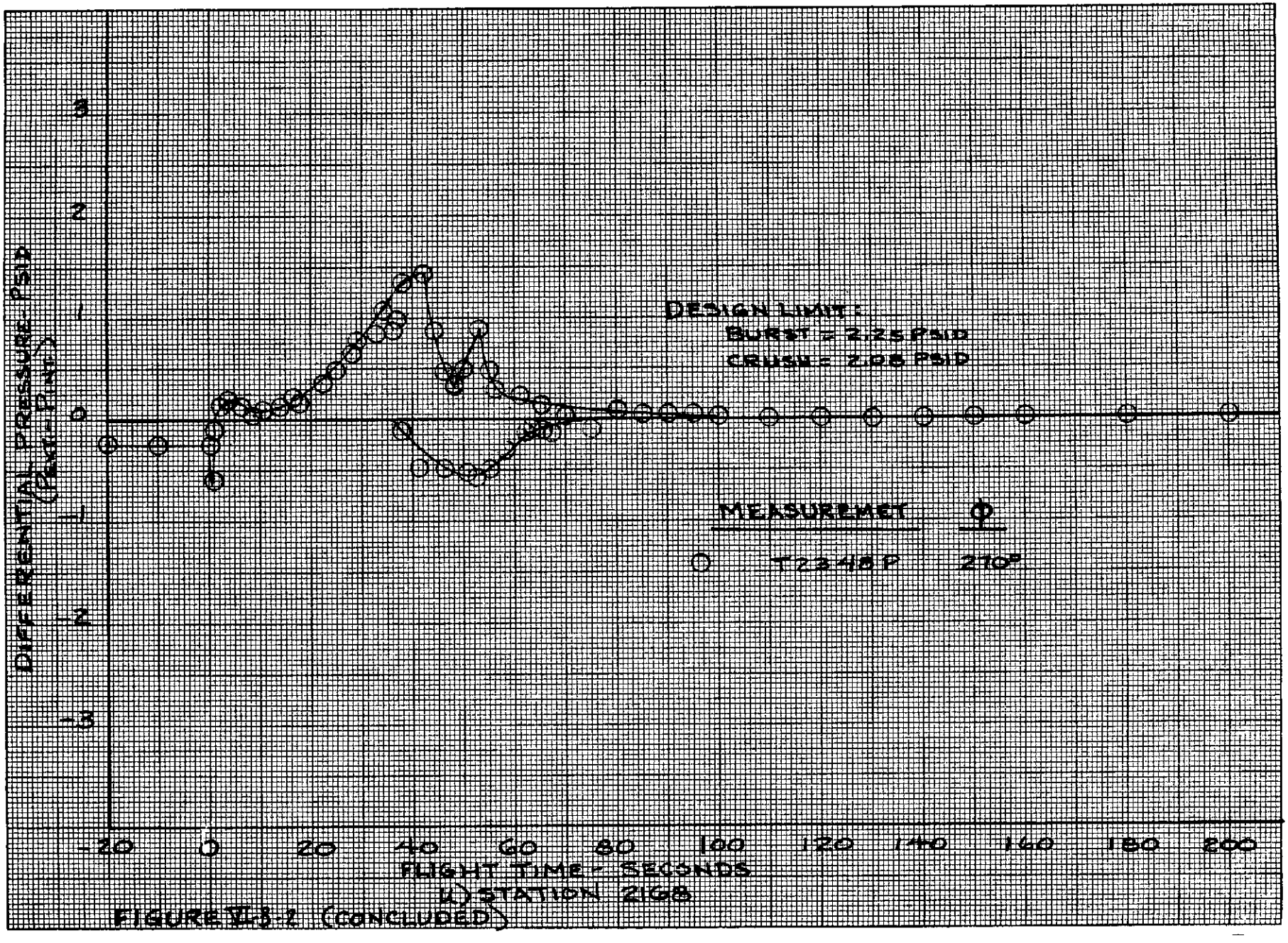

FIGURE VI-3-1 (CONCLUDED)

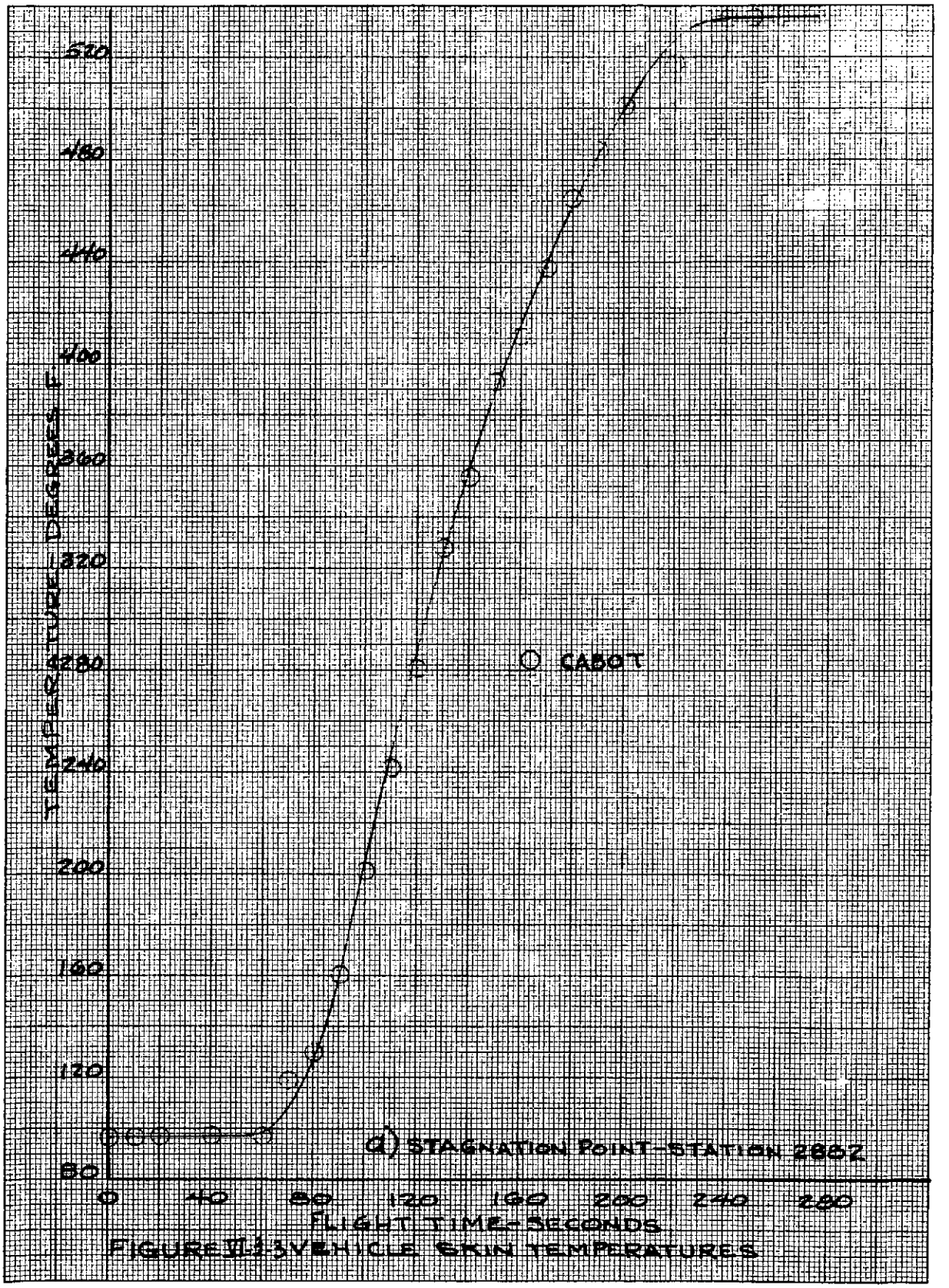

FIGURE VI-3 VEHICLE SKIN TEMPERATURES

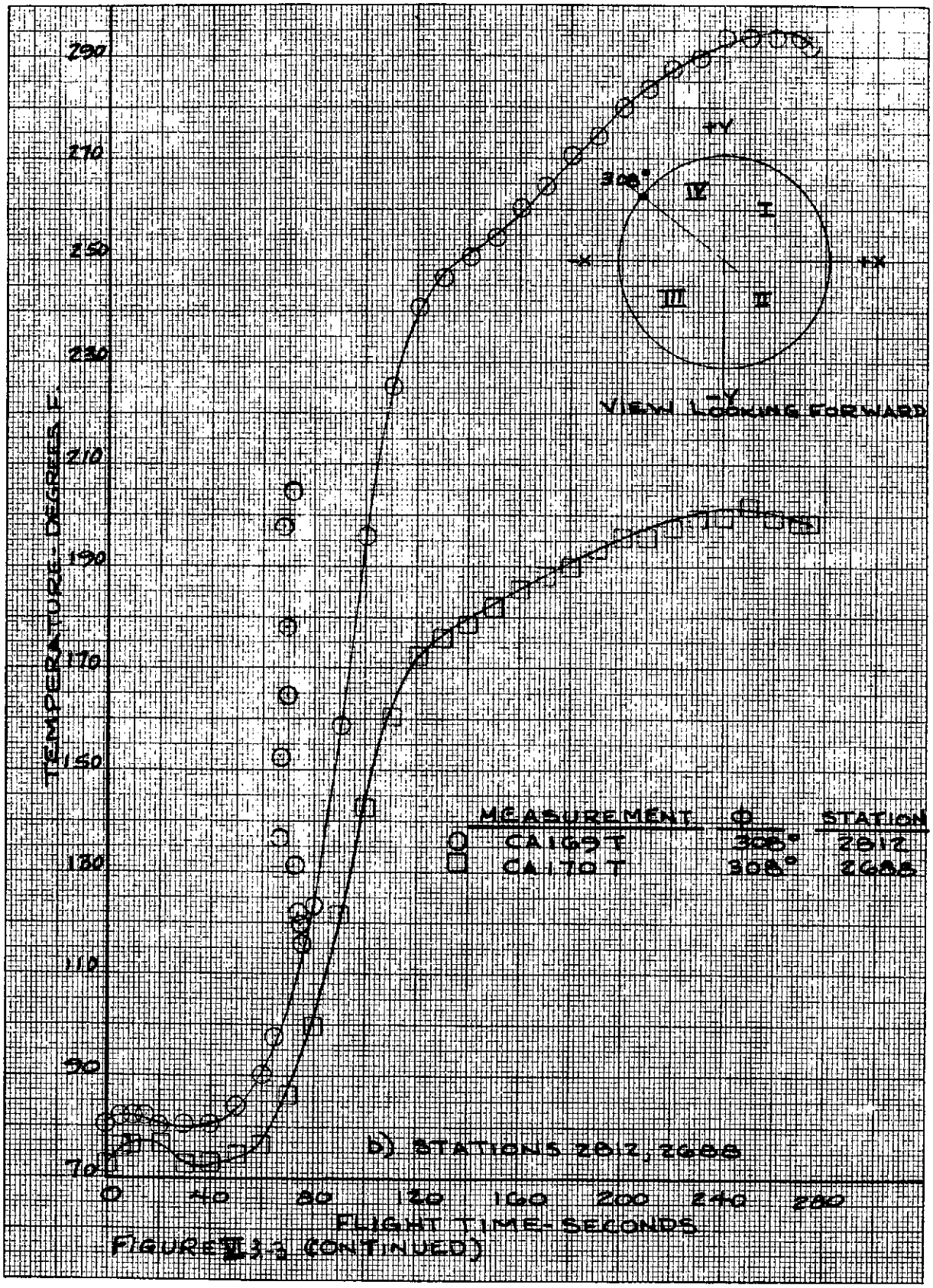

FIGURE VI-3-3 (CONTINUED)

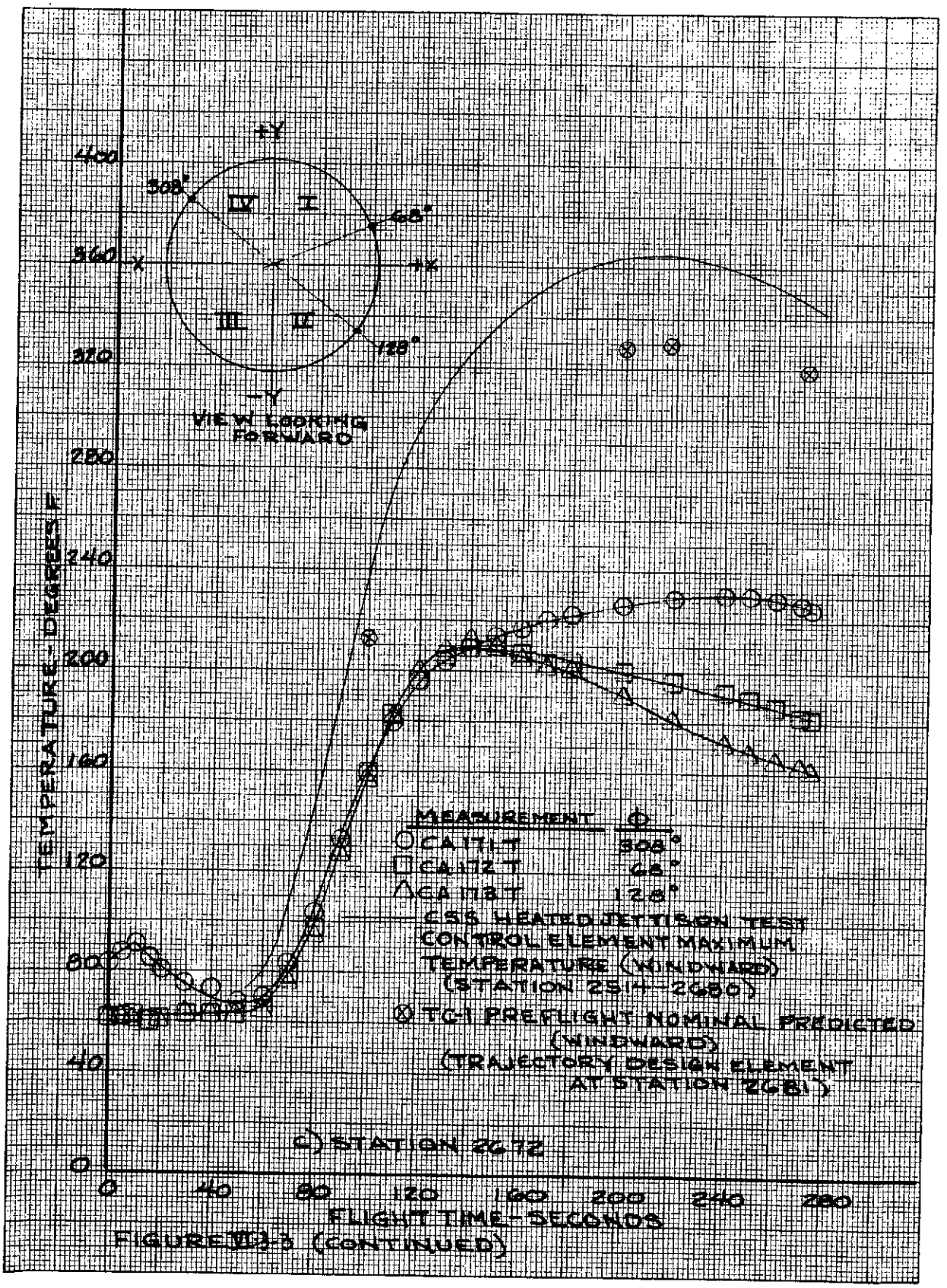

FIGURE VI-3 (CONTINUED)

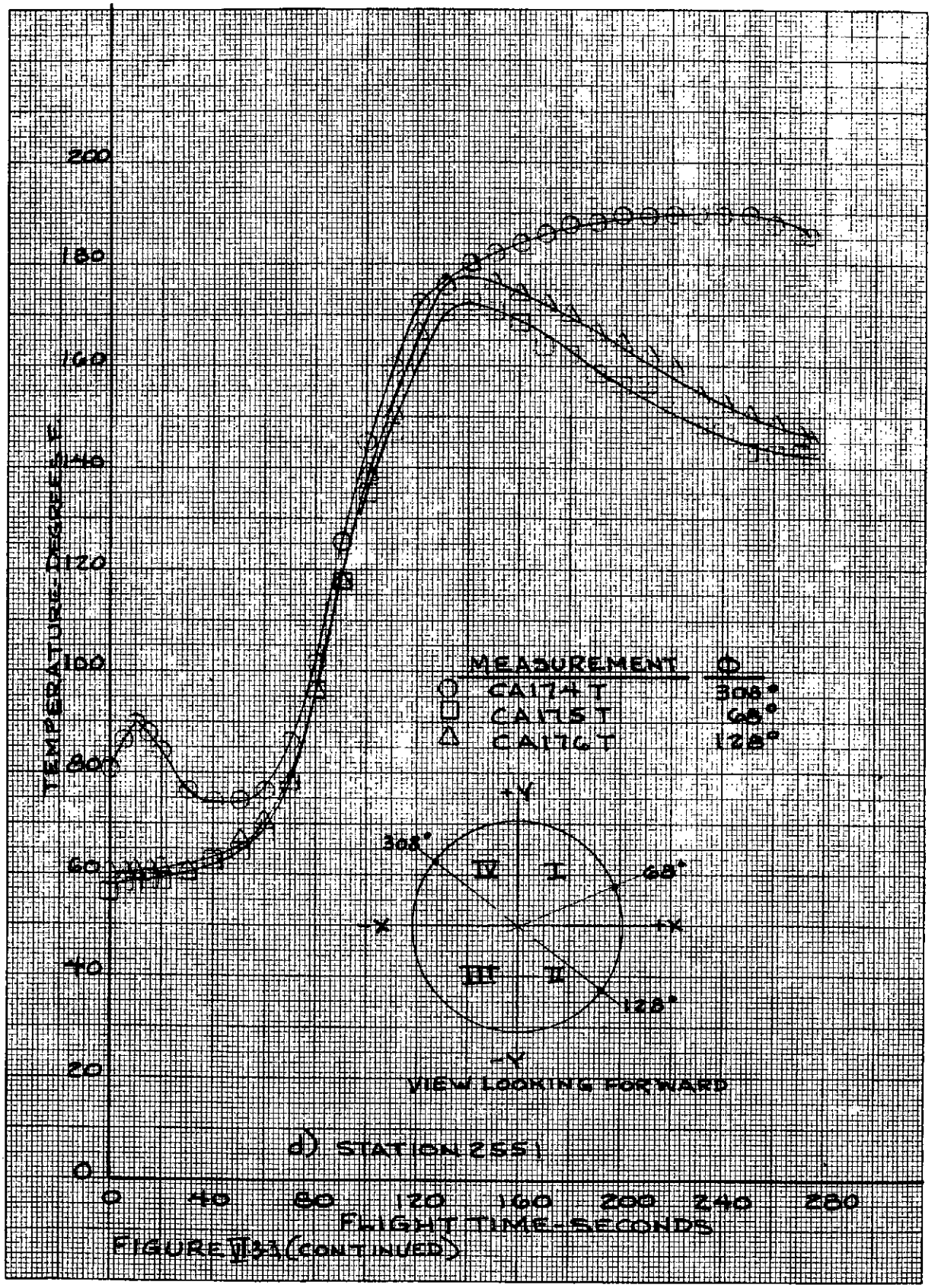

FIGURE VI-34 (CONTINUED)

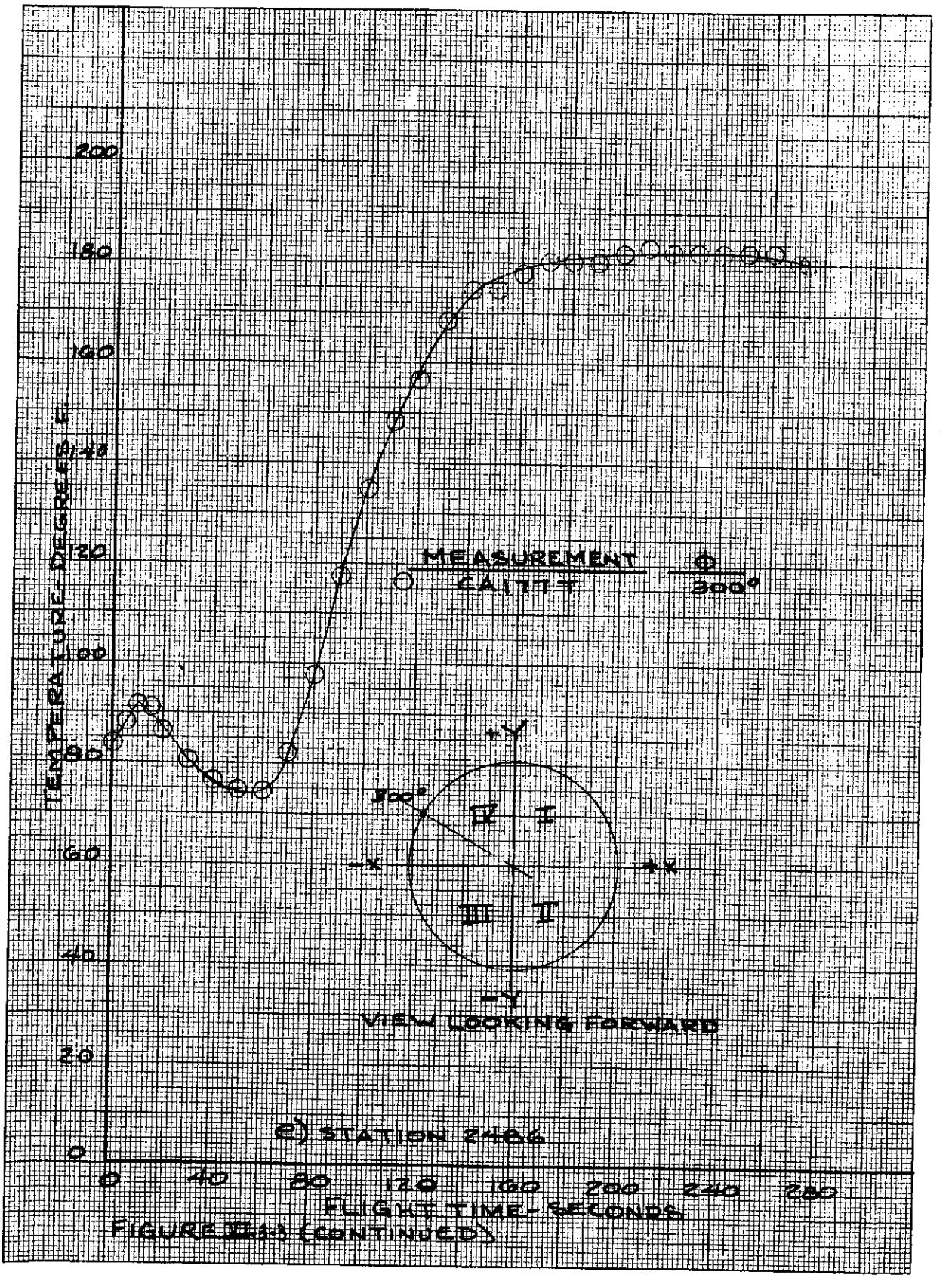

FIGURE VI-13 (CONTINUED)

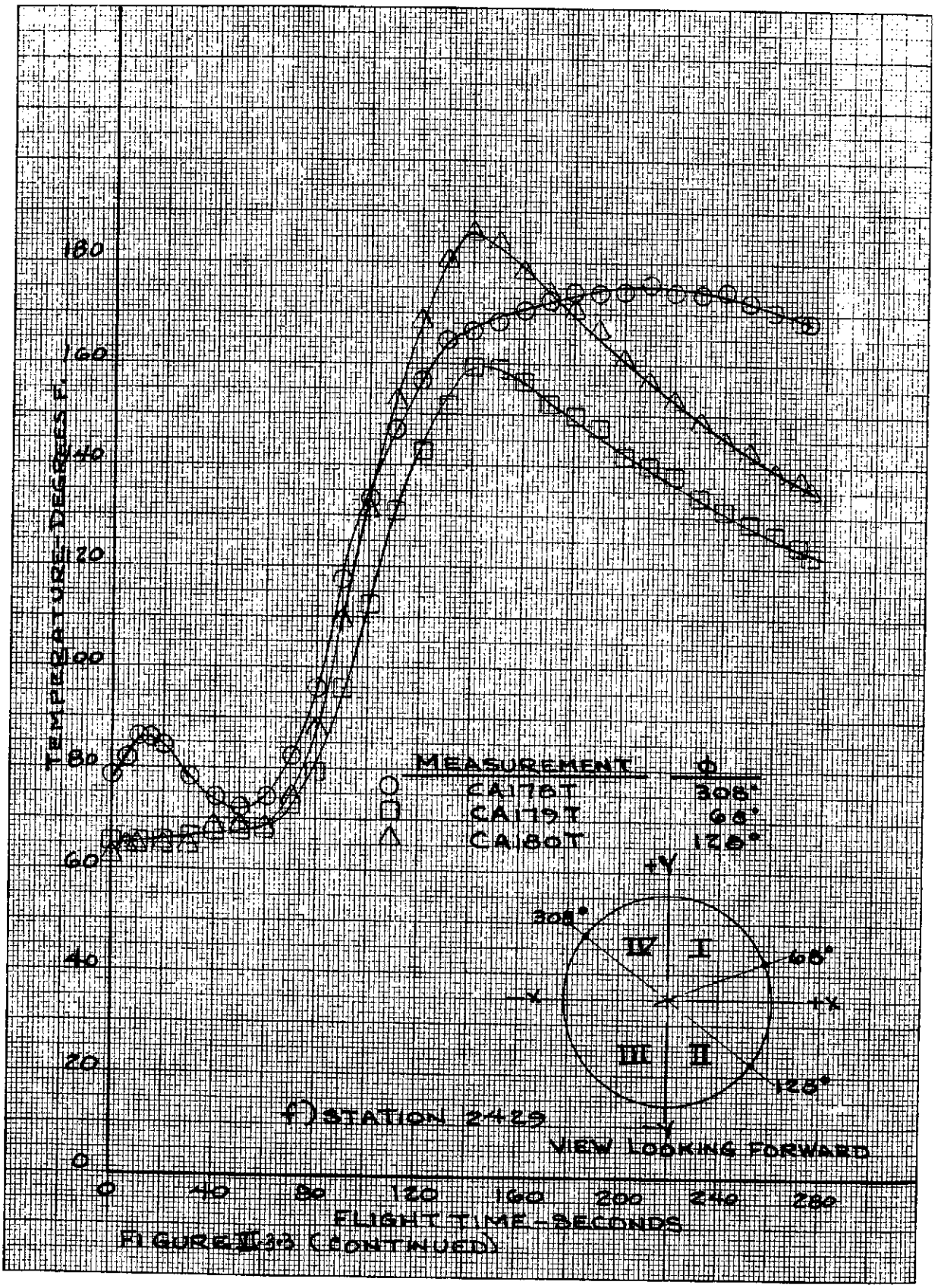

FIGURE VI-33 (CONTINUED)

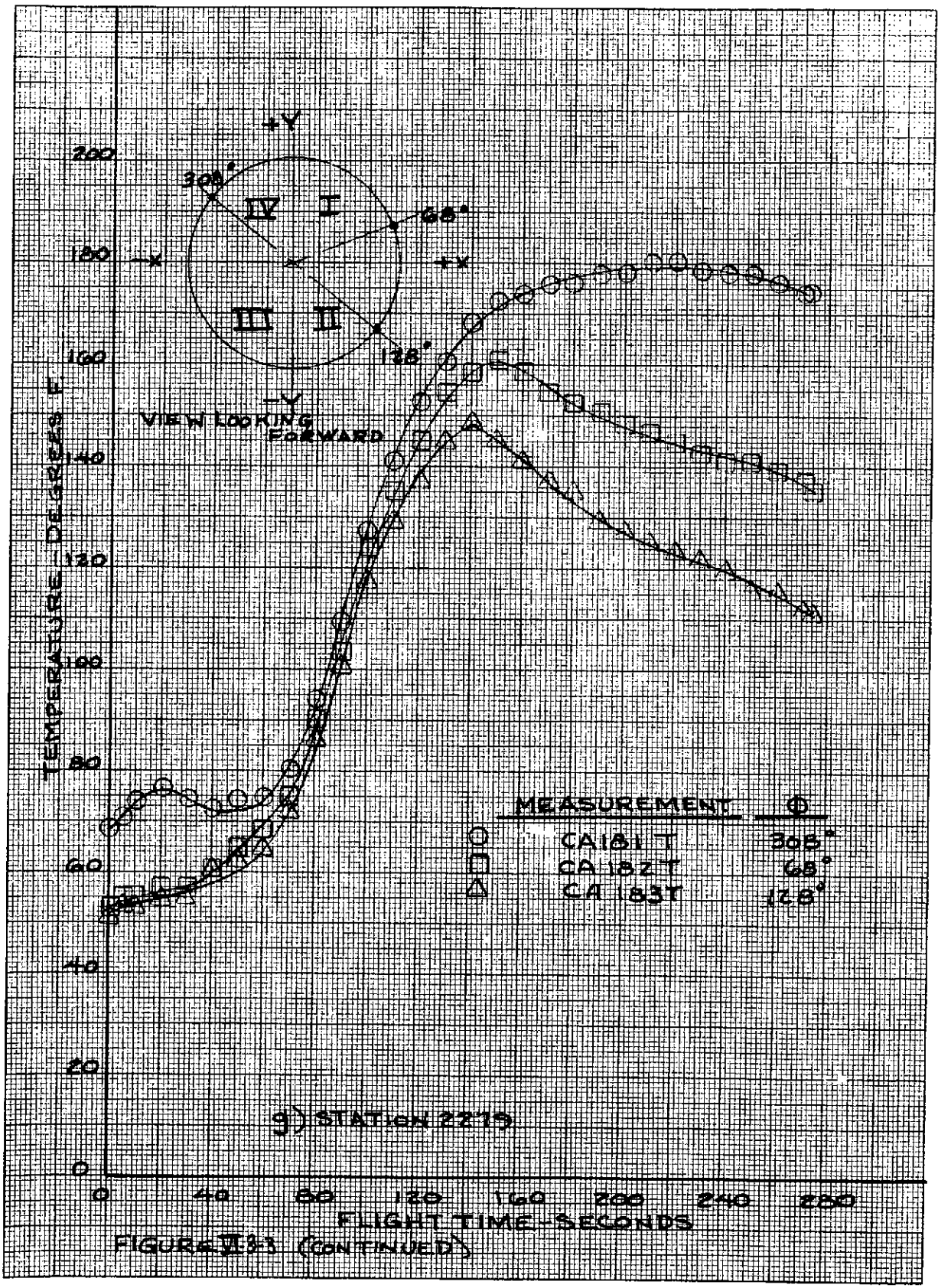

FIGURE VI-3-3 (CONTINUED)

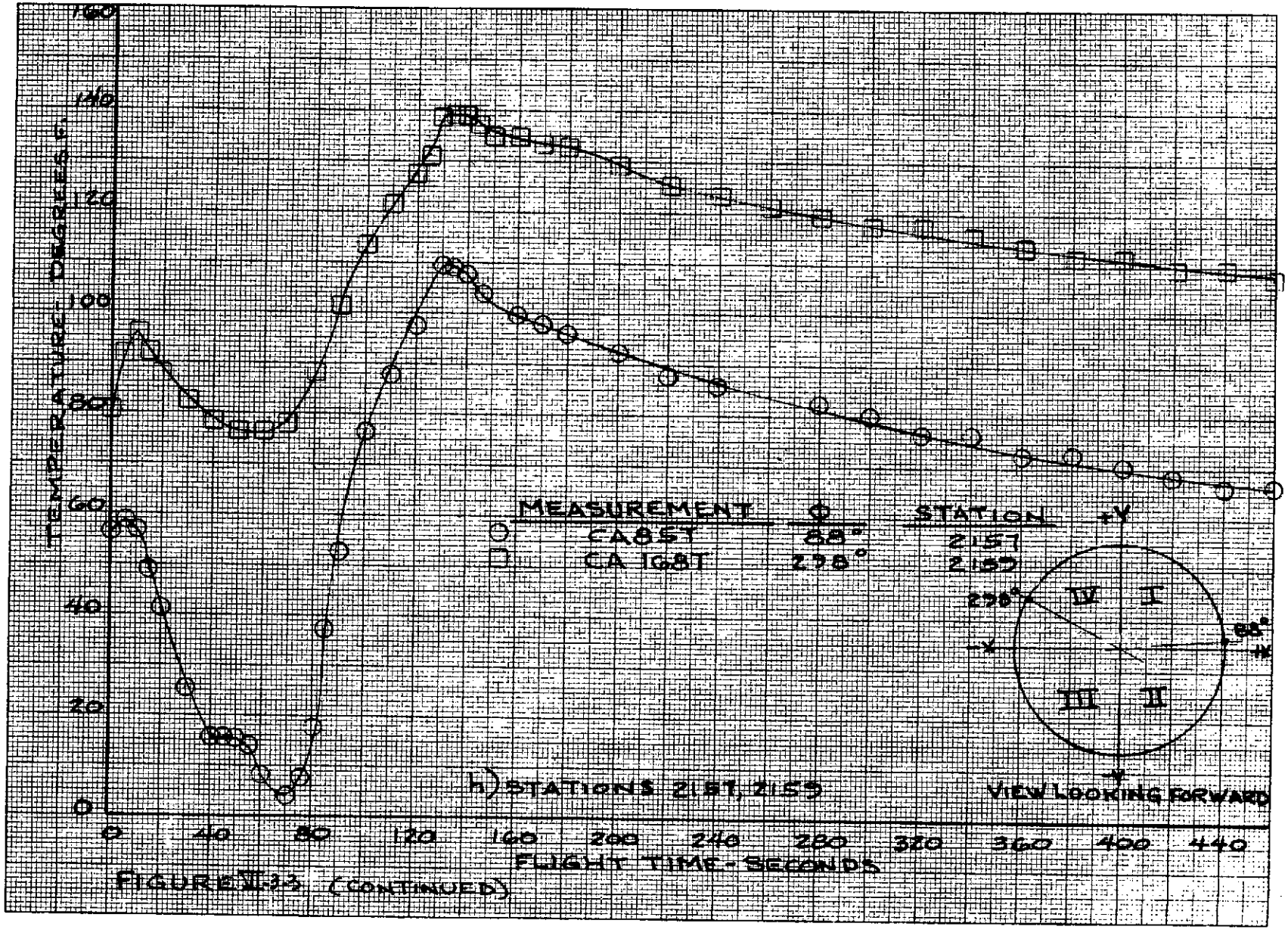

FIGURE XI-23 (CONTINUED)

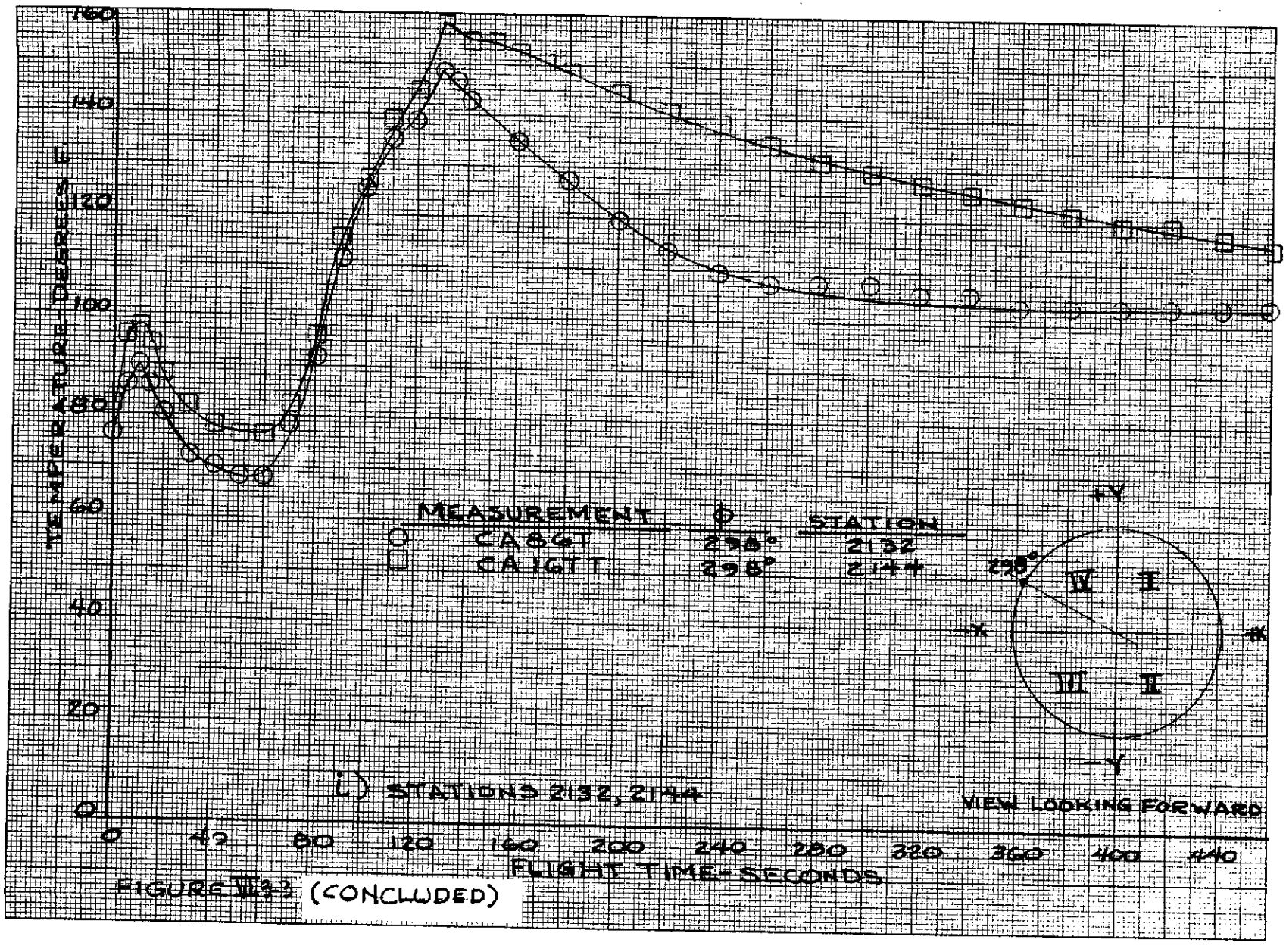

L) STATIONS 2132, 2144

FIGURE III-3 (CONCLUDED)

VI-4. CSS STRUCTURES

by C. W. Eastwood and G. S. Sarvay

Summary

Structural loading on the Centaur Standard Shroud from acceleration, wind loading, and dynamic pressure were all within allowable values. Stresses induced by thermal effects and differential pressures across the shroud walls were also below maximum design values.

Instrumentation

The flight loads both axial and bending moments on the shroud were calculated from structural strains that were sensed by strain measurements composed of strain gage arrays. Near the aft end of the shroud, four arrays were located at Station 2294 and spaced 90° apart at azimuths 24°, 114°, 204°, and 294° as shown in figure VI-4-1. Each array consisted of four uniaxial gages mounted on the exterior skin corrugations and connected electrically as shown in figure VI-4-2. The circuit compensated for temperature variations but, also, gave an augmented signal voltage output which was corrected by the data reduction equations. The strain measurements were installed on the shroud prior to build-up on the vehicle and were zeroes after erection on the launch pad. Consequently, the tare weight of the shroud (5000 lb) forward of the strain gages was nulled-out. Although the value is small compared to the flight maximum load, the data presented has been corrected to include the shroud tare weight.

The Centaur Standard Shroud (CSS) external skin temperatures were monitored by thermal transducers that were located on the inner surfaces of the shroud skins. The flight measurement locations are illustrated in figure VI-4-3.

The CSS external wall and compartment differential pressures were obtained by pressure transducers located internal to the shroud walls. Figure VI-4-4 illustrates the locations of the flight transducers for the various compartments within the shroud shell as well as those across the shroud outer walls.

Flight Performance

The maximum combined loads on the shroud at Station 2294 occurred at T + 46 seconds. The equivalent axial load at that time was 150 400 pounds on the compression side and 105 600 pounds tension load on the opposite side. Of this equivalent axial compressive load, 22 400 pounds were direct axial load and 128 000 pounds were from a bending moment of 5.38×10^6 inch pounds. The direct axial load was composed of 13 800 pounds of aerodynamic loading and 8600 pounds of inertia loading from the vehicle

acceleration of 1.76 g. The shroud effective compressive shear azimuth was 312°.

Axial equivalent loads, direct axial loads, and bending moments through transonic flight are listed in table VI-4-1. Loads applied to the test shroud with and without the FBR system installed also are included in the table for comparison. As shown, the flight bending moments and the total equivalent axial loads were less than 40 percent of limit load test maximum values.

The measured flight strains were small with the maximum value less than 15 percent of the instrument range. As a consequence, the normal instrument error of ±2 percent of full scale was a significant part of the measured strains. Because the strains were produced by a combination of axial load and bending moment, the error for either was correspondingly greater. In particular, the accuracy of the portion of the strain produced by the axial loads, being less that 4 percent of the instrument range, was severely reduced. The accuracies of maximum values were approximately ±50 percent for the axial loads and ±20 percent for the bending moments.

Temperatures. - The maximum flight values, including the circumferential distribution are compared with the maximum design values in table VI-4-2. An evaluation of the data shows that the maximum flight skin temperatures ranged between 33 to 51 percent below the maximum design values. Therefore, the actual flight environment did not appreciably degrade the structural material properties or induce any severe thermal stresses.

Pressures. - Tables VI-4-3 and VI-4-4 show the comparisons between maximum obtained flight values with maximum predicted and structural design values. A review of the data reveals that, in some instances, the flight values exceeded the preflight predictions, however, the flight values were well below the limit structural design values. Therefore, it is concluded from the evaluation of flight data, that the actual flight pressure load environment was below the Centaur Standard Shroud's performance capability.

TABLE VI-4-1. - CSS STRUCTURAL FLIGHT LOADS AND LIMIT TESTS LOADS AT STATION 2294 (INCLUDES WEIGHT OF SHROUD FORWARD OF STATION 2294 IN ALL AXIAL VALUES)

Flight event	Nominal time, sec	Total axial load, lb C=Compress. T=Tension	Bending moment, in. lb x10^{-6}	Vehicle acceleration, g	Total equivalent axial load at extreme fiber, lb	
					Compression	Tension
Zero reference	T - 1	5 000 C	0	1.00	5 000	-------
	T + 5	51 300 C	1.96	1.54	97 900	-------
Transonic	T + 46	22 400 C	5.38	1.76	150 400	105 600
	T + 64	43 600 C	1.31	1.88	74 800	-------
Test limit loads with FBR		24 300 C	14.0	1.00	357 600	309 000
Test limit loads without FBR		94 600 C	17.0	1.00	499 100	309 900

TABLE VI-4-2

CENTAUR STANDARD SHROUD SKIN TEMPERATURES

	MEASUREMENT NUMBER	STATION/AZIMUTH	FLIGHT TEMPERATURES °F (MAXIMUM)	DESIGN TEMPERATURES °F (MAXIMUM)
	CA80T	2822/0°	498	> 900
	CA169T	2812/308°	300	450
	CA170T	2688/308°	216	370
	CA171T	2672/308°	235	390
	CA172T	2672/68°	216	
	CA173T	2672/128°	216	
	CA174T	2551/308°	197	390
	CA175T	2551/68°	179	
	CA176T	2551/128°	184	
	CA177T	2486/300°	188	360
	CA178T	2429/308°	179	390
	CA179T	2429/68°	160	
	CA180T	2429/128°	188	
	CA181T	2279/308°	188	350
	CA182T	2279/68°	170	
	CA183T	2279/128°	150	
*	CA184T/CA185T	2812/0°	282/132	350
*	CA186T/CA187T	2688/0°	221/122	350

* SUPER*ZIP DOUBLERS TEMPERATURE.

CO-TA

TABLE VI-4-3

COMPARTMENT DIFFERENTIAL PRESSURES

MEASUREMENT NUMBER	COMPARTMENT Δ P	DIRECTION OF Δ P	MAXIMUM FLIGHT Δ P (PSI)	PREDICTED Δ P (PSI)	LIMIT STRUCTURAL DESIGN Δ P (PSI)
	(1) (2/3)	NO SPACECRAFT COMPARTMENT			
CA882P	(4A) (2/3)	FORWARD	1.20	0.95	3.0
CA877P	(4) (2/3)	FORWARD	1.00	0.95	2.9
CA883P	(4) (5)	AFT	0.60	1.20	2.8
TA2208P	(5) (6)	AFT	0.15	0.30	1.0

TABLE VI-4-4

CSS WALL DIFFERENTIAL PRESSURES

MEASUREMENT NUMBER	STATION	DIRECTION OF PRESSURE	FLIGHT Δ P (PSI) (MAX.)	PREDICTED Δ P (PSI)	LIMIT STRUCTURAL DESIGN Δ P (PSI)
CA421P CA422P CA423P CA424P	2750	CRUSH	1.70 1.60 1.80 1.40	0.60	4.0
CA419P	2678	BURST	5.30	5.85	6.95
CA418P	2597	BURST	2.84	3.50	5.50
CA126P CA127P CA128P CA129P	2485	BURST	1.25 1.25 1.40 1.40	2.20	3.45
CA417P	2380	BURST	1.82	—	3.8
CA411P CA412P CA413P CA414P	2221	BURST	0.1 0.2 0.1 0.0	—	2.0
CA411P CA412P CA413P CA414P		CRUSH	0.10 0.05 0.10 0.05	—	1.5

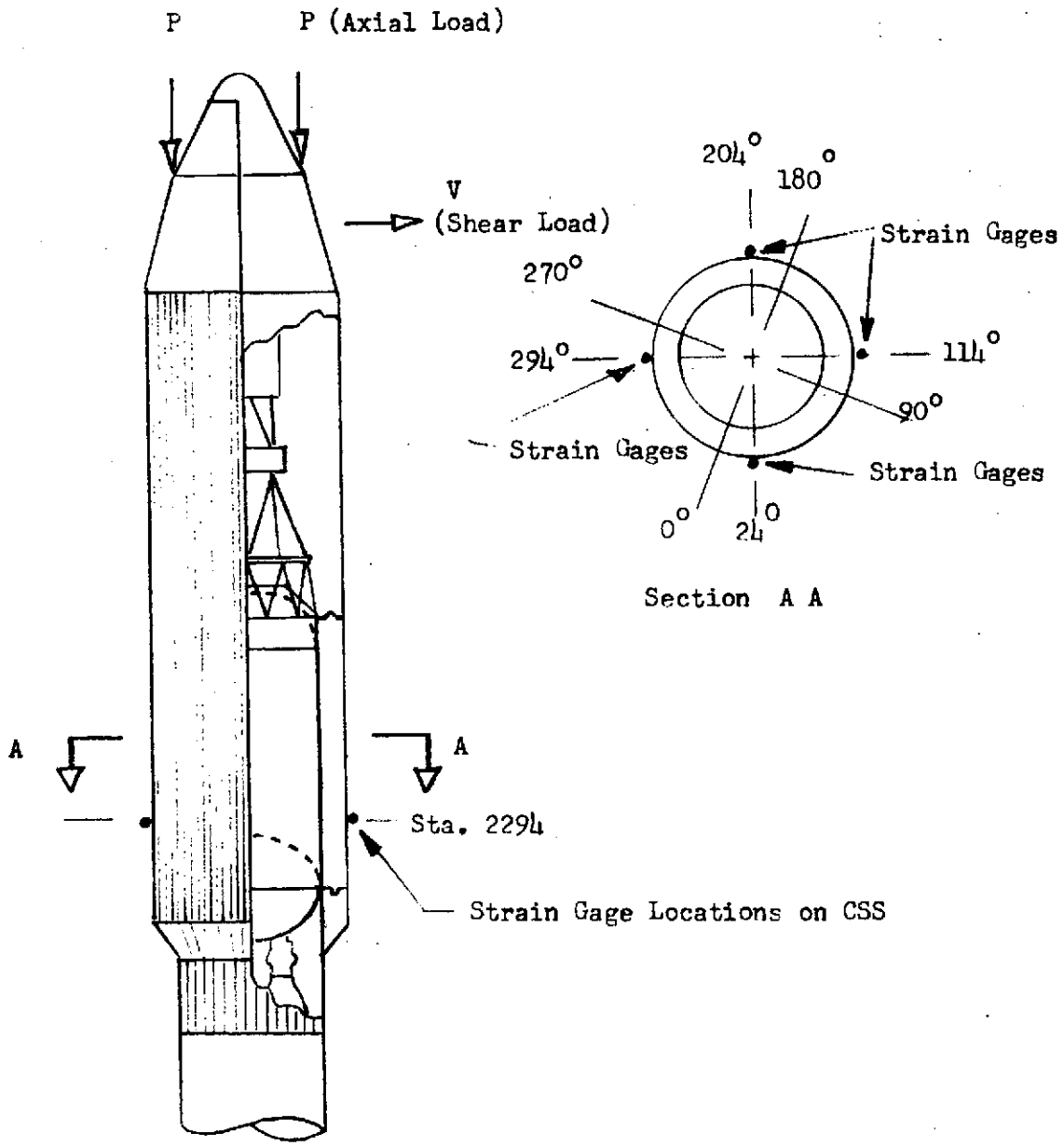

FIGURE VI-4-1 Structural Strain Measurement Locations on CSS.

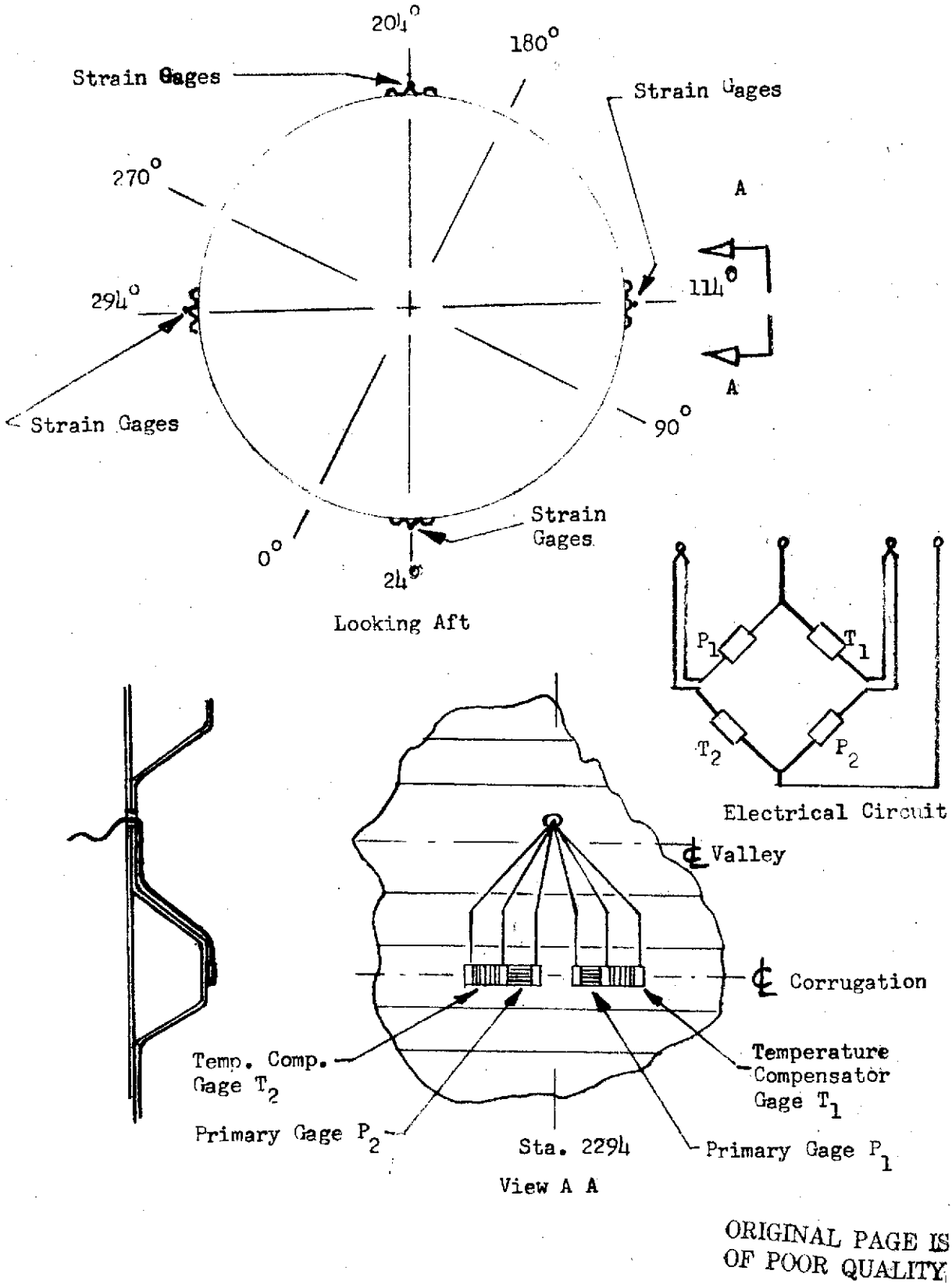

Figure VI-4-2 . Centaur Standard Shroud Structural Strain Gages.

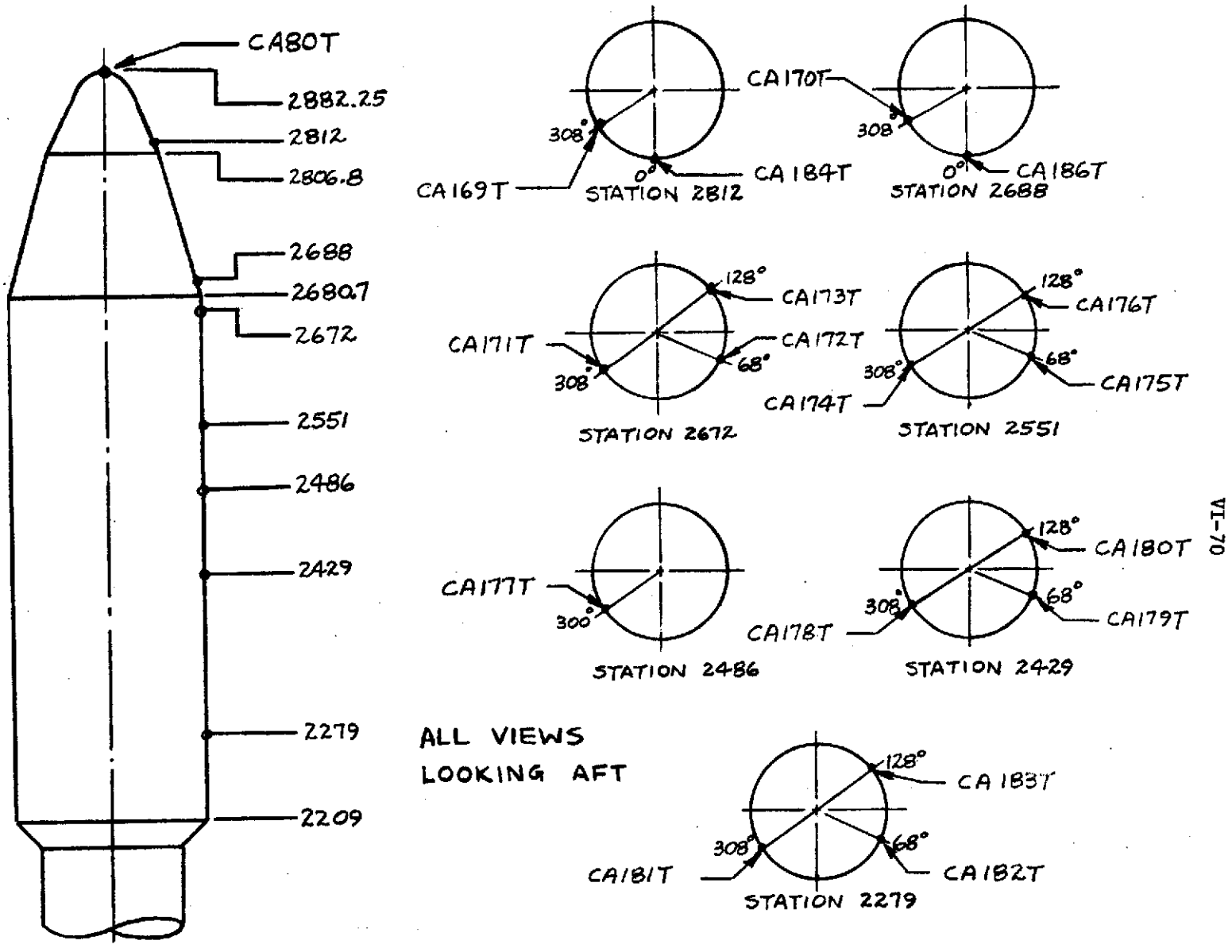

FIGURE VI-4-3 CSS SKIN TEMPERATURE MEASUREMENTS

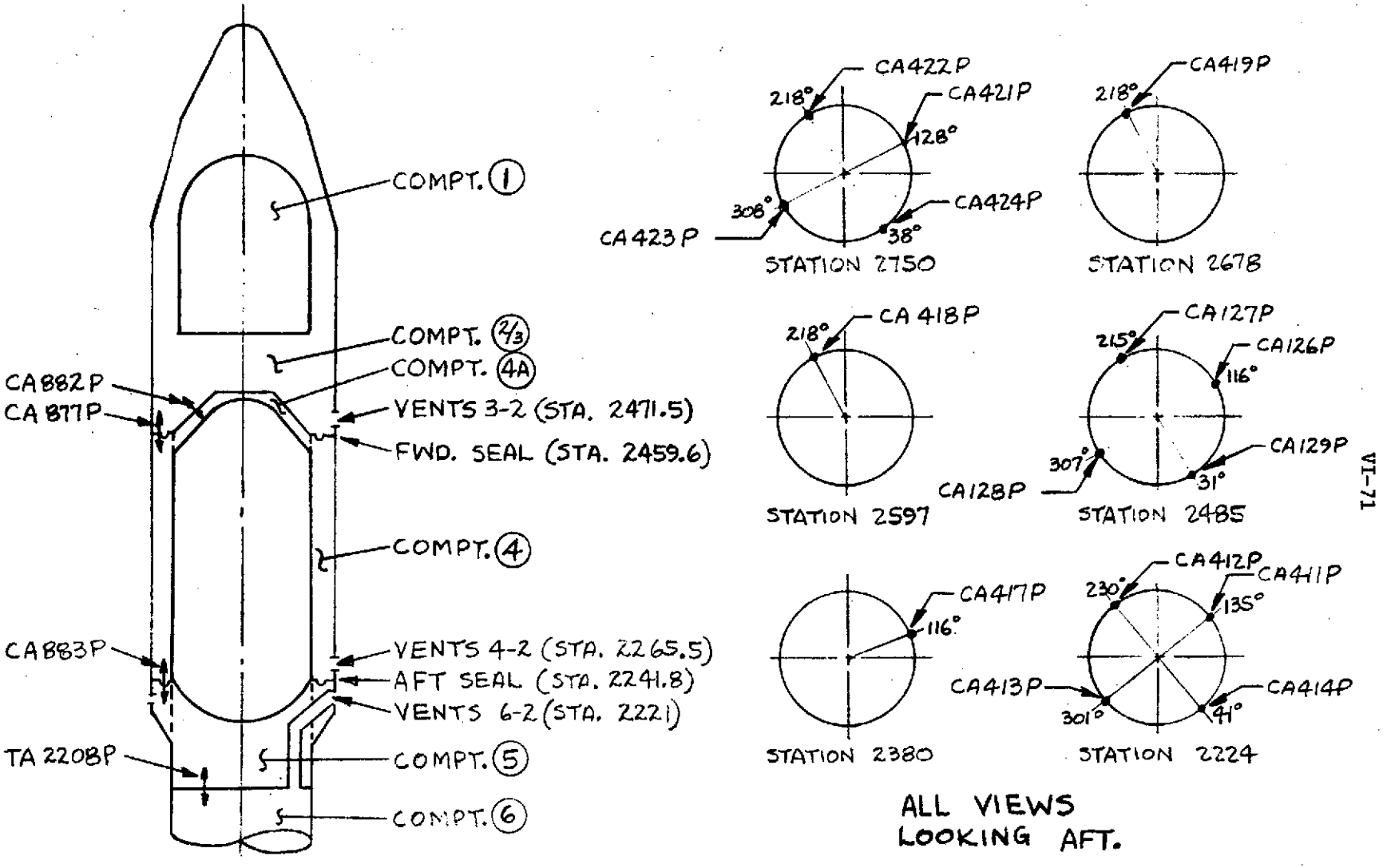

FIGURE VI-4-4 CSS COMPARTMENT AND WALL PRESSURE MEASUREMENTS

VI-5. CSS INFLIGHT EVENTS AND JETTISON

by T. L. Seeholzer and C. W. Eastwood

Summary

The CSS inflight events of forward bearing reaction strut separation and forward seal release were accomplished without incident. Separation of the pyrotechnic (Super-Zip) joints on the CSS and jettison of the CSS were also accomplished satisfactorily.

System Descriptions

Forward bearing reactor struts. - Separation of the six forward bearing reaction struts was accomplished by redundant explosive bolts as shown in figure VI-5-1. Following bolt separation, the strut halves were retracted against the CSS by a spring loaded retractor and against the stub adapter by a tension spring as shown in figure VI-5-2. Explosive separation bolts were located as shown in figure VI-5-2. Bolt separation was caused by actuation of two electro-explosive devices (cartridge). Firing of either cartridge will separate the bolts. Pressure produced by the cartridge was converted into a force by means of two pistons and a silicone rubber force amplifier. The resultant force fractured the bolts in the grooved area. This bolt had been successfully employed on the Atlas/Centaur vehicle for nose fairing separation.

Forward seal. - The forward seal, illustrated by figure VI-5-3 was located at Station 2454 between the CSS and Centaur stub adapter. The seal consisted of a silicone rubberized dacron fabric attached to the stub adapter by bolts and retained on the CSS forward bulkhead by a cable and retaining mechanism. A 5/16-inch diameter segmented teflon bead on the outboard edge of the seal held the seal under the cable.

A redundant explosive bolt was employed to release the seal. This is the same bolt as used for forward bearing reaction separation, see figure VI-5-1. Two bolts, one at each split line, were attached to the seal retaining cable as shown in figure VI-5-3. When the bolts separated the cable tension was relaxed and the seal released. Seal release assist retractors were located around the periphery of the seal to assist in raising the seal bead over the retainer lip as shown in figure VI-5-4. Two seal retractors were located at the LH_2 vent nozzles to insure seal retraction over the nozzles.

CSS separation system (Super-Zip). - The Super-Zip separation systems, both primary and secondary, are shown in figures VI-5-5 and 6. The systems incorporate a longitudinal and circumferential joint consisting of two explosive cords in a stainless steel tube as shown in figures VI-5-7 and 8. When either cord is ignited, the resultant pressure expands the tube and fractures the frangible doublers.

The secondary system is fired 0.5 second after primary command only in the event the primary system fails to separate the shroud. Each joint is redundantly actuated by electric detonators as shown in figures VI-5-9 and 10. At payload section, there are detonation transfer lines which bridge the field joint and fire the cord by means of nonelectric detonators.

Jettison of the CSS following joint separation is accomplished by eight jettison springs located at the base of the CSS and four helper springs on the split lines as shown in figure VI-5-11.

The shroud jettison strains were sensed by strain measurements and the strains converted to stress values. Because of the complexity of the jettison loads on the shroud hinges combined with the limitation of the available instrumentation, the loads on the hinges were assessed by comparing flight strains in the aft hinge support longerons to those experienced in the shroud jettison tests and the hinge static load tests.

Strain gage arrays were located on the aft hinge longeron webs. Each array consisted of four uniaxial gages centered on Station 2187 and electrically connected to compensate for temperature variations and to give augmented signal voltage output as shown in figure VI-5-12.

Systems Performance

Forward bearing reaction. - Forward bearing reaction (FBR) system separation was nominally programmed to occur at T + 100 seconds. At this time, the vehicle has passed through the period of maximum loading. FBR separation actually occurred at T + 99.7 seconds. Separation of all six struts was verified by breakwires across the strut separation planes.

FBR load, at time of separation, was estimated to be 1200 pounds from the CSS/payload extensiometers mounted from the forward end of the Viking Dynamic Simulator to the Centaur Standard Shroud.

Forward seal. - Forward seal release occurred at T + 214.8 seconds. Breakwires mounted across each explosive bolt housing verified the bolts separated at this time releasing the seal retaining cable. Nominal jettison of the Centaur Standard Shroud verified the seal had completely released.

CSS separation system and jettison. - At T + 273.63 seconds the Super-Zip primary system actuated and separated the CSS from the vehicle. The jettison springs rotated the CSS halves on the hinges until the shroud jettisoned free of the Titan/Centaur vehicle 2.8 seconds later. Reference table VI-5-I breakwires listed in table VI-5-I provided time for 3°, 8°, and 32° CSS half rotation. The time for 3° and 8° angles of rotation are approximately the same for each half indicating a nominal separation and jettison function. At 32° rotation the capped or heavy

half time is 0.2 second longer than the uncapped half which is normal performance.

Primary system separation of the CSS was verified by comparison of command times, accelerometer data, hinge strain data, and breakwire/disconnect data. Table VI-5-2 lists the command times for the primary and secondary systems. At T + 273.63 seconds accelerometers and hinge strain gages verify the Super-Zip primary system fired coincident with primary system command. The secondary system command occurred at 274.13 seconds (as programmed). Also, as per configuration, the secondary system did not fire since the CSS had already rotated over 8°, and disconnected the electrical lines which transmit power to the secondary detonators. This disconnect occurred at approximately 1.0° of CSS rotation.

Prior to shroud jettison, stresses in the aft hinge longerons were small in value as expected. The hinge longerons are designed primarily for loading at shroud jettison and only peripheral loads are transmitted to them in the course of the flight.

At shroud jettison the stresses in the four aft hinge longerons went from zero to maximum tension values in 0.04 second as follows:

Hinge longeron at 77° azimuth, 2200 psi tension
Hinge longeron at 103° azimuth, 2500 psi tension
Hinge longeron at 257° azimuth, 1800 psi tension
Hinge longeron at 283° azimuth, 1900 psi tension

These values compare to 2900 and 1950 psi maximum tension in the heated/altitude jettison tests numbers 1 and 2, respectively, and to 6080 psi maximum in the hinge static load test.

The hinge longeron stresses were oscillatory tension stresses during the initial phase of the jettison event as expected. The oscillations were at approximately 12 hertz with the amplitudes damping to zero by 0.6 second. From 0.6 second until the shroud separated from the vehicle, the hinge longeron stresses were compression stresses of varying magnitudes. The maximum compression stresses were:

Hinge at 77° azimuth, 1000 psi compression
Hinge at 103° azimuth, 1300 psi compression
Hinge at 257° azimuth, 800 psi compression
Hinge at 283° azimuth, 700 psi compression

By comparison, the maximum stresses in the aft hinge longerons in the numbers 1 and 2 heated/altitude jettison tests were 400 and 500 psi, respectively. The longeron maximum stress value in the hinge static load test was 7750 psi.

Shroud jettison loads as evidenced by aft hinge longeron strains started at T + 274.0 seconds and the last indication of longeron

strains which was associated with completed jettison of the shroud from the vehicle was at T + 276.8 seconds. The duration of shroud jettison was 2.8 seconds and compares to 2.7 seconds in the heated/altitude jettison tests.

Some unsymmetric loading on the hinges was evident from the strain measurement data after the tension loads had diminished. The capped half of the shroud exerted small compression loads on the 77° longeron first and then on the 103° longeron, alternating back and forth in diminishing amplitude for two cycles. The uncapped half developed small compression loads in the 257° longeron first and then alternated the loads with the 283° longeron in diminishing amplitude for $1\frac{1}{2}$ cycles. Data traces of the flight shroud jettison stresses in each aft hinge longeron against time are compared to curves from the heated/altitude jettison tests in figure VI-5-13. As shown, the traces are similar both in magnitude and in stress fluctuation.

The stresses in the aft hinge longerons during shroud jettison were of low value and compared well to the heated/altitude jettison tests data and were considerably less than half of the value of the stresses in the hinge static load test as shown in table VI-5-III.

Because the maximum stress values were only 10 percent of the instrumentation full range, the accuracy of the measurements based on instrument normal error was approximately ±20 percent.

TABLE VI-5-1

CSS BREAKWIRE SUMMARY

BREAKWIRE (ROTATION AND LOCATION)		ACTIVATION TIME (SEC)	SAMPLING RATE (HZ)
3^{o} QUAD I	CAPPED	274.03	697
3^{o} QUAD II		274.05	697
3^{o} QUAD III	UNCAPPED	274.02	697
3^{o} QUAD IV		274.03	697
8^{o} QUAD I-II	CAPPED	274.28	697
8^{o} QUAD III-IV	UNCAPPED	274.35	697
32^{o} QUAD I-II	CAPPED	275.65	139
32^{o} QUAD III-IV	UNCAPPED	275.47	139

TABLE VI-5-2

SUPER*ZIP ACTUATION TIMES

SYSTEM	NOMINAL FIRING TIME	ACTUAL FIRING TIME
PRIMARY	T + 273 SEC	T + 273.63 SEC CENTAUR COMMAND T + 274 SEC
SECONDARY	T + 273.5 SEC	NONE CENTAUR COMMAND T + 274.13 SEC

TABLE VI-5-3

Shroud Jettison Hinge Stresses

in Aft Hinge Longeron at Station 2187.

		Flight Actual				Plum Brook Tests		
		Capped Half (90°)		Uncapped Half (270°)		Heated/Altitude Jettison		Static Structural
	Time (Sec)	77° Hinge	103° Hinge	257° Hinge	283° Hinge	#1	#2	
Max. Tension	T+274.1	2200	2500	1800	1900	2900	1950	6080
Max. Compression	---	1000	1300	800	700	400	500	7750

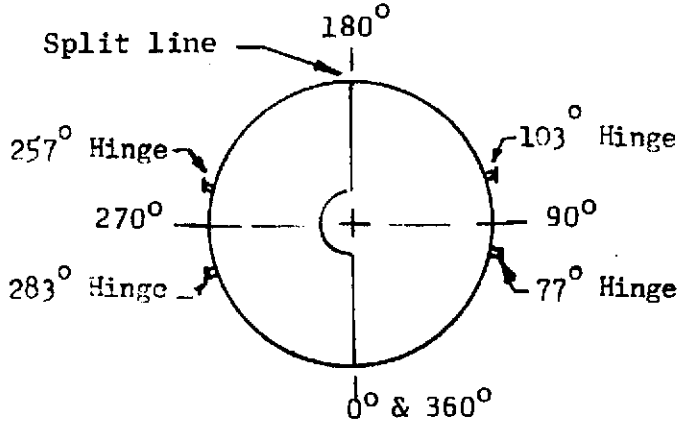

Looking Aft

Jettison Duration: Flight 2.8 Sec
Test 2.7 Sec

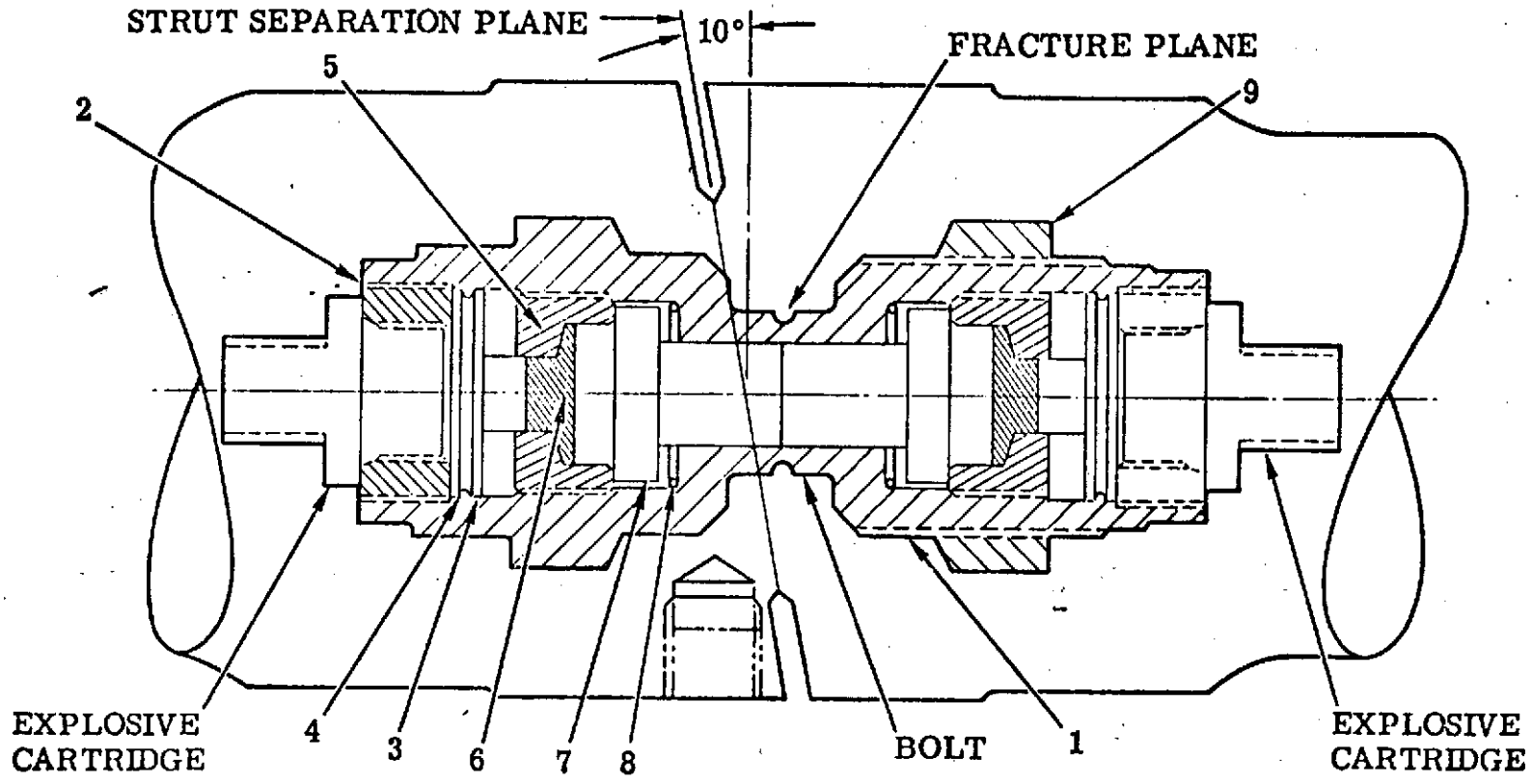

ITEM NO.	NOMENCLATURE	MATERIAL	QTY/ BOLT
1	HOUSING	STEEL	1
2	RETAINER	MAR. STEEL	2
3	PISTON - PRIMARY	MAR, STEEL	2
4	O-RING	TEFLON	2
5	INSERT	MAR. STEEL	2

ITEM NO.	NOMENCLATURE	MATERIAL	QTY/ BOLT
6	COUPLER	SILICONE RUBBER	2
7	PISTON - SECONDARY	MAR. STEEL	2
8	RING	COPPER	2
9	NUT	4340 STEEL	1

FIGURE VI-5-1 FORWARD BEARING REACTION SEPARATION BOLT LOCATION AND DETAILS

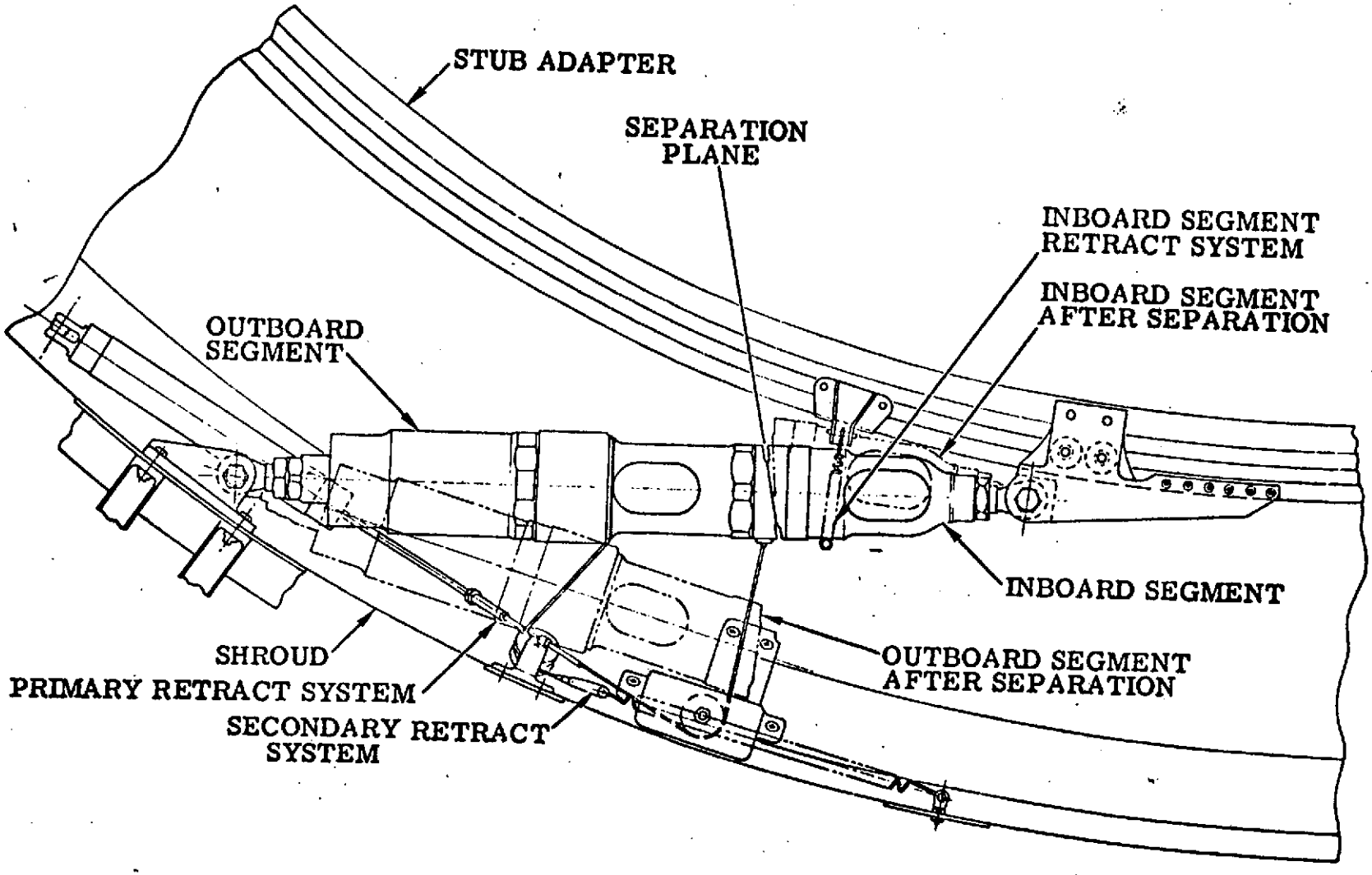

FIGURE VI-5-2 FORWARD BEARING REACTION STRUT INSTALLATION

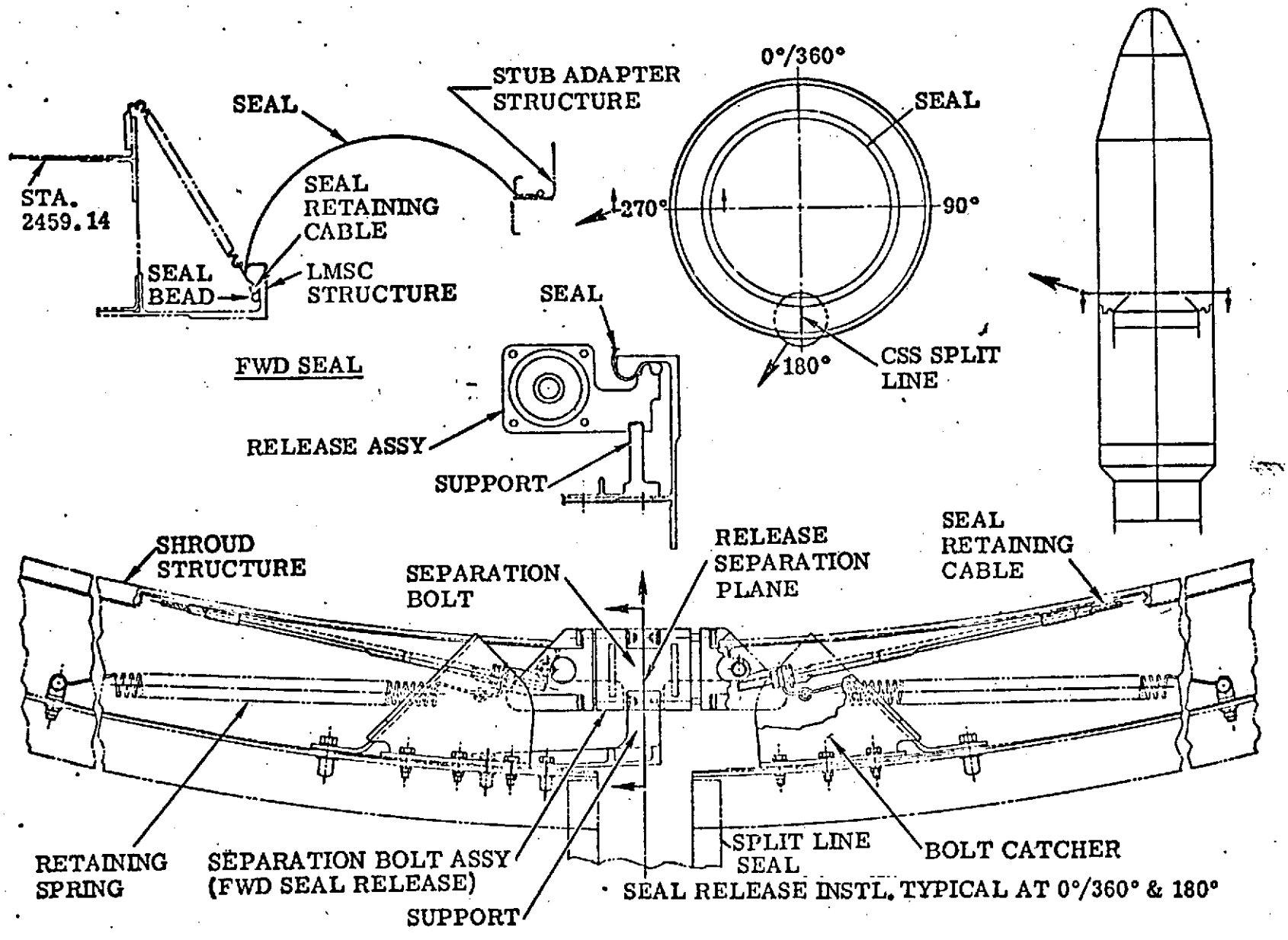

FIGURE VI-5-3 FORWARD SEAL

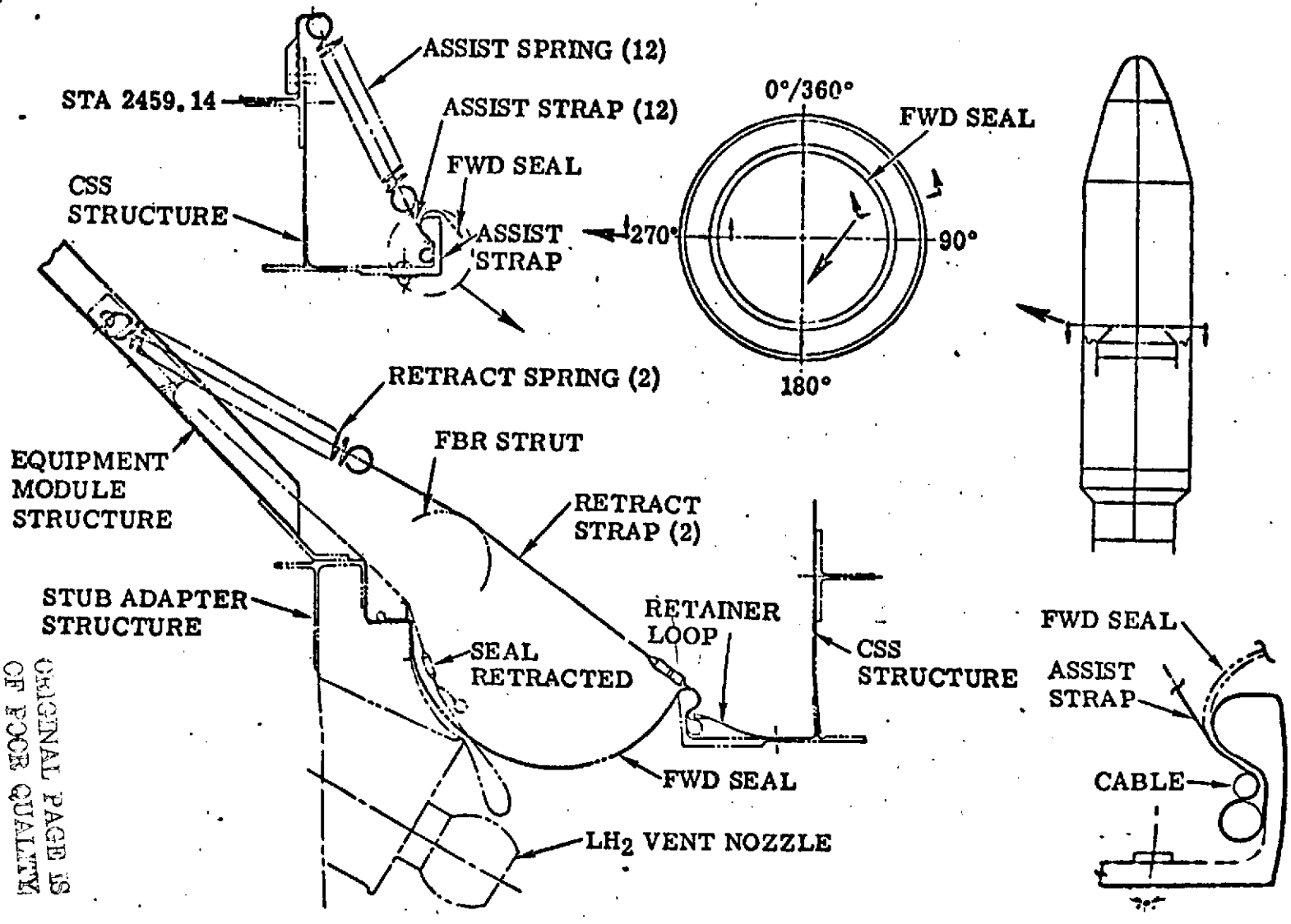

FIGURE VI-5-4 FORWARD SEAL RELEASE ASSIST SYSTEM

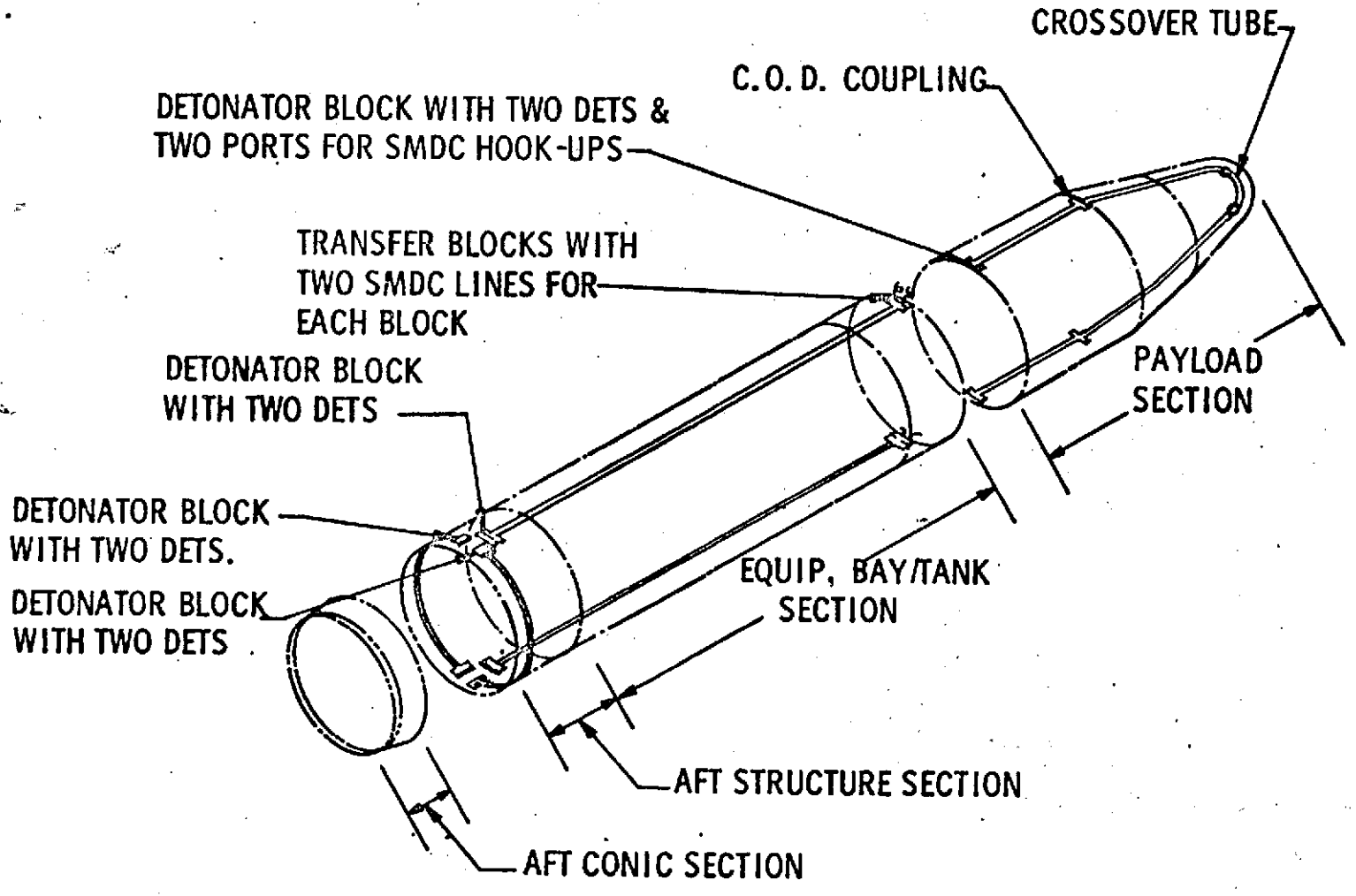

FIGURE VI-5-5 SUPER*ZIP SEPARATION SYSTEM

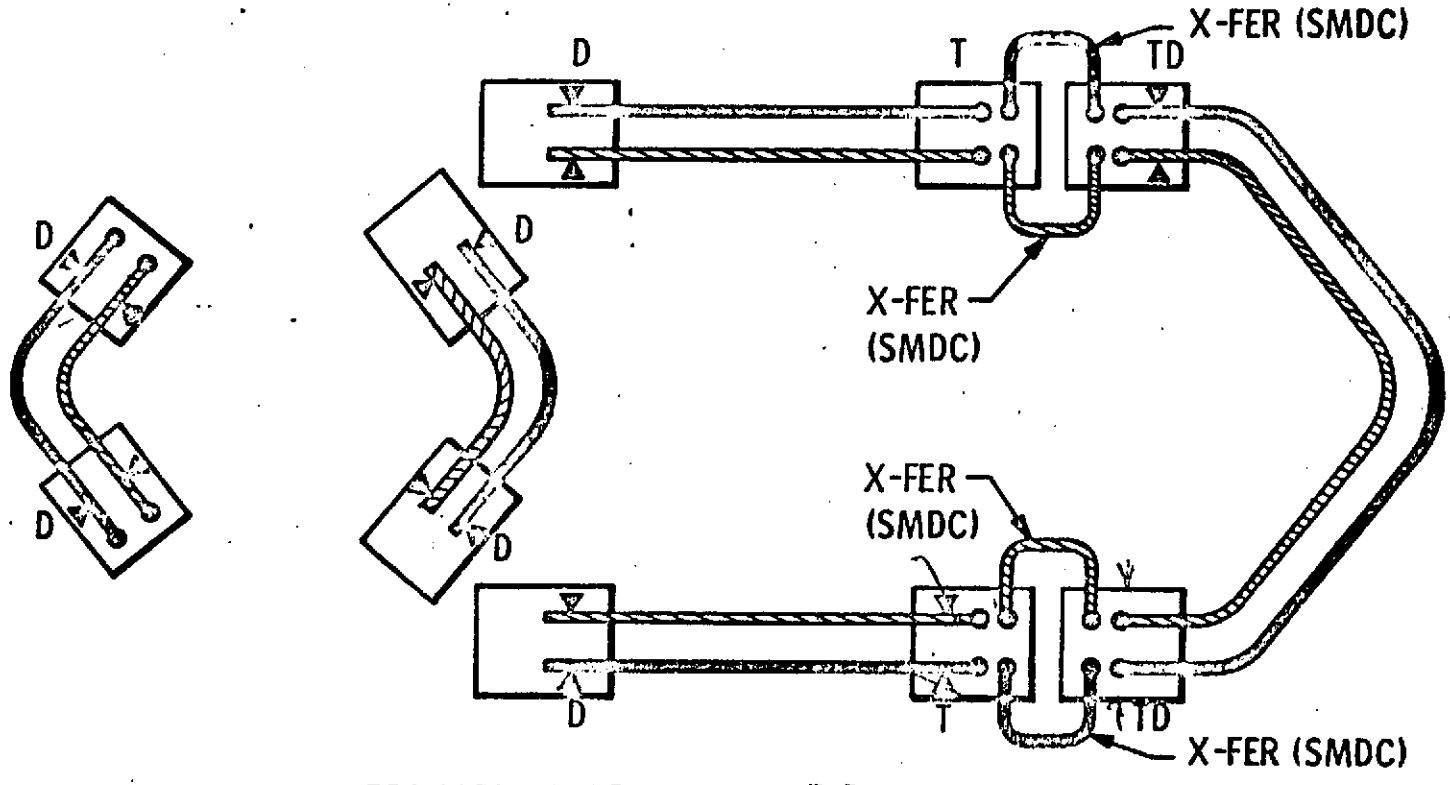

PRIMARY SYSTEM

SECONDARY SYSTEM

NON-ELEC. DET

ELECTRIC DETONATOR

E. D.	16
N. E. D.	16
DET. BLOCKS (D)	6
X-FER BLOCKS (T)	2
TRANS DET BLOCKS (TD)	2

FIGURE VI-5-6 SUPER-ZIP ORDNANCE SYSTEM

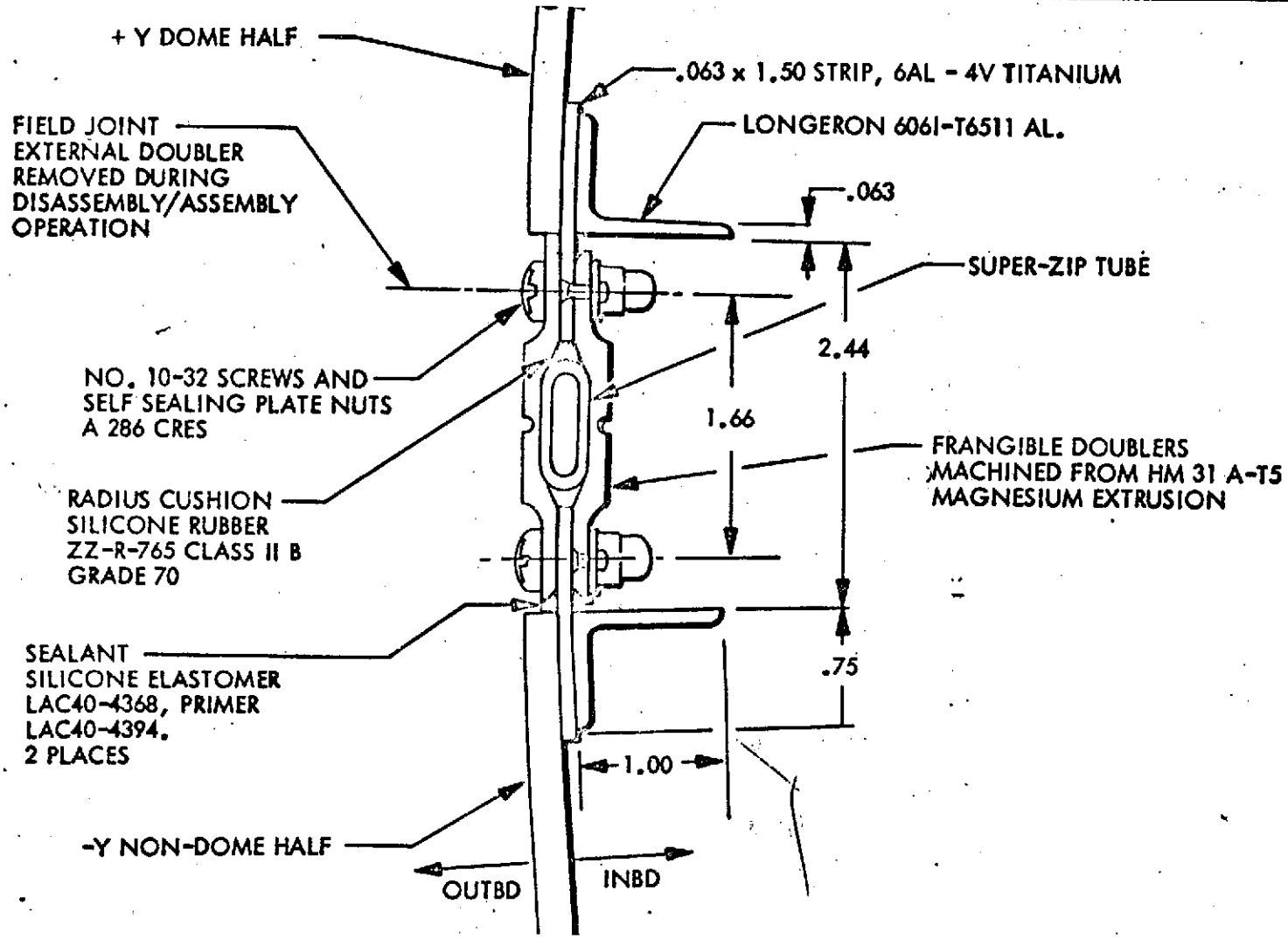

FIGURE VI-5-7 TYPICAL LONGITUDINAL PYRO JOINT

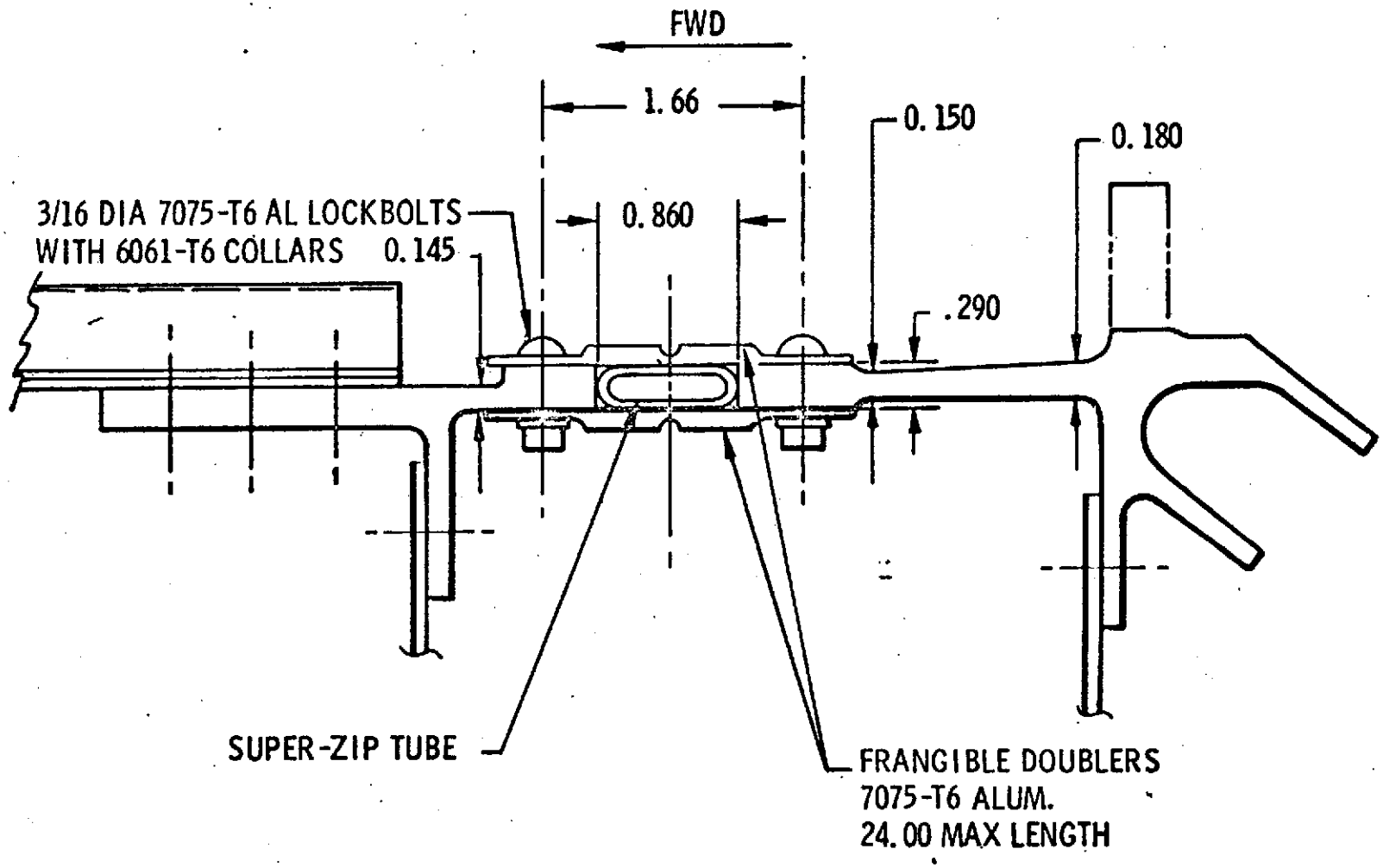

VI-86

FIGURE VI-5-8 TYPICAL CIRCUMFERENTIAL PYRO JOINT

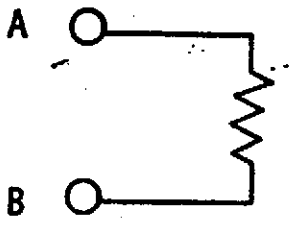

PRIMARY SYSTEM

- STANDARD CLOCKING ON INITIATOR END
- RIGHT HAND THREADS ON OUTPUT END

SECONDARY SYSTEM

- "W" CLOCKING ON INITIATOR END
- LEFT HAND THREADS ON OUTPUT END

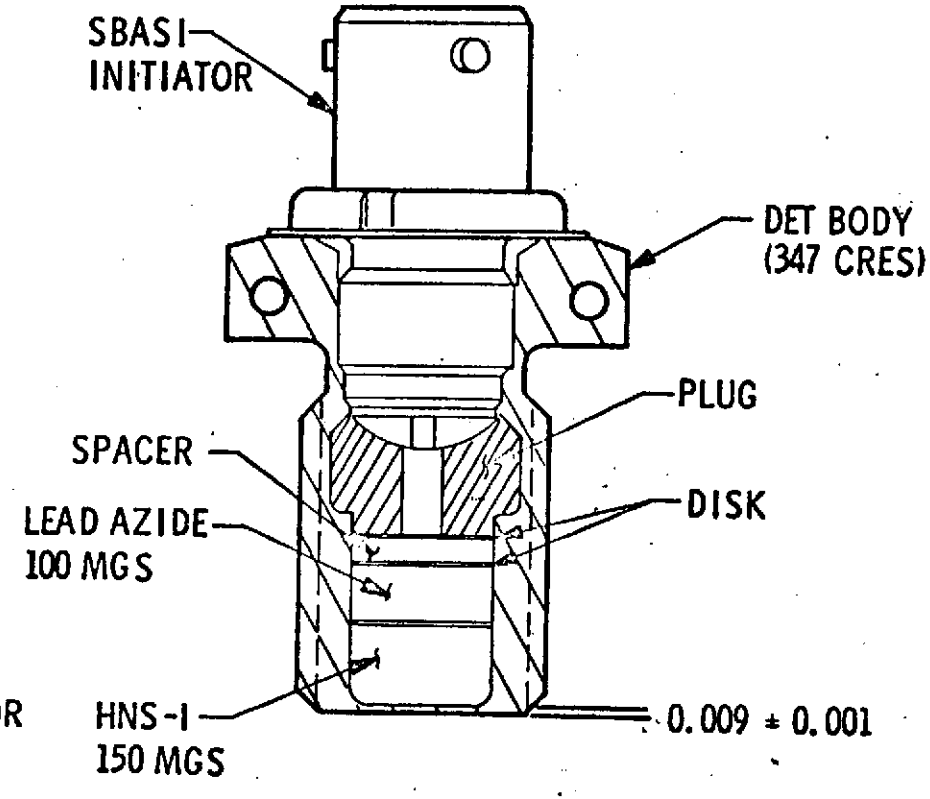

FIGURE VI-5-9 ELECTRIC DETONATOR

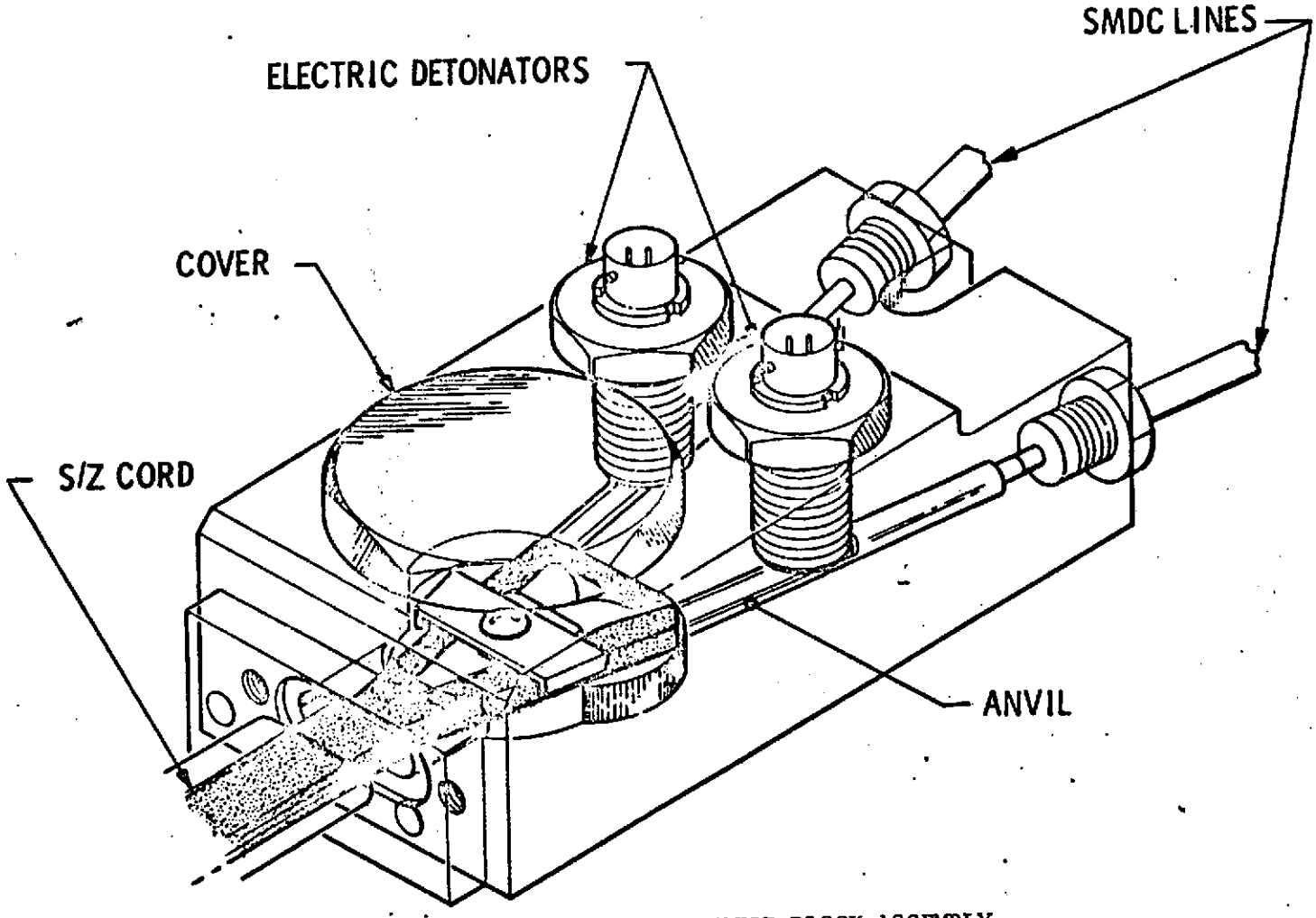

FIGURE VI-5-10 DETONATOR BLOCK ASSEMBLY

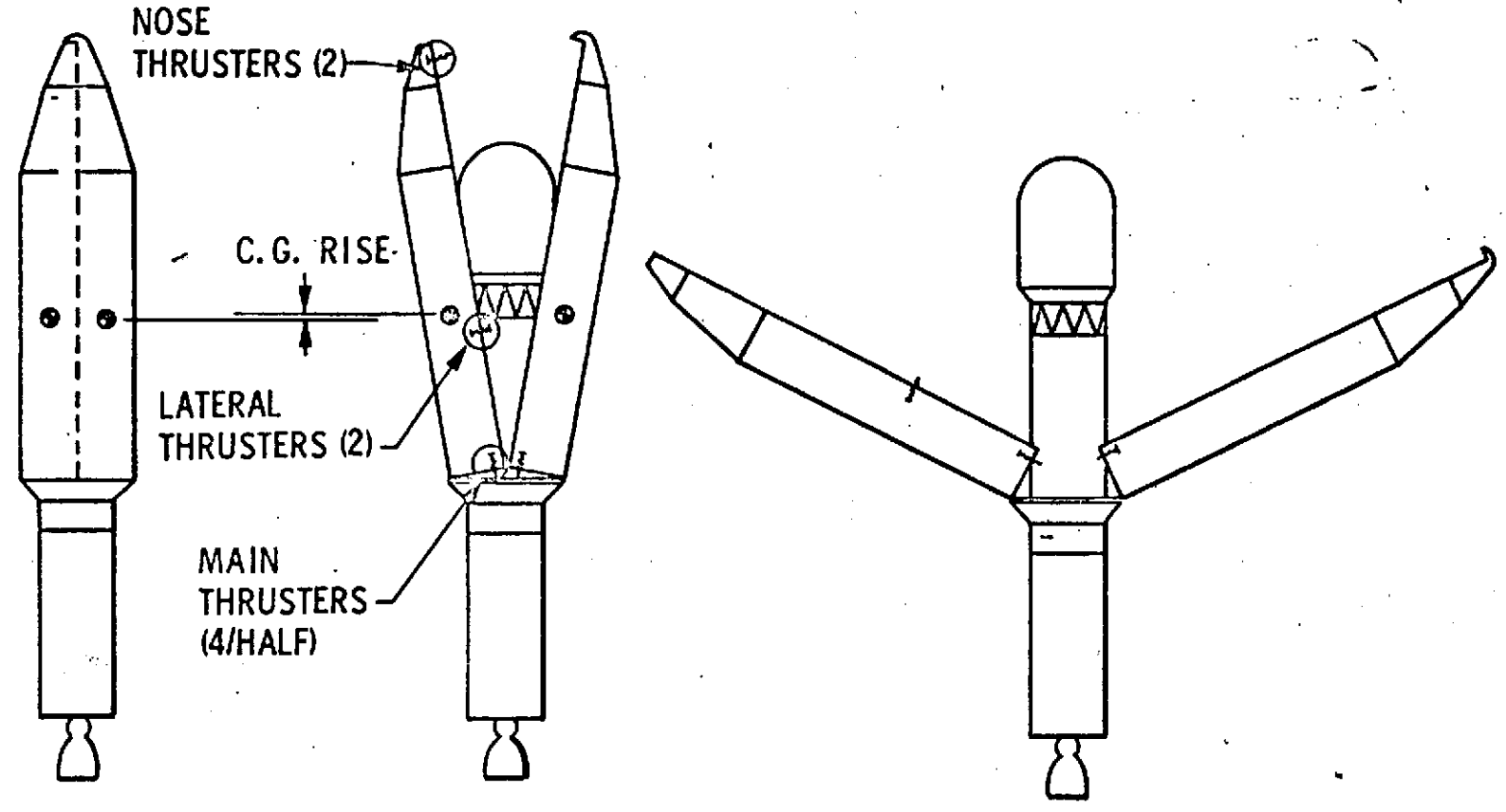

FIGURE VI-5-11 JETTISON SEQUENCE AND SPRING LOCATION

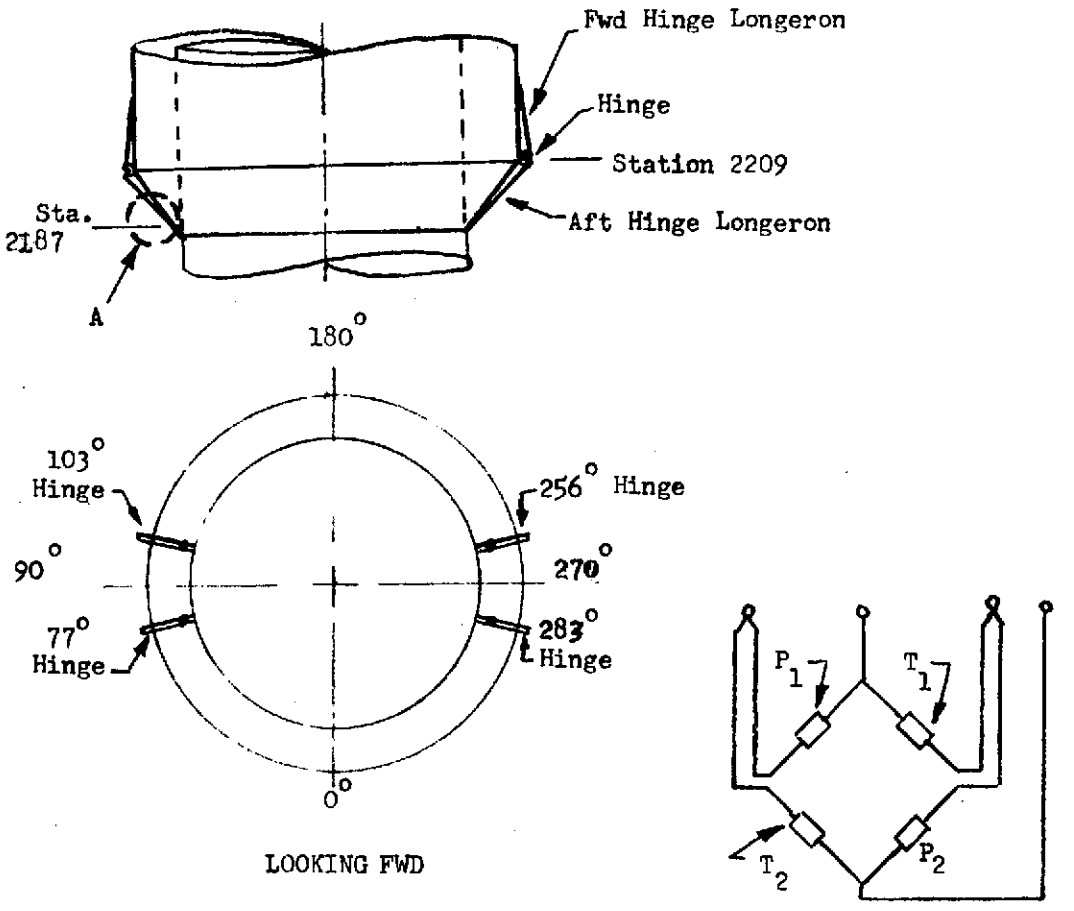

Fig. VI-5-12 Centaur Standard Shroud Hinge Longeron Strain Gages.

T = Tension
C = Compression

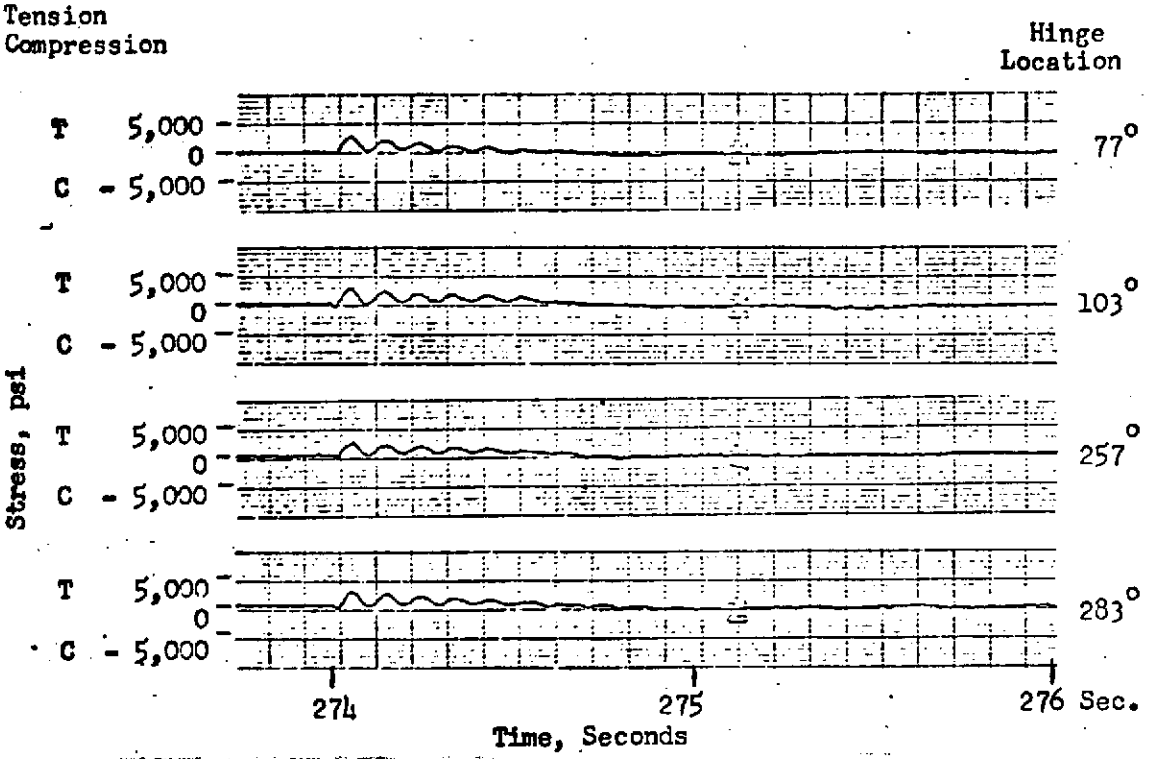

TC - 1 Flight Data

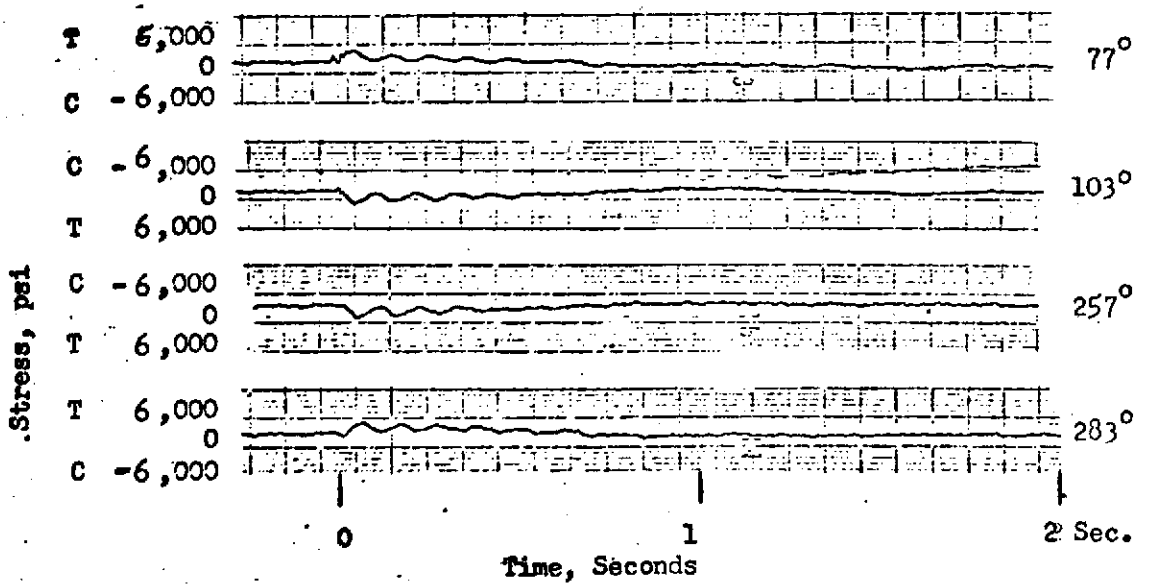

Heated/ Altitude Jettison Test No. 2.

Fig. VI-5-13 Aft Hinge Longeron Stresses at Station 2187 During Shroud Jettison.

VII. CENTAUR D-1T SYSTEMS ANALYSIS

VII-1. MECHANICAL SYSTEMS

VII-1A. Structures

by R. T. Barrett, R. C. Edwards, C. W. Eastwood,
J. O. Van Vleet, and T. L. Seeholzer

Summary

The ISA satisfactorily transferred all Centaur and CSS loadings onto the Titan skirt structure. The ISA forward ring was completely severed at Titan/Centaur staging and the vehicles separated at a constant acceleration.

The ullage pressures in the Centaur propellant compartments were within prescribed limits. Sufficient pressure was maintained to prevent buckling and maximum pressures did not exceed burst limits of the tank structure.

The structural components located on the forward portion of the Centaur tank satisfactorily supported the payload and electronic packages. The stub adapter structure safely withstood the tangential loading of the six FBR struts.

The forward bearing reactor struts successfully transferred flight loads from the CSS to the Centaur stub adapter. The magnitude of these loads was well within the demonstrated capability.

The TC-1 flight qualified the Centaur D-1T structural system for loading during the Titan boost phase of flight. No structural anomalies were noted. The ISA separation system was verified for the Titan/Centaur configuration.

Description and Performance

Interstage adapter. - The interstage adapter (ISA) provides a physical connection between the Titan forward skirt (at Station 2127.43) and the Centaur (at Station 2240.79). In addition, it provides a support ring for the Centaur Standard Shroud at Station 2180.48. The ISA is a 10-foot diameter spacer of aluminum skin, ring, stringer construction which is 113.35 inches long (see fig. VII-1A-1). It also serves as a mounting structure for various installations such as the air conditioning

system, panel disconnects, vent lines, umbilicals, and the Titan/Centaur separation system.

A separation monitoring device (potentiometer) was mounted between the ISA and the Centaur aft bulkhead (fig. VII-1A-2). This potentiometer extended for a total of 15 feet during Titan/Centaur separation to verify that separation was satisfactory.

The potentiometer data trace was very smooth (fig. VII-1A-3), indicating a normal Titan/Centaur separation. Since the ISA is 9.5 feet long and the total potentiometer travel is 15 feet, the ISA cleared the Centaur.

The flight loads, both axial and bending moments, on the forward section of the interstage adapter (ISA) were calculated from structural strains that were sensed by strain measurements composed of strain gage arrays. On the section of the ISA forward of the shroud/ISA interface, four strain gage arrays were located at Station 2208 and spaced 90° apart at azimuths 24°, 114°, 204°, and 294° as shown in figures VII-1A-4. Each array consisted of four uniaxial gages mounted on the stringers and electrically connected as shown in figure VII-1A-5. The circuit compensated for temperature variations and gave an augmented signal voltage output.

Prior to lift-off of the vehicle, the strain measurements were zeroed. This method of reference required the addition of the weight in a 1 g field of the Centaur and propellants, the forward adapters and equipment, and the VDS and the SPHINX spacecraft, totaling 43 450 pounds, to all axial loads on the forward ISA. Also, a calibration factor of 0.79 was applied to the indicated bending moments on the ISA. The calibration factor was determined from limit load static structural tests.

The maximum combined loads on the ISA at Station 2208 were at T + 261 seconds at maximum acceleration during stage I burn. The equivalent axial load at that time was 149 450 pounds on the compression side and 141 450 pounds compression on the opposite side. Of this equivalent axial load, 145 450 pounds were direct axial load and 4000 pounds were from a bending moment of 0.12×10^6 inch pounds.

The maximum bending moment on the ISA at Station 2208 was 0.8×10^6 inch pounds at T + 46 seconds. At that time the axial load was 67 350 pounds compression at Station 2208 on the ISA. The equivalent axial load was 94 000 pounds on the compressive side and 40 680 pounds compression on the opposite side. The effective compressive shear azimuth on the ISA at Station 2208 was 198°.

Axial equivalent loads, direct axial loads, and bending moments at the various event times during the flight are listed in table VII-1A-I. Loads applied to the test ISA with the FBR system installed also are included in the table for comparison. As shown, the flight maximum equivalent axial load was approximately 70 percent of the test maximum value

performed at Plum Brook Station. The value was less than 50 percent of the maximum test load applied in an ISA test conducted at the contractor's plant at an earlier date. The flight maximum bending moment was less than 20 percent of the test value maximum. The axial load at stage I maximum acceleration was almost twice the test axial load, however, as previously stated, the combined load was only approximately 70 percent of the test value.

Using the bending moments from the ISA at Station 2208 and from the shroud at Station 2294 , and correlating the values with the qualification test values, a bending moment value for flight on the ISA/ itan skirt interface at Station 2127 can be approximated within 20 percent. At T + 46 seconds of flight this value was 8.8×10^6 inch pounds compared to a test value of 22.9×10^6 inch pounds. The equivalent axial load at Station 2127 at T + 46 seconds, calculated by combining the correlated bending moment and the axial load , was 382 850 pounds compression compared to a test value of 869 600 pounds and 203 750 pounds tension compared to a test value of 658 400 pounds.

Accuracies of the ISA strain measurements were reduced by the large instrumentation range. The maximum axial loads were approximately 10 percent of the full range and the accuracy was ±20 percent. The maximum bending moments produced strains of approximately 6 percent of the measurement full range and the accuracy was ±33 percent.

Centaur tank. - The propellant tank forms the primary Centaur vehicle structure. The propellant tank is constructed of welded, thin walled, stainless steel, monocoque skins (fig. VII-1A-6). A double walled intermediate bulkhead separates the propellant tank into a fuel compartment and an oxidizer compartment.

A minimum internal pressure within each compartment is required for structural stability. The tensile strength of the tank material and welded joints determine the maximum allowable pressure in each compartment.

The tank locations and criteria which determine the maximum allowable and minimum required tank pressures during various phases of flight are described in figure VII-1A-7. These maximum allowable and minimum required tank pressure limits are compared to actual TC-1 propellant tank pressures in figure VII-1A-8. The pressure limits are not constant because of varying loading and ambient pressure during flight. The minimum required liquid hydrogen tank pressure is computed using maximum design loads (as opposed to actual flight loads) with appropriate factors of safety.

The maximum allowable liquid hydrogen tank pressure is governed by the pressure differential between the hydrogen tank and the cavity within the double walled intermediate bulkhead (see fig. VII-1A-7, location S2). The combined hydrogen ullage pressure and hydrostatic pressure of the liquid hydrogen cannot exceed 29.2 psia. During the flight, the combined

ullage and hydrostatic pressure was always less than 29.2 psia.

The minimum required liquid hydrogen tank pressure must be sufficient to prevent compression buckling of the pressure stabilized cylindrical skin at Station 2243.90. During flight the liquid hydrogen tank ullage pressure was always greater than the minimum required pressure.

The maximum differential pressure between the liquid oxygen and liquid hydrogen tanks is limited by the strength of the Centaur intermediate bulkhead. The maximum allowable differential pressure is 23.0 psi. The oxygen tank pressure must always be greater than the combined hydrogen tank pressure and hydrostatic pressure of the liquid hydrogen to prevent reversal of the intermediate bulkhead. During flight the oxygen tank pressure was always greater than the combined hydrogen ullage and hydrostatic pressures. The differential pressure between the propellant compartments did not exceed 23.0 psi at any time during flight.

The maximum allowable liquid oxygen tank pressure is determined by the following criteria:

(1) The pressure cannot exceed a differential of 48.0 psi, less hydrostatic pressure of liquid oxygen, between the oxygen tank and the cavity within the double walled intermediate bulkhead (see fig. VII-1A-7, location S3).

(2) The pressure cannot exceed a differential of 53.0 psi, less hydrostatic pressure of liquid oxygen, across the Centaur aft bulkhead (see fig. VII-1A-7, location S4).

During the flight, the liquid oxygen tank pressure was always less than the maximum allowable pressure.

The minimum required liquid oxygen tank pressure for aft bulkhead stability is always less than the previously mentioned minimum required oxygen tank pressure for intermediate bulkhead stability. Therefore, no flight comparison is necessary.

Stub adapter. - The stub adapter is a 10-foot diameter skin-and-stringer cylinder, 25 inches high, which attaches to the Centaur tank and provides a mounting platform for forward equipment and payloads.

The adapter was not instrumented for strain monitoring - no direct load data for the adapter is available. However, strain readings were taken on adjacent VSCA and PFLA structure, and these show that the stub adapter was lightly loaded relative to its design load.

Truss adapter. - The truss adapter is a 10-foot diameter cylindrical structure, 49 inches high, consisting of 24 tubular struts joined at twelve equally spaced points at each end of the adapter, as shown in figure VII-1A-9. The aft end attaches to the equipment module near the forward end of the stub adapter. The truss adapter forward end attaches to

the transition adapter. The function of the truss adapter is to support the payload and distribute payload loads into the top of the stub adapter.

The truss adapter was not instrumented for strain but does appear to have been lightly loaded.

Transition adapter. - The transition adapter is a rectangular torus 5 inches high by 3 inches deep, of 10 foot diameter. It attaches to the top of the truss adapter and provides the spacecraft-to-Centaur interface mounting plane, also as shown in figure VII-1A-9.

Strain gages attached to the VSCA struts immediately adjacent indicated that transition adapter loads were far below its design loads.

Equipment module. - The Centaur equipment module is a conical skin-stringer structure of 10-foot diameter base and 5-foot diameter top, 30 inches high, which attaches to the top of the stub adapter. Its function, for the proof flight, was to provide a mounting surface for the avionics packages and to act as a thermal insulating cap for the Centaur tank.

For certain other missions, the module also serves as a payload mounting platform, and thus is strong enough to transmit loads far in excess of the package loads present in the proof flight.

Viking spacecraft adapter and proof flight lander adapter. - The Viking spacecraft adapter and proof flight lander adapter are spacecraft support trusses. The VSCA (see fig. VII-1A-9) attaches to the transition adapter and supports the Viking orbiter dynamic simulator (VODS), whereas the PFLA attaches to the VODS and supports the Viking lander dynamic simulator (VLDS).

Both of these strut systems were strain instrumented as shown in figure VII-1A-9 for the proof flight. The maximum load recorded was less than 1/3 design limit load. See table VII-1A-II for data from these instruments.

Forward bearing reaction. - The CSS/Centaur forward bearing reaction provided load sharing and limited the relative deflection between the CSS and the Centaur vehicle during flight until the vehicle has passed through the area of maximum aerodynamic loading (approximately 100 sec after liftoff). The forward bearing reaction system, located at Station 2460, consisted of six spring loaded double action struts.

The basic strut system is illustrated in figures VII-1A-10 and VII-1A-11. The spring rate of the system, 19 500 per inch, was designed to be compatible with the stiffness of the CSS and the Centaur.

Conical steel spring washers were utilized to produce the required spring rate in tension and compression (fig. VII-1A-11). At T + 100 seconds the forward bearing reaction was separated. For a description of

the FBR separation system, see Section VI.

The forward bearing reaction system limited the deflection between the payload and CSS to a maximum of 0.36 inch during the maximum alpha Q phase of flight as listed in table VII-1A-III. This table also shows the relative motion between the payload and CSS during the above periods of flight. All deflections were within predicted limits. Extensiometers were located at the forward end of the Viking dynamic simulator. Relative motion at the CSS backbone (90^{o}) and split line (0^{o}) was measured.

This data was extrapolated to provide FBR deflections and loads. The maximum FBR deflection and load during the maximum alpha 0 phase were 0.36 inch and 7000 pounds. As indicated in the table, all loads and deflections were less than predicted values for the TC-1 flight.

TABLE VII-1A-1. - ISA STRUCTURAL FLIGHT LOADS AND LIMIT TEST LOADS AT STATION 2208 (INCLUDES WEIGHT OF CENTAUR, PROPELLANTS, ADAPTERS, EQUIPMENT, VDS, AND SPHINX SPACECRAFT FORWARD OF STATION 2208 IN ALL AXIAL VALUES)

[Station 2208 is Centaur/ISA mating station. (See Fig. VII-1A-4.]

Flight event	Nominal time, sec	Total axial load, lb C=Compress. T=Tension	Bending moment, in. lb $\times 10^{-6}$	Vehicle acceleration, g	Total equivalent axial load at extreme fiber, lb	
					Compression	Tension
Zero reference	T - 1	43 450 C	0	1.00	43 450	------
	T + 5	63 500 C	.06	1.54	65 500	------
Transonic	T + 46	67 350 C	.80	1.76	94 000	------
	T + 64	82 000 C	.56	1.88	100 700	------
SRM maximum acceleration	T + 108	109 750 C	.16	1.52	115 050	------
Stage I ignition	T + 115	91 950 C	.40	1.22	105 250	------
SRM jettison	T + 126	54 950 C	.08	1.06	57 650	------
Stage I maximum acceleration	T + 261	145 450 C	.12	3.42	149 450	------
Prior to CSS jettison	T + 273	2 850 T	.08	.74	0	5 500
Stage II maximum acceleration	T + 468	81 950 C	.07	1.90	84 250	------
Test limit loads with FBR		79 100 C	4.33	1.00	223 400	65 200

TABLE VII-1A-2

SPACECRAFT ADAPTER STRUT LOADS

MAX./MIN. (+) = COMPRESSION (-) = TENSION

ALL LOADS IN LB, RELATIVE TO 1.0 G STATIC COMPRESSION AXIAL LOAD; ADD 1.0 G AXIAL LOAD TO BELOW TO GET TOTAL LOAD IN MEMBER

	GAGE NO.	Design Limit Load	MEASURED LOADS AT VARIOUS TIMES OF FLIGHT								
			Stage Zero Ignition	Max. αq	SRM Burnout *	Stage I Ignition **	Steady Load Before POGO *	Max. POGO	Stage I Burn Out *	Stage I Separation	Stage II Ignition
PFLA	209	11050	1366	1639	1093	1366	820	2459	1639	546	0
		-11540	-820	-382	273	273		273	-273	-1366	
	210		1902	1902	1087	1359	815	1902	1631	1087	
			-815	-544	272	272		544	-544	-2174	
	211		1332	1332	533	799	533	1065	799	426	
			-1332	-1065	0	0		0	-266	-906	
	212		1249	1466	1087	1087	815	1629	1629	707	
			-1086	-815	0	0		543	-272	-1794	
	213		2067	1466	923	1086	816	2012	1632	815	
			-1795	-816	102	0		272	-272	-1901	
	214		1522	1359	272	816	272	1088	707	272	
			-1468	-1087	0	0		0	-272	-816	
VSCA	215	9100	1520	1925	760	1267	760	2128	1520	0	1013
		-7500	-1013	-912	253	253		152	-253		-760
	216	9180	1673	2027	1013	1267	760	2129	1774		253
		-7500	-1216	-1014	253	0		659	-507		-1014

NOTE: ALL ACTUALS ARE PEAK VALUES EXCEPT COLUMNS (*) AND MINIMUMS OF (**), WHICH ARE MEANS.

TABLE VII-1A-3

CSS/PAYLOAD EXTENSIOMETER DATA SUMMARY

EXTENSIOMETERS (STATION 2648)	FLIGHT PHASE	PREDICTED MAXIMUM DEFLECTION-INCHES	TC-1 MAXIMUM DEFLECTION, VECTOR SUM-INCHES	FLIGHT TIME-SECONDS
90° (CSS BACKBONE)	LAUNCH	.81	.76	T + .025
0° (CSS SPLIT LINE)	LAUNCH	.89		
--	--	--	--	--
90° (CSS BACKBONE)	MAX. Q	1.50	.80	T + 46
0° (CSS SPLIT LINE)	MAX. Q	1.50		
FBR LOADS AND DEFLECTIONS (EXTRAPOLATED)			--	--
DEFLECTION	MAX. Q	1.00 INCHES	.36 INCHES	T + 46
LOADS	MAX. Q	20,000 POUNDS	7,000 POUNDS	

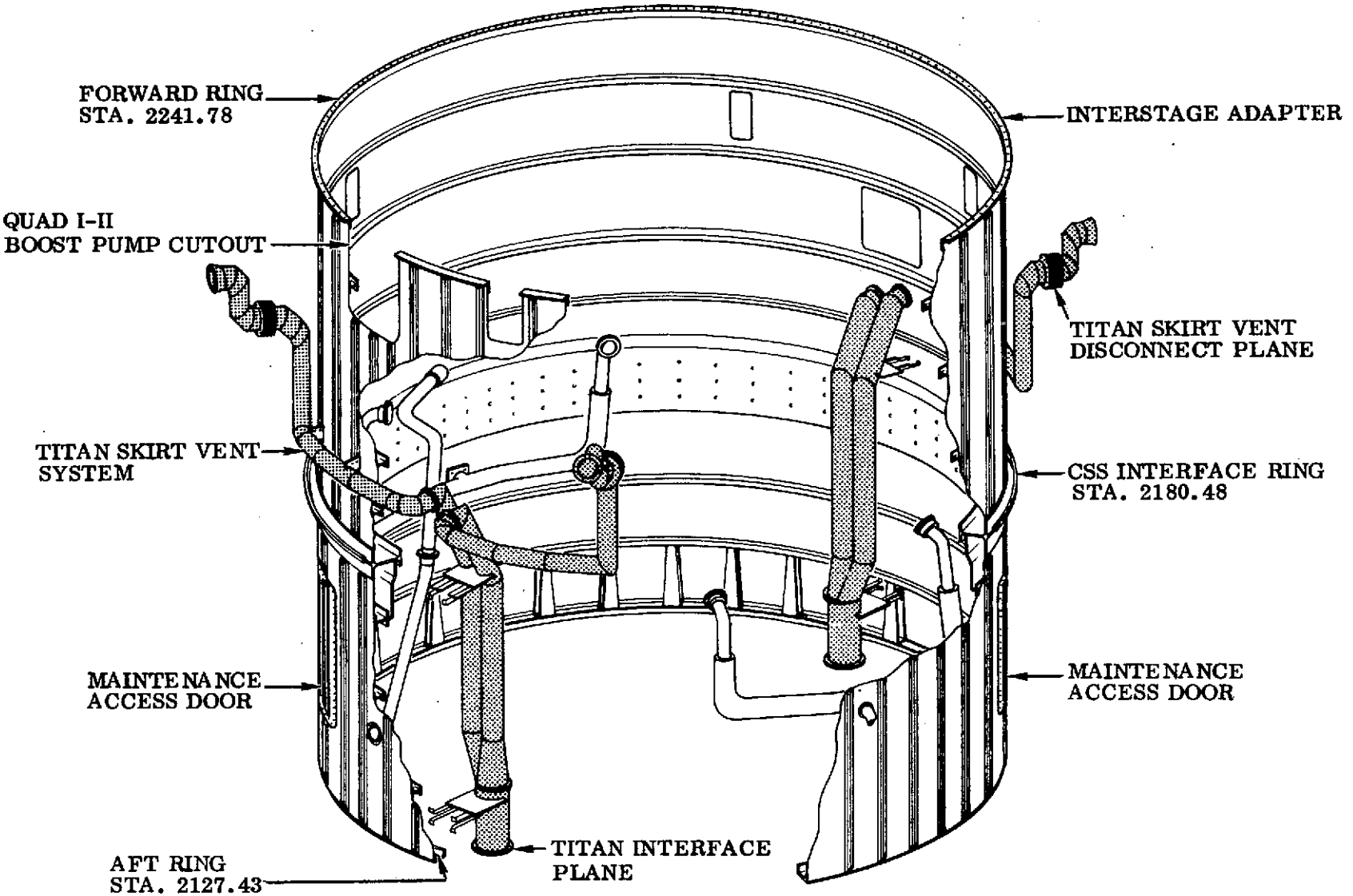

FIGURE VII-1A-1 TITAN/CENTAUR INTERSTAGE ADAPTER

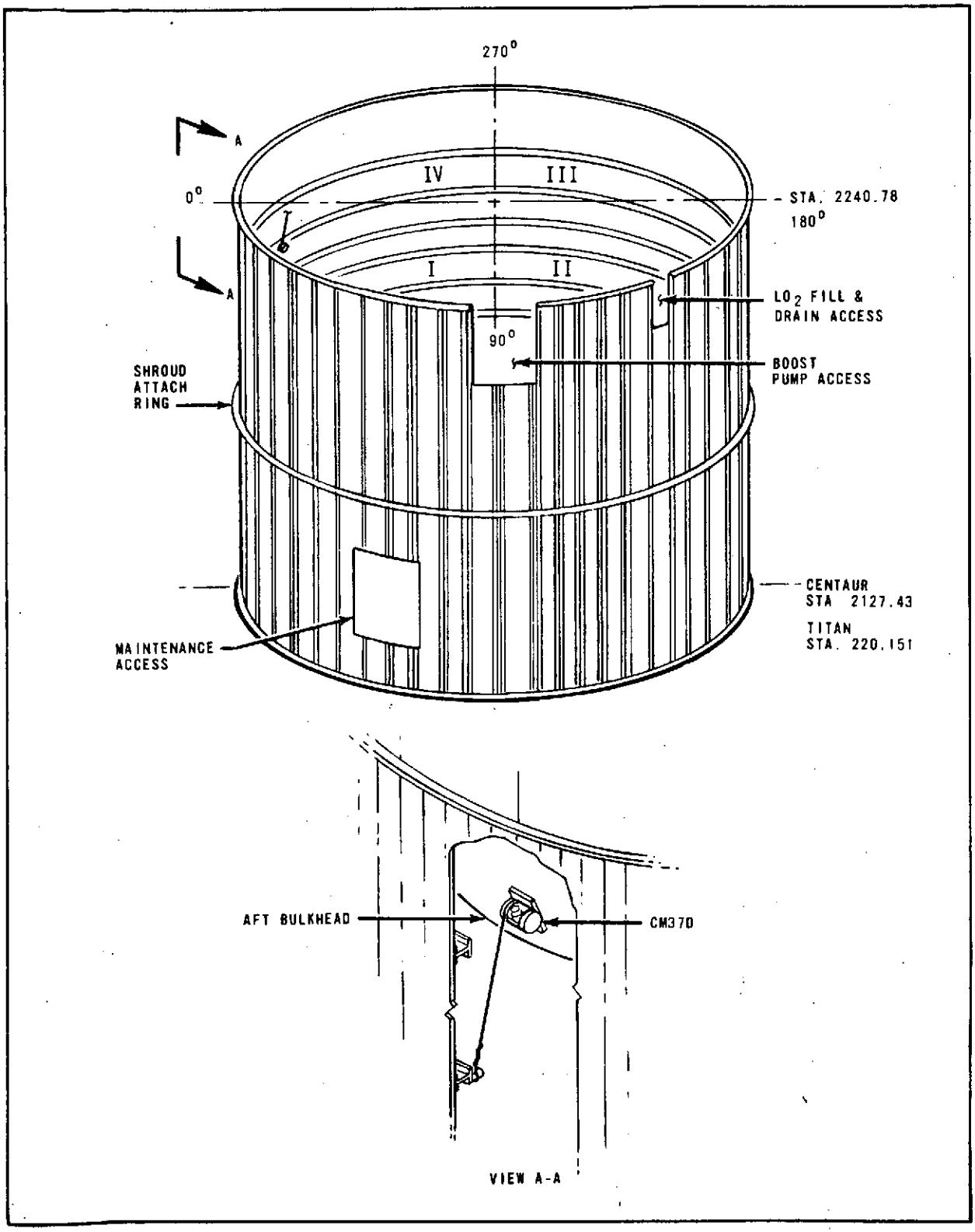

FIGURE VII-1A-2 TITAN/CENTAUR INTERSTAGE ADAPTER SEPARATION INSTRUMENTATION

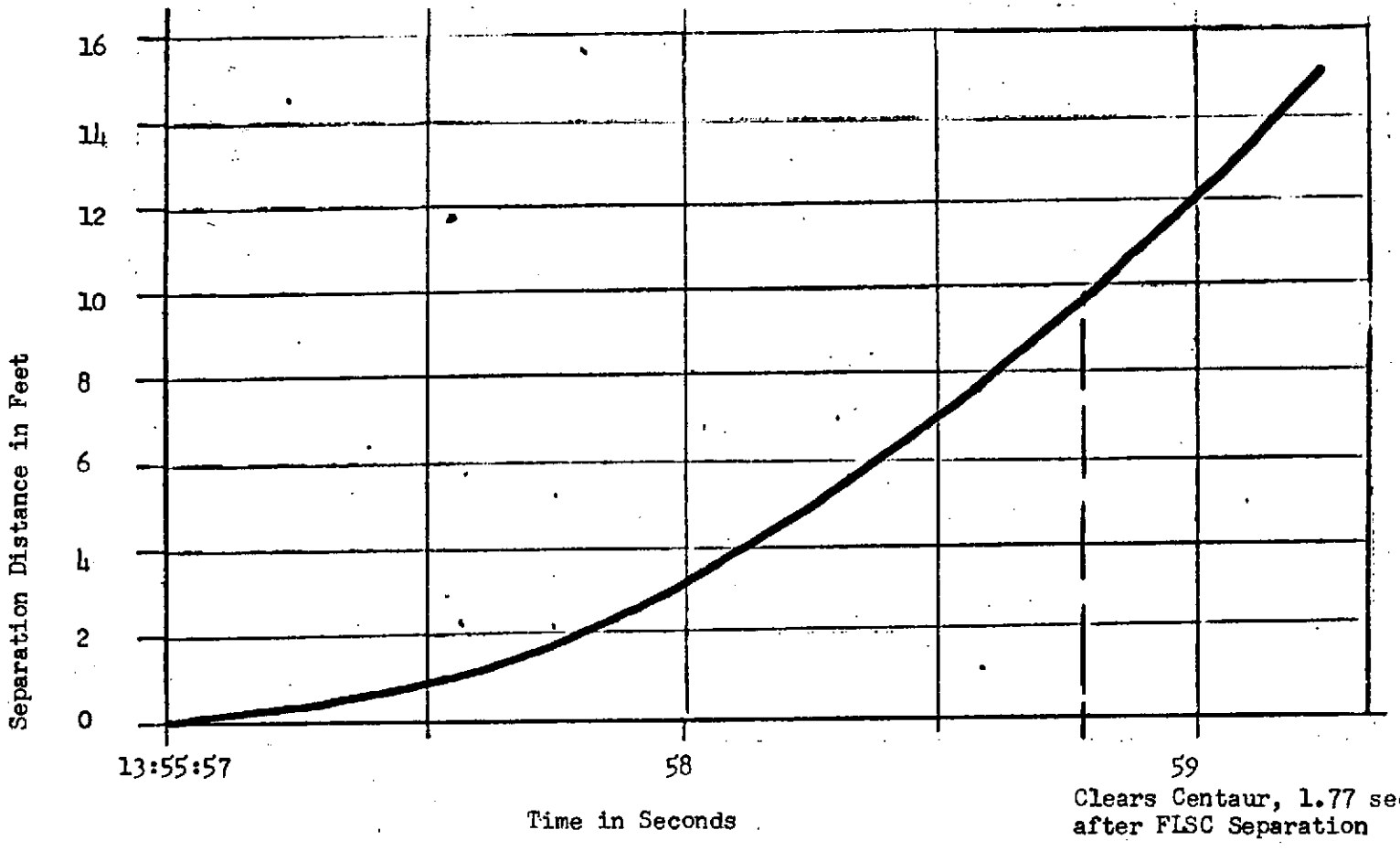

Figure VII-1A-3 Titan/Centaur Flight Separation Instrumentation Data TC-1

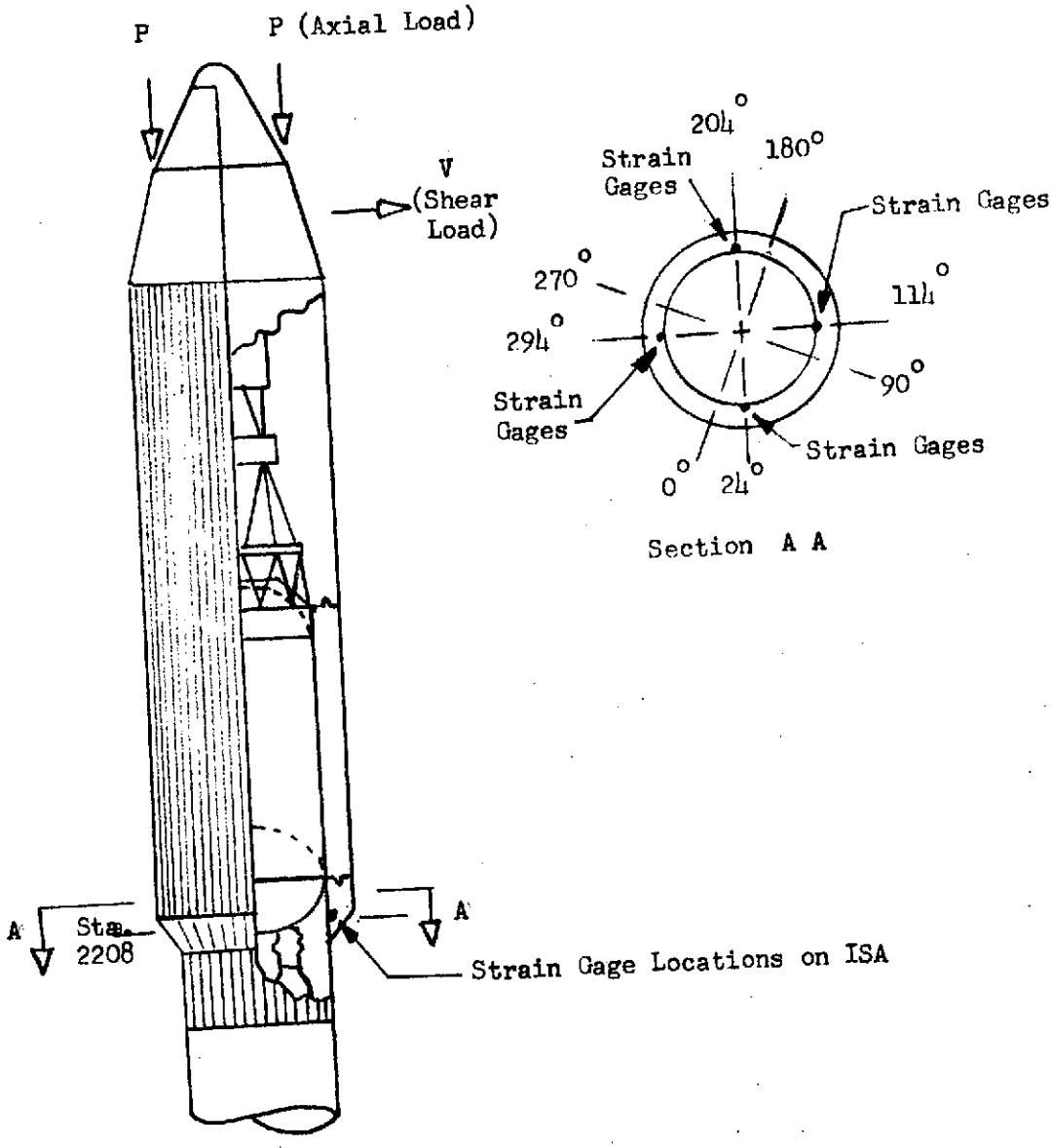

Fig. VII-1A-4 Structural Strain Measurement Locations on ISA.

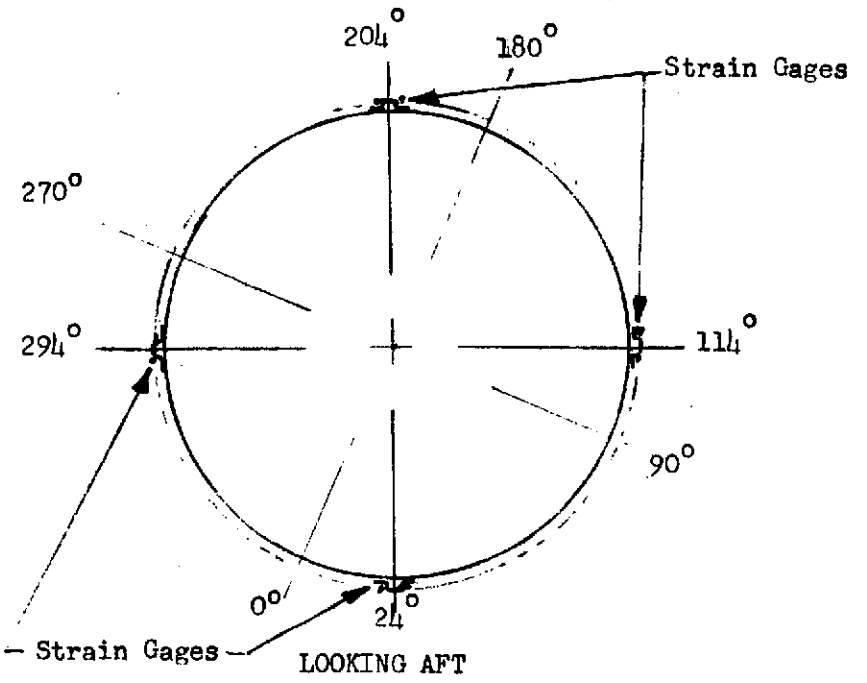

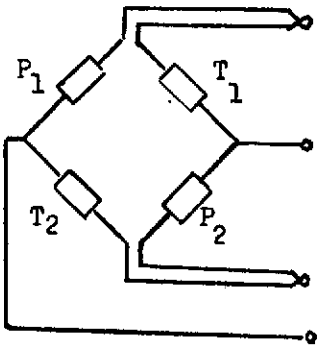

Electrical Circuit

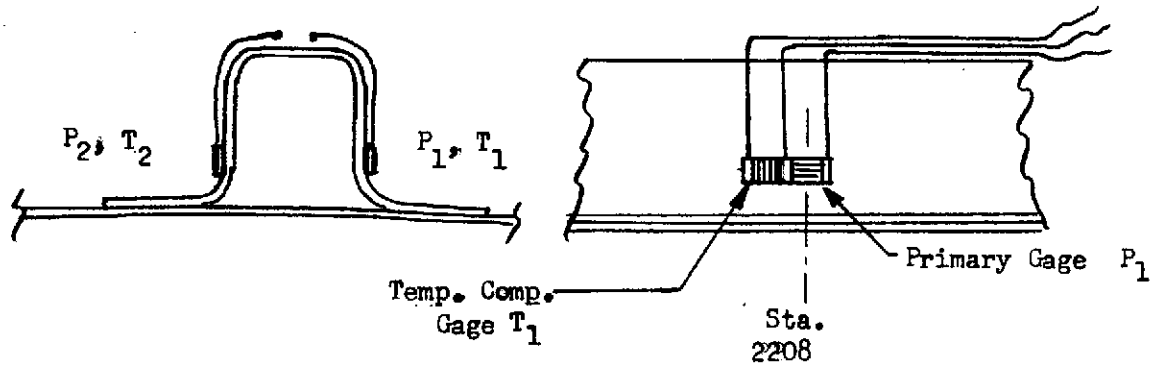

Typical Each Side of Stringer.

Fig. VII-1A--5 Centaur Interstage Adapter Strain Gages.

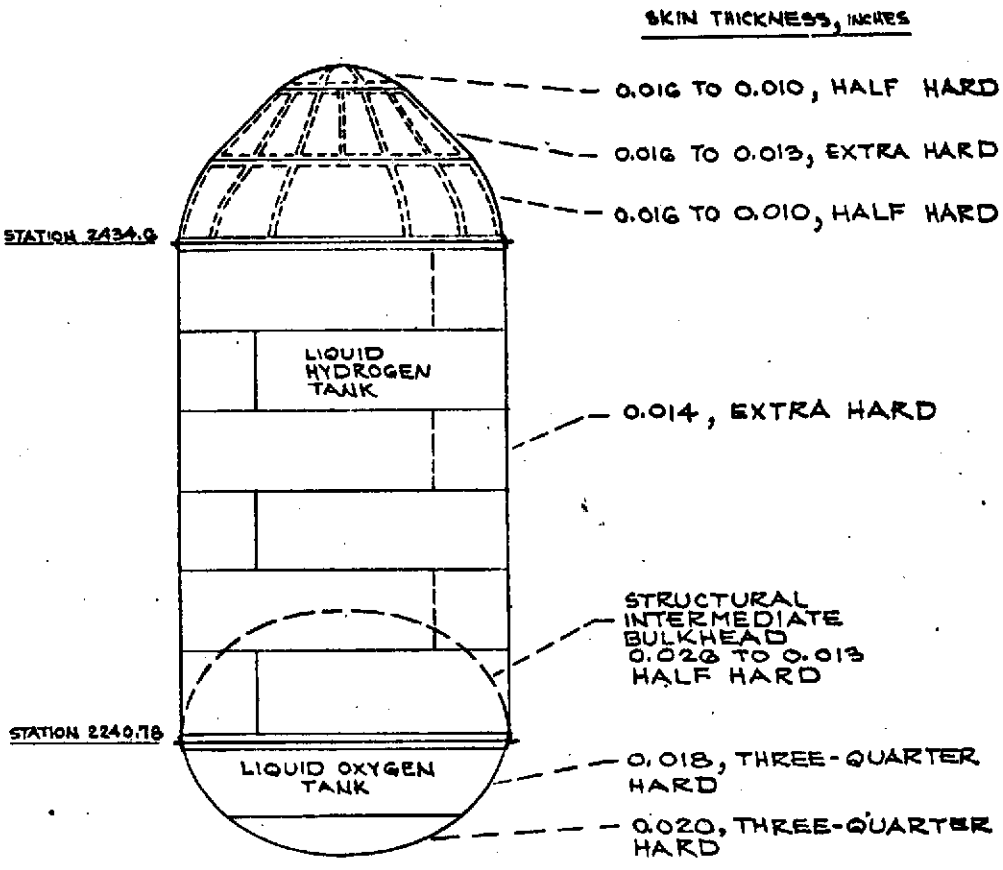

FIGURE VII-1A-6 CENTAUR PROPELLANT TANKS (ALL MATERIAL 301 CRES)

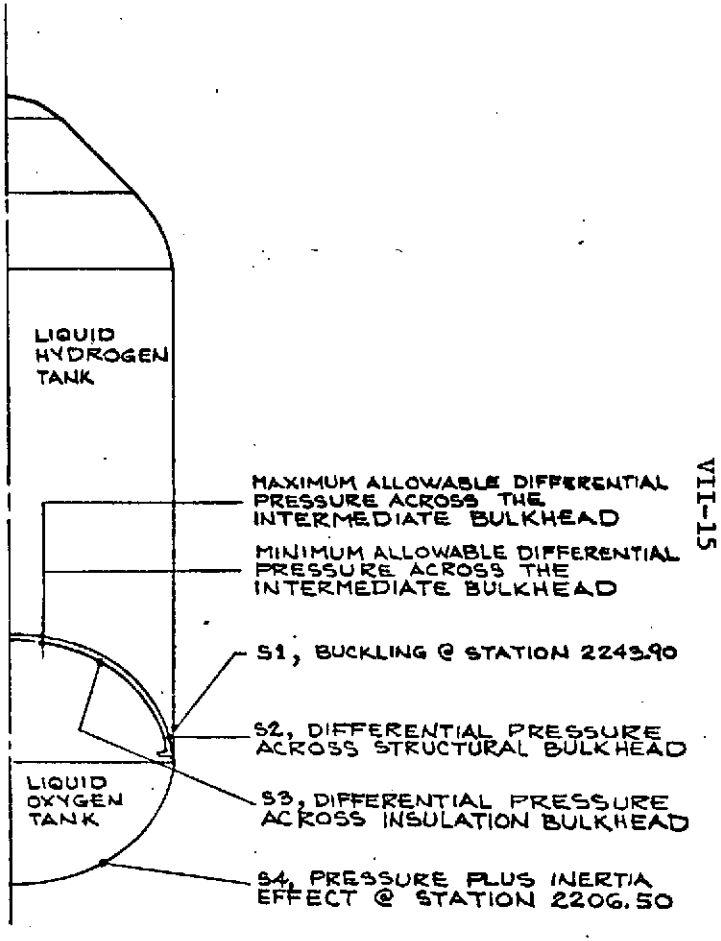

FIGURE VII-1A-7 TANK LOCATIONS AND CRITERIA WHICH DETERMINE ALLOWABLE PRESSURES

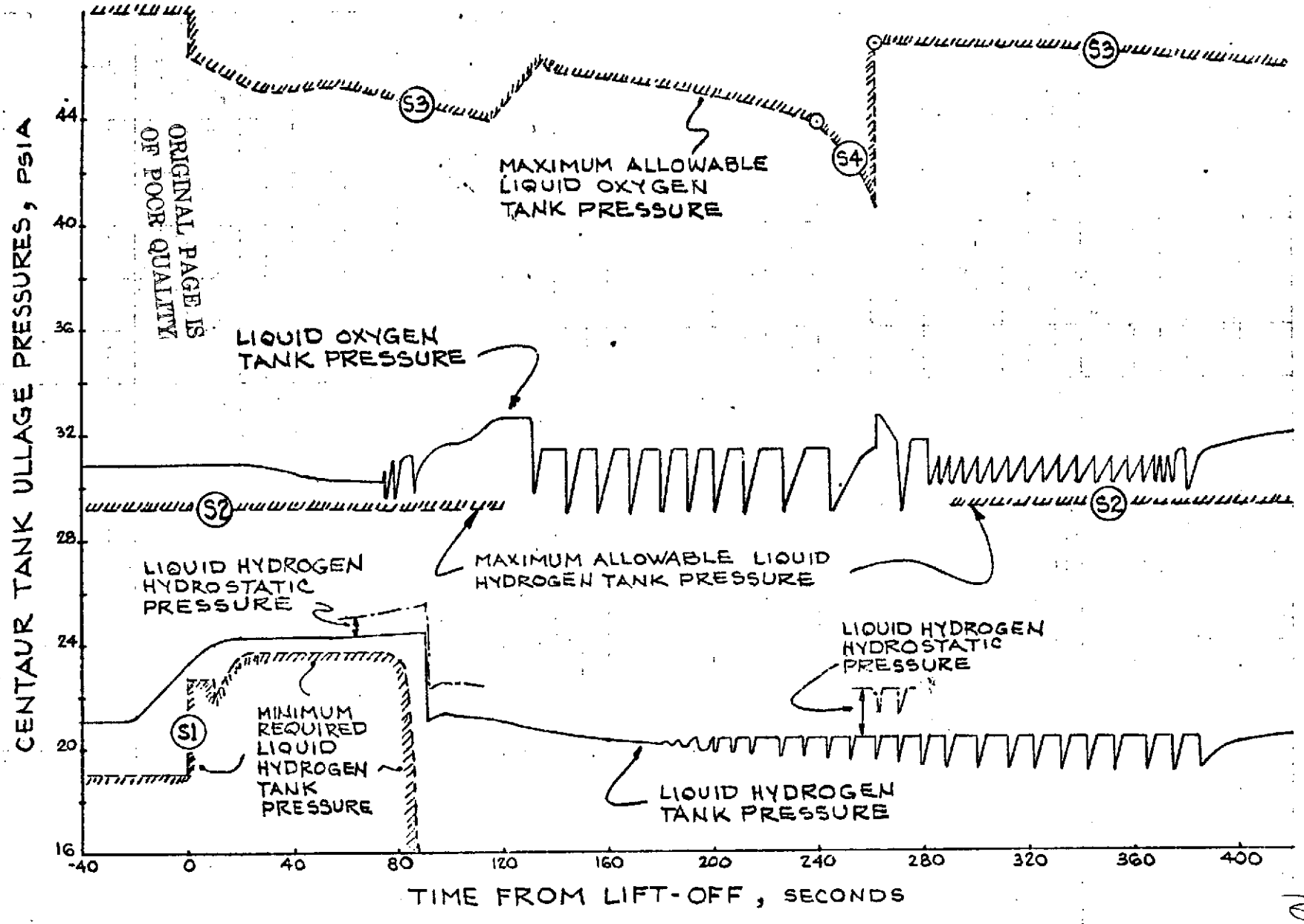

FIGURE VII-1A-8 CENTAUR TANK PRESSURE HISTORY

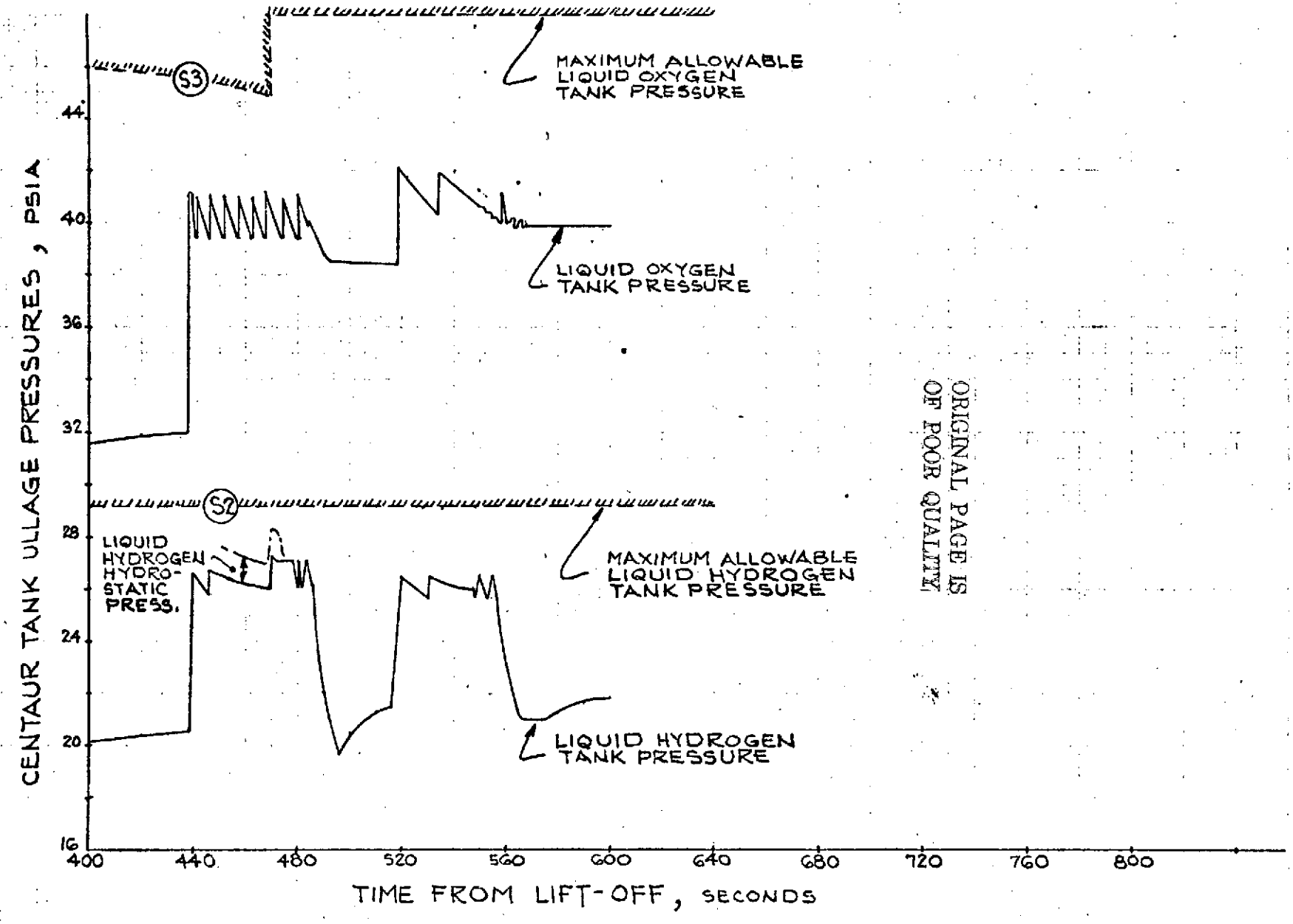

FIGURE VII-1A-8 CENTAUR TANK PRESSURE HISTORY

PAGE 2 OF 2

STRAIN GAGE LOCATIONS

● Denotes Strain Gage

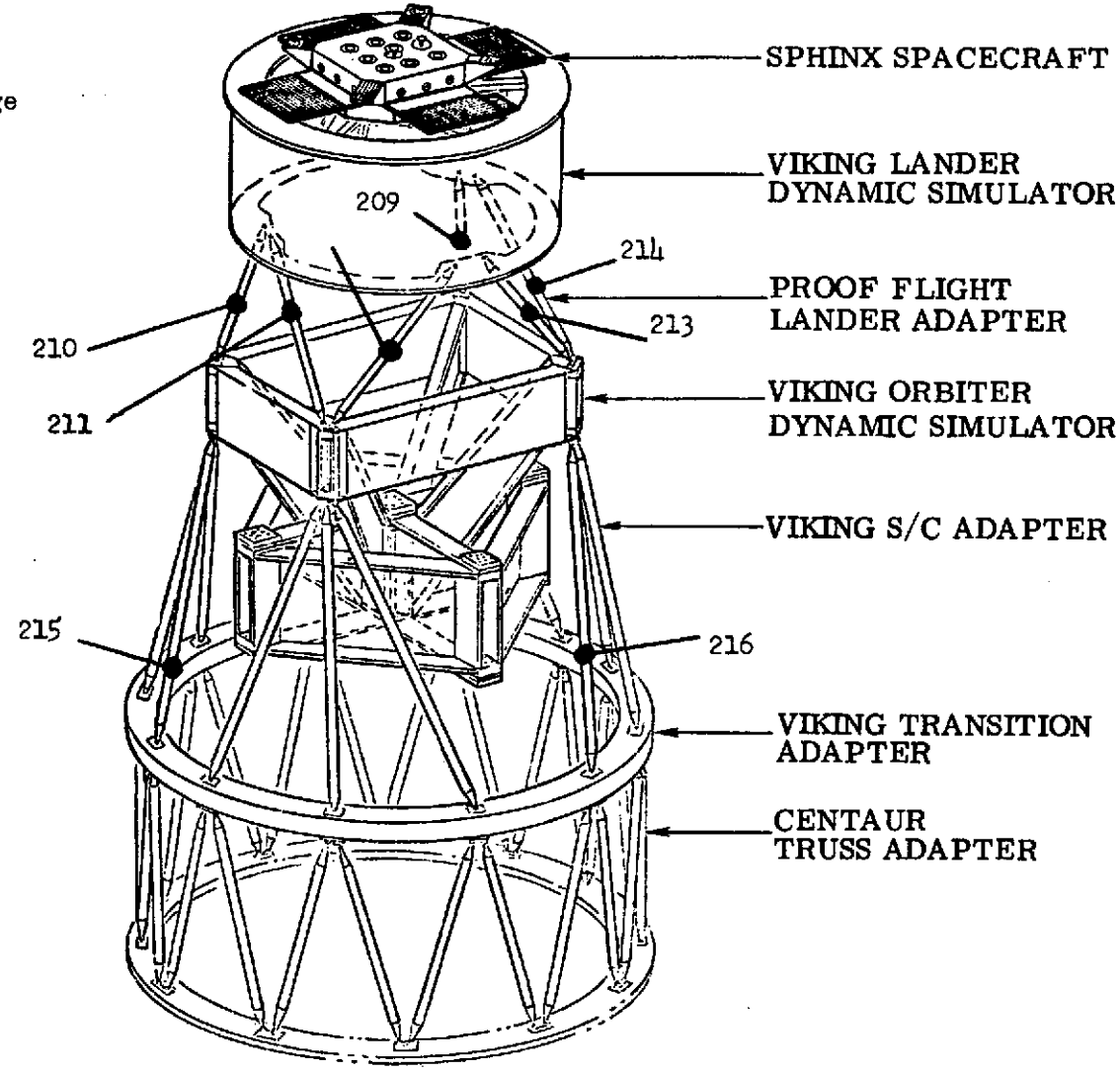

Figure VII-1A-9 Payload Adapters and Strain Gage Locations

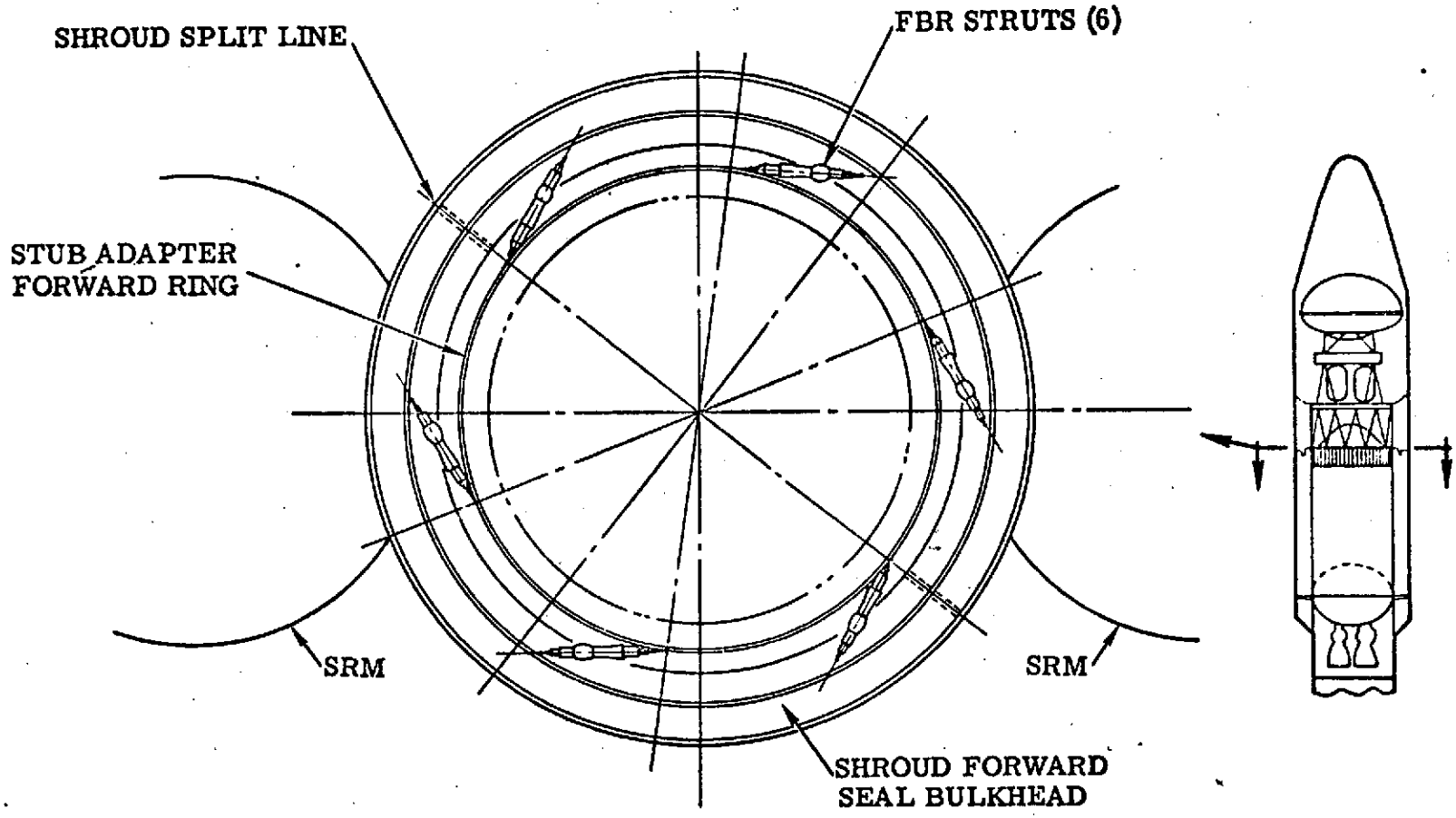

FIGURE VII-1A-10 - FORWARD BEARING REACTION SYSTEM

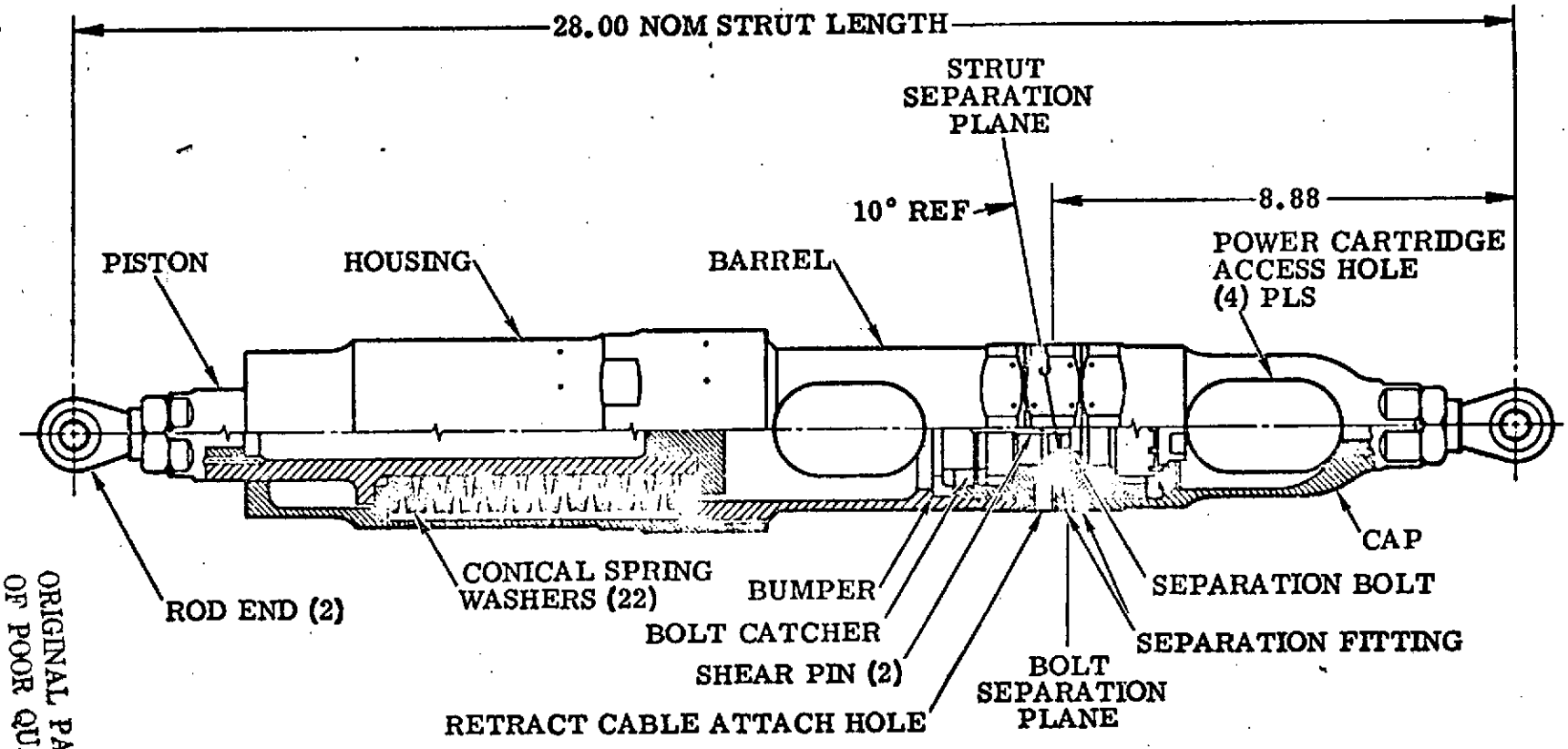

FIGURE VII-1A-II FORWARD BEARING REACTION STRUT

VII-1B. Centaur Propellant Feed System

by K. W. Band

Summary

The liquid hydrogen propellant feed system, including the boost pump operation, engine chilldown, and propellant flow to the engines was satisfactory.

The liquid oxygen propellant feed system operation was not proper. Failure of the LO_2 boost pump to start and reach rated speed and pressure rise caused improper engine chilldown, insufficient NPSP to the engine turbopumps, and subsequent failure of the engines to reach rated thrust.

Descriptions of hardware and presentation of flight data are presented here. For further information regarding the cause or causes of the LO_2 boost pump failure, refer to "Report of the TC-1 Review Board" Lewis Research Center, June 3, 1974.

System Description

Liquid oxygen feed system. - The liquid oxygen propellant feed system consists of a sump, boost pump, and turbine drive assembly, and supply ducts to transfer liquid oxygen from the Centaur tank to the inlet of the main engine liquid oxygen pumps as shown in figure VII-1B-1.

The sump is located at the aft end of the liquid oxygen tank. The liquid oxygen boost pump is mounted inside the sump (see fig. VII-1B-2), and operates while completely submerged in liquid oxygen. The pump is driven by a geared turbine-drive subassembly mounted external to the sump. A cutaway view of the liquid oxygen boost pump and turbine assembly is shown in figure VII-1B-3.

The major parts of the liquid oxygen boost pump are the inducer, centrifugal impeller, inducer housing, volute housing, shaft, shaft bearings (2), shaft housing, and bellows type dynamic shaft seals (2). The inducer and impeller housings, and the impeller are aluminum alloy castings. The inducer is machined from wrought aluminum alloy. The inducer and impeller are spline fitted to the pump shaft. The shaft and shaft housing are machined from 304 stainless steel. The volute and inducer housings each contain an interference fitted brass ring to absorb potential rub at the forward and aft ends of the impeller.

Leakage between the impeller and the pump housing is controlled by the clearance between the labyrinth grooves machined on the forward and aft rims of the impeller and the brass wear rings. The controlled leakage is directed back into the sump by way of three small holes in the

volute casting. The small quantity of volute bleed flow permits the pump to operate at near zero discharge flow.

Both pump shaft bearings are 440C steel ball bearing type, and are cooled by a small flow of liquid oxygen through each bearing. The coolant flow for the aft bearing is bled from the impeller discharge and routed through a small orifice into a drilled passage in the inducer casting, through the bearing, and exits back into the sump by means of a hole drilled in the pump shaft. The coolant flow for the forward bearing is bled from the backside of the impeller, through the bearing, and exits directly into the sump. The aft bearing is designed to absorb the thrust loads induced by the impeller.

The pump shaft dynamic seals are press fitted into the shaft housing. The forward seal is designated the primary seal. The aft seal is designated the secondary seal. Both seals are bellows spring loaded with a carbon nose piece rubbing against a carbon faced seal mating ring on the pump shaft. The bellows of each seal is Inconel-X. The primary seal is cooled, lubricated, and vibration dampened by the liquid oxygen on the forward side of the seal. The secondary seal, however, operates dry. A snubber spring is installed in the secondary seal to dampen vibration induced chatter between the sealing surfaces. Leakage past the primary seal is vented overboard by means of a port into the cavity between the primary and secondary seals (primary cavity). Leakage past the turbine output shaft seal is prevented from entering the primary cavity by venting the cavity between the pump secondary seal and the turbine output shaft seal (secondary cavity). Both seal cavities are provided with a gaseous helium blanket purge when LO_2 is tanked (see fig. 2). The purge is terminated at liftoff.

The turbine drive subassembly consists of a gas generator (catalyst bed), turbine wheel, and a 9.1 to 1 reduction gear-train. A cross sectional view of the turbine drive is shown in figure VII-1B-4. Hydrogen peroxide monopropellant (90 percent concentration) is directed into a silver plated nickel screen catalyst bed where it is decomposed into superheated steam and oxygen (approximately 1350° F). The hot gases are collected in a rectangular plenum chamber (referred to as the nozzle box), and then directed into the turbine wheel buckets by five convergent-divergent nozzles. The turbine is a single stage, impulse, partial admission type, with the five nozzles oriented in a 76 degree arc of the turbine wheel. The turbine wheel contains 79 cast buckets welded to the wheel disk. After passing through the buckets, the gases are collected in an exhaust casing, and routed overboard by an aft directed, 2 inch diameter, turbine exhaust duct. A continuous power, 40-watt, 28 volt d.c. coil heater is provided on the external surface of the catalyst bed housing to heat the bed and improve starting characteristics. The turbine operates at a constant power level as determined by the flow rate of peroxide through two orifices upstream of the catalyst bed. The orifices are installed in an orifice block (referred to as the "orifice holder") which is mounted on the nozzle box/exhaust casing flange by a bracket.

Details of the gear train are shown in figure VII-1B-5. The turbine wheel shaft is integral with the wheel. The wheel shaft is supported by two ball bearings and contains a 22-tooth pinion (first reduction pinion) spur gear which is spline connected to the shaft. The first reduction pinion drives the intermediate shaft assembly, which contains the first reduction spur gear (integral with the shaft) with 63 teeth and the second reduction pinion (spline connected to the shaft) spur gear with 17 teeth. The intermediate shaft is supported by a ball bearing on each end of the shaft. The second reduction pinion drives the output shaft which contains the second reduction (output) spur gear. The output gear has 54 teeth and is integral with the output shaft. The output shaft is also supported by a ball bearing on each end, and is internally splined to accept the drive-to-pump coupling. All gears are induction hardened 4340 steel with silver plate on the teeth of the first and second reduction gears. The gears and bearing are lubricated with 37 grams of wide temperature range grease which is applied during assembly.

The gear-case consists of an upper and lower cast aluminum alloy housing fastened together by a bolted flange design. An aluminum filler plate is sandwiched between the two halves of the gear casing to maintain proper grease distribution. Alinement between the two halves is maintained by three close tolerance "body-bound" bolts installed in the flanges.

The gear case is sealed from the turbine wheel by a double sealing arrangement: a labyrinth type seal around the shaft, and a bellows-type carbon nosed dynamic seal which rides on a shoulder machined on the shaft. The cavity between the two seals is vented overboard to prevent labyrinth seal leakage from entering the gear case.

The drive output shaft also contains a bellows-type carbon nosed dynamic seal which rides against a metal seal mating ring on the output shaft.

A pressure relief valve is installed in the gear case to prevent overpressurization. The relief valve is set to relieve when the internal-to-external pressure differential exceeds 5 to 9 psid.

Liquid oxygen is transferred from the boost pump to the main engines through a stainless steel feed duct assembly. The two branch legs (one to each engine) are 2.5 inches in diameter. The common leg connecting to the sump outlet is 3.0 inches in diameter. Each of the two branch legs contain three bellows covered gimbal joints to permit duct movement during engine gimbaling. The exterior surface of the duct assembly is covered with a closed cell, rigid, foam insulation to reduce heat transfer to the liquid oxygen while the vehicle is on the launch pad. The exterior surface of the foam is covered with a tight wrapping of aluminized mylar and white plastic tape to minimize radiation heat transfer during space flight.

A bleed line is connected to each branch leg of the feed duct near

the engine and routed back into the ullage space of the liquid oxygen tank. The bleed line provides a path for the trapped boiloff gas and warm propellant to circulate back into the tank. The circulation assists in chilling the ducts and maintaining liquid at the main engine pump inlets for engine start.

For the TC-1 flight, the LO_2 feed duct assembly was covered by a multilayer radiation shield blanket. Purpose of the blanket shield is to minimize the radiation heat transfer during extended coast periods.

Locations of the liquid oxygen propellant feed system instrumentation is shown in figure VII-1B-6. The instrumentation consisted of the following:

Measurement number	Description
CP120P	LO_2 boost pump headrise
CP15B	LO_2 boost pump turbine speed
CP26P	LO_2 boost pump turbine nozzlebox pressure
CP36T	LO_2 boost pump turbine bearing temperature
CP33T	LO_2 boost pump inlet temperature
CP59T,CP61T	C-1 and C-2 LO_2 pump inlet temperatures

Liquid Hydrogen Feed System. - The liquid hydrogen propellant feed system consists of the same basic elements as the liquid oxygen system: a sump, boost pump and turbine drive assembly, and supply ducts to transfer liquid hydrogen from the Centaur tank to the inlet of the main engine liquid hydrogen pumps (see fig. VII-18-1).

The sump is located at the aft end of the liquid hydrogen tank. The liquid hydrogen boost pump is mounted inside the sump and operates while completely submerged in liquid hydrogen. The pump is driven by a geared turbine-drive subassembly mounted external to the sump. A cutaway view of the liquid hydrogen boost pump and turbine assembly is shown in figure VII-1B-7.

Basic components of the hydrogen boost pump are the same as previously described for the liquid oxygen boost pump. The materials and design details of the liquid hydrogen boost pump are the same as the liquid oxygen boost pump with the following exceptions:

(1) The pump shaft and coupling are A-286 instead of 304 stainless steel.

(2) The impeller wear rings are carbon instead of brass.

(3) The aft bearing is grease lubricated instead of liquid cooled.

(4) Flow is from forward-to-aft whereas the liquid oxygen boost pump flow is from aft-to-forward.

(5) Inlet guide vanes are provided.

(6) The volute bleed flow is collected in an annular can and directed back into the tank by means of a small diameter line.

(7) The two dynamic bellows-type carbon seals are located at the aft end of the pump shaft housing instead of the forward end as for the liquid oxygen pump.

(8) The inducer and impeller are cantilevered from the forward shaft bearing.

(9) The forward bearing coolant bleed flow is directed from the bearing cavity into an orificed passageway in the volute casting, and exits into the lower end of the sump by means of a single hole.

The liquid hydrogen boost pump turbine drive subassembly is identical to the liquid oxygen subassembly with the following exceptions:

(1) The gear reduction ratio is 5.96 to 1 (the number of teeth on the second reduction pinion is 23, and on the output gear is 48).

(2) The first reduction pinion material is nitralloy-N.

(3) Two ports are provided to enable periodic regreasing of the two pinion gears.

(4) The turbine exhaust exit is directed aft at an angle of 45^{o} with the vehicle longitudinal centerline.

The liquid hydrogen feed duct and blanket radiation shield design is identical to the liquid oxygen duct design except for the length and routing of the duct segments. Liquid hydrogen bleed lines are provided and serve the same function as described in the liquid oxygen feed system. The liquid hydrogen duct bleed flow return line enters the tank at a location approximately 40 inches above the liquid hydrogen sump. The bleed flow is directed laterally across the tank. The flow velocity into the tank is reduced to minimize disturbance of the liquid by routing the bleed flow through an energy dissipator inside the tank (see fig. 1).

The boost pump volute bleed flow is returned to the liquid hydrogen tank by means of a 2-inch diameter line inside the sump and tank. An energy dissipator is connected to the end of the line to reduce the exit velocity, and consequently the propellant disturbances in low gravity. The exit flow is directed laterally across the tank just above the intermediate bulkhead.

Location of the liquid hydrogen propellant feed system instrumentation is shown in figure VII-1B-6. The instrumentation consisted of the following:

Measurement number	Description
CP121P	LH_2 boost pump headrise
CP16B	LH_2 boost pump turbine speed
CP28P	LH_2 boost pump turbine nozzlebox pressure
CP127T	LH_2 boost pump turbine bearing temperature
CP32T	LH_2 boost pump inlet temperature
CP60T,CP62T	C-1 and C-2 LH_2 pump inlet temperature

Propellant Feed System Flight Data

The liquid hydrogen (LH_2) boost pump appeared to start and operate normally during both attempted engine starts. However, the liquid oxygen (LO_2) boost pump did not rotate during either of the two attempted engine starts. Performance data for the LO_2 and LH_2 boost pumps during the first start attempt are shown in figures VII-1B-8 and VII-1B-9, respectively. Corresponding data for the second start attempt are shown in figures VII-1B-10 and VII-1B-11.

The boost pump turbine inlet pressure data indicated peroxide flow and decomposition within the catalyst beds was near normal for both turbines during each start attempt. The first indications of turbine inlet pressure increase was less than 2 seconds for each turbine and each start attempt. Steady state LH_2 turbine inlet pressure was 100 psia during both start attempts. Steady state LO_2 turbine inlet pressure was 100 psia for the first start attempt and 105 psia for the second start attempt. The 5 psi higher LO_2 turbine inlet pressure during the second start attempt is not totally explainable and may therefore be related to the failure to rotate. A slight increase in pressure normally occurs until the catalyst bed temperature reaches equilibrium. It is possible that the LO_2 turbine catalyst bed temperature had not stabilized by the end of the first start period, and the temperature therefore increased due to heat soak-back during the short coast period. However, the LO_2 and LH_2 turbine catalyst beds should reach thermal equilibrium at the same time since the design and peroxide flow rates are essentially identical. Since the LH_2 turbine inlet pressure showed no increase from the first operating period, its catalyst bed had apparently reached thermal equilibrium.

The LH_2 turbine inlet pressure data indicated short duration pressure perturbations during both engine start attempts. Perturbations occurred at three different times during the first start attempt, and once during the second start attempt. All but the first pressure perturbation exhibited a time-pressure signature that is characteristic of gas bubbles entrained in the peroxide flow through the orifices and catalyst bed. A gas bubble passing through the system normally results in a positive pressure spike followed immediately by a negative pressure spike. The first pressure perturbation occurred 5.5 seconds after boost pump start (BPS), and exhibited the positive spike, but not the negative spike

characteristic of a gas bubble. This first pressure perturbation was similar to perturbations noted on small peroxide engines during ground tests when delayed decomposition (temporary flooding) occurred during the starting transient.

The three latter LH_2 turbine inlet pressure perturbations were caused by trapping helium purge gas between two columns of liquid in the peroxide supply lines to the LH_2 turbine. A gaseous helium purge flows through the boost pump peroxide feed lines continuously at a rate of 250 + 50 standard cubic inches per minute except for the time periods when the boost pumps are operating. At first BPS, the two peroxide feed valves and the purge shutoff valve were energized simultaneously, which terminated the flow of purge gas and initiated flow of peroxide to the boost pump turbines. Peroxide flowed toward the LH_2 turbine by means of the two available flow paths, expelling the purge gas ahead of the liquid. Ideally the liquid flow would arrive at the common line to the LH_2 turbine simultaneously such that no purge gas would become trapped. However, opening response time for the two feed valves may not be identical and the two peroxide lines may not have the same length and pressure drop. Consequently, the liquid column in one of the two legs may arrive at the common line to the LH_2 turbine ahead of the other column, and a small pocket of purge gas becomes trapped. The gas pocket will then gradually migrate toward the LH_2 turbine and eventually be expelled through the turbine. The resultant turbine inlet pressure fluctuations on TC-1 were of such duration and amplitude that very little effect on turbine speed and pump headrise occurred.

The boost pump turbine speed measurements indicated no speed from either turbine during both start attempts. However, other instrumentation (pump headrise and engine inlet pressures) indicated that the hydrogen boost pump was operating in a normal manner. The lack of a speed indication for the LH_2 turbine was therefore concluded to be the result of an instrumentation failure.

The LO_2 boost pump either failed to rotate, or rotated at such low speed that it could not be detected by the instrumentation. Lack of rotation as indicated by the turbine speed measurement was supported by other instrumentation which indicated there was no pump pressure rise. The LO_2 boost pump headrise measurement (CP120P) remained at zero during both start attempts except for a small pressure spike shortly after main engine start (MES) command. The LO_2 boost pump headrise is normally approximately 75 psid at prestart (PS) and MES. The small pressure spikes indicated the CP120P pressure transducer was operative. The main engine LO_2 pump inlet pressure measurements (CP51P and CP53P) also showed no evidence of boost pump pressure rise. After the engine pump inlet valves were opened at prestart, the pressures were essentially the same as the LO_2 tank ullage pressure (approximately 40 psia). The engine LO_2 pump inlet pressures should be approximately 115 psia during the time period between prestart and MES.

The LH_2 boost pump headrise instrumentation (CP121P) indicated pump

operation was normal. The pump headrise was approximately 24 psid at prestart and 21 psid at MES for both start attempts. The headrise dropped to zero momentarily during the first engine start transient due to the high liquid hydrogen flow rate created by the main engines overspeeding.

The LO_2 and LH_2 turbine bearing temperature measurements (CP36T and CP127T, respectively) indicated normal values at first BPS. The LO_2 turbine bearing temperature at this time was 60° F, and the LH_2 turbine bearing temperature was 66° F. The LH_2 turbine bearing temperature increased at a normal rate of 0.3° F per second during the boost pump operating periods. However, the LO_2 turbine bearing temperature increased at an abnormal rate of approximately 0.1° F per second. The low LO_2 turbine bearing temperature rise rate was believed to be the result of the failure to rotate.

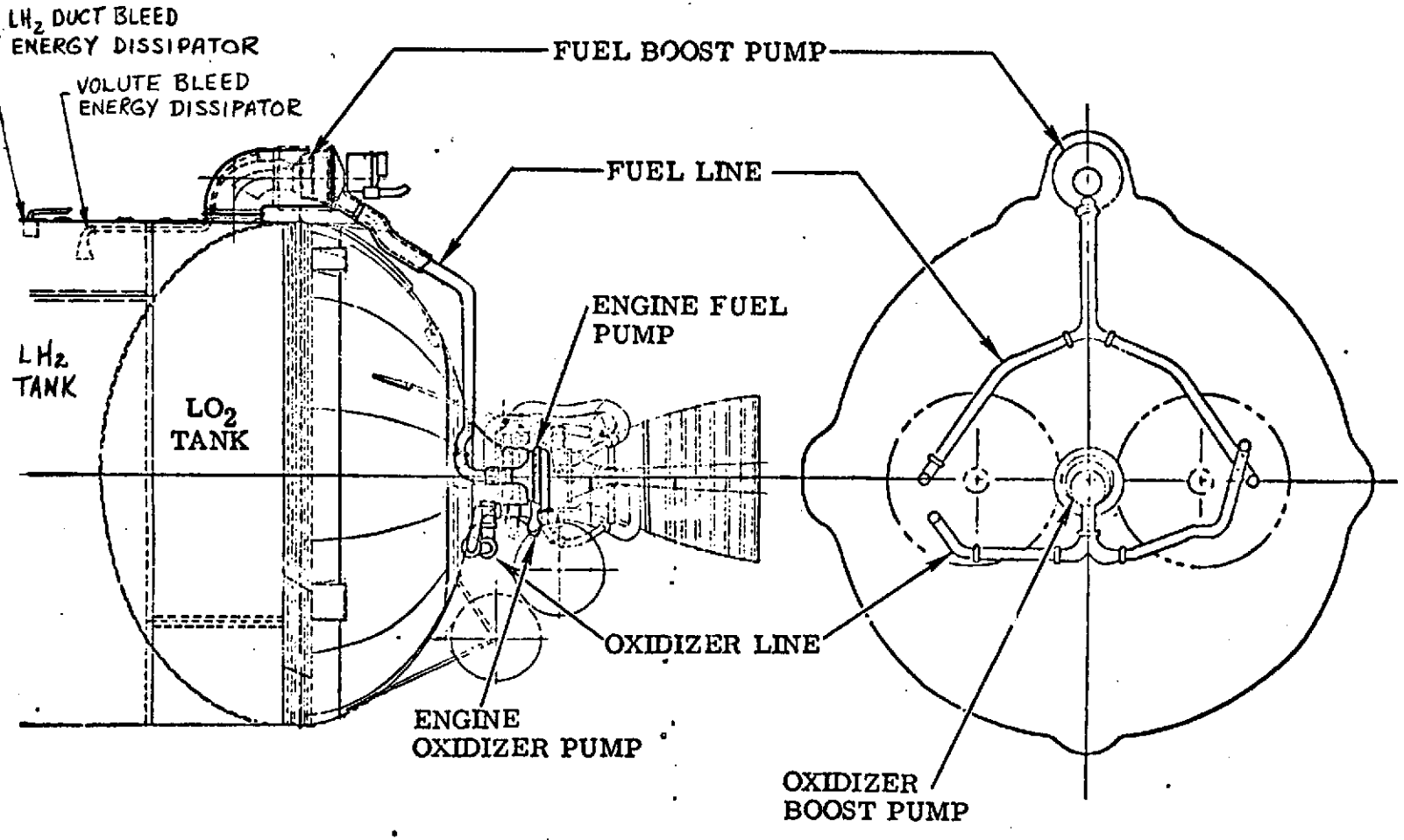

Figure VII-1B-1 Centaur Propellant Feed System

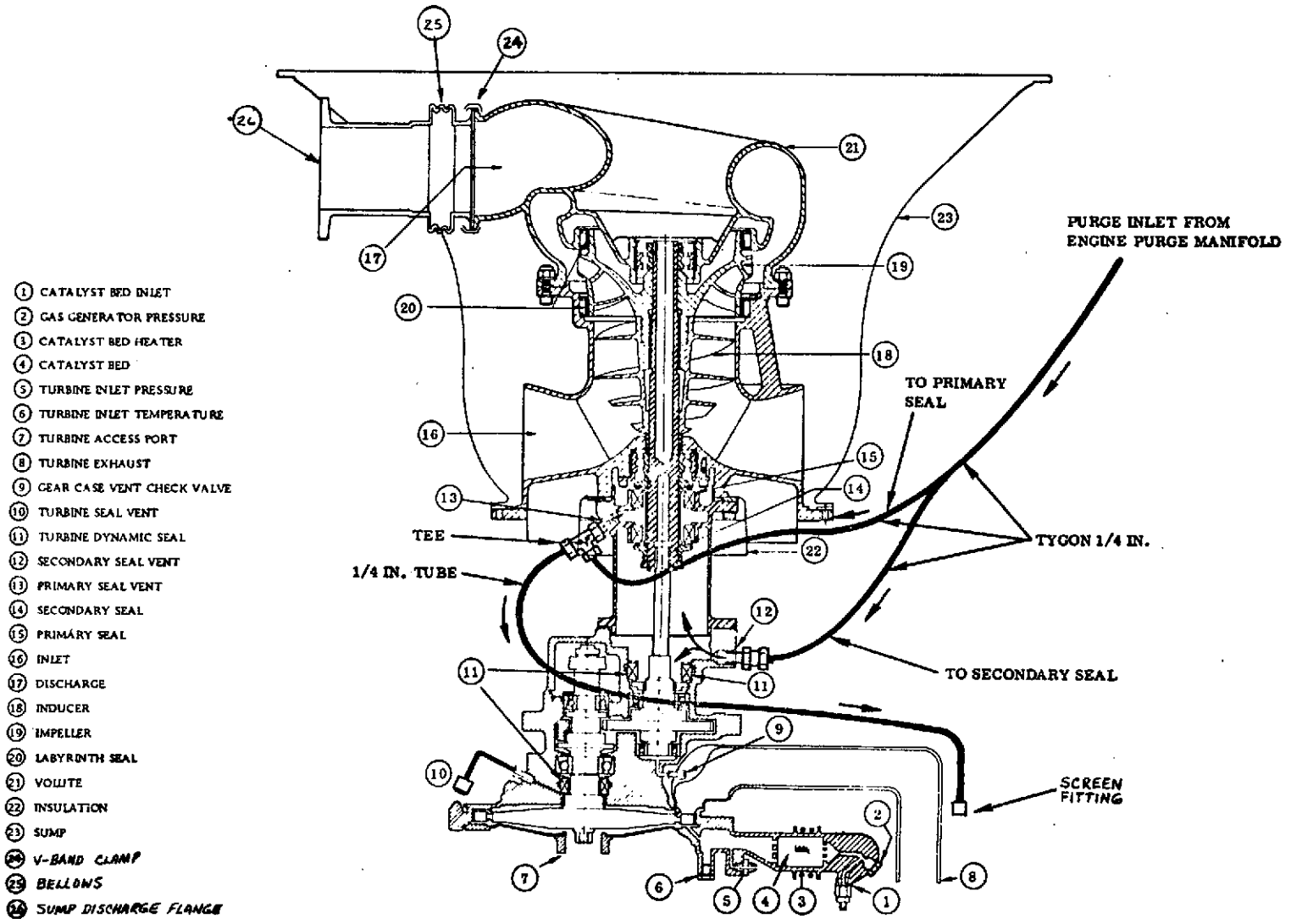

FIGURE VII-1B-2 CUTAWAY VIEW OF CENTAUR LO_2 BOOST PUMP INSTALLED IN SUMP

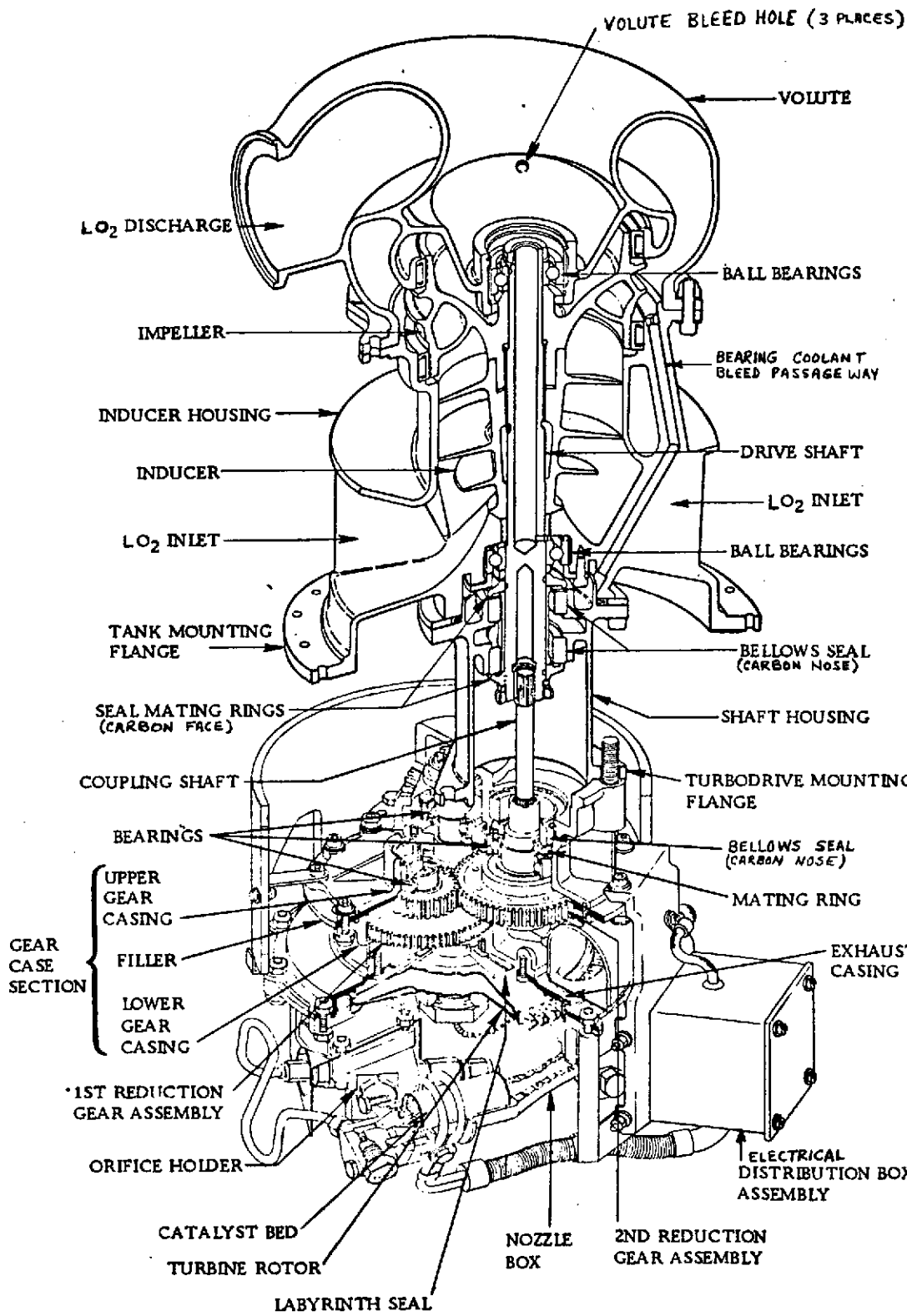

FIGURE VII-1B-3 CUTAWAY VIEW OF CENTAUR LO_2 BOOST PUMP AND TURBINE ASSEMBLY

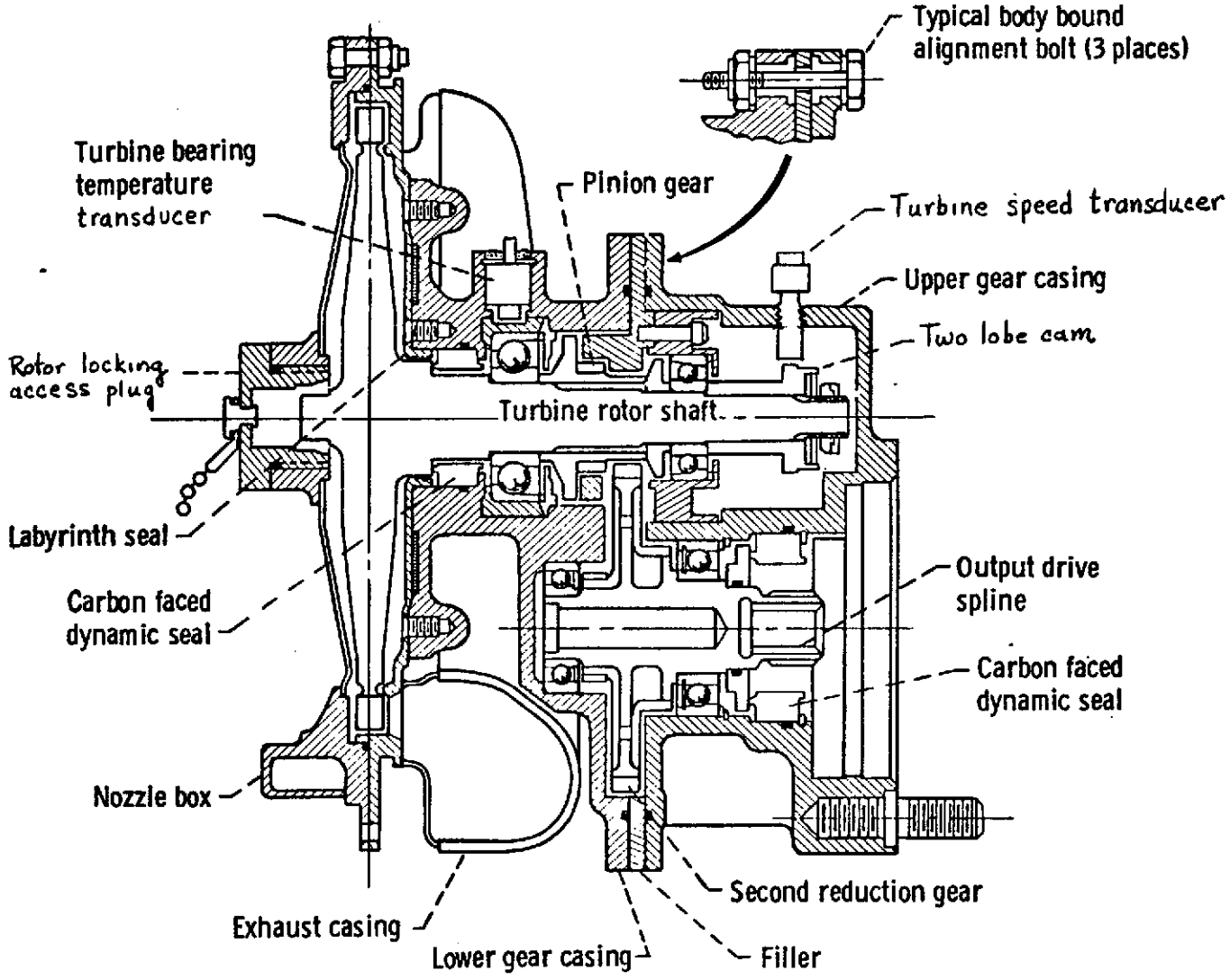

FIGURE VII-1B-4 CROSS SECTION VIEW OF CENTAUR BOOST PUMP TURBINE DRIVE

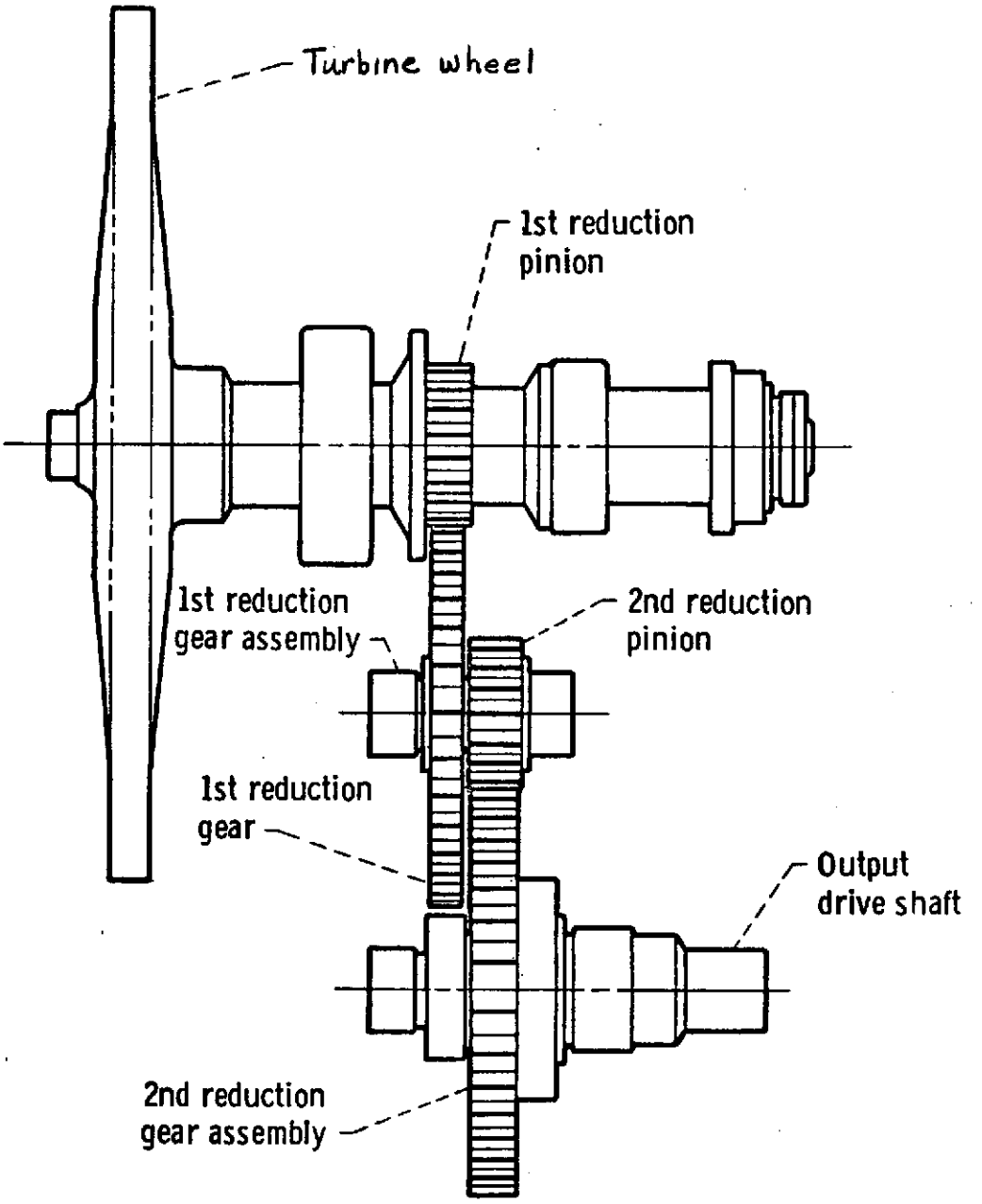

FIGURE VII-1B-5 CENTAUR BOOST PUMP TURBINE GEAR DRIVE TRAIN

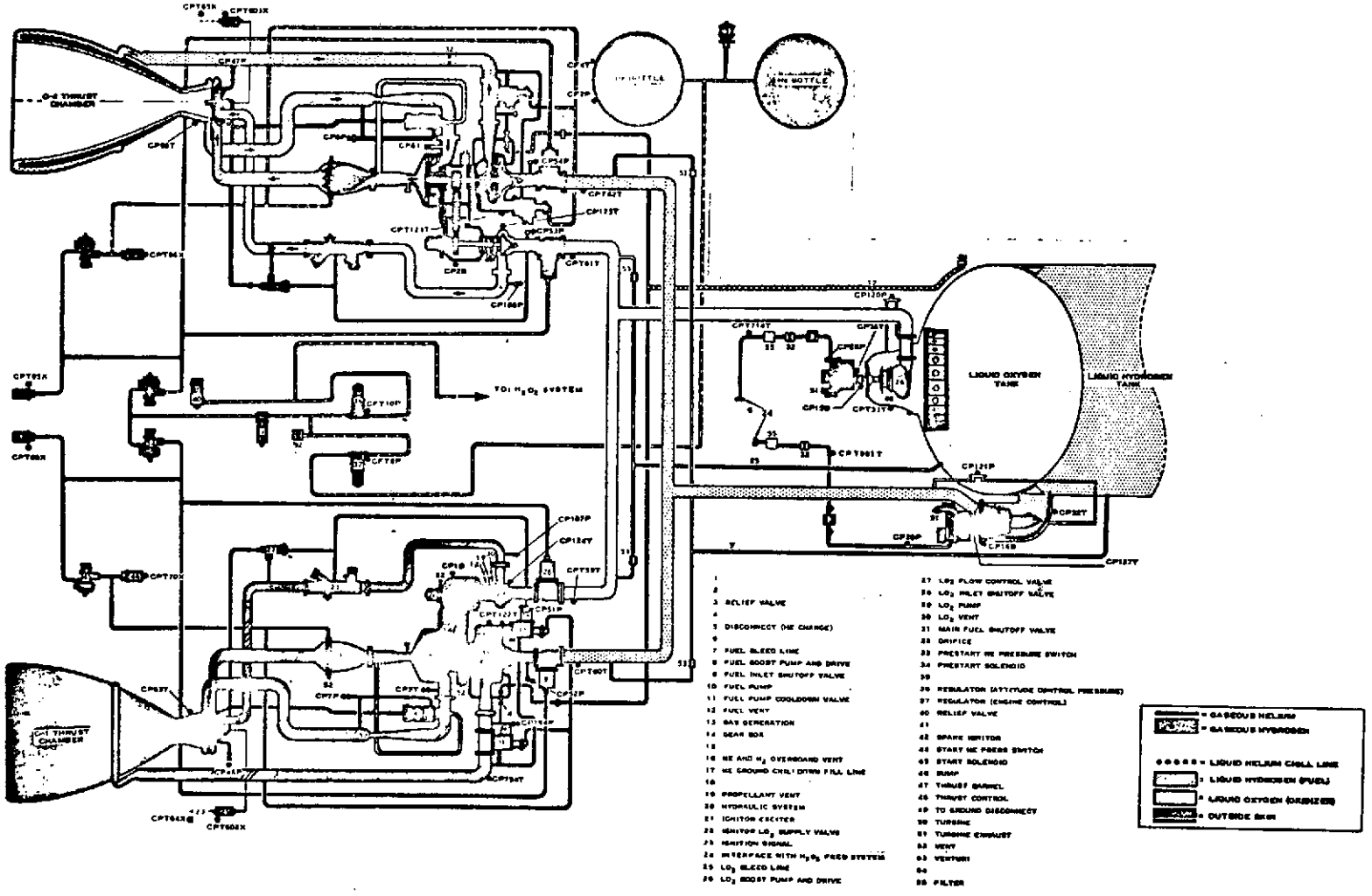

FIGURE VII-1B-6 CENTAUR PROPELLANT FEED SYSTEM INSTRUMENTATION LOCATIONS

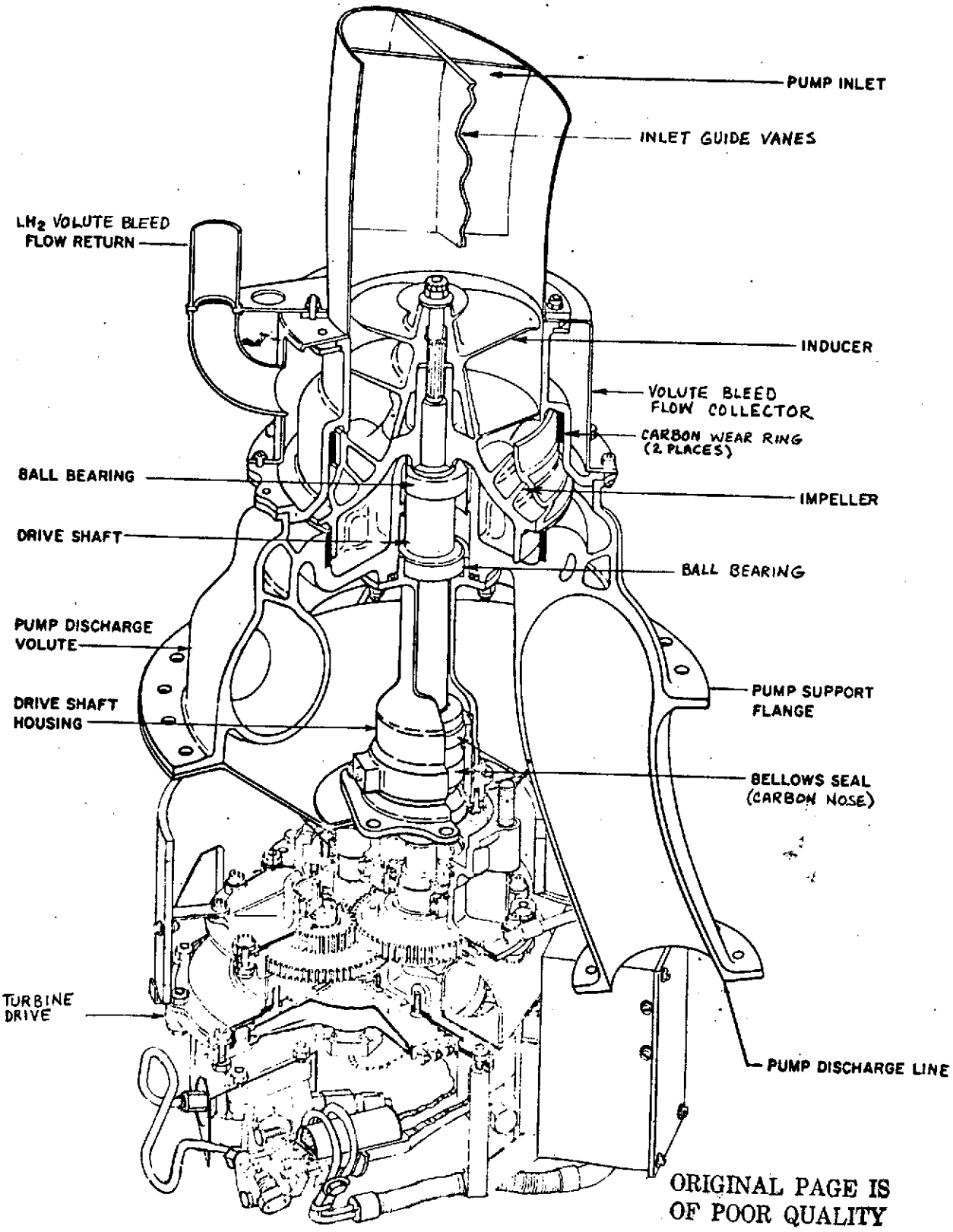

FIGURE VII-1B-7 CUTAWAY VIEW OF LIQUID HYDROGEN BOOST PUMP AND TURBINE DRIVE

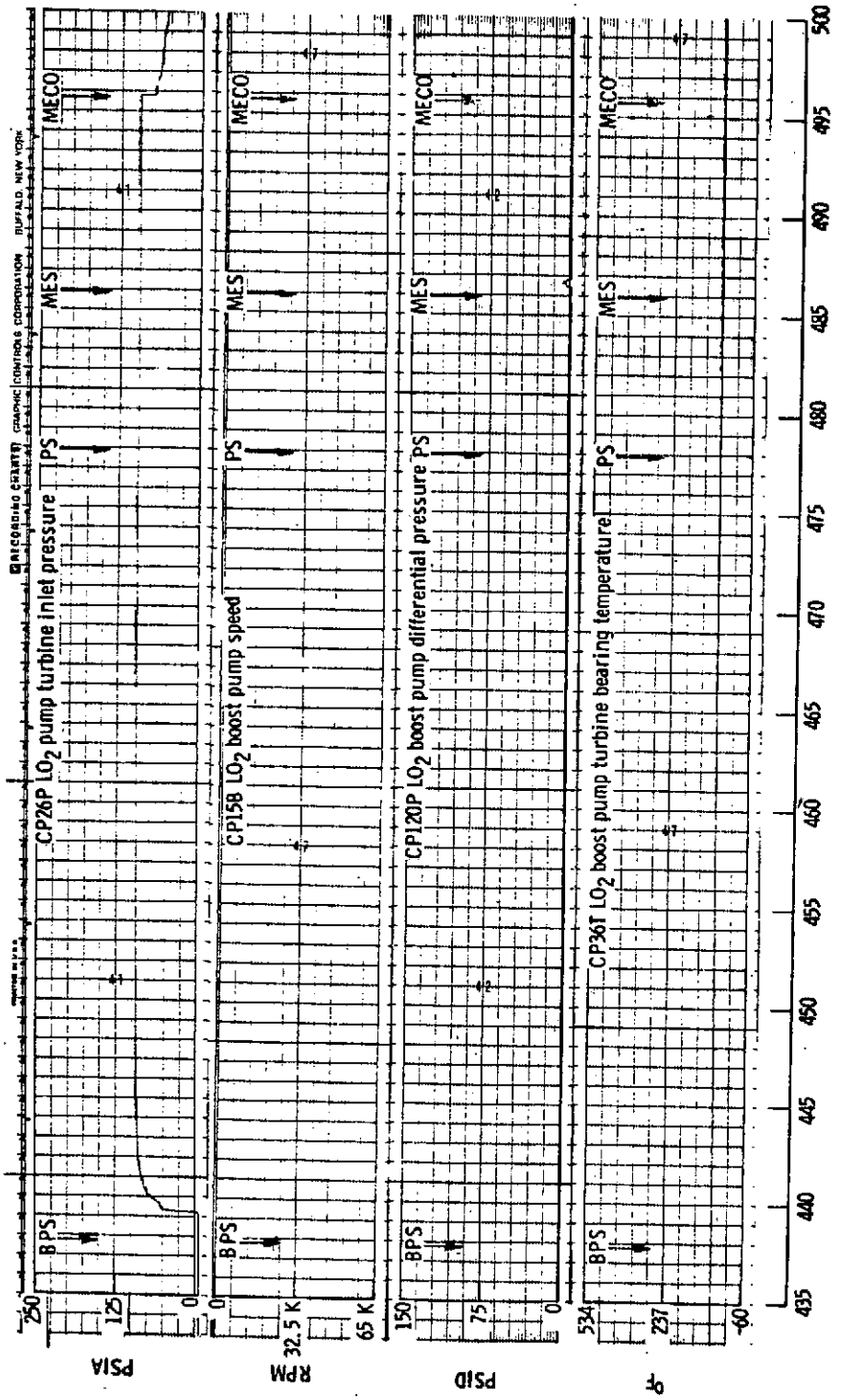

FIGURE VII-1B-8 CENTAUR LIQUID OXYGEN BOOST PUMP PERFORMANCE DURING FIRST START ATTEMPT

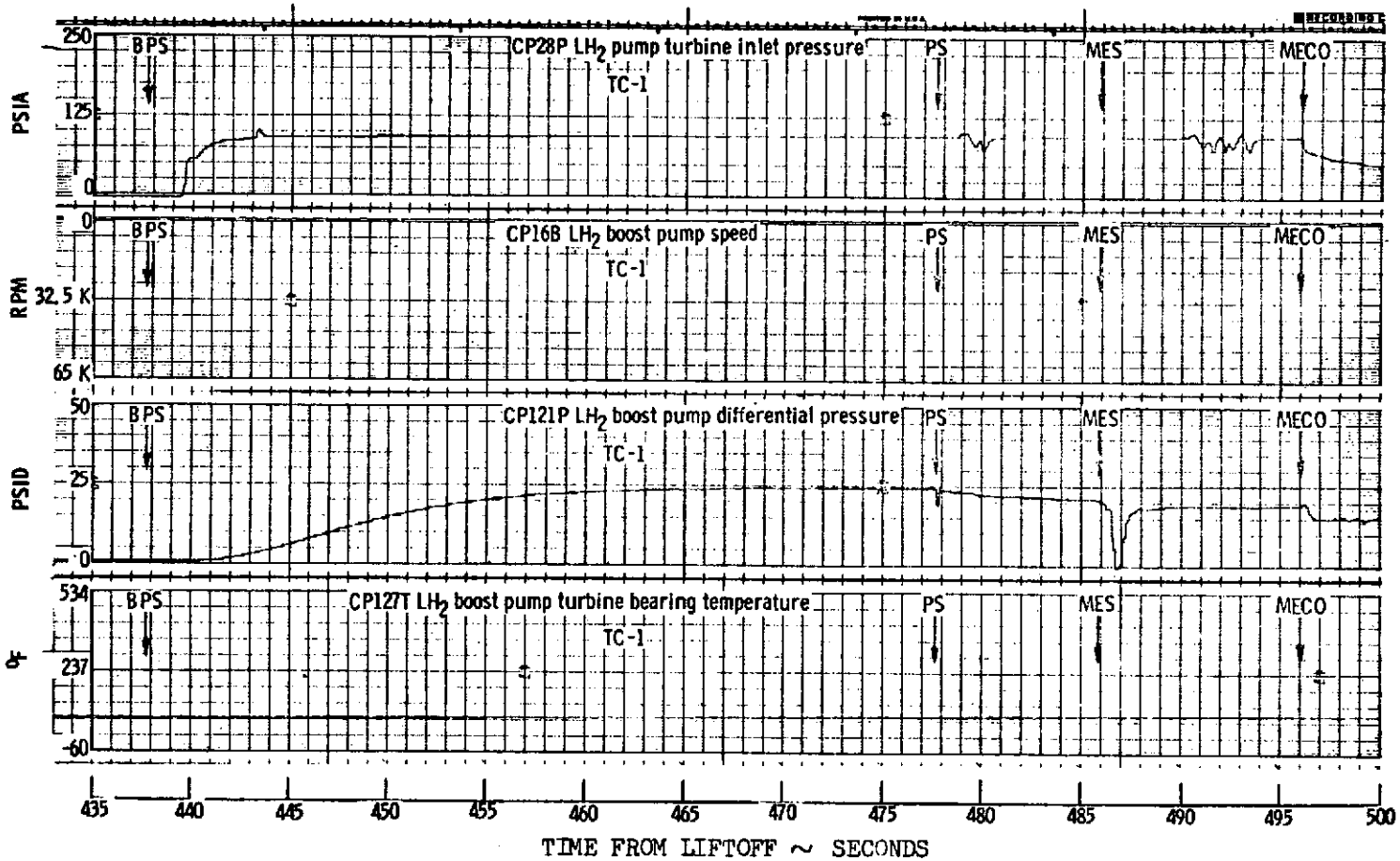

FIGURE VII-1B-9 CENTAUR LIQUID HYDROGEN BOOST PUMP PERFORMANCE DURING FIRST START ATTEMPT

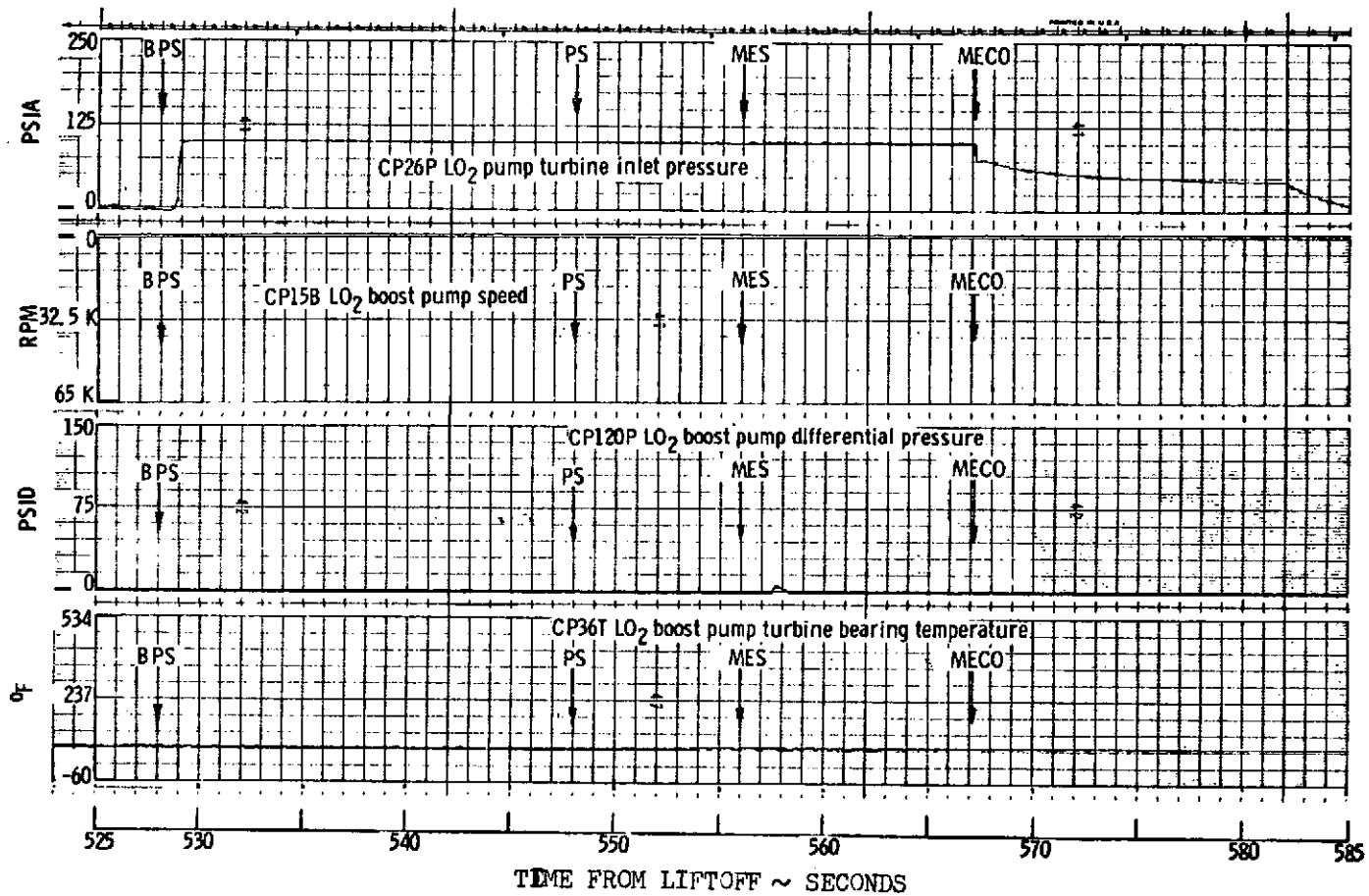

FIGURE VII-1B-10 CENTAUR LIQUID OXYGEN BOOST PUMP PERFORMANCE DURING SECOND START ATTEMPT

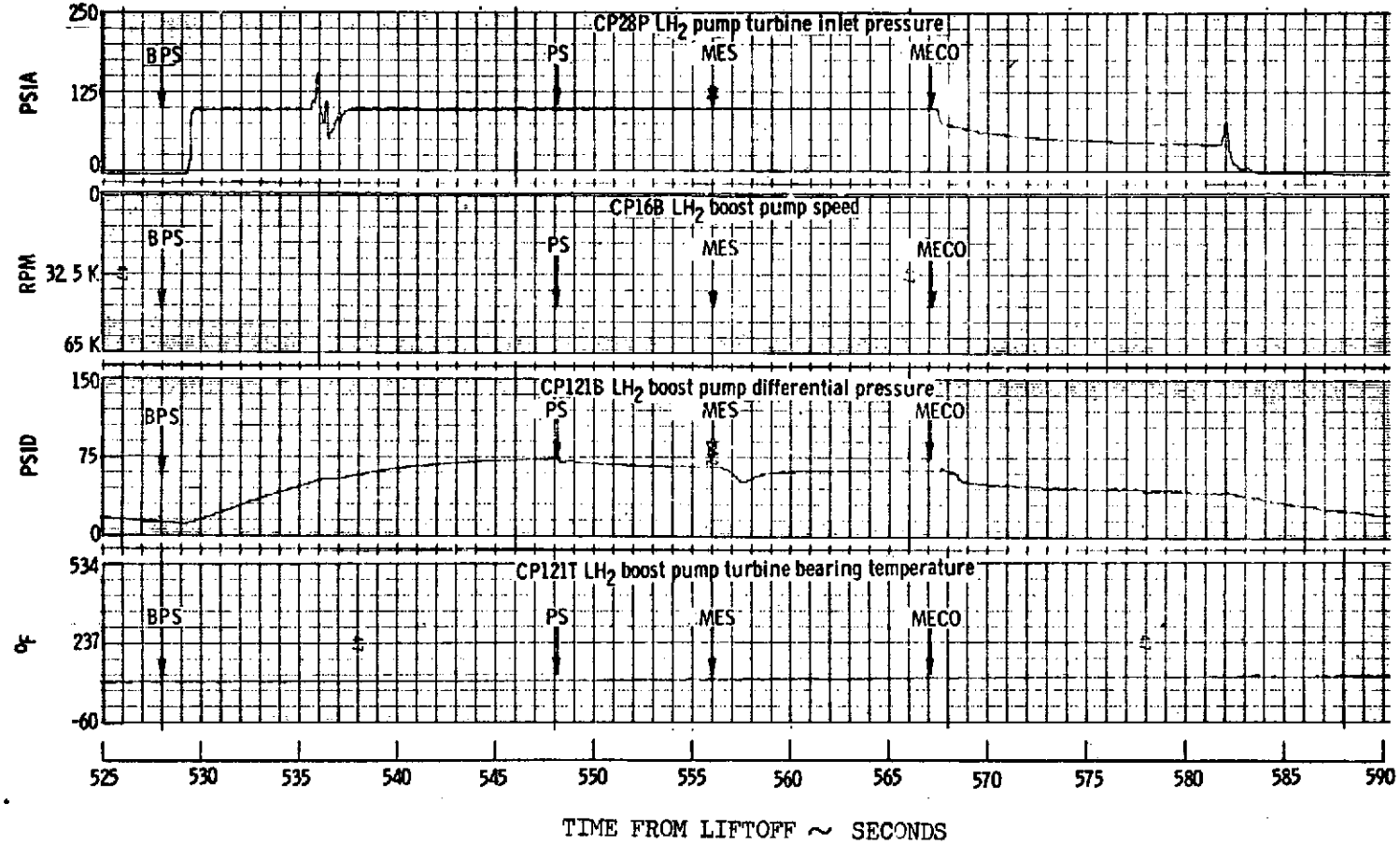

FIGURE VII-1B-11 CENTAUR LIQUID HYDROGEN BOOST PUMP PERFORMANCE DURING SECOND START ATTEMPT

VII-1C. Centaur Main Propulsion System

by W. K. Tabata

Summary

Analyses of the RL10A-3-3 engine flight data from the TC-1 launch indicate the following:

(1) Both engines operated as would be expected under the adverse oxidizer propellant inlet conditions.

(2) Ignition was normal on both engines on both MES #1 attempts.

(3) Engine valves operated normally during the aborted start transients.

(4) Both the C-1 and C-2 engine fuel pumps exhibited normal cooldown and acceleration during the start transient.

(5) Both the C-1 and C-2 engine oxidizer pumps exhibited abnormal cooldown and acceleration during the start transient.

(6) All special proof flight temperature measurements on the engines appear normal.

System Description

The Centaur D-1T main propulsion system is composed of two RL10A-3-3 engines. The engine systems are identical to that of the Centaur D-1A and the previous Centaur D. The RL10A-3-3 engines are regeneratively cooled, turbopump-fed rocket engines. The liquid oxygen and liquid hydrogen propellants are burned at a nominal mixture ratio (O/F) of 5.0 in the combustion chamber at a nominal chamber pressure of 400 psia. The nominal vacuum thrust and specific impulse are 15 000 pounds and 444 seconds.

Shown in figure VII-1C-1 is a flow schematic of the RL10A-3-3 engine. The operating sequence of the engine is the following:

(a) Ground prechill. - On the ground, 30 minutes prior to liftoff, the engine fuel pumps are prechilled with a ground supply of liquid helium. The requirement for a Titan/Centaur launch is that both engine fuel pump housing temperature probes indicate less than 100° R (-360° F) at least 10 minutes prior to liftoff and remain below 100° R until the liquid helium prechill is secured at 7 seconds before liftoff.

The liquid helium enters the engine through the prelaunch cooldown check valve. After flowing through the engine fuel pump, the cold helium is vented through the engine fuel pump interstage cooldown valve and the

fuel pump discharge cooldown valve into a manifold and vented overboard.

The ground liquid helium prechill is used to minimize the in-flight cooldown time required for the first-burn of Centaur.

(b) Prestart. - Prior to each engine start, the engine oxidizer and fuel pumps are cooled down during a programmed prestart period. During prestart, the engine prestart solenoid valve is energized allowing vehicle-supplied helium to actuate the engine fuel pump inlet shutoff valve and oxidizer pump inlet shutoff valve open. With the inlet valves open, liquid propellants are allowed to pass through the pumps and cool them.

The liquid oxygen flows through the single-stage oxidizer pump, through the oxidizer flow control valve, and overboard through the thrust chamber.

The liquid hydrogen flows through the first stage of the two-stage fuel pump. Part of the flow is vented overboard through the fuel pump interstage cooldown valve. The remainder of the flow passes through the second stage of the pump and is vented overboard through the fuel pump discharge cooldown valve. This prestart hydrogen flow is prevented from flowing through the thrust chamber regeneratively cooled jacket, the turbine, and out through the thrust chamber by the main fuel shutoff valve which is closed at this time. The main fuel shutoff valve is not a zero leakage valve by design. There is some leakage through the valve during prestart in order to keep the fuel manifold in the injector purged of oxygen.

(c) Start. - At engine start signal, the engine start solenoid valve is actuated. This allows vehicle-supplied helium to open the main fuel shutoff valve, close the fuel pump discharge cooldown valve, and partially close the fuel pump interstage cooldown valve. This now allows the hydrogen to pass through the regeneratively cooled jacket picking up heat energy and through the turbine. With flow through the turbine, both pumps start to rotate. The hydrogen leaves the turbine and passes through the main fuel shutoff valve into the combustion chamber.

Coincident to start signal, the engine spark plug igniter is energized for 4 seconds. Ignition normally occurs about 0.2 second after start signal.

With combustion established in the thrust chamber, the hydrogen picks up more heat energy in the regeneratively cooled jacket and the engine starts to accelerate to steady-state conditions.

The fuel pump interstage cooldown valve is fully closed when fuel pump pressure-rise becomes greater than 150 psi. This delay in closing is to prevent stall of the fuel pump first stage during the start transient.

The oxidizer flow control valve main poppet opens after the oxidizer

pump-pressure rise becomes greater than 75 psi.

(d) Steady-state. - After engine acceleration to steady-state (less than 2 sec), constant engine thrust is maintained by the engine thrust control valve. The thrust control senses engine chamber pressure and modulates the bypass flow around the fuel turbine in order to maintain a constant chamber pressure.

Flight Performance

The TC-1 flight data for the C-1 engine main engine start number 1 (MES #1) first attempt are shown in figure VII-1C-2. These data are copies of a strip chart recorder. The engine parameters and the instrumentation ranges are noted on each channel. Also marked on the trace is the time for prestart and start.

Analyses of these data indicate the following:

(1) At prestart signal, both the fuel pump inlet shutoff valve and the oxidizer pump inlet shutoff valve opened normally. This is evidenced by the step increase in C-1 pump LO_2 inlet pressure (measurement CP51P) and C-1 pump LH_2 inlet pressure (measurement CP52P). The C-1 pump LH_2 inlet pressure indicates approximately 50 psia at prestart and this value is normal. The C-1 pump LO_2 inlet pressure indicates approximately 40 psia which is LO_2 tank ullage pressure and this is abnormal. Normally the oxidizer pump inlet pressure should be approximately 120 psia at prestart.

The flow of propellants through the pumps are also indicated by the C-1 pump LO_2 discharge pressure (measurement CP107P), C-1 pump LH_2 discharge pressure (measurement CP194P), and C-1 fuel venturi inlet pressure (measurement CP7P) during the prestart period.

The rise in C-1 turbine inlet temperature (measurement CP5T) from approximately 385° to 415° R during the prestart period is normal and is caused by the slight leakage of hydrogen through the main fuel shutoff valve.

(2) At engine start signal, the main fuel shutoff valve opens normally as indicated by the rise in C-1 turbine inlet temperature (CP5T) and the acceleration of the C-1 pump speed (CP1B).

Right after start signal, the C-1 thrust chamber pressure (measurement CP46P) indicates a rapid increase to approximately 8 psia. This indicates engine ignition. Previous engine testing has indicated that a rapid increase in chamber pressure to this level or higher could only result if ignition occurs.

After engine start, the pump speed and the fuel pump discharge pres-

sure accelerate normally. Proper fuel pump acceleration is also indicated in the fuel venturi inlet pressure. Since the fuel side accelerated normally, it can be assumed that both fuel pump cooldown valves operated normally.

The oxidizer pump discharge pressure indicates a delay in pressure rise. Based on the pump discharge pressure and the pump speed, it appears that the oxidizer pump cavitated.

With normal fuel flow and abnormal oxidizer flow into the combustion chamber, the engine either flamed-out or had a very cold fire as evidenced by the sudden decrease of turbine inlet temperature to off-scale low about 1 second after ignition.

With the heat energy gone or drastically reduced, the engine pump speed immediately started to drop. With the drop in pump speed, the fuel pump discharge pressure also dropped.

The dip in fuel pump inlet pressure after start signal is still being evaluated. This pressure dip coincides with a dip in the hydrogen boost pump pressure-rise after start signal and probably is related to a higher than normal increase in fuel flow through the cold engine.

The initial pressure spikes in the oxidizer pump inlet pressure after start signal is probably caused by the 80 psia oxidizer pump discharge pressure surging back through the pump as the pump starts to decelerate. The subsequent pressure spikes in oxidizer pump inlet pressure and also oxidizer pump discharge pressure are caused by the oxidizer pump alternately starting and cavitating as the pump decelerated.

The engine shutdown signal was issued 10 seconds after start signal by the guidance system when vehicle acceleration was not sensed.

The flight data for the C-2 engine during the MES #1 first attempt is shown in figure VII-1C-3. The C-2 engine behavior is similar to the C-1 engine.

For comparison purposes, the successful MES #1 of the C-2 engine on Atlas/Centaur flight A/C-30 is presented in figure VII-1C-4.

The TC-1 engine data indicate that the reason for unsatisfactory engine start was caused by inadequate cooldown of the C-1 and C-2 engine oxidizer pumps. This inadequate cooldown was caused by abnormally low inlet pressure and low net positive suction pressure (NPSP) to the engine oxidizer pumps.

After the guidance system shut the engines down, one minute later the vehicle computer initiated a second engine start sequence.

The C-1 and C-2 engine data for this second attempt at MES #1 are shown in figures VII-1C-5 and 6. Again the inlet valves opened normally

at prestart signal, the main fuel shutoff valve opened normally at start signal, and both engines ignited as evidenced by chamber pressure.

On this attempt, since the engine thrust chambers were colder, pump speed acceleration was slower and peaked at a lower speed. The fuel pumps show normal pressure rise, but the oxidizer pumps again indicate cavitation. And again since the guidance system failed to sense vehicle acceleration, the engines were shutdown.

Inadequate cooldown of the oxidizer pump is also indicated in figure VII-1C-7 which is a plot of the C-1 and C-2 engine oxidizer and fuel pump housing temperatures. In the figure, TC-1 MES #1 first and second attempts are compared to the successful A/C-30 MES #1.

The TC-1 C-1 and C-2 engine oxidizer pump housing temperatures (measurements CP124T and CP125T) indicate normal temperatures at the initiation of prestart. The range in oxidizer pump housing temperature at MES #1 prestart from previous successful Atlas/Centaur flights has been 365° to 430° R. During TC-1 MES #1 first attempt prestart, the oxidizer housing temperatures decreased only 17 degrees from 382° to 365° R and 386° to 369° R indicating very little cooldown. A typical oxidizer pump cooldown during prestart is indicated by the AC-30 C-1 engine where the temperature decreased 165° R from 398° to 233° R during the prestart. On A/C-30, the C-2 engine oxidizer pump housing temperature probe exhibited a slow response and decreased only 37° R. This problem of slow response has been experienced on several successful Atlas/Centaur flights. The TC-1 oxidizer pump housing temperature probes could be suspected of slow response, but this is unlikely. Even if both probes had a response problem, the probes should have responsed by the time of initiating the second attempt MES #1 about a minute later.

During the MES #1 second attempt prestart, both C-1 and C-2 engine oxidizer pump housing temperature probes still indicate very little cooldown. The temperatures only decreased on C-1 engine 13° R from 345° to 332° R and on the C-2 engine 17° R from 357° to 340° R.

These data tend to confirm inadequate cooldown of both oxidizer pumps due to propellant inlet conditions to the engines.

The C-1 and C-2 engine fuel pumps indicate normal cooldown during the MES #1 first attempt prestart as shown in figure VII-1C-7. The C-1 and C-2 engine housing temperatures at initiation of prestart were 186° and 191° R. These temperatures are within the range of approximately 130° to 200° R experienced on previous Atlas/Centaur flights. The temperature transients during prestart are normal.

For the second attempt MES #1 prestart, both fuel pumps started at a colder temperature (56° and 59° R). During the second prestart period, the pumps both cooled to essentially liquid hydrogen temperature.

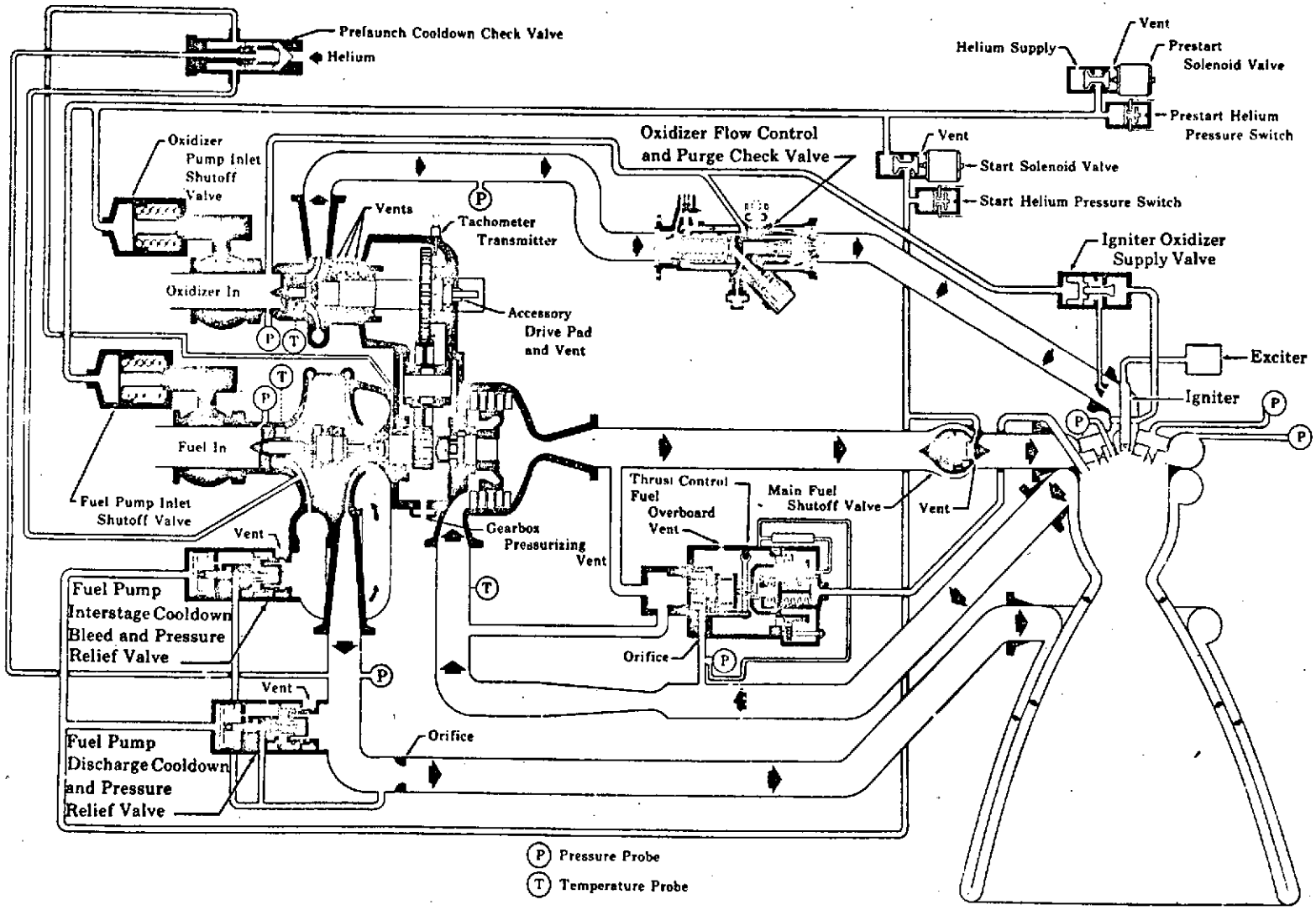

Figure VII-1C-1 RL10A-3-3 Engine Flow Schematic

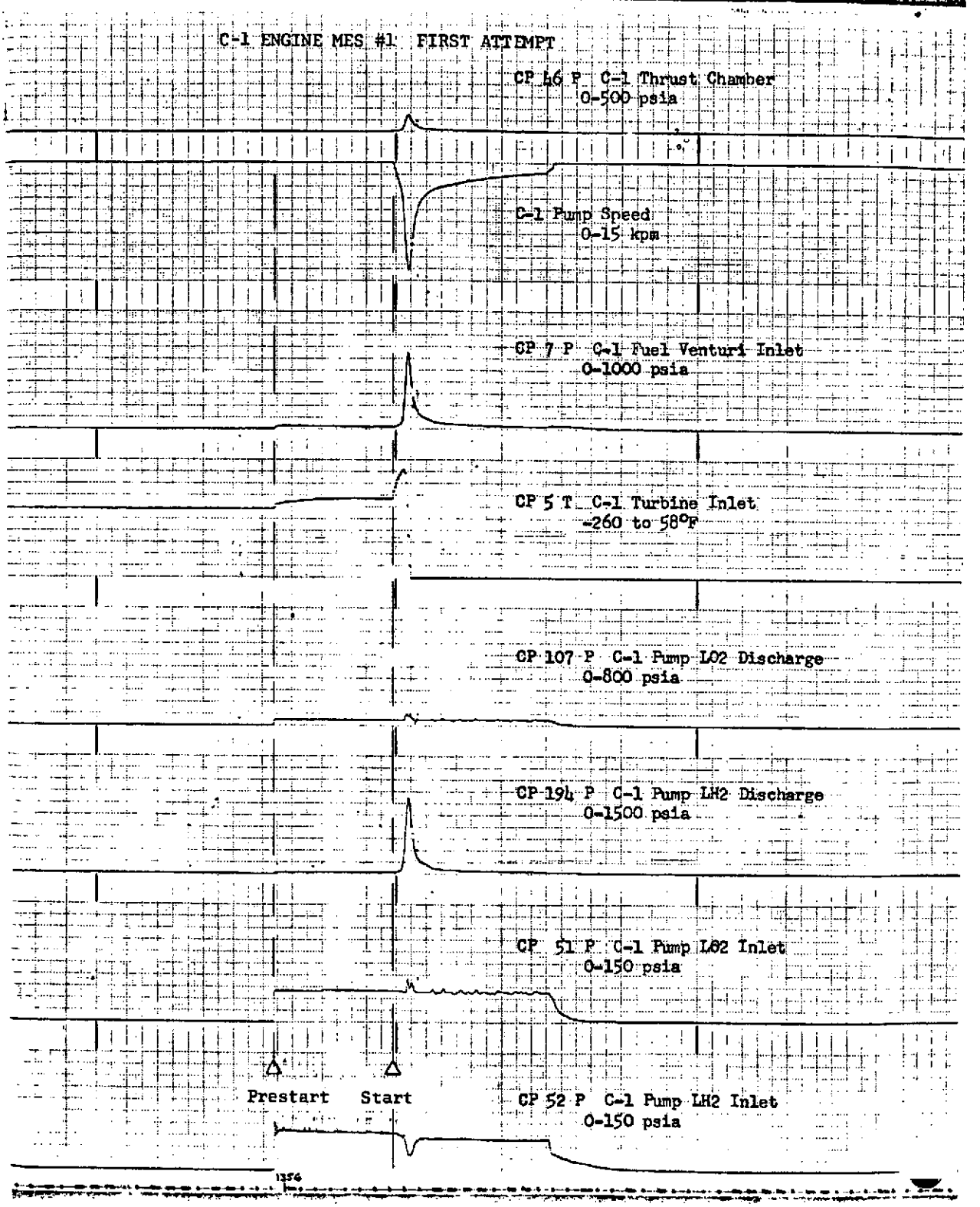

Figure VII-1C-2 C-1 Engine Data for TC-1 MES #1 First Attempt

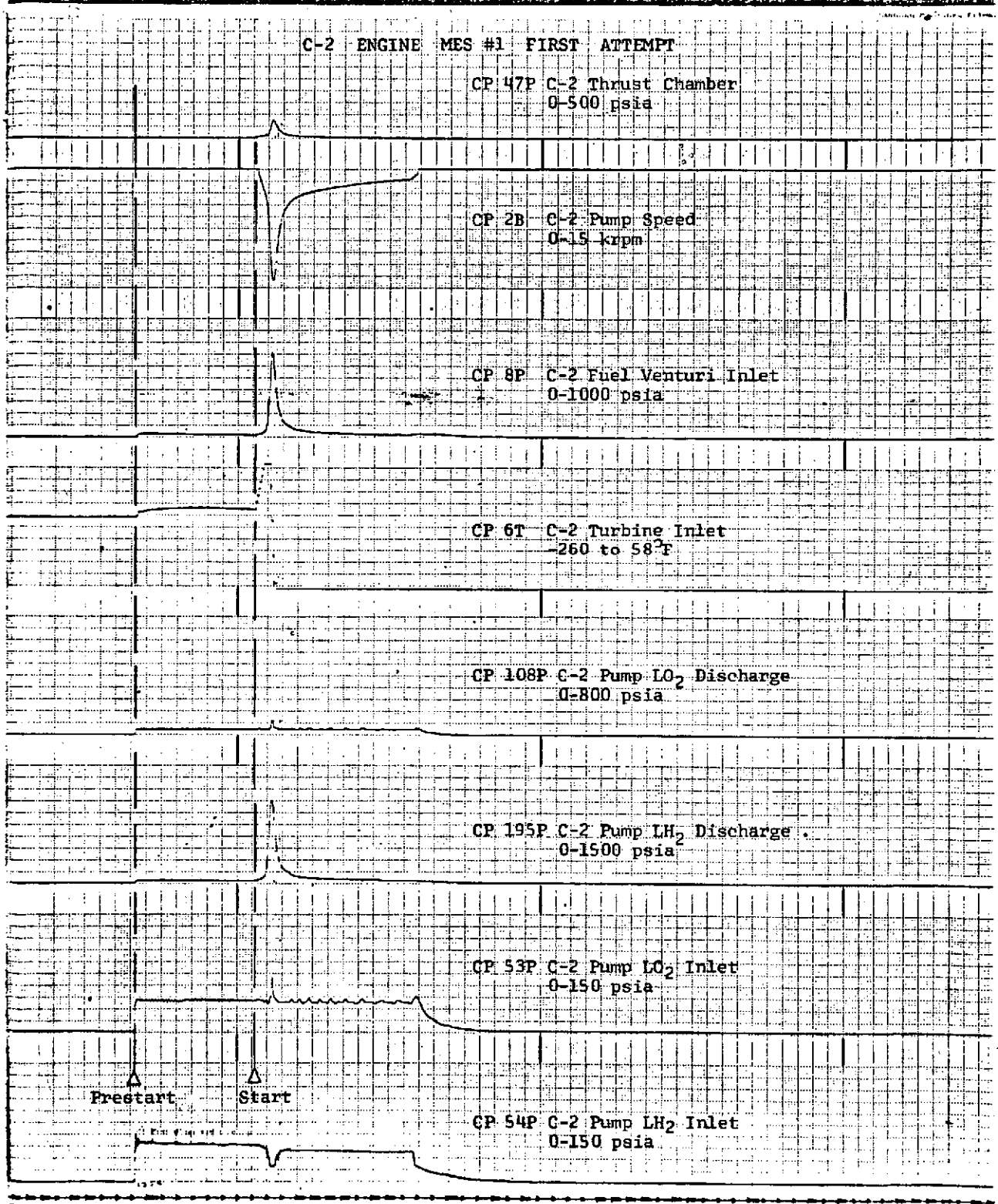

Figure VII-1C-3 C-2 Engine Data for TC-1 MES #1 First Attempt

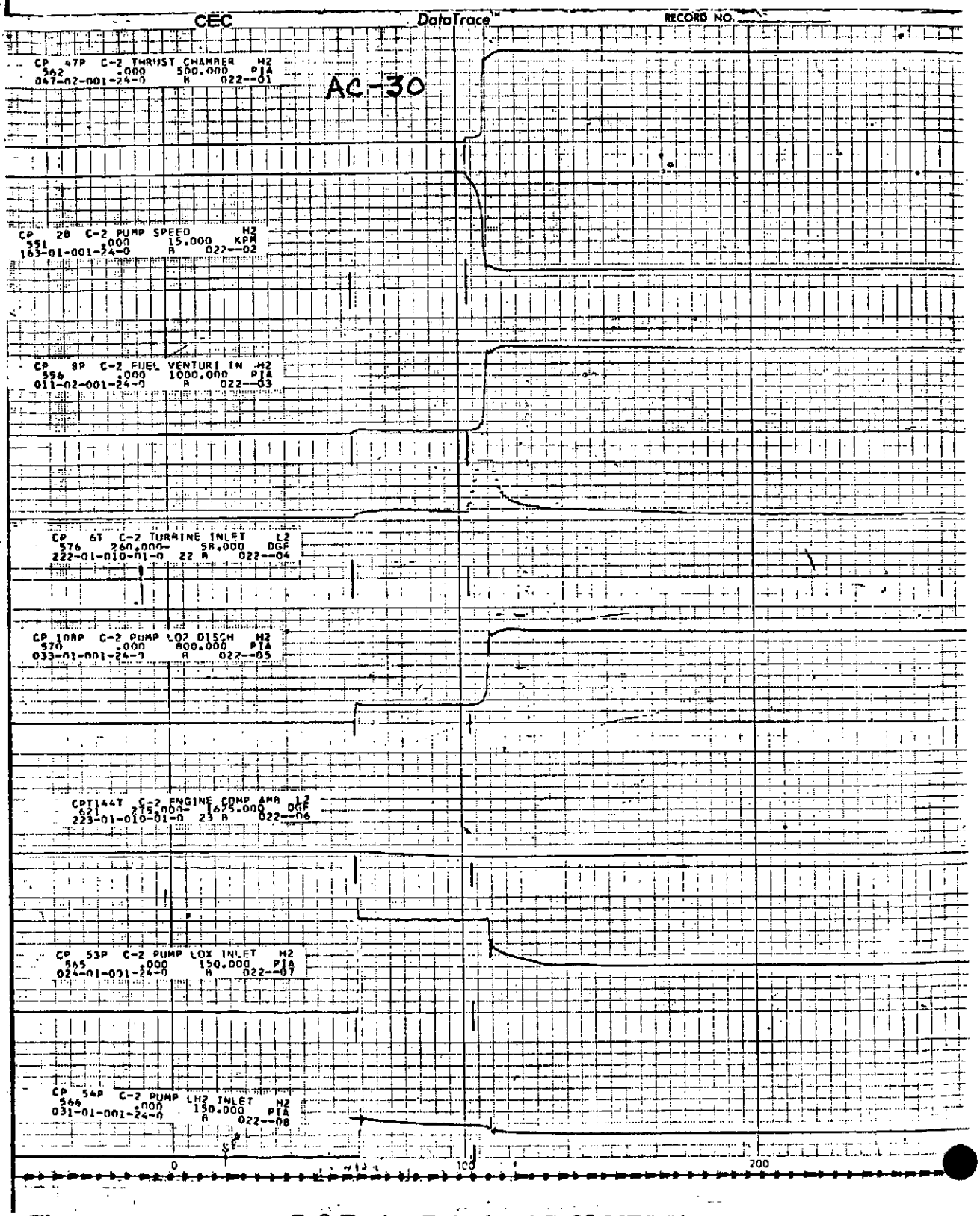

Figure VII-1C-4 C-2 Engine Data for AC-30 MES #1

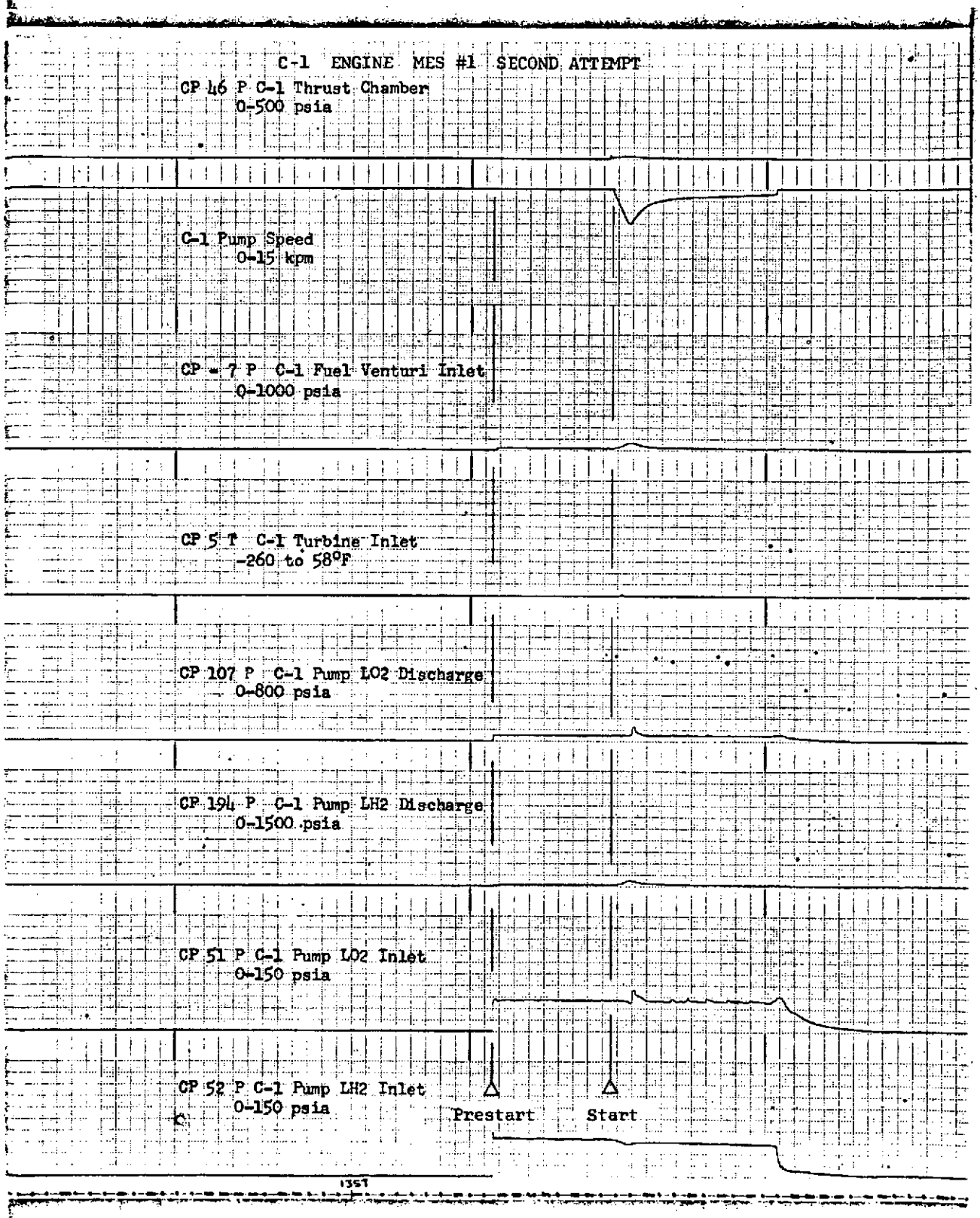

Figure VII-1C-5 **C-1 Engine Data for TC-1 MES #1 Second Attempt**

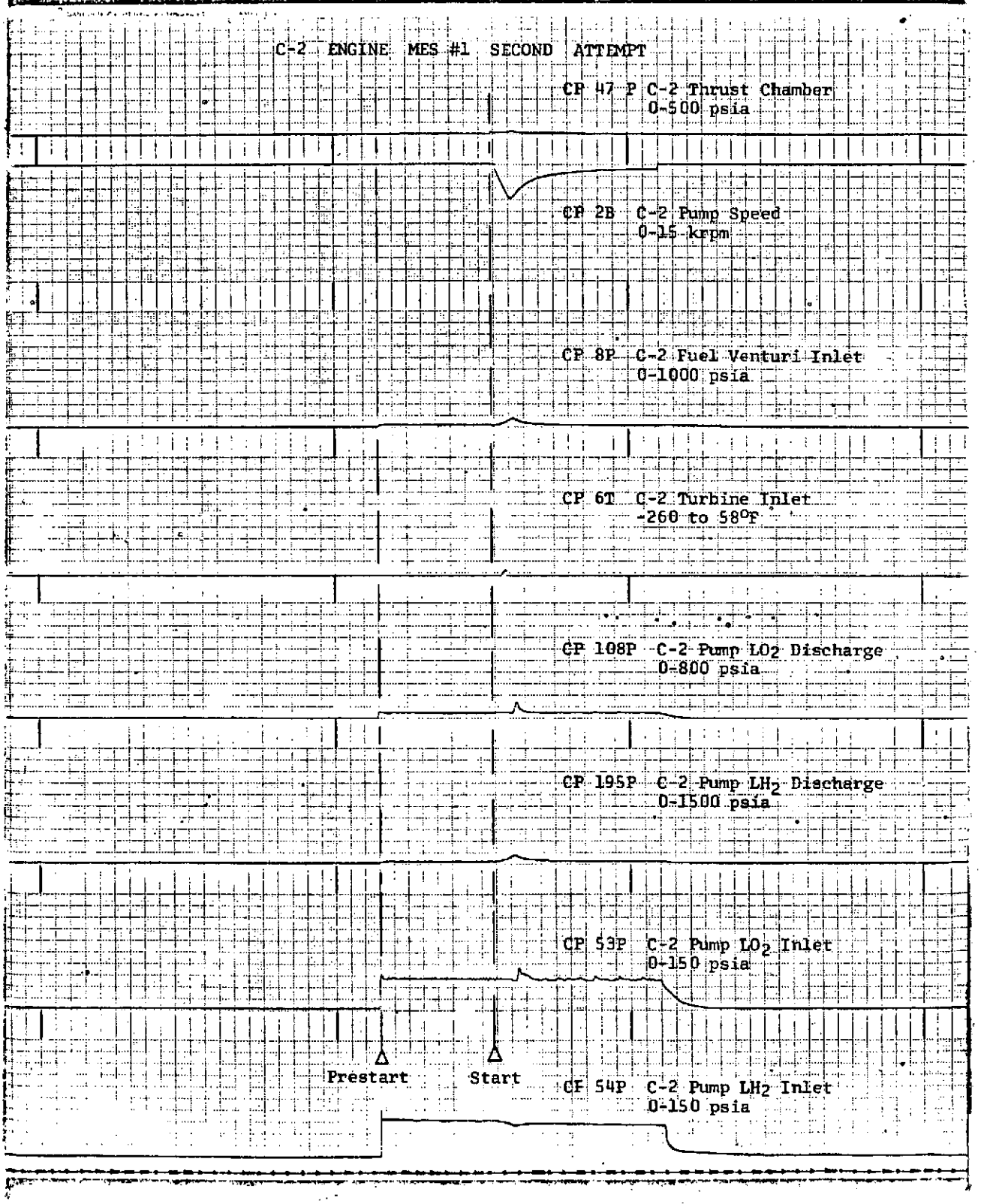

Figure VII-1C-6 C-2 Engine Data for TC-1 MES #1 Second Attempt

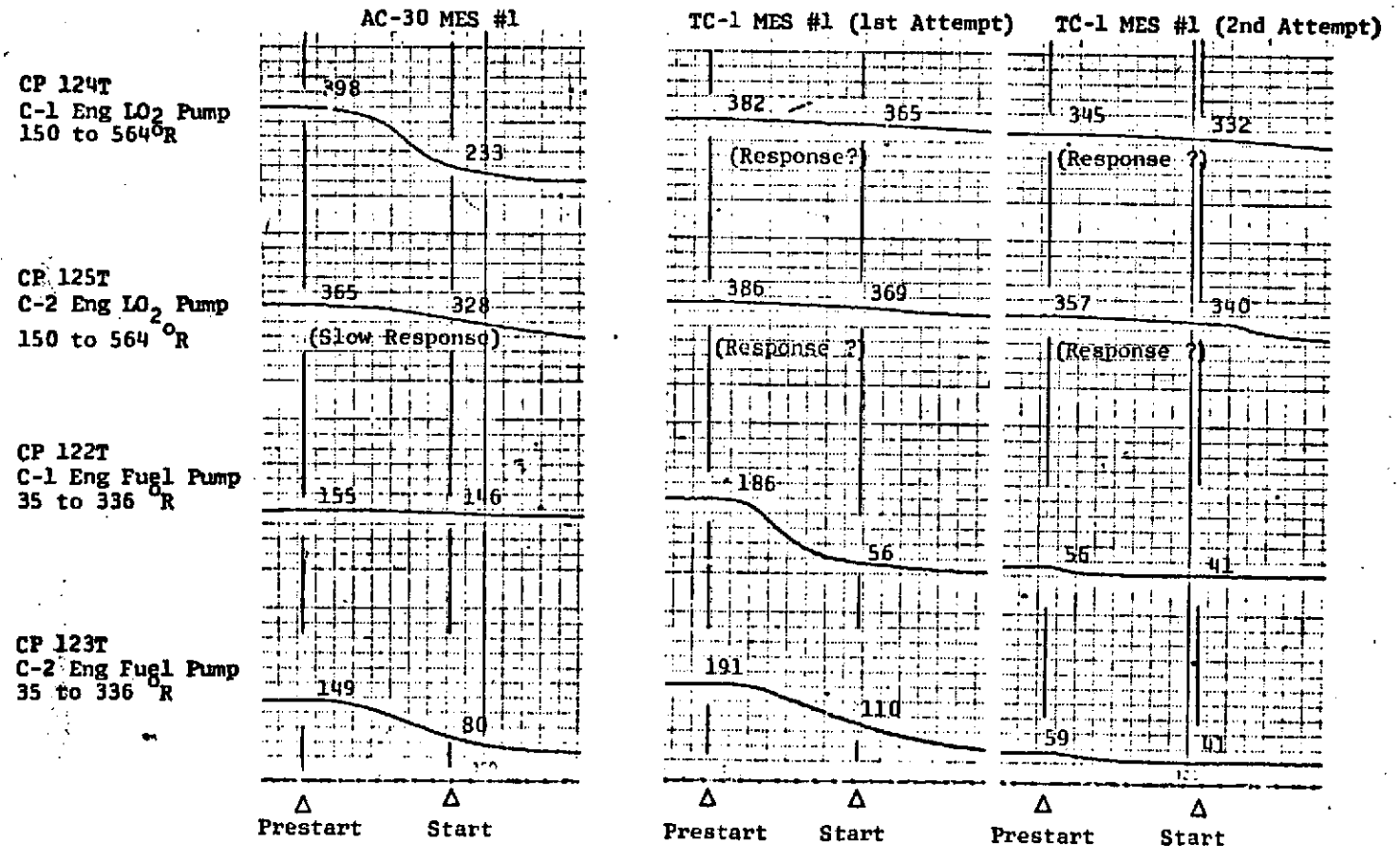

Figure VII-1C-7 Fuel and Oxidizer Pump Housing Temperatures During Prestart for AC-30 and TC-1 MES #1

VII-1D. Hydrogen Peroxide Supply and Reaction Control System

by K. W. Band

Summary

The hydrogen peroxide supply and reaction control system performed as expected, considering the failure to achieve Centaur main engine start. All system pressures and temperatures were within expected limits.

System Description

Reaction control system. - The reaction control system (RCS) consists of twelve individual engines rated at 6 pounds vacuum thrust. The engines use hydrogen peroxide (H_2O_2-90 percent concentration) monopropellant. Each engine consists of an integral solenoid valve, a decomposition chamber containing the catalyst bed, and a convergent-divergent expansion nozzle.

The engines are located on the Centaur aft bulkhead, and are grouped in clusters of two or four on manifold assemblies. The manifold assemblies (4) are located on the vehicle 45°, 135°, 225°, and 315° axis as shown in figure VII-1D-1. The manifold assemblies located in quadrants I and III contain two lateral directed thrust engines each. The manifold assemblies in quadrants II and IV contain two lateral and two aft directed thrust engines each.

The four aft directed engines (designated S2A, S2B, S4A, and S4B) provide axial thrust for propellant settling during coast periods, and for displacement of the Centaur away from the payload after separation. Two vehicle thrust levels (12 or 24 lb) are obtainable for these functions by using one or both pairs of axial engines.

The eight lateral directed engines provide thrust for vehicle pitch, yaw, and roll control during coast periods. The four lateral engines alined perpendicular to the vehicle pitch axis are designated P1, P2, P3, and P4. The remaining four lateral engines alined perpendicular to the vehicle yaw axis are designated Y1, Y2, Y3, and Y4.

The axial and lateral thrusters are identical in design except for the nozzle orientation. The axial engine nozzle is coincident with the engine centerline, whereas the lateral engine nozzle is alined perpendicular to the engine centerline. Each thruster consumes approximately 0.038 pound per second of propellant while firing in a continuous on mode. The nozzle is a conical design with an area ratio of 15 to 1. The nominal nozzle throat diameter is 0.1882 inch. The solenoid valve operates on 28 volts d.c. with a current of approximately 0.5 ampere.

Hydrogen peroxide supply system. - The hydrogen peroxide monopropel-

lant supply system consists of the storage bottles, valves, and plumbing for distribution of monopropellant to the Centaur reaction control engines and boost pump turbine drives. A flow schematic for the system is shown in figure VII-1D-2.

Major components of the system are:

(1) Two peroxide storage bottles with positive expulsion bladders, each having a usable capacity of 239 pounds of monopropellant

(2) A solenoid operated, three-way boost pump peroxide feed valve (BPFV-1)

(3) A solenoid operated, two-way boost pump peroxide feed valve (BPFV-2)

(4) A solenoid operated, two-way peroxide vent valve (VV-1)

(5) A solenoid operated, three-way peroxide vent valve (VV-2)

(6) A solenoid operated, three-way pneumatic pressurization valve

(7) A solenoid operated, three-way pneumatic vent valve

(8) A solenoid operated, three-way boost pump feed line purge shut-off valve

(9) A pressure relief valve

(10) A sintered purge orifice

(11) Heated and unheated peroxide and purge lines between the various components of the system and the reaction control engines and boost pump turbine drives

The two peroxide bottles are identical in design except the bottle closest to the boost pumps contains a dip tube to prevent entrainment of large quantities of trapped air or evolved gaseous oxygen (from the ullage space above the liquid) with the peroxide flow to the boost pump turbines. The bottle closest to the reaction control loop is designated the reaction control system (RCS) bottle, and the other is designated the boost pump (BP) bottle for identification purposes. The liquid side of both bottles are manifolded together which permits peroxide flow from either bottle to both the reaction control engines and the boost pump turbines. A cross sectional view of a peroxide bottle is shown in figure VII-10-3.

The two boost pump feed valves are mounted on the head of the BP bottle and utilize the heat capacity of the filled bottle for thermal control. The two valves provide a parallel flow path to the boost pump turbines which protects against the failure of one valve to open. Both valves are energized simultaneously to admit peroxide flow to the two

boost pump turbines, and de-energized simultaneously to stop peroxide flow to the turbines. Cross sectional views of the two- and three-way solenoid valves are shown in figures VII-1D-4 and 5, respectively.

The two peroxide vent valves are mounted on the head of the RCS bottle and also utilize the heat capacity of the filled bottle for thermal control. Each valve is energized to vent the liquid side of the bottles to atmosphere, and are de-energized to close the vent path. Neither valve is operated in flight. The primary seal is provided by vent valve number 1. Vent valve number 2 is plumbed in series with the number 1 valve to protect against liquid leakage in flight. A relief valve is connected to the normally open port of vent valve number 2 to preclude excessive pressure buildup due to any trapped liquid between the two closed vent valves. The relief valve cracking pressure is 350 to 380 psig; reseat pressure is 330 psig minimum.

The pressurization valve provides the primary means of pressurizing and venting the pneumatic side of the peroxide bottle expulsion bladders. The valve is de-energized to pressurize the bottles and energized to vent the pressurant gas. The pneumatic vent valve is plumbed in series with the pressurization valve vent port, and serves as a secondary seal against leakage of pressurant gas during flight. The pneumatic vent valve is de-energized to close the vent path, and energized to vent the pressurant gas. Neither of these two valves are actuated in flight. Both are mounted on a pneumatics panel on the Centaur aft bulkhead.

The peroxide supply lines to the boost pumps are internally purged during flight. The purpose of the purge is to quickly expel the residual peroxide from the lines downstream of the boost pump feed values immediately after each boost pump operating period. Replacement of the stagnant peroxide residuals with a flowing gas reduces the possibility of peroxide freezing in the lines during the long coast periods. A sintered metal purge orifice is provided to control the purge flow rate to 250±50 standard cubic inches per minute of gaseous helium. The purge gas line is connected to a tee at the inlet of the bottle pressurization line, and is routed to the purge shutoff valve located on the peroxide system pneumatics panel. The purge gas is then routed to the normally open port of BPFV-1. The purge shutoff valve is electrically connected to the same switch that controls BPFV-1, such that the two valves are energized and de-energized simultaneously. The purge valve is plumbed in series with the BPFV-1 normally open port, and thus serves as a second seal against purge gas leakage into the peroxide flow to the turbine during boost pump operation.

Each of the peroxide system solenoid valves (7) are operated by 28 volts d.c.. The ports on all valves contain a filter except for the outlet port of the two boost pump feed valves. The nominal rating of each filter is 70 microns.

The tubing and fittings in the peroxide supply system are 304 stainless steel. Tubing sizes used are 1/4, 3/8, and 1/2 inch outside diam-

eter with 0.20 inch wall thickness. All of the purge gas tubes between the airborne helium regulator and BPFV-1, and some of the peroxide flow tubes are heated (depending on the line length and location). A total of 18 tube assemblies are heated. Location of the heated tubes is shown in figure VII-1D-6. All of the tube assemblies have a single heater, except two heaters are provided on the tube between the quadrant I and IV engine manifolds, on the tube between the quadrant II and III engine manifolds, on the first tube downstream of BPFV-1, and on the first tube downstream of BPFV-2 because of the length of these tubes.

The peroxide supply system lines heaters are designed to provide 0.186 watt per square inch of external surface area. The heaters are constant power and operate on 28 volts d.c.. The nominal current for individual heaters varies from 0.196 to 0.571 ampere depending on the tube diameter and length. The outside surface of the heated tubes is coated with a white zinc oxide and potassium silicate mixture which has a high emittance to absorptance ratio for thermal control during space flight. The design temperature operating range for heated tubes is 40° to 120° F.

A cross sectional view of a typical heated tube is shown in figure VII-1D-7. A 1/8-inch (o.d.) tube is brazed to the main flow tube. The nichrome heater wire is installed inside the 1/8-inch tube, and the annular cavity between the wire and tube filled with heat conducting potting compound.

Instrumentation for RCS and hydrogen peroxide supply systems. - Instrumentation consisted of the two peroxide bottle temperature measurements CP93T and CP659T, and numerous temperature measurements located on the lines and components as shown in figure VII-1D-8.

Flight Performance

The hydrogen peroxide (H_2O_2) supply and reaction control system (RCS) performed as expected, considering the failure to achieve Centaur main engine start. The RCS was inactive during the time period from liftoff to first main engine cutoff (MECO #1) except for programmed firing of four RCS engines before boost pump start. The RCS flight data during the time period from liftoff through MECO #1 is discussed in this section, and the post-MECO #1 data are discussed in Section VIII, VEHICLE DYNAMICS.

The S2A, Y1, Y2, and S4B thrusters were fired in that order for 20 seconds each during the Titan boost phase. The S2A, Y1, and Y2 were fired in succession. The S2B engine was fired 43 seconds after termination of the Y2 firing. Temperature measurements on the S2A, Y1, and S2B engine chamber surfaces provided a direct indication that the programmed firing sequence for these three engines was accomplished in the proper order and duration. Proper operation of the Y2 engine was indirectly indicated by a temperature measurement on the interior of the interstage adapter (CA397T). The CA397T measurement was located directly opposite

the Y2 engine nozzle to measure the impingement heating resulting from the Y2 engine firing. The temperature data for the eight instrumented RCS engines (four engines were not instrumented) is shown in figures VII-1D-9 through VII-1D-12. The temperature data from measurement CA397T is shown in figure VII-1D-13. The temperature rise beginning at MECO #1 on the settling engine measurements, and followed shortly by a temperature rise on the lateral engine measurements, is due to the 4S-on plus pitch, yaw, and roll control mode which was initiated at MECO #1.

The H_2O_2 supply system temperatures were normal with the exception of apparent failure of measurement CP833T. The CP833T measurement increased linearly beginning at BPS #1 and eventually went off scale. It is believed that the transducer came loose from the H_2O_2 line.

The H_2O_2 supply system temperatures in the vicinity of the H_2O_2 bottles are shown in figure VII-1D-14. The H_2O_2 bulk temperature was approximately 83° F throughout the flight as indicated by measurements CP93T and CP659T. The lines and valves cooled slightly during the first 60 seconds of flight, and then gradually warmed during the remainder of the boost phase (measurements CP756T, CP831T, and CP834T). The latter three measurements reflected a temperature change at BPS #1 due to flow of H_2O_2 in the lines. A cooling trend was also evident on measurements CP756T and CP831T during the time period from prestart through MECO #1.

Temperatures in the vicinity of the boost pumps are shown in figure VII-1D-15. The LH_2 boost pump electrical connector (CP712T) and the LO_2 boost pump inlet line (CPT714T) were unheated and of small mass which resulted in a pronounced cooling trend during the first 100 seconds of boost. The lowest temperature recorded in the H_2O_2 supply system (20° F) occurred at the CPT714T measurement. The LH_2 and LO_2 orifice blocks (measurements CP710T and CP711T, respectively) also cooled during the boost phase, but not as pronounced because of their relatively large mass. Measurements CP712T and CP714T showed an increased temperature rise rate during the programmed RCS engine firings. At BPS-1 all of the temperatures increased rapidly due to flow of warm H_2O_2 through the lines and radiation heating from the hot turbines. The LH_2 boost pump electrical connector cooled during the time period from prestart to MECO #1.

Temperature data for the H_2O_2 supply lines to the RCS engines are shown in figure VII-1D-16. A very slight cooling trend occurred on all lines during the first 90 seconds of boost phase, and then slowly warmed. Flow of H_2O_2 in the lines caused noticeable changes in temperatures when the RCS engines were fired during the boost phase. A slight cooling trend was evident on most of the lines during the time period between prestart and MECO #1.

Temperature data for the boost pump H_2O_2 supply lines are shown in figure VII-1D-17. Temperatures on all of the lines showed a cooling trend during the first 100 seconds of boost phase. The most pronounced cooling occurred near the LH_2 boost pump. Most of the gaseous nitrogen in the interstage adapter is vented through the opening in the interstage

adapter at this location which results in more convective cooling of components in the immediate vicinity. The quadrant 2 and 4 line temperatures (CP157T and CP159T, respectively) showed an increased temperature rise rate during the programmed firing of the RCS engines. All temperatures increased due to the warm H_2O_2 flow at BPS #1. Measurements CP159T, CPT361T, CP157T, and CP158T show a pronounced cooling trend during the time period from prestart to MECO #1.

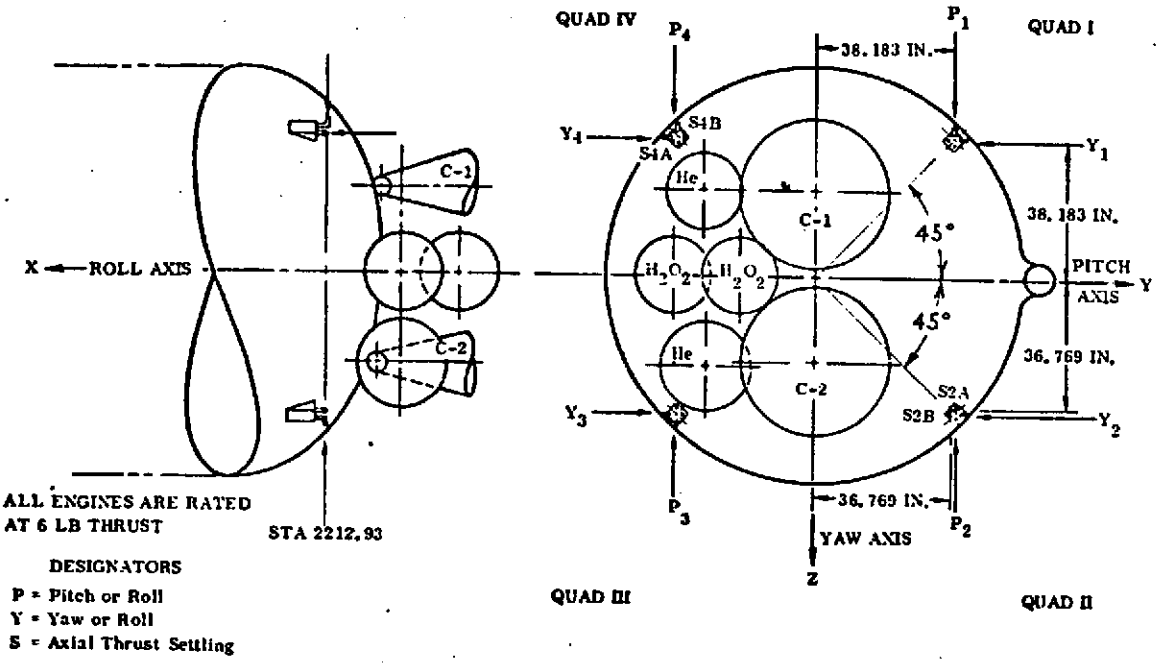

FIGURE VII-1D-1 REACTION CONTROL SYSTEM ARRANGEMENT ON CENTAUR AFT BULKHEAD

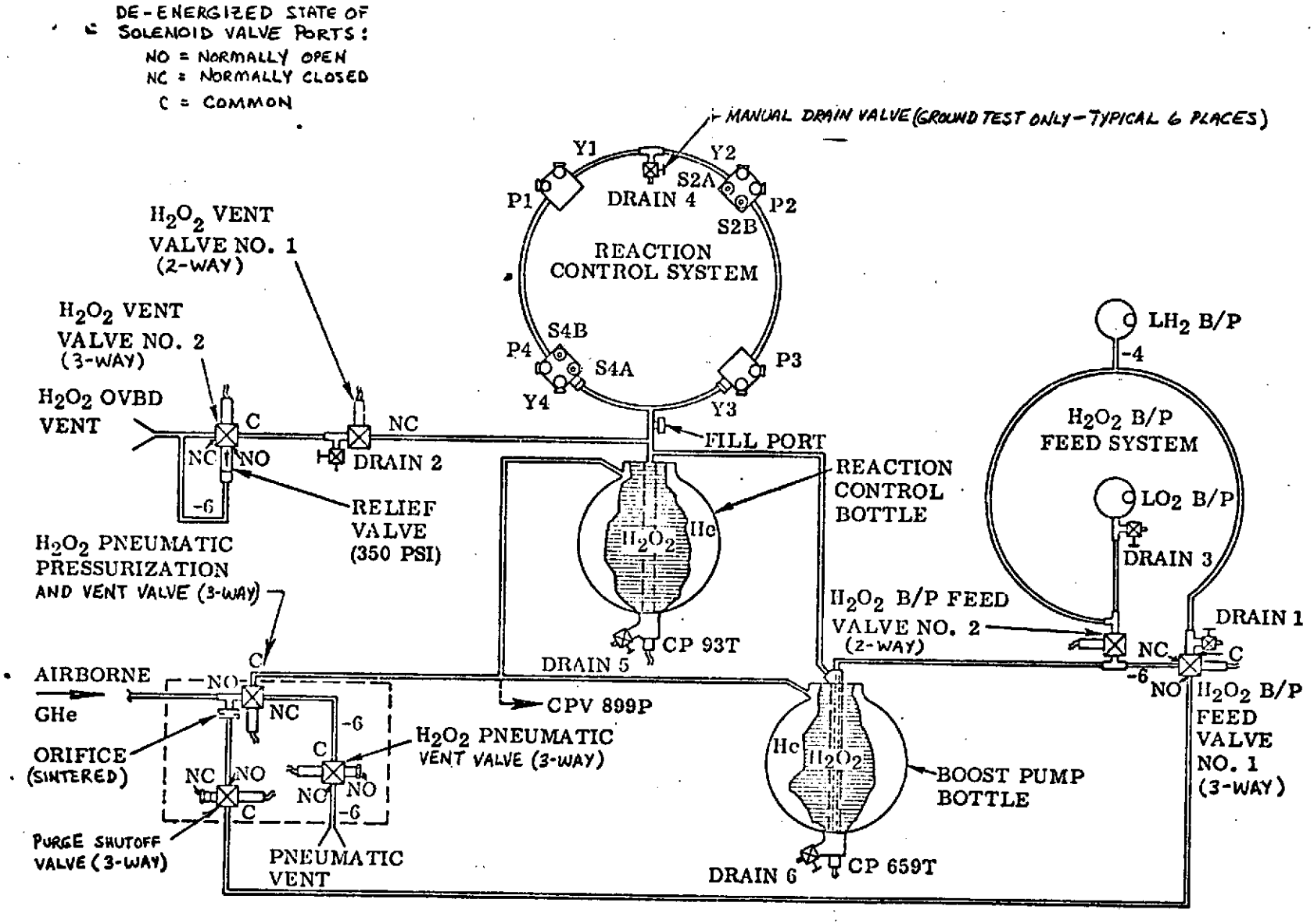

FIGURE VII-1D-2 CENTAUR HYDROGEN PEROXIDE SUPPLY SYSTEM FLOW SCHEMATIC

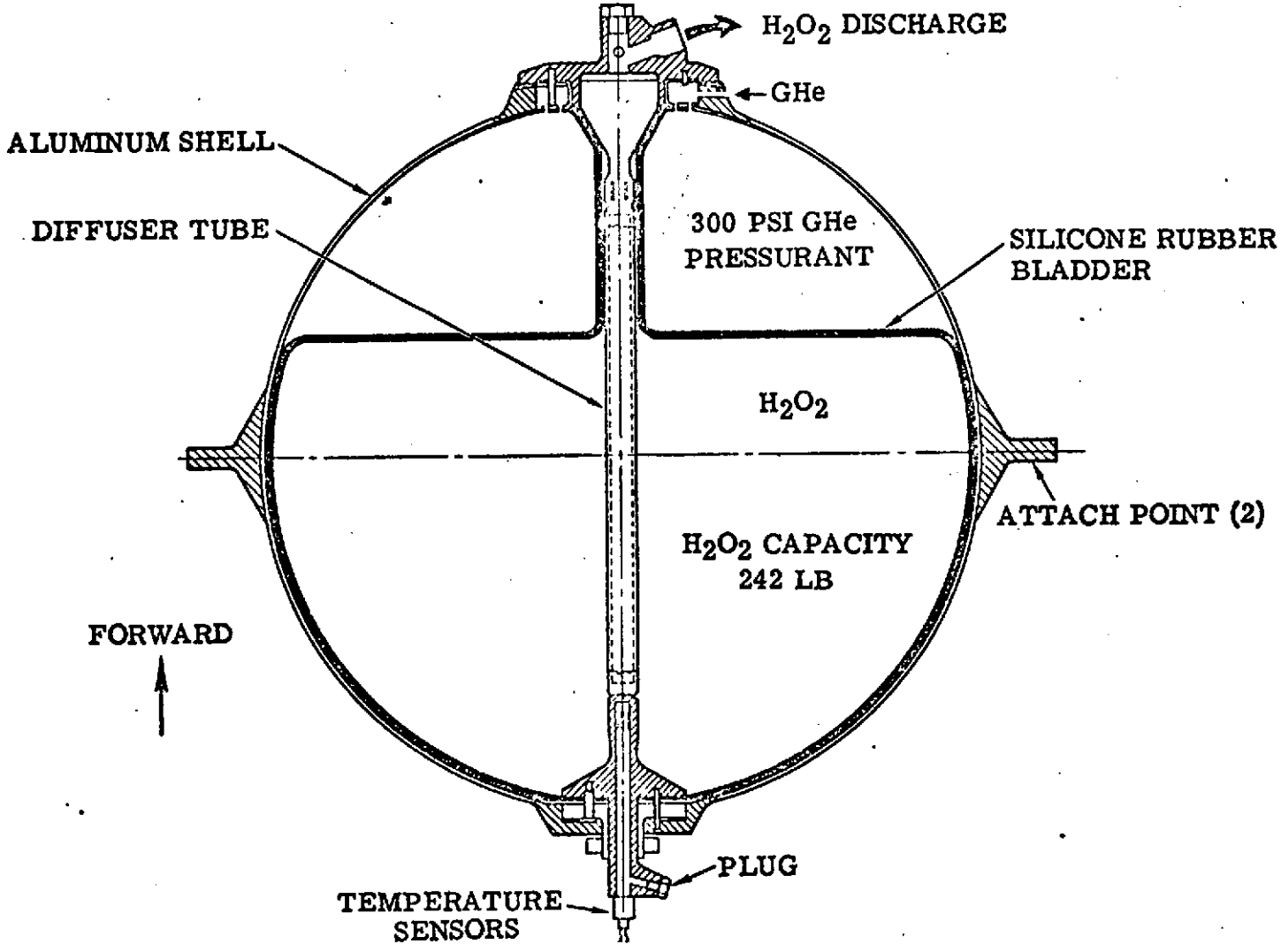

FIGURE VII-1D-3 CROSS SECTIONAL VIEW OF CENTAUR HYDROGEN PEROXIDE STORAGE BOTTLE

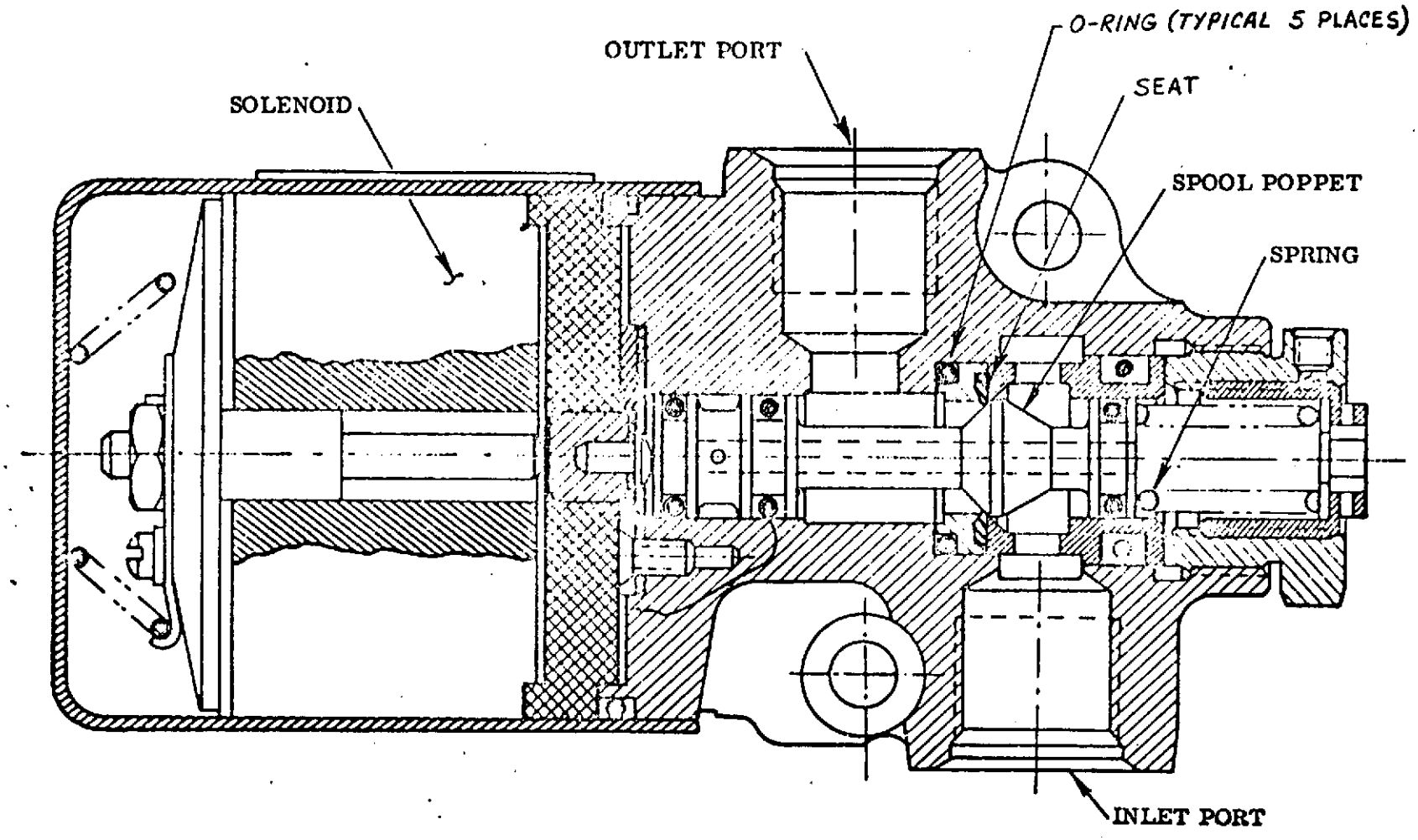

FIGURE VII-1D-4 CROSS SECTIONAL VIEW OF CENTAUR HYDROGEN PEROXIDE SUPPLY SYSTEM TWO-WAY VALVE

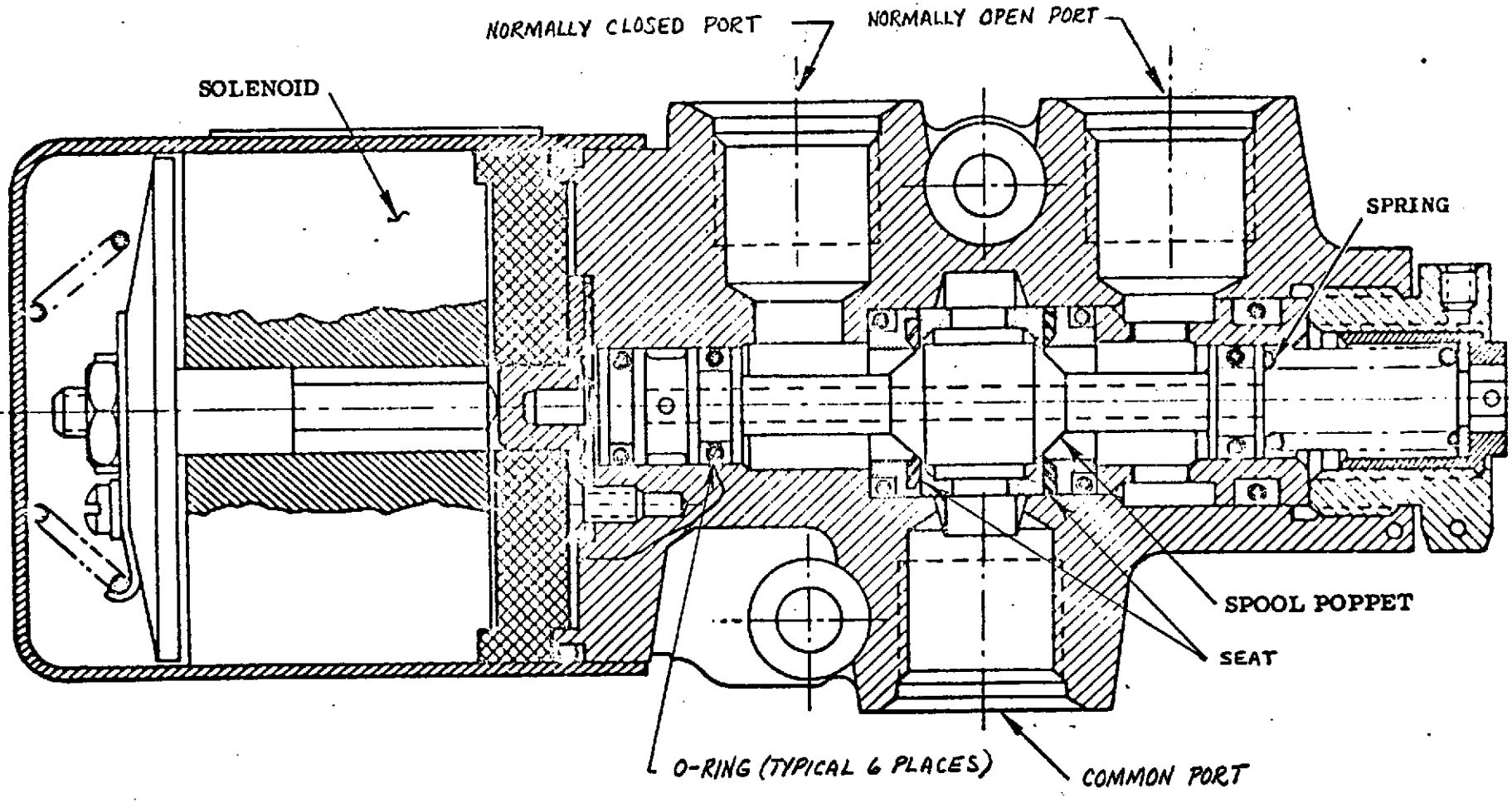

FIGURE VII-1D-5 CROSS SECTIONAL VIEW OF CENTAIR HYDROGEN PEROXIDE SUPPLY SYSTEM THREE-WAY VALVE

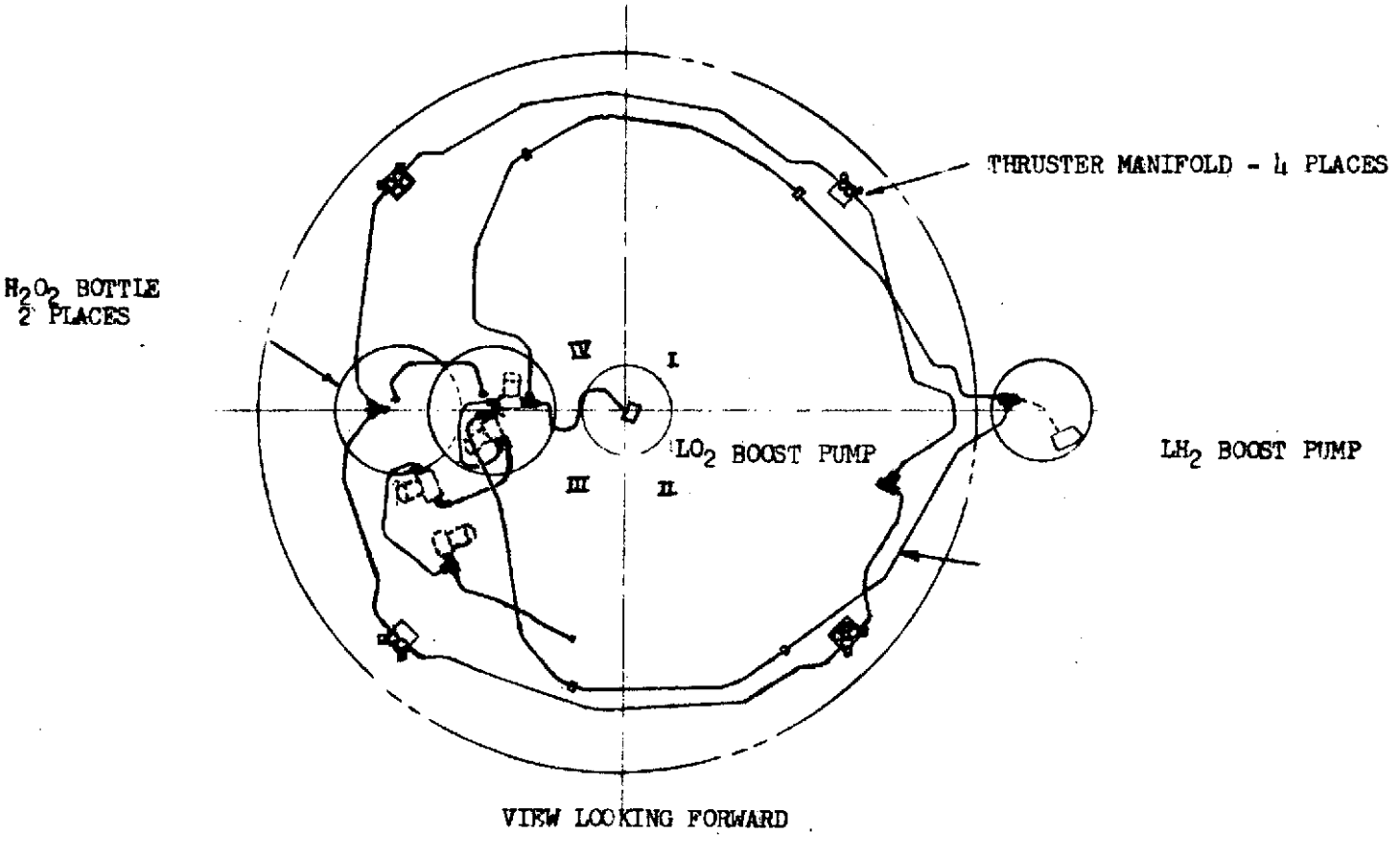

FIGURE VII-1D-6 LOCATION OF H_2O_2 SUPPLY SYSTEM HEATED TUBES

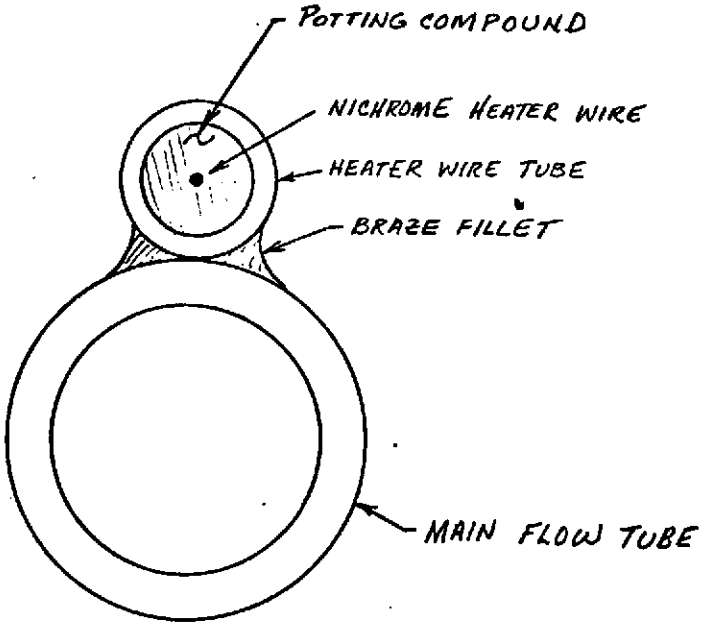

FIGURE VII-1D-7 CROSS SECTIONAL VIEW OF HEATED FLOW TUBE FOR CENTAUR HYDROGEN PEROXIDE SUPPLY SYSTEM

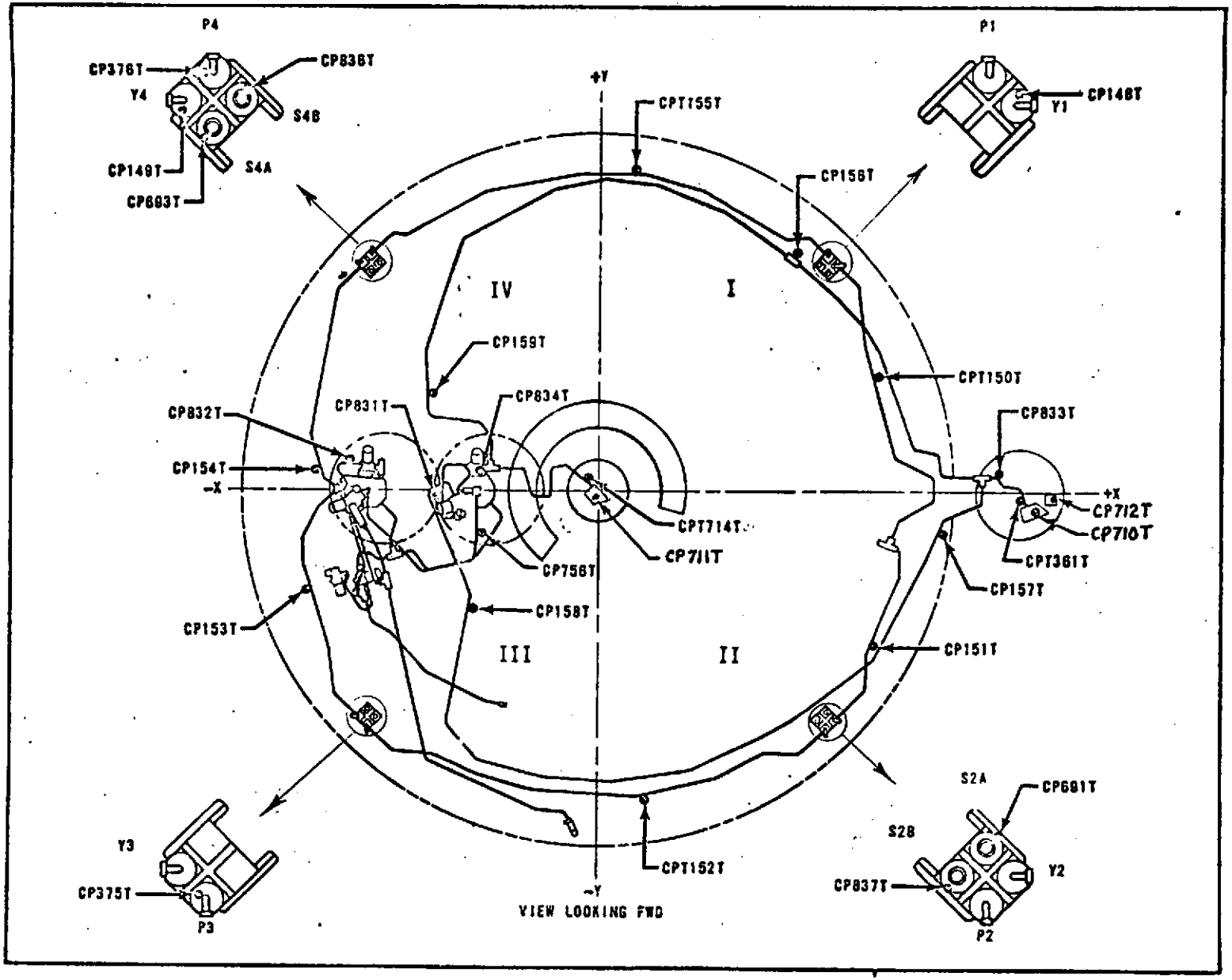

FIGURE VII-1D-8 TEMPERATURE MEASUREMENT LOCATIONS FOR CENTAUR REACTION CONTROL AND HYDROGEN PEROXIDE SYSTEMS

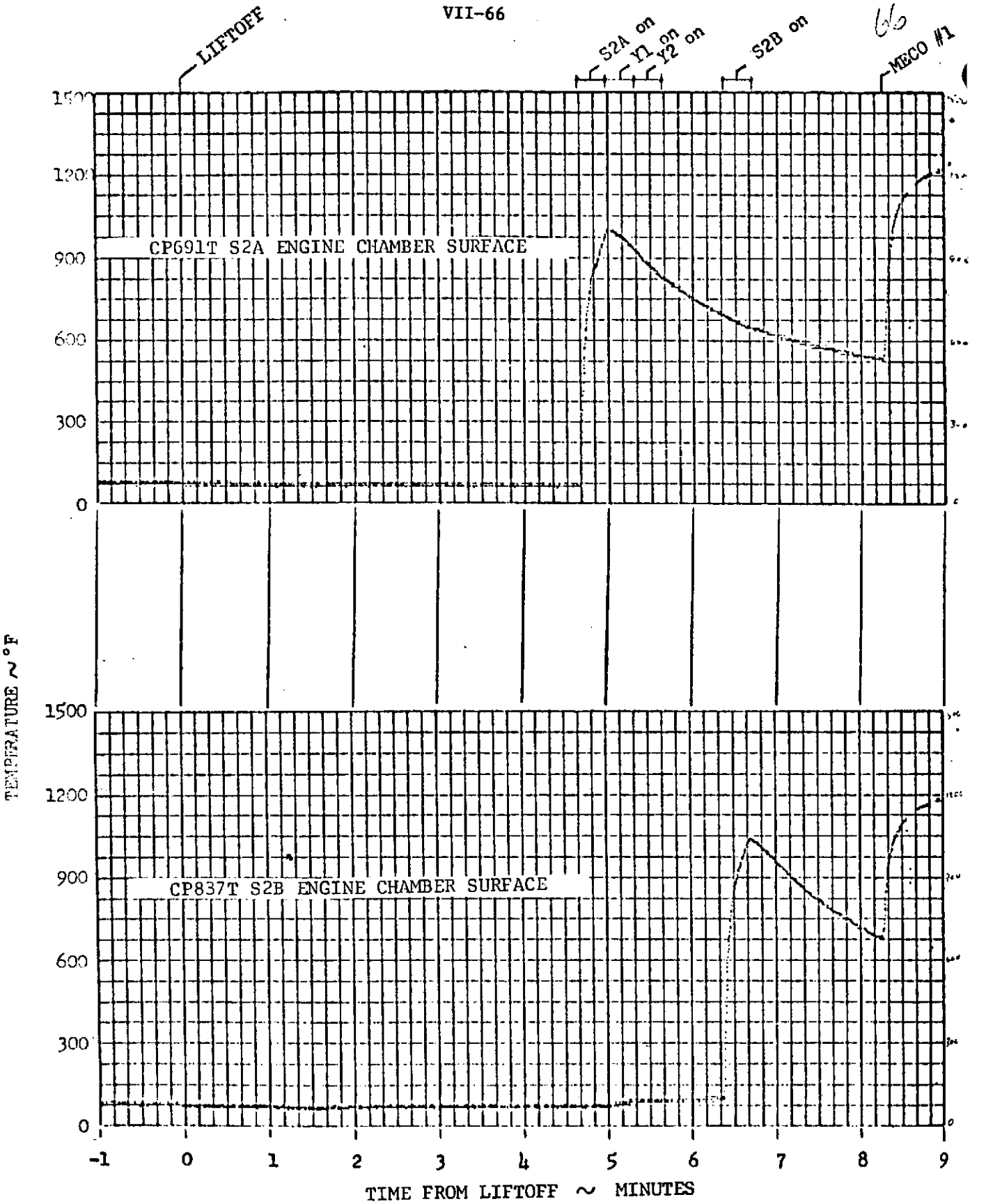

CENTAUR RCS SETTLING ENGINE CHAMBER SURFACE TEMPERATURES, QUADRANT 2

FIGURE VII-1D-9

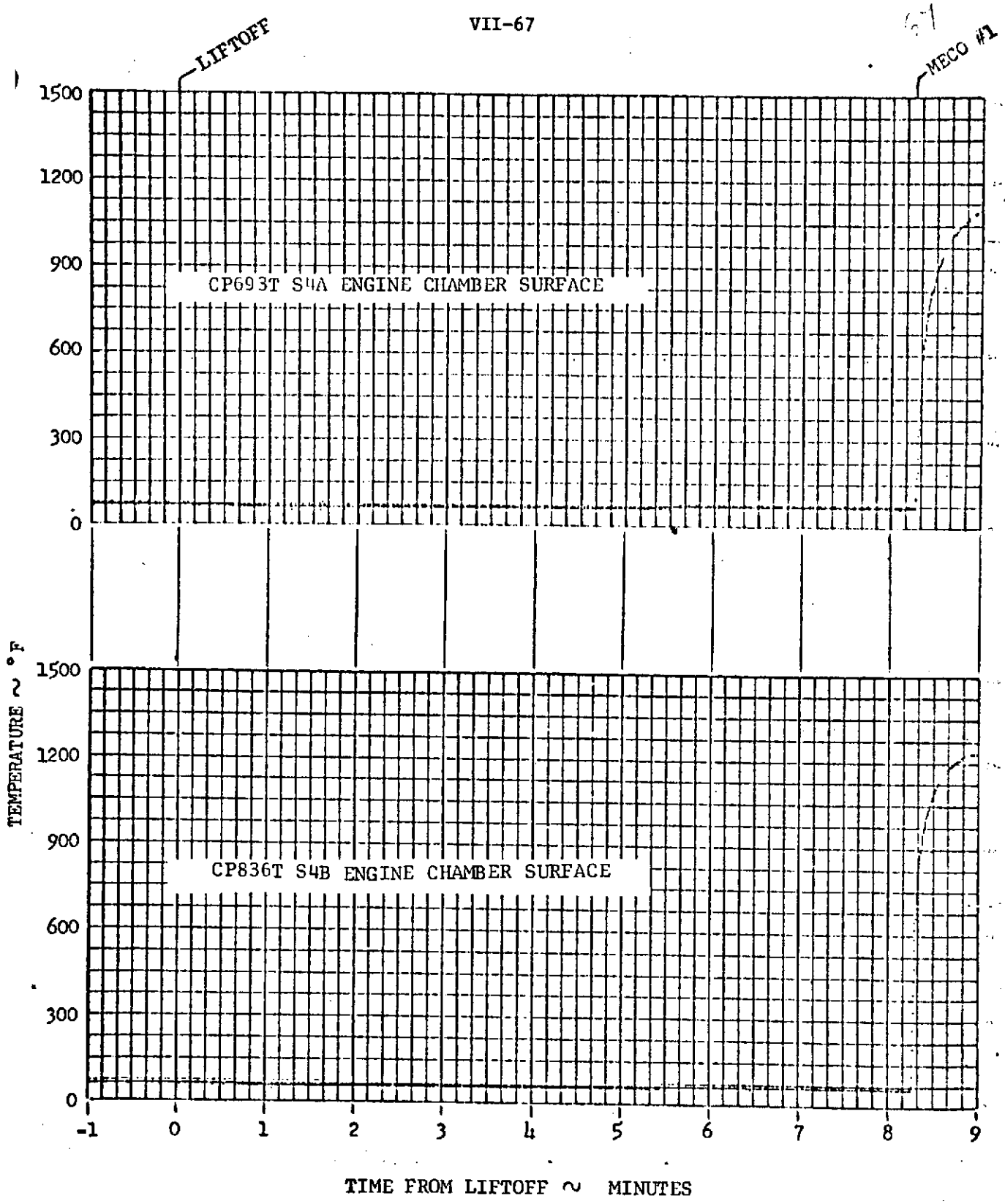

: CENTAUR RCS SETTLING ENGINE CHAMBER SURFACE TEMPERATURES, QUADRANT 4

FIGURE VII-1D-10

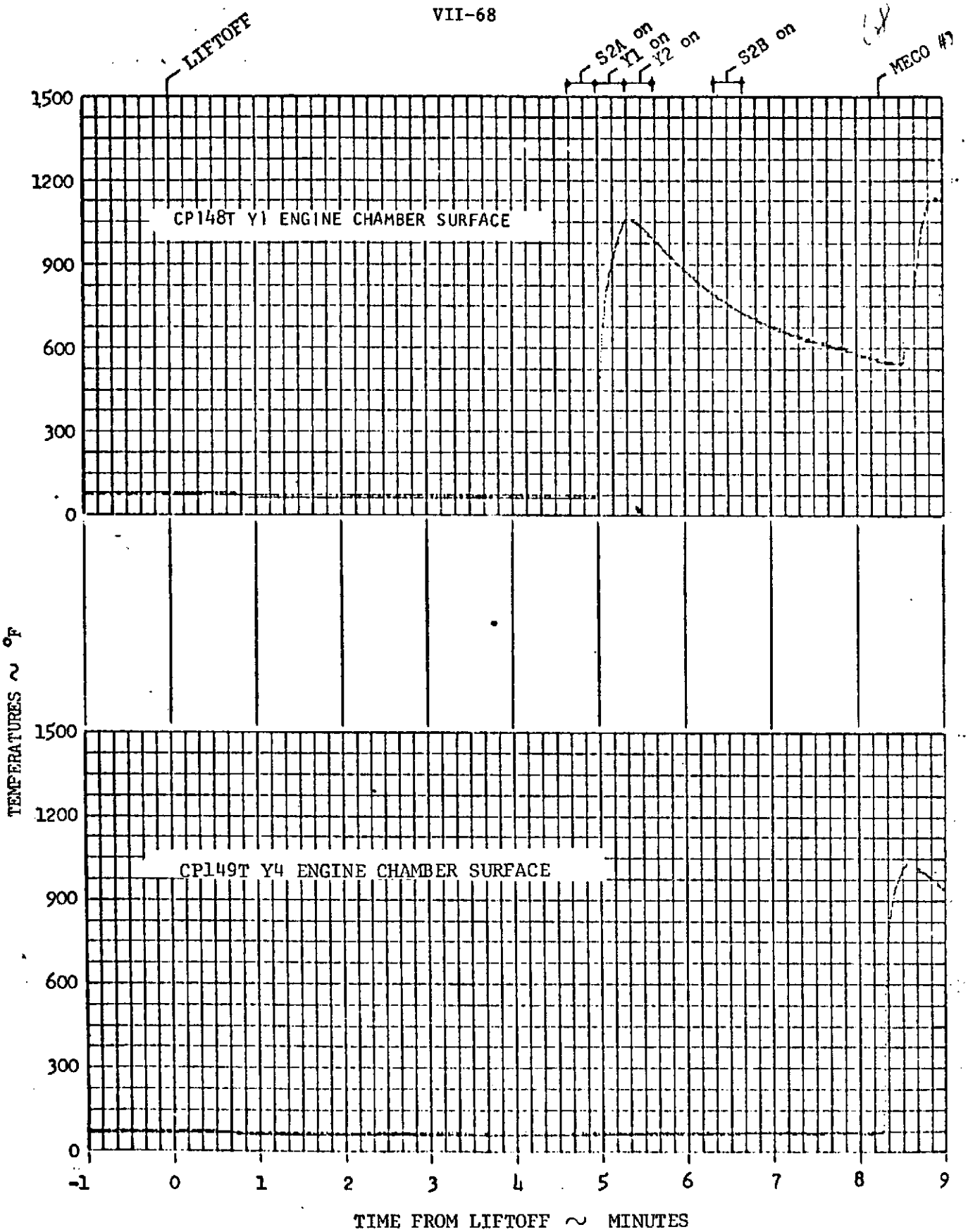

CENTAUR RCS YAW ENGINE CHAMBER SURFACE TEMPERATURES, QUADRANTS 1 and 4

FIGURE VII-1D-11

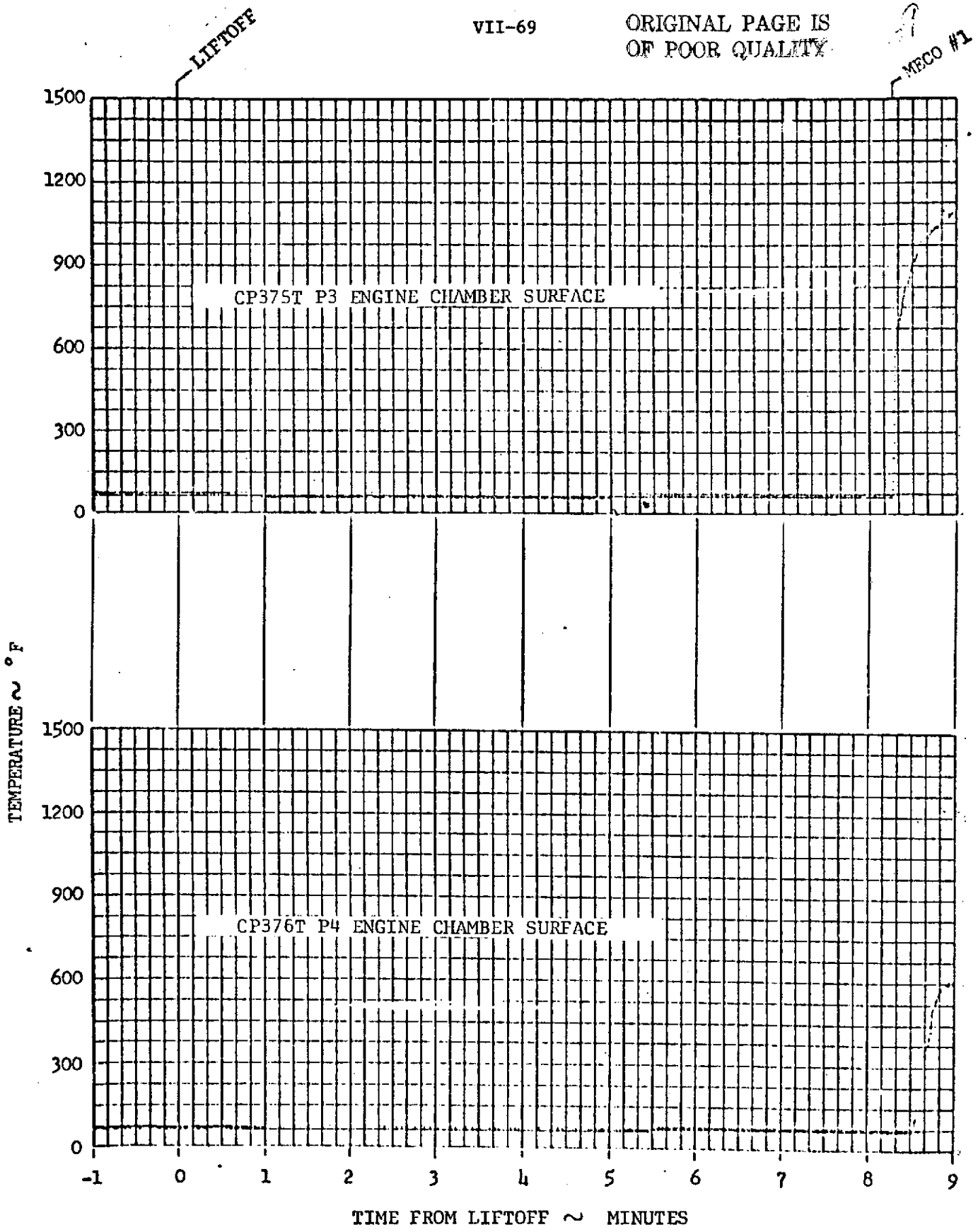

CENTAUR RCS PITCH ENGINE CHAMBER SURFACE TEMPERATURES, QUADRANTS 3 and 4

FIGURE VII-1D-12

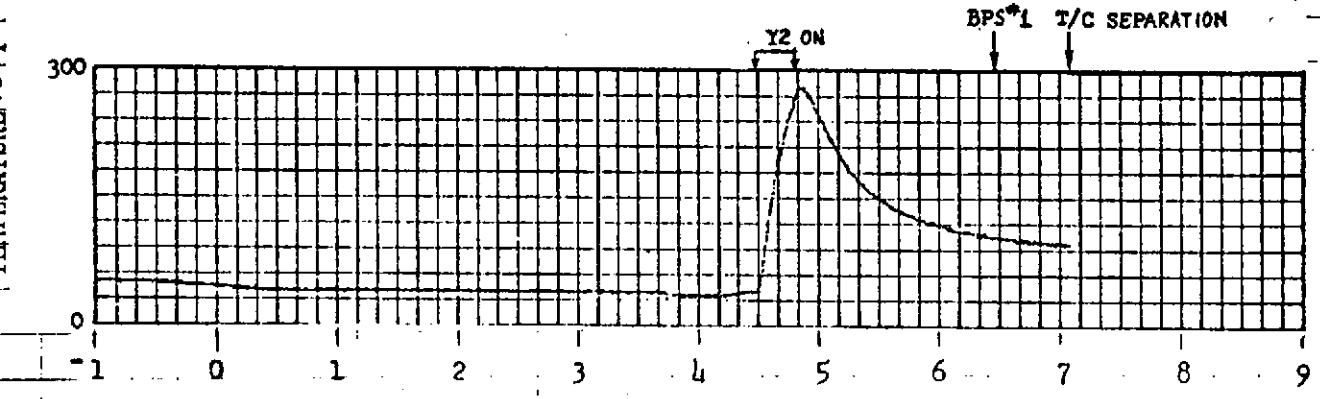

FIGURE VII-1D-13 IMPINGEMENT HEATING OF INTERSTAGE ADAPTER DUE TO Y2 ENGINE FIRING (MEASUREMENT CA397T)

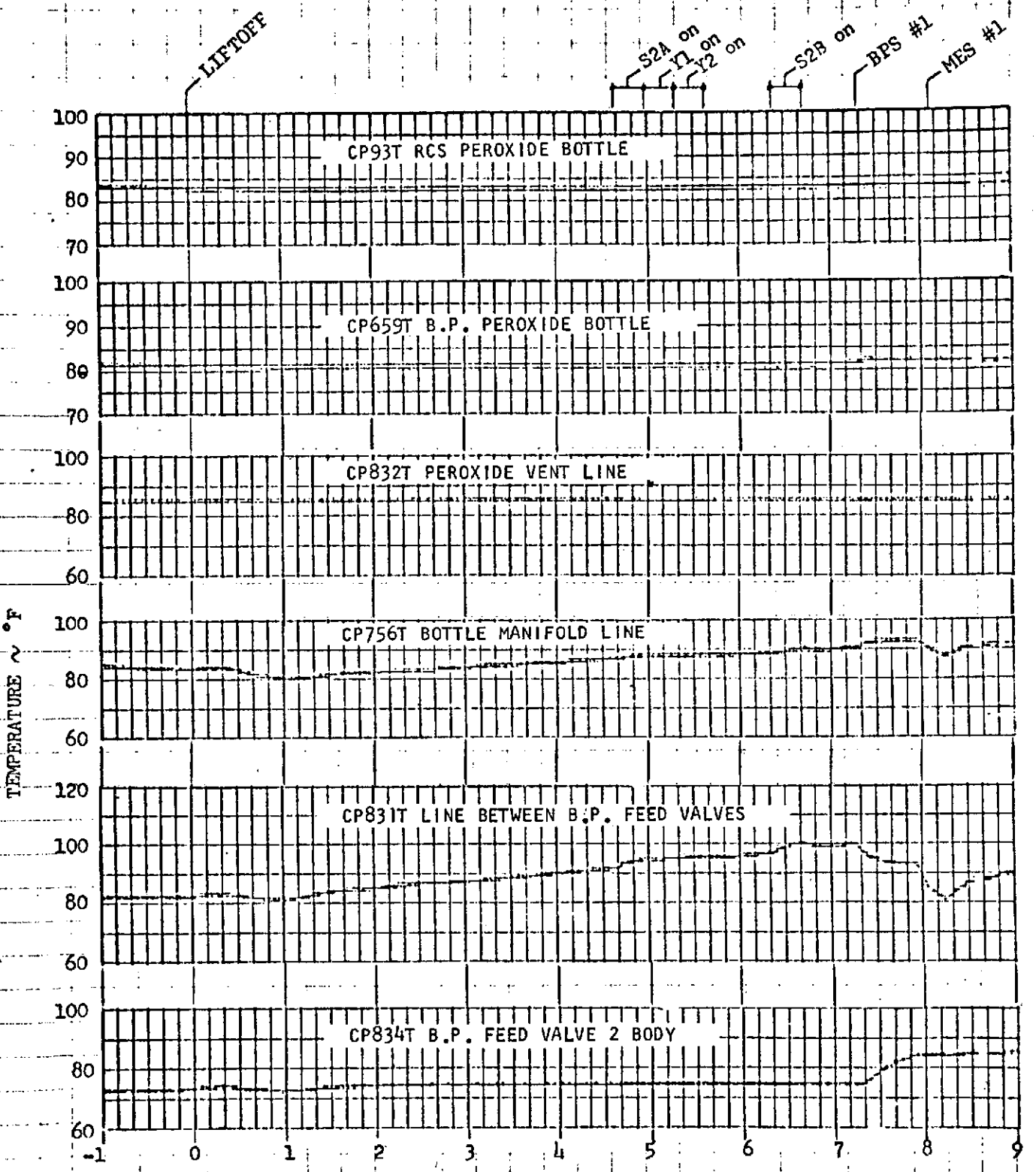

TEMPERATURES IN VICINITY OF HYDROGEN PEROXIDE SUPPLY BOTTLES

FIGURE VII-1D-14

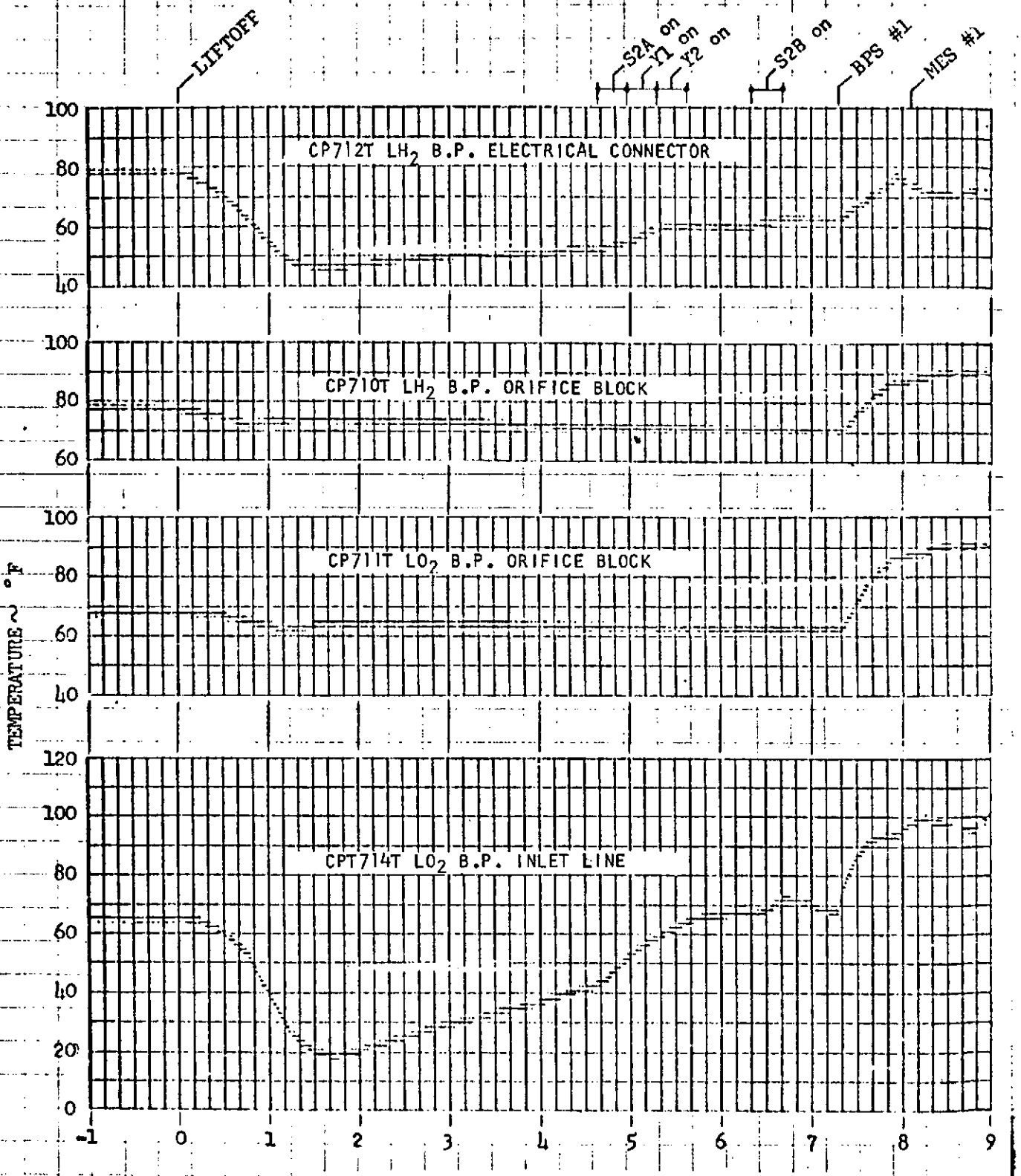

TEMPERATURES IN VICINITY OF CENTAUR BOOST PUMP TURBINES

FIGURE VII-1D-15

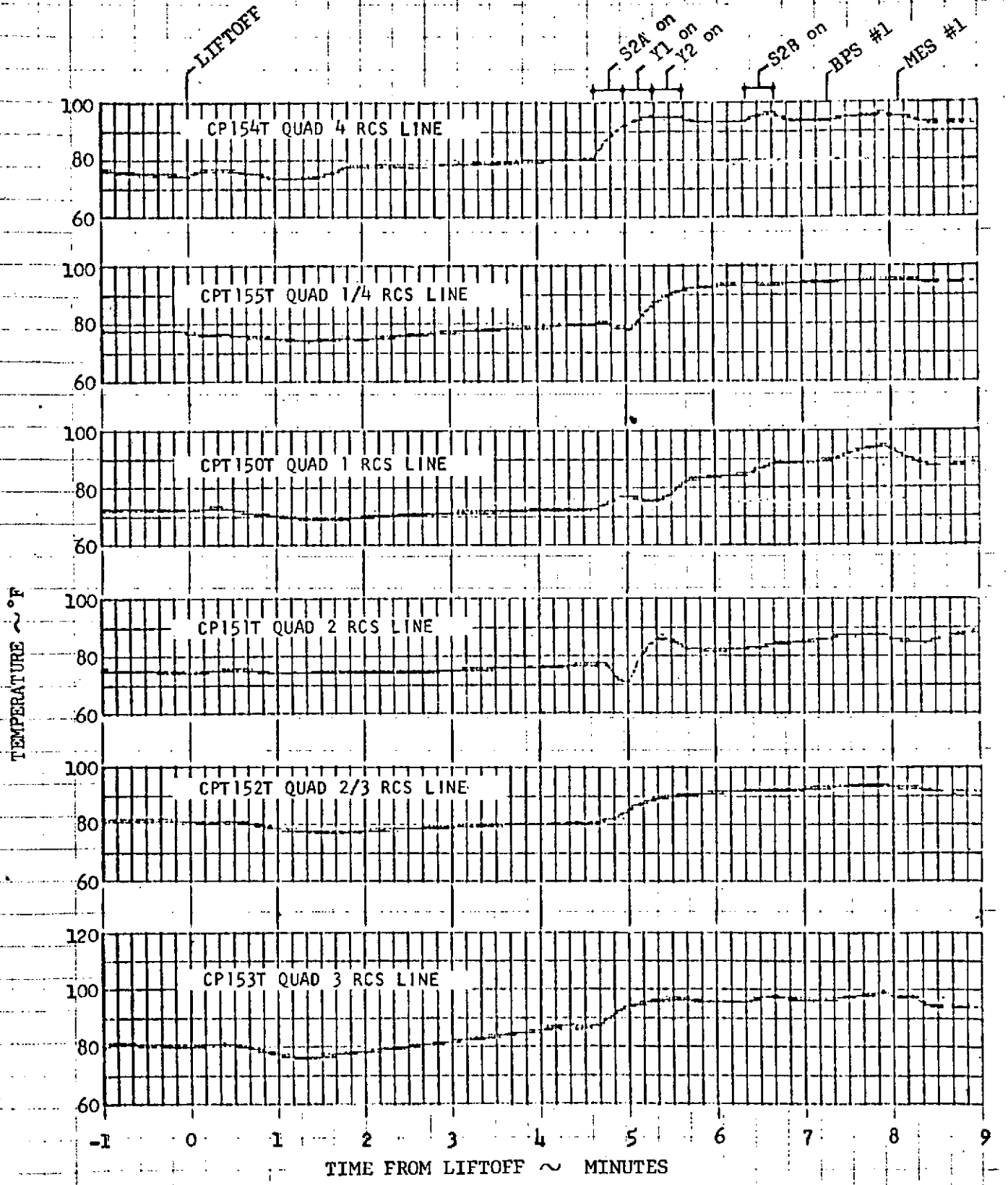

: TEMPERATURES OF HYDROGEN PEROXIDE SUPPLY LINES TO RCS ENGINES

FIGURE VII-1D-16

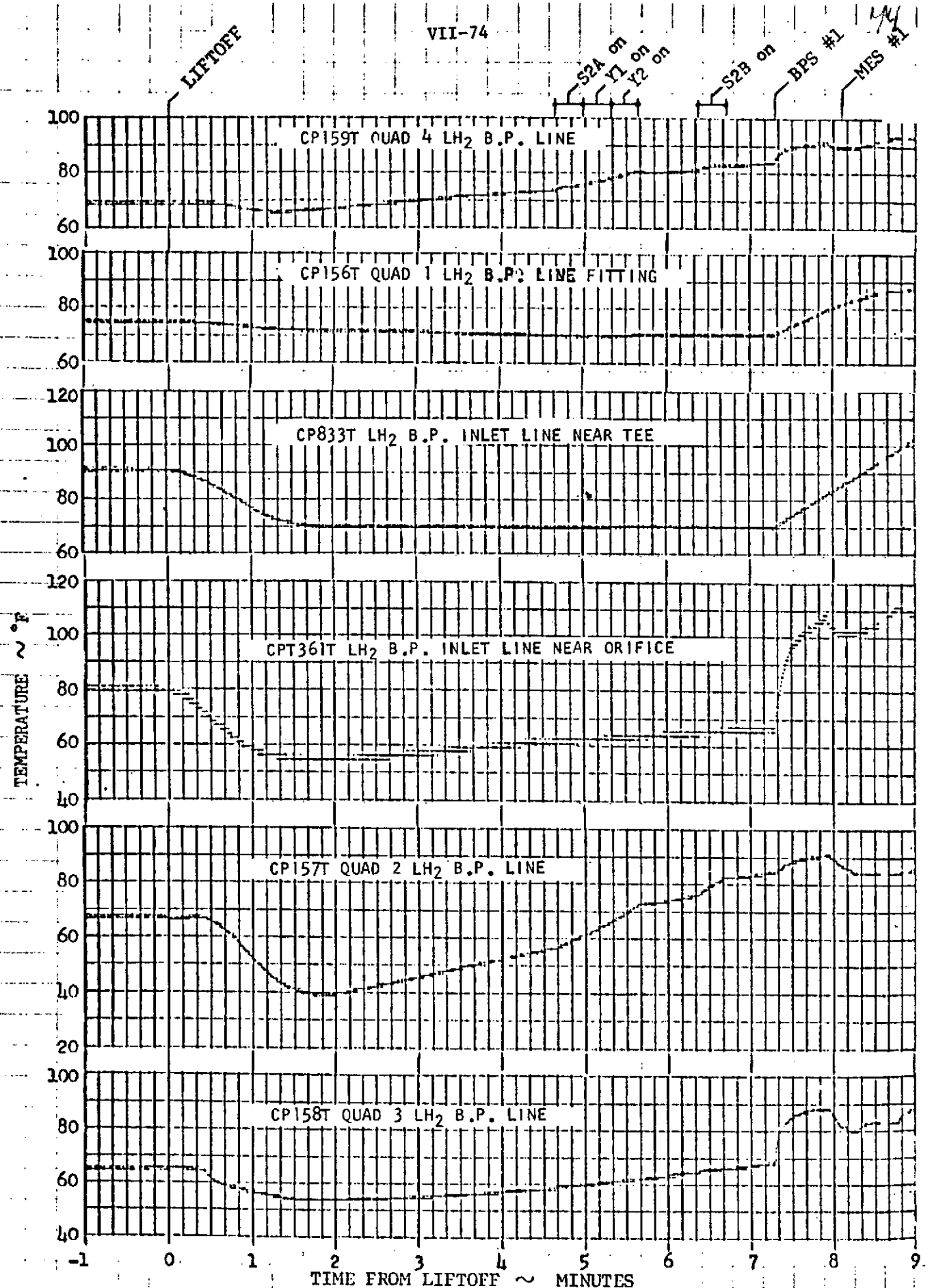

FIGURE VII-1D-17 TEMPERATURES IN VICINITY OF SUPPLY LINES TO BOOST PUMP TURBINES

VII-1E. Centaur Hydraulic System

by T. W. Godwin

Summary

Analysis of the limited hydraulic system operation flight data shows the following:

(a) Operation and sequencing of the Centaur hydraulic system was satisfactory in all respects except for the limitations imposed by the main engine start failure.

(b) Servoactuator response is improved for the new D-1 design with jet pipe servovalve and piston bypass orifice.

(c) The hydraulic system data does not supply any information as to the cause of engine start failure.

System Description

Two separate, but identical hydraulic systems (shown in fig. VII-1E-1) were used on the Centaur stage. Each system gimbaled one engine for pitch, yaw, and roll control, and consisted of an engine-coupled power package and two servocylinders. The power package contained vane type, constant displacement high and low pressure pumps, a reservoir, a bootstrap piston and two relief valves for pressure regulation. The high pressure pump was driven from the engine turbopump accessory drive shaft. The low pressure, or recirculation, pump was driven by a small electric motor and was used to provide low pressure for engine gimbaling requirements during prelaunch checkouts, for alinement of engines prior to main engine start, and for circulation of hydraulic fluid to equalize temperature gradients during coast periods. For the last purpose, the motor was actuated by thermostats on the hydraulic manifolds and on the actuator bodies. The servocylinders were controlled by two-stage, jet pipe type servovalves, which responded to signals from the flight control servoamplifier unit. These servovalves and a redesigned actuator incorporating a piston bypass orifice were new for TC-1. Maximum engine gimbal angle was $\pm 3.15^{\circ}$.

Flight Performance

Operation and sequencing of the hydraulic system was satisfactory in all respects except for limitations imposed by main engine start failure. Main pump operation was limited to approximately 18 seconds, of which only three seconds was at or near normal speed. On the first start attempt, main pump pressure rose to rated value for about one second and

slowly decayed: on the second attempt, pressure peaked to about 90 percent of rated value and decayed rapidly. The recirculation pumps operated for a total of 95 seconds during the two MES1 attempts. All system pressures and temperatures were within allowable limits. Servoactuator response to engine centering signals was very fast, requiring about 2 seconds to aline the engines. This is about twice the previous rate and is attributed to the fast response characteristics of the new jet pipe servovalves at low pressure. Hydraulic system data is summarized in table VII-1E-I.

TABLE VII-1E-1. - HYDRAULIC SYSTEM DATA

Parameter	MES #1	MES #2
CHT1P C-1 power pack pressure	1155 psi	1065 psi
CHT3P C-2 power pack pressure	1155 psi	1110 psi
CHT1P C-1 recirculation pressure	120 psi	120 psi
CHT3P C-2 recirculation pressure	122 psi	122 psi
CH7P C-1 P/P return pressure	65 psi	61 psi
CH8P C-2 P/P return pressure	62 psi	58 psi
CHT2T C-1 P/P temperature	64° F	67° F
CHT4T C-2 P/P temperature	63° F	65° F
CHT5T C-1 manifold temperature	69° F	69° F
CHT6T C-2 manifold temperature	63° F	63° F
CH9T C-1 recirculation motor housing temperature	58° F	60° F
CH10T C-2 recirculation motor housing temperature	55° F	57° F
CH33T C-1 yaw acting body temperature	83° F	80° F
CH36T C-2 pitch acting body temperature	74° F	73° F

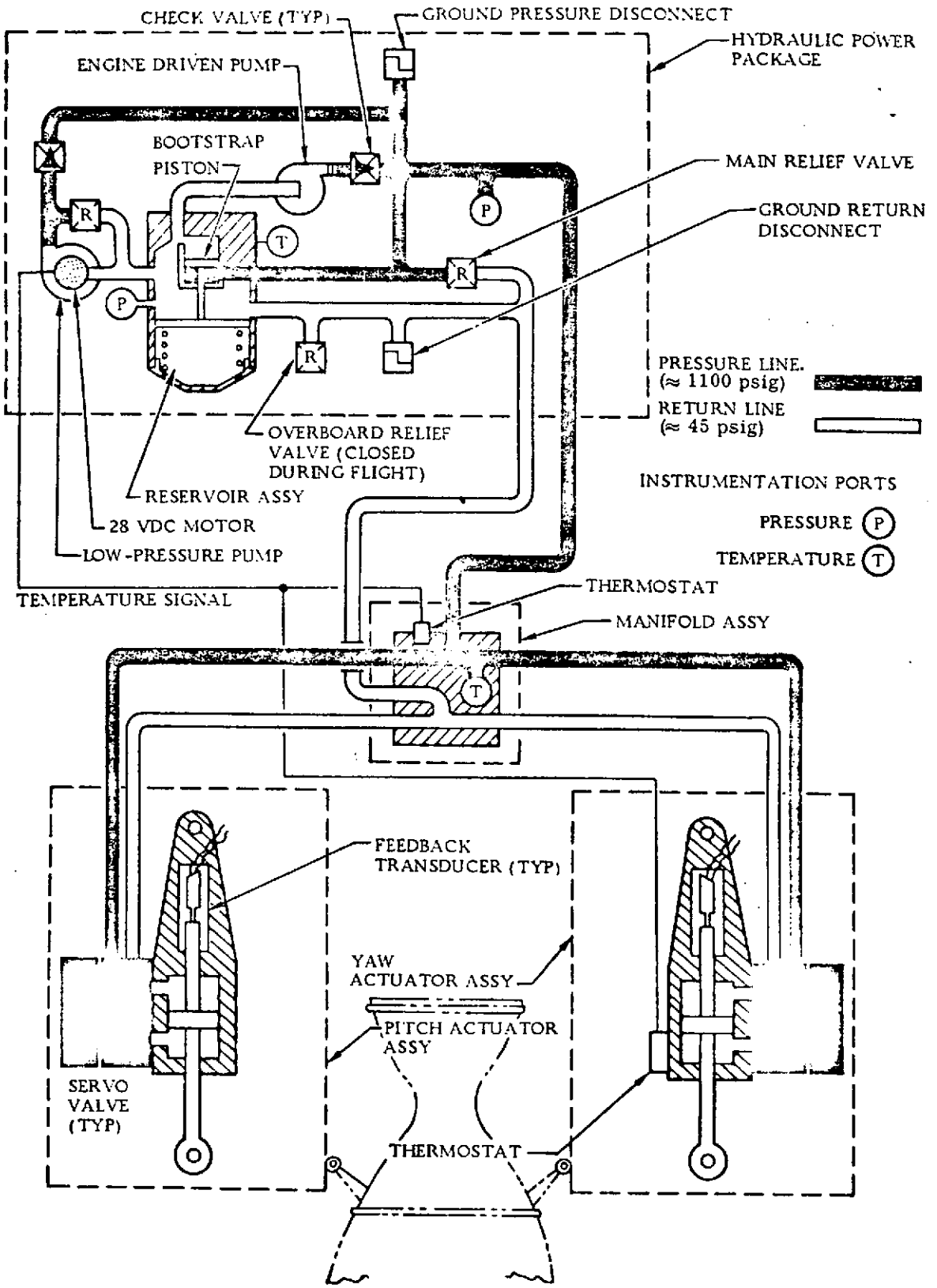

Figure VII-1E-1 Hydraulic system schematic.

VII-1F. Centaur Pneumatics Systems

by W. A. Groesbeck

Summary

The pneumatics system provided regulation of propellant tank pressures, during vent and pressurization sequences, and also provided a stable regulated supply of helium for the propulsion pneumatics and various subsystem purges. Regulation of tank pressures using the new computer controlled vent and pressurization system, CCVAPS, proved to be very accurate and responsive to system requirements. Tank pressure regulation during the boost phase vent control mode was not completely satisfactory. Liquid splashing into the vent standpipe in the oxygen tank resulted in abnormal behavior of the vent valve. The presence of liquid in the vent valve resulted in an unusually wide control band between crack and reseat pressures, and on two occasions the ullage pressure exceeded the upper specification control limit before venting down. The hydrogen and oxygen vent system design, including the vent disconnects, were new and both functioned properly.

System Description

The Centaur pneumatic and vent systems provided vent and pressurization control of propellant tank pressures and provided a regulated supply of helium for inflight purges and to operate propulsion system control valves. A helium supply for the airborne pneumatic system was provided by two helium bottles (one 7365 and one 4650 cu in.), mounted on the aft bulkhead in the Centaur thrust section. A schematic of the airborne Centaur pneumatics system is shown in figure VII-1F-1.

Tank pressurization subsystems. - The tank pressurization system comprised one flow control valve, six pressurization solenoid valves (three primary and three backup), six orifices, and three check valves installed as shown on two pneumatics panels mounted to the aft bulkhead. In addition, two pyrotechnic shutoff valves provided a redundant closure of the tank pressurization lines at umbilical disconnect. Pressurant gas is supplied to the oxygen tank through a bubbler located beneath the liquid surface. For the hydrogen tank the pressurant gas is diffused into the tank ullage through an energy dissipator. The bubbler and the energy dissipator as shown in figure VII-1F-2 are new designs for the Titan/Centaur vehicle.

The primary pressurization system provides two valves for hydrogen tank pressurization and one valve for oxygen tank pressurization. The dual valve and orifice configuration for the hydrogen tank is necessary to meet the pressurant gas flow rate requirements. One valve with an 0.089-inch diameter orifice is used for the first, second, and third burn engine start sequences. A second valve with an 0.157-inch diameter ori-

fice is used for the fourth burn engine test. The larger orifice is needed to provide the required pressurization rate under conditions with a large ullage volume and lowered helium bottle supply pressures. In the oxygen tank, using the bubbler pressurization, a single valve with a 0.046 inch diameter orifice suffices for all engine start sequences.

Tank pressurization is regulated by a new computer controlled vent and pressurization system known as CCVAPS. During pressurization control, ullage pressure data for each tank is fed to the computer from special high accuracy transducers. The computer logic compares the pressure with the preprogrammed requirements and then issues commands to open or close the respective tank pressurization valves. Pressurant gas flow rates are metered by orifices in the outlet ports of the valves.

The pressurization system is redundant with a backup set of pressurization valves and pressure transducers. If a valve failure is detected CCVAPS issues a command to close the main control valve and transfers pressurization commands to the redundant valves. Similarly if a transducer failure is detected, its output is rejected and the control input is switched over to a redundant transducer.

Propulsion pneumatics subsystems. - A regulated helium supply is provided to the propulsion system components by means of two regulators mounted on the aft pneumatic panel. One regulator supplies helium to the engine control valves at 440 to 481 psig. A second regulator downstream of the engine controls regulator steps the pressure down to 297 to 314 psig for pressurization of the hydrogen peroxide storage bottle and inflight purging of the boost pump feed lines. The system is protected against overpressurization by a relief valve downstream of each regulator.

Purge subsystems. - A forward and aft purge system, as shown in figure VII-1F-1 is used to provide environmental control of various system components during prelaunch ground operations. Helium gas for these purges is provided to the vehicle systems from a ground supply through umbilical disconnects. The forward purge system supplies helium to the compartment under the equipment module and to the tank shroud annulus. The purge rate can be regulated as required during cryogenic tanking and chilldown operations to maintain a given pressure level in the shroud annulus. The positive pressure in the shroud prevents contamination of the annulus due to wind inflow.

The aft purge system provides helium to the liquid helium chilldown ducts, the oxygen vent disconnect, the destruct box (which vents into the shroud annulus), the engine purge manifold and the hydraulic purge manifold.

An inflight purge is provided to purge the bubbler in the oxygen tank to keep it free of liquid. In addition a zero-g purge is included which supplies a purge to the standpipe in the oxygen tank, the oxygen tank pressure sense line and the hydrogen tank pressurization line. The purpose of the zero-g purge is to maintain the areas free of liquid dur-

ing a zero-g coast period. Helium for the inflight purges is provided from the airborne storage bottles.

Propellant tank vent systems. - The Centaur tank vent systems provided for tank pressure regulation and overboard venting of boiloff gases from the propellant tanks during all vent mode phases of ground and flight operations. Each tank is configured with ducting to discharge the vent gases external to the vehicle; and tank pressures were regulated within required limits by means of pilot operated vent valves.

The hydrogen tank vent system, as shown in figure VII-1F-3, comprised two vent valves mounted to the forward tank door, a 4-inch diameter cylindrical plenum, a 2.5-inch diameter ducting extending diametrically from each end of the plenum across the forward bulkhead and through the stub adapter, aft canted vent nozzles, inflight vent disconnects, and a vent fin mounted to the Centaur shroud. The main vent duct is indexed directly toward the vent fin and is attached to the forward bulkhead with a series of brackets.

The plenum and ducting are covered with an insulation blanket integral with the forward bulkhead insulation. The vent valves are painted white for thermal control, but are not covered with the insulation blanket. Differential motion between the shroud and tank is accommodated at the sliding seal interface of the vent disconnects, see figure VII-1F-4. All system components in the forward bulkhead compartment and in the tank cavity are in a helium purged environment during ground operations.

During prelaunch operations and the initial boost phase of flight, while the shroud is in place, hydrogen venting is through the one active leg of the vent system. The opposite leg of the vent ducting is passive until the cap is pulled off at shroud jettison. Once the shroud is jettisoned boiloff gases are vented evenly through both legs of the vent system to provide the balanced thrust vent configuration as required for the coast phase vent sequences. The vent nozzles are a convergent divergent design and are aft canted to provide a forward thrust component during venting.

Hydrogen tank pressures are regulated during the vent modes by means of two pilot operated vent valves; one primary and one secondary. The primary vent valve regulator tank pressure between 19 and 21.5 psia during prelaunch operations, boost phase, and coast phase venting sequences.

The secondary vent valve regulates tank pressure at a higher range between 24.8 and 26.8 psia. Both vent valves have locking solenoid control to inhibit venting during pressurization sequences, or to provide selective dual range pressure control during vent sequences. During the ascent boost phase the secondary valve is in the relief mode to protect against overpressurization while the primary vent valve is locked.

The oxygen tank vent system, as shown in figures VII-1F-3 and 4, comprised a single vent valve mounted at the base of the standpipe, a

vent disconnect and ducting to a flush exit in the interstage adapter. The vent ducting is insulated with 1/2-inch thick stafoam, and the duct sections are adjustable to permit optimum alinement of the vent thrust vector with respect to the vehicle center of gravity during coast phase venting. For TC-1 the vent nozzle was alined at 4^{o} 48' to the vertical. The vent valve is a pilot operated valve with a nominal pressure regulation from 29 to 32 psia. The valve also has a locking solenoid to inhibit venting during various pressurization and coast phase control modes. The vent valve was also painted white for thermal radiation control. The top of the vent standpipe inside the tank was covered with a screen to inhibit liquid entering the pipe during the zero-g coast.

Flight Performance

Tank pressurization. - Propellant tank pressures were controlled within specification by the computer controlled vent and pressurization system, CCVAPS, during the active control phases of the flight sequence. These control phases included the hydrogen tank liftoff pressure check prior to liftoff and the prestart tank pressurization during both attempted engine start sequences.

The liftoff pressure check was part of the terminal countdown sequence to verify that the hydrogen tank pressure would be between 22.7 and 24.4 psia at liftoff. CCVAPS accomplished this check by monitoring tank pressure rise, following the vent valve lockup at T - 21.3 seconds, and predicting a liftoff pressure. The final liftoff pressure prediction was made at T - 8 seconds and was within the required limits for a go condition. The actual pressure attained at liftoff was 23.3 psia. Following the last liftoff pressure check CCVAPS control was inactive until the start of tank pressurization during the engine prestart sequences.

Hydrogen tank pressure, as shown in figure VII-1F-5, continued to increase after liftoff, but at a slower rate. At about T + 30 seconds the pressure leveled off at 24.4 psia and then decreased slowly to 24.1 psia at T + 60 seconds. The pressure then increased slowly to 24.5 psia at T + 90 seconds when the vent valve was unlocked and tank pressure vented down to the control range of the primary vent valve.

The reduced pressure rise rate after liftoff, followed by an interval of slow pressure decay resulted from changes in tank heating rates, increase in tank volume, and vehicle acceleration. Heating rates, due to convection, reduced to zero as the tank shroud annulus volume vented to zero pressure during the ascent. This annulus pressure decay also resulted in an increased tank pressure differential causing the tank volume to swell. And the increasing vehicle acceleration acted to suppress liquid boiling and reduce the boiloff. The combined effect of these factors resulted in the reduced rates of self-pressurization.

Control for pressurization of the tanks preparatory to engine start was initiated at T + 436 seconds. At this time all vent valves were

locked and 2 seconds later CCVAPS commanded the pressurization valves open to begin pressurizing the tanks. A closing pressure for each tank was computed based on the initial tank pressure at vent valve lockup. The computed closing pressures and control selection criteria are listed in table VII-1F-1. In each tank the selection criteria considered structural limits and delta P requirements and then CCVAPS selected and controlled to the lesser value.

The tank pressure profiles during the pressurization sequences are shown in figure VII-1F-6. As shown, the hydrogen tank pressure was increased from 20.456 psia to an upper control range of 25.8 to 26.0 psia as limited by the maximum tank pressure limit of 26.0 psia. After Stage II shutdown the structural limits were increased to 27.1 psia and CCVAPS controlled to the computed tank delta P range of 26.256 to 26.456 psia which was the lesser of the two values.

The oxygen tank was pressurized from 32.015 psia to an upper control range of 39.456 to 39.656 psia as limited by the intermediate bulkhead structural limits. After Stage II shutdown the bulkhead delta P limits no longer pertained and the control range shifted upward to 39.575 to 39.775 psia.

At the second engine start attempt CCVAPS again regulated the tank pressurization to given control ranges based on applicable selection criteria. In the oxygen tank the structural limit of 40.5 psia dictated the control range of 40.3 to 40.5 psia. The structural limit of 26.0 psia also governed the selected control range of 25.8 to 26.0 psia in the hydrogen tank.

Pressurization to the given control ranges resulted in a significant but not unexpected pressure overshoot due to the high pressurant gas flow rates, small ullage volumes, and closing response times of the pressurization valves. A summary of the pressure data during CCVAPS regulation is given in tables VII-1F-2 and 3. The maximum overshoot above the upper control range pressure was 0.80 psi in the hydrogen tank and 1.69 psi in the oxygen tank. The pressure undershoot during the control cycles was not significant, less than 0.1 psi in either tank.

The duty cycle on the hydrogen tank pressurization valves was significantly increased at prestart. Liquid outflow from the tank increased the makeup gas requirement and additional repressurization cycles were required to maintain pressure. Prestart, however, had no effect on the oxygen tank pressurization requirements. Because of the failure of the oxygen boost pump, there was no significant liquid outflow from the tank.

Pressurant gas usage. - The helium usage for the controlled tank pressurization sequences at engine start is summarized in table VII-1F-4. The first pressurization sequence, including ramp and repressurization cycles, required 0.522 pound for the hydrogen tank and 0.134 pound for the oxygen tank. For the second start sequence the helium usage was reduced because of lower pressurization delta P requirements. The hydrogen

tank usage was 0.458 pound and the oxygen tank usage was reduced to only 0.030 pound.

Helium storage for the mission was provided from the two bottles pressurized to 3550 psia at liftoff. At this pressure the total initial helium loading was 15.27 pounds. The minimum required helium loading was 14.52 pounds. During the flight a very small quantity of helium (about 0.02 lb) was consumed for the inflight zero-g purge and the bubbler purge.

Propulsion pneumatics. - Pneumatic system regulation for the propulsion system was stable and within specification throughout the flight. The engine controls regulator provided a controlled output pressure of 442 to 444 psig (specification is 440 to 481 psig). The monopropellant regulator output was stable at 305 psig (specification is 297 to 314 psig).

Tank shroud annulus purge. - The forward and aft purge systems were used to supply helium purge gas to the shroud annulus. At high flow conditions of 169 pounds per hour a stable tank shroud annulus pressure of 0.165 psid was maintained through launch. The minimum delta P requirement based on wind conditions was 0.045 psid. Following lockup of the hydrogen tank vent valve at T - 213 seconds the shroud annulus pressure increased slightly to a maximum of 0.200 psid at T - 0. The shroud annulus purge was terminated at liftoff, after which the cavity pressure vented to zero during the ascent.

Tank venting control. - Propellant tank pressures were regulated by vent valve control during the Titan boost phase of flight. The pressure regulation, however, exhibited some abnormal characteristic and in some instances the pressures were out of specification. The unusual behavior during the vent control mode though did not adversely effect the flight performance.

The hydrogen tank vent valve maintained pressure within the specified control range of 19 to 21.5 psia; but the operating control range opened up and shifted downward during the ascent. See figure VII-1F-5. The first hydrogen venting occurred at T + 90 seconds when the primary vent valve was unlocked. As the valve opened tank pressure vented down normally to the control range of the primary vent valve. At about T + 180 seconds the blowdown was nearly complete and the valve started to limit cycle. Characteristically under vacuum conditions the valve no longer modulates but cycles rapidly between the crack and reseat pressure limits (limit cycling). This characteristic is normal and has been observed in ground test and on other Centaur flights. It has also been normal for the control range to open up and shift downward a little.

During the first part of the limit cycle the control band is about 0.6 psi between crack and reseat pressure, but after shroud jettison the control range opens up to about 1.3 psi. These characteristics may be explained in part by the response time of the valve in venting from a small ullage; about 20 to 25 cubic feet as compared to 40 to 50 cubic feet on previous Centaur vehicles. The vent cycle duration is less than

a second, but with a high vent flow capacity the pressure tends to undershoot before the valve can reseat. At shroud jettison the closed leg of the vent system opens up and, with less back pressure, additional gas is vented during each vent cycle causing an even larger pressure undershoot as noted. Prior to shroud jettison an average of about 0.30 pound of gas was vented per vent cycle. After shroud jettison the venting increased to about 0.40 pound per vent cycle.

Venting control of the oxygen tank shows some of the same characteristics only more extreme. The first limit cycle operation of the vent valve begins about T + 75 seconds, as the valve controlled between 29.7 and 31.1 psia. Tank pressure then increased slowly to 32.6 psia before venting occurred. Specification control range was 29 to 32 psia. When the valve did vent again the control range opened up to about 2.5 psi. There was one other occurrence of exceeding the upper cracking limit of the valve at T + 262 seconds; the pressure peaked out at 32.6 psia before the valve opened.

The unusual behavior of the oxygen vent valve was caused by liquid injection in the vent valve. The same characteristics have been observed in ground tests when liquid gets into the valve. Both cases in which the cracking pressure exceeded the upper control limit of 32 psia occurred at vehicle staging times, stage 0 and stage I shutdown. The abrupt reduction in acceleration caused the liquid to swell up, due to boiling, and overflow the top of the vent standpipe and down into the vent valve. Liquid in the valve inhibited its relief operation until the liquid boiled away.

The wide excursion in pressure during the other vent cycles was considered to be an undershoot condition related to the response times of the valve in venting from a very small ullage. Any slight liquid entrainment in the vent gas at this time would also aggravate this condition.

The total propellant boiloff gas vented overboard was calculated based on vent nozzle instrumentation in each vent system. The calculations do not include any liquid entrainment. In the hydrogen tank the total gaseous hydrogen vented during the boost phase was 46 pounds. For the oxygen tank the boiloff gas vented was about 32 pounds.

Table VII-1F-1 CCVAPS CONTROL PRESSURE SELECTION CRITERIA

BOOST PHASE OF FLIGHT PRIOR TO MES - 1		REPEAT ENGINE START ATTEMPT
Prior to Titan Stage II shutdown	After Stage II Shutdown	[sequencing same as for engine start following a settled propellant coast]
LIQUID OXYGEN TANK:		
$P_{close} = P_{max} = 40.5 = 40.500$	$P_{close} = 40.500$	$P_{close} = 40.5 = 40.500$ psia*
$P_{close} = P_{O_2} + P = 32.015 + 7.76 = 39.775$	$P_{close} = 39.775$*	$P_{close} = 38.422 + 7.76 = 46.182$ psia
$P_{close} = P_{H_2} + P_{blkhd} = 20.456 + 19.2 = 39.656$*		
LIQUID HYDROGEN TANK:		
$P_{close} = P_{max} = 26.000 = 26.000$*	$P_{close} = 27.100$	$P_{close} = 26.000 = 26.000$ psia*
$P_{close} = P_{H_2} + P = 20.456 + 6.000 = 26.456$	$P_{close} = 26.456$*	$P_{close} = 21.528 + 6.00 = 27.528$ psia

Note: 1. CCVAPS selects lowest pressure criteria for control set points during any given flight mode.

2. Control set points for pressurization indicated by (*). Also see tank pressure regulation data summary in Table .

Table VII-1F-2 : Oxygen Tank Pressure Regulation - CCVAPS

Event Sequence	Time From T - 0 sec	Ullage Volume ft³	Ullage Pressure psia	Controlled Pressurization Δp psi	Controlled Pressurization Δt sec	CCVAPS Control set points psia	Maximum Pressure after Cmd to close psia	Press Over-Shoot psi	Press Under-Shoot psi	Average Pressure Rise Rate psi/sec	Average Pressure Decay Rate psi/sec
FIRST START SEQUENCE:											
Ramp Prstn, B/P Start	437.8	8	32.015	7.64	0.88	39.456 - 39.656	41.027	1.37	-	8.90	0.56
Repress Cycle # 1	441.8		39.372	0.20	0.16	"	40.815	1.16	0.09	2.42	0.59
" " # 2	444.5		39.407	"	"	"	40.886	1.23	0.05	2.63	0.51
" " # 3	447.7		39.372	"	"	"	40.992	1.34	0.09	2.42	0.43
" " # 4	451.6		39.407	"	"	"	"	"	0.05	2.85	0.33
" " # 5	456.7		39.443	"	0.18	"	40.886	1.23	0.01	2.34	0.26
" " # 6	462.4		39.443	"	"	"	"	"	"	"	"
Stage II Shutdown	469.6		39.865	-	-	39.575 - 39.775	-	-	-	2.20	0.15
Repress Cycle # 7	473.5		39.513	0.20	0.18	"	41.308	1.53	0.06	2.35	0.25
Prestart	477.8		40.639	-	-	"	-	-	-	-	0.25
Repress Cycle # 8	481.0		39.548	0.20	0.18	"	41.097	1.32	0.03	2.35	0.21
Ignition (MES)	485.8		40.114	-	-	-	-	-	-	-	-
REPEAT START SEQUENCE:											
Ramp Pressurization	518.2	9	38.422	2.08	0.34	40.300 - 40.500	42.188	1.69	-	6.33	0.12
Boost Pump Start	528.1		40.710	-	-	"	-	-	-	-	-
Repress Cycle # 1	534.2		40.287	0.20	0.12	"	41.836	1.34	0.01	3.24	0.06
Prestart	548.1		41.062	"	-	"	-	-	-	-	0.09
Ignition (MES)	556.1		40.393	-	-	-	-	-	-	-	-

Table VII-1F-3 Hydrogen Tank Pressure Regulation - CCVAPS

Event Sequence	Time From T - 0 sec	Ullage Volume ft^3	Ullage Pressure psia	Controlled Pressurization Δp psi	Controlled Pressurization Δt sec	CCVAPS Control set points psia	Maximum Pressure after Cmd to close psia	Press Over-Shoot psi	Press Under-Shoot psi	Average Pressure Rise Rate psi/sec	Average Pressure Decay Rate psi/sec
FIRST START SEQUENCE:											
Ramp Pressurization	437.8	25	20.456	5.54	1.92	25.800 - 26.000	26.610	0.61	-	2.90	0.11
Repress Cycle # 1	447.2		25.766	0.20	0.20	"	26.697	0.70	0.03	1.58	0.03
Stage II Shutdown	469.6		26.188	-	-	26.256 - 26.456	-	-	-	-	-
Repress Cycle # 2	469.7		26.227	0.23	0.20	"	27.260	0.80	-	2.35	0.02
Prestart	477.8		27.137	-	-	"	-	-	-	-	0.44
Repress Cycle # 3	479.9		26.170	0.20	0.24	"	27.119	0.66	0.09	1.32	0.62
" " # 4	481.8		26.187	0.20	0.24	"	27.207	0.75	0.07	1.69	0.58
" " # 5	483.9		26.205	0.20	0.20	"	27.137	0.68	0.05	1.41	0.52
Ignition (MES)	485.8		26.328	-	-	-	-	-	-	-	-
REPEAT START SEQUENCE:											
Ramp Pressurization	518.2	40	21.528	4.47	1.60	25.800 - 26.000	26.557	0.56	-	2.88	0.13
Repress Cycle # 1	525.9		25.765	0.20	0.22	"	26.697	0.70	0.04	1.76	0.03
Boost Pump Start	528.1		26.557	-	-	"	-	-	-	-	-
Prestart	548.1		26.047	-	-	"	-	-	-	-	0.53
Repress Cycle # 2	548.8		25.765	0.20	0.24	"	26.557	0.56	0.04	1.39	0.53
" " # 3	550.8		25.748	"	"	"	26.574	0.57	0.05	1.32	0.50
" " # 4	552.9		"	"	"	"	26.592	0.59	"	"	0.51
" " # 5	555.0		"	"	"	"	26.557	0.56	"	1.39	0.50
Ignition (MES)	556.1		26.222	-	-	-	-	-	-	-	-

Table VII-1F-4 PRESSURANT GAS USAGE SUMMARY FOR TC-1 PROOF FLIGHT

	Event	Tank Ullage Volume ft^3	Prztn Orifice Dia. inch	Ullage Pressurization Δp psi	Ullage Pressurization Δt sec	Gas Usage lbs	Gas Flow Rate, ave lb/sec	Helium Storage pressure psia	Bottle Temp. oF
HYDROGEN TANK	FIRST START SEQUENCE:								
	Ramp Prztn	25	0.089	6.15	1.98	0.311	0.157	3532 - 3360	77
	Repress Cycle # 1		"	0.91	0.26	0.040	0.154	3360 - 3346	71
	" " # 2		"	0.93	0.26	0.040	0.154	3346 - 3332	68
	" " # 3		"	0.88	0.30	0.046	0.153	3318 - 3304	66
	" " # 4		"	0.99	0.30	0.046	0.152	3304,- 3290	66
	" " # 5		"	0.92	0.26	0.039	0.151	3290 - 3262	66
	Total Helium Usage					0.522			
	REPEAT START ATTEMP:								
	Ramp Prztn	40	0.089	5.03	1.66	0.246	0.148	3262 - 3150	66
	Repress Cycle # 1		"	0.91	0.28	0.041	0.145	3150 - 3125	62
	" " # 2		"	0.77	0.30	0.043	0.144	3125 - 3100	61
	" " # 3		"	0.79	0.30	0.043	0.144	3100 - 3080	59
	" " # 4		"	0.81	0.30	0.043	0.143	3080 - 3065	58
	" " # 5		"	0.81	0.30	0.043	0.142	3065 - 3045	57
	Total Helium Usage					0.458			
OXYGEN TANK	FIRST START SEQUENCE:								
	Ramp Prztn	8	0.046	9.01	0.94	0.051	0.0537	3532	77
	Repress Cycle # 1		"	1.37	0.22	0.011	0.0521	3360	73
	" " # 2		"	1.44	"	0.012	0.0521	3360	71
	" " # 3		"	1.55	"	0.011	0.0521	3346	70
	" " # 4		"	1.55	"	0.011	0.0521	3346	67
	" " # 5		"	1.44	0.18	0.010	0.0521	3346	67
	" " # 6		"	1.44	"	0.009	0.0521	3346	67
	" " # 7		"	1.79	"	0.009	0.0519	3332	66
	" " # 8		"	1.55	"	0.009	0.0516	3304	66
	Total Helium Usage					0.134			
	REPEAT START ATTEMPT:								
	Ramp Prztn	9	0.046	3.77	0.40	0.021	0.0507	3262	66
	Repress Cycle # 1		"	1.55	0.18	0.009	0.0490	3130	66
	Total Helium Usage					0.030			

1. Δt = time pressurization valve was open = Δt between valve open and closing commands + 0.060 seconds. (consideration for closing response time)
2. $\Delta p = P_{max} - P_{min}$ for each pressurization cycle, includes overshoot & undershoot.
3. Additional helium usage for
   a. engine control valves = 0.09 lbs per start sequence
   b. zero-g purges, LOX bubbler, H202 system = 0.02 lbs.
4. Helium loading at liftoff, (one large + one small bottle = 6.933 cu. ft.)
   a. minimum requirement = 14.52 lbs
   b. actual loading = 15.27 lbs

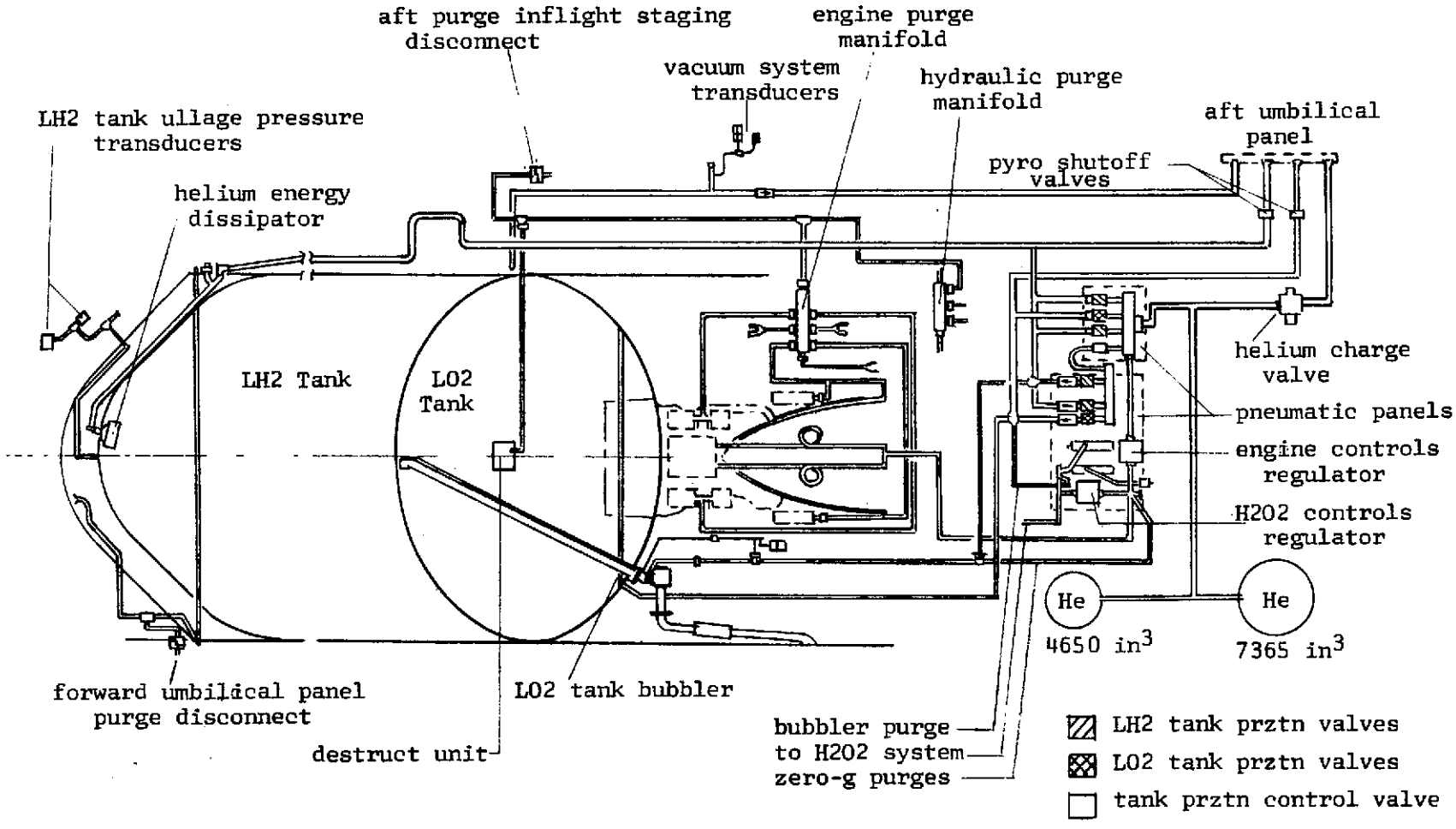

Figure VII-1F-1 Centaur Pneumatics System Schematic, TC-1 vehicle

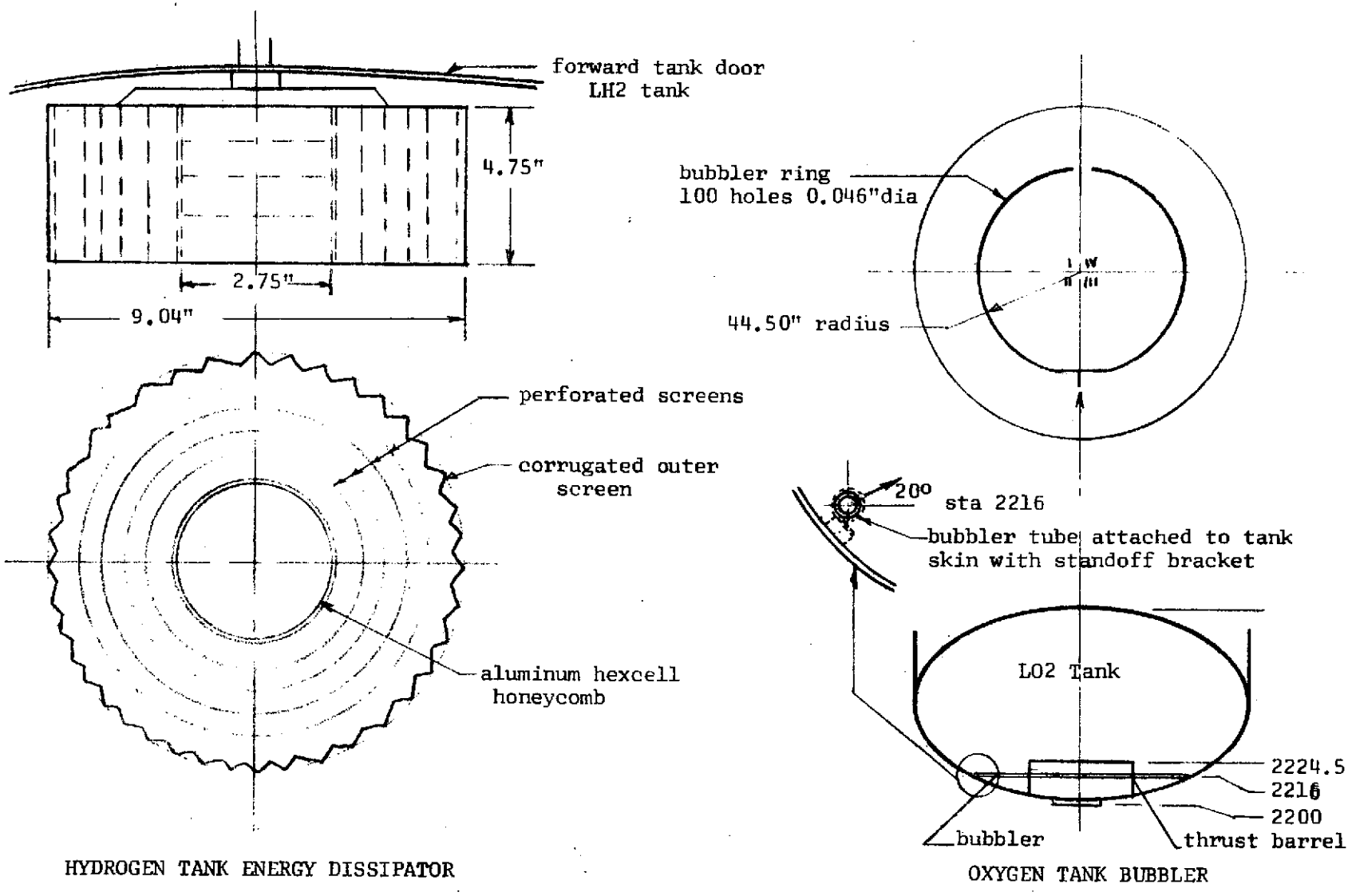

Figure VII-1F-2 LH2 TANK ENERGY DISSIPATOR AND LO2 TANK BUBBLER FOR PRESSURANT GAS INJECTION

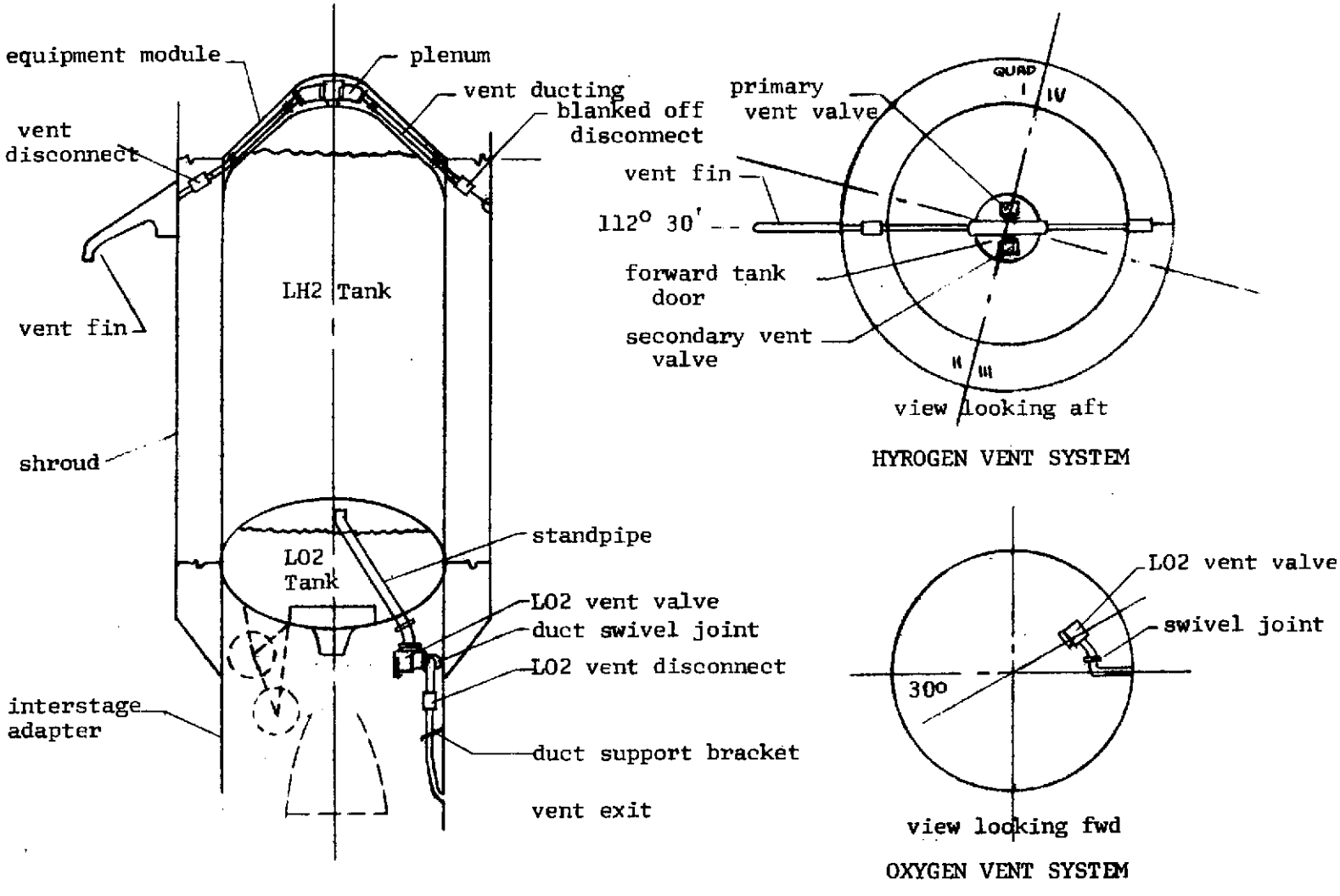

Figure VII-1F-3 PROPELLANT TANK VENT SYSTEMS FOR TC-1 VEHICLE

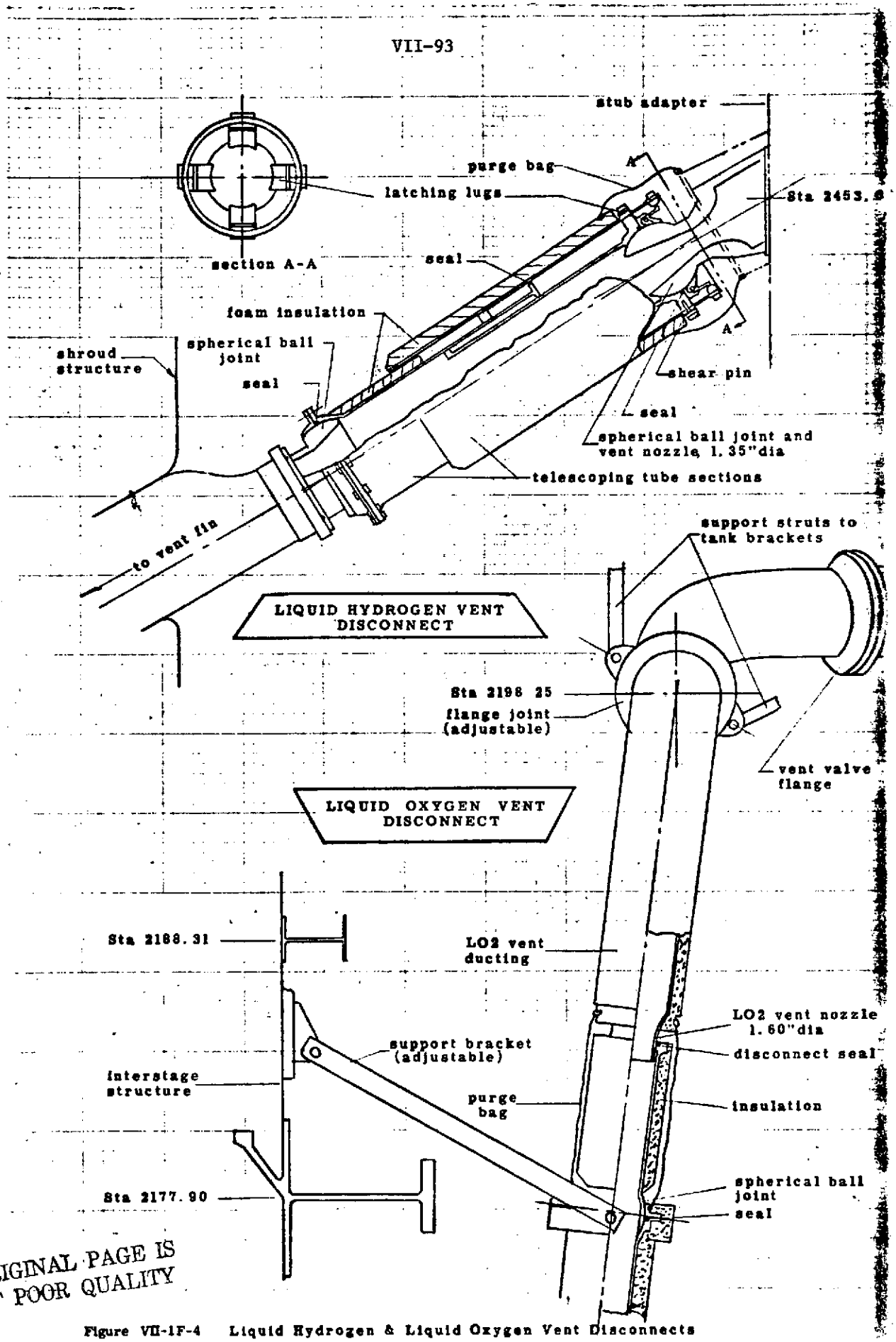

Figure VII-1F-4 Liquid Hydrogen & Liquid Oxygen Vent Disconnects

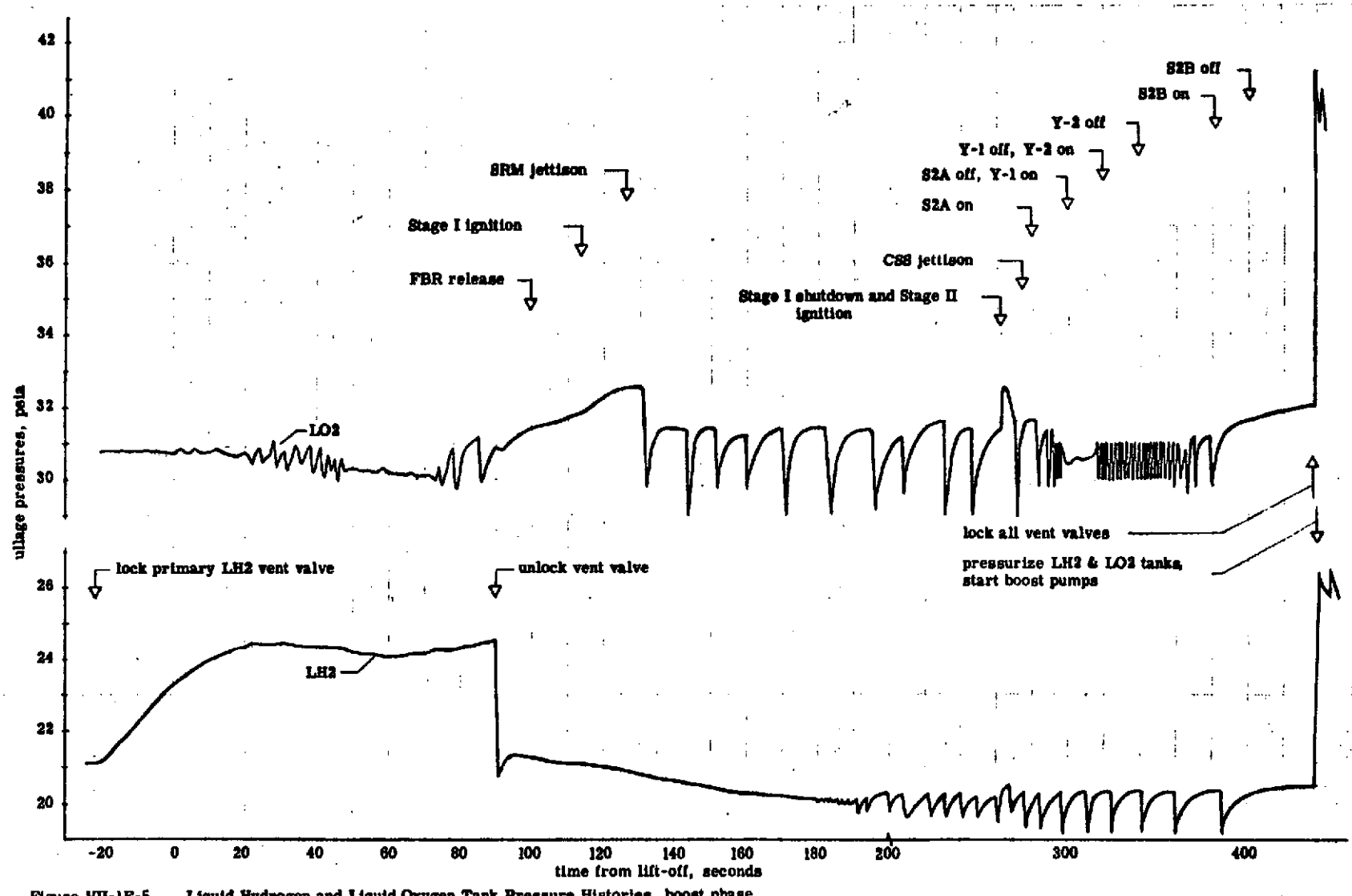

Figure VII-1F-5 Liquid Hydrogen and Liquid Oxygen Tank Pressure Histories, boost phase

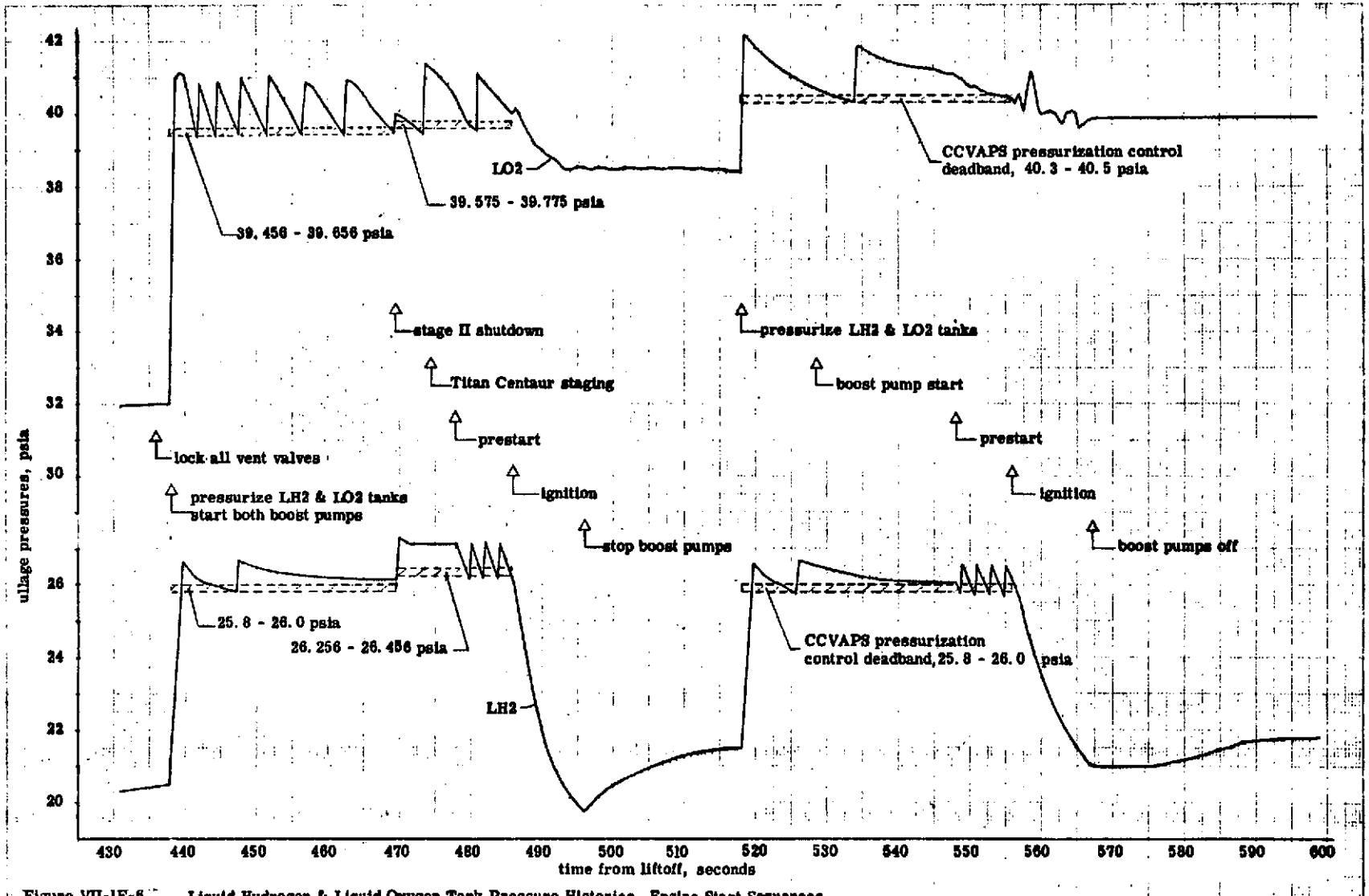

Figure VII-1F-6 Liquid Hydrogen & Liquid Oxygen Tank Pressure Histories, Engine Start Sequences

VII-2. CENTAUR D-1T AND CSS THERMAL ENVIRONMENTS, HEAT TRANSFER AND PROPELLANT BEHAVIOR

by R. F. Lacovic

Centaur Thermal Environment

One of the TC-1 flight objectives was to demonstrate the adequacy of the D-1T Centaur thermal environment in supporting missions with a space coast of up to 5.25 hours. A large number of thermal control modifications had been incorporated into the D-1T Centaur to accomplish this objective by controlling the component temperatures to within their allowable limits and by reducing propellant boiloff. These modifications generally consisted of radiation shielding, coating changes, and low wattage heaters. In addition, the flight plan was designed to include a thermal maneuver (a 180° vehicle roll every 28 min) during the coast, in order to provide uniform heating and cooling of the Centaur components, and the flight sequencing was designed to include periodic firing of the H_2O_2 thrusters to insure proper warming of the H_2O_2 thrusters and lines.

Because first MES was not achieved, an evaluation of the D-1T Centaur thermal environment for a space coast was not obtained. However, the thermal data from the boost phase was obtained, and is summarized as follows.

LH_2 Tank Thermal Environment

The LH_2 tank thermal environment consists of the tank sidewall radiation shielding, forward equipment module, CSS, and stub adapter. The temperatures of these components at selected times throughout the TC-1 flight are presented in table VII-2-I. The locations of these temperature sensors are shown in figure VII-2-1. The T - 0 temperatures obtained during the TCD and LRV are also listed in table VII-2-I, to provide a comparison of the T - 0 thermal environment between the three tankings. As shown by this comparison, the TC-1 liftoff temperatures were in good agreement with the TCD and LRV T - 0 temperatures, which indicates that the LH_2 tank heating rates, helium purge leaks, and overall thermal environment at liftoff were "as expected."

Between liftoff and CSS separation the LH_2 tank environmental temperatures reflect the various cavity venting responses to the external pressure drop during ascent. The rapid venting of the helium decreases the convection heating and produces a significant decrease in all of the radiation shield, equipment module, CSS insulation, and stub adapter temperatures (refer to table VII-2-I). The temperature decrease was expected and indicates the adequacy of the CSS insulation in attenuating the aerodynamic heating penetration to the LH_2 tank area.

After CSS separation the component temperatures began to increase or decrease as expected to achieve equilibrium with the space environment (refer to table VII-2-I). For example, as space heating begins to warm the LH_2 tank radiation shielding, the shielding will continue to vent down at a rate dependent on the outgassing rate and free molecular residual gas flow rate. The thermal behavior of the radiation shielding during this transient period was of concern in evaluating the shielding performance. A typical temperature history of the LH_2 tank radiation shielding throughout the flight is shown in figure VII-2-2. The figure shows both the cooling effect during the ascent venting and the transient warming after CSS separation. On the same figure is shown some GD/CA small scale test data on the shielding where the ascent venting and full solar heating were simulated. The test data and flight data are in good agreement, indicating that the LH_2 tank radiation shield venting and transient thermal performance were as designed. Unfortunately, the space coast was not long enough to determine the steady state performance and effectiveness of the radiation shielding.

The thermal behavior of the components located on the forward equipment module is also presented in table VII-2-I. These components were all well within their temperature limits at liftoff and remained essentially constant throughout the entire flight.

Centaur Aft End Environmental Temperatures

The Centaur aft end environmental temperatures consisted primarily of sensors located on the propulsion system, propellant feed system, aft bulkhead, and H_2O_2 system. These sensors provided a relatively complete survey of the aft end thermal behavior throughout the TC-1 flight. The sensor locations are shown in figure VII-2-3 and the flight temperatures at selected event times are listed in table VII-2-II. The T - 0 temperatures from the TCD and LRV are also listed in the table to provide a comparison with the TC-1 liftoff temperatures. As shown by this comparison, all of the aft end temperatures were as expected at liftoff.

Between liftoff and CSS separation the aft end temperatures respond to ISA compartment venting and the termination of LHe flow and begin to chill or warm accordingly.

At 5 seconds after CSS separation, four of H_2O_2 engines were fired in sequence into the ISA compartment in order to prime the H_2O_2 lines (TC-1 was the first vehicle to employ this priming sequence). The H_2O_2 engine exhaust impingement heating that resulted from the firings affected many of the aft end temperature sensors. The affected temperatures are designated by an asterisk in table VII-2-II, and their locations are shown in figure VII-2-4. The S2A, Y-1, Y-2, and S2B engines were each fired for 20 seconds at T + 279, 299, 319, and 382 seconds, respectively. The exhaust from these firings which consists of a mixture of 56 percent steam, 41 percent oxygen, and 3 percent H_2O_2 rebounds off the thermal barrier and fills the ISA compartment as a plenum, producing

heating of virtually all surfaces in the compartment as shown in figure VII-2-4.

The calculated maximum pressure that could result in the ISA compartment from the H_2O_2 firings is 0.013 psia. This pressure is considerably below the triple point pressure of water (0.089 psia). As the water vapor comes in contact with a cold surface (-60° F) it will sublime directly into the solid state. A typical response of some selected aft end temperatures to H_2O_2 exhaust impingement heating is shown in figure VII-2-5. As the steam from the H_2O_2 exhaust impinges on a cold surface the heat of sublimation is released and the surface temperature increases until it corresponds to the partial pressure of water vapor that exists in the compartment. The best example of this impingement heating behavior was given by CA305T as shown in figure VII-2-5. CA305T increased to an equilibrium temperature of -25° F which corresponds to a water vapor pressure of 0.0046 psia. Other sensors such as CP753T appear to be increasing toward the same equilibrium temperature. Only a small percentage of the water vapor sublimed onto cold components; the great percentage of vapor sublimed onto the LO_2 tank aft bulkhead. This was verified by the significant increase in LO_2 tank heating (as indicated by the LO_2 tank vent rate) that occurred during the H_2O_2 engine firing period. The LO_2 tank heating rate was about 66 000 Btu per hour during the firings as compared with 17 000 Btu per hour during the boost, and 44 000 Btu per hour during prelaunch. These impingement heating effects were expected, and were no more severe than the previous impingement heating experienced on Centaur D-1A aft components from the 50-pound thrust H_2O_2 engine exhaust. The most significant heating from the H_2O_2 engine firings for TC-1 was in local heating of the ISA. Measurement CA397T which was located on the ISA skin at the centerline of the Y-2 engine exhaust (only 4 in. away from the nozzle exit) indicated a maximum temperature of 293° F. This temperature was about 40° F greater than predicted.

Figure VII-2-5 also shows the effects of nitrogen sublimation during the first 100 seconds of boost. Measurement CP122T was probably covered with nitrogen frost at T - 0. When the LHe chill is terminated, the pump begins to warm until the nitrogen liquefies at its vapor pressure corresponding to the ISA compartment pressure. The temperature then remains at this level until the nitrogen is vaporized.

At boost pump start some aft end temperatures respond to the impingement heating from the LO_2 boost pump exhaust (as also shown in fig. VII-2-5) in a manner similar to the response from the H_2O_2 engine firings. At Titan/Centaur separation and prestart the aft end temperatures respond to the removal of the ISA compartment and to the flow of propellants.

The aft end equipment temperatures, and pneumatic system temperatures were essentially constant throughout the flight, as shown in table VII-2-II. The only anomaly was the LO_2 vent valve temperature, CF30T, which indicated a temperature colder than LO_2 temperature during

boost. This cold temperature is attributed to the venting of LO_2 which would flash to the ambient pressure in the vent ducting. This LO_2 venting affected the LO_2 tank vent valve behavior as discussed in section VII-1F. The H_2O_2 system temperatures were well within limits throughout the entire flight. The H_2O_2 fluid temperatures were essentially constant at 82° F.

Coast Phase Propellant Behavior

Liquid hydrogen. - The TC-1 LH_2 tank was internally instrumented with sixteen liquid/vapor sensors to monitor the liquid position and slosh behavior during the 12-minute settled coast, 80-minute zero gravity coast, and $5\frac{1}{4}$ hour zero gravity coast phases of flight. Because first MES was never achieved, none of the propellant behavior data relative to these expected coast periods was obtained. The limited LH_2 behavior data that was obtained is summarized as follows.

After the first MECO signal, the vehicle went into a restart sequence which resulted in a short 60-second settled coast period followed by a restart attempt for 10 seconds and then followed by another settled coast period of 182 seconds until vehicle destruct. The estimated LH_2 level during the 60-second coast was at Station 2465 at an ullage of 40 cubic feet. The estimated LH_2 level during the 182-second coast was at Station 2461 at an ullage of 55 cubic feet. The vehicle acceleration during both coast periods was 5.6×10^{-4} g provided by the four H_2O_2 settling engines.

The LH_2 behavior during these coast periods is presented in figure VII-2-6. Only two of the liquid/vapor sensors were in the tank ullage during the coasts, and these sensors were located in the center of the tank. Both of these sensors remained dry throughout the 60-second coast and during both LH_2 tank pressurizations and engine start attempts. However, because of the location of these sensors, significant sloshing could have taken place without activating the sensors.

At 62 seconds into the second coast period sensor CM241X, located 23 inches above the liquid surface, went wet (refer to fig. VII-2-6) indicating that LH_2 had probably reached the top of the tank. The sensor stayed wet for 12 seconds, went dry for 40 seconds, then went wet again for 24 seconds, and then dry for the remaining 44 seconds of flight. The lower sensor CM242X behaved in a similar manner. The type of behavior displayed by these sensors indicates a sloshing motion rather than bulk motion away from the tank bottom or splashing. The coast period was not long enough to show conclusively that the slosh motion would have decayed sufficiently to permit tank venting. The LH_2 tank upper slosh baffle, of course, was not located in the proper position to effectively dampen the slosh motion at this liquid level. The baffle was located 60 inches below the liquid surface at the level expected after a normal first engine firing.

Liquid oxygen. - The LO_2 tank was essentially full throughout the coast periods if no LO_2 prestart or engine start flow is assumed. The tank ullage was approximately 8 cubic feet throughout both coast periods. If a tank venting was commanded, liquid would probably have been vented.

TABLE VII-2-1. - CENTAUR LH_2 TANK ENVIRONMENTAL TEMPERATURE

Measured number	Location	Temperature, ∿°F						
		T - 0	CSS Sep'n	B/P Start 1	MES 1	MES 2	LRV T - 0	TCD T - 0
CA900T	VIK. trans. adpt.	54	44	44	43	43	N.A.	58
CA903T	Eq. mod. skin	41	32	30	32	32	44	41
CA905T	IRU out. mount	66	59	59	63	66	66	63
CA906T	FWD blkhd skin	-422	-424	-421	-416	-409	-417	-420
CA907T	FWD blkhd skin	-421	-423	-422	-422	-423	-417	-423
CA908T	FWD blkhd skin	-422	-423	-422	-422	-423	-418	-423
CA909T	FWD blkhd ins fx	-71	-102	-77	-71	-65	-69	-65
CA910T	FWD flkhd ins fx	-60	-106	-85	-79	-75	-56	-67
CA911T	FWD blkhd ins md	-272	-254	-254	-254	-254	-217	-233
CA912T	FWD blkhd ins md	-190	-254	-254	-254	-254	-190	-189
CA913T	FWD blkhd ins ex	-63	-112	-94	-91	-84	-64	-58
CA914T	Eq. mod. skin	46	35	33	33	35	52	48
CA952T	LH_2 tk rs out	-138	-342	-109	-71	-47	-211	-141
CA953T	LH_2 tk rs mid	-265	-380	-290	-275	-260	-285	-263
CA954T	LH_2 tk rs inr	-313	-402	-340	-330	-323	-333	-335
CA955T	LH_2 tk rs out	-368	-410	-109	-72	-44	-367	-368
CA956T	LH_2 tk rs mid	-395	-415	-313	-298	-283	-392	-393
CA957T	LH_2 tk rs inr	-412	-417	-387	-387	-385	-412	-410
CA960T	LH_2 tk rs out	-151	-355	-248	-226	-211	-225	-156
CA961T	LH_2 tk rs mid	-263	-382	-323	-310	-303	-285	-260
CA962T	LH_2 tk rs inr	-320	-405	-347	-343	-335	-342	-348
CA963T	LH_2 tk rs out	-385	-410	-129	-91	-56	-382	-383
CA964T	LH_2 tk rs mid	-402	-412	-355	-345	-330	-395	-400
CA965T	LH_2 tk rs inr	-415	-415	-377	-382	-385	-415	-415
CA966T	LH_2 sump rs out	-375	-362	-303	-270	-240	-377	-372
CA967T	LH_2 sump rs mid	OSH	OSH	OSH	OSH	OSH	-387	-385
CA968T	LH_2 sump rs inr	-402	-405	-375	-382	-395	-397	-395
CA969T	LH_2 sump rs out	27	-9	-46	-54	-66	15	38
CA972T	Stub adpt shld	-44	-126	-126	-112	-119	-27	-39
CA973T	Stub adpt shld	-86	-148	-156	-156	-158	-27	-25
CA974T	Stub adpt shld	-44	-128	-81	-69	-59	-24	-20
CA975T	Stub adpt shld	-41	-128	-71	-59	-46	-29	-25
CA976T	Stub adpt skin	-273	-337	-360	-360	-362	-256	-278
CA977T	Stub adpt skin	-168	-221	-226	-226	-228	-149	-174
CA978T	Stub adpt skin	-138	-153	-156	-158	-158	-119	-139
CA979T	Stub adpt skin	-49	-64	-59	-56	-56	-37	-49

TABLE VII-2-1. - Concluded.

Measured number	Location	Temperature, ∿° F						
		T - 0	CSS Sep'n	B/P Start 1	MES 1	MES 2	LRV T - 0	TCD T - 0
CA980T	Wire tnl	-186	-250	-188	-121	-146	-186	-154
CA981T	Wire tnl	27	-84	-96	-86	-99	22	33
CA982T	Wire tnl	-362	-372	-365	-362	-360	-365	-363
CA983T	Wire tnl	-372	-387	-387	-385	-382	-375	-370
CA984T	Wire tnl	-357	-360	-362	-360	-360	-360	-355
CA985T	Wire tnl	-372	-395	-395	-395	-395	-378	-375
CA987T	Recirc line	-415	-417	-420	-415	-415	-405	-415
CA988T	Destruct. mount	10	-109	-131	-136	-143	32	25
CA989T	Destruct. pod	12	-176	-206	-208	-208	35	25
CA188T	CSS frame in	72	256	N.A.	N.A.	N.A.	N.A.	82
CA189T	CSS frame in	68	144	↓	↓	↓	↓	80
CA190T	CSS frame in	82	133					80
CA191T	CSS rad shld	60	17					65
CA192T	CSS insul in	64	22					66
CA193T	CSS insul in	61	10					65
CA194T	CSS insul in	63	22					65
CA195T	CSS insul out	76	61					77
CA196T	CSS insul in	73	27					75
CA197T	FWD seal	19	18				28	30
CA198T	CSS frame in	64	106				63	65
CA199T	CSS diaph in	-37	-67				-28	-36
CA204T	CSS insul in	-27	-32				-15	-13
CA205T	CSS insul in	-83	-88				-206	-86
CA206T	CSS insul in	-66	-68				-49	-50
CA207T	CSS insul out	25	13				28	33
CA208T	CSS insul in	-52	-71				-13	-32
CA209T	CSS insul in	-310	-252				-308	-308
CA210T	CSS insul out	-81	-71				-71	-74
CA211T	CSS insul in	-325	-300	↓			-322	-320
CA397T	ISA H_2O_2 imping	65	51	117	↓	↓	68	73
CS811T	Siu skin	66	65	66	67	68	65	68
CT56T	Sig cond no. 1	61	60	60	61	61	62	62
CT58T	Eq. mod. mux 1	63	61	60	60	60	60	67
CT62T	S-band xmtr	76	78	80	82	82	74	75
CT75T	Eq mod instr box	66	64	64	64	64	65	68
CB1T	C-band xponder	66	70	72	72	72	68	67
CC202T	SCU housing	63	63	63	63	63	63	63
CL300T	IRU skin	82	82	84	86	86	69	84
CL316T	SEU internal	68	66	66	66	66	66	68
CK30T	DCU skin	82	82	87	88	88	77	80
CM47T	IRU gyro	80	80	80	80	80	80	83

TABLE VII-2-2. - CENTAUR AFT END ENVIRONMENTAL TEMPERATURES

Measured number	Location	Temperature, ∿°F						
		T - 0	CSS Sep'n	B/P Start 1	MES 1	MES 2	LRV T - 0	TCD T - 0
[a]CA302T	LH_2 duct rad sh	60	55	20	23	1	66	65
CA303T	LH_2 duct rad sh	55	41	-8	-4	-13	59	33
[a]CA304T	LO_2 duct rad sh	46	-13	10	14	64	42	45
[a]CA305T	Aft blkhd rad sh	0	-108	-58	-58	-81	-55	5
CA306T	Aft blkhd rad sh	-95	-203	-170	-167	-167	-115	-100
CA307T	LO_2 sump rad sh	41	-8	1	1	-22	31	33
CA308T	LO_2 sump rad sh	-36	-67	-67	-67	-76	-68	-73
CA309T	Aft blkhd rad sh	46	-8	5	10	5	50	55
[a]CA310T	Aft blkhd rad sh	-170	-90	-90	-85	-85	-176	-192
[a]CF30T	LO_2 vent vlv	-142	-202	-176	-149	-178	-135	-140
CF133T	Aft pneu pnl	66	61	58	58	55	67	66
CF134T	Aft pneu pnl	66	61	55	55	55	64	69
CP63T	C-1 thst chm jkt	71	60	60	54	-348	70	73
CP93T	Att cntrl H_2O_2	82	82	82	82	82	76	86
CP98T	C-2 thst chm jkt	48	48	48	42	-343	40	54
CPT122T	C-1 eng fuel pmp	-380	-295	-268	-380	-414	-400	-390
CPT123T	C-2 eng fuel pmp	-380	-290	-263	-330	-407	-400	-395
CPT124T	C-1 eng ox pmp	-57	-77	-81	-94	-127	-63	-80
CP125T	C-2 eng ox pmp	-48	-69	-81	-90	-123	-40	-50
[a]CP143T	C-1 comp amb	68	45	68	68	-27	80	78
[a]CPT144T	C-2 comp amb	68	68	68	-135	-275	80	68
CPT150T	QD1 a/c line	72	74	90	92	92	75	77
CPT151T	QD2 a/c line	74	76	84	84	84	80	73
CPT152T	QD2 a/c line	80	80	94	92	92	80	83
CP153T	QD3 a/c line	80	86	96	96	96	79	80
CP154T	QD4 a/c line	74	80	94	94	94	72	72
CP155T	QD1 a/c line	76	78	92	92	92	80	82
CP156T	B/P H_2O_2 ftg	76	70	70	82	88	77	78
[a]CP157T	B/P H_2O_2 line	64	55	64	88	84	69	72
CP158T	B/P H_2O_2 line	65	59	69	83	83	69	71
[a]CP159T	B/P H_2O_2 line	63	71	83	89	93	70	71
CPT361T	B/P sup ln orf	75	50	67	105	116	81	84
CP659T	B/P H_2O_2 btl	81	81	81	81	81	72	85
CF4T	He bottle 1	81	79	79	67	64	80	75
CF15T	He bottle 2	75	72	72	61	55	75	71
[a]CA980T	LH_2 sump tnl	-181	-240	-181	-121	-145	-186	-150
[a]CA981T	LO_2 tank tnl	22	-20	-30	-20	-97	22	37

[a]Measurement responds to H_2O_2 engine firing impingement heating.

TABLE VII-2-2. - Concluded.

Measured number	Location	Temperature, ∿° F						
		T - 0	CSS Sep'n	B/P Start 1	MES 1	MES 2	LRV T - 0	TCD T - 0
CP710T	LH_2 B/P orifice	75	72	72	81	81	84	83
CP711T	LO_2 B/P orifice	68	64	64	86	94	70	68
[a]CP712T	LH_2 B/P conn.	75	50	60	90	90	77	79
[a]CPT714T	LO_2 B/P line	64	39	64	94	94	67	70
[a]CP741T	C1 eng. bell	79	61	79	70	-250	87	72
[a]CP742T	C2 eng. bell	70	53	70	61	-225	87	71
[a]CP743T	C1 eng. bell	70	61	70	112	-140	85	71
[a]CP744T	C2 eng. bell	61	53	61	79	-182	85	71
CP745T	C1 eng. bell	61	53	61	53	-225	75	71
CP746T	C2 eng. bell	61	53	53	53	-182	71	71
CP750T	C-1 LO_2 duct surf.	-265	-265	-265	-265	-265	-280	-280
CP751T	C-1 LH_2 duct surf.	-400	-400	-400	-400	-400	-400	-400
[a]CP752T	C-1 LH_2 pmp dsch	-342	-232	-191	-325	-371	-330	-335
[a]CP753T	C-1 LH_2 pmp HSG	-338	-259	-170	-215	-294	-332	-345
[a]CP754T	C-1 LH_2 jckt line	-76	-85	-85	-243	-393	-130	-100
CP756T	H_2O_2 crossover	84	87	92	92	90	82	88
CP828T	C-2 eng. tb pmp	-393	-315	-288	-283	-393	-393	-393
[a]CP829T	C-2 pump shield	-27	-135	-52	-27	-27	10	20
[a]CP831T	LN btwn B/P FVS	80	90	98	84	86	82	88
CP832T	H_2O_2 vent ln	84	84	84	84	82	57	84
CP833T	LH_2 B/P line	84	68	68	82	104	101	102
CP834T	B/P fd vlv body	72	72	74	84	86	70	73
CT59T	Thr. sect. mux 2	75	75	75	75	75	80	75
CT76T	Aft instr. box	72	69	72	72	72	74	68
CT77T	C-2 instr. box	72	69	72	72	72	75	75
CU240T	C-1 servo psn HSG	66	66	69	69	68	61	66
CU241T	C-2 servo psn HSG	60	61	64	63	63	70	67
CA397T	ISA H_2O_2 imping	62	51	117	N.A.	N.A.	68	73

[a]Measurement responds to H_2O_2 engine firing impingement heating.

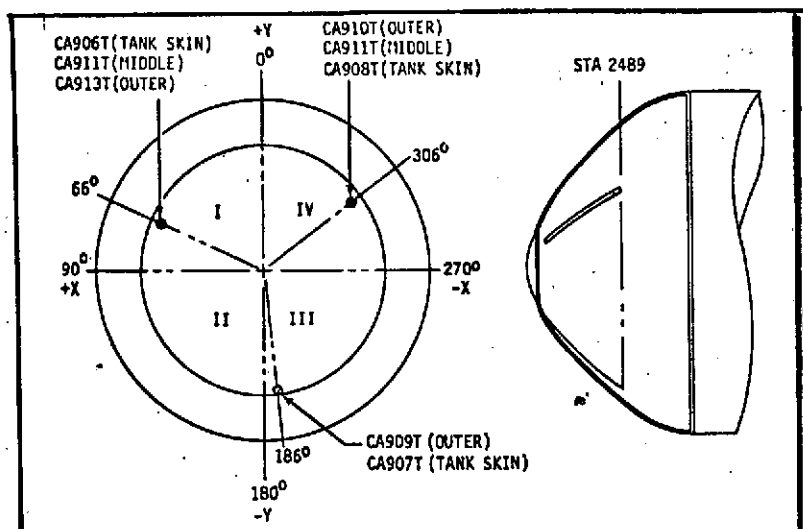

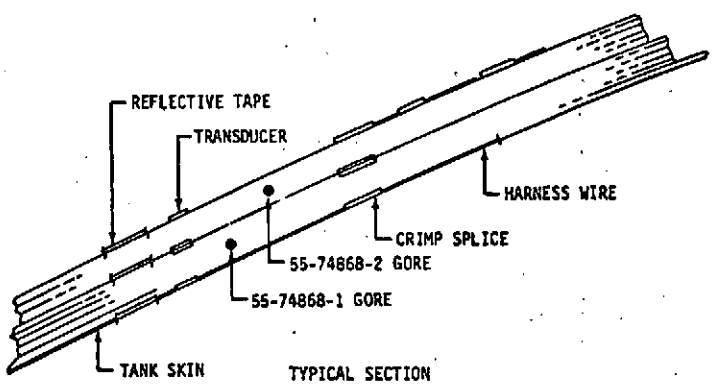

CENTAUR Forward Bulkhead Temperatures

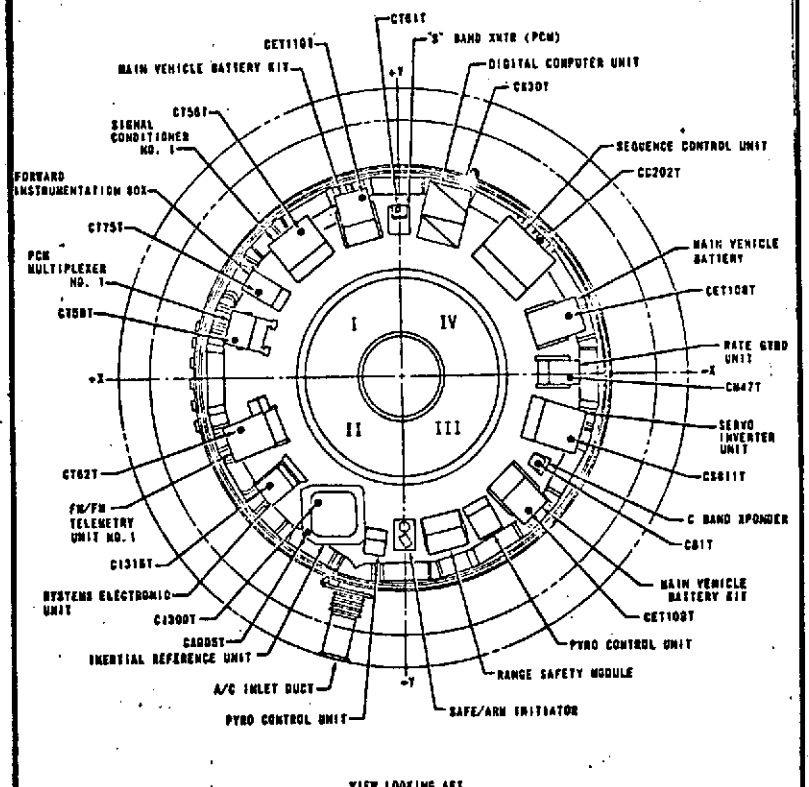

CENTAUR Forward Equipment Module

FIGURE VII-2-1a CENTAUR FORWARD AREA TEMPERATURE MEASUREMENTS

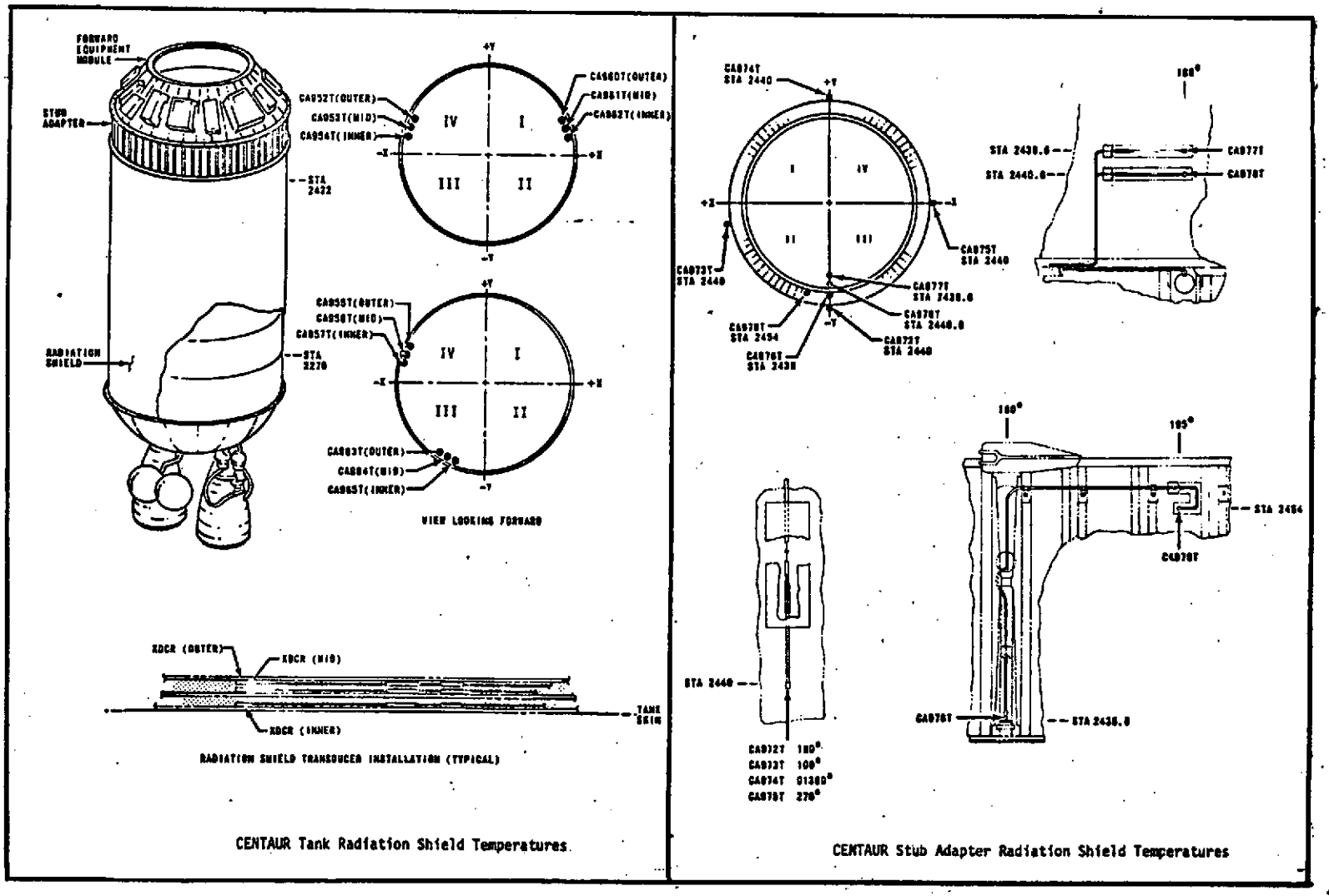

FIGURE VII-2-1b CENTAUR LH_2 TANK AND STUB ADAPTER RADIATION SHIELDING TEMPERATURE LOCATIONS

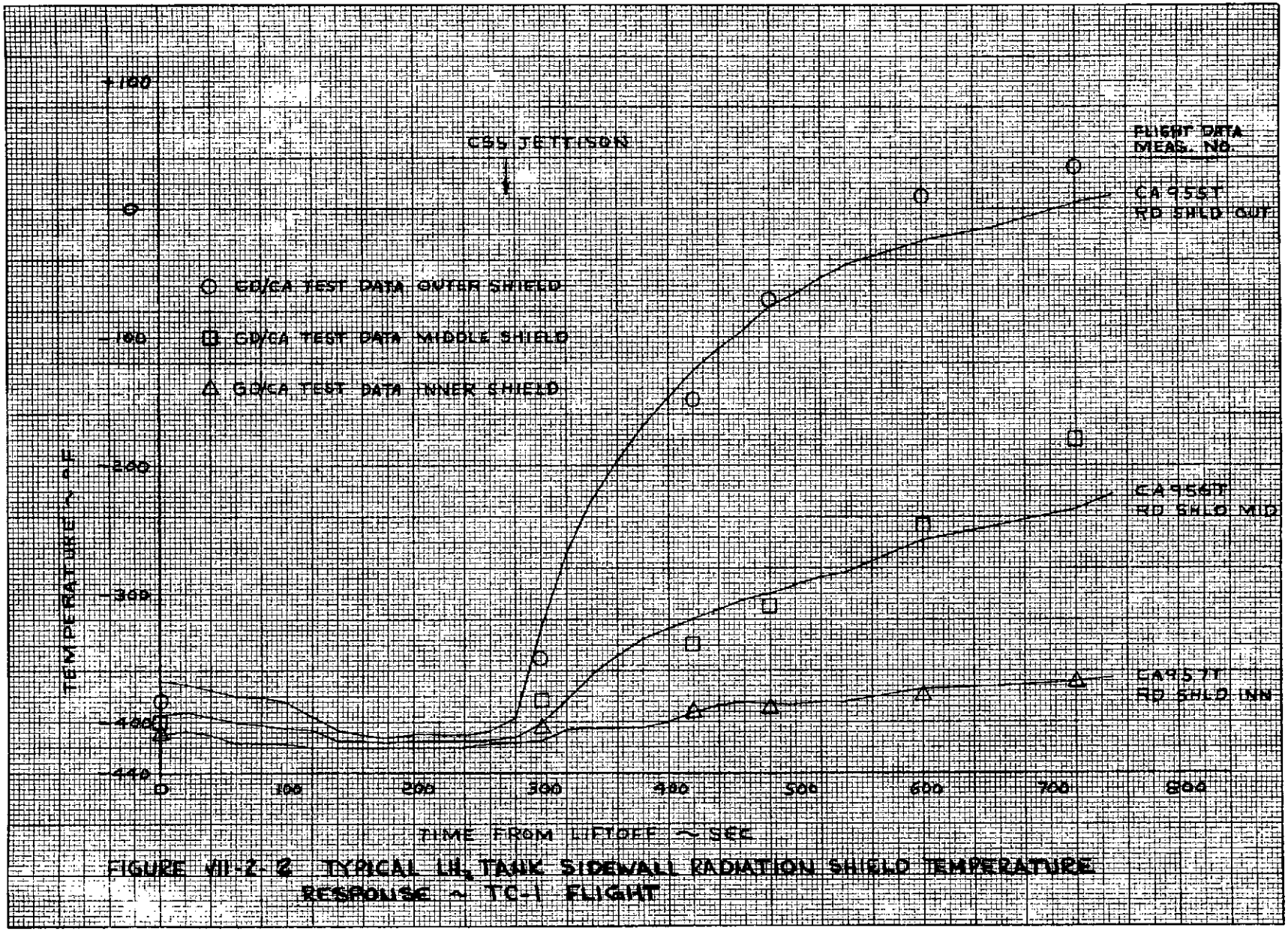

FIGURE VII-2-2 TYPICAL LH_2 TANK SIDEWALL RADIATION SHIELD TEMPERATURE RESPONSE ~ TC-1 FLIGHT

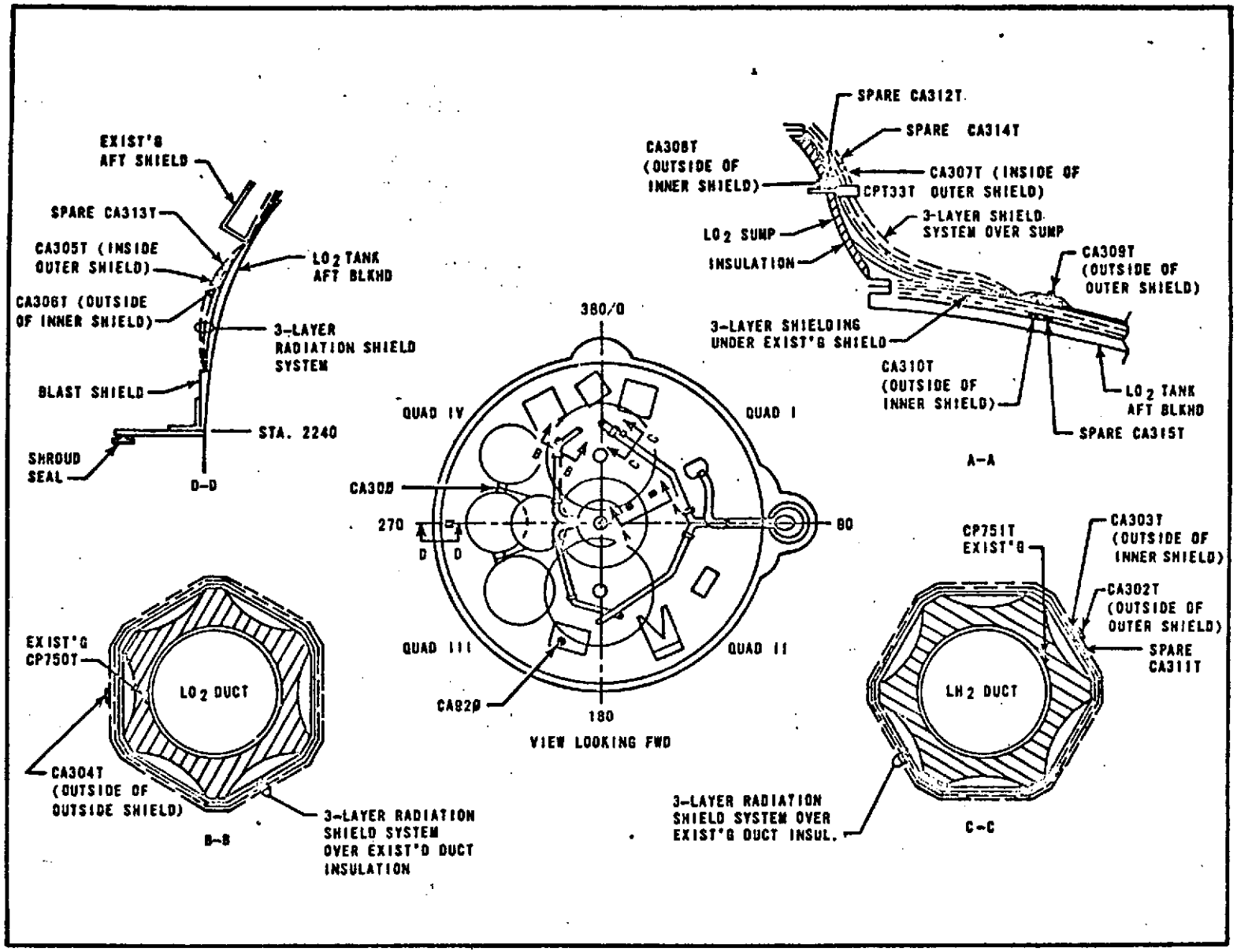

FIGURE VII-2-3a CENTAUR THRUST SECTION RADIATION SHIELD TEMPERATURES

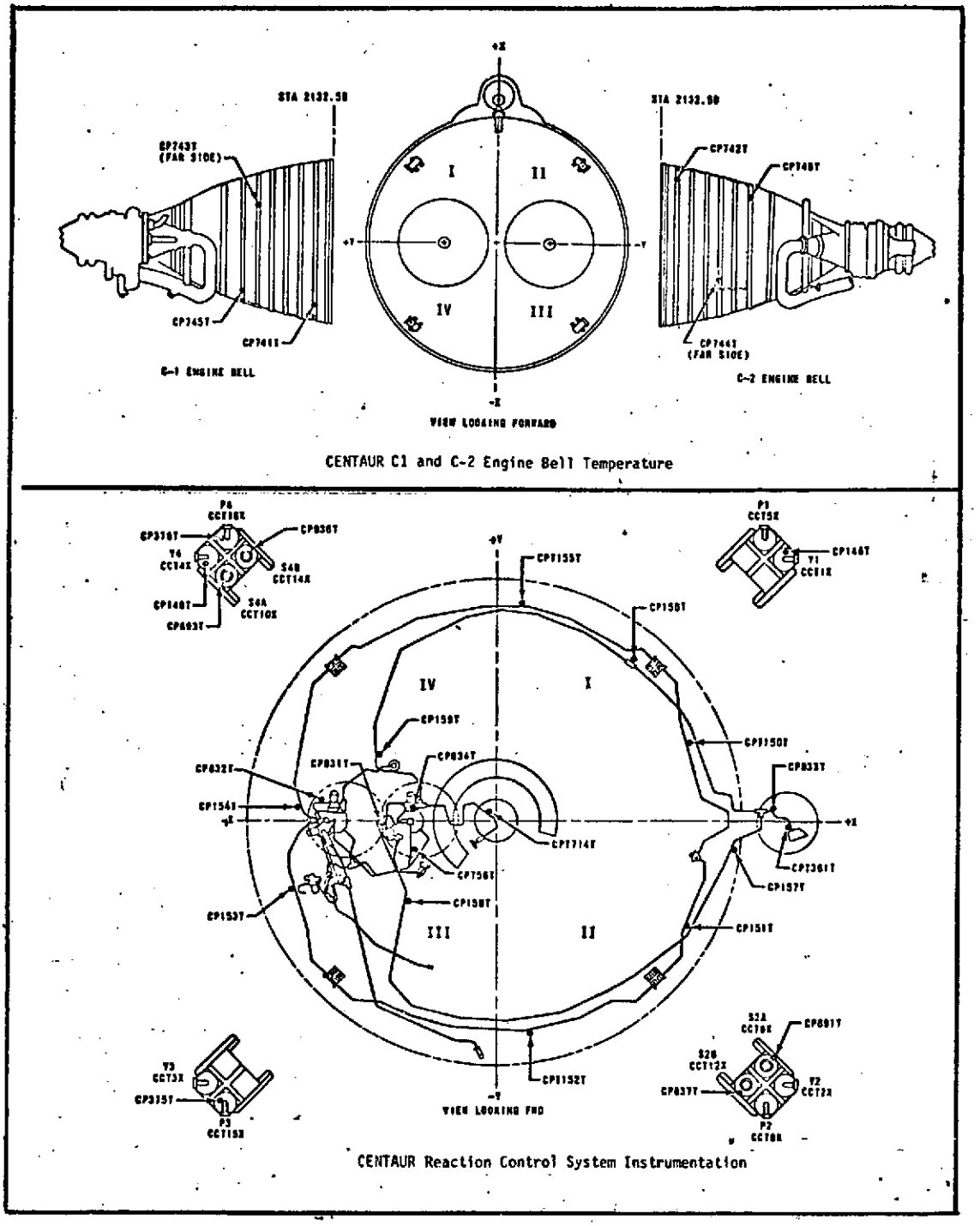

FIGURE VII-2-3b CENTAUR ENGINE BELL AND REACTION CONTROL SYSTEM INSTRUMENTATION

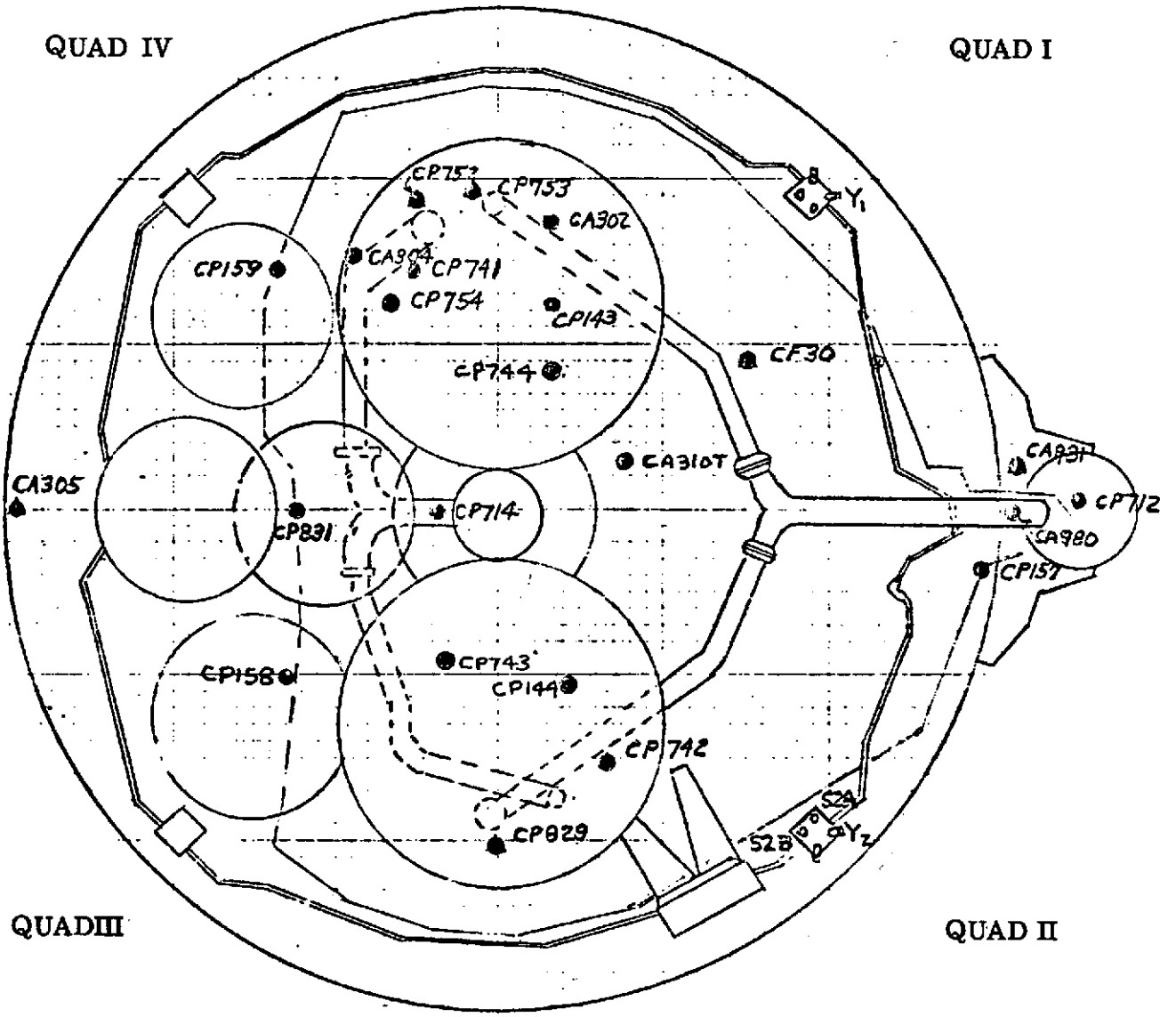

VIEW LOOKING FORWARD

FIGURE VII-2-4 CENTAUR AFT END TEMPERATURE MEASUREMENTS WHICH RESPONDED TO H_2O_2 ENGINE FIRING IMPINGEMENT HEATING

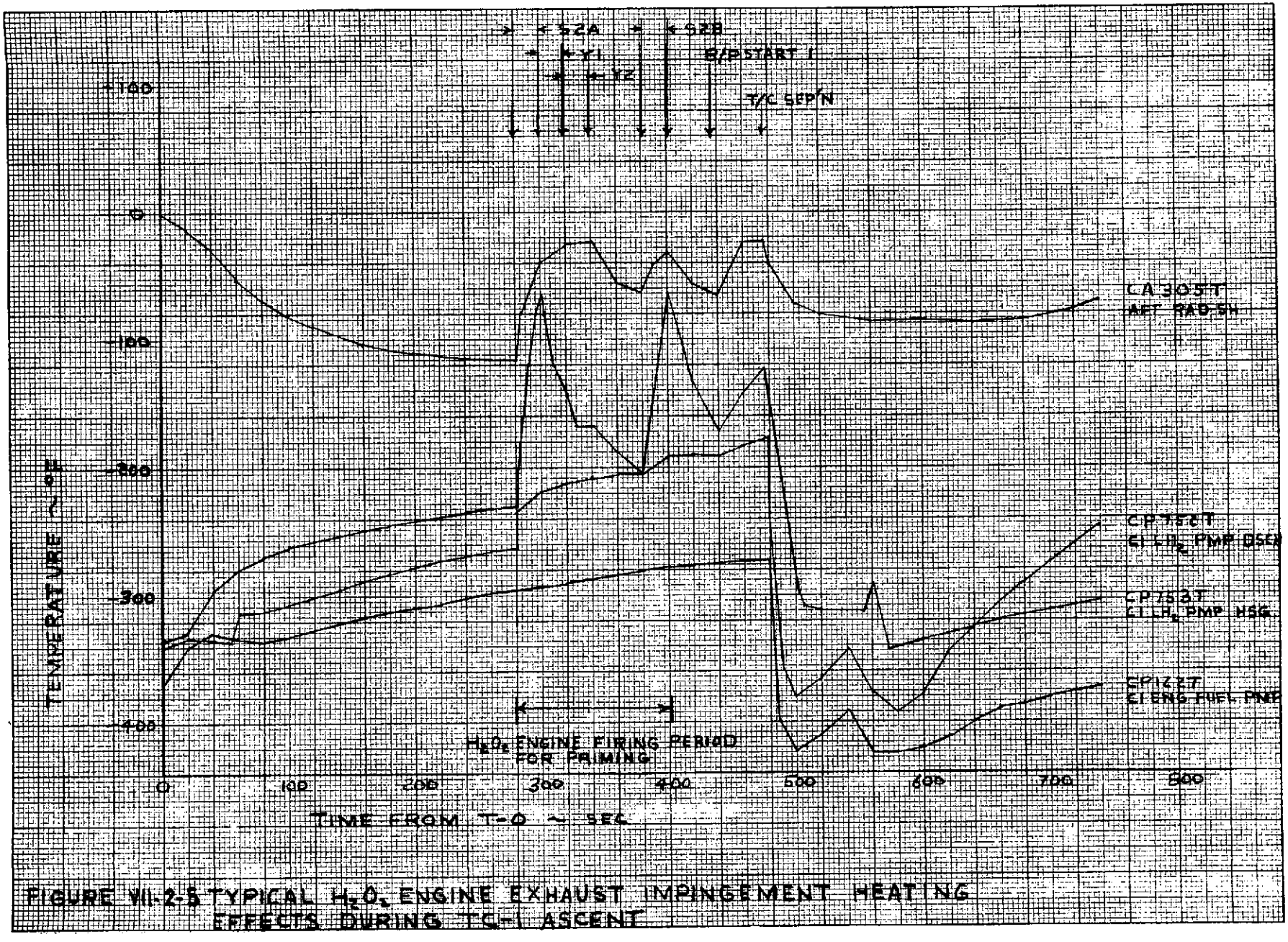

FIGURE VII-2-5 TYPICAL H_2O_2 ENGINE EXHAUST IMPINGEMENT HEATING EFFECTS DURING TC-1 ASCENT

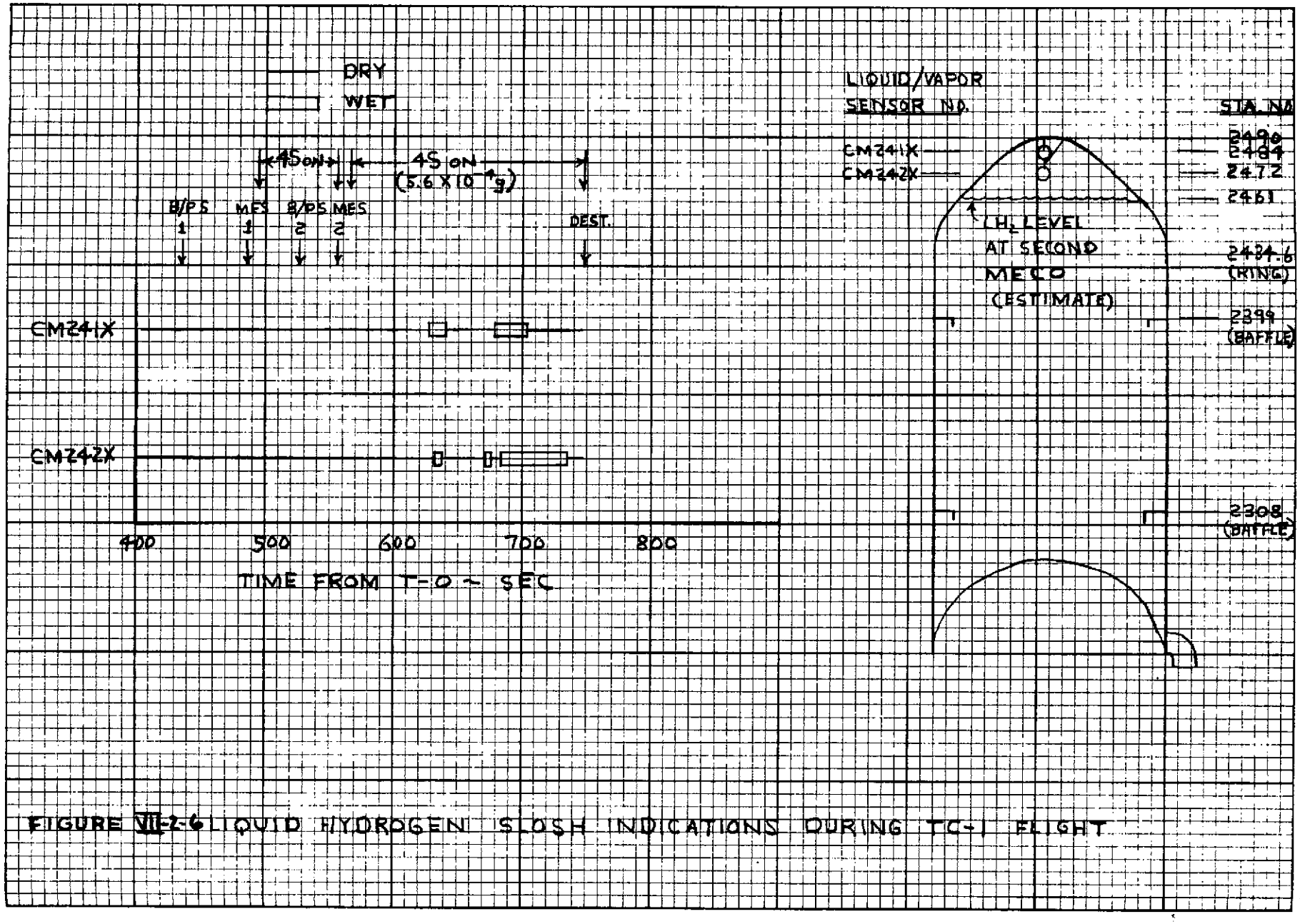

FIGURE VII-2-6 LIQUID HYDROGEN SLOSH INDICATIONS DURING TC-1 FLIGHT

VII-3. ELECTRICAL/ELECTRONIC SYSTEMS

VII-3A. Centaur Electrical Power System

by J. B. Nechvatal

Summary

The performance of the Centaur electrical system was satisfactory throughout all phases of flight. Vehicle battery bus voltages at liftoff were satisfactory. Current profiles measured were consistent with levels and profiles recorded during preflight tests.

System Description

The electrical power system as shown in figure VII-3A-1 consists of a power changeover switch (integral part of the sequence control unit), three main batteries (interconnected by a diode assembly), two independent range safety command (vehicle destruct) batteries, and a single 400 hertz inverter (the inverter is an integral part of the servo inverter unit).

Flight Performance

The performance of the Centaur electrical system was satisfactory until vehicle destruct was initiated. There were no unexpected system current demands noted during the programmed flight period. Transfer of the electrical load from external power to the internal batteries was accomplished at -116.5 seconds by the changeover switch and normal transfer characteristics were observed.

The three Centaur buses were supplied by separate 150 ampere-hour batteries, interconnected by a diode assembly. The diode assembly permitted bus number 2 battery to supply bus number 1 and bus number 3 power during surge loads and at depletion of capacity of bus number 1 and/or bus number 3 battery during the long proposed flight sequence. (Bus number 2 battery has the lowest programmed power drain.)

At liftoff the three (3) main battery bus voltages were 28.6, 28.9, and 28.6 volts for buses number 1, 2, and 3 batteries, respectively. (Battery data shown in table VII-3A-I.) Bus number 1 battery voltage was constant throughout the flight. Bus number 2 battery voltages reflected some of the bus number 3 flight current demands, but remained fairly constant up to vehicle destruct. Bus number 3 battery voltage reflected normal level changes resulting from the application and removal of electromechanical loads per the programmed sequence. A low of 27.4 volts was observed during main engine start sequence numbers 1 and 2 (a period of maximum load).

The total Centaur current (as measured by CE1C) was 46.5 amperes at liftoff as shown in table VII-3A-II. Peaks of 65.2 amperes at main engine first start sequence and 64.5 amperes at main engine restart sequence were recorded. The flight current profile was consistent with values recorded during preflight tests and no anomalies were observed. Battery current values with respect to flight programmed events is shown in table VII-3A-III.

The individual bus currents exhibited normal profiles. Bus number 1 remained steady between 9.6 and 10.0 amperes, exhibiting only the expected variations due to the DCU duty cycle and real time interrupts. Bus number 2 current was steady at 7.7 amperes with the exception of the period of P.U. control. Variations between 6.6 and 7.7 were noted during this time interval, which was nominal and as expected. Bus number 3 current exhibited changes throughout the flight in response to vehicle demands. The maximum current observed was 39.5 amperes at main engine first start attempt sequence.

Two individual electronic package currents (IMG and SCU) were monitored via telemetry. The IMG (Inertial Measuring Group) currently exhibited low level oscillation (as expected) following platform stabilization (prelaunch function). The load current varied between 6.6 and 7.1 amperes. The SCU (Sequence Control Unit) current also exhibited a normal output with a steady state load of 0.18 amperes and a strobe current of 0.88 amperes. The IMG and SCU are supplied by the bus number 1 battery and are part of the total bus number 1 load.

Performance of the two range safety command batteries was satisfactory. The voltages at liftoff were 32.2 volts for range safety command number 1 and 32.4 volts for range safety command number 2. Voltages remained steady throughout the flight until vehicle destruct was initiated. (See Range Safety Command System for detailed system performance.)

Vehicle a.c. power was supplied by the servo inverter unit. The voltage output of the inverter remained steady at 25.9 volts a.c. throughout the programmed flight as given in table VII-3A-2.

TABLE VII-3A-1. - CENTAUR BATTERY DATA

	Open circuit, V	T - 0 Lift-off, V	Load test amps against volts
Main battery, bus number 1	35.1	28.6	64 A at 27.2 V
Main battery, bus number 2	35.0	28.9	64 A at 27.5 V
Main battery, bus number 3	35.1	28.6	64 A at 27.3 V
RSC number 1 battery	33.7	32.2	10 A at 27.3 V
RSC number 2 battery	33.8	32.4	10 A at 27.5 V

TABLE VII-3A-2. - CENTAUR ELECTRICAL SYSTEM DATA

Measured number	Description	Units	T - 0	Stage number 1 shutdown	Shroud separation	Stage number 2 shutdown	MES	MECO	MES 2nd attempt	MECO	RSC destruct
CE1C	Centaur total load	Amps	46.5	44.5	43.5	58.3	65.2	53.3	64.5	50.7	48.5
CE142C	Bus number 1 current	Amps	10.0	10	10	10	10	10	10	10	10
CE143C	Bus number 2 current	Amps	7.7	7.7	7.7	7.7	7.7	7.7	7.7	7.7	7.7
CE144C	Bus number 3 current	Amps	14.0	12.0	12.1	21.5	24.4	16.5	24.0	16.5	16.4
CE97C	Bus number 3 partial current	Amps	5.0	5.0	4.2	5.8	4.9	4.4	4.9	4.4	3.9
CE28V	Bus number 1 voltage	VDC	28.5	28.3	28.3	28.2	28.1	28.2	28.2	28.2	28.3
CE600V	Bus number 1 battery voltage	VDC	28.6	28.4	28.4	28.1	28.1	28.2	28.2	28.2	28.3
CE609V	Bus number 2 battery voltage	VDC	28.9	28.9	28.9	28.6	28.4	28.7	28.4	28.9	28.9
CE610V	Bus number 3 battery voltage	VDC	28.6	28.6	28.8	27.8	27.4	27.8	27.4	28.1	28.2
CS844V	Inverter output voltage	VAC	25.9	25.9	25.9	25.9	25.9	25.9	25.9	25.9	25.9

TABLE VII-3A-3

TC-1 CURRENT PROFILE - CENTAUR

EVENT	TOTAL CURRENT MEAS. CEIC BEFORE	TOTAL CURRENT MEAS. CEIC AFTER	DELTA CURRENT LEVEL CHANGE ACTUAL	DELTA CURRENT LEVEL CHANGE EXPECTED	TIME (REF. TO LIFT-OFF) - SECONDS
T-0 (LIFT-OFF)	46.5	46.5	—	—	T-0
UNLOCK LH_2 VENT VALVE	46.3	44.5	-1.8	1.5/2.0	T+89.8
SEP. FWD. BRG. REACTOR	44.5	44.75	+0.25	0.2/0.3	T+99.9
SEP. FWD. BRG. REACTOR RST.	44.75	44.50	-0.25	0.2/0.3	T+101.9
FORWARD SEAL RELEASE	44.5	44.75	+0.25	0.2/0.3	T+215.0
FORWARD SEAL RELEASE RST.	44.75	44.5	-0.25	0.2/0.3	T+218.0
UNLATCH SHROUD & RF SW. DISC.	44.3	43.5	-0.8	0.7/1.0	T+274.0
UNLATCH SHROUD RESET	43.5	43.25	-0.25	0.2/0.3	T+275.5
H_2O_2 ENGINE - S2A ON	43.0	43.5	+0.50	0.45/0.5	T+278.9
S2A OFF; Y1 ON	43.5	43.5	0	0	T+298.9
Y1 ON, Y2 ON	43.5	43.5	0	0	T+318.9
Y2 OFF	43.5	43.0	-0.50	0.45/0.5	T+338.9
S2B ON	43.0	43.5	+0.50	0.45/0.5	T+381.9
S2B OFF	43.5	43.0	-0.50	0.45/0.5	T+401.9
LOCK ALL VENT VALVES (3)	43.0	49.0	+6.0	5.5/6.5	T+435.5
BOOST PUMP B/U & PRIMARY FEED VALVES ON; H_2O_2 PURGE VALVE ON; CONTROL VALVE ON; & PRESSURIZE LH_2 & LO_2 TANKS	49.0	55.0	+6.0	5.1/6.3	T+437.5
END LO_2 TANK PRESSURE	55.0	54.2	-0.8	0.7/0.9	T+438.4
END LH_2 TANK PRESSURE	54.2	53.5	-0.8	0.7/0.9	T+439.4
HYDRAULIC CIRC. PUMPS ON	53.3	58.3	+5.0	4.8/5.2	T+469.5
SLOW PU ZERO COMMAND	57.8	56.7	-1.1	0.8/1.2	T+475.4
PRESTART VALVES ON	56.5	59.2	+2.7	2.5/3.0	T+477.6
PU S/P_2 CCW OFF	59.2	59.7	+0.5	0.3/0.6	T+480.6
PU S/P_1 CCW OFF	59.7	60.2	+0.5	0.3/0.6	T+481.6
CONTROL VALVE OFF	59.8	59.0	-0.8	0.7/0.9	T+485.4
START VALVES & IGNITERS ON	59.0	65.2	+6.2	5.9/6.7	T+485.6
IGNITERS OFF	65.0	61.5	-3.5	3.4/3.7	T+489.6
MECO: PRESTART AND START VALVES OFF; BOOST PUMP PRIMARY & B/U FEED VALVES OFF; H_2O_2 PURGE VALVE OFF; PU S/P_1 & S/P_2 CW ON; H_2O_2 ENGINES ON. (4 ENGINES)	61.5	53.3	-8.2	7.0/8.8	T+495.9
H_2O_2 ENGINES ON (4 ENGINES)	53.3	55.2	+1.9	1.8/2.0	T+496.1
PU S/P_1 CW & S/P_2 CW OFF	55.2	56.2	+1.0	0.8/1.2	T+496.8
CONTROL VALVE ON; ENABLE LH_2 & LO_2 TANK PRESSURIZATION	55.0	57.3	+2.3	2.1/2.7	T+518
BOOST PUMP PRIMARY & B/U FEED VALVES ON; & H_2O_2 PURGE VALVE ON.	56.5	59.7	+3.2	3.0/3.6	T+528
PRESTART VALVES ON	58.0	60.8	+2.8	2.5/3.0	T+548
CONTROL VALVE AND H_2O_2 ENGINES OFF (4 ENGINES)	60.5	58.2	+2.7	2.3/2.9	T+555.7
MES: IGNITERS & START VALVES ON	58.2	64.5	+6.3	5.9/6.7	T+555.9
IGNITERS OFF	64.2	60.7	-3.5	3.4/3.7	T+559.9
HYDRAULIC CIRC. PUMPS OFF	60.5	55.5	-5.0	4.8/5.2	T+566.9
MECO: PRESTART AND START VALVES OFF; BOOST PUMPS PRIMARY & B/U FEED VALVES OFF; H_2O_2 PURGE VALVE OFF & H_2O_2 ENGINES ON (8 ENGINES)	55.5	50.7	-4.8	4.4/5.6	T+567.1
DATA PRIOR TO RSC DESTRUCT	48.5	48.5	0	0	T+748.4

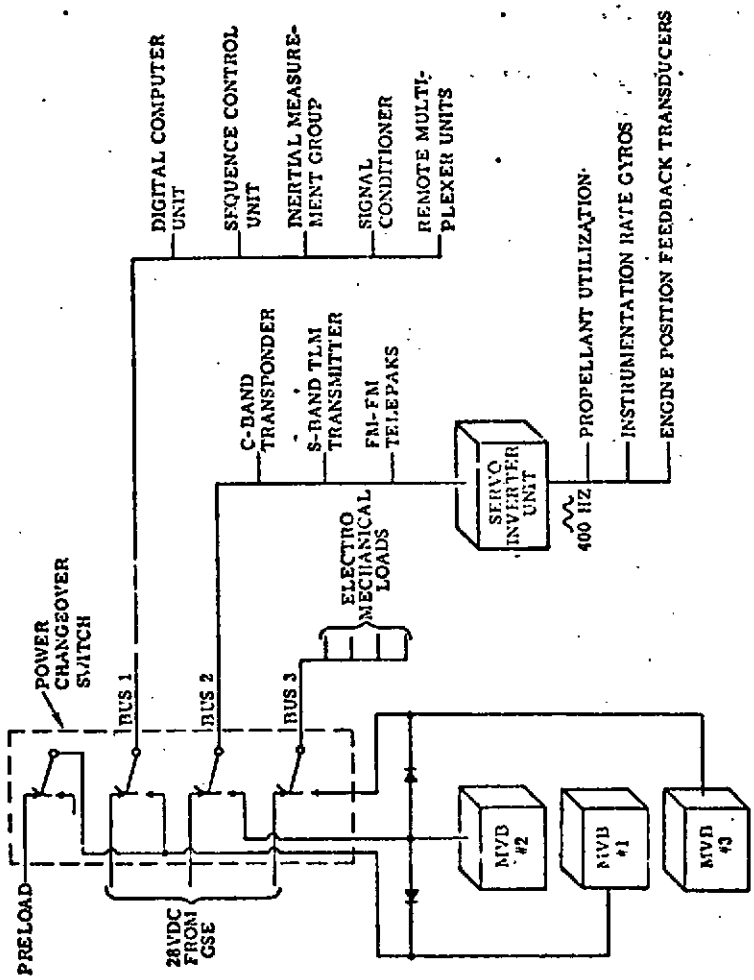

Figure VII-3A-1 Electrical power system (three-battery configuration).

VII-3B. Inertial Measurement Group

by P. W. Kuebelar

Summary

The Inertial Measurement Group (IMG) performance during the flight was satisfactory as evidenced by the accuracy of the trajectory, which is described in the Trajectory and Performance Section, and the telemetered data which is considered here.

System Description

The Inertial Measurement Group (IMG) consists of two packages: an Inertial Reference Unit (IRU) and a System Electronics Unit (SEU). The IRU consists of a vibration isolated four gimbal platform section and a hard-mounted electronics section. The four gimbals provide rotational motion isolation of the stable element for all vehicle attitudes. Three single-degree-of-freedom rate integrating gyros mounted in the stable element provide the references by which the stable element is maintained in a fixed orientation relative to inertial space. Three single-axis hinged-pendulum pulse-rebalanced accelerometers are orthogonally mounted in the stable element. The accelerometers and associated electronics measure thrust acceleration components along their respective input axes and provide incremental velocity information based on this measurement to the navigation equations in the Digital Computer Unit.

Another function, independent of measuring vehicle acceleration, is provided by resolvers installed between the gimbals. These resolvers are electrically connected so that electrical signals representing inertial referenced steering vectors generated by the guidance equations are transformed into steering commands (referenced to vehicle axes) to control engine thrust direction. The IRU also contains a crystal-controlled time standard which provides the real-time reference to the navigation equations. The SEU provides power line filtering, power supply outputs, and control circuitry for the IRU.

Flight Performance

The IMG transformed the desired vehicle pointing vectors into pitch, yaw, and roll steering commands to the vehicle autopilot. Maximum attitude errors in pitch, yaw, and roll were 3.1°, 2.9°, and 4.8°, respectively.

Gimbal loop performance was satisfactory. The stable element was maintained within 8 arcseconds of the gyro reference positions. The dynamic accuracy specification is 60 arcseconds.

At T + 268.4 seconds vehicle acceleration as computed from IMG accelerometer data was 3.54 g which compares with 3.6 g as measured by the vehicle axial accelerometer.

IMG current was normal throughout the flight. The SEU and IRU temperatures were 67° and 81° at lift-off and 65° and 85° at the end of the flight, respectively.

VII-3C. Flight Control Systems

by D. Bitler, R. Edkin, and E. Procasky

Summary

The Centaur flight control system performance was satisfactory throughout all phases of flight. Ten seconds after main engine start (MES) the Digital Computer Unit (DCU) computed the acceleration level to verify whether or not the engines started. The calculated acceleration was less than 0.19 g, and the software then assumed that the engines did not start. The DCU sequencer then went through a restart sequence which resulted in a second MES 60 seconds after the acceleration test. Ten seconds after the second MES attempt, the DCU again calculated the acceleration level to verify whether or not the engines started. The calculated acceleration was less than 0.19 g, and the software treated this second MES failure as a normal MECO and continued the flight program. The TC-1 flight was terminated at approximately 748 seconds after liftoff when the range safety transmitter issued the inflight destruct command.

System Description

The D-1T Centaur flight control system provides vehicle attitude stabilization and points the vehicle in response to guidance steering vectors. The sequencing system provides the discrete switching required by the vehicle. Elements which perform functions for these systems are:

Digital Computer Unit (DCU)
Inertial Reference Unit (IRU)
Sequence Control Unit (SCU)
Servo Inverter Unit (SIU)
Vehicle Main Engines
Reaction Motors

A block diagram of the flight control and sequencing system is shown in figure VII-3C-1.

To accomplish pointing and stabilization two guidance steering vectors (pitch axis command and roll axis command) in inertial coordinates are generated in the DCU, converted to a.c. analog voltages, and output to the IRU. The IRU "resolves" these vectors from inertial to vehicle coordinates. The outputs of the IRU now represent vehicle pitch, yaw, and roll attitude errors. The DCU digitizes these errors and converts them to engine commands.

During Centaur powered flight pointing and stabilization control torques are provided through the gimballing of the main engines. The DCU converts the computed engine commands to d.c. analog voltages which are

output to the SIU as pitch, yaw/-roll and yaw/+roll servo commands. In the SIU the servo commands are summed with the main engine feedback signals and the resultant "error" signals are fed to servo amplifiers for conditioning to be input to the main engine servo actuator valves. Current to these valves results in engine gimballing.

During Centaur coast, pointing, and stabilization control torques are provided by the "firing" of the reaction motors. Motor "firing" commands are transmitted from the DCU to the SCU via discrete output register. The output of this register is a 22 bit binary word + a strobe. The SCU decodes the words and actuates the proper relay(s) upon receipt of the strobe. The relays in the SCU control the solenoid valves in the hydrogen peroxide lines to the reaction motors. The DCU contains the logic which determine which motors are to be fired and the length of time they are fired.

The sequencing system provides all discretes required by the vehicle. The DCU determines the time an event should occur, transmits the command to the SCU via the discrete output register, and the appropriate relay(s) are actuated to provide the power.

The Centaur also provides the Titan with torquing commands and discretes via SCU relays. Titan power is routed through contacts of SCU relay(s). Torquing commands are sent to the Titan to provide pitch and yaw wind bias programs and the roll to azimuth shortly after lift-off during stage "0" and pitch and yaw closed loop steering commands during Stages I and II. The discretes provided are Centaur Standard Shroud Separation (and backup), Stage II engine shutdown and Titan/Centaur separation.

Flight Performance

The flight control and sequencing systems performed satisfactorily throughout the flight. All discretes, steering, and attitude maneuvering vectors, Titan wind bias and closed loop steering commands were properly generated. The flight control system responded satisfactorily to all commands except during main engine start and restart period when engine thrust level and hydraulic pressure were very low due to the failure of the main engines to start. Even though response time was severely degraded, vehicle attitude control was maintained through these 10-second periods. At the end of each start attempt, coast phase control was activated and vehicle attitude and pointing were properly controlled. The Digital Computer Unit and the Inertial Measrurment Group continued to operate after "destruct" until LOS. Evaluation of the powered and coast auto-pilot performance is contained in the Dynamics section of this report.

The sequencing system correctly generated and issued the vehicle discretes up until "destruct." Sequencing properly cycled throughout a restart sequence. Upon failure of the restart attempt, the sequencing system advanced to the first coast phase of flight until destruct.

TC-1 Flight Sequence of Events

The TC-1 flight sequence of events is presented in table VII-3C-I. This table shows the flight sequence of events issued by the Sequence Control Unit (SCU) to other vehicle systems. The SCU receives its input from the DCU and converts this input into commands usable by other vehicle systems. Other functions programmed by the DCU software are shown in the table to help in clarifying the flight sequence. The SCU commands were issued at the expected times and for the expected duration of time. The table also shows the planned time for "BEGIN DCU PITCH/YAW STEERING PROGRAM" as T + 10 seconds after lift-off. The actual time this event took place was at T + 11.0 seconds. This actual time is not late. The time for the DCU to issue the pitch/yaw steering command is dependent on two conditions taking place. The first condition is that the software must issue an enable at 10 seconds after lift-off. The second condition is that the Titan/Centaur must attain an altitude of 1050 feet before this steering command is issued. The Titan/Centaur had not attained this altitude when the enable was received. Thus, the command was not issued until the Titan/Centaur attained the required altitude at T + 11.0 seconds.

Table VII-3C-I uses as its GMT time base the "GO INERTIAL" SCU switch response to the DCU "GO INERTIAL" command. This time is 6 seconds prior to lift-off and 25 seconds after the Control Monitor Group (CMG) sends a signal to start the DCU count. The column headed "Sequence" in the table shows the time of the event from the start of each phase of flight. The column headed "Planned Time" shows the seconds after lift-off for each event based upon preflight actual launch time trajectory. The "Actual Time" column shows the seconds after lift-off that each command was issued by the SCU during flight. The "Command Source" column defines those commands for which the source is other than a timed event. If the command is timed from a phase change, the column is left blank.

TABLE VII-3C-1 TC-1 FLIGHT SEQUENCE OF EVENTS

SW	POS	EVENT	SEQUENCE	GMT	PLANNED TIME SEC	ACTUAL TIME SEC	COMMAND SOURCE
84 85 86	RS RS RS	GO INERTIAL	T-6	13:47:55.6	T-6	T-6	(1)
--	--	LIFT-OFF	T=0	13:48:01.6	T=0	T=0	(2)
59,60	S	BEGIN ROLL PROGRAM	T+6.5	13:48:08.1	T+6.5	T+6.5	
49,50	S	BEGIN DCU PITCH, YAW PROGRAM	T+10	13:48:12.6	T+10	T+11.0	
28	RS	UNLOCK LH_2 VENT VALVE	T+90	13:49:31.6	T+90	T+90	
34	S	SEP FWD BRG REACTOR	T+100	13:49:41.6	T+100	T+100	
34	RS	RESET FWD BRG REACTOR	T+102	13:49:43.5	T+102	T+101.9	
--	--	STG 0 SHUTDOWN	STG 0	13:49:56.6	T+114	T+115.0	(3)
39	S	RELEASE FWD SEAL	STG 0 + 100	13:51:36.6	T+214	T+215.0	
--	--	STG 1 SHUTDOWN	STG 1	13:52:25.6	T+263	T+264.0	(4)
61	S	UNLATCH SHROUD CMD 1	STG 1 + 10	13:52:35.5	T+273	T+273.9	
62	S	UNLATCH SHROUD CMD 2	STG 1 + 10.5	13:52:36.0	T+273.5	T+274.4	

S - SET
RS - RESET

(1) PHASE 1 OCCURS 25 SECONDS AFTER THE CONTROL MONITOR GROUP SENDS A SIGNAL TO START THE DCU COUNT.

(2) PHASE 2 NOTED BY DCU WHEN OBSERVED ACCELERATION IS GREATER THAN 1.4 g.

(3) PHASE 3 NOTED BY DCU WHEN OBSERVED ACCELERATION IS LESS THAN 1.5 g.

(4) PHASE 4 NOTED BY DCU WHEN OBSERVED ACCELERATION IS LESS THAN 1.5 g.

TABLE VII-3C-1 TC-1 FLIGHT SEQUENCE OF EVENTS

SW	POS	EVENT	SEQUENCE	GMT	PLANNED TIME SEC	ACTUAL TIME SEC	COMMAND SOURCE
8	S	S2A ON	STG 1 + 15	13:52:40.5	T+278	T+278.9	
8	RS	S2A OFF	STG 1 + 35	13:53:00.5	T+298	T+298.9	
1	S	Y1 ON	STG 1 + 35	13:53:00.5	T+298	T+298.9	
1	RS	Y1 OFF	STG 1 + 55	13:53:20.5	T+318	T+318.9	
2	S	Y2 ON	STG 1 + 55	13:53:20.5	T+318	T+318.9	
2	RS	Y2 OFF	STG 1 + 75	13:53:40.5	T+338	T+338.9	
12	S	S2B ON	STG 1 + 118	13:54:23.5	T+381	T+381.9	
12	RS	S2B OFF	STG 1 + 138	13:54:43.5	T+401	T+401.9	
24	S	LOCK LO_2 VENT VALVE	STG 1 + 171.6	13:55:17.3	T+434.6	T+435.7	
28	S	LOCK LH_2 VENT VALVE 1	STG 1 + 171.6	13:55:17.3	T+434.6	T+435.7	
31	S	LOCK LH_2 VENT VALVE 2	STG 1 + 171.6	13:55:17.3	T+434.6	T+435.7	
27	S	OPEN CONTROL VALVE	STG 1 + 173.6	13:55:19.3	T+436.6	T+437.7	
29	S	PRESS LO_2 TANK	STG 1 + 173.6	13:55:19.3	T+436.6	T+437.7	
32	S	PRESS LH_2 TANK	STG 1 + 173.6	13:55:19.3	T+436.6	T+437.7	
23	S	BOOST PUMPS ON	STG 1 + 173.7	13:55:19.3	T+436.7	T+437.7	
18	S	BOOST PUMPS ON - B/U	STG 1 + 173.7	13:55:19.3	T+436.7	T+437.7	

TABLE VII-3C-1 TC-1 FLIGHT SEQUENCE OF EVENTS

SW	POS	EVENT	SEQUENCE	GMT	PLANNED TIME SEC	ACTUAL TIME SEC	COMMAND SOURCE
--	--	STG 2 SHUTDOWN	STG 2	13:55:51.1	T+465.1	T+469.5	(5)
65	S	STG 2 S/D B/U	STG 2	13:55:51.1	T+465.1	T+469.5	
17	S	C1 CIRC PUMP ON	STG 2 + .1	13:55:51.1	T+465.2	T+469.5	
21	S	C2 CIRC PUMP ON	STG 2 + .1	13:55:51.1	T+465.2	T+469.5	
63 64	S S	T/C SEPARATION	SEP	13:55:56.9	T+471.0	T+475.3	(6)
19	S	OPEN PRESTART VALVES	SEP + 2.5	13:55:59.3	T+473.5	T+477.7	
27	RS	CLOSE CONTROL VALVE	SEP + 10.22	13:56:07.0	T+481.22	T+485.4	
29	RS	END PRESS LO_2 TANK	SEP + 10.22	13:56:07.0	T+481.22	T+485.4	
32	RS	END PRESS LH_2 TANK	SEP + 10.22	13:56:07.0	T+481.22	T+485.4	
--	--	MES	MES	13:56:07.4	T+481.5	T+485.8	(7)
22	S	IGNITERS ON	MES	13:56:07.4	T+481.5	T+485.8	
20	S	OPEN START VALVES	MES	13:56:07.4	T+481.5	T+485.8	
--	--	TEST FOR MES	MES + 10	13:56:17.6	T+491.5	T+496.0	(5R)
--	--	BEGIN MES RESTART SEQUENCE	MES + 10	13:56:17.6	T+491.5	T+496.0	

(5) PHASE 5 NOTED BY DCU WHEN OBSERVED ACCELERATION IS LESS THAN 1.0 g.
(6) PHASE 6 IS COMMANDED BY DCU WHEN OBSERVED ACCELERATION IS 0.01 g.
(7) PHASE 7 IS COMMANDED BY THE DCU BASED ON GUIDANCE COMPUTED TIME.
(5R) PHASE 5 RESTART COMMANDED WHEN ACCELERATION IS BELOW 0.19 g AND ENABLES MECO.

TABLE VII-3C-1 TC-1 FLIGHT SEQUENCE OF EVENTS

SW	POS	EVENT	SEQUENCE	GMT	PLANNED TIME SEC	ACTUAL TIME SEC	COMMAND SOURCE
--	--	MECO 1	MES + 10	13:56:17.6	T+491.5	T+496.0	
23	RS	BOOST PUMPS OFF	MES + 10	13:56:17.6	T+491.5	T+496.0	
18	RS	BOOST PUMPS B/U OFF	MES + 10	13:56:17.6	T+491.5	T+496.0	
20	RS	CLOSE START VALVES	MES + 10	13:56:17.6	T+491.5	T+496.0	
19	RS	CLOSE PRESTART VALVES	MES + 10	13:56:17.6	T+491.5	T+496.0	
8	S	S2A ON	MES + 10.1	13:56:17.7	T+491.6	T+496.1	
10	S	S4A ON	MES + 10.1	13:56:17.7	T+491.6	T+496.1	
14	S	S4B ON	MES + 10.1	13:56:17.7	T+491.6	T+496.1	
12	S	S2B ON	MES + 10.1	13:56:17.7	T+491.6	T+496.1	
68 72	RS RS	SP 1 PU SWITCHES OFF	MES + 10.9	13:56:18.6	T+492.4	T+497.0	
76 80	RS RS	SP 2 PU SWITCHES OFF	MES + 10.9	13:56:18.6	T+492.4	T+497.0	
--	--	PHASE 6 RESTART	MES + 11	13:56:18.7	T+492.5	T+497.1	(6R)
27	S	OPEN CONTROL VALVE	MES + 31.94	13:56:39.6	T+513.44	T+518.0	
29	S	PRESS LO_2 TANK	MES + 31.94	13:56:39.6	T+513.44	T+518.0	
32	S	PRESS LH_2 TANK	MES + 31.94	13:56:39.6	T+513.44	T+518.0	

(6R) PHASE 6 RESTART IS COMMANDED BY THE DCU 11 SECONDS AFTER MES 1.

TABLE VII-3C-1 TC-1 FLIGHT SEQ CE OF EVENTS

SW	POS	EVENT	SEQUENCE	GMT	PLANNED TIME SEC	ACTUAL TIME SEC	COMMAND SOURCE
23	S	BOOST PUMPS ON	MES + 42	13:56:49.6	T+523.5	T+528.0	
18	S	BOOST PUMPS B/U ON	MES + 42	13:56:49.6	T+523.5	T+528.0	
19	S	OPEN PRESTART VALVES	MES + 62	13:57:09.7	T+543.5	T+548.1	
1 3 2 4	RS	YAW ENGINES OFF	MES + 63	13:57:10.7	T+544.5	T+549.1	
5 15 6 16	RS	PITCH ENGINES OFF	MES + 63	13:57:10.7	T+544.5	T+549.1	
27	RS	CLOSE CONTROL VALVE	MES + 69.72	13:57:17.3	T+551.22	T+555.7	
29	RS	END PRESS LO_2 TANK	MES + 69.72	13:57:17.3	T+551.22	T+555.7	
32	RS	END PRESS LH_2 TANK	MES + 69.72	13:57:17.3	T+551.22	T+555.7	
8	RS	S2A OFF	MES + 69.8	13:57:17.3	T+551.3	T+555.7	
10	RS	S4A OFF	MES + 69.8	13:57:17.3	T+551.3	T+555.7	
12	RS	S2B OFF	MES + 69.8	13:57:17.3	T+551.3	T+555.7	
14	RS	S4B OFF	MES + 69.8	13:57:17.3	T+551.3	T+555.7	
--	--	MES RESTART	MES + 70.0	13:57:17.6	T+551.5	T+556.0	(7R)
20	S	OPEN START VALVES	RMES + 0	13:57:17.6	T+551.5	T+556.0	
22	S	IGNITERS ON	RMES + 0	13:57:17.6	T+551.5	T+556.0	
--	--	MES RESTART TEST	RMES + 10.00	--	T+561.5	--	
17	RS	C1 CIRC PUMP OFF	RMES + 10.060	13:57:28.6	T+561.56	T+567.0	
21	RS	C2 CIRC PUMP OFF	RMES + 10.060	13:57:28.6	T+561.56	T+567.0	

(7R) PHASE 7 RESTART IS COMMANDED BY THE DCU 70 SECONDS AFTER MES 1.

TABLE VII-3C-1 TC-1 FLIGHT SEQUENCE OF EVENTS

SW	POS	EVENT	SEQUENCE	GMT	PLANNED TIME SEC	ACTUAL TIME SEC	COMMAND SOURCE
1 5 2 6 3 15 4 16	S	PITCH & YAW ENGINES ON	RMES + 10.12	13:57:28.7	T+561.62	T+567.1	
1 5 2 6 3 15 4 16	RS	PITCH & YAW ENGINES OFF	RMES + 10.18	13:57:28.7	T+561.68	T+567.1	
--	--	MECO 2	RMES + 10.24	13:57:28.8	T+561.74	T+567.2	(8R)
23	RS	BOOST PUMPS OFF	MECO 2 + 0	13:57:28.8	T+561.74	T+567.2	
18	RS	BOOST PUMPS B/U OFF	MECO 2 + 0	13:57:28.8	T+561.74	T+567.2	
20	RS	CLOSE START VALVES	MECO 2 + 0	13:57:28.8	T+561.74	T+567.2	
19	RS	CLOSE PRESTART VALVES	MECO 2 + 0	13:57:28.8	T+561.74	T+567.2	
8 12 10 14	S	S2A, S4A, S2B, S4B - ON	MECO 2 + 0.1	13:57:28.8	T+561.84	T+567.2	
--	--	DESTRUCT VEHICLE	----	14:00:30	----	T+748.4	*

(8R) PHASE 8 RESTART (MECO 2) IS COMMANDED BY THE DCU WHEN RESTART IS UNSUCCESSFUL. DCU TREATS THE RESTART FAILURE AS A NORMAL MECO AND CONTINUES THE FLIGHT PROGRAM.

* RANGE SAFETY TRANSMITTER. DESTRUCT TIME WAS DETERMINED FROM ACCELEROMETER CA 30 ø.

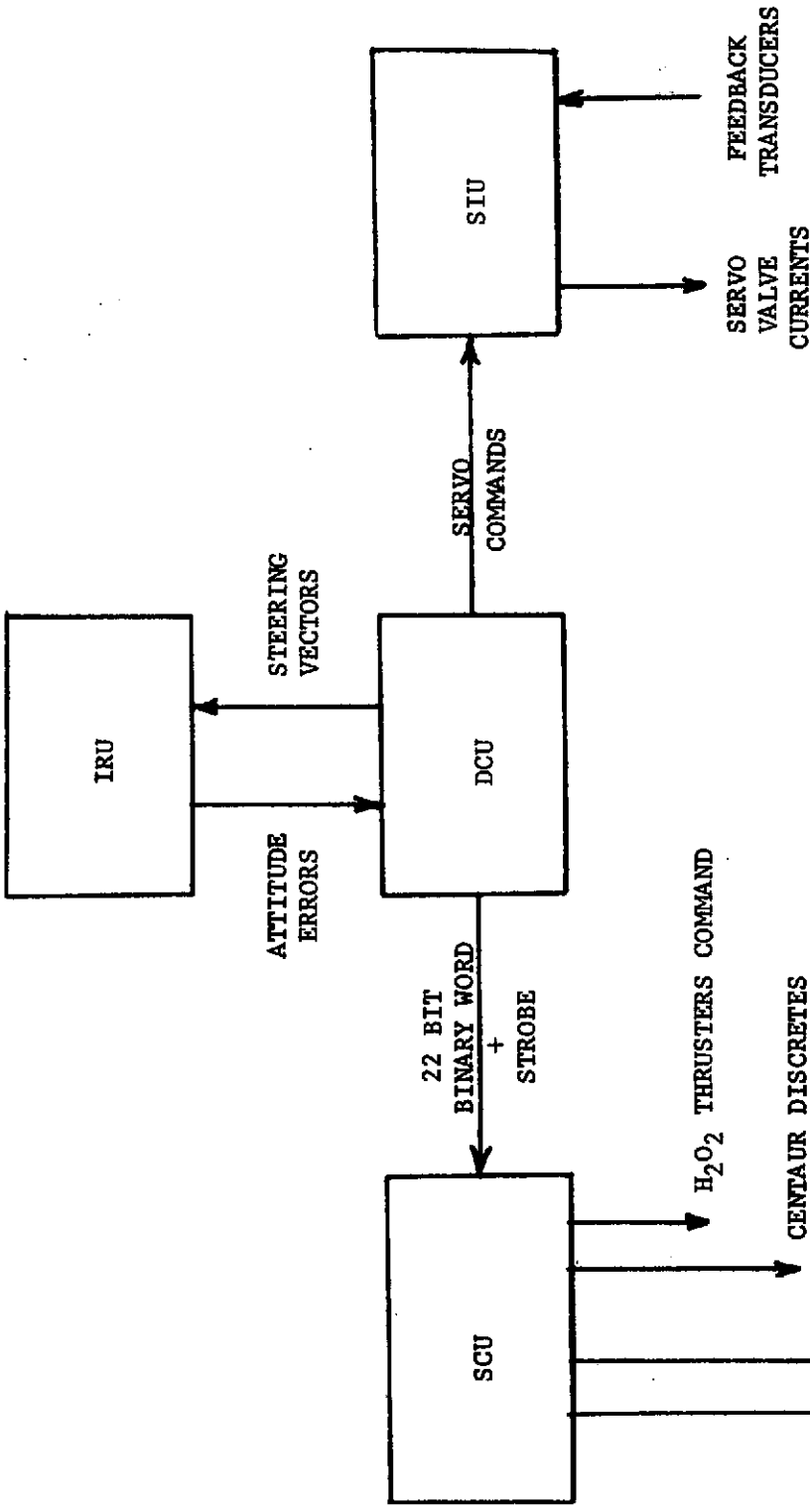

FIGURE VII-3C-1 FLIGHT CONTROL AND SEQUENCING SYSTEM - BLOCK DIAGRAM

VII-3D. Propellant Level/Propellant Utilization Systems

by R. C. Kalo

Summary

The propellant level-indicating system operated satisfactorily during the countdown. The Centaur PU system operated satisfactorily during both attempted Centaur main engine firings. The PU valves were driven to the proper fixed angles at the appropriate times.

System Description

Centaur propellant-level-indicating system. - This system utilizes three level sensors in the fuel (liquid hydrogen) tank and four level sensors in the oxidizer (liquid oxygen) tank as shown in figure VII-3D-1. The Centaur liquid propellant loading levels are determined from liquid sensors located at discrete points in the tank. The sensing elements are the hot-wire type made with platinum wire (0.001 in. diam), which has a linear resistance temperature coefficient. The sensors are applied with a near-constant current of approximately 200 milliamperes; the voltage drop across a sensor reflects the resistance value of the sensor. When uncovered, the wire has a higher resistance and therefore a high voltage drop. A control unit amplifies any change in voltage level and applies this signal to an electronic trigger circuit. When a sensor is wetted, a control relay is de-energized and a signal is sent to the propellant loading operator.

Centaur Propellant Utilization (PU) System. - The Centaur propellant utilization system, figure VII-3D-2, consists of contoured capacitance probes installed in the LH_2 and LO_2 tanks, the PU electronics incorporated in the Servo Inverter Unit (SIU), the Digital Computer Unit (DCU), the Sequence Control Unit (SCU), two engine mounted servo positioners, cables from the SIU to each capacitance probe and other related harnessing. A complete block diagram of harnessing is depicted in figure VII-3D-3. The system is used to reduce residual mass of one propellant at depletion of the other propellant. The system reduces errors caused by dispersions due to tanking, boiloff, propellant uncertainties, and engine performance uncertainties. In flight the SIU applies fixed voltages to the PU probes and receives a signal, which varies as a function of the mass of propellant in the tank. The SIU sums these signals in a bridge network and outputs and an error signal which is detected by the DCU via one of its A to D converters.

The DCU decides that a tank ratio change is necessary and commands a change in the positions of the PU valves on the engines by operating SCU switches through the normal DCU-SCU interface. The valves are motor driven and closed loop position control is provided by the DCU which receives position feedback signals through two of its A to D converters.

When the mass ratio is greater than 5 to 1, the liquid oxygen flow is increased to return the ratio to 5 to 1. When the ratio is less than 5 to 1, the liquid oxygen flow is decreased. The sensing probes do not extend to the top of the tanks, and therefore are not used for control until after the probes are uncovered, at approximately 110 seconds after Centaur main engine start. For the time period of MES + 5 seconds to MES + 110 seconds, the liquid oxygen flow control valves are maintained at predetermined fixed angles by the DCU which are independent of the PU error signal. The valves are also commanded to fixed angles 27 seconds after Centaur engine cutoff because the probes do not extend to the bottom of the tanks, and system control is lost when the liquid level depletes below the bottom of the probe. The fixed angles utilized at the end of the Centaur engine firing are based on a DCU computation of the valve angles required to minimize the residual error at MECO.

System Performance

Propellant level indicating system. - The Centaur level indicating system operated satisfactorily during the countdown. The total propellant tanked was approximately 5278 pounds of fuel (liquid hydrogen) and 25 444 pounds of liquid oxygen.

Propellant utilization system. - The Centaur PU system performance during the attempted Centaur main engine firing was satisfactory. The PU valves were positioned at null at approximately T + 482 seconds for the attempted MES1 firing at T + 486 seconds. The PU valves then moved to the fixed angles at MES1 + 5 seconds which were -6.5° for C-1 engine and -7.5° for C-2 engine. The PU system performance during the restart sequence was similar and proper.

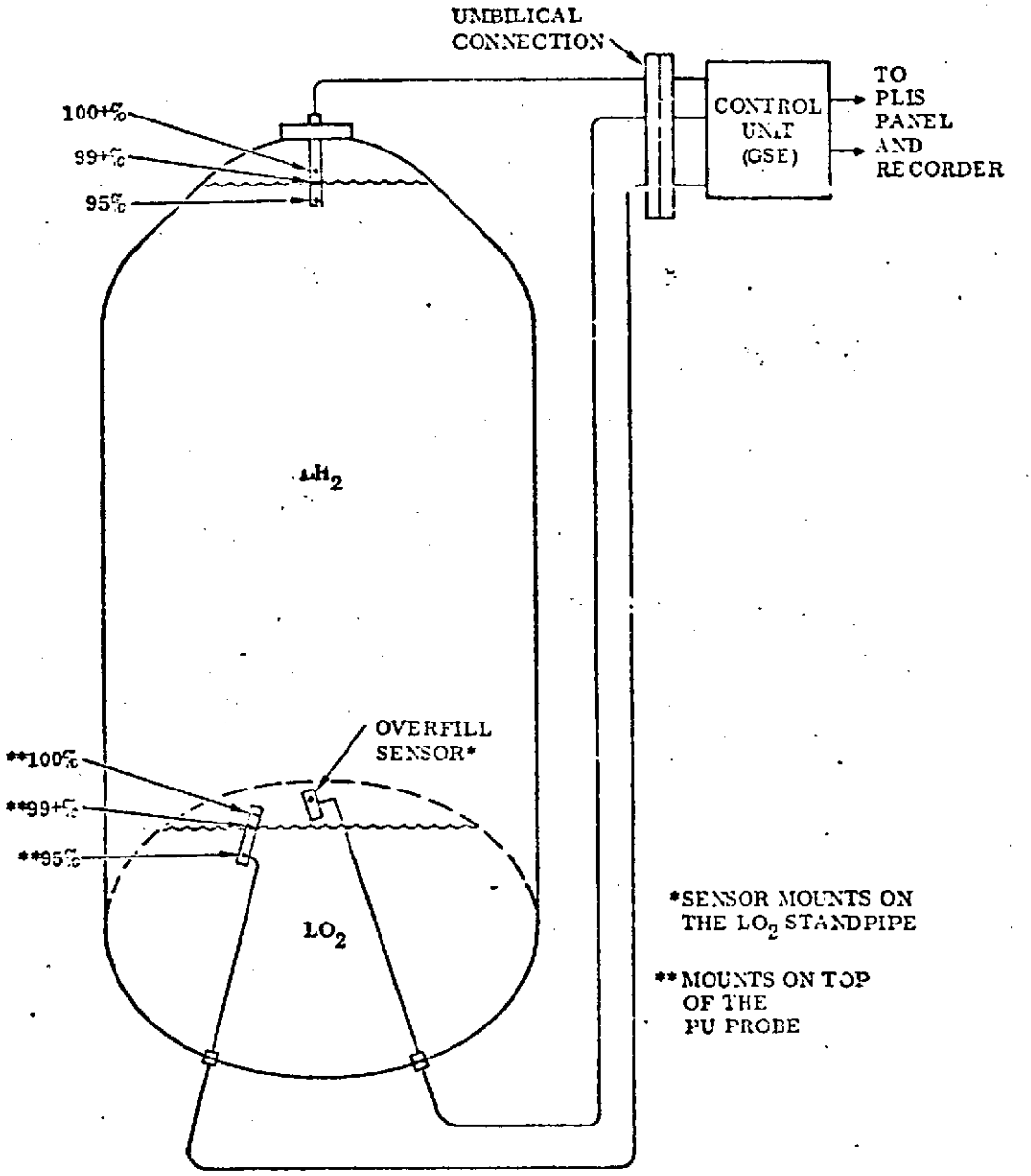

Figure VII-3D-1 Propellant Level Indicating System Schematic

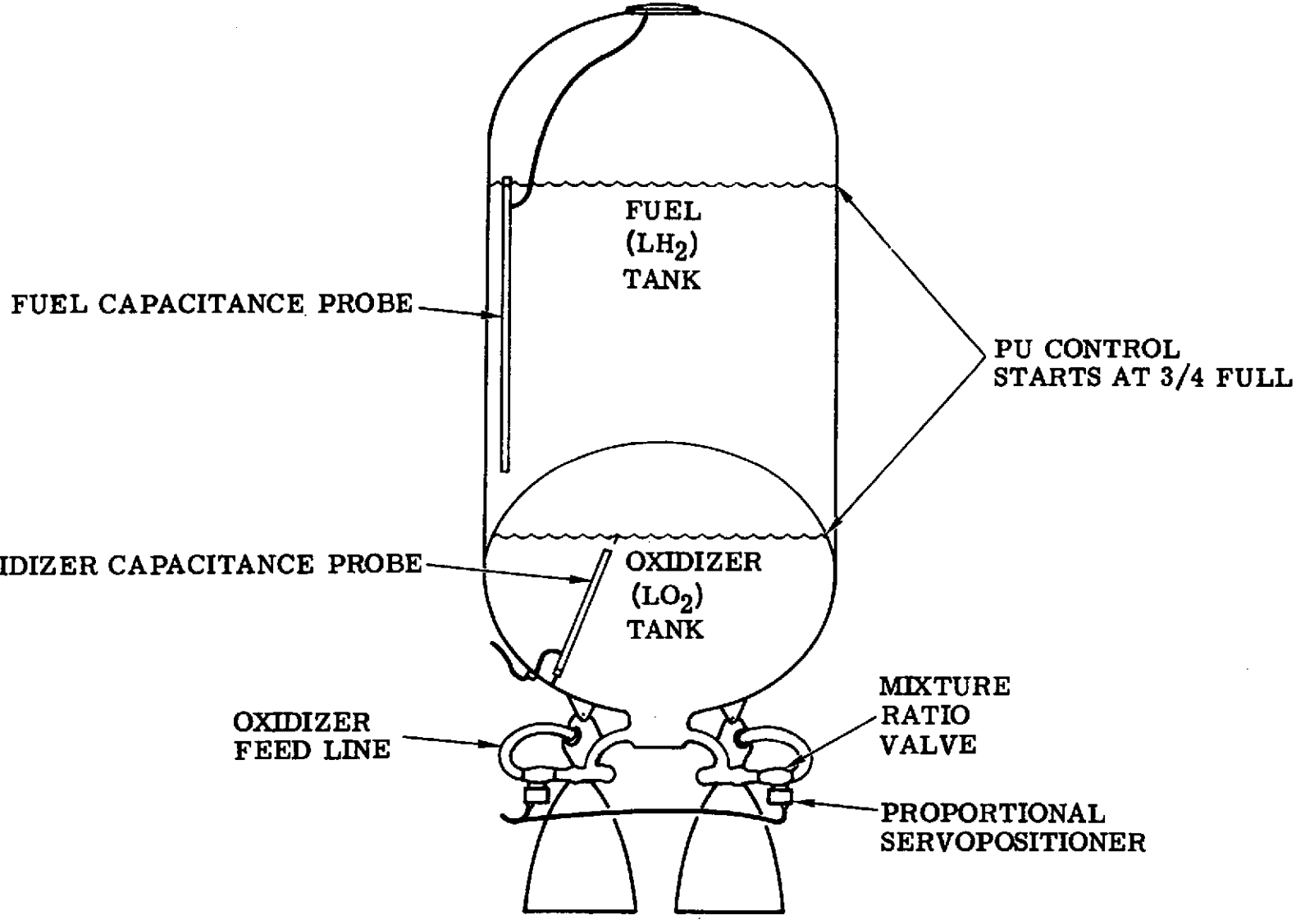

FIGURE VII-3D-2 CENTAUR PROPELLANT UTILIZATION SYSTEM MECHANICAL COMPONENTS

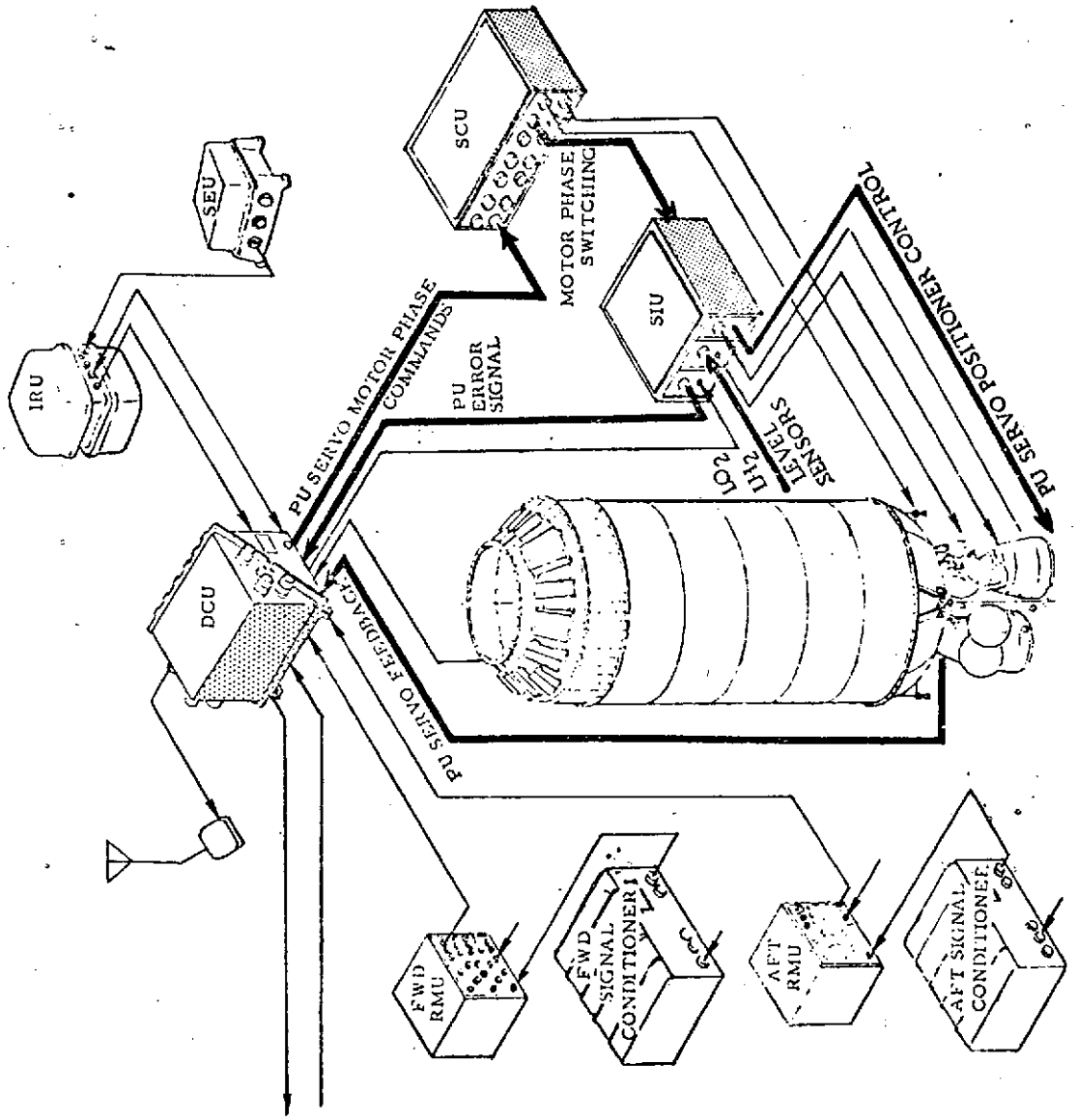

FIGURE VII-3D-3 CENTAUR PROPELLANT UTILIZATION SYSTEM ELECTRICAL DIAGRAM

VII-3E. Instrumentation and Telemetry System

by J. Bulloch

Summary

Operation of the instrumentation and telemetry system was satisfactory. Of 571 measurements on the TC-1 vehicle, only about 3 percent provided anomalous data or failed during flight.

System Description

The D1-T Centaur instrumentation and telemetry system consists of a pulse code modulation/frequency modulation (PCM/FM) and two frequency modulation/frequency modulation (FM/FM) systems. The PCM/FM system and the two FM/FM systems share common antennas and coaxial switches as shown in figure VII-3E-1.

The D1-T pulse code modulation/frequency modulation (PCM/FM) instrumentation system consists of transducers, two signal conditioners, two remote multiplexers (RMU's), a central control unit which is an integral part of the DCU, and a transmitter. The instrumentation and telemetry function collects, digitizes, and sends to the ground, measurements made on the airborne systems. These measurements are sent in a preprogrammed PCM format. During the prelaunch activity, this PCM data is used to check out and establish the flight readiness of most of the on-board astrionics. For this function, the data downlink is via a coax in one of the umbilical cables. During flight, the PCM data are sent to the ground by radio frequency (RF) link for postflight analysis.

Measurements, made directly or by transducers, are collected by the remote multiplexer unit (RMU). Analog signals are scaled by the signal conditioners before reaching the RMU's, where they are digitized. Event signals go directly to the RMU's. The RMU's identify signals by addresses, and when addressed by a central controller unit (CCU) send these measurements to a central controller unit.

The CUU, part of the DCU, determines the format (sequence of measurement addresses) by reading and interpreting a segment of the DCU memory. Measurements are put on the PCM bit stream by the CCU in the order of the format addresses. PCM bit stream goes to the transmitter and, before launch, by landline to the PCM ground station.

Two frequency modulation/frequency modulation (FM/FM) telemetry packages were installed. FM/FM telemetry package number 1 was installed on the Centaur for environmental measurements and FM/FM telemetry package number 2 was installed remotely for VDS measurements.

The FM/FM telemeter package (Telepak) provides excitation for and

accepts data signals from transducers, and conditions the signals into proper voltages compatible and proportional to the assigned subcarrier channel oscillator input. The conditioned signals are composited and used to frequency modulate an S-band transmitter carrier frequency. The resultant RF signal is fed from the S-band transmitter (mounted on the FM/FM Telepak) to a ring coupler which splits the signal and feeds the antennas.

Two S-band antennas are installed on the Centaur standard shroud for data transmission until the shroud is separated from the vehicle. After shroud separation, data transmission is accomplished with two antennas mounted on the stub adapter. In addition, two high-gain S-band antennas are mounted on the equipment module for use in deep space. Switching from one pair of antennas to the other is accomplished with coaxial switches.

Flight Performance

Of a total of 571 telemetry measurements only the following anomalies were noted:

CA967T (LH_2 sump radiation shield middle temperature Station 2247) went off scale high at approximately T - 60 minutes. The off scale high condition is characteristic of an open in the transducer or measurement circuitry.

CA884P (Payload/electrical compartment delta pressure 0 to 0.5 PlD) provided good data during the period of interest in the measurement; that is, prior to the time of separation of the payload encapsulation bulkhead. At that time the measurement dropped to approximately zero as it should. However, at approximately T + 43 seconds it began to drift upward and at approximately T + 77 reached the upperband limit where it stayed. It is not understood at this time what was responsible for the anomaly, but suspicion centers around: (1) partial obstruction of the filter on the high-pressure part of the transducer, or (2) failure of the transducer itself.

CA894P (interstage adapter ambient pressure 0 to 15 psia) indicate negative spikes of approximately 5 percent information bandwidth for about 1 second at approximately T + 7 seconds. This anomaly is indicative of wiper liftoff. No data was lost because of this anomaly.

CP16B (LH_2 boost pump speed 0 to 65 KPM) did not indicate pump speed rise. Other LH_2 pump performance measurements indicated the pump was operating during the MES attempts. The vehicle connector B101U3P10 used in conjunction with CP16B mates to signal conditioner number 2. This connector was demated and reworked on November 3, 1973 because of the added shroud edge accelerometer measurements CA998Ø and CA999Ø. Upon completion of the rework the added wiring was tested and the total system evaluated for data conditions during the remainder of the prelaunch activity.

There are six measurements for which data conditions during downstream testing activity would not discern an open or short failure mode in P10. The measurements are:

CP120P	LO_2 boost pump differential pressure
CP121P	LH_2 boost pump differential pressure
CP1B	C1 engine pump speed
CP2B	C2 engine pump speed
CP15B	LO_2 boost pump speed
CP16B	LH_2 boost pump speed

During the subsequent prelaunch activity, the transducer for CP121P was replaced and reverified. The remaining measurements were not reverified after the P10 rework so as to not further invalidate the instrumentation system or risk physical damage to other components during retest.

Past experience has shown that rework to harnesses utilizing a Deutsch RSM connector and H-film wire is difficult due to the stiffness of the wire. Developing malfunctions in other areas of the harness/connector interface during a rework cycle is not uncommon. All of the above listed measurements except CP16B provided data commensurate with flight events and other common supporting measurements. CP16B signal input leads are on P10-89 and P10-90 which are physically on the outer edge of the connector, and when installed, these wires are the shortest radius of the service loop.

Other components within the instrumentation system have been examined and found to be unlikely modes of the CP16B failure. It is concluded that during P10 disconnect rework cycle, CP16B wires received higher stresses and it is credible that one of them may have opened at the crimp joint.

CA26Ø (battery mount normal accelerometer ±10 g) showed an instantaneous positive displacement at 64.46 seconds from 50 percent information bandwidth to approximately 68 percent information bandwidth for approximately 2 seconds. The instantaneous nature of this offset, without subsequent indication of vibratory accelerations, and the evidence of undershoot recovering at an exponential rate which is characteristic of amplifier recovery, clearly indicates that this is an electrical phenomena unrelated to external mechanical excitation. Laboratory tests have demonstrated that this type of anomaly can be duplicated by minute changes in sensor/cable capacity or by introducing minute electrical charges into the sensor/cable circuit.

CA169T (shroud skin inner temperature at Station 2812/308) exhibited an unexpected increased output variation for approximately 10 seconds between 65 and 75 seconds of flight. The erratic output is not believed to be valid temperature data since peak temperature levels are higher than the stagnation temperature during this period and could not be a result of an aerodynamic phenomenon. The increased data levels indicate that additional resistance existed temporarily in the measurement circuit which

could have been caused by harness strain at the transducer/harness splice joint during transonics.

Measurement CM329A, axial acceleration fine (±1 mg) indicated data levels approximately 25 percent higher than expected and CM110A, axial acceleration (±10 mg) which uses the same transducer indicated data levels approximately 2.5 percent higher than expected. It is highly unlikely that the high levels of acceleration indicated by these measurements were actual. Since TC-1 never achieved a zero-g state, that inflight calibration is not available for data evaluation. It is concluded that the most probable cause of the high acceleration reading is the null offset of the accelerometer. The accelerometer provided excellent qualitative data.

CA419P (shroud aerodynamic differential pressure at Station 2678) was thought to be erratic for about 10 seconds beginning at approximately 35 seconds after lift-off. Further investigation, however, indicates that the measurement was probably responding to an unsteady flow phenomenon at that time. The pressure sensing port for this measurement is located 2 inches aft of the 15 degree "corner" of the shroud, where unsteady flow is likely to occur at that time in the flight. Not yet completely understood is a sudden data level shift of 20 percent bandwidth (corresponding to 2 lb pressure drop) at 37 seconds into flight, during the period of unsteady flow. The level then shifts back to the original level about 1.6 seconds later. This could conceivably be data caused by local separation of the air stream. Such an occurrence was not expected, but the possibility cannot be overlooked, especially since the data shift cannot be explained by any probable malfunction of the electrical portion of the instrumentation system. It remains for the data from this measurement on TC-2 to substantiate that it is valid data.

CY201Ø, VODS (accelerometer number 1 longitudinal ±20 g's) showed an instantaneous off-scale condition at 68.64 seconds, followed by a decremental recovery in the next 2 seconds. Since no vibratory acceleration data was recorded during the recovery period following the off-scale condition, it is concluded that the anomalous trace deflection was not due to mechanical shock excitation. Laboratory tests have demonstrated that a momentary break in the coaxial cable/connector circuits between the accelerometer, "T" calibrator, and charge amplifier will reproduce the condition recorded in flight. Therefore, it is concluded that the cause of this anomaly most probably was the result of a loose coaxial cable connector, defective connector pin/socket, or imperfect cable assembly.

CP753T (C-1 LH_2 pump housing second stage temperature) indicated unexpected heating during firing of the H_2O_2 five engines in the interstage adapter. Analysis of the data indicates that the bonding cement used to attach the transducer to the pump housing surface acted as thermal insulation and allowed the temperature sensor to heat up well beyond the surface to which it was bonded. The sensor cooled toward the surface temperature after the impingement heating was removed. Since the prime area of interest for this measurement is during long coast phases, this temporary sensor heating condition is acceptable.

CP833T (LH_2 boost pump H_2O_2 inlet line temperature data) indicated a linear rise from 70° F at first BPS (437 sec) to 120° F at 600 seconds. This measurement was expected to show a rise to a level consistent with H_2O_2 bulk temperature (approximately 92° F) in the 20-second period following BPS and to remain at that level.

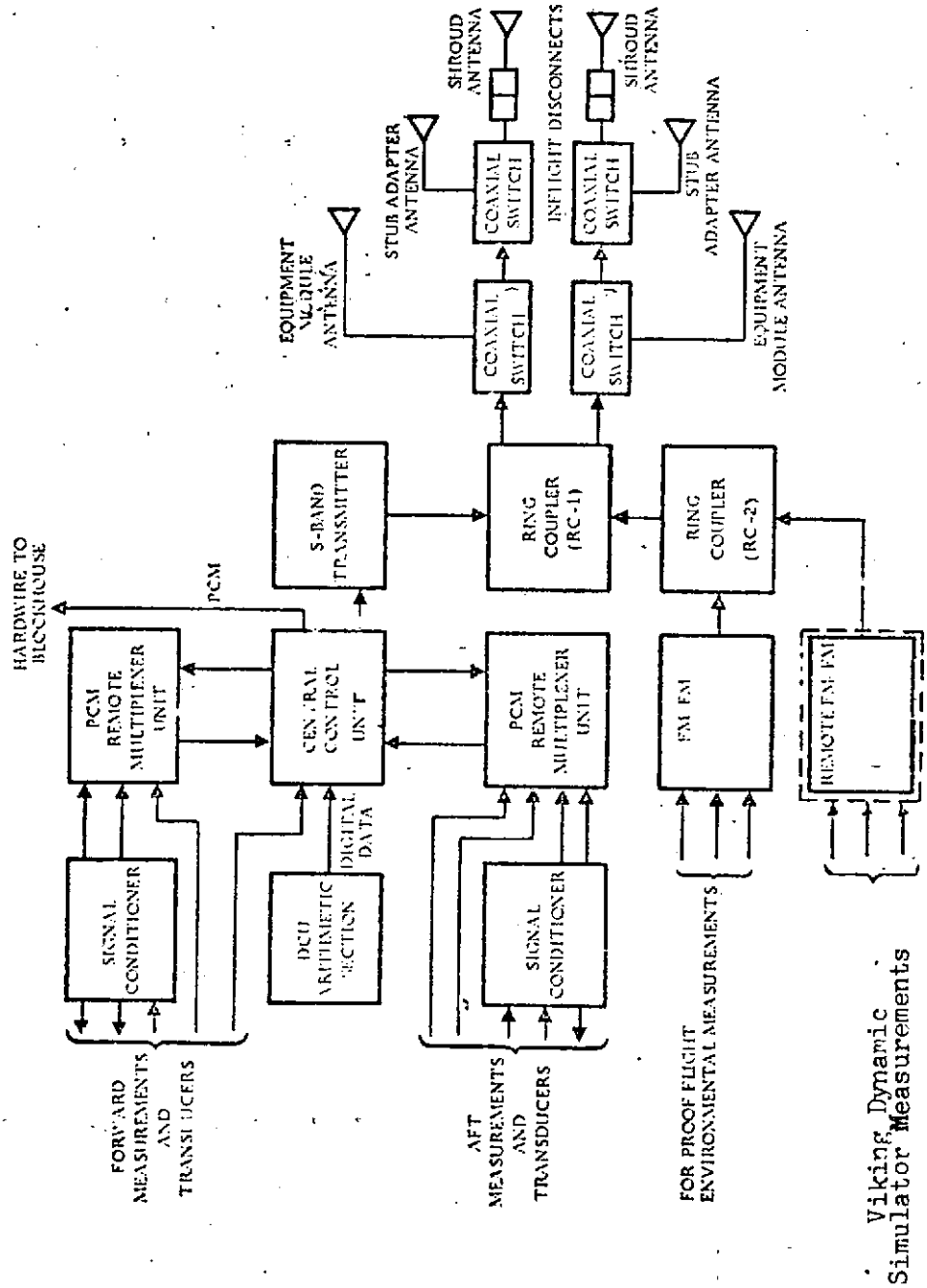

Figure VII-3E-1 Instrumentation and telemetry system.

VII-3F. Range Safety Command System

by J. Bulloch

System Description

The Centaur range safety command system provides a means of shutting down the engines or shutting down the engines and destroying the vehicle if commanded by appropriate radio signals from the range safety officer. To destroy the vehicle an explosive charge ruptures the propellant tanks at the bulkhead separating the two propellants. The Centaur range safety command system consists of redundant antennas, redundant receivers, redundant circuitry in the power control unit, redundant detonators in the destructors, and redundant batteries which operate independently of the main vehicle power system. Block diagram of the Centaur range safety system is shown in figure VII-3F-1.

Flight Performance

The range safety command system successfully received and executed the main engine cutoff command at approximately 743.480 seconds and the destruct command at approximately T + 748.210 seconds. Both commands were transmitted from Antigua. Signal strength was satisfactory. The following table depicts ground transmitter coverage.

Station	Carrier on, sec	Carrier off, sec
Cape Kennedy	-1948	160.5
Grand Bahama Island	160.5	181
Cape Kennedy	181	201
Grand Bahama Island	199.5	458.5
Antigua	457.5	775.5

After a successful destruct event, the range safety telemetry measurements for MECO and destruct were not as expected.

1. MECO (Main Engine Cutoff). CD3X (MECO command) indicated receipt of the MECO command at T + 743.480 seconds, a dropout at 748.210. It was then reactivated at T + 748.288 and dropped out again at 748.418 with no further activation. This should not happen since the MECO command latches up a relay in the ranges safety power control unit.

2. Destruct Number 1. CD5X (range safety destruct no. 1) had only one activation at T + 748.245 then dropping out at T + 748.259. This measurement was expected to remain on until the destruct command was removed at T + 764 seconds.

3. CD6X (Destruct No. 2) activated at T + 748.231 seconds, drops out at T + 748.260 seconds and activates at 748.289 seconds and drops out when the destruct command is removed at T + 764 seconds. This measurement was expected to remain on until the destruct command was removed at T + 764 seconds.

The preceding apparent telemetry data anomalies can be explained by the following. A single six wire harness from the RSC power control unit carries the affected measurements. Therefore, since the MECO measurement dropped out for several samples (long enough for the latching relays in the range safety power to transfer to the MECO condition) and reappeared for several samples, it is most probable that the MECO persisted but the measurement circuit was destroyed. A review of RSC battery voltage number 2 indicated RSC destruct number 2 operated successfully and the anomalous measurement dropout was indicative of the measurement opening up momentarily. RSC battery voltage number 1 data suggests that destruct number 1 was terminated as a result of a destruct that caused momentary open or short circuit which reduced the system voltage to the system number 1 command receiver to 18 volts or less. If the reduced voltage appears at the receiver for between 6 and 14 milliseconds after the receiver destruct logic is set, the receiver may terminate the destruct command output which cannot return unless an entire command sequence is retransmitted (only one command sequence was sent). RSC battery number 1 voltage rise immediately (after destruct) and stabilizes about 1/2 volt above the predestruct MECO level, thus confirming RSC receiver number 1 is no longer in a destruct mode. The fact that there is no voltage drop data to indicate the presence of a momentary short on system number 1 may be rationalized since the measurement is sampled at 176 millisecond intervals and was most probably of short duration such as a brushing of frayed wire strands resulting from the destructor detonation. Both RSC batteries exhibited a rise in voltage to predestruct valves following removal of the destruct command verifying that both receivers were operating in a normal fashion and that the received signal was adequate even beyond destruct.

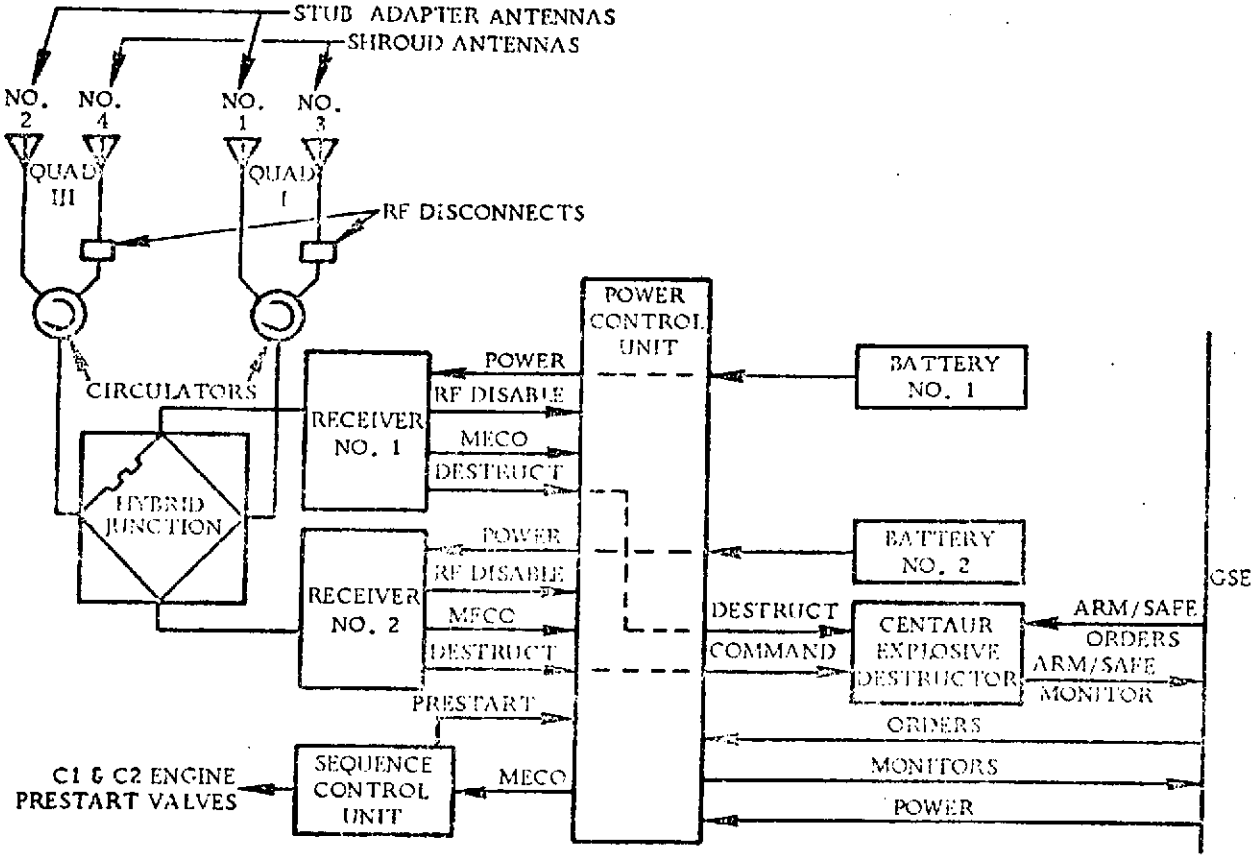

Figure VII-3F-1 Centaur Range Safety Command System Block Diagram

VIII. VEHICLE DYNAMICS

VIII-1. SYSTEM DYNAMIC RESPONSE

by T. F. Gerus

The dynamic response of the TC-1 vehicle was monitored by accelerometers mounted on the Viking Dynamic Simulator (VDS) as shown in figure VII-1-1 and on the Titan booster as shown in figure VII-1-2.

The response of the VDS observed in flight at significant events is presented in tables VIII-1-1 and 2, and is compared to maximum predicted levels where available. The acceleration levels were as expected except at launch and at T + 240 seconds. At launch both axial and lateral accelerations exceeded the predicted 3-sigma maximum expected values. While the observed values are well within structural capabilities, the deviation from expected is under study.

Beginning at about T + 200 seconds, a longitudinal oscillation of the VDS sprung mass began building up (see fig. VIII-1-3). The oscillation, having a frequency of 12 hertz, increased to a peak value of ±2.7 g's at approximately T + 240 seconds. The oscillation decreased to an amplitude of ±0.7 g at Stage I shutdown. Further excitation of the sprung mass was observed at Stage I jettison and CSS jettison. The loads resulting from the sprung mass oscillation were within allowables; however, this response was not expected. The cause of the sprung mass oscillation is under study and is believed, at this time, to be associated with low damping in the sprung mass structure.

The response observed on the Titan booster is presented in tables VIII-1-III through VIII-1-V along with appropriate comments. It must be noted that Titan accelerometer data is presented for information only since no preflight predictions are made for accelerations of Titan node points.

TABLE VIII-1-1. - VIKING DYNAMIC SIMULATOR DYNAMIC RESPONSE

Measurement	Location	Launch		Maximum αQ		FBR separation		Stage I ignition		SRM jettison	
		Flight	Maximum expected	Flight	Maximum expected	Flight	Maximum expected	Flight	Maximum expected	Flight	Maximum expected
CY201φ	VS/CA Axial	+2.2 +.6	+2.20 +.76	+2.2 +1.8	+3.2 -.8	[a]+2.4 -6.8	---	----	---	Data dropout	---
CY202φ	Bus Axial	+2.3	+2.20	+2.2	+3.2	+2.8	---	+2.0	---		---
CY203φ	Bus Axial	+2.3 +.7	+2.24 +.76	+2.2 +2.0	+3.2 -.8	+2.6 +2.5	---	+2.3 +2.1	---		---
CY204φ	Bus Axial	+1.80 +.48	+2.21 +.78	+1.8 +1.6	+3.2 -.8	+2.4	---	+2.0 +1.9	---		---
CY205φ	Bus y axis	+0.6 -.6	+0.49 -.30	±0.4	±1.33	±0.2	---	±0.1	---		---
CY206φ	Bus y axis	+0.7	+0.52	±0.4	±1.33	±0.2	---	±0.1	---		---
CY207φ	Bus x axis	+0.5 -.5	+0.62 -.45	±0.3	±1.33	±0.1	---	±0.1	---		---
CY208φ	Sprung mass axial	+2.44 +.20	+2.41 +.58	+2.4 -1.4	-----	+2.5	---	+2.4 +1.8	---	+1.8 +1.1	---

[a]High frequency, greater than 30 Hz. All values in g's. Peak to peak.

TABLE VIII-1-2. - VIKING DYNAMIC SIMULATOR DYNAMIC RESPONSE

[All values in g's. Peak to peak.]

Measurement	Location	T + 240 sec		Stage I shutdown		CSS jettison		Stage II shutdown	
		Flight	Maximum expected	Flight	Maximum expected	Flight	Maximum expected	Flight	Maximum expected
CY201ϕ	VS/CA Axial	±0.8	---	---	+4.55 -2.73	----	---	-----	---
CY202ϕ	Bus axial	+3.6 +2.5	---	+3.8 -.3	+4.56 -2.75	+0.8	---	2±0.2	---
CY203ϕ	Bus axial	+3.6 +2.5	---	+3.8 -.2	+4.62 -2.97	+0.9 +.6	---	2±0.1	---
CY204ϕ	Bus axial	+3.0 +2.5	---	+3.8 -.3	+4.63 -3.05	+0.8 +.4	---	2±0.1	---
CY205ϕ	Bus y áxis	0	---	±0.4	+0.60 -.57	±0.2	---	±0.1	---
CY206ϕ	Bus y axis	0	---	±0.3	+0.65 -.64	±0.2	---	±0.1	---
CY207ϕ	Bus x axis	0	---	±0.3	+0.18	±0.2	---	±0.1	---
CY208ϕ	Sprung mass axial	+5.4 +.2	---	+4.2 -1.0	+6.34 -5.77	+1.5 +.2	---	2±0.2	---

TABLE VIII-1-3. - TITAN DYNAMIC ENVIRONMENT - SOLID

ROCKET MOTOR PHASE OF FLIGHT

	Stage I G's P-P	Stage II G's P-P	Remarks
Lift-off			
Long	5.5 (HI)	1.4 (5)	5 Hz longitudinal response on
Long AC		2.0 (HI)	stage II is typical of first
Yaw	4.3 (HI)	>5.0 (HI)	axial mode excitation.
Pitch	3.0 (HI)	>5.0 (HI)	Lasted 1 sec
Transonic			
Long	1.5 (HI)	0.8 (HI)	65 sec of transonic buffeting
Long AC	---------	>2.0 (HI)	began sooner and lasted
Yaw	1.5 (HI)	>5.0 (HI)	longer than expected.
Pitch	2.5 (HI)	>5.0 (HI)	
Fire FBR			
Long	0	.1 (HI)	Typical response to Pyro
Long AC		.4 (HI)	shock. Nothing unexpected.
Yaw		2.0 (HI)	
Pitch		2.8 (HI)	
Peak acceleration was 2.5 g			Typical

TABLE VIII-1-4. - TITAN DYNAMIC ENVIRONMENT - STAGE I PHASE OF FLIGHT

	Stage I G's P-P	Stage II G's P-P	Remarks
Ignition			
Long	3.0 (HI)	0.2 (9)	Normal levels. 9 Hz osc. is response in the vehicle first axial mode
Long AC		.3 (HI)	
Yaw	2.4 (HI)	.3 (HI)	
Pitch	2.5 (HI)	.6 (HI)	
SRM jettison			
Long	.3 (HI)	.3 (9)	Data dropout as expected. Typical response in axial mode.
Long AC		.2 (9)	
Yaw	---	---	
Pitch	---	---	
Long. response			
Long	1.5 (12)	---	12 Hz axial osc. was not typical. Indicates payload influence on vehicle first mode.
Long AC	---	.3 (12)	
Yaw	---	---	
Pitch	---	---	
Engine shutdown			
Long	2 (20)	.5 (20)	20 Hz long. response was typical of ox depletion condition.
Long AC		1.2 (HI)	
Yaw	---	1.2 (HI)	
Pitch	---	.7	
Peak acceleration was 3.5 g			Typical.

TABLE VIII-1-5. - TITAN DYNAMIC ENVIRONMENT - STAGE II

PHASE OF FLIGHT

	Stage II	Remarks
Ignition		
Long	2.0 (HI)	Typical response.
Long AC	>2.0 (HI)	
Yaw	3.5 (HI)	
Pitch	3.4 (HI)	
CSS jettison		
Long	1.0 (HI)	As expected. The 9 Hz response is in agreement with IMSC predictions.
Long AC	1.0 (HI)	
Yaw	5.0 (9)	
Pitch	5.0 (HI)	
Engine shutdown		
Long	1.5 (32)	32 Hz response is typical of first axial mode excitation.
Long AC	2.0 (32)	
Yaw	.5 (32)	
Pitch	1.0 (32)	
Peak acceleration was 1.9 g		Typical
Staging		
Long	1.0 (HI)	As expected for Pyro shock.
Long AC	2.0 (HI)	
Yaw	4.0 (HI)	
Pitch	3.4 (HI)	

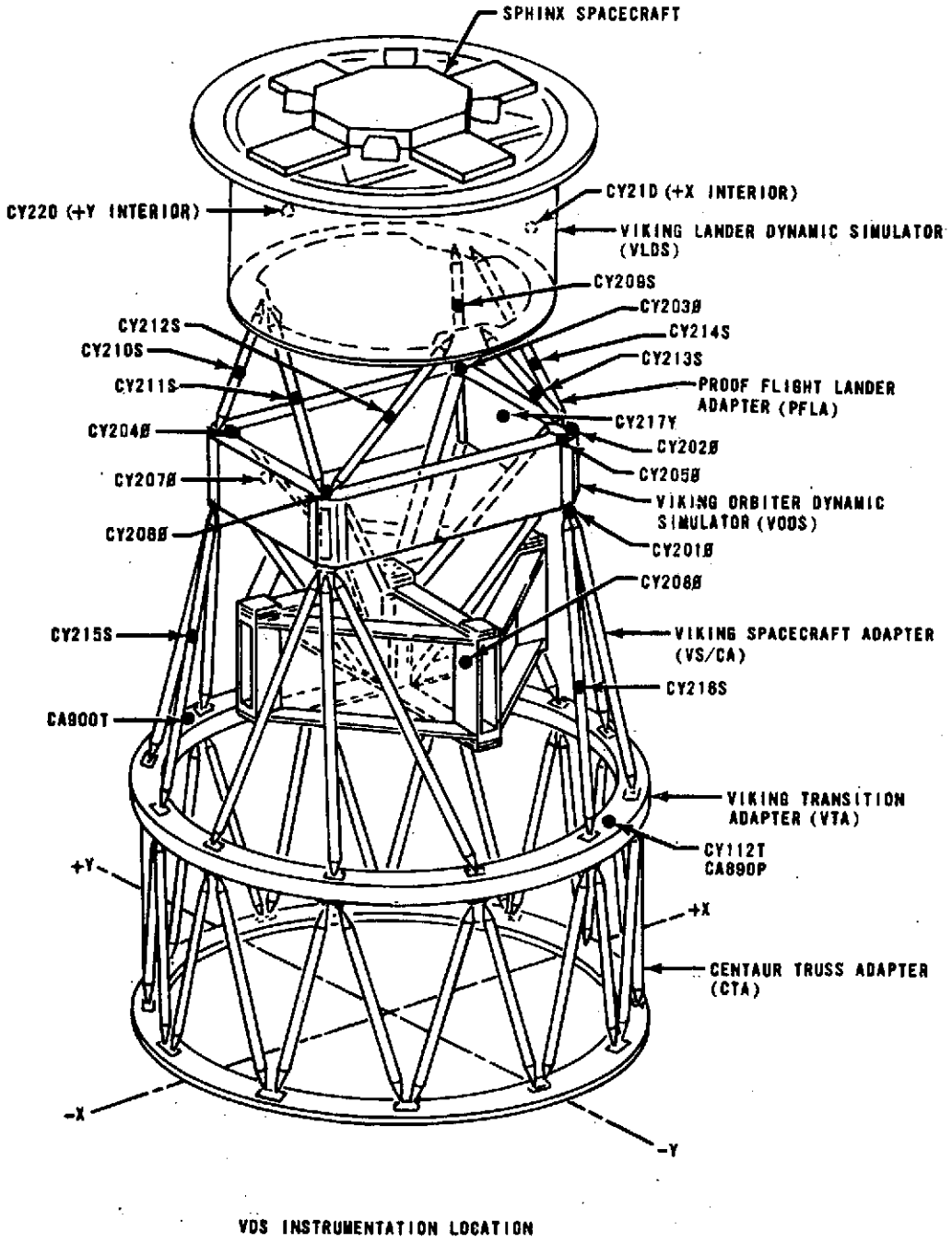

FIGURE VIII-1-1 VIKING DYNAMIC SIMULATOR INSTRUMENTATION

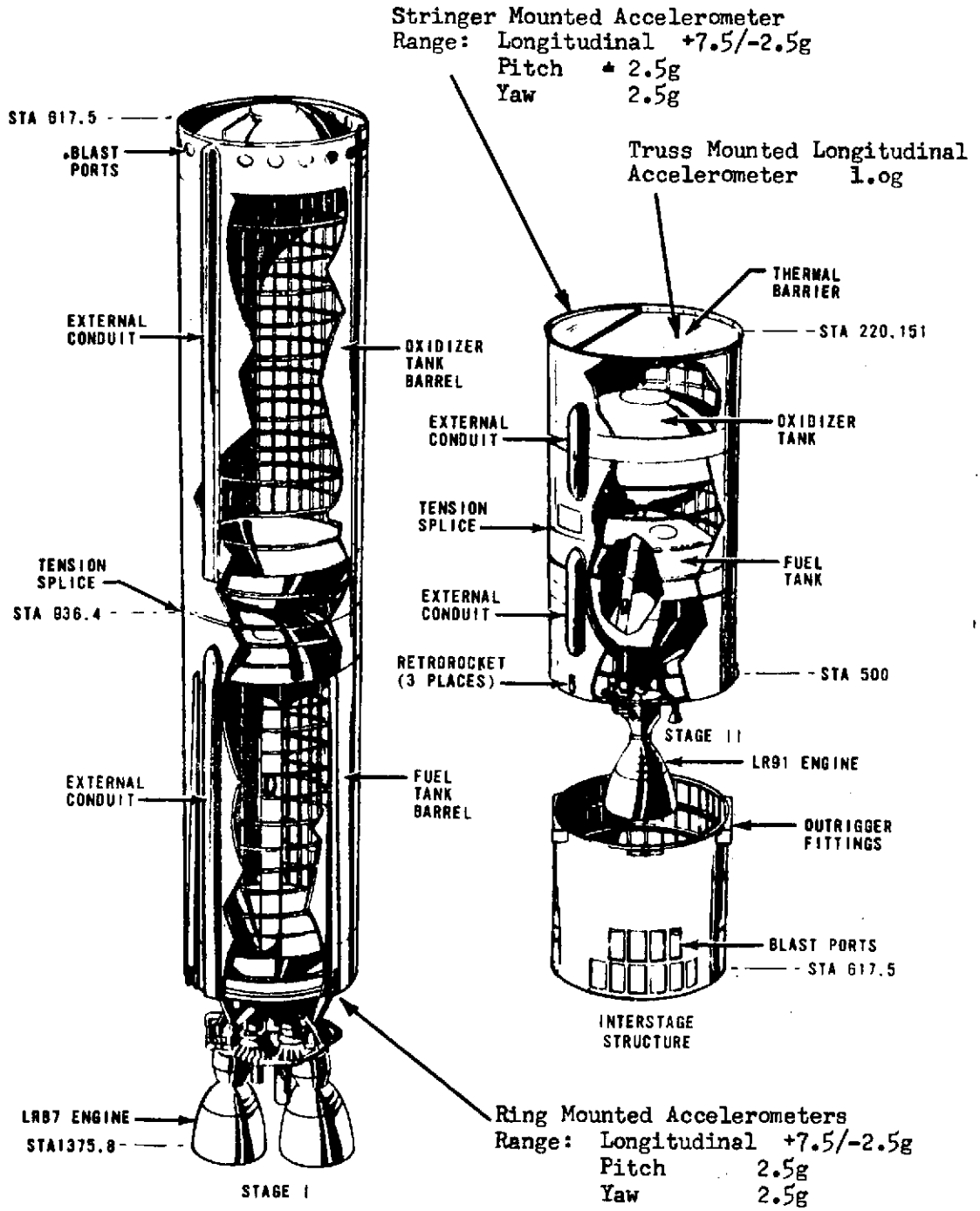

FIGURE VIII-1-2 TITAN ACCELEROMETER LOCATIONS

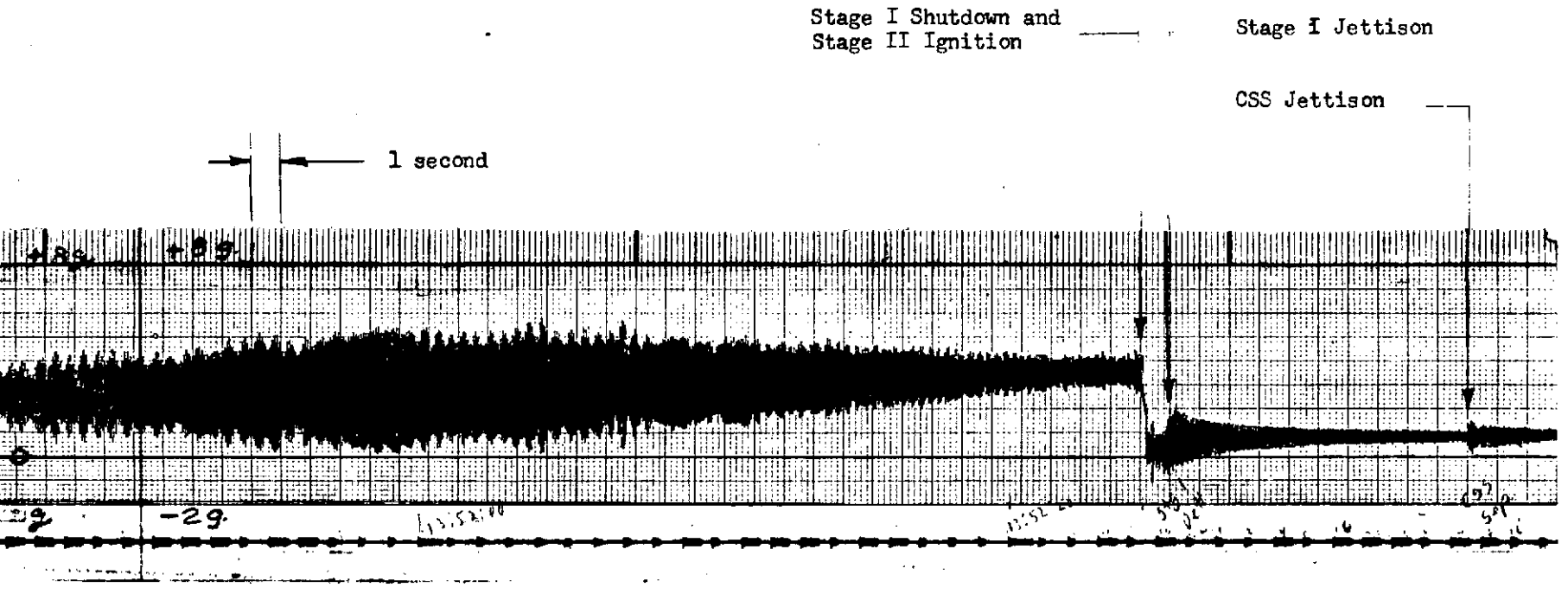

FIGURE VIII-1-3 SPRUNG MASS LONGITUDINAL ASCILLATION PRIOR TO STAGE I SHUTDOWN

VIII-2. TITAN/CENTAUR SEPARATION

by C. R. Finkelstein

Summary

Titan/Centaur separation occurred as expected and the interface specification requirements were met. All four retrorockets appear to have operated satisfactorily, and a review of Titan Stage II accelerometer data showed no evidence of impact between Titan and Centaur during separation. The Centaur engine bells were clear of the interstage adapter (ISA) at Centaur engine prestart.

System Description

Retrothrust for Titan/Centaur separation is provided by four retrorockets mounted on Titan Stage II as shown in figure VIII-2-1. The retrorockets are recessed to reduce structural loads during the maximum airload regime of flight and are canted outboard at 30° to direct the thrust vectors approximately through the center-of-percussion of the empty stage. The purpose of this latter arrangement is to offset interface rotation with translation if one of the retrorockets fails to fire. This provides the capability to separate the two vehicles without impact if only three retrorockets fire. Each retrorocket develops 499±26 pounds of thrust and burns for about 2.5 seconds. The primary command for Titan/Centaur separation is issued by the Centaur stage. Accelerometers in the Centaur Digital Computer Unit (DCU) sense the tailoff acceleration during Titan Stage II flight. When this acceleration has decayed to a nominal level of 0.01 g, the DCU sends a discrete to a relay in the Centaur Sequence Control Unit (SCU). The DCU discrete closes the SCU relay to which Titan power is connected. Titan power then closes a relay on the Titan side of the interface, which connects power to Silicon Controlled Rectifiers (SCR) in the Squib Fire Circuits (SFC) and turns the rectifiers on. Turning on the SCR's connects the pyro battery to the retrorocket igniter squibs and fires the retrorockets.

Separation is guided for approximately the first 9 inches of travel by four bumpers mounted on the Centaur stage. After this guided travel, both stages are free bodies.

Flight Performance

The command to separate the Centaur stage from Titan Stage II was issued at T + 475.24 seconds by the Centaur Sequence Control Unit (SCU). Based on data, shown in figure VII-1A-3, from the separation monitoring device (yo-yo), the Centaur engine bells cleared the interstage adapter (ISA) in 1.77 seconds. The nominal time predicted by MMC for the case of all four retrorockets operating is 2.15 seconds. These two data points

indicate that all four retrorockets operated satisfactorily. Based on the clearance time of 1.77 seconds, it also appears that the Centaur stage was clear of the ISA at Centaur engine prestart, which occurs nominally at 2.5 seconds after the separation command is issued.

Based on the Centaur Digital Computer Unit (DCU) data, the vector sum of Centaur pitch, roll, and yaw rates was approximately 0.32 degree per second when the Centaur stage cleared the ISA. According to the Titan/Centaur interface specification, this rate should not exceed 2 degrees per second. The actual rate was less than the allowable rate. Based on Titan Stage II gyro data and DCU data, the angle between the two stages was calculated to be 1.48° when the Centaur stage cleared the Titan Stage II. The interface specification requires that this angle not exceed 5 degrees. The actual angle was less than the allowable angle. Titan Stage II and Centaur stage attitudes and rates at separation are shown in tables VIII-2-I and VIII-2-II.

Data from a set of triaxial accelerometers mounted on the Titan Stage II were reviewed to see if there was evidence of impact between the vehicles during separation. There was no evidence of any impact.

VIII-2-1

TABLE VIII-2-1 . CENTAUR DISPLACEMENTS AND RATES DURING T/C SEPARATION

Parameter	Retro Ignition	Retro Mid-Point	Centaur/ISA Clearance
Roll - Deg	1.78 CW	1.78 CW	1.78 CW
Roll Rate - Deg/Sec	0.09 CW	0	0
Pitch - Deg	1.61 Nose Up	1.78 Nose Up	1.85 Nose Up
Pitch Rate - Deg/Sec	0.10 Nose Up	0.14 Nose Up	0.14 Nose Up
Yaw - Deg	0.35 Right	0.67 Right	0.94 Right
Yaw Rate - Deg/Sec	0.28 Right	0.28 Right	0.28 Right

TABLE VIII-2-2 TITAN DISPLACEMENTS AND RATES DURING T/C SEPARATION

Parameter	Retro Ignition	Retro Mid-Point	Centaur/ISA Clearance
Roll - Deg	0.96 CW	0.24 CW	0
Roll Rate - Deg/Sec	0.14 CW	0.72 CCW	0.96 CCW
Pitch - Deg	0.72 Nose Up	0.72 Nose Up	0.45 Nose Up
Pitch Rate - Deg/Sec	0.12 Nose Up	0.24 Nose Down	0.54 Nose Down
Yaw - Deg	1.44 Left	1.62 Left	1.44 Left
Yaw Rate - Deg/Sec	0.24 Left	0.36 Right	0.50 Right

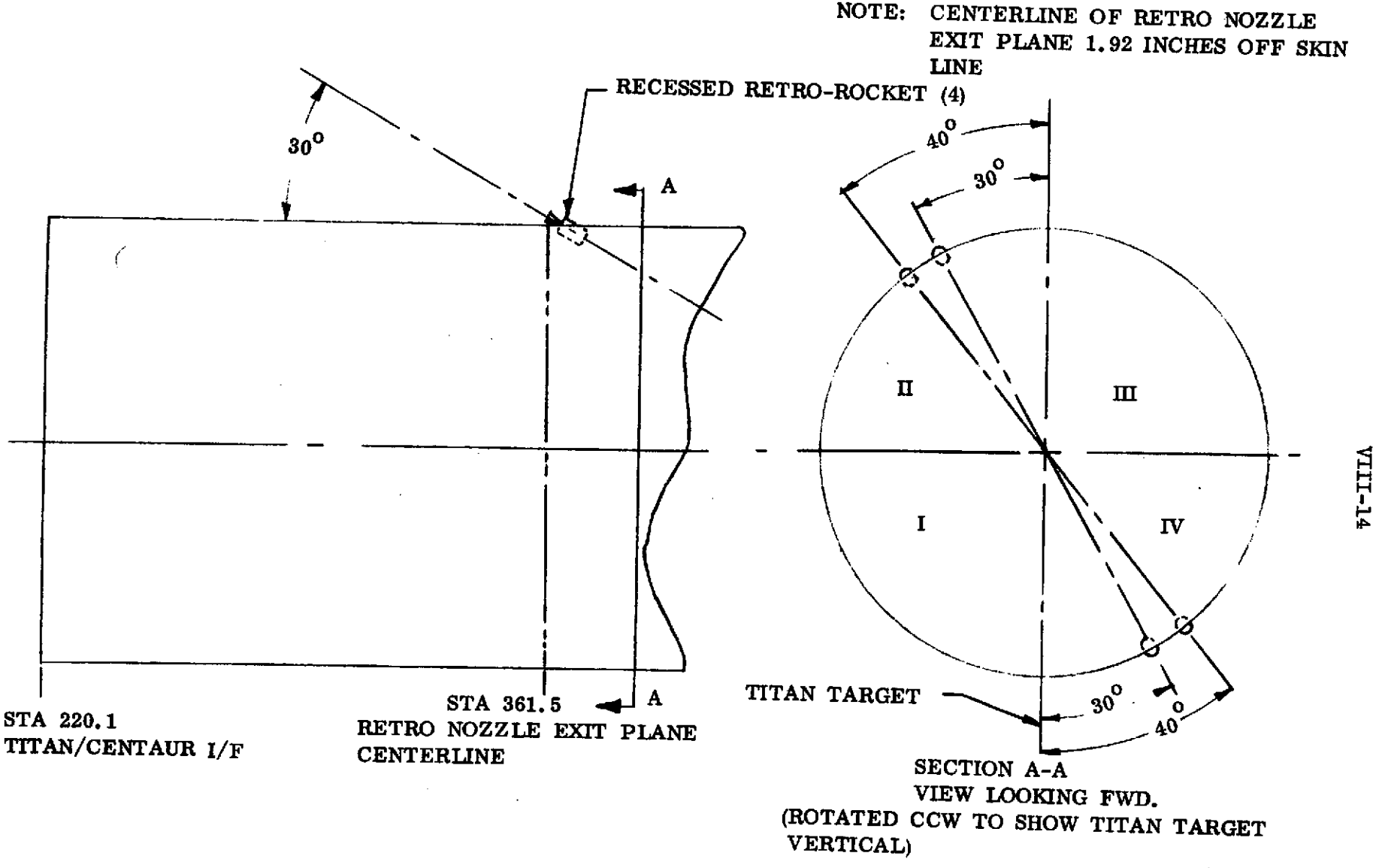

FIGURE VIII-2-TITAN STAGE II RETROROCKET LOCATION

VIII-3. CENTAUR FLIGHT DYNAMICS

by C. Rawlin

Summary

Centaur phase of flight may be described, for this mission, as the period from Titan/Centaur separation until destruct. During this time the Centaur autopilot performed as programmed as demonstrated by analysis of the following flight data: attitude error, DDR (digital derived rate of attitude error), instrumentation rate gyros, Centaur main engine commands, engine gimbal angle feedback, coast phase attitude control engine commands, and digital autopilot word output. The Centaur control system responded correctly to steady state and transient conditions. Although "low main engine thrust" precluded normal vehicle control capability, the powered autopilot functioned properly by causing the required engine commands. The coast autopilot damped disturbances from the powered phases and generally maintained control properly during settled coast phases.

System Description-Flight Control Software

The Centaur flight control system maintains vehicle stability and control during the Centaur phase of flight. The attitude reference is provided by the inertial guidance system. Pitch, yaw, and roll attitude error signals from the inertial platform are admitted into the autopilot. Rate information is obtained by digital differentiation of the attitude error signal. The digitally derived rate (DDR) is computed using a variable time base algorithm. Discrete changes in attitude error are divided by the time between these changes. Additional features were added to the system to provide noise saturation. The flight control system software contains the logic and equations for vehicle powered and coast phase control. Pointing vectors in the powered phase autopilot are supplied by the guidance equations and steering module together. Autopilot gains vary as a precomputed function of thrust acceleration. Powered phase autopilot computes and outputs engine actuator commands.

The steering module provides the pointing vectors in the coast phase autopilot. Attitude error signals are tested against thresholds which are a function of attitude error and DDR. The control engine on-off commands are generated by the pitch and yaw engine logic module. The Centaur D-1T coast phase attitude control system and propellant settling engine system is different from that of Centaur D and D-1A vehicles. The D-1T consists of twelve 6-pound thrust engines: eight lateral for pitch, yaw, and roll control, four axial exclusively for propellant settling. (See figs. VIII-3-1 and VIII-3-2).

Vehicle Dynamic Behavior

DDR computations were begun at phase =5, coincident with DCU detection of stage II shutdown (469.54 sec). The small disturbance from stage II shutdown (peak angular transient rate approximately 0.3 deg/sec) introduced an attitude error (approximately 1.6 degree in pitch and roll, 0.4 degree yaw) which was present at the time of Titan/Centaur separation.

The powered autopilot is turned on at Phase 6 (475.24 sec) coincident with Titan/Centaur separation, although engine commands are not computed until MES-1. Centaur separation from the Titan vehicle was smooth as predicted. A comparison of rate traces for this flight and AC-31 showed them to be very similar. Table VIII-2-I summarizes the rates from Titan/Centaur separation to MES-1. At separation a high frequency oscillation of approximately 25 hertz was observed (on TC-1 and AC-31); this is believed to be the natural frequency of the rate gyro package mounting. These oscillations did not exceed 0.5 degrees per second and were of brief duration.

At 478.04 seconds the prestart valves were opened. An oscillation on the yaw rate trace and a negative acceleration on the roll rate trace were observed. A steady-state clockwise roll torque ensued until MES-1 which yielded an acceleration of approximately 0.26 degrees per second^2. (The source of the torque is not known; however, this acceleration could be produced by a force of approximately 0.8 pound at either main engine gimbal point.) Also at this time (478.0 sec) null was set, that is, guidance began putting out the null pointing vector (which causes the vehicle to aline to the velocity vector), and the powered autopilot word (PASQ = 00012000), which contains the gains, logic flags, and D/A scaling coefficient, was verified. Attitude error data confirmed the periodic 2 second null output. A 24-inch-pound clockwise roll to torque was present during prestart; this was well within the average value seen on previous D flight. Pitch and yaw rates remained small and nearly constant until MES-1 (as shown in table VIII-3-I).

At MES-1 (attempt) Phase 7 and PASQ = 11120000. Oscillations of approximately 10 hertz were observed in all three rate channels with the maximum occurring in roll (0.6 deg/sec). Computation of main engine commands was initiated and engine gimbaling began. A comparison of actual and computed engine commands verified the fixed gain control law. Calculations were made in an attempt to verify the autopilot integral function; the short period of operation precluded an accurate check.

Approximately 2.26 seconds after MES-1, null was set equal to zero and the output of the guidance attitude error was verified. The values of the attitude errors immediately before and after vector output are presented in table VIII-3-II. Autopilot response to the vector output was observed on engine gimbal angle command and engine feedback data. The C_1 and C_2 engine yaw/roll output was saturated (exceeded 3.537°) 8 seconds after MES.

(The Centaur body axes were "skewed" on Titan; the large errors were actually in the pitch plane.) Average vehicle rates during the interim from MES transient decay until MECO were small: +0.2, +0.24, -0.52 degree per second in pitch, yaw, and roll, respectively. The acceleration test for engine start was performed at approximately MES + 10 and MECO - 1 was enabled at 496.02 seconds. Coincident with MECO, steering was inhibited and PASQ was set, and, because this was a MES - 1 restart sequence, Phase = 5. One tenth second later powered autopilot was turned off, coast autopilot was turned on and its parameters were set (table VIII-3-III), and the 4S engines turned on for 24 pounds of settling thrust. (At RMES 1-59, Phase = 6.)

Attitude errors in pitch, yaw, and roll at MECO were $+0.67^{\circ}$, $+4.35^{\circ}$, and -2.48°, respectively. The coast phase autopilot (using parameters in tables VIII-3-III and IV) commanded the attitude control engines as required to reduce the MECO errors and control torques resulting from the firing of the 4S engine; Y_3Y_4 engines were on for approximately 15 seconds following MECO to correct for the yaw error incurred during the "powered phase." Vehicle angular rates varied between small positive and negative values until RMES-8. The prestart valves were opened, coast autopilot was turned off (KMODE = 0), powered autopilot was turned on (with last set PASQ), and null = 1 at 548.02 seconds. Vehicle rates increased during the interim until RMES with the only significant increase being in the roll plane, as expected. Roll rates increased from -0.04° per second to $+0.62^{\circ}$ per second (clockwise roll torque of nearly 74 in.-lb) due to increased flow of colder propellant lines.

RMES occurred at 556 seconds at which time the PASQ was set and engine commands were verified. RMES disturbances were small; a frequency of 10 hertz was observed in all three axes with a maximum peak-to-peak oscillation of 0.28° per second in roll. DCU data verified guidance attitude error output at 558 seconds, followed in 6 seconds by guidance enable. The control system issued engine commands in proper response to guidance, but lack of thrust caused an error buildup. At approximately RMES + 10 the acceleration test for engine start was again performed. Failure to pass this test again resulted in issuance of all remaining commands prior to and including MECO. By the time of issuance of MECO, the following attitude errors were observed: -1.17 degree pitch, +13.93 degree yaw, and +7.68 degree roll; angular rates were within 0.1 degree per second. At MECO the powered and coast autopilot parameters were set; the 4S engines were turned on at MECO + 0.1. Steering was inhibited at 568.02 and the guidance attitude error was output 2 seconds later; no noticeable transients were observed.

With a positive yaw rate at MECO, yaw attitude error reached its peak of 14.13 degrees 2.4 seconds after MECO. Pitch attitude and rate were within switching line limits during this time, while engine firings caused the MECO roll error to rapidly decrease. It was nearly 22 seconds before the yaw negative command was first turned off, but a considerable duty cycle continued.

The later portion of this post-MECO 4S on-mode was the only period of this flight suitable for steady state disturbance determination. The observed torques were probably due to S engine impingement upon main engine bells and aft mounted equipment. Because the propellant tanks were nearly full, the observed torques were somewhat different from that expected for the planned first coast. Average duty cycles during the last 100 seconds of this period (prior to destruct) were -15.9, -1.6, and +0.2 percent in pitch, yaw, and roll, respectively. Calculation using predicted impingement disturbances, adjusted to the mass properties for this flight, yielded duty cycles close to those observed. There was cross coupling primarily into roll from firing pitch and yaw engines. The coupling of pitch into roll was in a direction opposite to the impingement originated torque in roll, lessening its apparent effect.

Fifty hertz data from the GD/CA Telemetry Reduction Analysis Program (TRAP) enabled the verification of coast phase control logic software including inhibit, minon, switchlines, and firing logic. Of the 20 possible engine control logic commands, 13 were exercised between the two coast phase periods. Only two axis control logic was employed on this flight.

TABLE VIII-3-1 ANGULAR RATES AT T/C SEPARATION AND MES-1 (DEGREES/SECOND)

Control Axis	T/C Separation	MES-1
Pitch	+ .14	+ .16
Yaw	+ .24	+ .31
Roll *	+ .02	+ .08

* Dips down to -.08 at approximately T/C separation +4 seconds.

TABLE VIII-3-2 ATTITUDE ERRORS IMMEDIATELY BEFORE AND AFTER GUIDANCE VECTOR OUTPUT (DEGREES)

	494.1 seconds	494.2 seconds
Pitch	+ 1.05	+ 0.64
Yaw	+ 2.01	+ 4.09
Roll	- 2.48	- 1.43

TABLE VIII-3-3 COAST AUTOPILOT PARAMETERS

	Switchline Set		Minon Time Set		Inhibit Set		DDR Set	
	Roll	Pitch/Yaw	Roll	Pitch/Yaw	Roll	Pitch/Yaw	Roll	Pitch/Yaw
Prestart Set (used during Restart Attempt)	1	4	1	4	1	1	1	1
Settling Set (used Following Unsuccessful Restart)	1	1	1	1	1	1	1	1

TABLE VIII-3-4

COAST PHASE AUTOPILOT CONSTANTS

	UNITS	ROLL k = 1			PITCH AND YAW k = 2, 3				
		SET 1	SET 2	SET 3	SET 1	SET 2	SET 3	SET 4	SET 5
SWITCHLINE PARAMETERS									
K_{HC_k}	deg/sec	- 0.5	- 0.5	- 1.0	- 0.2	- 0.2	- 0.5	- 0.2	
K_{LC_k}	deg/sec	- 1.5	- 1.5	- 2.0	- 1.0	- 1.0	- 1.0	- 1.0	
K_{PC_k}	deg/sec	0.8	2.25	0.8	0.5	1.2	0.1	.25	
K_{L_k}	sec	10.0	20.0	10.0	20.0	20.0	20.0	20.0	
K_{Q_k}	sec	4.0	4.0	4.0	8.0	8.0	6.0	6.0	
DDR PARAMETERS									
ADDR	deg/sec	0.10	0.20	0.2	0.10	0.15	0.20		
FDDR	deg/sec	0.01	0.01	0.1	0.001	0.03	0.01		
TAU	N.D.	0.9	0.9	0.9	0.9	0.9	0.9		
MINON PARAMETER									
τ_{M_k}	sec	0.1	0.1	-	0.5	0.4	0.1	0.2	
RATE INHIBIT PARAMETER									
τ_{C_k}	sec	.240	.50	1.20	.240	-	-	-	

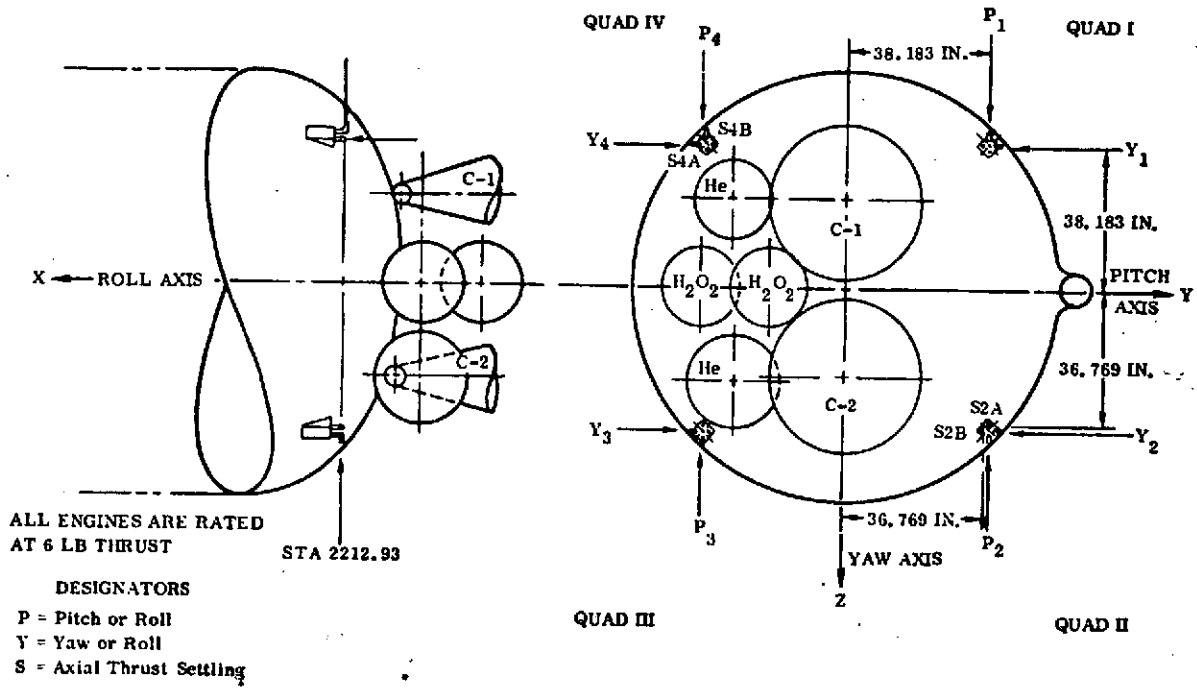

Figure VIII-3-1 - Centaur D-1T H_2O_2 engine geometry.

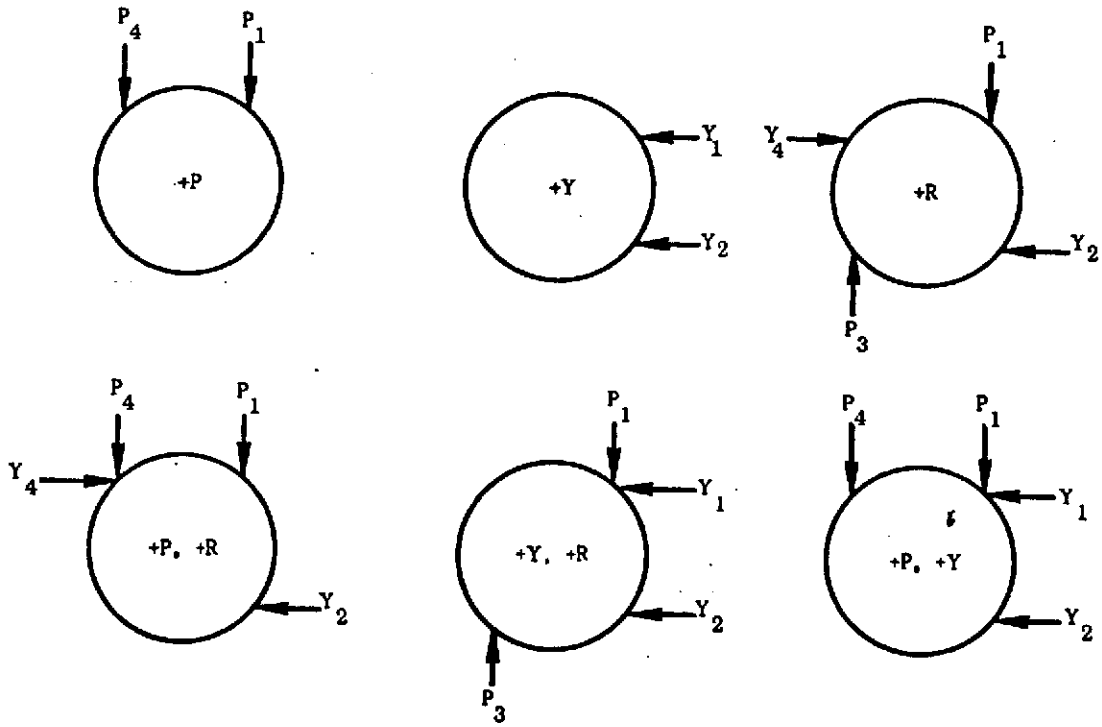

Figure VIII-3-2 Attitude control engine firing modes for positive polarity.

IX. FACILITY AND AEROSPACE GROUND EQUIPMENT

INTEGRATE-TRANSFER-LAUNCH FACILITY

by F. Gue

Description

In the ITL concept, the Titan and Centaur stages are received, assembled vertically on a rail transporter, and checked out in the Vertical Integration Building (VIB). Figure IX-1 shows an overall view of the ITL Facility. Rail vans are used to house aerospace ground equipment (AGE) for the launch vehicle. The vans are connected in the VIB and remain connected during all operations through launch. After checkout in the VIB the Titan and Centaur stages are transported to the Solid Rocket Motor Assembly Building (SMAB) where the two solid rocket motors are assembled to the vehicle and checked out.

The launch vehicle is then transported to Launch Complex 41 for final integrated vehicle tests, Range tests, propellant servicing, and launch. For the TC-1 launch, the payload consisting of the encapsulated Viking Dynamic Simulator and SPHINX, was installed at the complex.

The ground system equipment used for the Titan/Centaur program is a combination of Titan equipment and added Centaur equipment similar to that in use at Complex 36 which has been adapted for use at ITL.

Electrical Launch Control and Checkout Equipment

The electrical launch control and checkout equipment for Titan/Centaur consists of modified Titan items, new Centaur items, and the Computer Controlled Launch Set (CCLS) at Complex 36. Equipment required for remote control of the launch is located in the VIB. Required test support equipment is located in the mobile vans, or in the complex AGE Building.

Titan Electrical Systems Modifications

The integrated Titan/Centaur countdown is controlled and monitored by the Titan Launch Control Console (LCC) and Control Monitor Group (CMG) which have been modified to accommodate the Centaur interface. Countdown

holds, status, and major functions are displayed on the LCC. The interfacing CMG has been modified to control the integrated countdown on a time and event sequenced basis.

The Vehicle Checkout Set (VECOS) provides the capability for checking out the Titan flight control, hydraulic and electrical systems. For the Titan/Centaur program a new unit of the Titan IIID design has been installed. A remote control and monitor panel has been added to allow checkout and malfunction isolation from the VIB after pad evacuation.

The Titan Data Transmission System (DTS) and Data Recording System (DRS) have been modified to transmit high-speed data from the new VECOS and to handle the Centaur command/monitor signals between the VIB and LC-41. A new hard wire system is used to transmit critical Centaur signals between LC-41, VIB, and LC-36. The DRS has been modified to provide recording of Titan and Centaur functions.

The Titan ground instrumentation equipment (GIE) located in the instrumentation van and VIB instrumentation room has been modified to signal condition, encode, and transmit new Centaur measurements. A real time display and magnetic tape recordings of Titan/Centaur PCM and landline data has been provided. An additional capability to rapidly display Titan/Centaur data was provided by the implementation of the Kennedy Space Center's Central Instrumentation Facility (CIF).

Centaur Electrical System Additions

Newly installed Centaur electrical AGE provides separate control of Centaur operations but utilizes the existing Titan ground instrumentation, data transmission/recording and launch control systems. Isolation of Titan and Centaur power functions is maintained for all integrated systems.

Eight (8) Centaur Launch Control Consoles in the VIB provide remote control of checkout and launch operations. The Mobile Transfer Room (MTR) contains launch control, instrumentation, system test equipment, and other electrical equipment required to interface with the Centaur vehicle, Complex 41 systems, CCLS, VIB Control Room, and instrumentation room. Local control and monitoring of Centaur systems is provided on the MTR.

Centaur electrical AGE installed in the Complex 41 AGE Building includes eleven racks of electrical equipment required for control of Centaur systems at Complex 41, power supplies, and data recording equipment.

LAUNCH CONTROL AND VEHICLE POWER SYSTEMS

by J. Nestor

Two separate power systems are used to support system and countdown operations for the Centaur vehicle at ITL-41 as shown by figure IX-2. The first power system furnishes 28 volts d.c. for control of AGE and GSE at the launch pad. The power supply is located in the AGE Building equipment room, and receives its input power from commercial sources. Battery backup for d.c. power is supplied from a set of batteries in the same building. During assembly and checkout operation at the VIB, this power is furnished from an alternate power source in the VIB.

The second system provides 28 volts d.c. power to the vehicle buses and the SCU until the time the changeover switch switches to internal power. The primary and backup supplies are located in the MTR. Primary input power is commercial; backup power input is provided from a diesel generator. During preliminary checkout operations at the VIB, vehicle power is furnished from a MMC power source in the VIB. This power supply also furnishes power to the LCC and the isolation relays.

The interfacing Titan and Centaur facility a.c. power systems were extensively modified and include the use of commercial and diesel generator power.

Three diesel generators are used to assure critical power requirements were met. At the complex, one 100 kilowatt generator was used as the primary source for Titan/Centaur critical launch systems and one 500 kilowatt generator was used as the primary source for the Centaur Environmental Control System.

At the VIB, one 100-kilowatt generator is used as the primary source for critical LCC systems. Appropriate switching has been installed to use backup commercial power in event of diesel failure.

RANGE SAFETY COMMAND SYSTEM

by J. Nestor

Ground support equipment and support hardware associated with the Range Safety Command System is shown in the block diagram (fig. IX-3). Control and monitoring of the system is from the RSC control panel in the VIB. Power for the airborne receivers is furnished from the two RSC power supplies in the MTR up to the time RSC power is switched to internal at approximately T - 4:20 minutes.

The Test Set in the MTR provides the capability for closed loop testing of the system. The RF switches are remotely controlled from the test set to permit selection of any one of the four vehicle borne RSC antennas for closed loop tests, and between the test set and the receiving antenna for Range tests. Transmitted Range commands are monitored at the control panel in the VIB to correlate received commands and resultant RSC system response.

LANDLINE INSTRUMENTATION SYSTEM

by J. Nestor

This system provides the recording and display capability required to support system and vehicle checkout procedures, countdown, and launch. Data recording and display devices are provided in the MTR, the AGE Building, and at the VIB in the DTS, Instrumentation and Launch Control Rooms.

Landline signals are multiplexed in the Titan instrumentation van for transmission via coaxial cables (A2A lines) to the VIB, Complex 36 CCLS, and to CIF.

A parallel but independent system installed in the MTR provides a landline data link with the CIF and Complex 36 CCLS directly rather than through the instrumentation van. This second system serves as a backup during countdown and launch, in addition to providing the required instrumentation capability when the instrumentation van is not otherwise needed, as in some preliminary checkout procedures.

RF SYSTEMS

by J. Nestor

Telemetry

The telemetry system at LC-41 supports two functions: (1) RF link operations via S-band antennas on the stub adapter and shroud and (2) the PCM/CCLS hard link operation to Complex 36 via a coaxial cable in the Centaur umbilicals.

For the RF link, signals from the S-band antennas on the vehicle are routed by cable through an RF coupling to reradiate antennas on the umbilical tower. These antennas in turn beam the signals to receiving antennas at the VIB, Complex 36, Hangar AE, and the CIF. At the VIB, receiving equipment detects the RF signals for decommutation and signal conditioning, or tape recording. Predetection signals may also be transmitted to Complex 36 from the VIB via the GEEIA transmission link.

At Complex 36 the antenna receiving system receives radiated or reradiated signals beamed from Complex 41 or from the VIB. The receiving equipment predetects these signals for tape recording, or detects the RF signals for PCM decommutation and signal conditioning.

The hard link to the CCLS is accomplished by routing coaxial cable from the umbilical interface to the GEEIA interface rack (GIR) in the MTR, then by coaxial cable to the GEEIA rack in the AGE Building. From the GEEIA rack the RF signals are transmitted to the VIB by A2A lines, and patched to Complex 36 for recording on magnetic tape, CCLS interface, or decommutation for PCM to landline stripout.

GROUND MECHANICAL

by G. S. Pablic and M. Proskine

The mechanical modifications and additions required to provide the Titan/Centaur capability encompass all areas of ITL. Discussion here is limited to the Centaur systems. Operation of the existing Titan systems remains essentially unchanged and a Titan IIIC launch capability has been retained. Installation of the systems required to provide the Centaur services necessitated considerable mechanical, facility, structural, and electrical effort. In addition to the Complex 41 area, the Umbilical Tower, Transporter/Mast, and AGE Building were effected. The following systems have been incorporated.

1. Liquid Hydrogen System. - The new system includes a 28 000 gallon liquid hydrogen dewar, vaporizer, and control equipment installed in the new LH_2 Holding Area. Vacuum jacketed LH_2 transfer piping is routed from the LH_2 Holding Area to the base of the umbilical tower and up the tower to the level required for loading the Centaur fuel tank. The system includes a H_2 vent system with a vent stack and burner near the LH_2 storage area and another vent stack on top of the umbilical tower. LH_2 transfer operations are controlled remotely from the Launch Control Center after the launch complex has been evacuated. The vent stack on top of the Umbilical Tower is used only during transfer operations. Figure IX-4 provides a simplified diagram of the system.

2. Liquid Oxygen System. - The new system will include a 13 000 gallon LO_2 dewar with the necessary transfer control equipment in the LO_2 Holding Area. The vacuum jacketed transfer piping has been routed through the trench across the launch deck to the base of the Umbilical Tower and up the tower to the proper level for loading the Centaur oxidizer tank. LO_2 transfer operations are controlled remotely from the Launch Control Center after the launch complex has been evacuated. Figure IX-5 provides a simplified diagram of the system.

3. Liquid Helium System. - The system consists of a mobile LHe dewar parked in the LHe Holding Area and vacuum jacketed piping from the Holding Area through the tunnel to the base of the Umbilical Tower and up the tower to the level required for Centaur engine chilldown. The system is remotely operated and controlled from the Launch Control Center. Figure IX-6 shows the LHe system.

4. Centaur and Spacecraft A/C System. - The Centaur and spacecraft air conditioning system at LC-41, shown by figure IX-7, consists of an air conditioning unit installed in the air conditioning shelter and ducting through the tunnel to the base of the Umbilical Tower and up the tower to the proper levels to provide conditioning to the Centaur thrust compartment, the Centaur equipment compartment and to the payload shroud. The system can operate with either air or dry gaseous nitrogen as the conditioning medium. The air intake for the system is connected into the existing remote air intake system which allows intake air to be drawn

from either of two remote air intake structures. Prior to start of tanking cryogenics into the Centaur vehicle the system will be switched from air to dry GN_2. The GN_2 will be supplied to the air conditioning system from the air conditioning gas storage.

5. Centaur Gas Systems (LC-41). - The Centaur pressurization, purge, and routine gas requirements are supplied from the expanded gas storage area located in the northeast quadrant of the Launch Complex. High pressure (5000 psi) helium and nitrogen gases is delivered from the gas storage area to Centaur pressure control equipment in the basement of the AGE building, as shown in figure IX-8. Distribution piping for the Centaur vehicle and equipment has been routed through the tunnel from the AGE Building to the base of the Umbilical Tower and up the tower to the proper levels for usage.

6. Intermediate Bulkhead Vacuum System. - The system consists of a vacuum pump, control panel, and piping located on the Umbilical Tower at the level required to service the Centaur vehicle.

7. H202 Vacuum Drying System. - The vacuum drying system consists of a vacuum pump, a liquid nitrogen cryogenic cold trap, and the necessary piping to interface with the Centaur attitude control system components. The entire system has been installed on the Mobile Service Tower at the level of usage.

8. H202 Transfer System. - The transfer system consists of a portable transfer cart, spill control basin, platform scale, dilution basin, and drain. The system is located in the Mobile Service Tower and is locally controlled.

9. Centaur Umbilical Retract System. - The Centaur umbilical retract system installed on the transporter umbilical mast, shown by figure IX-9, includes both pneumatic cylinder retract and static lanyard systems for the Centaur forward and aft umbilicals, as located in figure IX-10.

The system includes the flexible umbilical lines extending from the umbilical tower to the vehicle disconnect interfaces, retract actuators, lanyards and supporting electrical, instrumentation, and pneumatic equipment.

FACILITY AND SITE OPERATION

by M. Crnobrnja and E. Timmons

All facility systems required for the TC-1 vehicle performed satisfactorily during countdown and launch. The launch damage other than fire-related is typical of other Titan launches and is not considered significant. During the countdown and launch no power outages occurred. Diesel generator operation was satisfactory.

At T - 332 minutes a report was made on the communications network that a power drop had occurred at the GD/CA Mobile Transfer Room (MTR). Investigation of the stripchart recorder connected to the incoming line at the AGE Building indicated that a voltage drop of approximately 20 volts had taken place on the incoming 480 volt a.c. supplied by Florida Light and Power. The dip was reported to have lasted about 10 seconds. Since critical launch control equipment is connected to a diesel generator throughout the countdown, there was no effect on the countdown.

Further investigation of the charts after launch showed that this power dip occurred four times during the countdown at approximately 1 to $1\frac{1}{2}$ hour intervals from 2:15 a.m. to 5:45 a.m.. Each occurrence resulted in two or three voltage dips in a period of 1 to 3 minutes, then a return to stable conditions for a minimum of 55 minutes. The cause of these transients on the commercial power system is unknown.

Also of major importance during launch was proper operation of the facility water system. Because of the extraordinary demand on this system during the post-launch transporter fire, a review of system operation is being performed. Further discussion is beyond the scope of this report.

LAUNCH CONTROL AND GROUND INSTRUMENTATION SYSTEM

by E. Timmons

The countdown and launch of Titan/Centaur 1 had no major problems relative to ground systems. Table IX-I provides a list of minor anomalies discussed in the following paragraphs. The count picked up at the T-565 minute mark at 10:28 p.m. EDST on February 10, 1974.

At approximately T - 372 minutes Centaur landline measurement COS-6P began to experience problems. This is the measurement which monitors the interstage adapter air conditioning duct pressure. The measurement was breaking up on the strip chart display and the panel operator's meter such that the true value of the pressure could not be determined. This measurement problem persisted on and off throughout the countdown. Since the measurement was not a redline and since other measurements in the same duct such as temperature were still reading properly and were within expected limits, no attempt was made to repair the problem since repair would have necessitated disabling other measurements also. Initial diagnosis indicated a shorted diode in the stripping gate within the digital-to-analog converter supplying the stripchart recorder and panel meter.

At approximately T - 371 minutes, the lamp test button was pressed on the Titan Launch Control Console (LCC) to insure that all the indicators on the panel were operative. Although the action of pressing this button normally only applies +28 volts d.c. to all the panel lamps, a shorted diode in one of the lamps allowed this +28 volts d.c. signal to be sent through the AGE system. The signal simulated the action of someone pressing the control switch on the panel which closes the airborne prevalves on the Titan. The "close prevalve" signal was present for 9.05 seconds, the duration of the lamp test exercise. As can be seen from figure IX-11 this action had no effect on the airborne prevalves since there was no path for current to flow to the prevalve motor. The path is open by virtue of the circuitry which routes motor current through the closed limit switch on the valve. Since the valve was already closed, this limit switch was in the position shown in the figure. There was no effect on the countdown. The diode was replaced after launch following normal component replacement procedures.

At approximately T - 306 minutes the programmable PCM decommutator in the VIB ground station used to decommutate Centaur telemetry data dropped out of synchronization. This decommutator is used to strip various redline measurements out of the telemetry data stream for display on the GD/CA consoles in the VIB. Loss of synchronization in the equipment results in display readings that are not representative of the actual data.

The decomm was immediately reset and returned to sync for about 6 minutes. At T - 300 approximately, the same problem recurred. The decision was made to replace the bit synchronizer in the decomm. The bit

synchronizer is used to recondition the bit train and provide a synchronization function to insure that the PCM bits are stored in register properly prior to being converted to an analog signal.

Change-out of the bit synchronizer was accomplished in about 5 minutes. During this time, all strip charts and panel meters which were reading measurements from the Centaur telemetry were inoperative. Once the bit synchronizer was restored to proper configuration, the system operated normally until approximately T - 120 minutes when the same problem occurred. The decommutator was manually reset. It again functioned properly until approximately T - 73 minutes when it again dropped out of sync. It was again manually reset and continued to operate properly for the remainder of the launch. Since the problem was obviously within the decomm post-launch trouble shooting was instituted.

Since this failure had the potential of scrubbing the launch, a backup plan was formulated after the bit synchronizer replacement was completed. The backup plan entailed the use of a secondary data system to evaluate Titan telemetry data so that the PCM decommutator normally assigned to Titan could be switched over to decommutate the Centaur data. This plan would be feasible since Titan real time analog data evaluation is limited to seven measurements, all relatively steady and quiescent; Centaur requires approximately 87 measurements to be evaluated in real time, too many to be handled on the secondary system.

At T - 190 minutes a Titan automatic vehicle verification (AVV) was started. This is a test of the flight controls system in Titan automatically conducted under the control of a tape in the Vehicle Checkout Set (VECOS). The tape contains 641 discrete flight controls tests and 32 VECOS self-tests. Anytime a NO-GO occurs during a particular test, the VECOS stops testing and displays a NO-GO indication along with an analog value related to the response of the flight control system to the particular test.

A NO-GO was received at frame 7 of the test tape. Frame 7 is a test of the autopilot +20 volt source. The limits on the voltage are 19.100 to 20.100. At the time of the NO-GO, the VECOS analog meter was reading 20.17 volts. However, a telemetry readout of the same voltage showed a value of 19.91 volts, well within the limits. It was decided to rerun the test and see if the same hold would be generated again. A rerun was successful and the remainder of the AVV continued on to the last frame with no other anomalies. The problem was attributed to noise on the VECOS sense lines and was recorded as an unverified failure.

PROPELLANT LOADING SYSTEM OPERATIONS

by G. S. Pablic

Titan vehicle propellant loading was initiated on F - 3 day and completed on F - 2 day. A simplified diagram of the Titan propellant loading system is provided by figure IX-12. System operation was satisfactory.

Centaur propellants were tanked during the launch countdown. Significant system operation event times are provided by table IX-II. Table IX-III provides the system flow rates, temperatures, and quantities consumed. The propellant loading system operation was satisfactory and all Centaur tanking requirements were met.

LIQUID HELIUM SYSTEM OPERATIONS

by G. S. Pablic

Liquid helium flow for chilldown of the Centaur vehicle propellant turbopumps was initiated at T - 30 minutes during the countdown and continued to T - 6.97 seconds. The nominal flow rate was 8 gallons per minute and total liquid helium usage was 260 gallons. System operation was satisfactory.

UMBILICAL SYSTEMS OPERATION

by M. H. Proskine

The Titan vehicle umbilicals (six total) are disconnected by static lanyard pull at vehicle liftoff. Disconnect times are provided by table IX-IV. The data shows that the Titan umbilical disconnect sequence did not occur as planned. The Solid Rocket Motor Umbilical (LB1E and RB1E) should have disconnected before the first Titan vehicle core umbilical (1C1E).

The Centaur umbilical retract system consists of both pneumatic actuator and static lanyard system. Table IX-V provides a listing of all Centaur umbilicals with the planned release times and release modes identified.

Event times for system actual operation are provided by tables IX-VI through IX-IX.

Operation of the Centaur umbilical retract system was satisfactory. Based on event times the primary retract mode was used for release of all umbilicals. A minor discrepancy was a 190 millisecond delay in separation of the liquid hydrogen line. The retract time for this umbilical was well within the T - 0.5 to T + 0.5 allowable time. Most probable cause was slower actuating cylinder operation.

CENTAUR ENVIRONMENTAL CONTROL SYSTEM OPERATION

by A. Hahn

The Centaur Environmental Control System provides conditioned air or gaseous nitrogen to the payload, Centaur equipment module, and interstage adapter compartment. System operation was switched from air to GN_2 prior to start of Centaur propellant loading. Table IX-X provides information on the GN_2 portion of the system.

System operation was satisfactory, except for malfunction of one instrumentation pressure transducer which had no effect on countdown or launch.

PNEUMATIC GROUND SYSTEMS OPERATION

by A. C. Hahn

Pneumatic systems include the primary helium, emergency helium, purge helium, and routine nitrogen systems. The three helium systems are peculiar to Centaur. The routine nitrogen storage supplies both the Titan and the Centaur nitrogen systems. No anomalies occurred in the systems during launch countdown. System parameters were as follows:

System	Supply pressure, psig			Remarks
	Start 1 hr hold	Liftoff	Minimum allowable	
Primary helium	5310	4290	2200	
Emergency helium	5520	5280		
Purge helium	5550			
Routine GN_2 (oxidizer side)	5250	4200	2200	Centaur only for countdown
Routine GN_2 (fuel side)	5500	3500 (T + 1 hr)	2000	Titan only

TITAN AIR CONDITIONING SYSTEM OPERATION

by A. C. Hahn

The core air conditioning system, shown by figure IX-11, supplied conditioned air to compartment 2A and to the start cartridges. No anomalies occurred in the system during launch countdown. System parameters at the end of the hard duct on the umbilical tower for compartment 2A were as follows:

	Actual at T - 100 min	Required
Temperature	64° F	65±3° F
Flow	124 lb/min	124±5 lb/min

TABLE IX-1 - LAUNCH CONTROL AND INSTRUMENTATION ANOMALIES

TIME	PROBLEM	CAUSE
T-372	Measurement COS-6P providing ISA air conditioning pressure erratic through CD	Shorted Diode
T-371	Inadvertent "Close Prevalve" signal sent when LCC "Lamp Test" button depressed	Shorted Diode
T-306 T-300 T-120 T-73	Programmable PCM decommutator dropped out of synchronization	Not Known
T-190	Titan autopilot + 20V NO-GO during automatic vehicle verification	Test Rerun Satisfactory. Cause Unknown

TABLE IX-2

PROPELLANT LOADING SYSTEM EVENTS

	PLANNED TIME FROM LIFTOFF MIN:SEC	ACTUAL TIME FROM LIFTOFF MIN:SEC
Start LO_2 Transfer Line Chilldown	T-105	T-106
Start LO_2 Tanking	T-98	T-99
Start LH_2 Chilldown	T-90	T-90
Start LH_2 Tanking	T-70	T-70
LO_2 at Flight Level	T-8	T-32
LH_2 at Flight Level	T-8	T-34
Secure LH_2 Tanking	T-0:90	T-0:81
Secure LO_2 Tanking	T-0:75	T-0:65

TABLE IX-3

LO_2 AND LH_2 SYSTEM NOMINAL FLOW RATES

	LH2 #/MIN	LO2 #/MIN
Chilldown	100 #/min	50 #/min
Main Transfer	590 #/min	2540 #/min
Topping	10 1/2 #/min	9 3/4 #/min

LO_2 AND LH_2 TEMPERATURES AT F&D VALVES (NOMINAL)

	^{o}F
LO_2 - Measurement CJS-12T	-282.4
LH_2 - Measurement CJS-14T	-420

LO_2 AND LH_2 QUANTITIES

	GALLONS
LO_2 - Total Usage	6,000
LH_2 - Total Usage	16,000

TABLE IX-4 - TITAN UMBILICAL EJECT TIMES
(Time Referenced to CMG T-0)

PLANNED SEQUENCE	ACTUAL SEQUENCE	DRS CHANNEL NO.	TIME SECONDS
LB1E	1C1E	111	T+0.40
RB1E	LB1E	140	T+0.43
1C1E	RB1E	142	T+0.43
2A1E	2A1E	035	T+0.44
2A2E	2A2E	015	T+0.49
2C1E	2C1E	011	T+0.55

TABLE IX-5 - CENTAUR D-1T UMBILICAL TIMING

UMBILICAL	PLANNED RELEASE TIME	RELEASE PRIMARY	MODE BACKUP
AFT UMBILICALS			
Aft Panel	T-4 sec	Pneu. Actuator	None - Abort
LO_2 & LH_2 F&D	T-0.50 sec	Pneu. Actuator	None
ISA A/C Duct	T-0	Pneu. Seal	Static Lanyard
Aft He Purge	L/O	Static Lanyard	None
FORWARD UMBILICALS			
P1	T-4 sec	Pneu. Actuator	Break Away
P2	T-4 sec	Pneu. Actuator	Break Away
P3	T-4 sec	Pneu. Actuator	Break Away
P4	L/O	Static Lanyard	Break Away
P5	L/O	Static Lanyard	Break Away
Helium Purge Line	L/O	Static Lanyard	None

TABLE IX-6 - CENTAUR UPPER UMBILICAL EJECTION
(Time Referenced to CMG T-0)

	MEASUREMENT	TIME SECONDS
CMG Eject Signal Sent (T-4 Signal)		T-3.97
Centaur MTR T-4 Relay Actuation	CNS 36X	T-3.96
P-3 Umbilical Ejected Signal	CMV 56X	T-3.02
P-2 Umbilical Ejected Signal	CMV 55X	T-2.83
P-1 Umbilical Ejected Signal	CMV 54X	T-2.62
P-4 Rise-Off Disconnect	CMV 57X	T+0.71
P-5 Rise-Off Disconnect	CMV 58X	T+0.82

TABLE IX-7 - CENTAUR AIR CONDITIONING DISCONNECT

	MEASUREMENT	TIME SECONDS
CMG Signal (T-0)		T-0
Centaur MTR Relay Actuation		T+0.04

TABLE IX-8 - CENTAUR AFT PANEL EJECTION
(Times Referenced to CMG T-0)

EVENT	MEASUREMENT	TIME SECONDS
CMG Aft Plate Eject Signal	CNS 20X	T-3.97
Centaur MTR Relay Actuation	CNS 35X	T-3.96
Aft Door Closed Signal (Switch Closure)	CMV 60X	T-2.47
Aft Plate Ejected to CMG	CMV 31X	T-2.47
Overall Time Span Required		1.50

TABLE IX-9 - FILL AND DRAIN VALVE EJECTION
(Times Referenced to CMG T-0)

EVENT	MEASUREMENT	TIME SECONDS
CMG Signal Eject F&D Valves	CJS 197X & 199X	T-.48
Centaur MTR Relay Actuation	LO_2 CNS 38X & 39X	T-.43
	LH_2 CNS 40X & 41X	T-.43
Disconnect Signal Received by CMG	LO_2 CJS 197X	T-.09
	LH_2 CJS 199X	T+.09
Overall Actuation Time		.39 & .57

TABLE IX-10

ENVIRONMENTAL CONTROL SYSTEM OPERATION
TC-1 LAUNCH COUNTDOWN

EVENT	TIME G.M.T	INLET TO PAYLOAD COMPARTMENT			INLET TO EQUIPMENT MODULE COMPARTMENT			INLET TO INTERSTAGE ADAPTER COMPARTMENT			GN_2 SUPPLY PRESSURE-PSIG		GN_2 SUPPLY POUNDS
		TEMP.-DEG.F (REQUIRED= 47-51)	PRESS. INCHES H_2O	FLOW RATE #/MIN. (REQUIRED= 115-125)	TEMP.-DEG.F (REQUIRED= 70-75)	PRESS. INCHES H_2O	FLOW RATE #/MIN. (REQUIRED= 85-95)	TEMP.-DEG.F (REQUIRED= 115-125)	PRESS. INCHES H_2O	FLOW RATE #/MIN. (REQUIRED= 125-135)	HIGH PRESSURE SYSTEM	LOW PRESSURE SYSTEM	
CHANGE EQUIPMENT MODULE GAS TO GN_2	1010	48.5	25.5	120	72	18.5	90	116	35.5	130	5850	2240	218,919
CHANGE INTERSTAGE ADAPTER GAS TO GN_2	1011	48.5	26	READ ON PANEL METER	72	17.5	READ ON PANEL METER	116	35.5	READ ON PANEL METER	5850		218,919
CHANGE PAYLOAD GAS TO GN_2	1012	48.5	26		71	17.0		115	34.5		5850		218,919
START LO_2 TANKING	1159	48	24.5		71.5	17.5		118	34.5		3790		177,522
START LH_2 CHILLDOWN	1208	48	24.5		71.5	17.5		118	34.5		2660		176,632
START LH_2 TANKING	1228	48	24.5		71.5	17.5		118	34.5		3330		169,693
START LHe CHILLDOWN	1318	48	24.5		71.5	17.5		118	INSTRUMENT MALFUNCTION		2720		150,721
T-0	1348	48.5	24.5	120	71.5	17.5	90	119		130	2340	2240	139,508

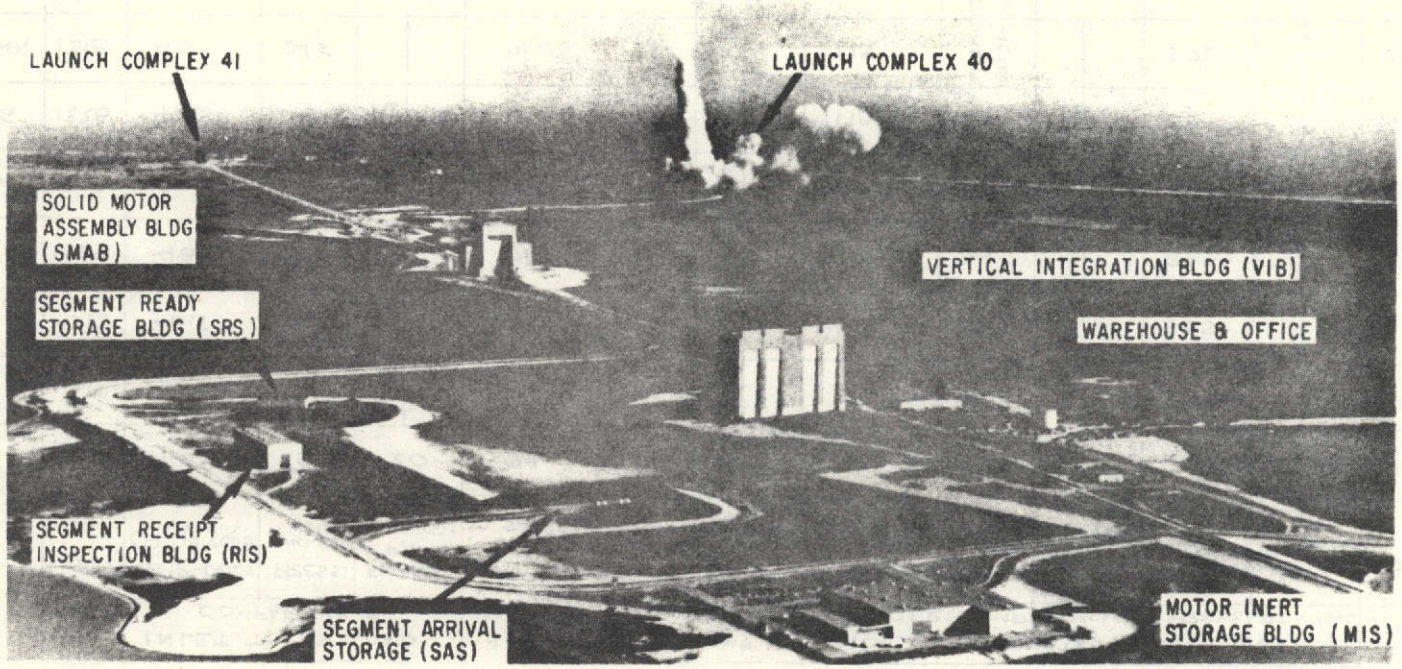

FIGURE IX-1 CKAFS INTEGRATE-TRANSFER -LAUNCH FACILITIES

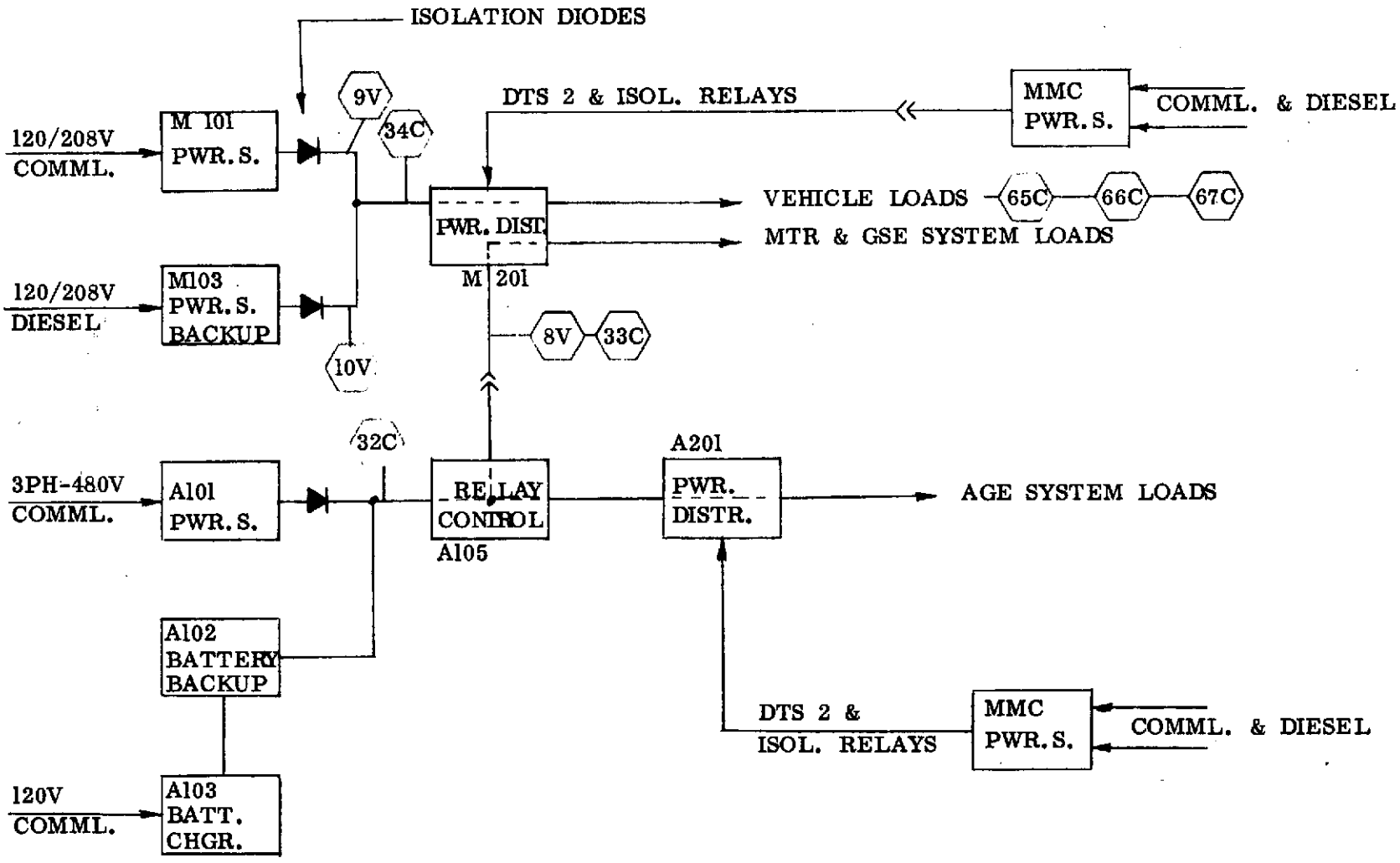

FIGURE IX-2 - 28VDC POWER SYSTEM AT CX41 LAUNCH PAD

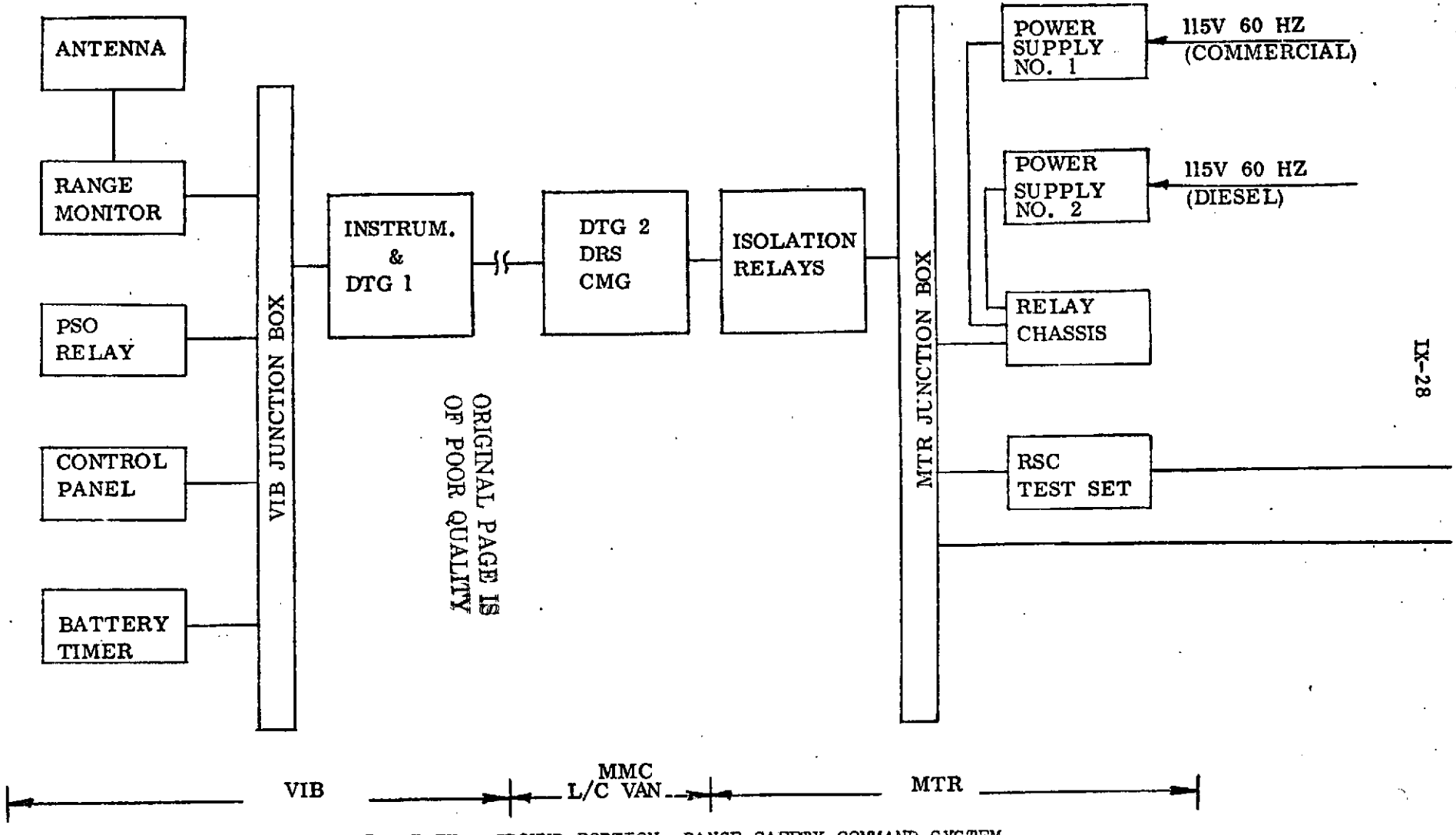

FIGURE IX-3 GROUND PORTION, RANGE SAFETY COMMAND SYSTEM

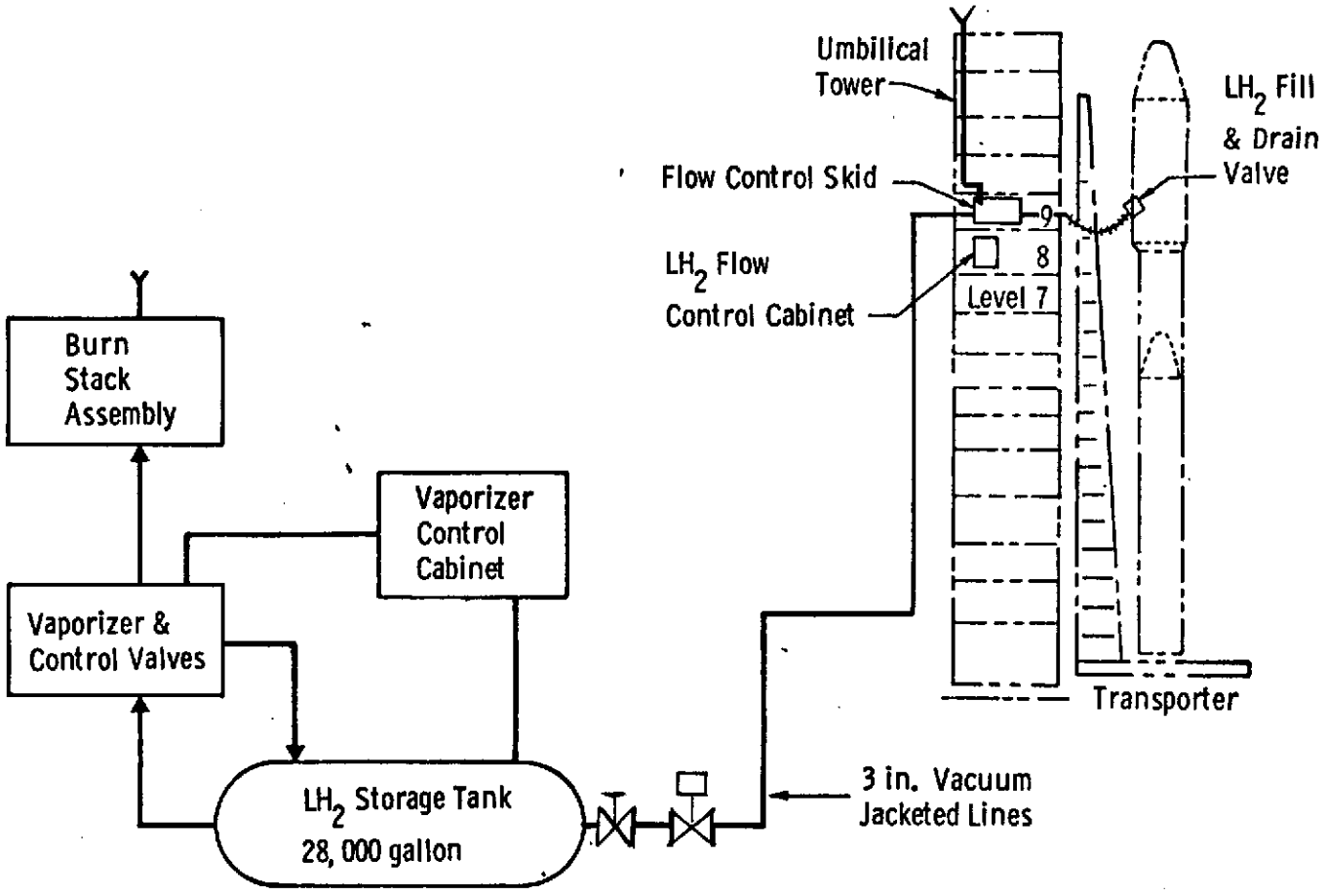

FIGURE IX-4 - LIQUID HYDROGEN SYSTEM

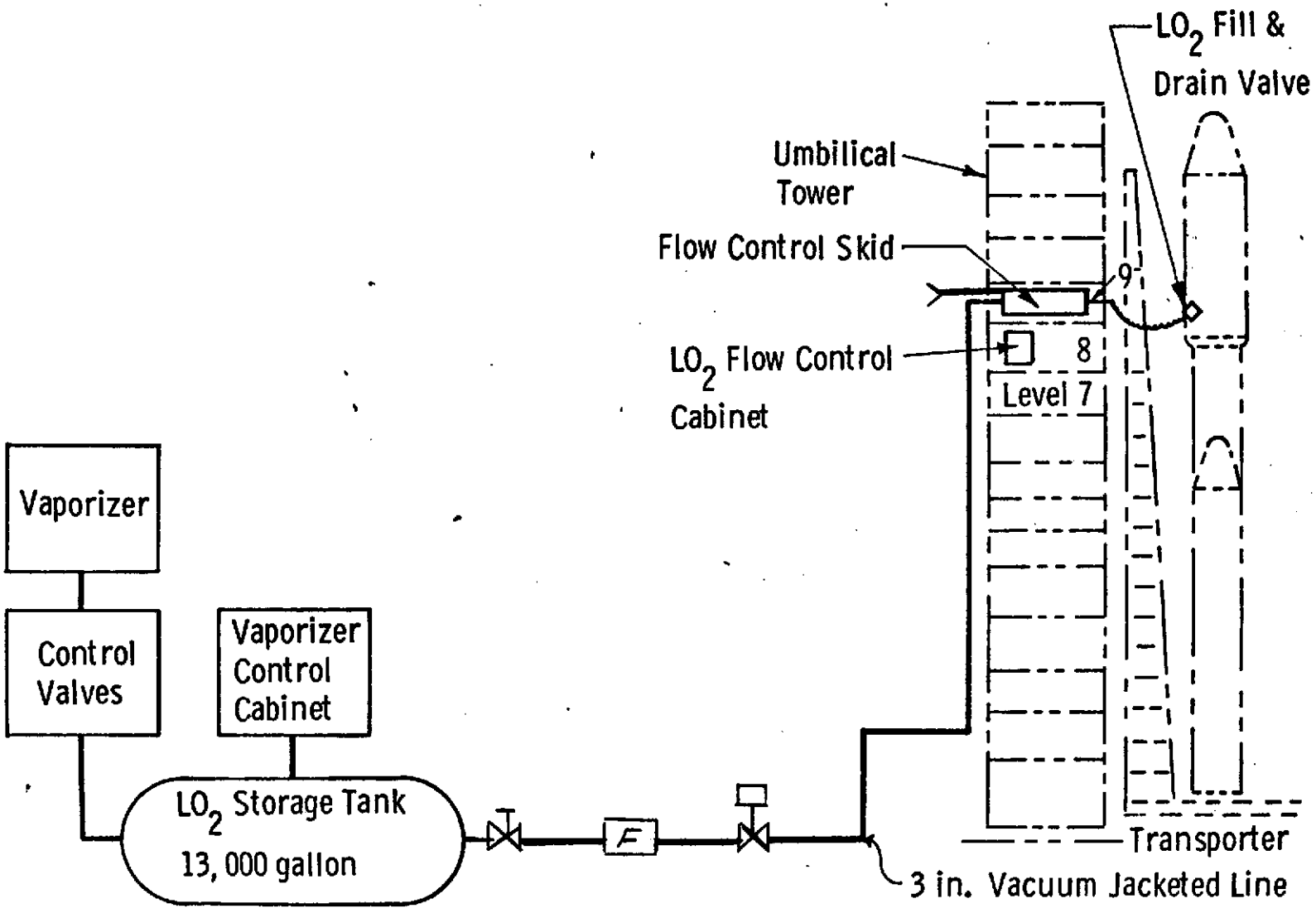

FIGURE IX-5 - LIQUID OXYGEN SYSTEM

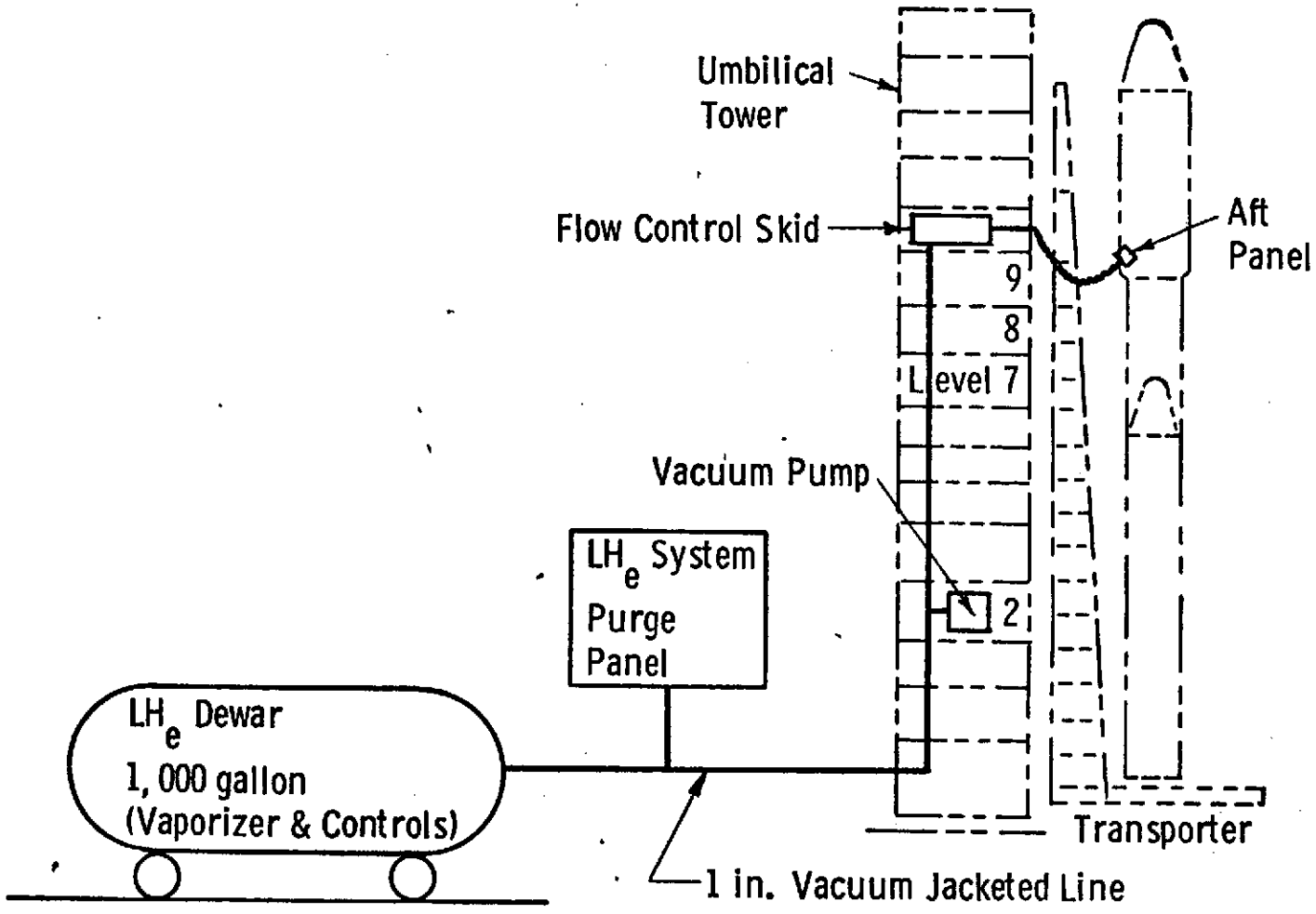

FIGURE IX-6 - LIQUID HELIUM SYSTEM

System Flow Rate and Temperature Capabilities Are:

	Payload	CEM	ISA
Flow: Air	120 ± 5	90^{+5}_{-25}	130 ± 30
(Lb/Min) GN_2	120 ± 5	90 ± 5	130 ± 5
Temp: Air	49 ± 2	60 ± 5	110 ± 5
(°F) GN_2	49 ± 2	70^{+5}_{-0}	120 ± 5

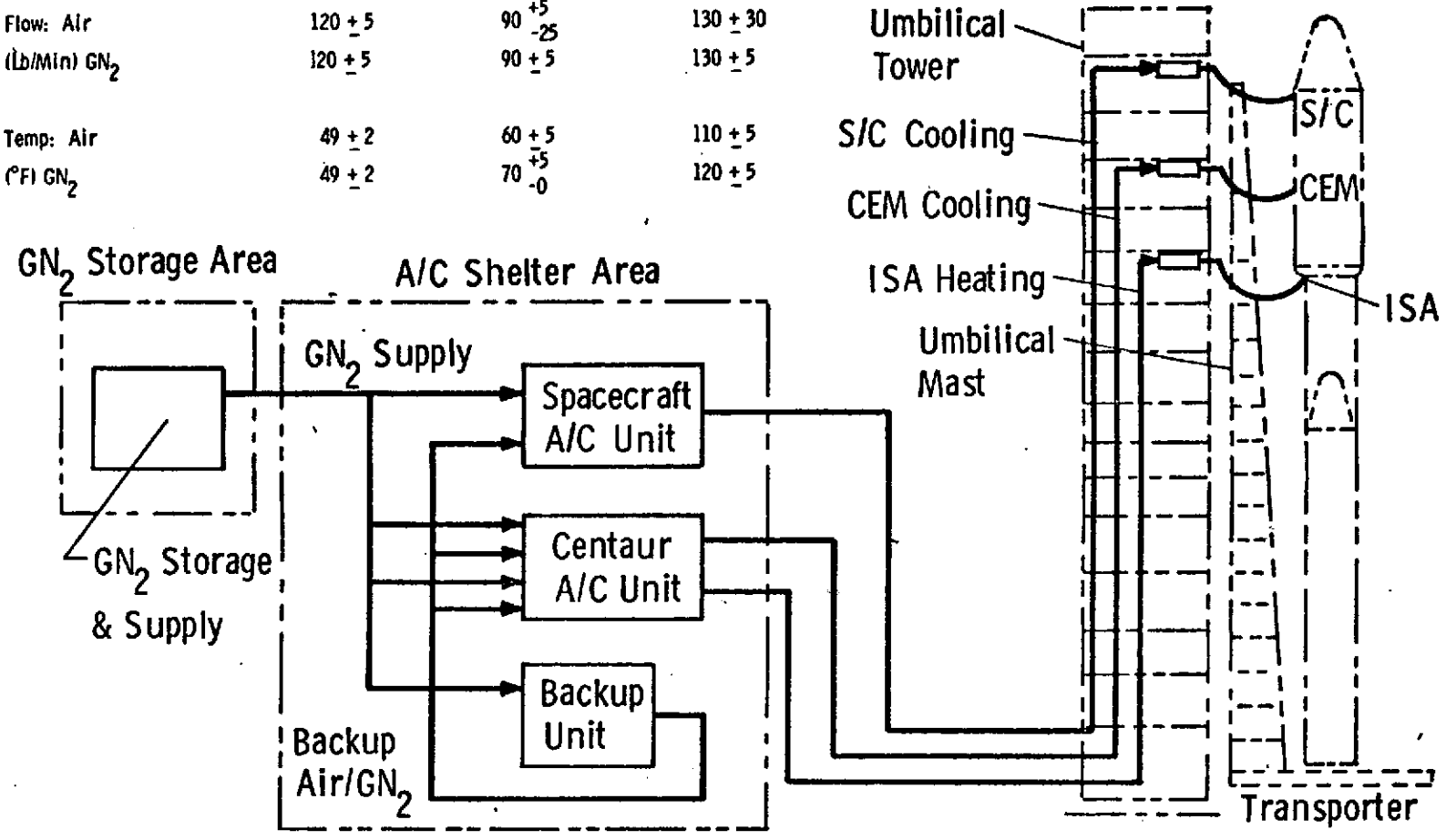

FIGURE IX-7 - CENTAUR ENVIRONMENTAL CONTROL SYSTEM

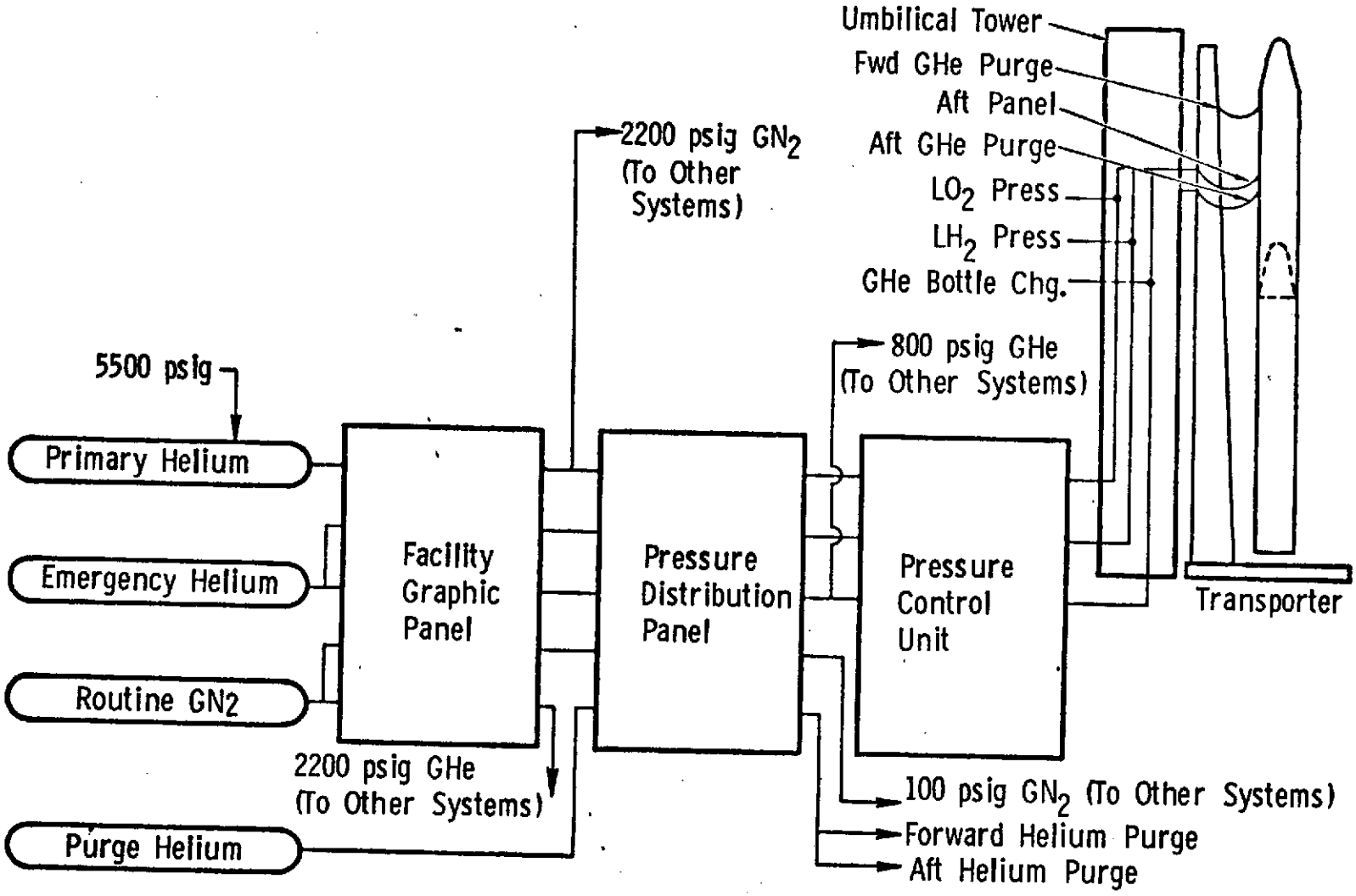

FIGURE IX-8 - CENTAUR PNEUMATIC SYSTEM

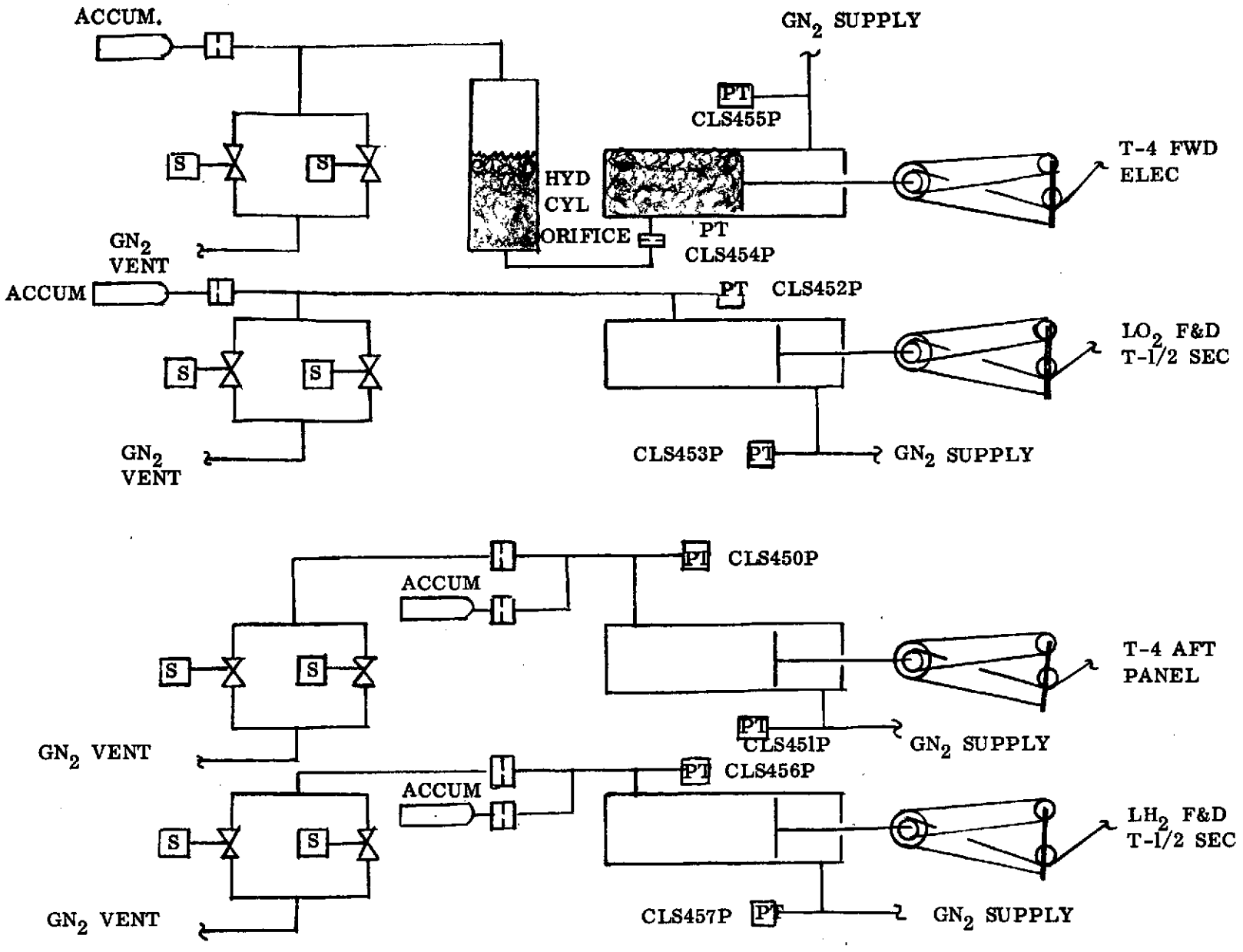

FIGURE IX-9 - UMBILICAL RETRACT SYSTEM SCHEMATIC

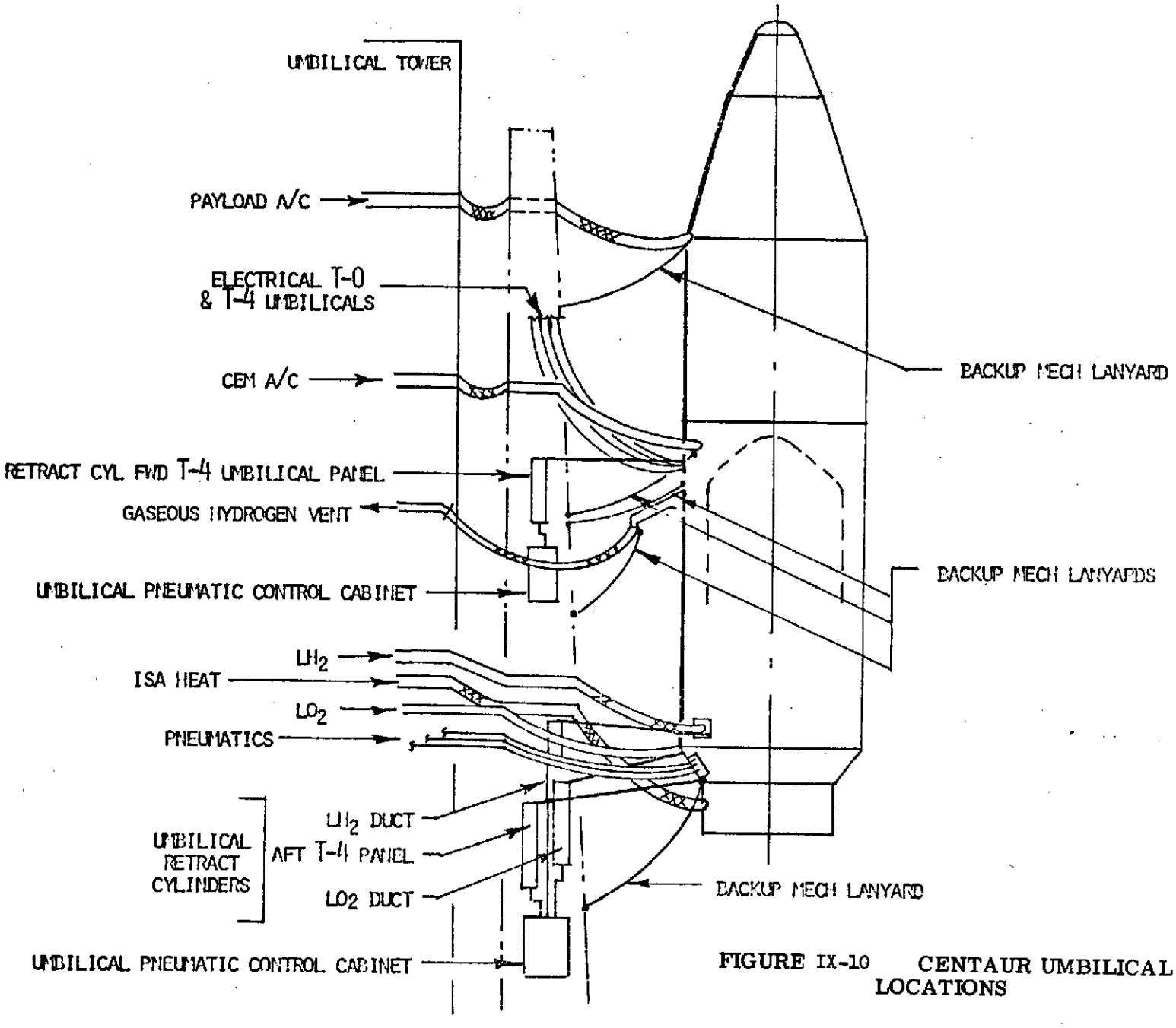

FIGURE IX-10 CENTAUR UMBILICAL LOCATIONS

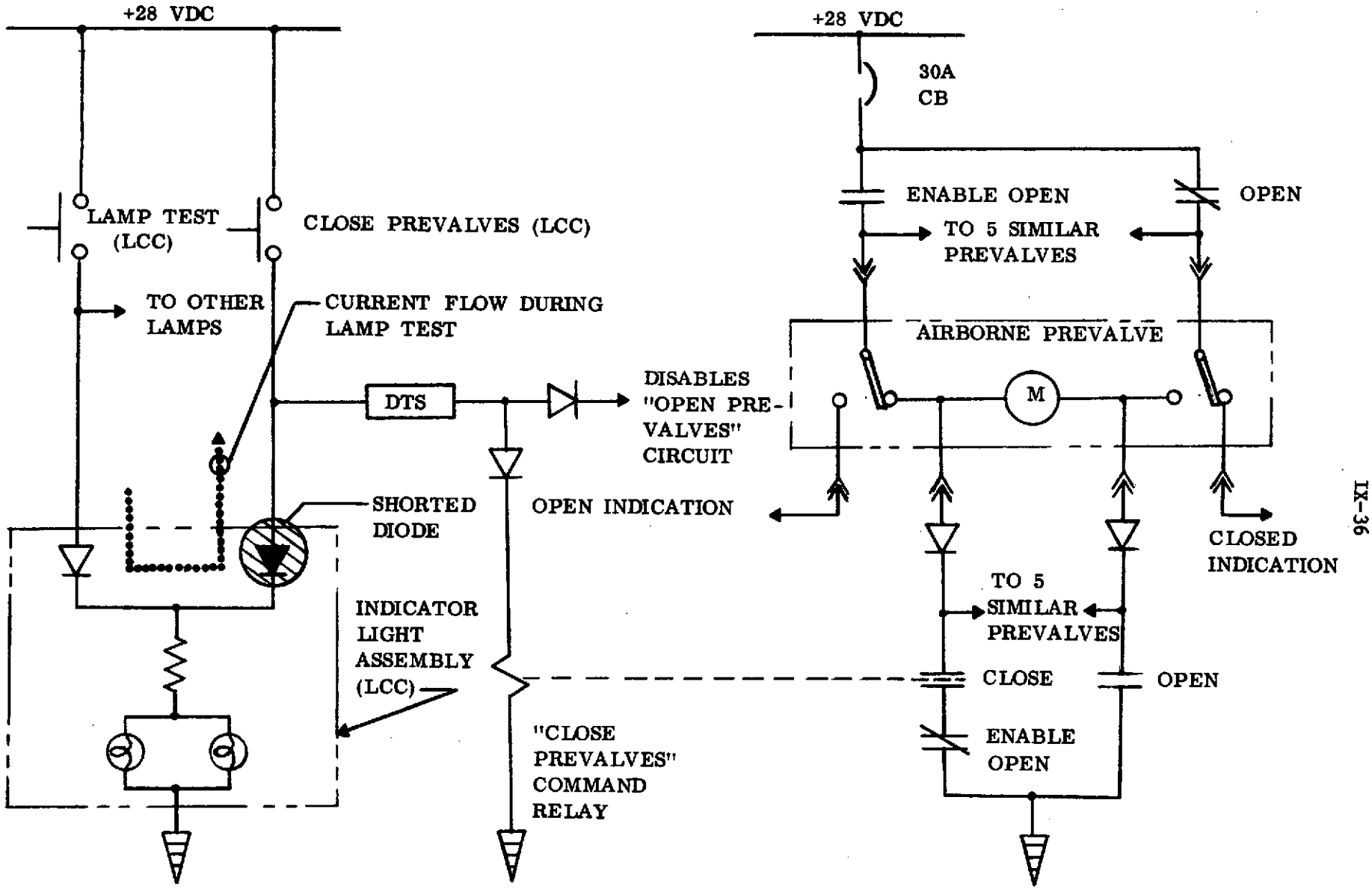

FIGURE IX-11 - PARTIAL SCHEMATIC DIAGRAM - CLOSE PREVALVES CIRCUIT